Understanding the Holocene explosive eruption record of the Tongariro Volcanic Centre, New Zealand

---

A thesis presented in partial fulfilment of the requirements for the degree of

Doctor of Philosophy

in

Earth Science

at Massey University, Palmerston North

New Zealand

Massey University

Anja Moebis

2010

This thesis is dedicated to my partner and best friend

Gert Lube

Ngauruhoe viewed from the west

Abstract

The Tongariro Volcanic Centre has experienced many VEI 1-4 eruptions over the last 12 000 cal. yrs. B.P., dominantly from Ruapehu, Ngauruhoe and Red Crater. The historic record of 150 years alone is insufficient to provide a robust understanding of future volcanic hazard, necessitating a quantification of eruption parameters from the geological record. The major obstacle to this is untangling a complex sequence of interdigitating, fine-grained and poorly distinguishable tephras from the three source volcanoes. With detailed mapping and using volcanic glass chemistry, tephras from the three sources were discriminated. This has led to a revision of the age of Ngauruhoe to be at least 6500 cal. yrs. B.P., around 4000 years earlier than previously thought. It also provides the most detailed explosive eruption frequency and magnitude record from the area since 12 000 cal. yrs. B.P. Ruapehu and Ngauruhoe tephras were characterised by initial phreatomagmatic explosions that transformed into dry magmatic (strombolian) phases. Magma-water interaction is shown by basal layers of pale-brownish-grey fine ash, containing blocky glass shards with small isolated spherical vesicles, and exhibiting surface conchoidal and step-like fractures. The magmatic phase ash is microlite-rich, with dark glass containing elongate vesicles with thin bubble walls and irregular surfaces. The largest eruption recognised from Ngauruhoe, produced a distinct dark purple tephra, with a well-constrained volume of 26.6 $x10^6$ m^3, and a probable eruption column height of about 15 km. The total tephra volume from Ngauruhoe is estimated to be 952 x 10^6 m^3, around 50% of the known lava volume. A climactic eruption period of Ngauruhoe occurred between ~ 2900 and 2700 cal. yrs. B.P., during which 64% of its known explosive eruptions occurred, including its largest known events. This phase, representing 3% of the volcano's lifespan, produced 57% of its pyroclastic output. Over the last 12 000 cal. yrs. B.P., the frequency of Ruapehu eruptions appears to have increased about 2000 yrs B.P., but this may reflect better preservation and exposure of the more recent tephras. Bursts in Ruapehu explosive activity have occurred out of phase with those from Ngauruhoe. The minor pyroclastic cone of Red Crater represents an eruption site that was active for at least ~ 4000 cal. yrs. B.P. and has mainly been characterised by effusive events. Since around 900 cal. yrs. B.P. minor explosive events have occurred from this location, increasing in magnitude from 400 cal. yrs. B.P.

Acknowledgements

This thesis would not have been possible without the help and encouragement of many wonderful and beautiful people whom I would like to thank here with all my heart.

I wish to thank my chief supervisor Prof. Shane J. Cronin (Massey University) for his guidance and encouragement through the research process and also for allowing me to fulfil all my ideas I had during these last few years writing my PhD. I would like to thank him for giving me the financial support for expensive analysis along with travel money for field work and international conferences, especially for the 2010 Tephra conference in Japan, where I had the chance to see my first eruption at Sakurajima volcano. He also helped me to secure funding from the New Zealand Earthquake commission to support my PhD-studies.

I also thank my co-supervisors Prof. Vince E. Neall (Massey University), Assoc Prof. Ian Smith (University of Auckland), Dr. Bob Stewart (Massey University) and Dr. Károly Németh (Massey University) for always answering all sorts of questions and for the useful discussions along the way as well as giving good advice on structuring my thesis. I would like to thank Vince for always finding the references I needed and for helping me to present my thesis in proper English and not in English with German grammar. Bob and Ian I would like to thank for the help in interpretations of chemical data and Ian I thank deeply for the special arrangements to use the electron microprobe in Auckland. Without this analysis, it would have not been possible to achieve the outcome of my study. And thank you Ian for always being so enthusiastic about my work. Károly, thanks for sharing his expertise in phreatomagmatic processes and particle shape analyses and for providing me with ash samples from Ambae and Yasur/Vanuatu.

I am very grateful to Prof. Richard Price (Waikato University) for analysing the strontium isotopes in my volcanic glasses from Ngauruhoe and for very useful discussions about the correlation of these data to strontium analysis on Ngauruhoe lavas.

Prof. Mark Bebbington (Massey University) I would like to thank for the age calculations (spline fit) of individual tephras in the sediment core of Lake Rangatauanui.

Over the course of my study I have cherished the friendship of my fellow students Deborah Crowley, Natalia Pardo, Marco Brenna, Susan E. Cole, Anke Zernack, Kat Holt and Jonathan Procter. Thanks for the thousands of fruitful discussions about volcanoes and about my research, the pub-nights and also for being there in the most difficult times throughout my PhD. Jon Procter and Matt Irwin I thank in particular for providing me with maps that included all my special wishes. The greatest thank you goes to my friend, flatmate and colleague Michael B. Turner. Thanks for the best BBQs, the Sunday soups, tea on the front wall, trips through the North Island, such as to Cape Palliser, and for introducing me to the scary cows on his parents farm. I am very glad to know you. Janine Krippner I would like to thank for her discussions about Ngauruhoe and especially for providing me with stunning photographs of Ngauruhoe eruptions from her grandfather John A. Krippner. Thanks also to Emma Phillips for assisting with running my samples through the Laser Particle Analyser.

A very special thanks goes to Ritchie Sims, at University of Auckland, who made the mostly monotonous and long hours on the microprobe a fun experience. He was always there when the smallest problem occurred, but mostly I thank him for just being a friend. His fantastic sense of humour and his interest in music from the 60s and 70s made the time in Auckland in his “office” very enjoyable.

Dr. Phil Shane (University of Auckland) I would like to thank for his expertise and all the discussions about analyses of volcanic glasses and also for providing me with useful papers in Tephrochronology.

Kate Arentsen, Moira Hubbard and also Liza Haarhoff, you are special. Thank you for all the help during all the administrative problems I had to face during my PhD and answering all sorts of questions regarding the University system, providing me with stationery and helping me to scan images and for helping me to format my thesis.

Thanks to the staff of the Soil and Earth Science Group in INR such as Alan Palmer, Bob Toes, Ian Furkert, Anne West, Glenys Wallace and Ross Wallace for their help in

the laboratories, for explaining instruments, providing me with lots and lots of H_2O_2 and sample bags, and helping with general sample preparations and discussions. A special thanks goes to Mike Bretherton who helped me patiently through all my attacks of hysteria when my computer did not want to do what I wanted. And it was always a pleasure to discuss with him all sorts of food recipes and to exchange seeds and vegetable plants. Furthermore, I would like to thank Dr. Clel Wallace for his support throughout my study, especially in the lab on sample preparation along with long discussions about specific problems regarding the interpretation of data. Thanks to Doug Hopcroft, who taught me the beautiful technique of scanning electron microprobing.

Thanks also to a special friend from Vanuatu: Douglas Takai Charley. Not only did he teach me how to prepare Kava, he also gave me one of the best volcanology lessons ever, when we climbed Ngauruhoe together.

I am grateful to the Department of Conservation, in particular to Harry Keys and Jimmy Johnson, for permission to work in this spectacular field area and to stay in the huts. I also would like to thank various hut wardens, especially Amy, who made me always feel welcome with a nice hot cup of tea. I also am grateful to the iwi of Ngati Rangi, who gave us permission to core their sacred Lake Rangatauanui, which delivered valuable pieces of information on the TgVC volcanoes and Mt Taranaki.

This PhD was supported by the Earthquake Commission (EQC) with a full doctoral scholarship and I also would like to thank Education New Zealand for a New Zealand Postgraduate Study Abroad Award, and INTAV for funding my travel to international conferences in Iceland and Japan. Additionally, I would like to thank the Tongariro Natural History Society and the Helen E. Akers Scholarship for funding my research.

Finally I want to thank my family. I am very grateful to Uwe Kratz and Edith Stein for their support throughout the entire process of my coming to New Zealand and also during the time of my study. They always made me feel very welcome at their home, especially the million times I was in Auckland for microprobing.

I want to thank my family back home in Germany, especially my parents Eckhard and Christiane Möbis, who supported me with their interest in my study, financially, with their love and also accepted my craziness in becoming a volcanologist on the other side of the world. You were, and are always, there for me when I needed you and listened to my German, which has got progressively worse over the last few years. Thank you.

I save my final thank you for Gert Lube. I can't really describe how thankful I am to know you, being allowed to love you and having you in my life. I think I could not have done any of this without you; your support, calmness, listening and your love. Thanks that you are a part of my life and for your patience during this rollercoaster PhD.

Table of Contents

List of Tables

List of Figures

List of Abbreviations

cpx	Clinopyroxene
DP	dark purple
EMPA	Electron microprobe analyses
F. or Form.	Formation
hb	Hornblende
hyp	Hypersthene
LPA	Laser Particle Analysis
MtF	Mangatawai Formation
MF	Mangamate Formation
NF	Ngauruhoe Formation
Ng	Ngauruhoe
ol	olivine
opx	orthopyroxene
OVC	Okataina Volcanic Centre
Ox	oxides
PF	Papakai Formation
PP	pale purple
plg	plagioclase
px	pyroxene
Rua	Ruapehu
RC	Red Crater
SEM	Scanning electron microscope
TgVC	Tongariro Volcanic Centre
tm	Titanomagnetite
TNP	Tongarioro National Park
TTF	Tufa Trig Formation
TVC	Taupo Volcanic Centre
TVZ	Taupo Volcanic Zone

Chapter 1

Introduction

1.1. Introduction

Successful mitigation of volcanic hazards requires precise information of the frequency, magnitude and nature of potential hazard impacts on communities and its support structures. Our geological knowledge of volcanic eruptions from the Tongariro Volcanic Centre (TgVC) includes a well-developed stratigraphy of major pyroclastic eruptions from Ruapehu (Donoghue *et al.,* 1995; 2001), Tongariro (Topping, 1973) and Ngauruhoe (Hobden *et al.*, 2002). However, this record is biased toward the largest and most easily mapped units and does not represent the full eruptive spectrum or frequency of events from TgVC. In addition, very little detailed physical information has been collected for pyroclastic deposits from which models of eruption-column heights; vent conditions, associated hazard processes, and eruptive-sequence reconstructions can be developed. Physical information on eruption styles, shapes and heights of eruption columns, and the mechanism of tephra deposition are known only from witnessed eruptions over the last 150 years (Gregg, 1960b) and are not well constrained for prehistoric eruptions. These data are critical for developing effective and accurate volcanic event scenarios for emergency management and hazard mitigation planning (Blong, 1984). It is well known that large plinian eruptions can produce volcanic ash clouds to great heights (up to 50 km) and deposit ash several hundred kilometres away from vent, depending on wind conditions during an eruption. The ash cloud during the Mt. St. Helens eruption in 1980, travelled a distance of ~900 km within the first 10 hours, and at 2000 km from source up to 1 cm of ash was deposited (Sarna-Wojcicki *et al.*, 1981), creating a hazard for agriculture and economic infrastructure over an enormous area. On a much smaller scale, ash clouds from Ruapehu in the night of 11/12 October 1995 reached a height of 10-12 km and "distributed at least 25 million m^3 of tephra over a broad area east-north-east of the volcano" (Cronin *et al.*, 2003). For

instance, ash deposits in Gisborne (220 km away) were up to 2 mm thick. Apart from the 17 June 1996 event, most of the other events of this eruption sequence produced lower columns and more restricted ash deposits. Eruptions, especially from Ruapehu in 1945 and 1995-96, caused local-scale intense damage and economic losses associated with agriculture (animals and plants), public health, infrastructure and transportation, water supplies and electricity, buildings and facilities, and the ski and tourism industries (Johnston *et al.*, 2000).

Studies of large scale eruptions are common world-wide; for example the historical eruptions from: Krakatau 1883, Indonesia (Simkin *et al.*, 1983), Mt. Pelee 1902, Martinique (Fisher *et al.*, 1980; Bourdier *et al.*, 1989), Mount St. Helens in 1980 ,USA (Lipman and Mullineaux, 1981) , El-Chichon 1882, Mexico (Scolamacchia and Macias, 2005), and Pinatubo 1991, Philippines (Koyaguchi and Ohno, 2001; Wiesner *et al.*, 2004); along with "classic" large-scale ancient eruptions, such as: Laacher See 12.900 B.C., Germany (Schmincke *et al.*, 1999), Santorini 1600-1626 B.C., Greece (Friedrich *et al.*, 2006), Vesuvius A.D. 79, Italy (Sigurdsson *et al.*, 1982) and Taupo 1850 B.P., New Zealand (Wilson and Walker, 1985). By contrast, small-scale eruptions, that were less dramatic or spectacular have been generally overlooked. As a result, hazard scenarios are typically biased toward reproducing large-scale events such as those mentioned above (Lirer *et al.*, 1997; Spence *et al.*, 2004).

Geological work on the pyroclastic volcanic record of the TgVC in the past has provided a robust stratigraphy of major volcanic events from both, Ruapehu and Tongariro. In addition, basic geochemical information such as tephra composition, ferromagnesian mineral assemblages and bulk chemistry, as well as glass chemistry, have been collected and used for correlation purposes. Those have led to the realisation that there have been numerous different types of eruption at TgVC on a variety of scales. The spectrum of event types ranges from large sub-plinian events represented by the Bullot and Mangamate Formations (Nairn *et al.*, 1998; Donoghue *et al.*, 1999), through to vulcanian and strombolian eruptions with minor or variable influences due to the involvement of external water (Houghton and Hackett, 1984). By contrast, small-scale eruptions of the TgVC have been mostly overlooked due to the difficulties of studying and sampling them. Studies of such "minor" events are likely to reveal a

higher frequency of potentially hazardous eruption episodes from these volcanoes, which will allow a more accurate estimate of risk for tephra fall hazards in surrounding areas.

The benefits of understanding the record of minor events from potentially active volcanoes is demonstrated from Merapi volcano, one of the most active volcanoes in the world (Andreastuti *et al.*, 2000; Newhall *et al.*, 2000). The stratigraphic record from Merapi is similar to that at Ruapehu and Tongariro, and even here small eruptions are underestimated and need to be incorporated into new hazard maps and evacuation plans around the densely populated volcano (Andreastuti *et al.*, 2000). The social importance of "small" eruptions is demonstrated by Itoh *et al.* (2004), where several people were killed on Tokachidake volcano, even during its smallest eruptions. Hence, while small-scaled eruptions as individual events may be overlooked in importance in favour of the largest events possible, collectively they may still cause significant damage and unpredictable outcomes over the long term.

1.2. Objectives

Despite having a well-established record of major eruptions at the Tongariro Volcanic Centre (TgVC), much of the detailed volcanic history of events between these episodes is hidden within soil and fine-ash deposits. Hence little is known about the mechanisms, chemistry and frequency of small eruptions from the major TgVC volcanoes (Ruapehu and Tongariro). In this thesis I show that this "hidden" record accounts for the numerical majority of eruptions at these two volcanoes, and consequently by understanding this record, we in turn can begin to understand the full potential eruptive behaviour and related volcanic hazards at TgVC.

For this reason the main objective of this study is to understand the eruption record and to collect information about small eruptions within the TgVC, particularly over the last ~12 000 cal. yrs. B.P., over which the most detailed record can be put together. My aim is to develop a better understanding of eruption frequency, magma composition,

vesiculation and fragmentation processes and the role of magma/water interaction. This leads to the characterisation of the range in possible eruption styles and transport mechanisms that may be expected from these volcanoes. Furthermore, by understanding and interpreting the individual tephra layers, eruption magnitudes (volumes, column heights etc.) can be better constrained, together with a record of eruption frequencies of individual volcanoes. With this knowledge a more representative understanding of volcanic hazards will be gained. For a better understanding of eruption mechanisms it is also necessary to compare the deposits of these small TgVC eruptions to those derived from modern, analogous eruptions with a known source and observed fragmentation and transport mechanisms, such as ash from Ruapehu 1995-1996 and Ngauruhoe in 1954 and 1975.

1.3. Geological Setting

1.3.1. The Taupo Volcanic Zone (TVZ)

New Zealand is situated at the south western part of the Pacific "Ring of Fire", which represents the almost complete encirclement of convergent plate margins surrounding the Pacific Ocean (Neall and Trewick, 2008). East of North Island of New Zealand, the Pacific Plate (oceanic) is subducted westwards beneath the Indo-Australian Plate (continental) with convergence rates between 42 to 50 mm/year (DeMets *et al.*, 1994; Bibby *et al.*, 1995). This active subduction zone, represented by the Hikurangi Trench, is the southern extension of the Tonga-Kermadec-New Zealand arc system, which stretches over 3000 km in the South Pacific (Ballance *et al.*, 1999) (Figure 1.1). The subduction zone of the North Island of New Zealand is characterised by a clockwise rotation (Wallace *et al.*, 2004) causing changes in subduction styles in the Central North Island (Reyners *et al.*, 2006). Stratford and Stern (2006) calculated that the subducted plate, the Hikurangi Plateau, has a lower density then the normal mantle, based on the uplift of the Central North Island, and is subducted to a depth of 65 km immediately west of Taupo caldera (Reyners *et al.*, 2006). The subducted plate of the Hikurangi

Plateau consists of a fragment of oceanic flood basalt which was connected with the Manihiki and Ontong Java Plateaus and after formation was separated by Cretaceous seafloor spreading (Taylor, 2006). Farther west, the subduction reaches depths of 300 km and according to Boddington *et al.* (2004), activity of the subduction zone has been recognised 600 km below Mt. Taranaki. According to Reyners *et al.* (2006), the crust below the central TVC is ca. 35 km thick, and increases to a thickness of 45 km southwest of Ruapehu. According to Stratford and Stern (2006) the crust-mantle boundary beneath the southern TVZ and therefore the region of the TgVC, has a depth ranging from 15 to 20 km.

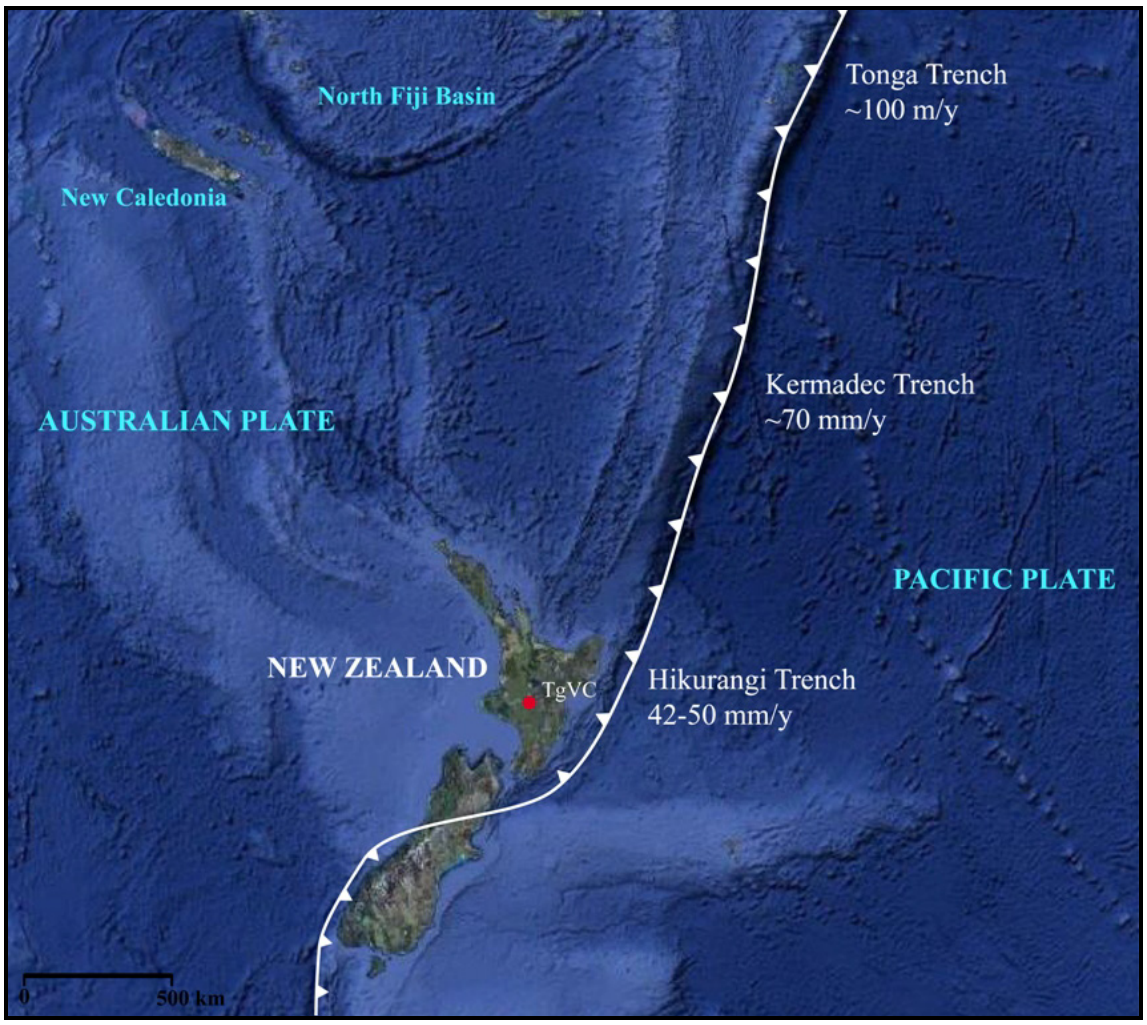

Figure 1.1: Topographic map showing the Tonga-Kermadec-New Zealand subduction zone. The subduction rate describe the present day convergence (DeMets *et al.*, 1994; Bibby *et al.*, 1995; Parson and Wright, 1996). Map from Google Earth 2009 (Data SIO, NOAA, U.S. Navy, NGA, GEBCO). The red dot represent the study area of the Tongariro Volcanic Centre.

The Taupo Volcanic Zone (TVZ) is 300 km long (with its northern limit, ~100 km offshore) and about 60 km wide, stretching from Ohakune to White Island on a SSW-NNE trend (Wilson *et al.*, 1995) (Figure 1.2.). The volcanic activity in the TVZ started around 2 million years ago with andesitic volcanism, while rhyolitic activity began around 1.6 Ma (Wilson *et al.*, 1995). Volcanism of the TVZ shows a large diversity in composition, with c. 80% of magmas being rhyolitic (Wilson *et al.*, 1995) and the remaining 20 % comprising basaltic, andesitic and dacitic compositions. Andesitic volcanism makes up c. 2.5% of the surface-represented volcanism of the TVZ and occurs mainly in the Central Plateau (95%) with minor occurrences in the Bay of Plenty (Graham *et al.*, 1995; Rowland and Sibson, 2001). The total magma production of the TVZ is at least 15 000 km^3 during *c.* 2 Ma lifetime (Allan *et al.*, 2008). This accounts for 90 % of known Late Pliocene to Quaternary eruptions in New Zealand (Wilson *et al*., 1995). The clockwise rotation of the forearc causes an extension of the northern part of the TVZ with a rate of 4-10 mm yr-1 (Darby and Meertens, 1995; Villamor and Berryman, 2001).

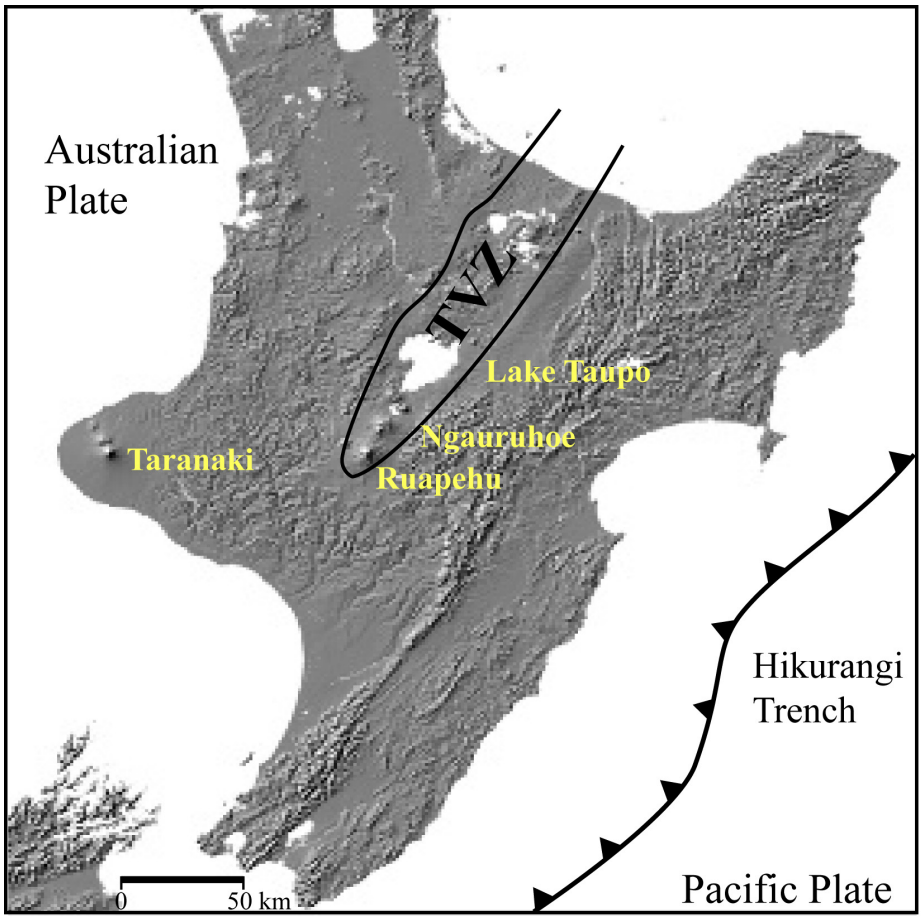

Figure 1.2: DEM of the Central North Island showing the boundary of the Taupo Volcanic Zone (TVZ), the volcanoes Ruapehu, Ngauruhoe, Taranaki and Taupo and its relationship to the subduction zone.

1.3.2. Tongariro Volcanic Centre (TgVC)

The Tongariro Volcanic Centre (TgVC) is situated at the southern end of the TVZ, south of Lake Taupo. Volcanism in the TgVC has occurred since at least 300 ka, defined by andesitic pebbles, originating from Mt Ruapehu within the Brunswick Formations at the Wanganui Basin (Fleming, 1953; Pillans, 1990; Parish, 1994). It includes two major stratovolcanoes, Mt. Ruapehu and Mt. Tongariro, with Mt. Ngauruhoe being the highest and youngest cone associated with the latter (Figure 1.3).

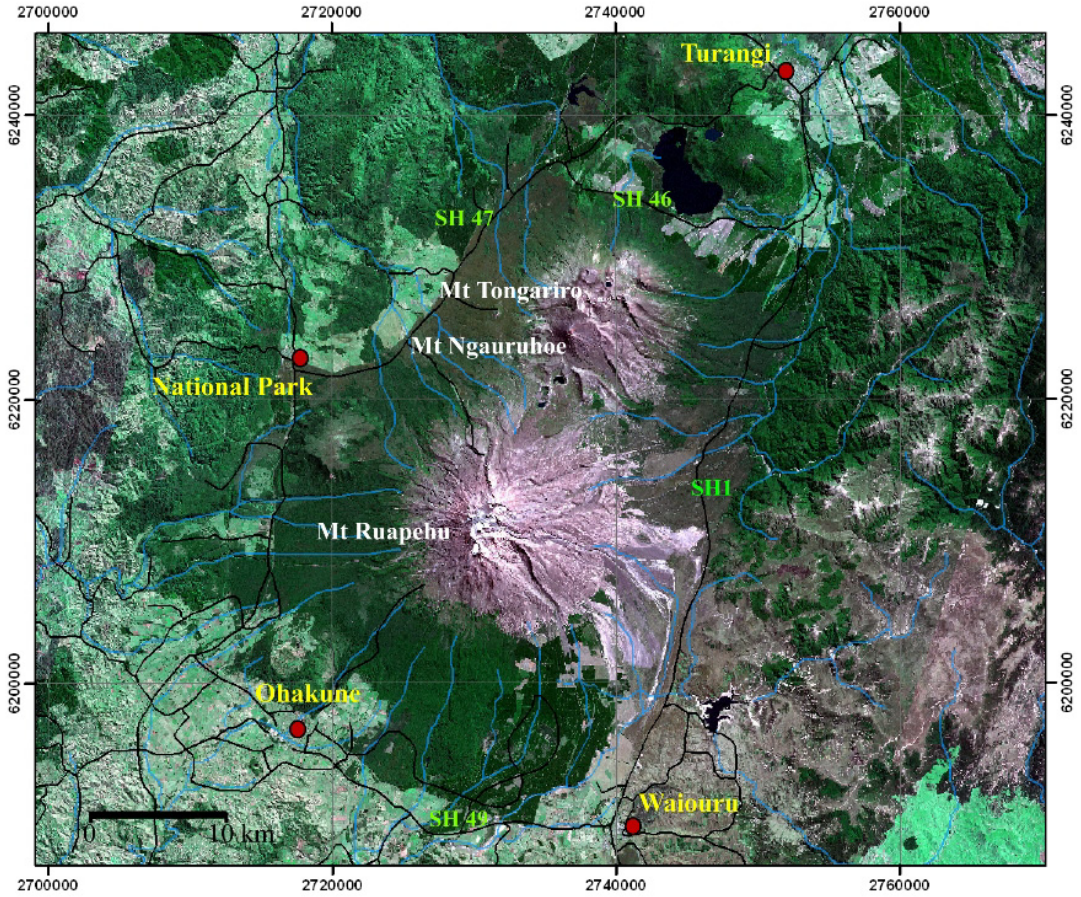

Figure 1.3: Satellite map of the Tongariro Volcanic Centre illustrating the main volcanoes, towns and main roads.

The wider and older part of the TgVC also includes smaller andesitic centres, such as Mt. Hauhangatahi to the west of Mt. Ruapehu, Pihanga, and Mt. Kakaramea to the north (Figure 1.4). In addition, several satellite cones of basaltic and andesitic composition are also included in the TgVC, such as Pukeonake (west of Ngauruhoe), Saddle Cone (on the northern flank of Ruapehu) and the Ohakune craters to the south-east of Ruapehu. The TgVC is surrounded by a ring plain consisting of a range of volcaniclastic sedimentary units including lahar, debris-avalanche and fluvial deposits with lava flows and widespread thin tephras (Topping, 1974; Donoghue, 1991; Cronin, 1996). These units are collectively up to 800 m thick in the Tama Lakes area, in the centre of the TgVC (Cassidy *et al.*, 2009). The ring plain overlies a basement of Mesozoic greywacke and argillite (Cole, 1978; Bibby *et al.*, 2002) covered by Tertiary sand- and mudstone (Grant, 2006).

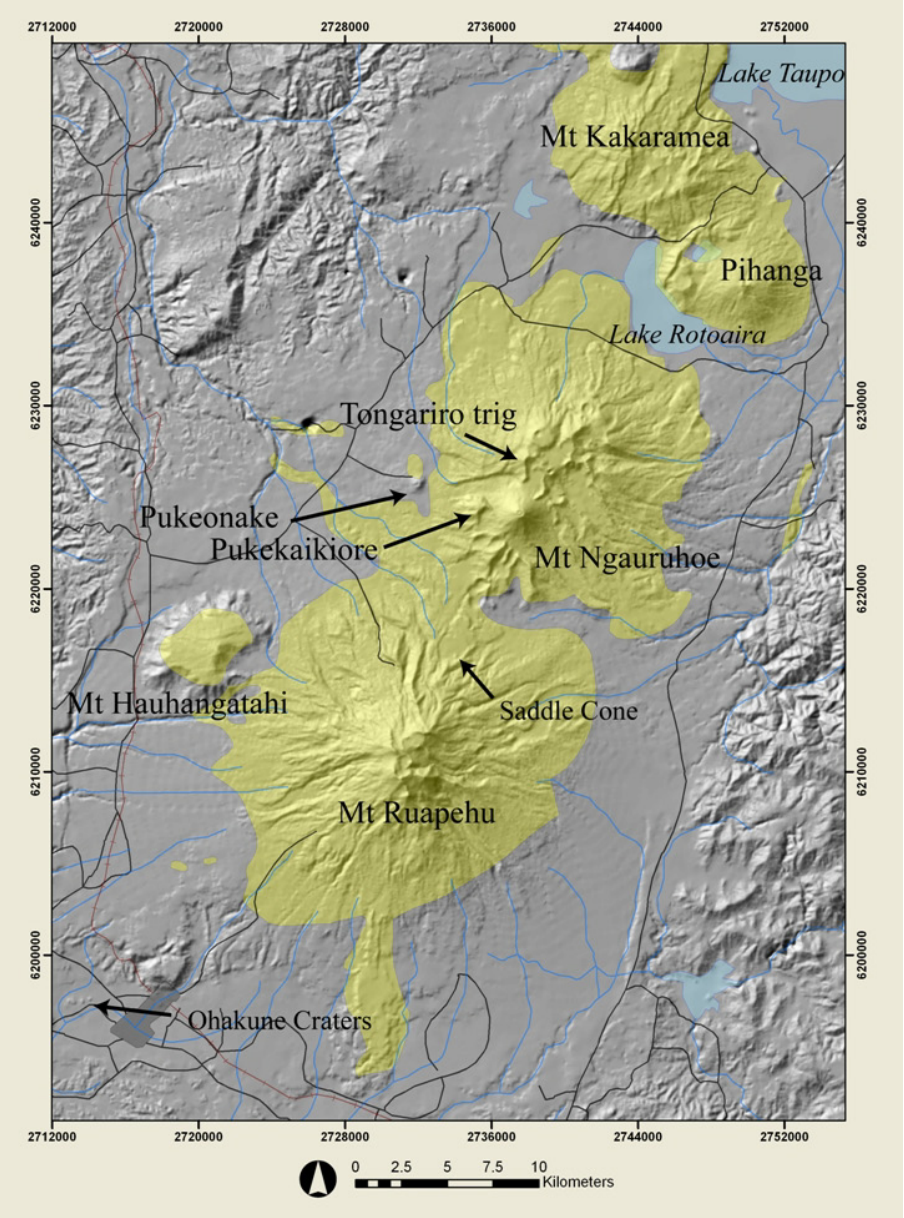

Figure 1.4: DEM showing the volcanic edifices of the Tongariro Volcanic Centre (TgVC).

Villamor and Berryman (2006), described the study area as including three main fault systems: the Ruapehu Graben (NS-trending), the Karioi fault (NE-trending) and Ohakune-Raetihi fault (WNW-ESE to W-E). The Ruapehu Graben is 40 km wide, and is defined by the Rangipo Fault to the east and the Raurimu Fault to the west of Ruapehu. This Ruapehu Graben has been extending since ~400 ka and is currently widening at a rate of 2.3 ± 1.2 mm/a (Villamor and Berryman, 2006) (Figures 1.5 and 1.6).

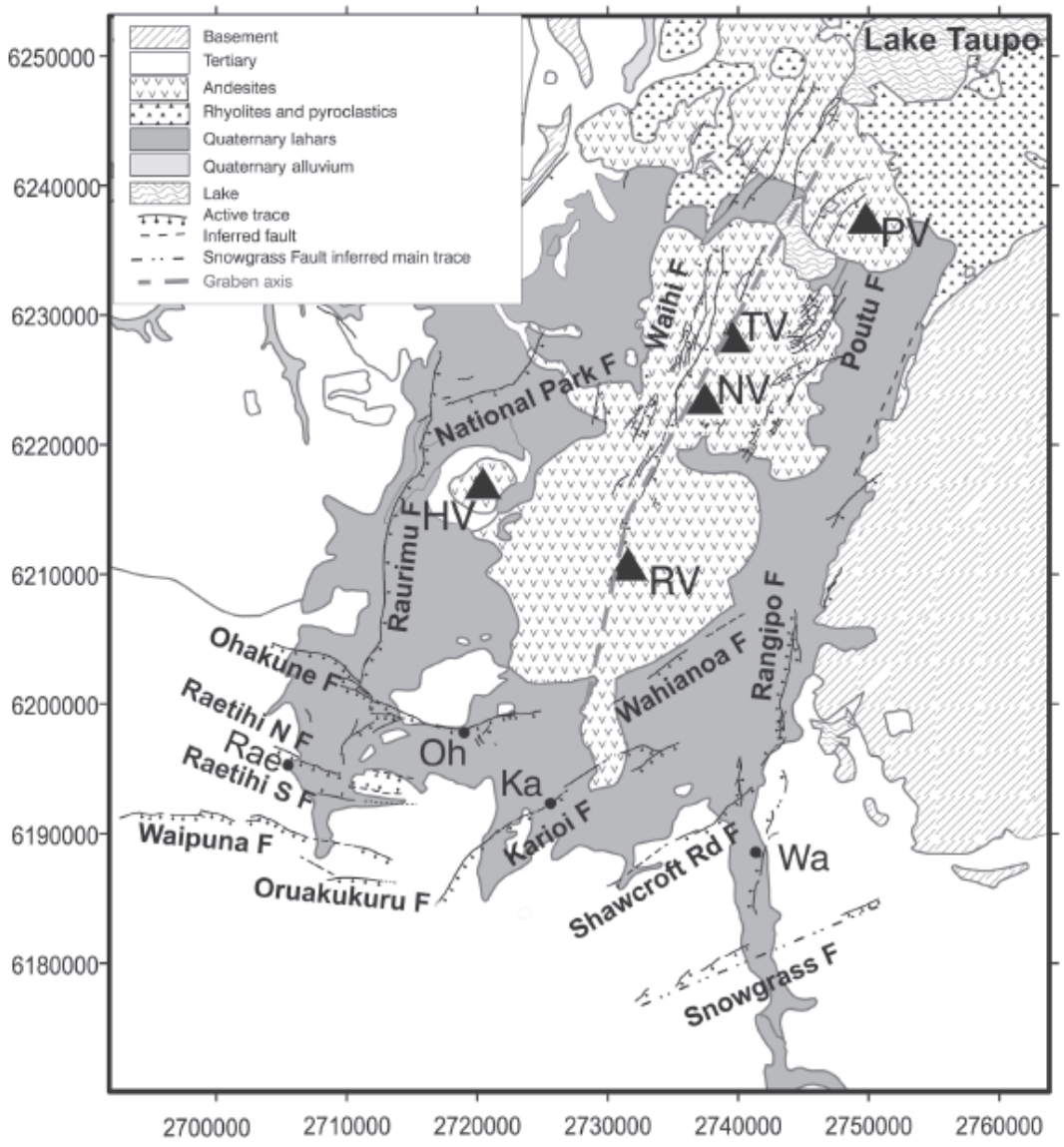

Figure 1.5: Fault system of the southern TVZ at the TgVC, from Villamor and Berryman (2006), PV = Pihanga, TV = Tongariro, NV = Ngauruhoe, HV = Hauhangatahi, RV = Ruapehu, Oh = Ohakune, Wa = Waiouru

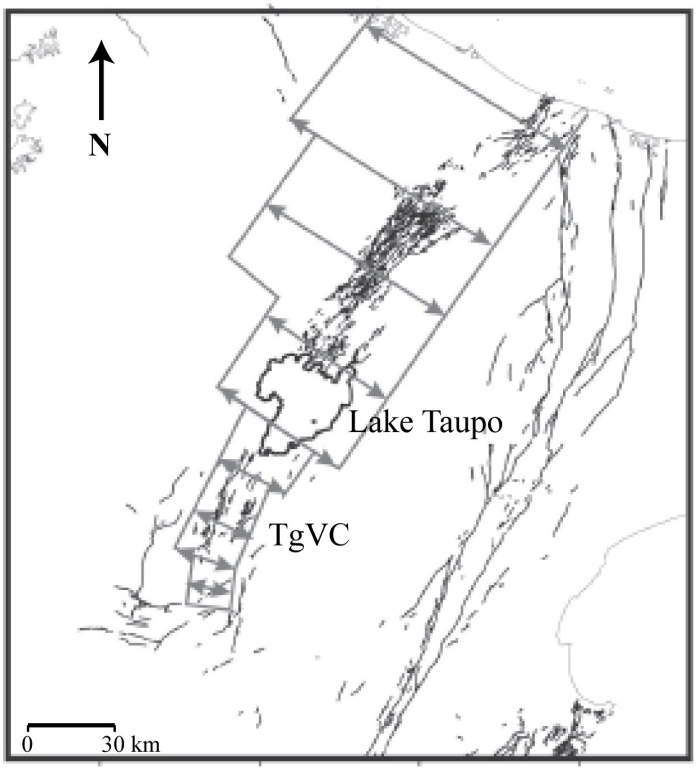

Figure 1.6: Spatial and temporal evolution of the Taupo Fault Belt modified after Villamor and Berryman (2006). Gray arrows indicate the opening of the rift- system towards the north-east.

Of the two major volcanic edifices of TgVC, Mt. Tongariro is the most complex, being an amalgamation of at least 17 overlapping vents, which collectively comprise a 13 km long and 5 km wide, *c.* 60 km^3 complex, (Hobden *et al.*, 1999). Mt. Tongariro has been active since at least 250-275 ka (Hobden *et al.*, 1996; Gamble *et al.*, 2003) and its history has been grouped into younger (<20 ka) and older (20-275 ka) eruption episodes (Cole *et al.*, 1986; Hobden *et al.,* 1999). The older stage includes eruptions around the Tama Lakes, while the eruptions comprising the younger episode include those along a NE-SE trend from North Crater, Red Crater to Ngauruhoe. According to Hobden *et al.* (1999), the active period of the individual cones was "short", occurring over <10 ka to 50 ka of activity. Post-20 ka activity is characterised by frequent eruptions with small volumes (<0.1 km^3) indicating small and short-lived magma batches below the volcanic complex (Hobden *et al.*, 1999).

The largest volcanic edifice in the TgVC is Ruapehu, 15 km south of Ngauruhoe. It has been active since at least 300 ka (Pillans, 1990; Parish, 1994) and has undergone several eruption pulses at 200, 134, 45, 22 and <15 ka B.P. (Gamble *et al.*, 2003). Geochemical

variation of the andesitic glass groundmass and in xenoliths indicate the interaction of mantle-derived arc magmas with the lower crust, and the variation in Sr-isotopes suggest that the magma is migrating to the surface through a plumbing system containing several small individual magma storage bodies and complex dyke-systems (Price *et al.*, 2005). Nakagawa *et al.* (1999) came to a similar conclusion by analysing scoria and bombs of the Ruapehu 1995-1996 eruptions, showing that mixing of different magma pockets occurred at "lower" (*sic*) depth and an upper crustal magma storage system, which comprised a plexus of dykes, sills and magma pockets occurred, where each small magma body evolved effectively individually.

1.4. Geographical Setting of the TgVC

1.4.1. Regional Setting

Most areas of the TgVC are included within the Tongariro National Park (TNP), which covers an area of 796 km² (Harlen, 1999). This is the oldest National Park in New Zealand, being founded in 1887, after Te Heuheu Tukino IV (Horonuku), the chief of Ngati Tuwharetoa gifted the land of his forefathers (2630 ha) to the Crown so it could not ever be sold or divided (Greenway, 1998). In 1984 the Tongariro National Park became a UNESCO World Heritage Site.

1.4.2. Flora and Fauna

The flora of the TgVC plays an important role in this study. The harsh alpine climate of this area has fluctuated considerably over the Late Quaternary (McGlone and Topping, 1977). Eruptions of Ruapehu and Tongariro have had localised impacts on the flora and fauna of the TgVC, however, major ignimbrite-producing eruptions from the Taupo caldera have devastated many parts of the area, including the *c.* 27 000 cal. yrs. B.P. (Lowe *at al*. 2008) Kawakawa Tephra and the 1717 ± 13 cal. yrs. B.P. (Lowe *et al.*

2008) Taupo Ignimbrite. Between 11 470 – 5700 cal. yrs. B.P., most parts of the TgVC were covered with forest such as *Nothofagus sp*. (beech), *Dacrydium cupressinum* (rimu), *Cyathea* and *Dicksonia* (tree ferns) *Weinmannia*, *Sphagnum moss* and *Ascarina*, indicating a milder and wetter climate than that of the present day (McGlone and Topping, 1977; Horrocks and Ogden, 2000). Between 5700 and 1717 cal. yrs B.P. *Leptospermum* (tea tree) and *Dacrydium colensoi* were more abundant, indicating a cooler and drier climate, similar to the present day. Leaves and pollen of these trees are interbedded in the tephra deposits from the TgVC volcanoes (Topping, 1973). Following the 1717 cal. yrs. B.P. Taupo eruption, a desert-like landscape prevailed, which is slowly recovering at the present time. Colonising species such as *Pteridium sp.* (fern), *Lycopodium* (moss), and *Taraxacum* (dandelion) increased in population immediately after the last Taupo eruption. *Nothofagus sp*. survived only in small patches and is only slowly recovering.

The TgVC today has a unique fauna and flora which is very sensitive to its environment. In lower regions the most commons trees are beech (*Nothofagus sp*.), rimu (*Dacrydium cupressinum*), as well as manuka (*Leptospermum scoparium)* and kanuka (*Kunzea ericoides)*, along with epiphytic ferns and tussock. At the highest elevations, lichen, moss and very small and fragile flowering plants grow, such as mountain harebell (*Wahlenbergia pygmaea*), silver raoulia (*Raoulia albo-sericea*), gentian (*Gentiana bellidifolia*), eyebright (*Euphrasia cuneata*), several Orchid varieties, and the North Island Edelweiss (*Leucogenes leontopodium*) (Tongariro Natural History Society, 1996). In the course of European settlement many exotic species were introduced, including the invasive pine tree (*Pinus contorta*), introduced in 1927, as well as the rapid spreading heather (*Erica sp.*) (Hobden, 1997). Damage to the endemic vegetation has occurred from the introduction of mammals such as rabbit, pig and deer, but also due to burning of the vegetation by the Maori and early European settlers to make the land utilisable for e.g. bracken and sheep farming (Hobden, 1997).

The volcaniclastic deposits as well as paleosols are today a fundament for recent vegetation and are also habitat for small vertebrata. Root systems as well as cavities from insects disturb the original bedding character of individual thin tephras. Additionally, tephras of the TgVC were deposited over a wider forested area between

~3700 and 1700 cal. yrs. B.P., and this also influences the bedding characteristics of individual tephras. For example, tree trunks have lead to discontinuity within tephra deposits and foliage had an impact on the internal structures of the fine grained, thinly bedded tephras (Chapter 5).

1.4.3. Climate

The climate of the TgVC has a large impact on vegetation and fauna, and also on the preservation, weathering and erosion of pyroclastic deposits. The climatic influence on vegetation was used by McGlone and Topping (1977; 1983), to identify changes in the climate during the Late Quaternary within the TgVC (Table.1.1). Mathews (1967) and Topping (1974) identified three glacial valleys on the Tongariro massif, recognising till deposits with a minimum age of 15 000 years, defined by overlying Rerewhakaaitu Ash (17,625 ± 425 cal. yrs. B.P. Lowe *et al*., 2008). Topping, (1974) also described glacial valleys on Mt. Ruapehu, such as the Wahianoa Valley, where tills cover the valley walls. Tills were also found on the Ohakune Mountain Road and southern side of Mangatoetoenui Stream.

Table.1.1: Climate changes in the Tongariro region, after McGlone and Topping (1977)

Age Range (yrs. B.P.)	Approx. cal. yrs. B.P.	Interpreted climate (McGlone and Topping, 1977; 1983)
14 000-10 000	16 670- 11 470	colder (up to˚C lower annual temperature) and drier then present
10 00-5000	11 470 - 5700	warmer and wetter than the present, but with marked fluctuations
5000-3500	5700 - 3777	cooler and drier, possibly approaching present conditions
3500-1800	3777 - 1700	a recovery to slightly wetter and perhaps milder conditions
1800-0	1700-0	no reliable data

The climate and weather in New Zealand is not only important for understanding the tephrostratigraphical record of a volcano, but also for hazard assessment of future eruptions. Today the area of the TgVC has an alpine climate with annual summer

temperatures ranging between 6 to 15˚C (max) and 0 to 6 ˚C (min) and winter temperatures between -4 to 7˚C (max) and -7 to 1˚C (min) (Thompson, 1984) depending on the altitude and slope orientation. The predominant winds within the TgVC are westerlies (from the SW-NW quarter) with wind speeds mostly <11 knots and common gales (>30 knots) in higher elevation regions (Thompson, 1984). Volcanic ash from historical eruptions of Ruapehu and Ngauruhoe was mainly transported towards the east, north-east and north, at times reaching as far as the Bay of Plenty (Reed, 1945; Self, 1975; Donoghue, 1991; Cronin *et al.*, 1998; Johnston *et al.*, 2000). Isopachs of pre-historic tephra deposits from Mt. Ruapehu and Mt. Taranaki are also mainly distributed towards the east and north-east (Donoghue *et al.*, 1995; Alloway *et al.*, 1995). The region east of the volcanoes and also south of Mt Ruapehu tends to be drier due to orographic effects and the westerly airflow. By contrast, the western flanks of the mountains have the highest rainfall (Table 1.2).

Table 1.2: Measured rainfall normals for 5 stations around Mt. Ruapehu and calculated value for the Rangipo Desert; after Purves (1990).

Station	Altitude (m)	Rainfall Normals (mm)	Grid reference
Chateau Tongariro [1] (north -west slope of Ruapehu)	1119	3965	S20/293196
Waikune [2] (north-west slope of Ruapehu)	744	2476	S20/176190
Ohakune Junction [1] (south-west of Ruapehu)	629	1564	S20/166956
Karioi [1] (south of Ruapehu	648	1189	S20/262923
Rangipo Desert (south-east of Ruapehu	1050	2000	T20/415055
Waiouru [1] (south-east of Ruapehu)	823	1048	T21/410890

[1]N.Z. Meteorological Service Miscellaneous Publications 145 (1973)

[2]N.Z. Meteorological Service Miscellaneous Publications 177 (1980)

A combination of weather conditions, coarse-grained and loosely packed soils prone to wind erosion (Fig. 1.7), along with the effect of large-scale eruptions and human disturbance have led to extremely patchy vegetation cover and consequently variable preservation of Holocene tephras immediately east of Mt. Ruapehu and Tongariro (Fig. 1.8). Tephras deposited after the Taupo eruption, 1717 cal. yrs. B.P., are mainly

preserved within dune sands (Makahikatoa Sands of Purves, 1990). Preservation is maximized in dunes and soils covered and protected by vegetation, including *Phyllocladus alpines* (mountain toatoa), *Hebe tetragona* (whipcord hebe) and *Chionochloa rubra* (red tussock).

Figure 1.7: An example of a small dust storm within the Rangipo Desert, a process that occurs semi-continuously throughout the summer months (photographer: Daniel Farley).

Figure 1.8: Tephra sheets in the eastern Ruapehu area, eroded by wind and water into "islands" that, if covered by vegetation, may be capped by dunes of Makahikatoa Sands, preserving late Holocene tephras (photographer: Gert Lube).

Up to 18 glaciers have been recognised on the upper flanks of Mt Ruapehu (Chinn, 2001), with the three largest being the Whangaehu, Mangatoetoenui, and the Summit Plateau Glaciers. The behaviour, stability and size of these glaciers have a great influence on the level of Crater Lake and therefore influence eruptions either directly or by controlling the amount of water perched over the active vent of Mt. Ruapehu. Collapse of glacial ice has been implicated in at least two past major lahars, including the 1953 lahra that resulted in the Tangiwai disaster (Odell, 1955; Hodgson, 1993; Cronin *et al.*, 1997c). Large proportions of tephra fall deposits from small-medium eruptions have been deposited on either seasonal snowpack or glaciers throughout Mt. Ruapehu's history (Figures 1.9 A+B)). This has led at times to rapid reworking following rainfall and poor preservation of proximal tephras (Manville *et al.*, 1998).

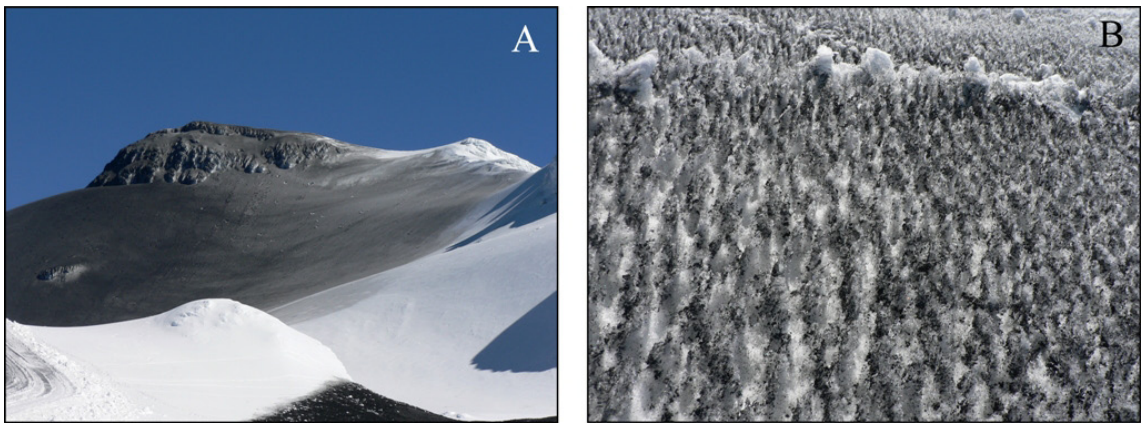

Figure 1.9: Ash deposited covering snow during the 2007 eruption from Mt. Ruapehu.

1.4.4. Soils

Volcanic soils tend to have a high natural fertility as a consequence of their being a weathering product of volcanic ash and rocks. This occurs mainly through the disaggregation of volcanic glass (Neall, 2006). Volcanic soils are termed Andosols (or Andisols), characterized by a low bulk density and ≥ 60% volcanic ash. The excellent phusical properties of volcanic soils allow them to be used for a wide range of purposes from farm land (dairy, sheep and beef) to forestry and a range of crops.

Soils within the TgVC are divided into five main groups which all developed from andesitic tephra. Recent soil development is represented by the Ngauruhoe series formed by tephras derived from Ngauruhoe and Ruapehu, after the last Taupo eruption (Cronin, 1996; Molloy, 1998). This coarse-textured highly erodible soil accommodates subalpine flora along the Desert Road, on the eastern side of the volcanoes. To the north-east of Tongariro, the Turangi series overlies the Taupo Pumice with lesser andesitic ash above and which thins rapidly towards the north-east. This soil has been used as farmland for cattle and sheep by the Rangipo and Tongariro prisons. Closer to Mt. Tongariro on its north-eastern flank and also along the northern Desert Road, the Turangi soils grade into the Rangipo soils (Cronin, 1996). Here, forestry has been developed on these Rangipo soil. In the southern part of the TgVC around Ruapehu, the soil has largely developed from tephras from Ruapehu and Tongariro deposited approximately 9000 – 20 000 years ago, and also from recent weathering of these older deposits. The loamy texture of the soils, the cooler climate and the high rainfall around Ohakune allows excellent growth of root vegetables. Within sub-soils of the study area there are many allophanic-rich horizons. Upon drying these shrink to produce vertical cracks down which more recent tephras may gravitationally fall to produce 'mixed' provenance horizons.

Within the course of this study, soil accumulation rates of a few paleosols within the lithostratigraphic Papakai Formation (between c. 11 000 and ~ 3500 cal. yrs. B. P.), Mangatawai Formation (between ~3500 and 1717 cal. yrs. B.P. and the Ngauruhoe series have been used in order to date some of the individual tephras (Chapters 5 and 6).

1.4.5. Land-use

The Tongariro National Park (TNP) has been extensively used for tourism for generations, with the main activities being, skiing, climbing and hiking. One of the most famous day walks in New Zealand is the Tongariro Crossing, which has up to 12 000 people per month crossing it (Martelli, 2007). Mt. Ruapehu had up to 410 000 people (average) on its upper slopes during each ski season from late June to late October in 2004 until 2009 (Ruapehu Alpine Lifts Limited, 2009). During summer month the

upper slopes of Ruapehu accommodate up to 18.000 people. The track of the Tongariro Crossing follows the Mangatepopo Valley towards South Crater to the east, crossing the Ngauruhoe 1954 lava flows and the pyroclastic flows deposits from the 1975 eruption of Mt. Ngauruhoe. A sudden eruption from the volcano in the future could lead to a major loss of life especially in high season. The 2007 eruption from Mt. Ruapehu also showed the danger of a blue sky eruption when surge deposit occurred and nearly killed two men staying at Dome Shelter which was destroyed during this very small phreatic eruption (Kilgour *et al.*, 2008; Christenson *et al.*, 2010). Snow slurry lahars also travelled down the Whangaehu River (east) and toward the Whakapapa ski-field (north) (Lube *et al.*, 2009) during this event.

Four small townships are located around Tongariro National Park (Figure 1.10). Turangi, a forestry, prison and tourism-based township with a local population of around 3240 (http://www.stats.govt.nz/Census/2006CensusHomePage), is located on the northern side of the TNP and was built in the 1960s during construction of a major hydro-electric power scheme (Electricity Corporation of New Zealand Limited, 1994). This town and the much older nearby Maori village of Tokaanu are destinations for trout fishing, rafting and boating on the lakes and rivers of the area. The Tongariro and Rangipo Prisons near Turangi, are low security prisons that include river reserves, native forest, wetlands and at least 4200 hectares of forestry, and 2400 hectares of pastoral farmland. The tourism service centre of National Park is situated on the western side of the TNP with a population of 240. On the north-western flanks of Ruapehu, Whakapapa Village is located at around the *c*. 1100 m contour and further up, Iwikau Village at 1600 m, is made up of ski chalets where people are accommodated during the ski season. Both villages are also active in the summer, with visitors using them as staging points for climbing and hiking in the area, including the popular hike to Ruapehu Crater Lake. Ohakune, with a population of 1100, is situated south-west of Mt. Ruapehu, and is an agricultural service town that doubles as a base for skiing, hiking and climbing. Waiouru, a service centre for State Highway 1 travellers and the NZ Army base is located south-west of Mt. Ruapehu. This town, with a population of 1380 including approximately 500 stationed soldiers (Mark Heys, pers. com. 2010), is on the boundary of the NZ Army Training Area that comprises 86,818 hectares to the east and south-east of Ruapehu. The army uses this land for training purposes within 10 km of

Mt. Ruapehu. Between these towns, the southern Tongariro National Park boundary is adjoined by the Karioi Forest, an exotic pine forest which covers an area of 10 554 ha (Jamieson, 1974). The first timber trees were planted in 1927, and since the late 1960s the wood has been processed at the Winstone Pulp Mill at Karioi and the Tangiwai Saw Mill.

The Tongariro River has its source in the Kaimanawa Mountains and is fed by several smaller rivers from the eastern side of the TgVC volcanoes as well as the northern Kaimanawa Mountains to its east, before it drains into Lake Taupo. This catchment plays an important role in New Zealand's electricity generation. The Tongariro Power Scheme uses water from 26,000 km^2 of catchment including most of the rivers on the southern slopes of Ruapehu. Waters from southern Ruapehu flanks are fed into the Wahianoa Aqueduct (Figure 1.10), which discharges into Lake Moawhango (travelling beneath the lahar-prone Whangaehu River). From this point a network of tunnels and canals leads the water in and out of the Tongariro River, through Lake Rotoaira and into Lake Taupo, passing through two power stations along the way. The Tongariro Power Scheme produces around 4% of New Zealand's annual power requirements.

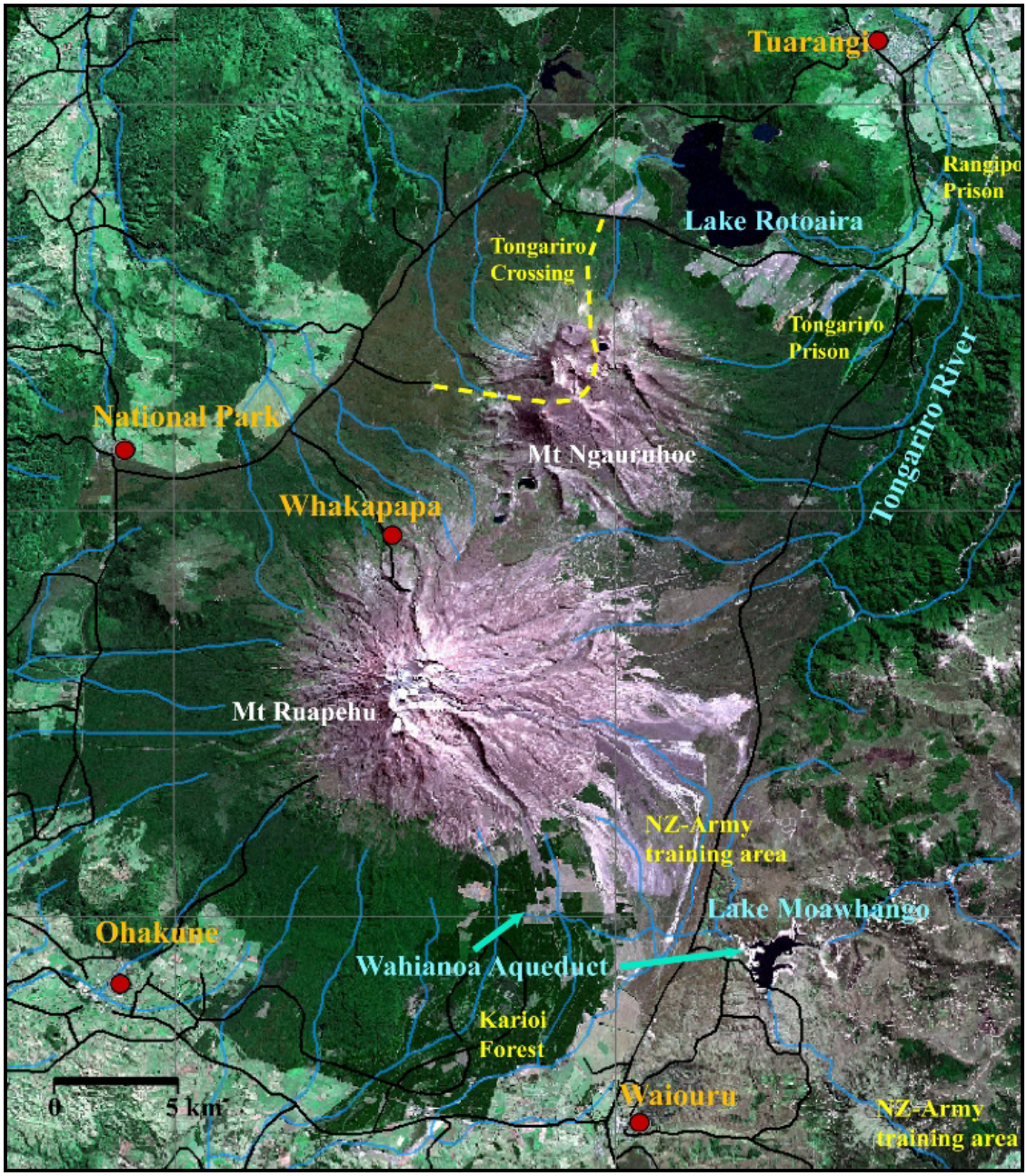

Figure 1.10: Satellite map of the major land-use areas within the TgVC and surroundings.

1.5. Thesis Outline

This thesis comprises a further 8 chapters. Chapter 2 describes the methods used in this study while Chapter 3 provides an overview of the tephrostratigraphical record of the study area from both TgVC and distal sources, based on the findings of previous workers, but with additions and corrections based on the present study. Chapter 4 is focused on discussing geochemical analyses (mainly Electron Microprobe determinations) of glass and mineral phases which have been used for differentiating the three main local sources of Holocene eruptions from TgVC: Mt. Ruapehu, Mt. Ngauruhoe and Tongariro's Red Crater. Further means to distinguish between TgVC-sourced and Mt. Taranaki-derived andesitic tephras are presented. Chapter 5 delivers new results focusing on Ngauruhoe that are the basis of the most complete tephrostratigraphical record of the entire known history of Mt. Ngauruhoe. Additionally new results from Red Crater and Te Maari craters will be discussed. This chapter also includes an interpretation of the insights revealed from volcanic glass geochemistry of all known products from these vents. In Chapter 6, the tephrostratigraphical record of Mt. Ruapehu over the last ~25.000 cal. yrs. B.P. is explained along with a comparative interpretation of microprobe geochemical data. Chapter 7 focuses on analysing the eruption styles and fragmentation processes occurring during small-medium Holocene eruptions from Mts. Ruapehu, Ngauruhoe and Red Crater. In Chapter 8 the explosive eruption magnitude (volume and column height) and frequency and grain size analysis for Holocene activity of the TgVC will be presented. Chapter 9 completes the thesis summarising previous chapters and concludes with the key findings. Additionally, ideas for extending this type of work in the future will be presented.

Chapter 2

Methodology

This chapter explains the methodologies used to fulfill the objectives of this study outlined in Chapter 1.

2.1. Field Studies

Detailed field stratigraphic studies were conducted to unravel the complex stratigraphy of tephra deposits grouped collectively as the Mangatawai, Ngauruhoe, and Tufa Trig Formations. The procedures for this are outlined below. Once the stratigraphic relationships were established, these formed the basis for the sampling of tephras for petrological, granulometric and geochemical analyses.

2.1.1. Study area and key sampling localities

Field studies for this thesis were carried out in a 1500 km^2 area encompassing Tongariro National Park (TNP), the Tongariro and Rangipo Prisons, the western Kaimanawa Mountains, New Zealand Army Training Land, Karioi Forest and private and Maori-owned land (Figure 2.1.). Across this area the distribution of individual and multiple sequences of tephra layers was mapped to produce isopach maps, and to define the best locations for detailed studies. Most of the > 110 locations sampled in this study are situated along the main roads, or along walking tracks inside TNP (Figure 2.1, Appendix 1). Road cuttings were preferred for sampling in order to protect the ecologically sensitive environment within the National Park. Only a few specific off-road locations were needed to obtain the most comprehensive stratigraphic sequence. It was necessary to find a large number of locations to determine the overall characteristics of the tephras and to understand their variations with distance and

direction from source. For each previously defined Tephra Formation (Topping, 1973; Donoghue, 1991) new reference sections needed to be selected, because the original locations were in poor condition, or did not show all features and variations necessary for reconstruction of eruption properties (Table 2.1; Figure 2.2). These locations collectively span the last c. 12 000 cal. yrs. B.P., including tephras from Mt. Ruapehu, the most complete tephra stratigraphy of the entire eruption history of Mt. Ngauruhoe, and tephras from Red Crater erupted since *c.* 1000 cal. yrs. B.P. The main reference site, Loc. 12, is situated along the Desert Road south of Waihohonu Stream; it represents the medial accumulation area of studied volcanic ash from Ruapehu and Tongariro along the most favourable wind dispersal direction. In total, 9 samples of the Mangamate Formation (MF), 14 tephra and soil samples of the Papakai Formation (PF), 63 tephra units from the Mangatawai Formation (MtF), and 16 soil and tephra layers of the Tufa Trig Formation (TTF) were collected and chemically analysed, representing a total distal eruption record over the last *c.* 11 200 cal. yrs. B.P. On the opposite side of the volcanoes at Loc. 6, near the head of the Mangatepopo valley, 64 tephra and soil samples were analysed of the MtF, TTF and the PF to correlate individual tephra beds and packages to Loc. 12, around 15.5 km to the south-east. At a third site (Loc. 63) on the northern slope of Pukekaikiore, 2.5 km west of Mt. Ngauruhoe, proximal fall deposits from Mt. Ngauruhoe are found, along with medial tephras derived from Mt. Ruapehu. Here, 86 samples were taken, representing tephras from Ngauruhoe, Ruapehu and Red Crater erupted over at least the last ~ 1000 years. A further location (67) on the northern slope of Ngauruhoe collectively represent proximal tephras from Mt. Ngauruhoe and Red Crater and distal fall units of Ruapehu for at least the last *c.* 4500 years. At the northern edge of the Karioi Forest, Donoghue *et al.*'s (1997) reference section 2 was also sampled (here Loc. 56). This site contains primarily Tufa Trig Tephras of the last *c.* 1700 yrs.

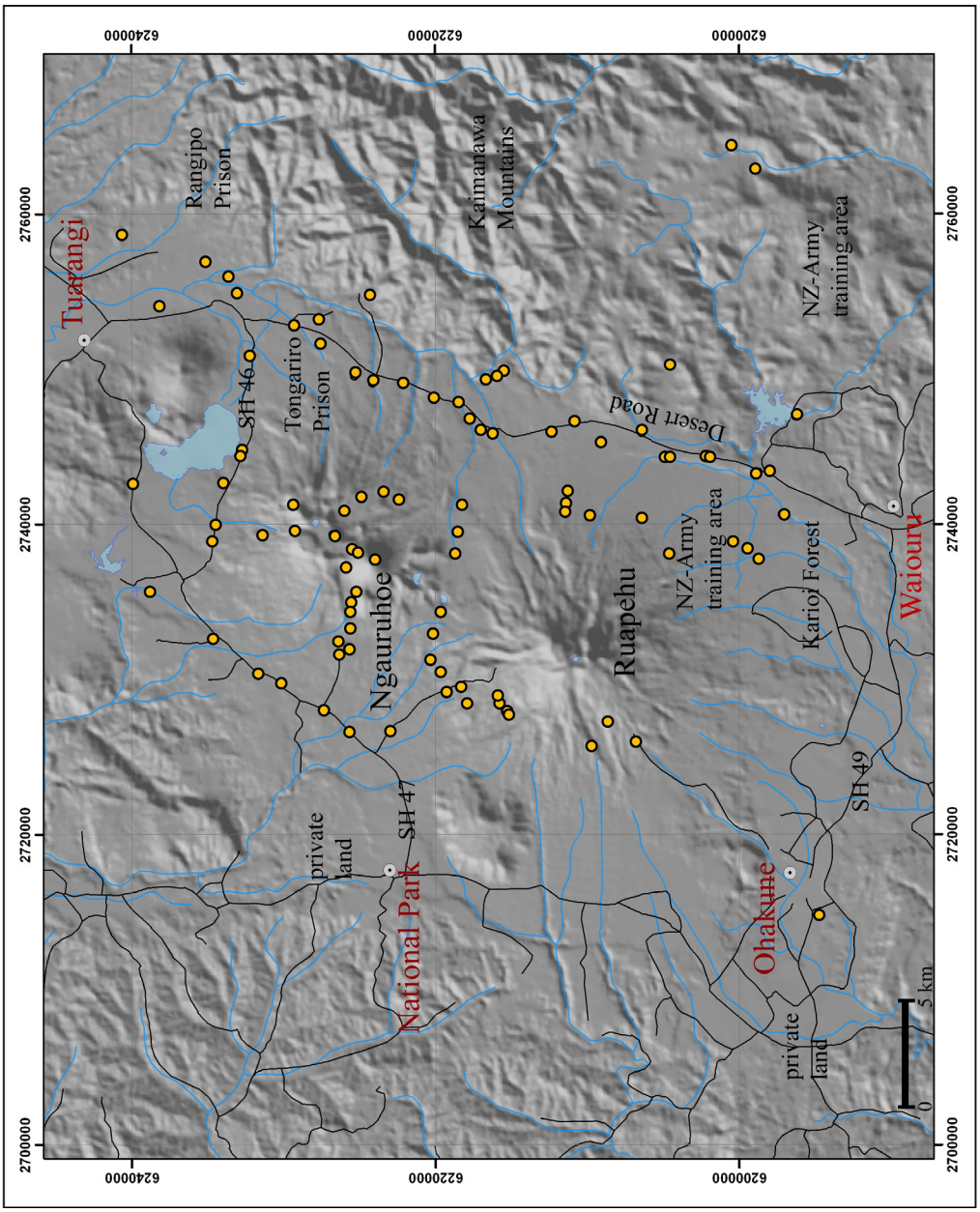

Figure 2.1: Field locations analysed in the course of this study. Detailed descriptions of individual locations are listed in Appendix 1.

In addition, a series of cores were collected from Lake Rangatauanui, located 2.5 km south-west of Ohakune (Figure 2.2), and 23 km south-west of Crater Lake on Ruapehu. This location also contained tephras from Taupo Volcano (c. 62 - 100 km north-west) and Mt. Taranaki, c. 115 km to the west. The lake has a maximum water depth of 4 m, and is 152 m wide (north-south) and 253 m long (west-east). Five cores were taken in a transect along the long-axis, providing a consistent stratigraphy extending back over ~25 000 cal. yrs. B.P. Detailed descriptions from each of the key field locations are listed in Appendix 1.

Table 2.1: Locations of the main reference locations used in this study.

Location number	Grid reference (NZMG series 260)	Location description	Units best represented
6	T19/331256	Mangatepopo valley	medial (Ngauruhoe) and distal (Ruapehu) Mangatawai Formation
12	T20/462173	Desert Road, south of Waihohonu Stream	distal Mangatawai Form.
56	T20/378047	Reference Section 2 at Tufa Trig (Donoghue, 1991)	medial Tufa Trig Formation
63	T19/355251	northern face of Pukekaikiore	proximal Ngauruhoe Formation and distal Tufa Trig Formation
67	T19/384251	northern slope of Mt. Ngauruhoe	proximal Mangatawai Formation
73	T20/475069	NZ army training Area Paradise Road	distal Tufa Trig
Lake Rangatauanui	S20/148940	south of Ohakune	-

Exposures of the Tufa Trig Formation (TTF) were identified within the Rangipo Desert east of Mt. Ruapehu and within the Army-land training area east of the Desert Road, approximately 32 km east and south-east of the volcano. Along the Desert Road the TTF was recognised in this study from as far north as near Loc. 12 to just south of Loc. 2. In addition, members of the TTF were identified to the south-west at the Ohakune Mountain Road and within the sediment cores of Lake Rangatauanui and in the Mangatepopo Valley, to the north of Mt. Ruapehu. Discrete tephras of the Ngauruhoe Formation (NF) were identified on the northern face of Pukekaikiore (Loc.63), South Crater (Loc.75) and within the inner crater of Mt. Ngauruhoe. Possible tephras of the NF were recognised on the northern edge of Oturere lava flow as previous described by

Topping, (1974). In addition NF was identified along the northern Desert Road as soil derived from ash accumulations of Ngauruhoe. The Mangatawai Formation (MtF) is exposed along the Desert Road from near the Waihianoa Aqueduct in the south to as far north as the Tongariro and Rangipo Prisons on Airstrip Road, north-east of the TgVC. It is also preserved to the north along SH 46 as well as to the west along SH 47. The westernmost locations are found along the *Around the Mountain Track* and possibly within the Hauhungatahi wilderness between Ruapehu and Hauhungatahi. In the south MtF is so far only found in proximal sites, along the Ohakune Mountain Road (around the 14 km marker) and within the Karioi Forest. In detail it is difficult to draw isopachs of individual tephra layers within the Formation due to the problem of correlating specific units between locations.

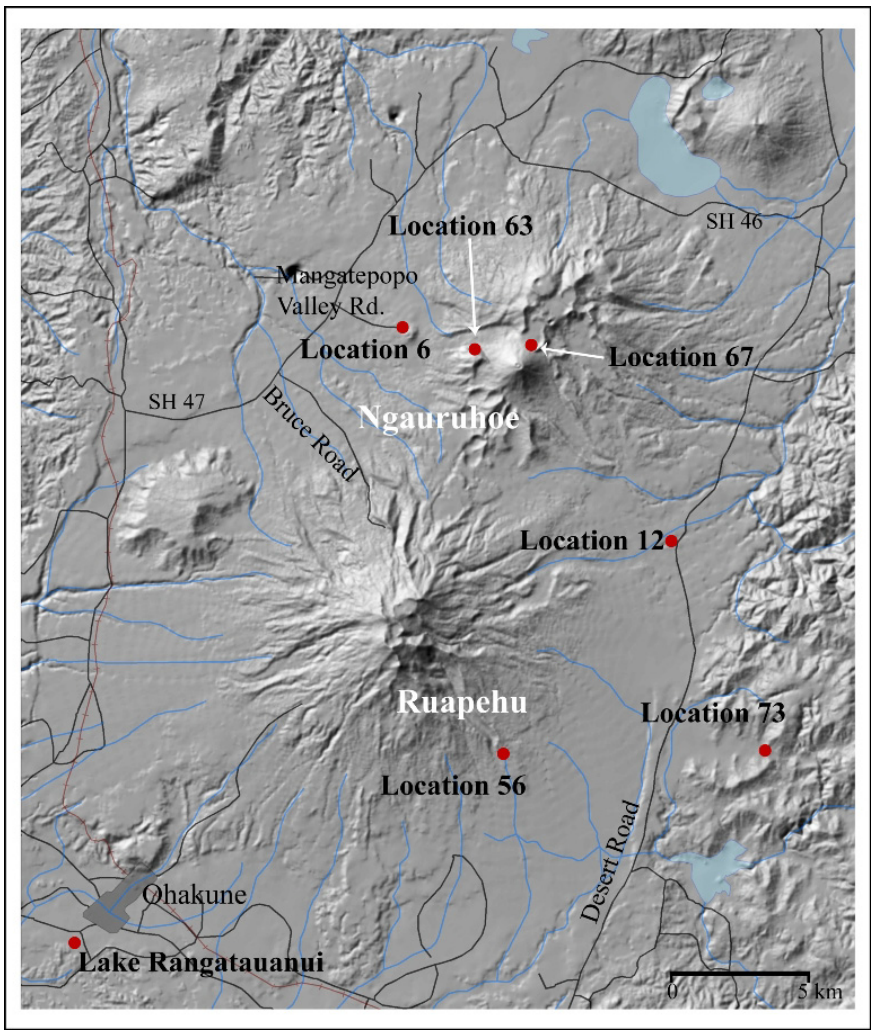

Figure 2.2: Main reference Locations used in this study to describe the most complete tephrostratigraphical record of Mt. Ngauruhoe, Mt. Ruapehu and Red Crater.

2.1.2. Sampling

To geochemically fingerprint eruption sources in the TgVC and to draw conclusions about eruption behaviour by analysing particle shapes and composition of tephras, samples of each individual tephra from the above named exposures were collected and analysed in different laboratories.

Each outcrop was cleaned by spade to make a new cut beneath any plants and shallow surface weathering. Individual tephra layers were photographed and described in terms of thickness, colour, grain size, texture, internal bedding structures, grading, content of organic material and vesiculation. The thickness of individual tephra beds or packages, varied markedly over very short distances. Depending on thickness and grain size, a representative amount of tephra was sampled. In some cases the individual tephra layers were too thin for sampling without contamination and were sampled as bulk samples.

Swamp or shallow lake core samples were taken with a ”D-section” corer (50 mm diameter and 0.5 m long). Deeper lake sediment sequences were collected with a Livingston-piston corer (35 mm diameter and 1 m long). Intact cores were transferred to electical trunking tubes and refrigerated before X-ray imaging and detailed sampling in the laboratory.

2.2. Laboratory work

Most core and soil samples were treated with H_2O_2 (hydrogen peroxide) to dissolve organic matter, followed by washing with distilled water through a 32 µm sieve to remove the finer silt and clay fraction. In some cases the <32 µm fraction was kept for XRD-analysis. After the samples were oven dried at 50˚C, some were dry hand sieved at one phi-intervals for heavy liquid separation, Scanning Electron Microscopy (SEM) analysis and optical microscope-based point counting.

The cores from Lake Rangatauanui were imaged by X-Ray at the Institute for Veterinary Sciences at Massey University. The most complete record in Core 4 contained around 100 individual mineral layers which were separately sampled. Photographs and descriptions taken in the field also helped to identify the individual tephra layers in these and the D-section cores from swamp sites. Organic samples for radiocarbon dating were taken from important stratigraphic positions throughout the core (usually below distinctive tephra layers) to allow construction of a robust depth/age profile.

2.2.1. Electron Microprobe Analysis (EMPA)

Electron Microprobe Analysis (EMPA) provides major elemental analyses of small areas (2-20 μm) of polished mineral phases, metals, or glass. In the framework of this study, EMPA was mainly used to analyse volcanic glass and titanomagnetite from the reference sites described above and thus help to identify the source of each individual tephra. For this purpose it was necessary to obtain samples from known sources to be used as reference samples. In addition to volcanic glass analysis, titanomagnetites from each individual tephra within a core from Lake Rangatauanui and Loc. 12 were analysed (data in Appendix 2). Furthermore, volcanic glass shards from rhyolitic tephras were sampled within the Papakai Formation and from the lake sediment cores.

For EMPA, volcanic glass shards from ~450 individual tephra and soil layers from six main reference locations were handpicked from grain size 500 μm - 1 mm and 250 μm - 500 μm, while titanomagnetites were extracted from the 32 μm - 63 μm fraction with a magnet. Subsequently, the samples were embedded in a two component epoxy plug (EPOTEK 301). The plugs were polished on a Struers Planopol-3, using Kemet diamond paste (6, 3 and 1 μm), a water-based lubricant (Akasel) and Struers MD-Pan polishing cloth.

In all cases, EMPA were collected from 10 glass shards and/or 10 titanomagnetites in each sample. The analytical work was carried out at the University of Auckland, with a Jeol JXA-840A electron microprobe. The analytical spectra were collected using a

Princeton Gamma Tech Prism 2000 Si(Li) EDS X-ray detector. An accelerating voltage of 15 kV, beam current of 600 pA and 100 seconds live time count were used. A defocused beam, at least 20 μm in diameter, was used for the volcanic glass, while a 2 μm focused beam was used for titanomagnetite analysis. Results were calibrated using a suite of Astimex™ mineral standards (R. Sims, University of Auckland, pers. comm.). The standard analytical errors for glasses were: SiO_2 (< 0.13%), TiO_2 (< 0.10%), Al_2O_3 (< 0.75%), FeO (< 2.5%), MnO (< 25%), MgO (< 10%), CaO (< 2.5%), Na_2O (< 1.5%), K_2O (< 2%), Cl (< 10%). The error associated with analyses depends on elemental abundance and is lower at higher concentrations. In this study, P_2O_5, SO_3, Cr_2O_3 and NiO were not used for correlation purposes because measured levels were often near detection limits. Also, all analyses were normalised to 100% before correlating analysis. Titanomagnetite analyses were standardised using Astimex™ magnetite standards. A constant calibration factor was employed to correct FeO (total) values. Detection limits of oxides under EMPA varying according to atomic mass (Table 2.2).

As part of an inter-laboratory EMPA project (64 participating laboratories), basaltic glass was analysed by the University of Auckland instrument, showing very low deviation from accepted compositions (Table 2.2; R. Sims, unpublished data).

Table 2.2: Detection limit of major oxides measured at the EMP (University of Auckland) including the deviation from a reference glass composition.

Dectetion limit	SiO_2	TiO_2	Al_2O_3	FeO	MnO	MgO	CaO	Na_2O	K_2O	P_2O_5	SO_3	Cl	Cr_2O_3	NiO
1σ [wt.%]	0.11	0.08	0.06	0.07	0.07	0.07	0.04	0.11	0.03	0.07	0.06	0.03	0.06	0.10
3σ [wt.%]	0.32	0.23	0.18	0.20	0.20	0.21	0.13	0.32	0.10	0.20	0.19	0.08	0.17	0.30

International Round-Robin Inter-lab EPMA project (64 participating labs):
Difference to reference values of re-fused basaltic glass composition

SiO_2	TiO_2	Al_2O_3	FeO	MnO	MgO	CaO	Na_2O	K_2O	P_2O_5
-0.18	0.12	-0.05	-0.04	-0.01	0.17	-0.02	0.05	0.02	0.01

The most common problems during EMPA include instrument failure, incorrect sample preparation, or incorrect sampling. To reduce these, the following conditions were adhered to:

a) Plugs (24 mm diameter of Epoxy resin), containing up to 20 individual samples, were highly polished and treated to obtain a consistent coat of carbon.

b) The beam current was monitored and kept stable, and any significant deviation led to the analysis being stopped.
c) A defocused (10-20 μm diameter) beam makes analysis of small mineral grains and highly vesicular glasses very difficult. Even with a focussed beam, only some of the larger titanomagnetites from the TgVC tephras could be analysed.
d) Weathered tephra can also cause errors. Andesitic glass alters rapidly to allophanic clay and other phases (e.g., Platz *et al.*, 2007) and it is not always possible to visually recognise this; hence all analyses have to be carefully screened. Neall (1977) demonstrated that in EMPA-results from major element compositions of volcanic glass derived from Mt. Taranaki, there is a decrease of SiO_2 and an increase of Al_2O_3 with greater age of the tephra deposit, showing the increase of allophanic material with time.
e) Another characteristic of andesitic glass is a high content of microlites (Sharp *et al.*, 1996). These fine-scale crystallites are usually identifiable with a back-scatter electron image of the glass shard, but sometimes occur with such a high density that it is very difficult to analyse pure glass with a ~20 μm beam (Platz *et al.*, 2007; Turner, 2008). Despite this limitation, no major problems occurred with identification of glass in the tephras derived from TgVC volcanoes.

2.2.2. Scanning Electron Microscopy (SEM)

Scanning Electron Microscopy (SEM) was used to take surface images of pyroclasts with precise nm-range imaging. This was used to determine the pyroclast shapes, surface properties and fracturing patterns, providing information relevant to interpret eruption styles and fragmentation processes, as well as to help understand how the ash has been transported and deposited (Dellino *et al.*, 2001; Dellino and Kyriakopoulos, 2003; Heiken and Wohletz, 1985).

For SEM, the entire <63 μm fraction was analysed to provide an overview of the sample and to compare with handpicked glass shards from the >250 μm fraction (images Appendix 7). Shards were handpicked depending on their colour (light vs. dark-black) and variation in morphology under a binocular microscope. The samples were not

cleaned ultrasonically because adhering dust can be a characteristic feature of phreatomagmatic eruptions and can also create secondary surface textures and abrasions on glass shards and mineral. After the individual shards were placed on a ~10 mm wide stub, they were gold sputter-coated and placed in an FEI Quanta 200 SEM instrument. The sample was analysed in a high vacuum mode, with a voltage of 20 KV and a 3 μm beam. The distance between the beam and the sample was 10 mm.

Samples were chosen to be representative of the entire late Holocene period, all volcanic sources and all ranges in tephra colour and appearance. Samples from known eruption types were used to compare with the unknown units. For example, Ruapehu 1995-96 tephras were examined because they were products of observed complex magmatic and phreatomagmatic fragmentation (Cronin *et al.*, 2003). Samples from Yasur Volcano, Vanuatu show typical strombolian fragmentation (Lardy and Tabbagh, 1999; Oppenheimer *et al.*, 2006) and those of 2005 from Ambae volcano, surtseyan phreatomagmatic fragmentation (Nemeth *et al.*, 2006) (Appendix 7).

Shape characteristics of volcanic glass

To differentiate between magmatic (dry) and phreatomagmatic (wet) eruptions styles, measurements were made of vesicle content, vesicle- and grain-shape geometry and glass-surface structures (Heiken, 1972; Wohletz and Krinsley, 1982, Dellino *et al.*, 2001). Particles of magmatic eruptions are mostly irregular in shape, sometimes drop-like, and there is a high volume of tubular and contorted vesicles with smooth bubble walls and generally smooth surfaces (Heiken and Wohletz, 1985). In hawaiian and strombolian eruptions, characteristic glass particles such as Pele's hair or tears also occur (Heiken and Wohletz, 1985). In contrast to these features, particles from phreatomagmatic fragmentation are blocky with linear edges and show few or no ovoid and isolated vesicles. Here, because of the interaction of hot magma with external water, surface structures such as quenching cracks and step-like fractures also occur, along with common conchoidal fractures (Heiken, 1972, Pardo *et al.*, 2009). Features that reflect transport mechanisms and alteration processes of the grain (Freundt and Rosi, 2001) include: rounding, v-shaped depressions, chipped edges, grooves and

scratches especially where particles collide. Particles transported passively in tephra plumes show fewer features of violence and vesicle fillings, clay minerals, glass hydration and cracks in grain skins indicate alteration processes (Freundt and Rosi, 2001).

2.2.3. Laser Particle Analysis (LPA)

Tephra samples from Locations 12, 56, 63, and 67 were analysed to determine the variation in grain size for different tephras from a single source at a fixed distance from vent. In addition, two distinctive Ngauruhoe-sourced tephras, the dark purple (DP) and the pale purple (PP) units were sampled in a very narrow grid on the eastern side of the volcanoes Ruapehu and Tongariro. DP consists of a single bed, whereas PP is a multiple, thinly bedded/laminated deposit. The samples for this analysis were dried in an oven at about 50ºC and split with a riffle-splitter down to a representable size of 5 mg – 10 g, depending on the coarseness.

The samples were analysed by a Laser Scattering Particle Size Distribution Analyser (PSDA), model Partica LA 950V2 made by Horiba. This instrument measures a particle range of 10 nm to 3 mm by using two light-source wavelengths; long wavelength to measure coarser particles (>0.01 μm) and a short wave length to analyse particles <0.01 μm. For correct measurements it is also necessary to know the refractive index of the sample, which was calculated at 1.53 using Ruapehu-derived tephras.

For samples with components > 2 mm fraction, the coarser particles were dry sieved in half phi steps and weighed to then be combined for a total grain-size analysis of the full sample, using the program Gradistat Version 4.0, by Simon Blott. Results are listed in Appendix 3.

2.2.4. Point counting

The content and ratio of crystals, juvenile clasts (volcanic glasses (pumice, scoria) and crystals), accidental lithics (e.g. from wall rock or country rock from deep-seated pre-volcanic stratigraphic successions) and cognate lithics (fragments derived from previous eruptions of the same volcano) in tephras depends on the fragmentation and vesiculation processes occurring in the erupting magma, along with the transport and depositional mechanisms (Fisher and Schmincke, 1984; Cas and Wright, 1988). Secondary effects may also relate to environmental processes, such as changes of weather condition during the eruption, especially wind patterns, as well as post-depositional diagenetic or weathering processes (Fisher and Schmincke, 1984).

In the course of this study, the ratio and quantity of clinopyroxene (cpx), orthopyroxene (opx), olivine (ol), hornblende (hb), volcanic glass (dark vs. light shards), lithics, and in some cases sulphur-spherules were determined (Appendix 4). To obtain a representative sample, 300-500 grains from the fractions 1-2 mm, 0.5-1 mm, 0.25-0.5 mm for each targeted tephra sample were counted under a low-power binocular microscope and using a point counter.

2.2.5. Radiocarbon dating

New radio carbon dates were obtained to get an age control between the numerous thinly bedded tephras within the Mangatawai Formation and also to possibly obtain a new age when Ngauruhoe's explosive activity began. Furthermore samples for radio carbon dating were collected from the sediment core of Lake Rangatauanui to establish a depth age curve and also to determine the sediment accumulation rate within the lake and to have an age control on tephras identified within the core.
Radiocarbon dating requires collection of organic carbon such as charcoal (30-100 mg), peat (1-3 g) or wood (50-300 mg). Several tephras contain interbedded leaves and pollen, and these materials, where well preserved could be analysed by Accelerated Mass Spectrometry methods (AMS). From the cores of Lake Rangatauanui, organic

sediment and peat materials between tephras were analysed. All radiocarbon dates were carried out at the Rafter Radiocarbon Laboratory at the GNS Science in Lower Hutt using AMS methods. Results are listed in Appendix 6.

All ages, not obtained in this study, were calculated to cal. yrs. B.P. with the program OxCal 4.1, if not different noted. This correction was necessary to be able to compare obtained ages from previous works in New Zealand to the new dates of this study, but also to be up to standard in the world, where cal. yrs. B.P. are used to present the same kind of data. This program is calibrating radiocarbon ages including the changes in ^{14}C-isotopes prior 1950. The ages for individual tephras are listed in Appendix 5.

2.2.6. ICP-MS

To analyse for Sr-isotopes, twelve selected samples weighing 60-80 mg of volcanic glass were handpicked from the >500 µm-250 µm fraction following heavy liquid separation using Sodium Polytungstate. Sr-isotopes analyses were carried out at the University of Melbourne. After acid leaching (6M HCl, 100̊, 60 min) the samples were dissolved on a hotplate (110˚) in closed Savillex beakers with 2ml of 3:1 HF-HNO_3 for two days and 6M HCl for one day. The strontium was extracted using a combination of anion exchange (AGI-X8, 100-200 mesh, HBr-HCl) and EICHROM RE-LN- and SR-resin chromatography. The Sr-analyses were than obtained with a Nu Instruments® multi-collector (MC) Inductively Coupled Plasma Mass Spectrometry (ICP-MS) to a CETEC Aridus desolvating nebulizer with a sensitivity of 100-150 v/ppm Sr. The instrumental mass bias was normalised to $^{86}Sr/^{88}Sr = 0.1194$ using the exponential law and typical internal precisions were $\leq \pm 0.000020$ Sr. External precisions were estimated from the internal precisions with ± 0.000040 Sr (±2 std dev). Run precisions for all $^{87}Sr/^{86}Sr$ isotope measurements are between 0.000014 and 0.000020.

Chapter 3

Tephrostratigraphy of the Tongariro Volcanic Centre (TgVC)

Subdividing the stratigraphic record of multitudinous tephras into collective 'tephra formations' has been an important first step towards providing overviews and maps of the pyroclastic deposits of the Tongariro Volcanic Centre (TgVC), and to provide broad stratigraphic marker packages, given the relatively low resolution of available dates from the area. Definition of these local tephra formations has been helped by chronological constraints provided by interbedded and bounding tephras from outside TgVC, especially the distinctive rhyolite tephras from the Taupo and Okataina Volcanic Centres. A major issue in this approach, however, is that some of the formations have inadvertently combined tephras from different source volcanoes. To understand the eruption history of the individual TgVC volcanoes (Ruapehu, Ngauruhoe, Red Crater), and discern any possible interrelationship in their eruption frequencies, it is important to identify the source of all individual tephras. This information can be subjected to statistical analysis and provides the foundation of a robust record of prehistoric eruption events from an individual volcano, which help to forecast the probability behaviour of future eruptions.

New data collected during the course of this study will demonstrate that some of the established tephrostratigraphy has been based on false correlations of at least two of the distal tephras interbedded within the TgVC deposits. New analyses and detailed study of some of the late Holocene tephra formations have provided the basis of new correlations for these previously determined TgVC tephras. This chapter will present detailed information about the tephrostratigraphy of the Tongariro Volcanic Centre over the last approximately ~12 000 cal. yrs. B.P, elucidating the individual tephra deposits from different sources (Table 3.1) along with the new findings based on this study such as new tephra correlations.

Table 3.1: Tephrostratigraphical record of tephra layers found within the Tongariro Volcanic Centre after Donoghue (1991; 1995) and new findings of this study. Italicised entries are sourced from rhyolitic centres outside TgVC.

Formation	Member	Source	Age in Cal yrs B.P.	Reference of member and age
Tufa Trig Fm. & Ngauruhoe Tephra F. Stage 4	Tf16- Tf19	Ruapehu Ngauruhoe	0-295 cal yrs B.P.	this study
Burrell lapilli		*Mt Taranaki*	*1655 A.D. (295 cal yrs B.P.)*	*Druce (1966)*
Tufa Trig Fm. & Ngauruhoe Tephra F. Stage 4	Tf6-Tf15	Ruapehu Ngauruhoe		
Tufa Trig Fm. & Ngauruhoe Tephra F. Stage 4	Tf5	Ruapehu Ngauruhoe	between 611 ± 65 and 790 ± 119 cal. yrs. B.P.	Donoghue (1991)
Tufa Trig Fm. & Ngauruhoe Tephra F. Stage 4	Tf3-4	Ruapehu Ngauruhoe		
Tufa Trig Fm.	Tf2	Ruapehu	1338 ± 45 cal yrs B.P.	**this study**
Tufa Trig Fm.	Tf1	Ruapehu	1555 ± 135 cal. yrs. B.P.	**this study**
Taupo Tephra	*Taupo Ignimbr*	*TVC*	*1717 ± 13cal. yrs. B.P.*	*Lowe et al. (2008)*
Mangatawai F	MtF 62 (informal)	Mt Ruapehu		this study
Mangatawai Fm. Stage 3 **Mangatawai Fm.** Stage 3	MtF 58 (informal) MtF 46 (informal)	Ngauruhoe Ngauruhoe	2766 ± 226 cal yrs. B.P. 2810 ± 70 cal yrs B.P.	 **this study**
Maketawa Tephra		Taranaki	3058 ± 268 cal. yrs B.P.	Alloway *et al.* (1995)
Manganui Tephra		Taranaki	3550 ± 145 cal. yrs. B.P.	Alloway *et al*. (1995)
Mangatawi Fm Stage 2 **Mangatawai Fm.**	MtF 9-45 MtF 1-8 (informal)	Ngauruhoe Mt Ruapehu	3694 ± 133 cal. yrs B.P. 3592 ± 89 cal yrs. B.P.	 **this study**
Papakai Formation		TgVC		
Inglewood Tephra		Taranaki	3924 ± 224 to 4060 ± 231 cal. yrs B.P.	
Mangatepopo lapilli Stage 1	informal	Ngauruhoe		**this study**
Stent Tephra Korito Tephra	*Q*	*TVC* Taranaki	*4323 ± 174 cal yrs B.P.* 4647 ± 230 cal. yrs B.P	*Alloway et al. (1994)*
Papakai Formation Stage 1	soil+black ash	Ngauruhoe/ Ruapehu		**this study**
Papakai Formation	black ash-2	Mt Ruapehu		Donoghue (1991)
Papakai Formation	black ash-1	Mt Ruapehu	5562 ± 268 cal yrs B.P.	Donoghue (1991)
Hinemaiaia Tephra	*K*	*TVC*	*5120 ± 150 cal. yrs B.P.*	*Lowe et al. (2008)*
Papakai Formation				
Tariki Tephra		Taranaki	5277 ± 305 cal. yrs. B.P.	Alloway *et al.* (1995)
Papakai Formation	orange lapilli-2 orange lapilli-1	Mt Ruapehu Mt Ruapehu		Donoghue (1991) Donoghue (1991)
Whakatane Tephra Wk		*OVC*	*5530 ± 60 cal. yrs. B.P.*	*Lowe et. al. (2008)*
Waipuku		Taranaki	6025 ± 255 cal yrs. B.P.	Alloway *et al.* (1995)

Papakai Formation	Pp	TgVC		
Motutere Formation	*G-H*	*TVC*	*6122 ±185 cal yrs. B.P.*	*Froggatt and Lowe, (1990)*
Papakai Formation	Pp	TgVC		
Rotoma		*OVC*	*9505 ± 25 cal yrs. B.P.*	*Lowe et. al. (2008)*
Kaponga		Taranaki	9998 ± 388 cal. yrs. B.P.	Alloway *et. al.* (1995)
Opepe Tephra	*E*	*TVC*	*10 075 ± 155 cal yrs B.P.*	*Lowe et. al. (2008)*
Mangamate Form	Mm Poutu Lapilli Wharepu Teph.	Tongariro Tongariro Tongariro	11,165 ± 31 cal yrs B.P.	Topping (1973)
Poronui Tephra	*C*	*TVC*	*11,190 ± 80 cal. yrs. B.P.*	*Lowe et al. (2008)*
Mangamate Form.	Ohinepango T. Waihohonu La. unnamed Teph. Oturere Lapilli Te Rato Lapilli	Tongariro Tongariro - Tongariro Tongariro	11,242 ± 578 cal. yrs. B.P.	Topping (1973)
unnamed Tephra	unnamed tephra	-		
Karapiti Tephra	*B*	*TVC*	*11,410 ± 190 cal.yrs B.P.*	*Lowe et. al. (2008)*
unnamed Tephra		-		
Pahoka Tephra	Pa	Tongariro	max. 12,079 ± 76 cal yrs. B.P	
Bullot Formation (upper)	Bt Ngamatea L-2 Ngamatea L-1 Okupata Memb. Pourahu Memb. L18- L17 Shawcroft Lap. L16	Mt Ruapehu Mt Ruapehu Mt Ruapehu Mt Ruapehu Mt Ruapehu Mt Ruapehu Mt Ruapehu Mt Ruapehu	c. 11500 cal yrs B.P.	Donoghue (1991)
Waiohau Tephra	*Wh*	*OVC*	*13.635 ± 165 cal. yrs. B.P.*	*Lowe et. al. (2008)*
Bullot Formation (upper)	L15 – L8	Mt Ruapehu		
? Rotorua Tephra (a)	*Rr*	*OVC*	*15.425 ± 325 cal. yrs. B.P.*	*Lowe et al. (2008)*
Bullot Formation (upper)	Bt	Mt Ruapehu		
Rotoaira Lapilli (a)	Rt	Tongariro	16.501 ± 939 cal. yrs. B.P.	Topping (1973)
Bullot Formation (upper)	L15 – L8	Mt Ruapehu		
Rerewhakaaitu Tephra		*OVC*	*17.625 ± 425 cal. yrs. B.P.*	*Lowe et. al, (2008)*
Bullot Formation (middle)	L7b – L4	Mt Ruapehu		
Okareka Tephra	*Ok*	*OVC*	*21,800 ± 500 cal yrs. B.P.*	*Vucetich and Pullar, 1969)*
Bullot Formation (lower)	L3 – L1	Mt Ruapehu		
Kawakawa Tephra Fm.		*TVC*	*27,097 ± 957 cal. yrs. B.P.*	*Lowe et. al. (2008)*

[a]Exact stratigraphic position of these tephras relative to Bullot Formation Members is unknown

All dates, except Lowe *et al. (*2008), were calculated in OxCal using provided ages from reference

Stges only relate to Ngauruhoe-sourced tephras

3.1. TgVC Andesitic Tephrochronology

Previous researchers mapped the TgVC and grouped volcanic deposits into Formations, to broadly classify the eruption record (Thomas, 1889; Grange and Williamson, 1930; Grange, 1931; Baumgart, 1954; Gregg, 1960a; Gregg, 1960b; Mathews, 1967). Topping (1973) combined all tephras derived from Tongariro Volcanic Centre, from the base of the c. 16.5 ka cal. yrs. B.P. Rotoaira Tephra up to the present soil surface, within the Tongariro Subgroup (Table 3.2.; Figure 3.1). This was later refined by Donoghue (1991) who defined a younger boundary for the Subgroup at the base of Pahoka Tephra (now Mangamate Formation, c. ~11 ka cal. yrs. B.P.). This boundary is more readily marked by the distinctive Pahoka Tephra, whereas the Rotoaira lapilli has only been reliably identified in the northern part of the Tongariro Volcanic Centre (Topping, 1973). Donoghue (1991) also defined the Tukino Subgroup (Table 3.2), combining all tephras derived from the TgVC older than the Pahoka Tephra but younger than the Kawakawa Tephra Formation (27,097 ± 957 cal. yrs. BP. (Lowe *et al.*, 2008)).

Table 3.2: Classification of Tephra Formations derived from the TgVC into subgroups

	Topping (1973)	***Donoghue (1991)***
Tongariro Subgroup		Tufa Trig Formation
	Ngauruhoe Tephra	Ngauruhoe Formation
	Mangatawai Tephra	Mangatawai Tephra
	Papakai Tephra	Papakai Formation
	Mangamate Tephra	Mangamate Formation
	Okupata Tephra	
	Rotoaira Lapilli	
Tukino Subgroup	-	Okupata Tephra
	-	Rotoaira Lapilli
	-	Bullot Formation

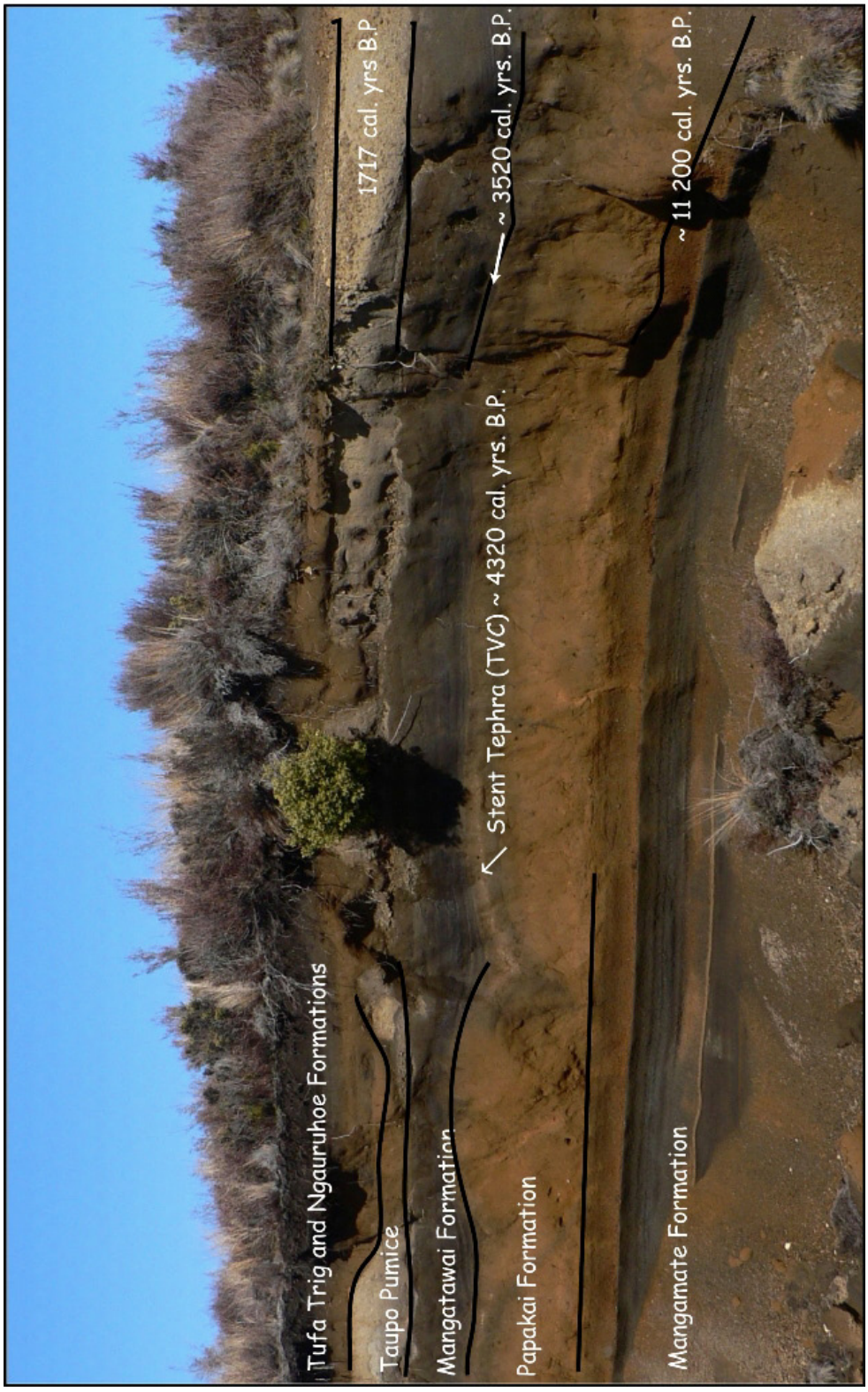

Figure 3.1: Typical exposure on the eastern ring plain (Desert Road), showing the main TgVC-sourced tephra formations (Tufa Trig, Ngauruhoe, Mangatawai, Papakai and Mangamate Formations), combining tephras from both volcanoes: Ruapehu and Tongariro over the last ~12 000 cal. yrs. B.P. Two rhyolitic marker-horizons: Taupo Pumice and Stent tephra,-sourced from the TVC, are also illustrated.

3.1.1. Ngauruhoe Formation (NF)

Definition, Description and Age

The post-Taupo Pumice (1717±13 cal. yrs. B.P. (Lowe *et al*. 2008)) tephra record from Ngauruhoe is here mapped as the Ngauruhoe Formation (NF). The "Ngauruhoe ash" was originally defined by Grange (1931) for "andesitic ash and scoria from Ngauruhoe". Later, Topping (1973) redefined it as the Ngauruhoe Tephra Formation because it "…contains scoriaceous lapilli horizons closer to Mount Ngauruhoe and Mount Ruapehu", and he defined a type section on the Desert Road, south of Mangatawai Stream, where the contact with the underlying Taupo Ignimbrite is visible. The Formation is attributed to multiple ash falls from the Te Maari craters, Red Crater, Ngauruhoe and Ruapehu; it is also locally over-thickened due to wind redistribution. Vucetich and Pullar (1973), also emphasised the collective nature of the "Ngauruhoe ash" (*sic*.) derived from multiple sources and ash fall events. Donoghue (1991) and Donoghue *et al.* (1995) re-defined the formation in order to separate out all Ruapehu-derived lapilli and ash units, which were combined into the new Tufa Trig Formation. Donoghue *et al*. (1995) suggested that the name Ngauruhoe Tephra Formation was "...inappropriate and even misleading for tephras from this source."

In this study, the "Ngauruhoe Formation" is re-defined to include tephras from Mt. Ngauruhoe, Red Crater and Te Maari Craters i.e., all major vents of Tongariro Volcano erupted since 1717 cal. yrs. B.P. Close to the volcano discrete tephras are visible, including distinctive ash and lapilli layers from Red Crater and the 1954 and 1975 eruptions of Ngauruhoe.

The newly described informal tephras members within the Ngauruhoe Formation (annotated in Chapter 4), enable us to make further insights into the eruptive behaviour of the Tongariro Volcano over the last ~1700 years, particularly with respect to eruption sizes, styles and frequency from Ngauruhoe and Red Crater.

3.1.2. Tufa Trig Formation (TTF)

Definition, Description and Age

The Tufa Trig Formation (TTF; Donoghue *et al.*, 1997) is situated above the distinctive Taupo Pumice (1717 cal. yrs. B.P.) and comprises 19 tephras sourced from Ruapehu volcano, defined as individual members along with unnamed, less distinctive, interbedded tephras. The tephras within the TTF are "…black to dark grey, coarse ash to lapilli grade tephras" (Donoghue, 1991), which are mainly preserved within dunes of windblown material (the Makahikatoa Sands of Purves (1990)). The absence of stable vegetative cover and the severe windy, montane climate of the Rangipo Desert causes rapid remobilisation of volcanic ash and surficial sediments, meaning that primary tephras are seldom preserved and are thus difficult to correlate. Although there have been a few distinctive marker beds, partial isopach maps have been created for Tf5, Tf8 and Tf14 (Donoghue, 1991; Donoghue *et al.,* 1997). Further distinct layers of the TTF include Tf1 and Tf2, which are characterised by brown and beige scoriaceous lapilli and lithics. Due to their grain size, colour and composition Tf1 and Tf2 are easily distinguishable from the other members of the TTF. Donoghue (1991) and Donoghue *et al.* (1997) dated peat below Tf5 in Ngamatea Swamp at 790 ± 119 cal. yrs. B.P. [Wk 1489], with peat above being 611 ± 65 cal. yrs. B.P. [Wk 1488].

3.1.3. Mangatawai Formation (MtF)

Definition, Description and Age

The Mangatawai Formation (MtF) was originally named by Gregg (1960a, 1960b), to describe a "thinly bedded dark grey andesitic ash containing leaves." This was later formalised by Topping (1973), with a type location on the Desert Road just north of the Mangatawai Stream. At the type location, it was described as "dark brown fine ash, ... , dark medium ash interbedded dark grey and very dark grey medium ash containing *Nothofagus sp.* leaves". Here the MtF underlies the Taupo Pumice and overlies the Papakai Formation. Topping noted that several units within the MtF contained lapilli where they occurred closer to Ngauruhoe. Topping and Kohn (1973) described the unit

as andesitic tephra overlying the Waimihia Lapilli (Taupo-sourced) and having the Whakaipo Tephra (Taupo-sourced; Vucetich and Pullar, 1973) interbedded within it. Donoghue (1991) described the type section where it "comprises an upper, well developed dark greyish brown greasy, … ,paleosol over multiple bedded black and dark purplish-grey coarse ash beds containing beech leaves and dark yellowish brown greasy sandy loam-textured ash." Based on isopach maps constructed from data on the eastern side of the volcanoes of the TgVC, Topping (1973) and Donoghue (1991) considered that the Mangatawai Tephra was mainly derived from Mt. Ngauruhoe. Vucetich & Pullar (1973) also noted that part of the tephras may have been derived from other vents of Mt Tongariro. At the base of the Mangatawai Formation, beech leaves interbedded in the tephra were radiocarbon dated at 2568 ± 508 cal. yrs. B.P. [NZ 186] (Fergusson and Rafter, 1959). The age of the overlying Taupo Pumice gives the Mangatawai Formation a minimum age of 1717 ± 13 cal. yrs. B.P. (Lowe *et al*., 2008).

The MtF is considered to be the most vigorous period of volcanism in the history of Mt. Ngauruhoe. Hence, studying the tephras of the Mangatawai Formation will help to define the largest scale explosive eruptions from Mt. Ngauruhoe and provide a more accurate history of eruption frequency and magnitude. Activity from this phase can be compared to the lower-magnitude eruption behaviour that characterised Mt. Ngauruhoe post-1717 cal. yrs. B.P.

3.1.4. Papakai Formation (PF)

Definition, Description and Age

The Papakai Formation is described by Grange (1931) as the Tongariro Shower or Tongariro ash (Gregg, 1960a). Topping (1973) named the unit after its type location south-east of Papakai (N112/125924) and defined the Papakai Tephra Formation as "a paleosol on ash and lapilli beds". According to Topping (1973), "its top is defined either by the first appearance of Waimihia Lapilli", or of horizontal "cracking and interspersed lapilli". The Papakai Tephra Formation is underlain by the Poutu Lapilli, the youngest tephra member of the Mangamate Tephra Formation. Vucetich & Pullar (1973), describe the same interval as an unnamed weakly weathered andesitic ash between the

Hinemaiaia and the Waimihia Tephras (both Taupo-sourced). The unit was renamed the Papakai Formation by Donoghue (1991) and "comprises all andesitic tephra erupted from TgVC, and possible tephric loess which overlies Mangamate Tephra and underlies the andesitic Mangatawai Tephra." The PF was originally defined by Topping (1973), as having been deposited between *c.* 11 000 cal. yrs. B.P., based on a wood sample above the Poutu Lapilli and 3410 ± 40 cal. yrs. B.P. (Lowe *et al*., 2008), where the upper boundary is defined by the Waimihia Lapilli. Donoghue (1991) redefined its upper boundary correlation to the Mangatawai Tephra Formation with an age of 2568 ± 508 cal. yrs. B.P. [NZ 186]. The Papakai Formation contains three rhyolitic tephras, thought to be derived from the Taupo Volcanic Centre: the Waimihia, Hinemaiaia and Motutere Tephras (Table 3.1). The unit also contains several distinct andesitic tephra layers, thought to be derived from Ruapehu due to their resemblance to the Tufa Trig Formation and their distribution pattern. Donoghue (1991), described four informal members within the Papakai Formation:

- Black Ash-2 (ba-2), below Waimihia Tephra, at Tufa Trig R.S.2 comprising a 10 mm-thick black pocketing coarse ash.
- Black Ash-1 (ba-1), below Black ash-2 and above Hinemaiaia Tephra, at Tufa Trig Reference Section 2, comprising a 10 mm-thick black pocketing coarse ash. This is also found below the Mangaio Formation (Ruapehu-sourced diamicton) in the Rangipo Desert, where peat has been radiocarbon dated at 5592 ± 268 cal. yrs. B.P. [NZ7532].
- Orange Lapilli-2 (or-2), below the Hinemaiaia Tephra, at Tufa Trig R.S.2, comprising an 80 mm-thick, strong brown, pumiceous fine and medium lapilli.
- Orange Lapilli-1 (or-1), below Orange Lapilli-2 and Hinemaiaia Tephra and above Motutere Tephra, at Tufa Trig R.S.2 comprising a 300 mm-thick, strong brown, fine and medium pumice lapilli.

The Papakai Formation was investigated in this study to enable correlation with the tephras contained in the sediment core collected at Lake Rangatauanui and to constrain the sources of individual tephras within it. In particular, any evidence for older Ngauruhoe-sourced tephras (i.e., below the Mangatawai Formation) was sought.

3.1.5. Mangamate Formation

Definition, Description and Age

The Mangamate Tephra Formation as defined combines "several andesitic tephras underlying Papakai Tephra Formation and overlying a thin rhyolitic marker bed, Papanetu Tephra" (Topping, 1973). The Formation consists of six named members, as well as other undefined tephras (Table 3.3). Donoghue *et al.* (1995) renamed it as the Mangamate Formation. The Karapiti Tephra (TVC; 11 410 ± 190 cal. yrs. B.P. (Lowe *et al*., 2008)) was found below the Mangamate Formation in the Tongariro area (Froggatt, 1981c), providing a maximum age (Table 3.3). Topping (1973) dated peat immediately underlying the oldest member at 11 242 ± 578 cal. yrs. B.P [NZ 1372]. The uppermost member, Poutu Lapilli, was dated at 11 165 ± 31 cal. yrs. B.P., based on peat accumulation rates using a radiocarbon date of 10 891 ± 297 cal. yrs. B.P. [NZ 1335] from peat 90 mm above the unit (Topping, 1973; Hitchcock, 2005). Later, Nairn *et al.* (1998) combined the former Ohinepango and Waihohonu members into a single unit (PM4a and PM4b) and added an older dacitic/andesitic unit, the Pahoka Tephra as member PM1. They defined sources for the individual members as being the Tama Lakes and proto-Ngauruhoe (Nakagawa *et al.*, 1998), as well as the possible vents of Saddle Cone and Half Cone (Figure 3.2).

The members of the Mangamate Formation were sampled at Loc. 12 and their glass analysed by electron microprobe for comparison to tephras within the sediment core at Lake Rangatauanui, as well as for comparison to the younger Tongariro-sourced tephras.

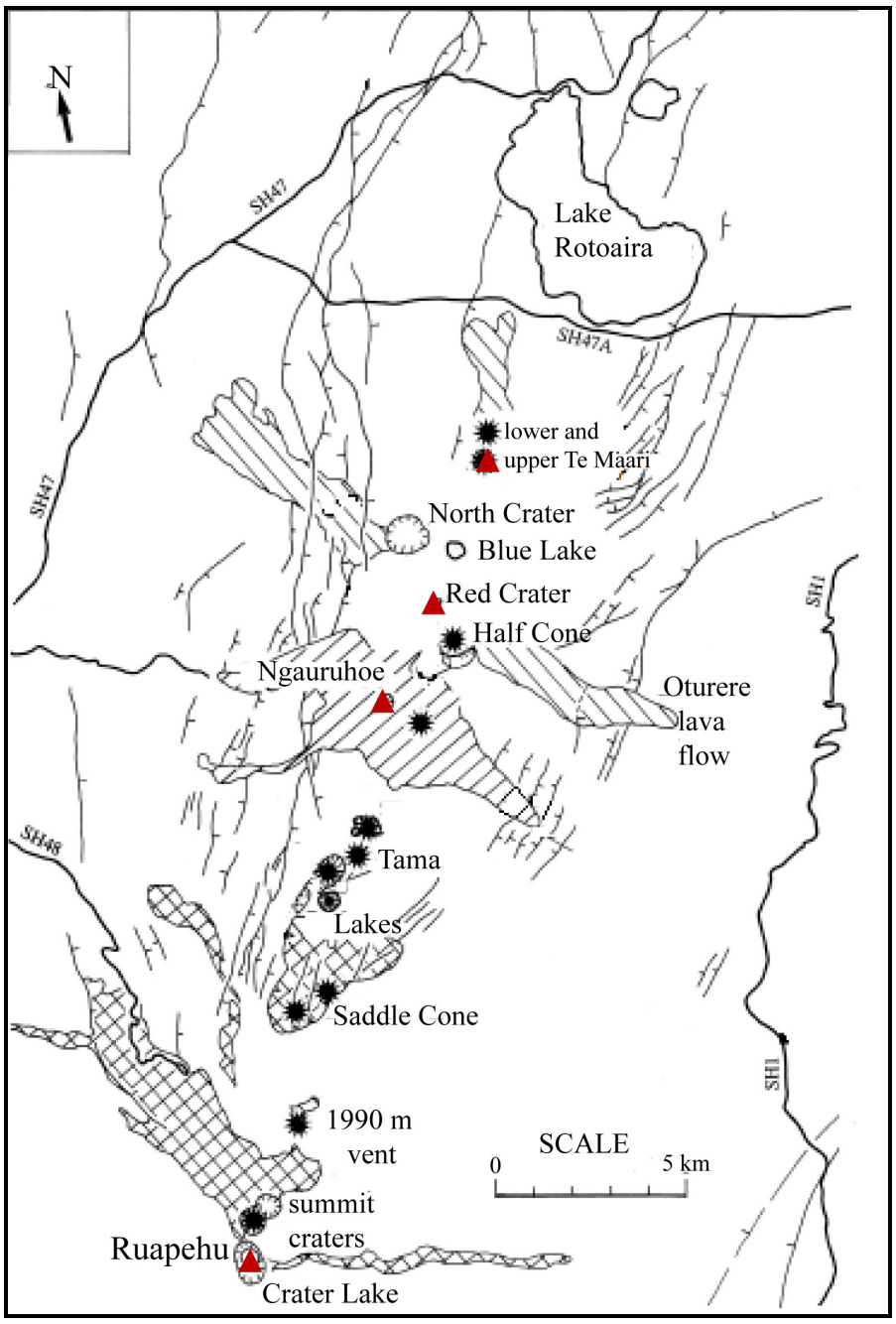

Figure 3.2: Map showing the active volcanic vents of the TgVC (red) and older dormant eruption vents (black), modified after Nairn *et al*. (1998).

Table 3.3: Radiocarbon ages for dated members of the Mangamate Formation

Member	Ages after Topping (1973)	Ages after Donoghue *et al.* (1991)	Ages after Nairn *et al.* (1998)
Poutu Lapilli	10 891 ± 297 cal. yrs. B.P. (N112/545; NZ 1335) minimum age		
Wharepu Tephra		11 173 ± 78 cal. yrs. B.P. (Froggatt and Lowe, 1990) age of underlying Poronui Tephra	
Ohinepango Tephra			11 173 ± 78 cal. yrs. B.P. (Froggatt & Lowe, 1990) age of underlying Poronui Tephra
Waihohonu Lapilli			
Unnamed Tephra			
Oturere Tephra			
Te Rato Lapilli	11 131 ± 693 cal. yrs. B.P. (N112/551; NZ 1373) maximum age 11 241 ± 577 cal. yrs. B.P. (NZ 1372) maximum age		11 241 ± 577 cal. yrs. B.P. (NZ 1372)
Pahoka Tephra			min. age 11 244 ± 360 cal. yrs. B.P. from the overlying Karapiti Tephra

all ages were calculated with OxCal 4.1.

3.1.6. Pahoka Tephra

Definition, Description and Age

The Pahoka Lapilli was first recognised by Topping (1974) as a lapilli unit below the Mangamate Formation. Donoghue (1991) redefined it as the Pahoka Tephra, indicating that it was a distinctive marker bed below the Mangamate Formation and above the Bullot Formation. Topping (1974) suggested that the unit was derived from North Crater, Mt. Tongariro, and Donoghue *et al*. (1995) defined a type section on the Desert Road (DR.16) where three beds within the unit are recognised and described. Later, Nairn *et al.* (1998) included the Pahoka Tephra within the Mangamate Formation, suggesting that Saddle Cone (Figure 3.1) was a more likely source. The minimum age of Pahoka Tephra is defined by the overlying rhyolitic Karapiti Tephra with a minimum

age of 11 410 ± 190 cal. yrs. B.P. (Lowe *et al*, 2008), and its maximum age with 12 079 ± 76 cal. yrs. B.P. defined by the underlying Okupata member of the Bullot Formation (Donoghue *et al.*, 1999).

3.1.7. Bullot Formation (BF)

Definition, Description and Age

The Bullot Formation was defined by Donoghue (1991) as comprising all tephra fall deposits erupted from Mt. Ruapehu older than the Pahoka Tephra (Mangamate Tephra), but younger than the Kawakawa Tephra Formation 27 097 ± 957 cal. yrs. B.P. (Lowe *et al*. 2008). The Bullot Formation was divided into three parts, split by distal-sourced rhyolitic marker units, and contains 18 informal members, and five which were formally defined (Table 3.1) (Donoghue, 1991; Donoghue *et al.*, 1999). Cronin (1996) described further andesitic lapilli derived from Ruapehu occurring below the Kawakawa Tephra Formation, which could be either included into the Bullot Formation or be defined as a new tephra formation. The Bullot Formation is distributed primarily to the east of Mt. Ruapehu with excellent exposures found throughout the Rangipo Desert, the Karioi Forest, and toward the Kaimanawa Mountains to the east. Members of the Bullot Formation are also identified north of Mt. Ruapehu on Pukeonake and along the Waihohonu Track in the vicinity of the Tama Lakes and also north of Mt. Tongariro, around Lake Rotoaira (Figure 3.1).

Tephras of the Bullot Formation are recognised within the sediment core of Lake Rangatauanui and comprise products representing the largest known explosive eruptions from Mt. Ruapehu (Donoghue *et al.,* 1995).

3.2. Rhyolitic Tephras

3.2.1. Rhyolitic Tephras sourced from Taupo Volcanic Centre

Holocene tephras sourced from the Taupo Volcanic Centre (TVC) were collectively combined in the Taupo Subgroup (Healy, 1964) with the youngest member being the Taupo Pumice Formation (1717 ± 13 cal. yrs. B.P.(Lowe *et al*. 2008)) and the oldest the Karapiti Tephra (11 410 ± 190 cal. yrs. B.P. (Lowe *et al.* 2008)). Baumgart (1954) had earlier defined 26 individual tephras within the Taupo Ash Sequence (Table 3.4).

Table 3.4: Members of the Taupo-Subgroup, References: #Sparks *et al.* (1995); * Vucetisch and Pullar (1973); ♦Froggatt and Lowe (1990); ○ Froggatt (1981b); ● Lowe and Hogg, 1986); [&]Wilson (1993); [@] Turner (2008)

Tephra unit	Baumgart (1954) Healy (1964) members	Wilson (1993) units	Age in ^{14}C yrs. B.P.	Age in cal. yrs. B.P. (Lowe *et al*. 2008) and Oxcal
Taupo Pumice	1-8	Y	1850 ± 100 [NZ515] 232 AD [#]	1717 ± 13
Mapara Tephra	9 and 10	X	min age 2010 ± 60 [NZ 1068] * max age 2150 ± 48 [NZ1069] *	1975 ± 148 (Oxcal) 2156 ± 154 (Oxcal)
Whakaipo Tephra	11 and 12	V	max age 2730 ± 60 [NZ1071] *	2760 ± 20
Waimihia Tephra	13 - 15	S	3280 ± 20 ♦	3410 ± 40
Hinemaiaia Ash	16b and 16c	N-R	3950 to 4200[&]	4419 ± 9 (Oxcal) to 4771 ± 63 (Oxcal)
		Q	4050, 4130 ± 70, 3920 ±59[@]	4323 ± 174 (Oxcal)
		I-M	4500 to 5200[&]	5250 to 5950[&]
		K	4650 ± 80○	5120 ± 150
Motutere Tephra	16d	H	5370 ± 90 [NZ 4846] ○	6050[&]
		G	5800[&]	6650[&]
unknown		F	6150[&]	7050[&]
Opepe Tephra	17 and 18	E	8850 ± 1000 [NZ 185] *	10 075 ± 155
unknown		D	9780[&]	11380[&]
Poronui Tephra	20- 22	C	*c*. 9900 [Wk 351; 352, 491] •	11 190 ± 80
Karapiti Lapilli	23-25	B	9910 ± 130 ○	11 410 ± 190
unnamed		A	14 200 - 17 000	17102 ± 287 – 20168 ± 208

Previous studies of the TgVC described several interbedded tephras of the Taupo subgroup (Topping, 1973; Topping and Kohn, 1973; Donoghue, 1991; Lecointre *et al.*, 2004b). The most distinctive rhyolitic marker horizon is the Taupo Pumice Formation 1717 cal. yrs. B.P. (Lowe *et al*. 2008), comprising members 1-8 of the Taupo Subgroup.

Froggatt (1981c) redefined the 8 members of the Taupo subgroup, into Taupo Ignimbrite (members 1-2), Taupo lapilli (member 3), Rotongaio Ash (member 4) and Hatepe Tephra (members 5-7). Of these, the Taupo Ignimbrite member is the main unit found in the TgVC, represented by a poorly sorted, non-welded, white, pale grey or pink ignimbrite unit that lies above the andesitic Mangatawai Formation (MtF) and below the Tufa Trig and Ngauruhoe Formations. Mapara Tephra (1975 ± 148 to 2156 ± 154 cal. yrs. B.P.) was recognised by Donoghue (1991) within the MtF at Tufa Trig Reference Section 2 and at Ngamatea Swamp as a white to pale brown discontinuous fine ash. Furthermore, Topping and Kohn (1973) identified the Whakaipo Tephra (2760 ± 20 cal. yrs. B.P.; Lowe *et al*. (2008)) as a pale yellow ash within the MtF in the northern part of the TgVC. Donoghue (1991), on the other hand interprets this as Waimihia Tephra (Table 3.5). Several radiocarbon dates of the Waimihia Tephra range from 3332 ± 251 cal. yrs. B.P. [NZ 180] (Healy, 1964) to 3610 ± 216 cal. yrs. B.P. [NZ505] (Pullar and Heine, 1971) and even up to 4471± 46 cal. yrs. B.P. [Wk 1032, Wk 1259] (Alloway, 1989). Lowe *et al.* (2008) presents a calibrated ^{14}C-date for the Waimihia Tephra 3410 ± 40 cal. yrs. B.P. The Waimihia Tephra was described as being interbedded within the Papakai Formation along the Desert Road and within the Rangipo Desert (Donoghue, 1991), where it comprises yellow to pale yellow fine ash. The Hinemaiaia Tephra (unit K) 5120 ± 150 cal. yrs. B.P. (Lowe *et al*. 2008), was described within the TgVC by Topping and Kohn (1973), and Donoghue (1991), but the latter re-defines Topping and Kohn's "Hinemaiaia Tephra" as being the Motutere Tephra (Table 3.5). Donoghue, (1991) describes the Hinemaiaia Tephra as an olive yellow and white coarse pumiceous ash (coarser than both the Waimihia and Motutere Tephras) within the Papakai Formation along the Desert Road and the southern Rangipo Desert. The Motutere Tephra was documented within the TgVC by Donoghue (1991) as a distinctive pinkish brown fine ash with scattered pumice fragments in the lower part of the Papakai Formation. Opepe Tephra (10 075 ± 155 cal. yrs. B.P. (Lowe *et al*. 2008)) was identified by Topping and Kohn, (1973) in peats along the Otamangakau Canal (at N112/109984). The Poronui Tephra was identified by Topping and Kohn (1973), and Donoghue (1991) in the northern part of the TgVC, along Access 10 Road, the Poutu Canal, and the Desert Road north of Mt. Ruapehu. The Poronui Tephra (11 620 ± 80 cal. yrs. B.P. (Lowe e*t al.*, 2008)) was recognised by Donoghue (1991), as a

white to yellow fine ash between the Mangamate members Wherapu and Ohinepango tephras. The Karapiti Lapilli (11 410 ± 190 cal. yrs. B.P. (Lowe *et al*., 2008)) was identified by Topping and Kohn (1973), in the northern part of the TgVC at Kepa Road underlying the Te Rato Lapilli. Donoghue (1991), however, identified Karapiti Tephra at the Mangatoetoenui Quarry (T20/459153) and the northern end of the TgVC as a discontinuous white to pale grey fine ash below the Oturere Lapilli Member and above the Pahoka Tephra.

Table 3.5: Comparison of the rhyolitic TVC-sourced tephras preserved in the TgVC

Topping (1973) **Topping & Kohn (1973)**	**Donoghue (1991)**	**this thesis**
Taupo Pumice	Taupo Pumice	Taupo Pumice
-	Mapara Tephra	-
Whakaipo Tephra	Waimihia Tephra	Stent Tephra (Q)
Waimihia Lapilli	Hinemaiaia Tephra	Hinemaiaia Tephra (K?)
Hinemaiaia Ash	Motutere Tephra	Motutere Tephra (G)
Opepe Tephra	-	Opepe Tephra *
Poronui Tphra	Poronui Tephra	Poronui Tephra *
Karapiti Tephra	Karapiti Tephra	

* in this study identified in sediment core Lake Rangatauanui

In this thesis, the post-12 000 cal. yrs. B.P. tephrostratigraphic record was studied in soil sequences of the TgVC, and a post-25 000 cal. yrs. B.P. record obtained from the cores of Lake Rangatauanui. The youngest TVC-sourced tephra, clearly identified during this study, was the Taupo Pumice. As Topping and Kohn (1973) and Donoghue (1991) describe, this marker horizon appears as a distinctive white and partly pink ash-lapilli, containing charcoal and is stratigraphically situated between the Mangatawai Formation (MtF) (below) and TTF and NF (above). The Taupo Pumice was also identified within the cores from Lake Rangatauanui.

Within the Papakai Formation, several rhyolitic tephras sourced from the TVC were also identified. The youngest of these rhyolitic tephras is at Loc. 12, a 40 mm-thick discontinuous pale white to pale yellow fine ash, c. 100 mm below the top of the formation within medial ash with strong paleosol development. New radiocarbon dates and age calculations based on soil accumulation (presented in Chapter 4) from the basal

MtF, show a min. age of 3523 cal. yrs. B.P. (Appendix 5). This excludes the possibility that the youngest identified rhyolitic tephra within the Papakai Formation is the Waimihia Tephra (3410 ± 40 cal. yrs. B.P.; Lowe *et al.*, 2008) as was postulated by previous workers. This age and stratigraphic position suggests a more likely correlative is the Stent Tephra (Alloway *et al.*, 1994), with a combined calendrical age of 4323 ± 174 cal. yrs. B.P. The Waimihia Tephra, if present in the TgVC, should be found within the MtF; however, no rhyolitic tephras have been identified within the MtF in the course of this study. Given the strong easterly dispersal axis of the Waimahia Tephra (Vucetich and Pullar, 1964), it is hereby considered unlikely that this unit is indeed preserved in the TgVC.

A rhyolitic tephra at the same stratigraphic position as the Stent Tephra at Loc. 12 was identified within a core from Lake Rangatauanui. Its age, based on a spline fit to radiocarbon-dating constrained deposition rates (see Chapter 6), is 4407 ± 417 cal. yrs. B.P., meaning that it also likely represents the Stent Tephra.

The Hinemaiaia Tephra was also identified by previous workers (described above), deeper within the Papakai Formation weathered medial ash. It occurs as a distinctive 50-80 mm-thick band of pale yellowish coarse ash and fine lapilli that is scattered within the brown medial ash. Within the core of Lake Rangatauanui, Hinemaiaia Tephra could not be clearly identified. About 150 mm below the Hinemaiaia Tephra on the ring plain and 10 mm below the Orange Lapilli 1, the Motutere Tephra was identified along the Desert Road. This unit was also recognised by previous workers as a pale yellow to pink fine ash, at times containing fine lapilli. The TVC-sourced tephra at similar stratigraphic position of the Motutere Tephra has a calculated age of 6907 ± 250 cal. yrs. B.P. and is therefore assumed to be Wilson's (1993) unit G.

Two further TVC-sourced tephras were identified in the Rangatauanui Core (Tab 3.6) with radiocarbon-date constrained deposition ages of 10 095 ± 275 cal. yrs. B.P. and 10 167 ± 251 cal. yrs. B.P. These ages imply that the units most likely correlate to the Opepe Tephra. In older parts of the core detrital glass has a signature implying it was

reworked from the TVC-sourced, Oruanui Ignimbrite (Kawakawa Tephra Formation (Wilson, 2001)).

Table 3.6: Identified rhyolitic tephras sourced from the TVC (italic) and OVC (bold) within the core from Lake Rangatauanui; S = sediment which has been dated; ages of tephras in yrs B.P. and cal. yrs. B.P. from previous workers, for spline fit see Chapter 6.

Soil	Tephra	Depth in mm	Lab-code	Age in yrs. B.P.	Age in cal. yrs. B.P.	Age in cal. yrs. B.P. splint fit
S-1		90-111	NZA-29191	1885 ± 35	1718 ± 107	
	Taupo Pumice (TVC)	*309-329*	*[NZ515]*	*1850 ± 100*	*1717 ± 13*	*1779 ± 45*
S-2		635-670	NZA29186	3325 ± 30	3487 ± 88	
	Stent Tephra (TVC)	*820-836*	*NZ 6702A*	*3580 ± 80*	*4323 ± 174*	*4407 ± 417*
			WK 1259-A	*3940 ± 70*		
			WK 1032	*3870 ± 110*		
	Motutere Tephra (TVC)	*1202-1209*	*NZ4846A*	*5370 ± 90*	*6122 ± 185*	*6907 ± 250*
	Mamaku (OVC)	1419-1429	N 77/ 554	**7250 ± 20**	**8005 ± 45**	**8075 ± 94**
S-3		1429-1440	NZA29190	7403 ± 40	8165 ± 141	
	Rotoma (OVC)	1678-1694	N 77/ 554	**7330 ± 235**	**9505 ± 25**	**9516 ± 25**
	Opepe Tephra (TVC)	*1809-1815*	*WK 492*	*8710 ± 80*	*10 075 ± 155*	*10 095 ± 275*
	Poronui Tephra (TVC)	*1826-1832*	*NZ185*	*9810 ± 50*	*11 190 ± 80*	*10 167 ± 251*
S-4		1980-1994	NZA29188	9581 ± 35	10 881 ± 210	
S-5		2121-2185	NZA29187	10 377 ± 40	12 309 ± 249	
	Waiohau Tephra (OVC)	2400-2410		**11 850 ± 60**	**13 635 ± 165**	**13 681 ± 259**
S-6		2737-2799	NZA29173	13 046 ± 60	15 438 ± 315	
	Rerewhakaaitu (OVC)	2985-2986		**14 700 ± 110**	**17 625 ± 425**	**17 891 ± 639**
	?? (OVC)	3003-3004				**18 095 ± 575**
S-7		3076-3215	NZA29172	13 406 ± 65	15 945 ± 392	
		3490-3500	NZ 716			
	Okareka Tephra (OVC)	3490-500	NZ 523	**20 700 ± 450**	**24850 ± 1158**	**20 430 ± 1015**
S-8		3500-3612	29171	13 522 ± 70	16 089 ± 400	
S-9		3933-3988	29175	18 880 ± 100	22 404 ± 186	

3.2.2. Rhyolitic Tephras sourced from Okataina Volcanic Centre

Tephras sourced from the Okataina Volcanic Centre (OVC) following the eruption of Rerewhakaaitu Tephra at 17 625 ± 425 cal. yrs. B.P. (Lowe *et al.,* 2008) were placed within the Rotorua Subgroup (Vucetich and Pullar, 1973). Later, Howorth and Ross (1981) expanded the Rotorua Subgroup to combine all OVC-sourced tephras younger than the TVC-sourced Kawakawa Tephra Formation (27 ka cal. yrs. B.P.). Hence, it

oldest member is now Te Rere Tephra (c. 25 271 ± 779 cal. yrs. B.P., Lowe *et al*., 2008). The youngest OVC sourced member of this subgroup is the Tarawera Formation, 1886 A.D. (Walker *et al.*, 1984). Deposits older than Kawakawa Tephra Formation are combined in the Mangaone Subgroup; both subgroups form the Okataina Group (Howorth and Ross, 1981).

Several OVC tephras have been identified in the TgVC (Tab.3.7). According to Donoghue (1991), a 10 mm thin pocket of fine white ash interbedded in reworked tephras and soils of the Tufa Trig Formation (Ohakune Mountain Road) and Makahikatoa Sands was correlated to the Kaharoa Tephra (636 ± 12 cal. yrs. B.P.; Lowe *et al.* (2008)). The white tephra correlated to fit between Tf5 and Tf8 of the Tufa Trig Formation with bracketing radiocarbon dates of 611 ± 65 cal. yrs. B.P. [Wk 1488] and 790 ± 119 cal. yrs. B.P. [WK 1489]. Furthermore, Donoghue (1991) identified the Whakatane Tephra (5530 ± 60 cal. yrs. B.P.; Lowe *et al.* (2008)) within the southern ring plain as a 5 mm thin layer of white fine cream cakes within Manutahi Formation volcaniclastic sediments (lahar deposits). Older OVC-sourced tephras were also identified by Topping and Kohn (1973), who identified the Rotoma Ash (9505 ± 25 cal. yrs. B.P. .; Lowe *et al.* (2008)) in a swamp cut by the Otamangakau Canal. Waiohau Tephra (13 635 ± 165 cal. yrs. B.P.; Lowe *et al,* (2008)) was identified by Donoghue (1991) at the Wahiona Aqueduct and along the Whangaehu River as a distinctive white ash layer below the Shawcroft lapilli (Ruapehu-sourced). Topping and Kohn (1973), identified the Rotorua Ash (15 425 ± 325 cal. yrs. B.P. ; Lowe *et al.* (2008)) as a fine yellow rhyolitic tephra with a maximum thickness of 60 mm, between the Te Rato Lapilli and Rotoaira Lapilli as far west as Moerangi and as south as Waiouru. Donoghue (1991) suggested that the Topping and Kohn "Rotorua Ash" was in fact the Waiohau Tephra (Tab. 3.7), due to a lower than expected content of biotite. Donoghue (1991) identified Rotorua Tephra only at Oturere Trig as a pocketing white fine ash. The Rerewhakaaitu Tephra, erupted at 17 625 ± 425 cal. yrs. B.P. (Lowe *et al.,* 2008) was identified by Topping and Kohn (1973) and Donoghue (1991), as a discontinuous thin (10 mm) white ash along the Bullot Track (Tukino Ski-field Road), the Desert Road, along the Whangaehu River and around Lake Rotoaira, to the north. Okareka Tephra is the oldest known eruption episode from Mt Tarawera 24 850 ± 1158 cal. yrs. B.P. [NZ

523] and appears as a pinkish brown fine – coarse ash (Vucetich and Pullar, 1969, Pullar *et al.*, 1973). The tephra consist of at least nine units of which the oldest consist of basaltic scoria and is overlain by rhyolitic tephras (Darragh *et al.*, 2006). Donoghue (1991) identified Okareka Tephra at one site south of Tukino Ski-field Rd as a 10 mm "white fine ash, interbedded with brown and black andesitic ash".

Table 3.7: Comparison of the rhyolitic OVC-sourced tephras preserved in the TgVC, Donoghue's (1991) Kaharoa Tephras was in this study identified as the Taranaki sourced Burrell Lapilli (italic),

Topping (1973) Topping and Kohn (1973)	**Donoghue, 1991)**	**this study**
-	Kaharoa Tephra	*Burrell Lapilli*
-	Whakatane Tephra	
		Mamaku Tephra*
?Rotoma ash	-	Rotoma Tephra
?Rotorua Ash	Waiohau Tephra ?	Waiohau Tephra
?Puketarata Ash	Rotorua Ash ?	Rotorua Ash*
Rerewhakaaitu Ash	Rerewhakaaitu Ash	Rerewhakaaitu Ash
	Okareka Tephra	Okareka Tephra

*only identified in the core from Lake Rangatauanui

In the course of this study OVC-sourced tephras were only identified in the cores from Lake Rangatauanui. The white tephra layer that Donoghue *et al.* (1995) identified as Kaharoa Tephra was re-analysed in this study. The glass composition, matches more closely to a Mt. Taranaki source, and in particular correlates to the tm-chemistry of the 1655 A.D. Burrell Lapilli (notably a biotite-bearing eruptive with dacitic glass; Druce, 1966; Platz *et al*., 2007). At the Bruce Road, Pukekaikiore and Oturere lava flow a white layer in a similar stratigraphic position showed an identical correlation. Within one of the cores from Lake Rangatauanui, six tephras from the OVC were clearly identified (Tab 3.6), between radiocarbon-date constrained depositional ages of 8075 ± 94 and 8106 ± 83; 9516 ± 25; 13 681 ± 259; 17 891 ± 639 and finally of 20 430 ± 1015 cal. yrs. B.P. This implies the units recorded include the Mamaku, Rotoma, Waiohau, Rerewhakaaitu and Okareka Tephras.

Chapter 4

Identification of volcanic sources using geochemical and mineralogical fingerprinting

4.1. Introduction

The correlation of tephras and the identification of their volcanic source(s) is one of the most important steps needed to build a history of the eruption behaviour for any volcano. The traditional way to determine the source of a particular tephra has been to map the tephra deposit to produce a fine grid of thickness points from which isopachs may be constructed, which typically thicken toward the eruptive vent (Healy, 1964; Vucetich and Pullar, 1964; Topping, 1973). Difficulties encountered, even when exposure and deposit preservation is good, can be caused by: a) many tephra beds not being correlated due to lateral and longitudinal facies variation, particularly for thin and fine-grained units; b) petrological and chemical properties of many tephras may be very similar, particularly within the andesitic Tongariro Volcanic Centre (TgVC); (Donoghue, 1991) and c) with numerous closely located eruption vents and variable wind directions, such as within the Taupo Volcanic Zone (TVZ) and TgVC, tephra isopachs may still be ambiguous as to their source vent.

Some of the most reliable correlation methods have focussed on the mineralogy and chemistry of tephras, identifying subsets of features that are unique for each volcano and possibly for individual tephras (Self and Sparks, 1980; Lowe, 1988; Froggatt and Lowe, 1990; Shane, 2000). Reasons for the chemical variations may result from variations in the evolution of basaltic-andesitic magma systems, including mantle/crustal sources, crustal interaction and assimilation, different melting depths, variations in the rate of ascent and resulting fractional crystallisation as well as magma

mixing/mingling processes (Gill *et al.*, 1993; Lundstrom *et al.*, 1995; Zellmer *et al.*, 2003; Price *et al.*, 2005; Turner and Costa, 2007).

As described in Chapter 1, the volcanism of the TVZ is up to 80% of rhyolitic composition and is only primarily andesitic at its most south-western end. Rhyolitic tephras from the major active caldera systems of the TVZ, such as Taupo Volcanic Centre (TVC) and the Okataina Volcanic Centre (OVC; which includes Mt Tarawera), provide very good marker beds within the dominantly andesitic ring-plain deposits of TgVC (Topping and Kohn, 1973; Donoghue, 1991; Cronin *et al.*, 1997d). The greatest difficulty in applying stratigraphic ages from these, however, is being able to distinguish individual rhyolitic tephras. Even with highly sensitive analytical methods and use of trace elements, many tephras from the same source are extremely difficult to discriminate (Shane and Froggatt, 1994; Cronin *et al.*, 1996d; Cronin *et al.*, 1997d). The main parameters for tephra fingerprinting include the use of ferromagnesian mineral assemblages, mineral chemistry, and volcanic glass chemistry typically measured by use of the electron microprobe.

4.1.1. Ferromagnesian Mineral Assemblages

Rhyolites

Ewart (1963; 1967;1971) and Kohn (1973) used ferromagnesian assemblages to identify and distinguish tephras sourced from the TVZ. They recognised five characteristic ferromagnesian assemblages (Table 4.1). Lowe (1980) and Froggatt and Lowe (1990) updated this classification by refining and extending the mineral assemblages.

Tab. 4.1: Definitive ferromagnesian assemblage groups for Late Quaternary rhyolitic tephra deposits in the Central North Island, New Zealand. hb = hornblende; hyp = hypersthene.

Group	*Ewart (1963, 1967, 1971) Kohn (1973)*	*Lowe (1980)*	*Froggatt and Lowe (1990)*
1	hypersthene	hyp+augite	hyp±augite ±hb
2	hyp+augite	hyp±cummingtonite+hb	hyp+hb±augite
3	hyp+calcic±hb	biotite+hb±hyp	hyp+hb+biotite
4	hyp+cummingtonite		hyp+cummingtonite±hb
5	biotite+calcic hb±hyp		hyp+augite±hb
6		Aegerine	aegirine±riebeckite± aenigmatite±olivine±tuhualite

Some of these mineral assemblages can be related to specific volcanoes (Lowe, 1980; Froggatt and Lowe, 1990). Furthermore, some individual tephra layers within a volcanic centre also have unique mineral assemblages. Rhyolitic tephras derived from the TVC post-27 ka cal. yrs. B.P. typically contain hypersthene ± augite ± hornblende while older tephra deposits (from the TVC) comprise hypersthene + hornblende ± augite. In addition some of the Taupo-sourced tephra layers contain biotite, olivine and amphibole (Ewart, 1963). OVC-sourced tephra deposits can be subdivided into 4 groups consisting of a) hypersthene + hornblende ± augite, b) hypersthene + hornblende + biotite, c) hypersthene + cummingtonite ± hornblende and d) hypersthene + augite ± hornblende. Group 6 of the ferromagnesian mineral assemblage from Froggatt and Lowe (1990) are the tephras from Tuhua Volcanic Centre (Mayor Island, New Zealand).

Andesites

The ferromagnesian mineral assemblages of andesitic volcanoes have also been studied but are less useful as discriminants. Mt Taranaki has a mineral assemblage containing plagioclase, clinopyroxene, hornblende, titanomagnetite, and traces of olivine, with higher abundance of hornblende being its most distinctive feature. Gow (1968) identified five typical ferromagnesian assemblages in Taranaki lavas, which were updated by Neall *et al.* (1986) and Price *et al.* (1999) by adding phases such as biotite and orthopyroxene. Shane (2000) described the most typical ferromagnesian

assemblage for Mt Taranaki tephras as: clinopyroxene + hornblende ± orthopyroxene. For the TgVC, Lowe (1988), Green and Lowe (1985) and Froggatt and Roger (1990) identified tephra mineral assemblages comprising: orthopyroxene (opx) + clinopyroxene (cpx) ± olivine (ol) ± hornblende (hb). Donoghue (1991) also defined four ferromagnesian mineral assemblages from 23 andesitic tephras derived from Ruapehu and Tongariro.

a) opx > cpx
b) opx > cpx ± ol ± hb
c) ol > cpx >> opx ± hb
d) hb >> opx > cpx ± ol

Clinopyroxene and opx were present in all of her analysed tephras, whereas ol and hb are only present in small amounts (<1%). Olivine was characteristic for Tongariro-sourced tephras, while hb and ol mainly occur in trace quantities in Ruapehu-sourced tephras.

In addition, Hobden (1997) defined three mineral assemblages for lavas of the Tongariro Complex:

a) plag + ol + cpx + opx + ox (rare ap, qtz)
b) plag + cpx+ opx ± oxide (rare ap, qtz)
c) plag + cpx + opx + hbl + oxide (rare ol, ap, qtz)

The major problem with modal analysis of ferromagnesian mineral contents in tephras is the common variability in their sorting during transport due to differences in mineral density, size and shape. Typically, heavy minerals are enriched close to source while low-density particles are carried farther and are more abundant in distal deposits. Specific particle shapes, such as biotite flakes, give rise to extremely high efficiencies of distribution; hence these are often enriched in distal deposits. The type and size of an eruption must also be taken into account. Different eruption styles have diverse fragmentation processes that may also affect the content and distribution of various mineral phases.

4.1.2. Titanomagnetite

Titanomagnetite (tm) chemistry has been successfully used to correlate rhyolitic tephras from the TVZ (Kohn, 1970; Cronin *et al.*, 1996d; Turner, 2008). Kohn analysed titanomagnetites from OVC and TVC spectrographically for Ti, Mg, Mn, Ca, V, Cr, Co, Ni, Zr, and Cu and was able to identify each analysed tephra by a specific combination of Ti/V, V/Mn and Co/Mn ratios. Kohn and Neall (1973) used tm compositions to confirm the identity of tephras derived from Taranaki, for developing ring-plain volcaniclastic stratigraphy. They also observed that titanomagnetite compositions from Taranaki tephras were distinct from those of TgVC. Cronin *et al.* (1996d) showed how tm and hb compositions could be used to identify and differentiate andesitic tephra from Mt. Taranaki and volcanoes of the TgVC, with the application of canonical discriminant function analysis. The latter statistical technique helped to distinguish individual tephras from Taranaki, but not in all cases those from TgVC. Turner (2008) and Turner *et al.* (2008b) were able to identify a systematic and characteristic cyclicity within the magma chemistry of Mt. Taranaki, that was also reflected in tm chemistry. This cyclic pattern could be used to correlate tephras in conjunction with independent stratigraphic information (Turner *et al.*, 2009).

4.1.3. Volcanic Glass

One of the most successful methods applied to distinguishing volcanic sources in New Zealand is the micro-geochemical analysis of volcanic glass using methods such as emission spectrography and electron microprobe analysis. Rankin (1973), for example used the micro-element composition of volcanic glass to distinguish rhyolitic tephras derived from the TVC and OVC. Since then, numerous studies have been carried out on the geochemistry of volcanic glass shards (Lowe, 1988, Froggatt and Lowe, 1990; Froggatt and Rogers, 1990; Shane and Froggatt, 1992; Shane *et al.*, 1998; Shane, 2000, Lowe *et al.*, 2008). These have aimed to identify tephras from different volcanic centres, but more recently to specifically identify and distinguish individual tephra beds within an individual volcanic centre (Smith *et al.*, 2005; Shane *et al.*, 2007). Stokes *et*

al. (1992) applied discriminant function analysis (dfa) to glass compositions to correlate rhyolitic tephra deposits derived from both the Taupo and Okataina Volcanic Centres and Cronin *et al.* (1997d) also used dfa to distinguish Quaternary rhyolitic tephras within the TgVC.

To analyse volcanic glass of andesitic origin is not easy. Platz *et al.* (2007) noted the high microlite content and high variability in glass composition within individual particles as being hindrances to obtain unique and narrow clusters of chemical analyses. In addition, the glass composition is strongly influenced by crystallinity. The glass composition of andesitic tephras from Mt Taranaki and TgVC has mostly been used to distinguish andesitic tephras from rhyolitic ones. Neall (1977) used andesitic glass chemistry of Taranaki-derived tephras to describe the genesis of andosols and "suggests a half-life of andesitic glass" of those tephras of around 7000 years in the soil environment. Shane and Hoverd (2002) were able to differentiate andesitic tephras from the TgVC and Mt. Taranaki within cores from the Onepoto Basin in Auckland using glass chemistry. Because andesitic tephras rarely show distinctive geochemical characteristics and because of the difficulty in preparing and analysing andesitic glass, its chemistry has not been previously used for correlation purposes within the TgVC.

4.2. Geochemical Tephra Fingerprinting of TgVC

Within the TgVC, a wide range of pyroclastic eruption types and scales have occurred, and their deposits have been typically grouped into "Tephra Formations". These, as described in Chapter 3, may contain the products of many individual and separate eruptions (even some from separate sources). For some, such as the Bullot Formation, tephras are clearly derived from Mt. Ruapehu between *c.* 25 000 and 12 000 cal. yrs. B.P. (Donoghue *et al.*, 1995). For others, particularly those containing the products of multiple smaller eruptions, single stratigraphic formations used in regional mapping have assumed that all tephra contained therein are derived from an individual source. However, new results from Donoghue (1991) and from this study (see below) show that the Mangatawai and Ngauruhoe Formations contain tephras from multiple sources. The

following sections outline how the source vents were identified for individual, indistinctive, fine-grained and often very thin deposits, using the geochemical fingerprinting of volcanic glass.

4.2.1. Volcanic Glass

Within the Tongariro Volcanic Centre, tephras are both locally and distally derived and include the distal rhyolitic tephras from centres such as TVC and OVC. The following sections present volcanic glass characteristics from the diverse volcanic fields.

4.2.1.1. Geochemistry of Ruapehu vs. Tongariro tephras

The active vents of Mts. Ruapehu and Tongariro/Ngauruhoe are located only 15 km apart. Hobden *et al*. (1999) and Price *et al.* (2005) suggested that despite this small distance, magma influx is disparate, and suggested small volume (<0.1km^3) and short-lived ($\leq$ 1 ka) magma batches apparently derived from non-communicating crustal magma storage zones beneath both Mts. Tongariro and Ruapehu. This petrological fact leads to the high probability of there being a distinct chemical variation between the effusive and explosive eruptive products of Mt. Ruapehu and Mt. Tongariro, as well as of individual eruptive vents within the Tongariro massif, such as Mt. Ngauruhoe and Red Crater.

To classify the source of unknown tephras in the eruptive sequence, 10 glass shards were analysed for each sample with the Electron Microprobe. Analyses of glass from the two main locations (12 and 63) in this study show, two or three, distinctive non-overlapping compositional fields on plots of K_2O vs. FeO (Fig. 4.1).

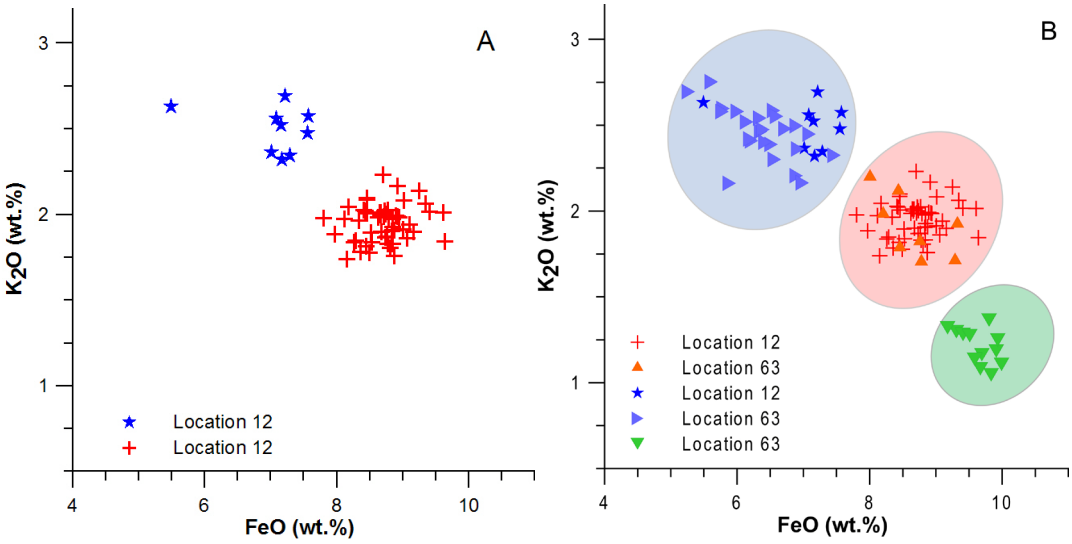

Figure 4.1: Average volcanic glass chemistry of major elements from A) 62 individual tephras of the Mangatawai Formation at Location 12 (Desert Rd.) and B) 85 individual tephras from Loc. 63 (northern slope of Pukekaikiore) and Loc 12., representing tephras younger than 1717 cal. yrs. B.P. The ellipsoids represent the three different compositional fields. Each point represents the average of 10 separate glass-shard analyses for each analysed tephra layer.

To identify the source for each of the compositional fields in Figure 4.1.B, EMP-analyses of volcanic glasses from recent eruptions of known source were obtained. For this purpose reference volcanic glass shards were sourced from the 1995-96 and the 2007 eruptions of Mt Ruapehu, 1954 and 1975 eruptions of Ngauruhoe, and deposits from the inner crater wall of Red Crater. The three separate compositional fields from unknown sources in Figure 4.1., correspond clearly to those individual modern Ruapehu, Ngauruhoe and Red Crater sources using both sample-average data and all individual analyses (Fig. 4.2 and 4.3). This demonstrates a distinctive chemical signature, characterising each of the volcanoes of the TgVC, at least during the last *c.* 10 ka. Other oxide pairs show varying degrees of separation, but none as strong as the K_2O/FeO pairing (Fig. 4.4). Because the K_2O/FeO ratios are so distinctive, this two-element plot is sufficient for correlation, without the need to use more complex discriminant function analyses (Stokes *et al.*, 1992; Cronin *et al.*, 1997d). In general, Ruapehu tephras are higher in K_2O (1.4 – 4%) and lower in FeO (3.7 – 8.3 wt %) than those derived from all Tongariro vents. Ngauruhoe tephra glass has intermediate K_2O and FeO concentrations between those of Red Crater and Ruapehu.

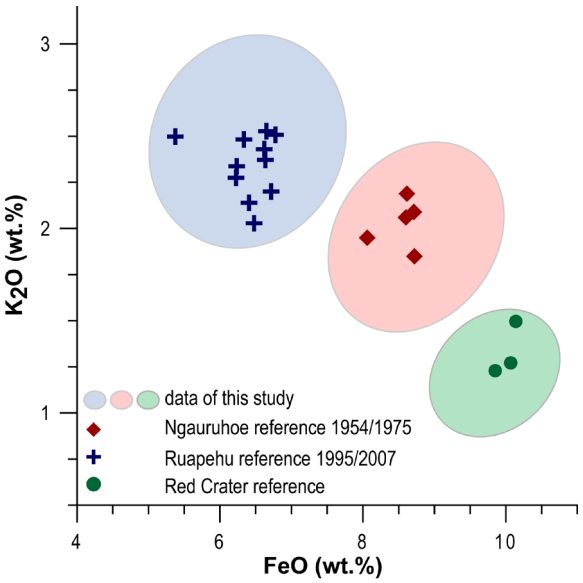

Figure 4.2: Average volcanic glass chemistry of the major elements K_2O and FeO from two main locations (ellipses as also shown in Figure 4.1.B) in comparison with reference volcanic glass chemistry of known recent eruptions such as Ruapehu 1995/96 (blue), Ngauruhoe 1954/1975 (red) and also volcanic glass from the crater facies pyroclastics of Red Crater (green).

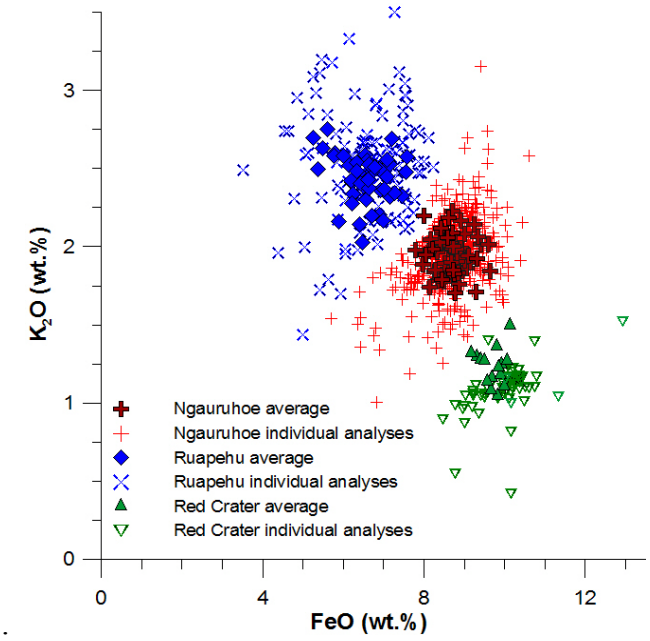

Figure 4.3: Volcanic glass chemistry of the major elements K_2O and FeO from two main locations (Loc. 12 and 63) and historic eruptions such as Ruapehu 1995/1996; Ruapehu 2007; Ngauruhoe 1975 and Red Crater (crater rim). The plot shows three discrete fields differentiating the three volcanic vents containing raw data (8-10 out of 10 analyses for each individual analysed tephra deposit) in comparison to average data.

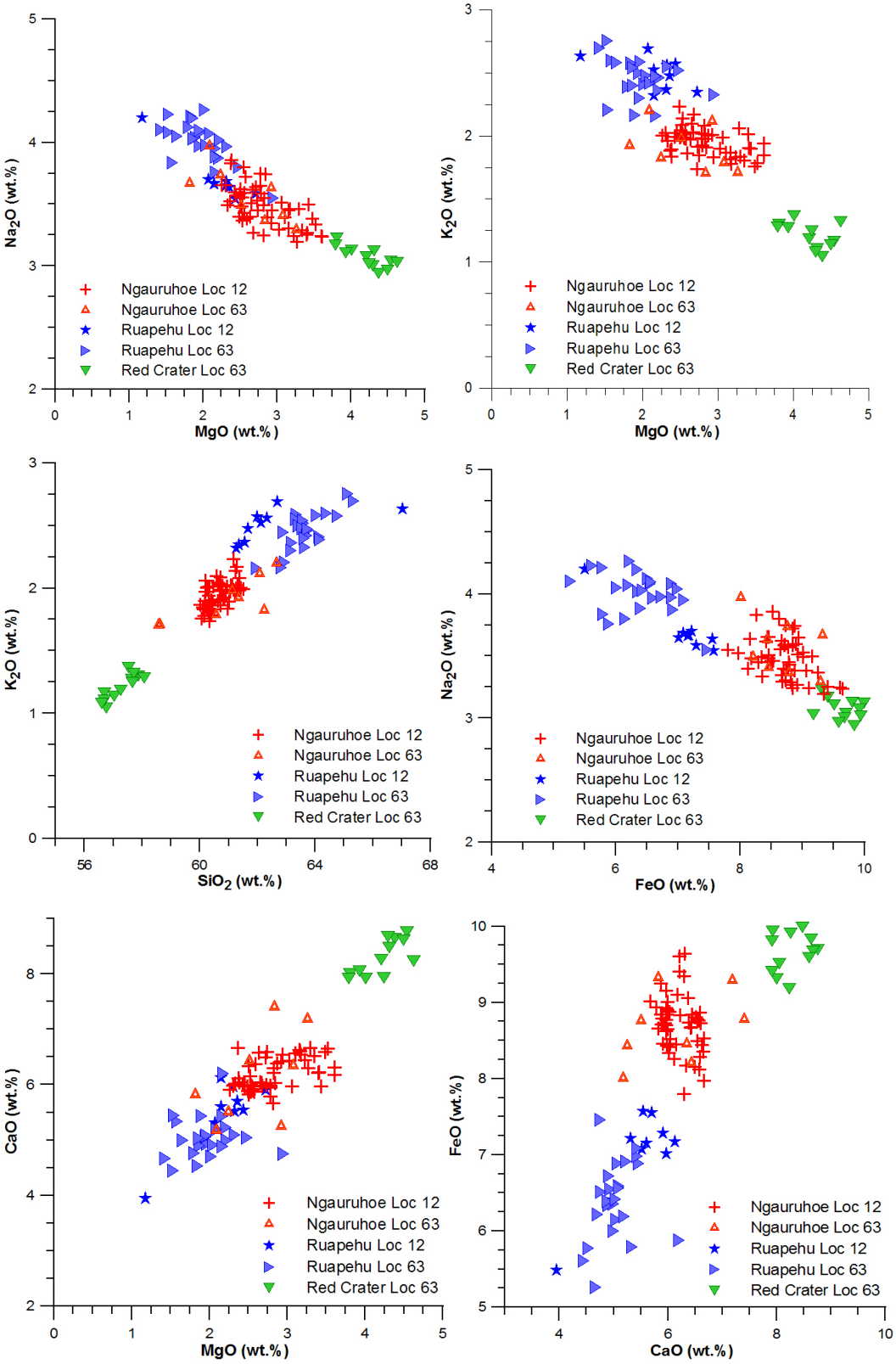

Figure 4.4: Average major element composition of volcanic glass comparing Ruapehu- vs. Ngauruhoe-derived tephras at Loc. 12, 63 and known recent eruptions from Ruapehu 1995/96 (blue), Ngauruhoe 1954/1975 (red) and also volcanic glass from the crater facies pyroclastics of Red Crater (green).

The trend of decreasing K_2O and increasing FeO corresponds to the geographic trend from Ruapehu northward through Ngauruhoe to Red Crater. A similar trend is also observed in the TAS diagram (Figure 4.5). The most northern vent analysed, Red Crater, has the most primitive glass compositions (55.5 – 58.5 wt% SiO_2). Ngauruhoe, just 2.7 km southwest, has dominantly andesitic glass (58.2 – 63 wt % SiO_2) and the most evolved magma is at Ruapehu 15 km farther southwest, where glass components range up to dacitic glass compositions (61.0 – 68.5 wt % SiO_2).

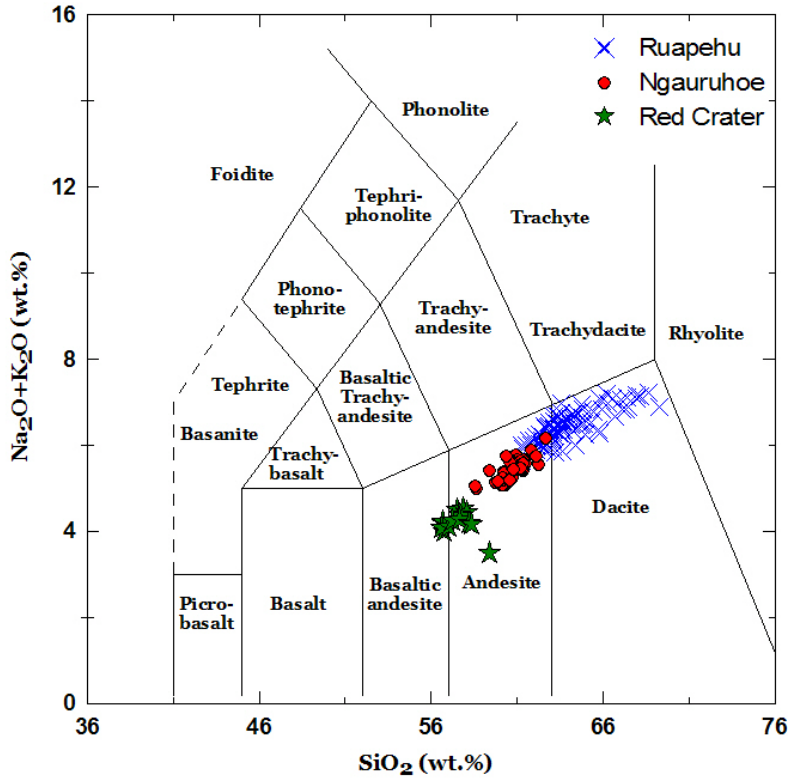

Figure 4.5: TAS discrimination diagram (after Le Maitre *et al.*, 1989) used to classify bulk-rock analysis show analysed volcanic glasses with ranges in composition from basaltic andesite to andesite for Red Crater, andesite for Ngauruhoe and andesite to dacite for Ruapehu.

For distinct macroscopic tephras, such as at Loc. 12, 66% had homogeneous glass populations indicating a single source. In some cases eight (9% of the tephras) or nine (25%) shards indicated one source, whereas the remaining shards indicated another origin within the TgVC. This could be due to:

- Some stacked individual thin tephra layers being sampled collectively
- Simultaneous or near-coincident eruptions from two volcanoes.

- Pedogenetic processes and disturbance of the tephra/soil profile by cryoturbation at the high altitude of this area as well as bioturbation due to soil and surface animals, along with plant root growth and decay.
- Ongoing wind dispersal of tephra-derived silt and sand from high-altitude non vegetated parts of the ring plain, including volcanic loess (Alloway *et al.*, 1988).

At proximal locations such as South Crater (65 and 75) and on Pukekaikiore, tephras from smaller (<VEI 1) eruptions could also be preserved. Here, the occurrence of "mixed" deposits, where volcanic glass from several TgVC sources was found, was more common. There are some "mixed" deposits containing shards from 2-3 sources, equally proportioned (21.5 % of the deposits), and there are 32% deposits with 1/10, 14% with 2/10 and 14% with 3/10 shards from a different source as at Loc.12. Only 17% of tephras were found to be homogeneous with shards indicating one single source. This is possibly because these sites are on higher slope angles with less-dense vegetation cover, leading to greater soil creep, colluvial action and higher rates of wind dispersal of reworked volcaniclastic particles.

The geochemical signature for the three volcanoes Ruapehu, Ngauruhoe and Red Crater as introduced above, is only clearly recognized for tephras deposited within the last *c.* 12 000 cal. yrs. B.P. The chemical composition of glass shards from older deposits such as from the Bullot (Ruapehu) and Mangamate (Tongariro) Formations show a wider variation and partly overlap (Figure 4.6).

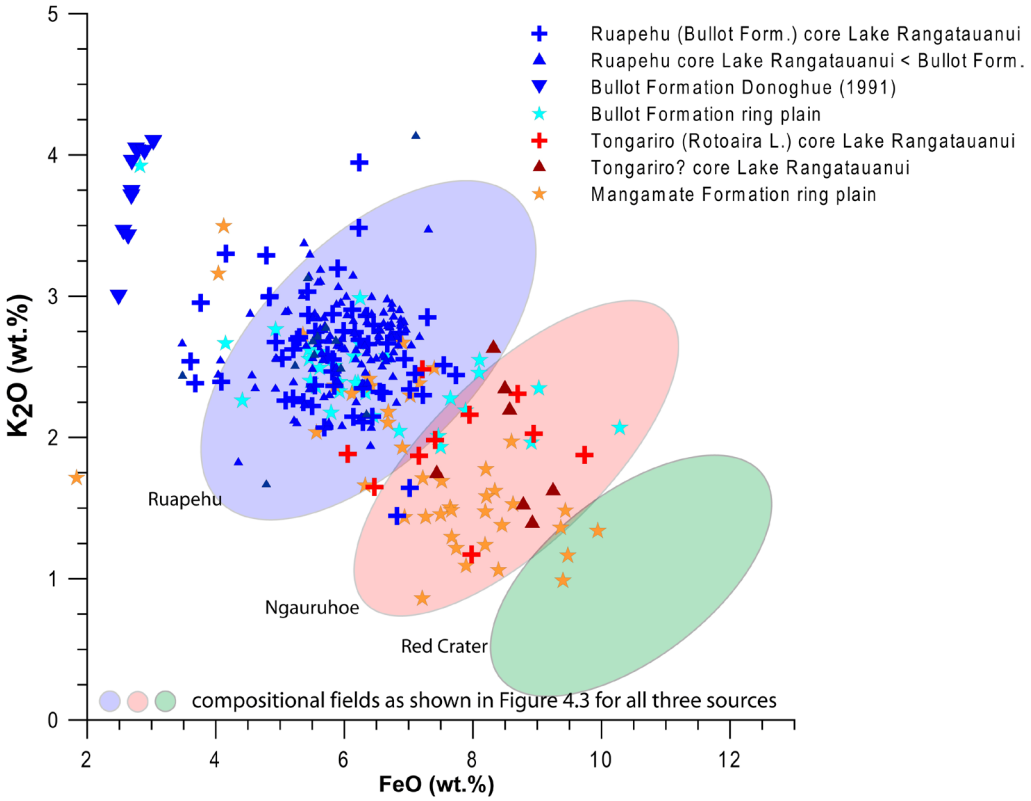

Figure 4.6: Volcanic glass chemistry of the major elements K_2O and FeO comparing Ruapehu and Tongariro sourced tephras younger than *c.* 12 000 cal. yrs. B.P. (ellipsoids) with tephras of the Bullot (Ruapehu (blue)) and Mangamate Formations (Tongariro (red)), which are older than 12 000 cal. yrs. B.P. The older deposits show a wider range and an overlapping in glass composition between both volcanoes.

4.2.1.2. Geochemistry of TgVC vs. Taranaki tephras

Mt. Taranaki is situated about 130 km east of Mt. Ruapehu and 135 km east of Mt. Ngauruhoe. The geological record suggests that the majority of Mt. Taranaki tephras were distributed north-east and east of the volcano (Grange and Taylor, 1933, Franks, 1984; Neall, 1972, Alloway *et al.*, 1995). Hence, it is highly likely that tephras from Mt. Taranaki were also deposited in the TgVC and could possibly be used as distinctive marker horizons.

In this study, however, a white to pale grey very fine-grained tephra layer was recognised at four to five locations on the western and central areas of the TgVC, including Pukekaikiore (Loc 63), Bruce Road (Loc 20) and Ohakune Mountain Road, Oturere lava flows (66), and South Crater (67). Geochemical analysis of the major

element composition of glass from this tephra indicates a distinctive Mt. Taranaki source (Fig. 4.7). The main characteristic for Taranaki-derived tephras is a high K_2O content in glasses (3.25 – 5.5 wt%; Turner, 2008) and lower FeO contents. These Taranaki tephra occurrences in the TgVC can all be considered a single depositional unit that can be directly correlated to the 1655 A.D. Burrell Lapilli (Druce, 1966; Platz, 2007; Turner, 2008).

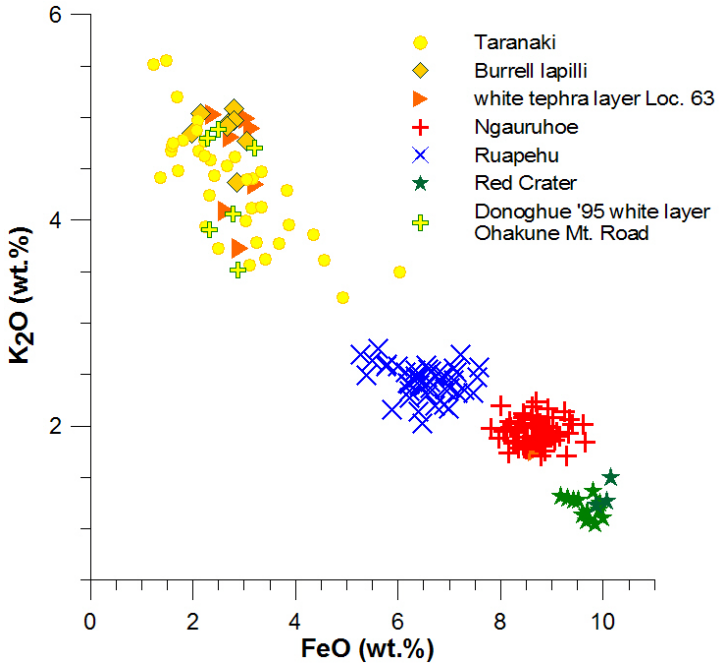

Figure 4.7: Volcanic glass chemistry of major elements from the three sources: Ruapehu, Ngauruhoe and Red Crater of the TgVC in comparison to Taranaki-sourced ash layers (Platz, 2007; Turner, 2008).

A tephra was identified at the Ohakune Mountain Road by Donoghue (1991) as the OVC (Mt. Tarawera)-sourced Kaharoa Tephra (Vucetich and Pullar, 1964). The chemical signature of this tephra also shows that its source is Mt. Taranaki, and due to its stratigraphic position and glass and tm chemistry, this unit was also correlated to the Burrell Lapilli (Figure 4.7).

4.2.1.3. Andesitic vs. rhyolitic tephra deposits

Within the area of the TgVC several rhyolitic tephra deposits are recognised and sourced to the Taupo and Okataina Volcanic Centres (Topping and Kohn, 1973,

Froggatt and Lowe, 1990, Donoghue *et al.*, 1995). In this study TVC-sourced rhyolitic tephras have been identified in several locations by their light-brown or white colours, stratigraphic positions and geochemical compositions. These beds were used as marker horizons for correlation purposes and time control. Volcanic ash derived from the OVC was not identified in the Holocene-soil/tephra sequences described here, but is contained within the cores taken from Lake Rangatauanui.

Chemical analyses of rhyolitic glass shards have been collected within many past studies (Froggatt, 1981a; Lowe, 1986, 1988; Froggatt and Rogers, 1990; Stokes *et al.*, 1992; Alloway *et al.*, 1994; Carter *et al.*, 1995; Eden and Froggatt, 1996; Shane, 2000; Shane and Hoverd, 2002; Smith *et al.*, 2005; Shane *et al.*, 2007 and Lowe *et al.*, 2008). These data, together with those collected in this work (Fig. 3.7), show that OVC-sourced tephras overlap part of the range of K_2O contents for Mt. Taranaki units, but have lower FeO contents (Fig. 4.8). TVC units, typically also have low FeO, but a narrow, intermediate range in K_2O between Taranaki and Ruapehu units.

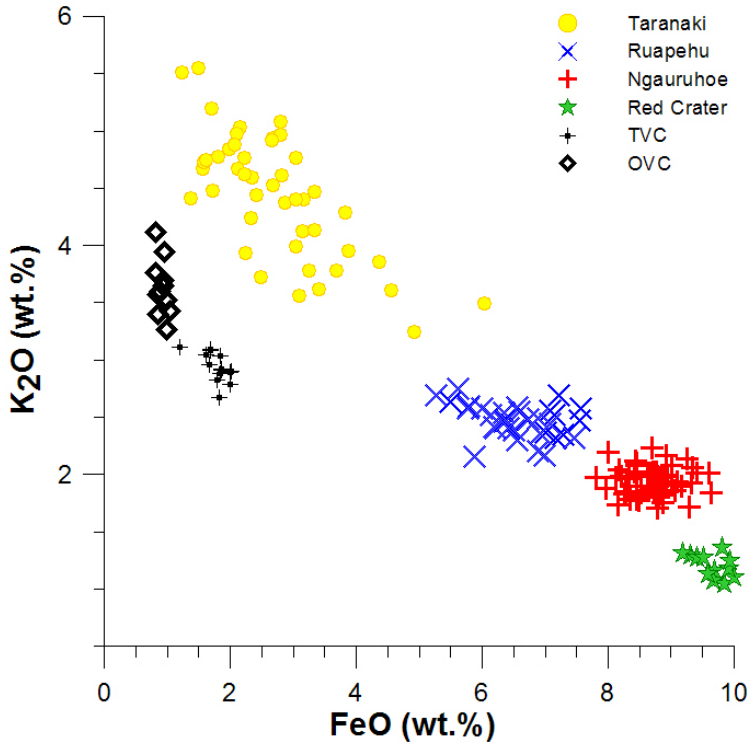

Figure 4.8: Volcanic glass chemistry of major elements from the four andesitic volcanoes Taranaki (yellow), Ruapehu (blue), Ngauruhoe (red) and Red Crater (green) in comparison to new and published data (see references in body text) from two rhyolitic centres TVC and OVC (black).

Several rhyolitic tephras derived from the TVC and OVC can be clearly identified from samples collected in the TgVC and Lake Rangatauanui (Fig. 4.9). The geochemical fingerprinting can be used to identify source, but the correlation of individual tephras to specific known events is possible only when stratigraphic position within the core or exposure is also taken into account. For example, tephras derived from the TVC can be distinguished from OVC and TgVC-sourced tephras by their lower FeO-content in volcanic glasses, but only due to its stratigraphic position e.g. Hinemaiaia Tephra can be distinguished from Stent Tephra or Taupo Pumice. The chemical composition of TVC-sourced and OVC-sourced tephras is too homogeneous to make distinctions between individual eruptions from the same source.

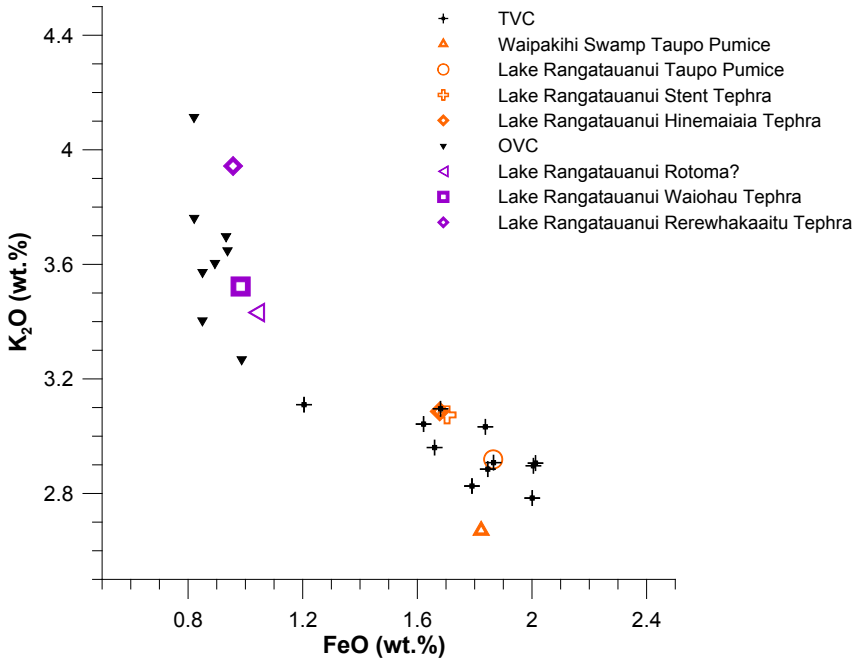

Figure 4.9: Unknown rhyolitic tephras sampled and analysed in this study (orange and purple symbols) plotted together with the known glass chemistry for rhyolitic tephras in the same stratigraphic interval from Taupo and Okataina Volcanic Centres (Froggatt, 1981a; Lowe, 1986; Lowe, 1988; Froggatt and Rogers, 1990; Stokes *et al.*, 1992; Alloway *et al.*, 1994; Carter *et al.*, 1995;Eden and Froggatt, 1996; Shane, 2000; Shane and Hoverd, 2002; Smith *et al.*, 2005; Shane *et al.*, 2007 and Lowe *et al.*, 2008).

4.2.2. Titanomagnetites

Several studies have used titanomagnetite (tm) for identification of source and individual tephras, as well as being used to determine oxygen fugacity and temperature estimates of the parental magma (Kohn, 1970; Gromme, 1982; Julian *et al.*, 1988; Cronin *et al.,* 1996d; Shane, 1998 and Suzuki, 2006). Cronin *et al.* (1996d) showed that individual Taranaki-sourced tephras can be discriminated by their tm chemistry. In addition, Turner *et al.* (2008b) and Turner *et al.* (2009) correlated individual Taranaki tephras between core sites, as well as identifying regular cyclic patterns in magma chemistry of this volcano using tm chemistry. These successes led to application of this method to the TgVC-sourced tephras. In this study, this method was used to identify the Taranaki-sourced Burrell lapilli, which tm-chemistry differs from older larger (0.6 km^3) Taranaki tephras such as Kaupokonui, Maunganui (Eg-1) and Maketatwa Tephras (Turner, 2008).

By contrast to the Taranaki tephras, the TgVC units contain only rare and mostly small (5 - 125 μm) titanomagnetite phenocrysts and micro-phenocrysts, mainly within Ruapehu-sourced tephras. More titanomagnetites are <100 μm-long and also occur as microlites within volcanic glass (Figure 4.10). These small crystals are extremely difficult to analyse on the EMPA, hence most major element compositions obtained from TgVC tephras at Loc. 12 and within the core from Lake Rangatauanui are highly variable. Tm's in rare units, mostly from Mt. Ruapehu could be successfully analysed, but not enough were in this category to allow tm to be used as a reliable phase for correlation of units within the TgVC. Of the successfully analysed units, tephras from Mt. Ruapehu could easily be distinguished from Mt. Taranaki tephras (Fig. 4.11). Titanomagnetites derived from Mt. Taranaki have lower TiO_2 and higher FeO (total) values. Rhyolitic tephra titanomagnetites from TVC and OVC overlapped each other, as well as the compositional range of Taranaki units and part of Ruapehu's range (Fig. 4.11).

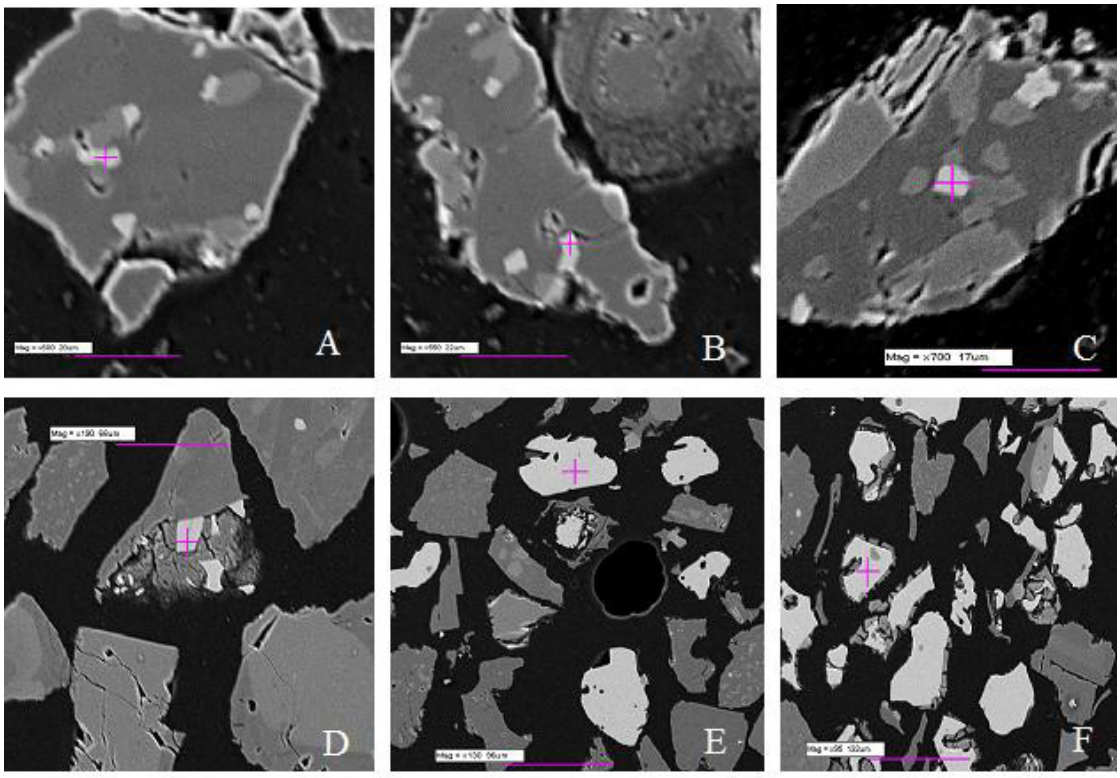

Figure 4.10: Back-scattered images of titanomagnetites in: A-C) Ngauruhoe-sourced glass shards (Loc. 12); D) Ruapehu-sourced glass shard (Lake Rangatauanui core); E) Taranaki-derived tephra (Lake Rangatauanui core); F) TVC-sourced rhyolitic tephra (Lake Rangatauanui core). The size of the titanomagnetites crystals range between 1-6 µm at Ruapehu and Ngauruhoe samples, between 50 and 100 µm for Taranaki samples and between 80 and 120 µm for TVC-sourced tephras.

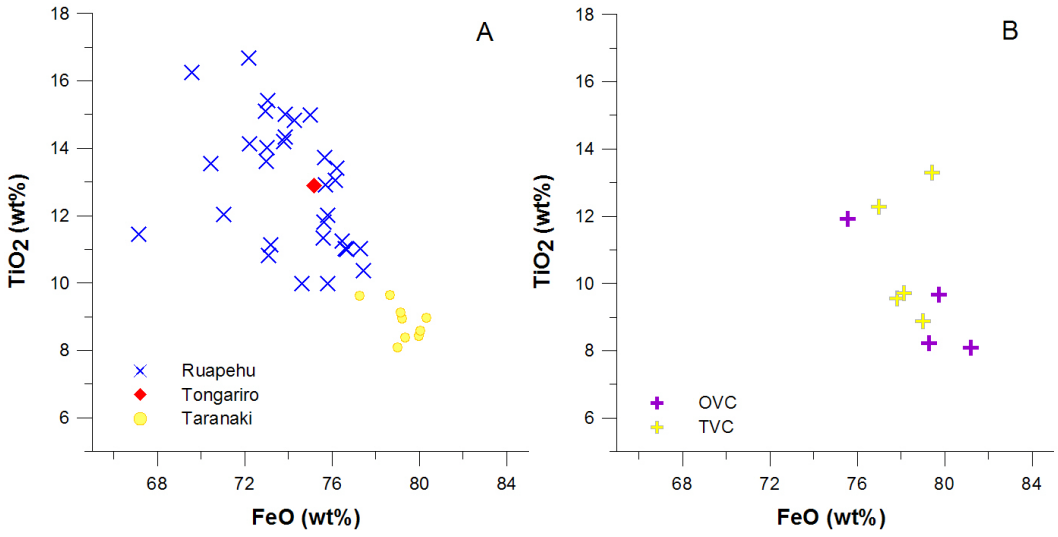

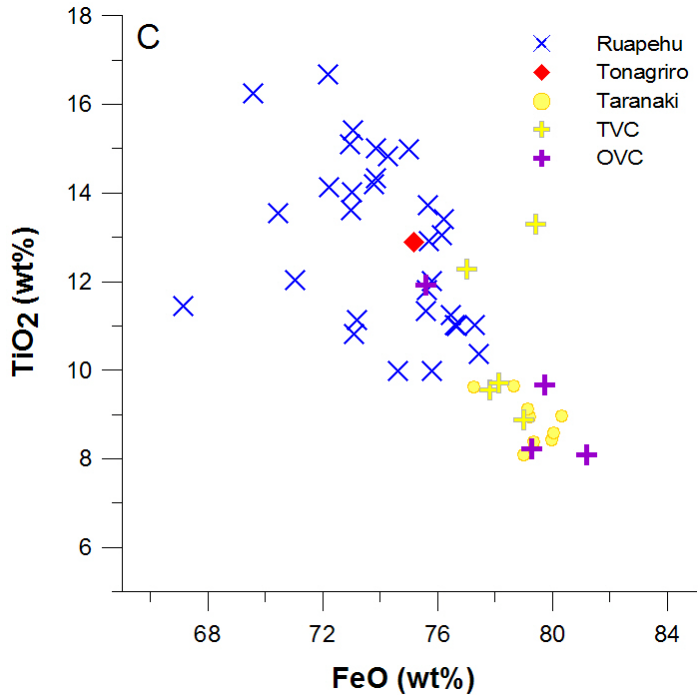

Figure 4.11: Major element composition of titanomagnetites of a core taken at Lake Rangatauanui, comparing (A) Ruapehu- and Taranaki-sourced tephras; (B) OVC vs. TVC derived tephras; and (C) andesitic vs. rhyolitic tephras.

Of the rare cases, when reliable, individual tm compositions could be collected from Ngauruhoe tephras, these revealed little differentiation from Ruapehu compositions (Fig. 4.12).

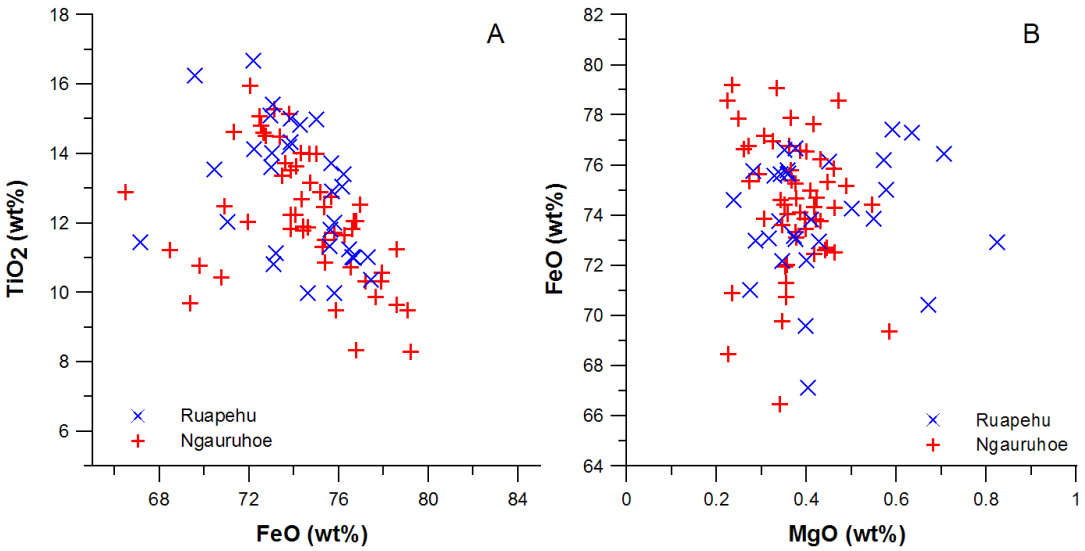

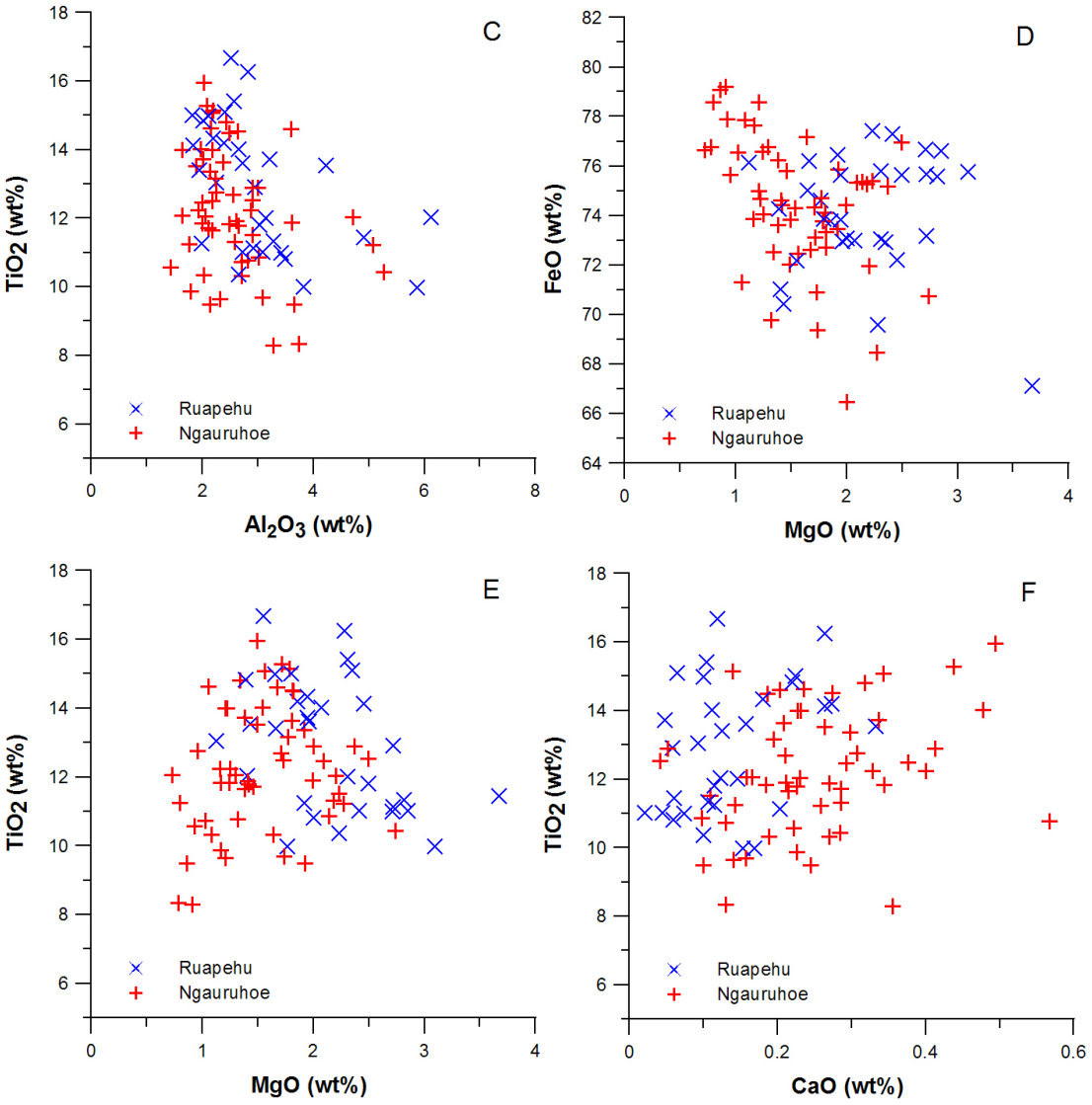

Figure 4.12: Major element composition of titanomagnetites from EMP analyses of this study, comparing Ruapehu vs. Ngauruhoe-derived tephras.

4.3. Conclusions resulting from fingerprinting

Identification of distinctive glass chemistry within tephras for each of the volcanoes of the TgVC, along with detailed stratigraphic description and sampling, allows for the first time a robust discrimination of thin tephras from closed-spaced, simultaneously erupting vents, and provided the main criteria to envisage the eruption frequency for each of the individual volcanoes (Chapter 8).

Noting the distinctive glass chemistry of tephras from Ngauruhoe, the oldest identifiable, macroscopic tephra that can be associated with the volcano, is found at ~4700 cal. yrs. B.P. within the Papakai Formation. This defines a new minimum age of the volcano that extends its previously estimated age (Topping, 1973) (Chapter 5).

Two locations from this study (Loc. 12 and 63) encapsulate the most complete tephra record of Mt. Ruapehu for the last ~12 000 cal. yrs. B.P. and the entire history of Mt. Ngauruhoe (Fig. 4.13). Along with tephras from the TgVC, units from three other volcanic centres have been chemically identified and stratigraphically placed: Mt. Taranaki, TVC and OVC (the latter only in the core from Lake Rangatauanui). Of the interbedded rhyolitic tephras already identified in past studies (Topping, 1973, Vucetich and Pullar, 1964; Donoghue, 1991), the only different correlations made here has been that the earlier identified Waimihia Tephra, is far more likely to be Unit Q of Wilson (1993), or the Stent Tephra of Alloway *et al.* (1994) and Donoghue's (1991) Kaharoa Tephra was interpreted to be the 1655 Taranaki-sourced Burrell lapilli.

Location 12 is 11 km south-east of Ngauruhoe and 16 km east north-east of Ruapehu and is a distal deposition site for tephras from primarily >VEI 2 sized eruptions of Ruapehu and Ngauruhoe. Tephras from eruptions of <VEI 2 appear to have been incorporated into the accumulating soils of the area, and produce no discrete, macroscopic units.

Using these correlation methods, it can be seen that the distribution of Holocene tephras from Ruapehu and Ngauruhoe differs markedly around the ring plain. Location 6 is situated north of Ruapehu and it appears that a greater number of Ruapehu tephras are interbedded throughout the Ngauruhoe-dominated sequence than at Loc. 12 (Fig. 4.14).

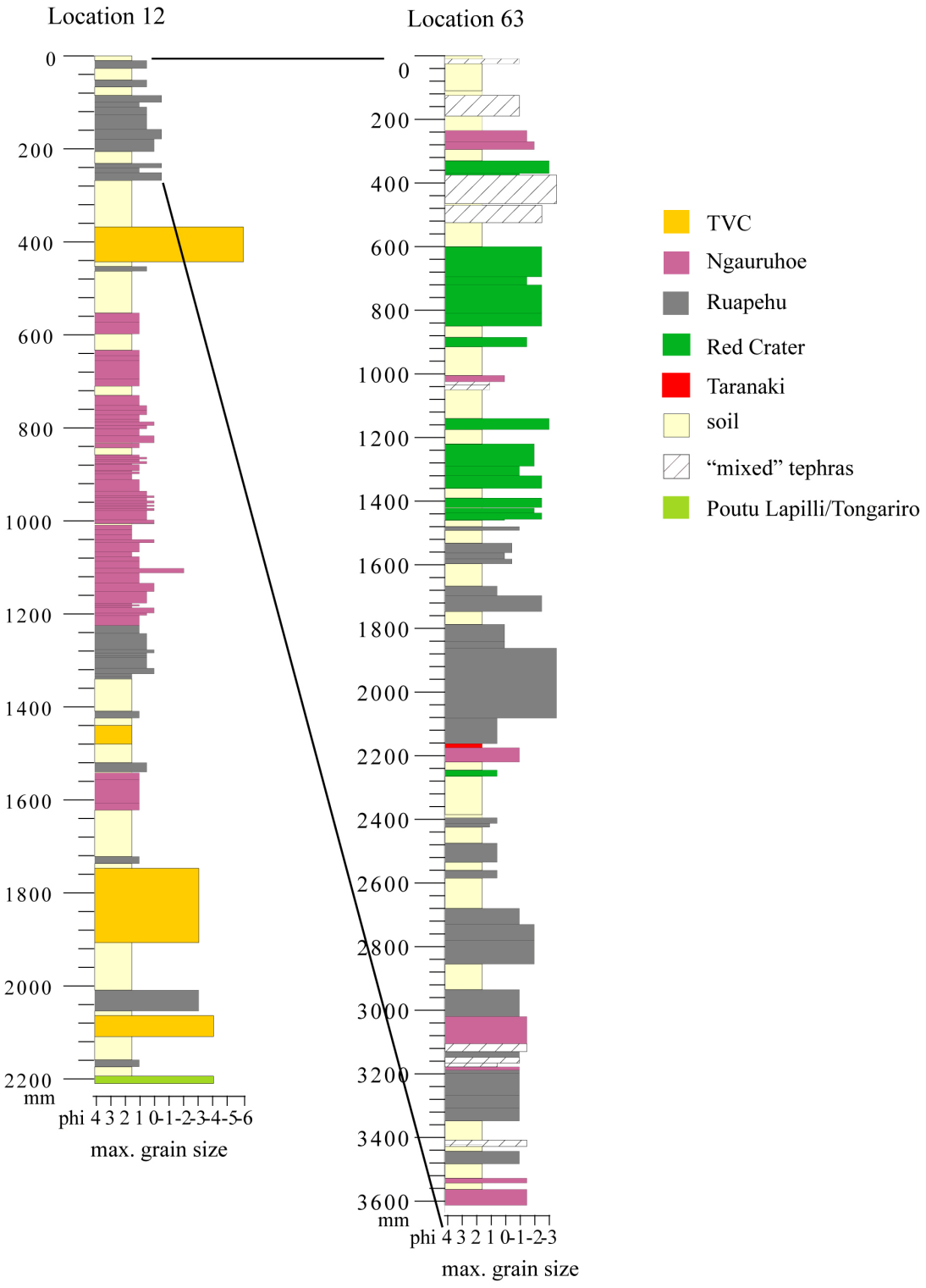

Figure 4.13: Stratigraphic profiles with tephras correlated to source from key reference sections: left, Loc. 12, Desert Road, south of Waihohonu Stream; Right, Loc. 63, northern slope of Pukekaikiore.

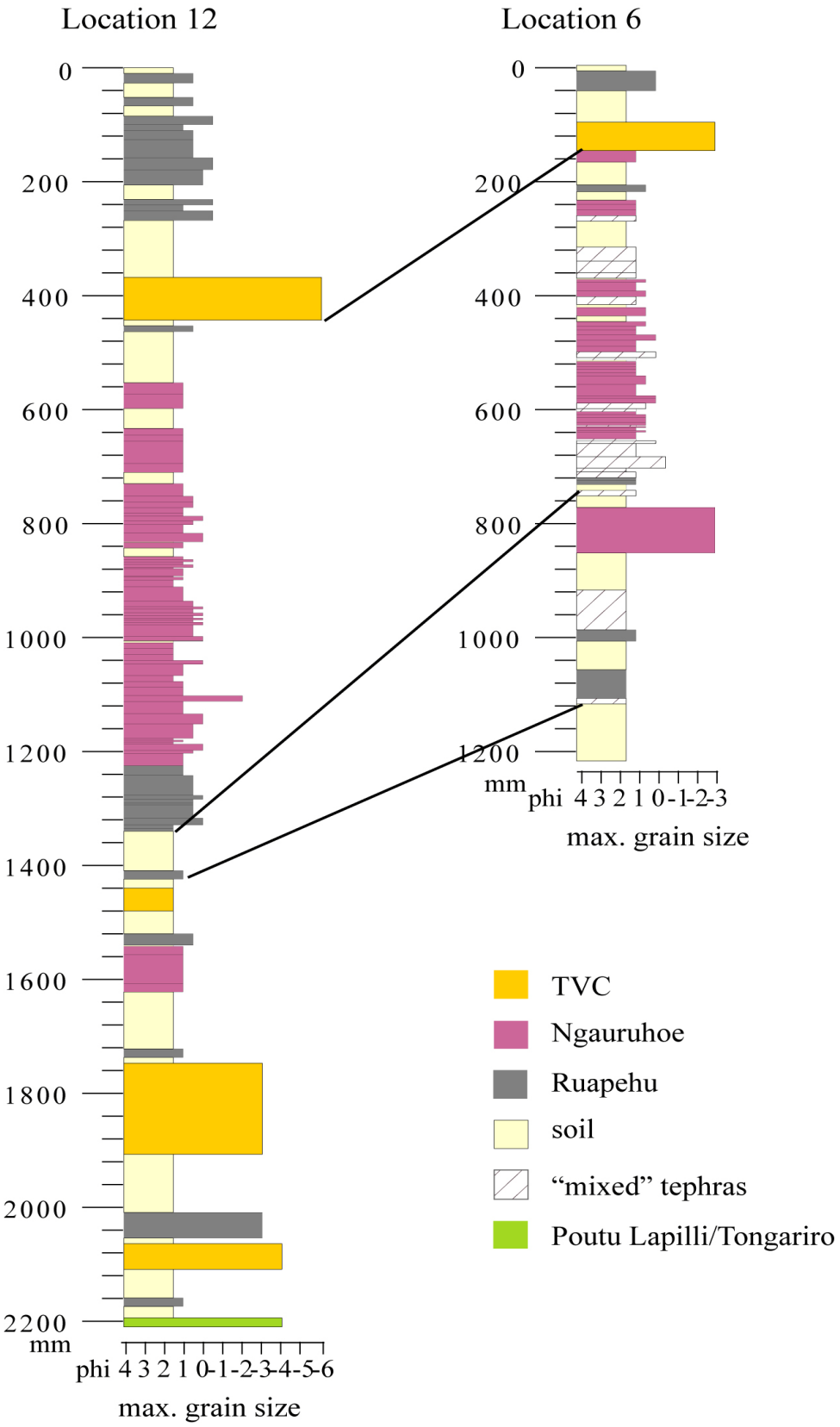

Figure 4.14: Right: Stratigraphic profile of Location 6, car park Mangatepopo Valley. Left: Stratigraphic profile of Location 12, Desert Road, south of Waihohonu Stream. Both columns show the source for each tephra layer based on glass chemistry. The locations are 15.5 km apart.

Chapter 5

Late Holocene tephras of Mt. Tongariro

This chapter contains a new interpretation of the recent eruption history of Tongariro based on revised and more detailed stratigraphy and geochemistry of the youngest active vents of the Tongariro volcanic complex, specifically Ngauruhoe, Red Crater and the upper Te Maari Crater. The focus is on Ngauruhoe, by far the longest lived and most active vent, which also has the most complete tephra record.

Mt. Tongariro (1967 m) is a 13 km long and 5 km wide volcanic complex with a present volume of 75 km^3. It is an unusually shaped stratovolcano in that it consists of at least 17 overlapping vents (Hobden, 1997; Hobden *et al.*, 1999). Discrete vents include: Te Maari Craters, North Crater, Central Crater, South Crater, Blue Lake, Emerald Lakes, Lower Tama Lake, 'proto'-Ngauruhoe, Pukekaikiore and Pukeonake (Figures 5.1a and 5.1b). At least three further unnamed, horseshoe-shaped cones are situated to the east of Te Maari Craters and Red Crater, between Oturere and Mangahouhounui Valleys (Mathews, 1967). Historic eruptions are known from Ngauruhoe, Red Crater and the upper Te Maari Craters. In addition, the geothermal area of Ketetahi, on the northern flanks of Tongariro, west of Te Maari Craters, has been the locus of periodic hydrothermal eruptions. The growth of this complex structure began with six episodes of volcanic activity, resulting in extensive lava flows; the oldest is exposed around the Tama Lakes and is dated at 273 ka (Hobden *et al.*, 1996). Since the onset of activity several episodes of volcanism have occurred, with the best known from the last *c.* 20 000 years of tephrochronological records (Topping, 1974; Donoghue *et al.,* 1995). Major explosive eruptions recognised from this period include the Rotoaira Lapilli (Shane *et al.*, 2008), and the Mangamate Tephra Formation of c. 12 079 ± 76 cal. yrs. B.P. that involved at least six major eruptions of VEI 4 and above (Nairn *et al.*, 1998). Since that time the explosive activity of Mt. Tongariro has been characterized by smaller eruptions (several orders of magnitude lower), although several lava flow eruptions have also occurred over this time, including the major Oturere lava flow (Stevens, 2002). In late Holocene times, the source of eruptions has dominantly been

attributed to Ngauruhoe (Topping, 1973). Mt. Tongariro's Holocene tephras are collectively mapped within the Papakai, Mangatawai and Ngauruhoe Formations (Donoghue *et al.*, 1995).

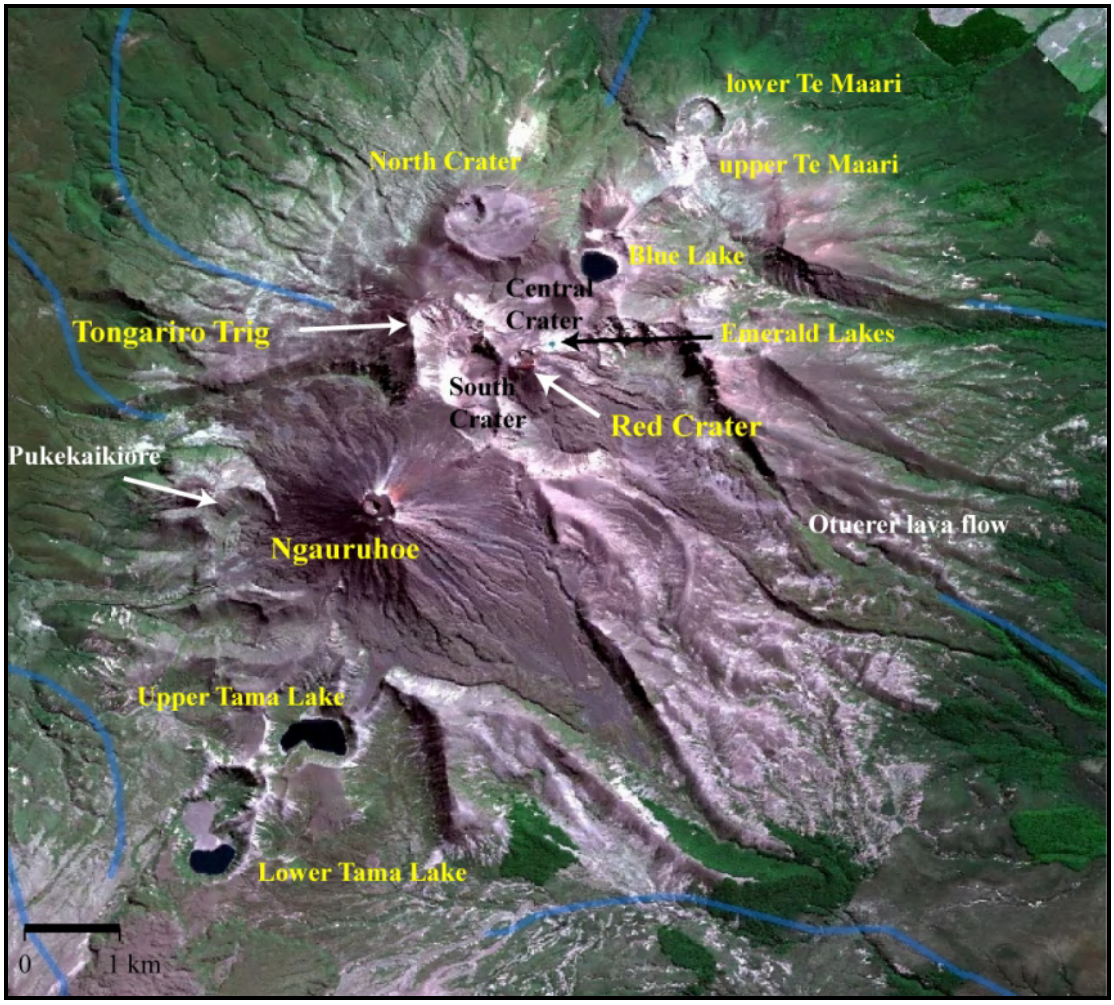

Figure 5.1a: Satellite image of the Tongariro Volcanic Complex.

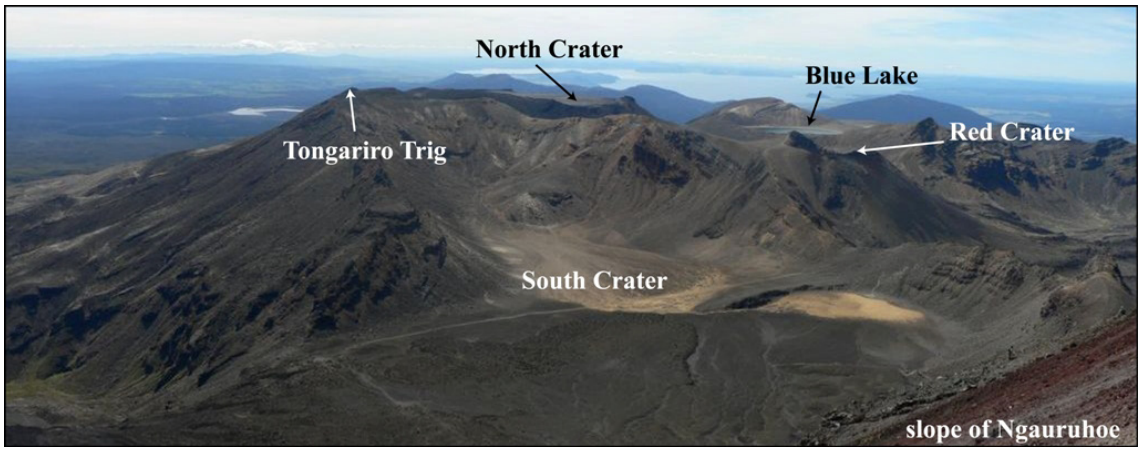

Figure 5.1b: Northern part of Tongariro volcanic complex, viewed from Ngauruhoe towards the north-east.

5.1. Mt. Ngauruhoe

5.1.1. Introduction

Mt. Ngauruhoe (2287 m) is the most active vent system of the Tongariro volcanic complex and was considered to have grown during the last 2500 years through repeated small strombolian, vulcanian and sub-plinian eruptions of andesitic and basaltic-andesitic magma (Hobden *et al.*, 2002) (Figure 5.1.1). The 900 m high and >30˚ sloping cone of Ngauruhoe has a volume of ~2.2 km^3 and consists of basaltic andesitic to andesitic lavas and pyroclastic deposits. It is constructed over older cones, including part of upper Tama Lake and Pukekaikiore (Hobden, 1997). The south-eastern flank appears to be inherited from an older feature, referred to as 'proto'-Ngauruhoe (Nairn *et al.*, 1998; Nakagawa *et al.*, 1998), which has been described as a *somma* ring (Cotton, 1944 *in:* Topping, 1974). According to Nairn *et al.* (1998), some of the large sub-plinian eruptions of the Mangamate Formation were sourced from 'proto'-Ngauruhoe, providing a minimum age of the burial or destruction of this structure at *c*. 12 000 years ago.

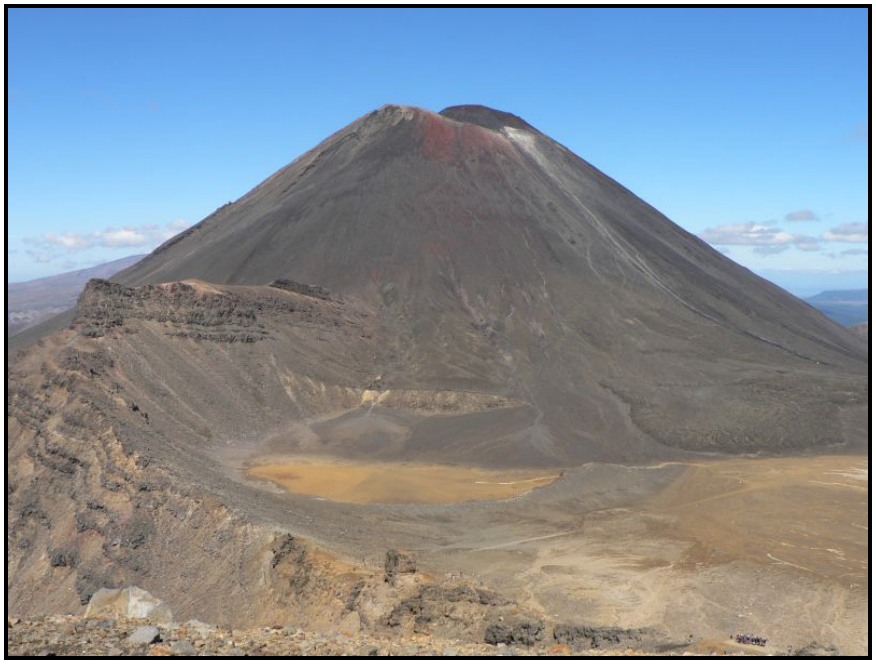

Figure: 5.1.1: Ngauruhoe, view across South Crater towards the south-west.

The proximal stratigraphy of Ngauruhoe is mostly based on lava and pyroclastic-flow deposits, with distal pyroclastic products being mapped as the Mangatawai Formation. The base of the Mangatawai Formation has until recent been dated at 2568 ± 508 cal. yrs. B.P. (Fergusson and Rafter, 1959), leading Hobden *et al.* (2002) to define this as the maximum age of the edifice. Pyroclastic deposits above the distinctive Taupo Tephra (1717 ± 13 cal. yrs. B.P.; Lowe *et al.,* 2008) are collectively mapped as the Ngauruhoe Formation. Lava flows originating from Mt. Ngauruhoe were divided into 5 groups depending on field relationships, chronology and chemical distinction. These are dominantly basaltic andesites (64%) with the remainder being andesite, with SiO_2 contents of 54.2 to 58.6 wt% (Hobden, 1997). Ngauruhoe's older lava flows tend to occur at low elevations and have travelled greater distances (5-6 km) from their source than younger flows.

5.1.2. Previous work

The early studies on Mt. Ngauruhoe and its surrounds were carried out by Grange (1931), and Gregg (1960a; 1960b). Gregg (1960a) produced the first isopach maps of Mangatawai Ash and Ngauruhoe Ash and compiled a comprehensive eruptive history of the last 150 years at Ruapehu and Tongariro volcanoes, including the youngest and most prominent cone of the Tongariro complex, Ngauruhoe (Gregg, 1960b). Later, Topping (1973) identified distal rhyolitic tephra beds erupted from Okataina, Rotorua and Taupo in the Tongariro area and from these chronohorizons developed an andesitic tephrostratigraphy for the Tongariro National Park. He defined and described major tephra formations by their appearance, source, best locations, age and distribution. Topping defined new tephra formations, and redefined existing formations that grouped products of small-scale eruptions, such as the Mangatawai Tephra and Ngauruhoe Tephra. Cole (1978) and Cole *et al.* (1986) described the petrology, mineralogy, chemistry and petrogenesis of the lavas from all volcanoes of the TgVC.

The 1974-1975 Ngauruhoe eruptions and their products were described in detail by Self (1975), Nairn (1976) and Nairn and Self (1978). The larger pyroclastic events of the Mangamate Formation were also studied in detail by Nairn *et al.* (1998), who identified their possible source vents, eruption mechanisms and relationship to tectonic behavior.

Nakagawa *et al.* (1998) described the petrological characteristics of this major eruptive sequence, interpreting the high phenocryst content of the products as an indication of shallow magma chambers (<4 km in depth) that experienced mixing with magma from deeper parts of the system. They concluded that the distinctive chemical composition of magmas from different vents of the TgVC suggested the presence of individual magma bodies with diverse storage systems, at different depths and with individual transport systems.

Donoghue (1991), and Cronin (1996), mapped and developed a detailed Late Quaternary stratigraphy of the pyroclastic deposits from Ruapehu and Tongariro. Extensive studies and K-Ar dating on Tongariro volcanic complex and specific magmatic studies on Ngauruhoe were carried out by Hobden (1997) and Hobden *et al.* (1996; 1999; 2002). Hobden *et al.* (1999) developed a model of small and short-lived magma batches to explain the variation in compositions of Ngauruhoe magmas erupted over very short intervals. Additionally, Hobden *et al.* (2002) considered that most of Ngauruhoe's cone was built over the first 700 years of its life; its average eruption rate was considered to be 0.9 km^3 ka^{-1}.

Ngauruhoe became an international type locality for distinctive low-volume scoria and ash flows produced by collapsing scoria piles and vulcanian eruption plumes following the 1974-75 eruption and the resultant deposit descriptions of Nairn and Self (1978). These units were later reanalysed by Lube *et al.* (2007), to provide detailed physical parameters of the pyroclastic density currents that emplaced them. Martelli (2007) evaluated the Titan2D model for predicting the path and distribution of future scoria and ash flows from Ngauruhoe and analysed the hazards associated with these flows. Krippner (2009) described the morphology of Ngauruhoe's inner crater and concluded that it was created by the 1954-1955 eruption series and was subsequently modified by the 1974-75 eruptions involving a range of eruption styles that included strombolian, vulcanian and hawaiian types. Krippner (2009) recalculated the average growth rate of Ngauruhoe as c. 0.6 km^3 per 1000 years using a new radiocarbon age at 3470 cal. yrs. B.P. (Moebis *et al.*, 2008) and a cone volume of 2.2 km^3 (Hobden *et al.,* 2002).

5.1.3. Historic Eruptions

Ngauruhoe is still frequently cited as one of the world's most active volcanoes, despite it having not erupted since 1977. This reputation stems from direct observations of almost continuous steam emissions and frequent vulcanian, strombolian and sub-plinian eruptions that occurred over the previous 130 years (Figure 5.1.2). According to Bebbington and Lai (1996) and Krippner (2009), at least 73 eruptive episodes have occurred since 1839. Gregg (1960b) described the characteristics of 60 historic eruptions (including fumarolic activity) from February 1839 to June 1959. Changes in the configuration of the Ngauruhoe summit area during the last 150 years were summarized in sketches by Gregg (1960b). The historic eruption record of the TgVC becomes less reliable in the 19th Century, because the region was isolated with few European visitors.

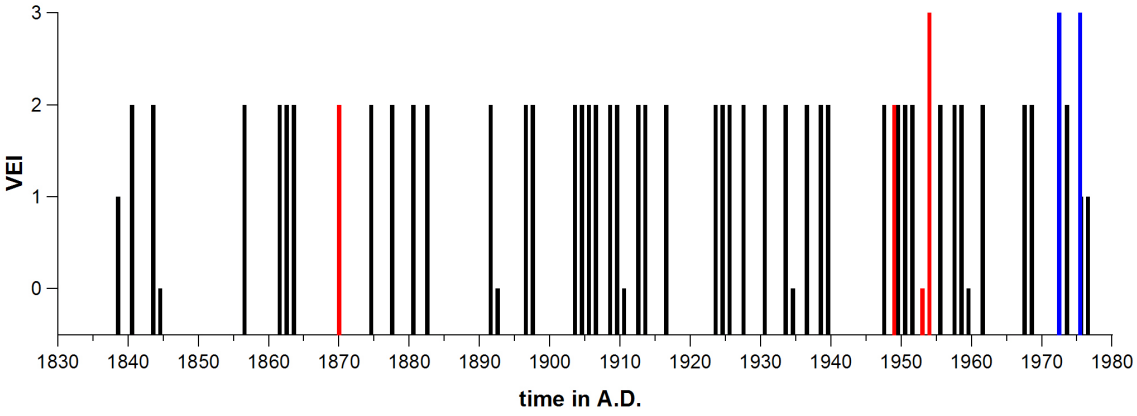

Figure 5.1.2: Known historic eruption record and their VEI of Ngauruhoe since 1839. Columns represent observed ash eruptions (black), lava flows (red) and pyroclastic flows (blue), summarised after Gregg (1960b) and Hobden *et al*. (2002).

The earliest Ngauruhoe eruption was described by Bildwill (1841), who witnessed an eruption on 3 March 1839 that produced strong rumbling and a "thick column of black smoke" rising above the volcano and spreading out like a mushroom. Between 1841 and 1865 several small phreatic and possibly magmatic ash eruptions occurred at irregular intervals of 1-10 years. Major eruptions of Ngauruhoe occurred in 1870 and possibly also a year earlier. Several sources, summarised in Gregg (1960b), describe a lava flow on 7 July 1870, followed by rising steam from the crater rim and the lower slopes. According to Hector (1887), the 1870 Ngauruhoe eruption "was more important than

the Tarawera eruption of 1886" with 'great lava and steam eruptions' continuing 'for a considerable time'. From 1875 to 1940 numerous small eruptions occurred (Figure 5.1.3) with intervals of up to a maximum of seven years.

Figure 5.1.3: Ngauruhoe eruption in 1928 observed from the western side. Image: with permission from the Alexander Turnbull Library ref.: 1/2-057225-F, photographer: unknown.

The small strombolian eruption of 30 April 1948 was typical for Ngauruhoe, ejecting blocks and bombs the size of small houses, and also producing a lava flow on the north-western rim from a breached lava lake (Allen, 1948) (Figure 5.1.4). From May of the same year small ash eruptions continued until February 1949, when a three-week, vent-clearing, vulcanian eruption occurred (Allen, 1949; Cloud, 1951). On 9 February 1949, small pyroclastic flows travelled down the north-western slopes into the Mangatepopo Valley. On 10 February the Crater was filled with lava, which overflowed to the north-west, and ash eruptions took place until 21 February, before activity ceased on 3 March (Figure 5.1.5). Allen (1949) and Cloud (1951) reported steaming fumaroles on the February pyroclastic-flow deposits until May 1949.

Figure 5.1.4: Ngauruhoe eruption of 1948 viewed from the west, showing ash clouds moving to the north. (Photo courtesy of John A. Krippner, private collection).

Figure 5.1.5: Ngauruhoe in eruption in 1949 observed from the Desert Road, south-east of the volcano (image: with permission from the Alexander Turnbull Library, ref.: 35mm-00709-D-F, photographer: Bruce Valentine Davis).

The eruption series from 1954-55 (Figures 5.1.6 and 5.1.7) was described by Gregg (1956) and Krippner (2009). It started with an explosion on 13 May 1954, followed by

large steam and strombolian ash eruptions accompanied by lava flows. The first lava flow was observed on 4 June, with additional lava flows in July, August and September. During this time lava fountains constructed a new cone within the old crater and reached a maximum height of 300 m above the crater on 30 June. Ash emissions, lava production and intermittent lava fountains continued until the end of September. On 16 September 1954 pyroclastic flows were also observed on the western slopes of the volcano. By the end of September the ash clouds rising above Ngauruhoe were large enough to deposit ash 65 km north-eastward in Taupo. The activity decreased until December 1954, when explosive eruptions of vulcanian style began that continued until February 1955. By the end of January, severe short explosions along with ash emission occurred and there was some of fire fountaining. The last eruption of this sequence was documented on 10 March 1955. During the 1954-1955 episode at least 11 lava flows were emplaced on the NW-flank with a volume of 3 million m^3 (Sanders, unpublished data *in* Krippner, 2009).

Figure 5.1.6: Ngauruhoe eruption in 1954 viewed from the west, with the eruption cloud moving towards the north-east (Photo courtesy of John A. Krippner, private collection).

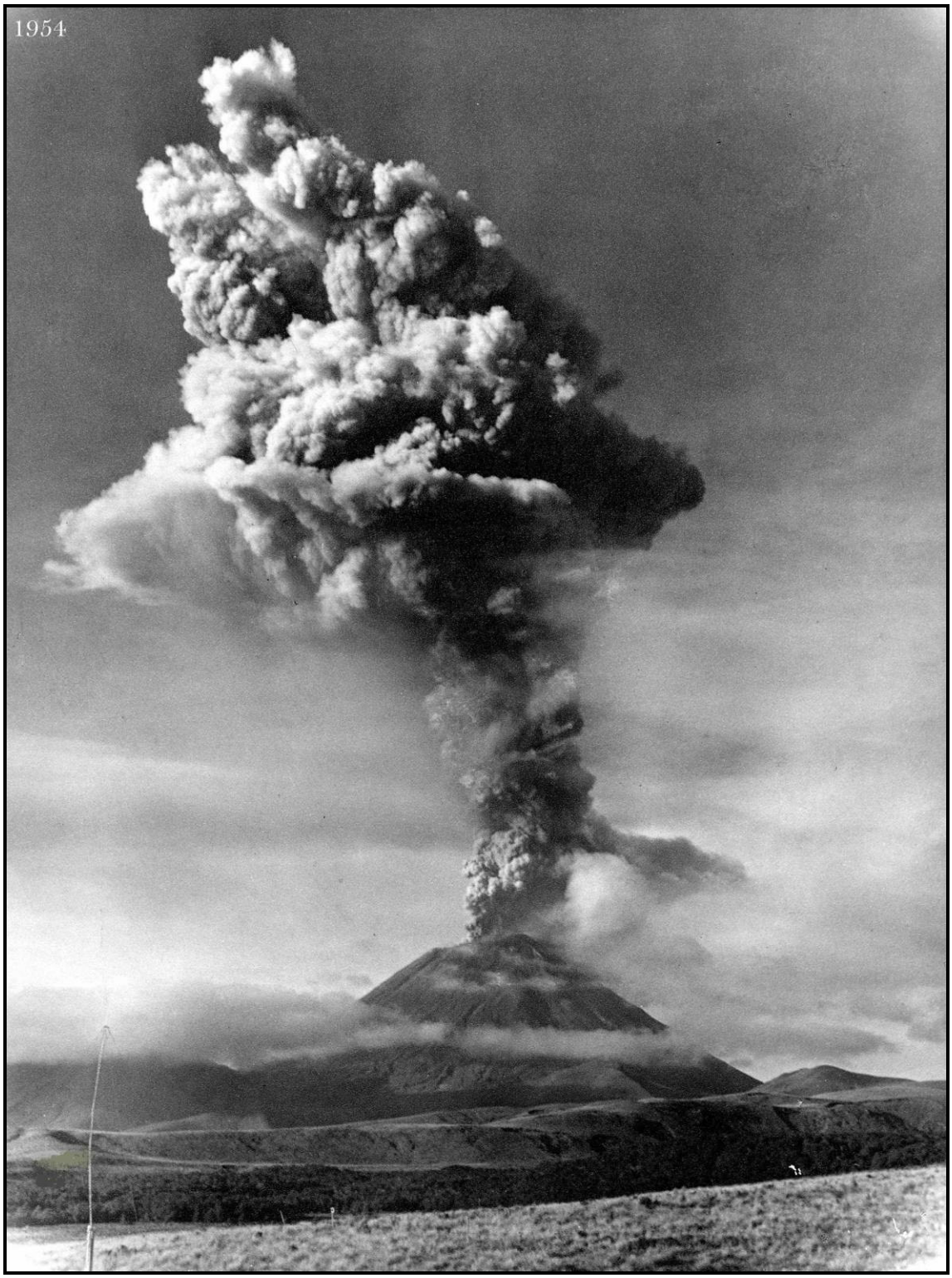

Figure 5.1.7: One of the major vulcanian eruptions from Ngauruhoe in 1954 as viewed from the west to south-west (Whakapapa area). The eruption column reached an estimated height of ~4.5 km (Photo courtesy of John A. Krippner, private collection).

The most recent eruption series of Ngauruhoe took place between January 1974 and February 1975, and was observed and described by Nairn (1976); Self (1975); Nairn and Self (1978) and summarised in Lube *et al.* (2007) and Krippner (2009). The first activity of the 1974-75 eruptions occurred on 22 January 1974 and formed an ash cloud 600 m above the crater with intermittent cyclic plumes occurring over the next few days. The eruptive phases produced bombs and ejecta that rolled down the slopes to the accompaniment of small earthquakes. On 26 January a convoluting ash column rose 1500 m above the crater and partly collapsed to generate pyroclastic flows (Nairn, 1976). Later in March, an eruption column rose 1700 m above the crater, producing a dense ash fall over Mt. Tongariro (Self, 1975). During this event a shockwave reached the Chateau on the north-western slopes of Ruapehu; large bombs were ejected and the north-western sector of the inner crater wall collapsed (Nairn, 1976). The largest eruption occurred on 28-29 March 1974 with a plume rising 2500 m above the crater before drifting towards the north-west (Self, 1975; Nairn *et al.*, 1976). The 1975 eruption sequence started on 12 February with ash eruptions that rose in intensity until 19 February. Major changes occurred within the crater area during this time (Nairn and Self, 1978). Along with the explosive vulcanian eruptions, several earthquakes were recorded. On 19 February the eruption cloud rose up to 6000 m above the crater and pyroclastic avalanches were generated from its collapsing margins onto the northern slopes of the volcano (Figures 5.1.8 and 5.1.9). The ash cloud travelled towards Taupo and finer particles were carried up to 150 km northward to Hamilton and 170 km north-east to Tauranga. Later in the day several of the explosive eruptions were accompanied by shock waves, visible in the steam-rich air, as well as small earthquakes (Nairn and Self, 1978). The eruption ended on the same night.

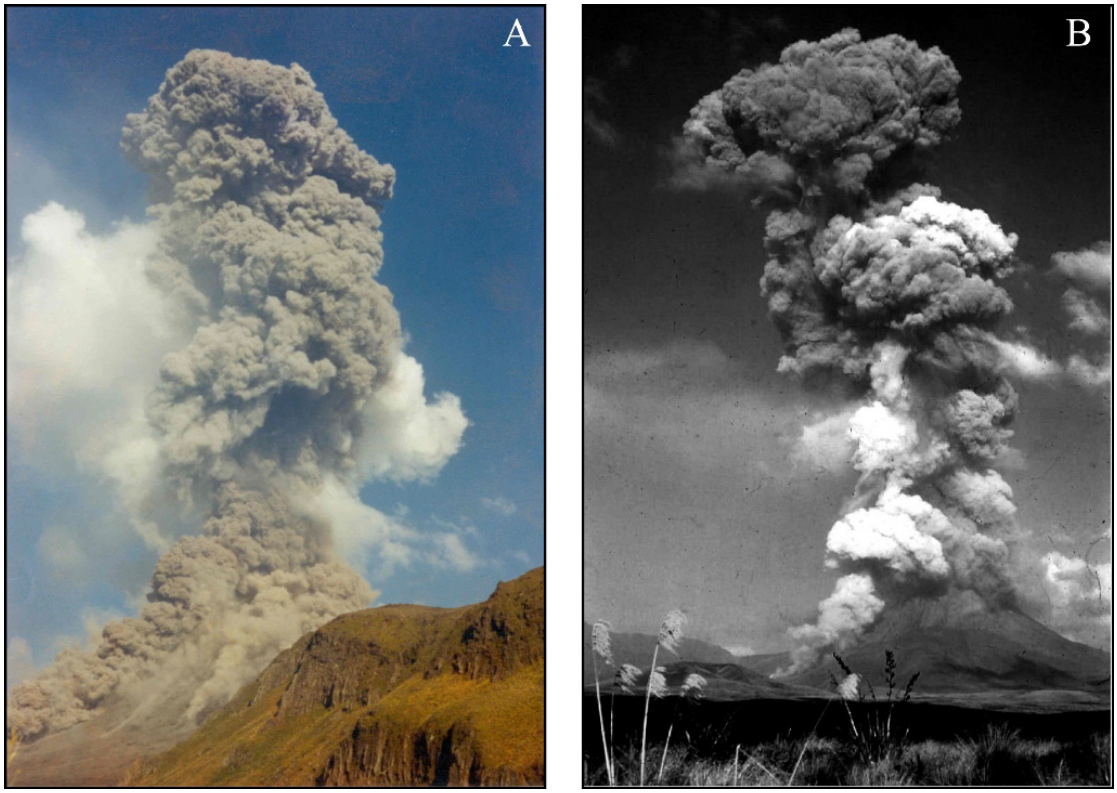

Figure 5.1.8: Ngauruhoe eruption from the 19 February 1975 with a partial collapse of the eruption column, producing a pyroclastic flow into the Mangatepopo Valley (images: (A) photo courtesy from Lloyd Homer with permission from "© Institute of Geological and Nuclear Sciences Limited [1975]" and (B) photo courtesy of John A. Krippner, private collection.

Figure 5.1.9: Ngauruhoe eruption on 19 February 1975 at $18^{h}10^{m}$ local time, showing an expanding eruption column (photo courtesy from Lloyd Homer with permission from "© Institute of Geological and Nuclear Sciences Limited [1975]"). The black spots are imperfections on the original negative.

5.1.4. Tephrochronological Record of Ngauruhoe

It has been postulated that the history of Mt. Ngauruhoe's growth is represented by two pyroclastic (ash-dominated) stratigraphic units. The older is collectively termed the Mangatawai Formation (Topping, 1973; Donoghue *et al.,* 1995). This formation lies stratigraphically below the Taupo Pumice Formation (1717 ± 13 cal. yrs. B.P. (Lowe *et al.* 2008)) with a defined maximum age from beech leaves of 2568 ± 508 cal. yrs. B.P. (NZ 186; Fergusson and Rafter, 1959). The younger part of the volcanic history of this cone is represented by a similar collective unit of small-scaled tephras, the Ngauruhoe Formation (post-1717 cal. yrs. B.P.).

In this study, Ngauruhoe's history is divided into four stages based on re-interpretation of the tephra record. Stages 1-3 represent the eruption history of Ngauruhoe prior to the Taupo Eruption at 1717 ± 13 cal. yrs. B.P., and deposits representing these stages are best preserved along the Desert Road, State Highway (SH) 46, SH 47, Bruce Road and in the Mangatepopo Valley (Fig. 5.1.10). These deposits are widely recognisable around Tongariro National Park and surrounding area. Stage 4 combines tephras younger than the Taupo eruption, collectively named Ngauruhoe Formation. Discrete tephras were only clearly identified at Loc 63, on the foot of the northern slope of Pukekaikiore, and on the northern slopes (Loc 67) and the crater of Ngauruhoe (Loc 68). Traces of Ngauruhoe-sourced glass were also identified at the type locality of NF, approximately 11.5 km east of Ngauruhoe (Loc 24). Here, no visually discrete tephras derived from Ngauruhoe were recognised.

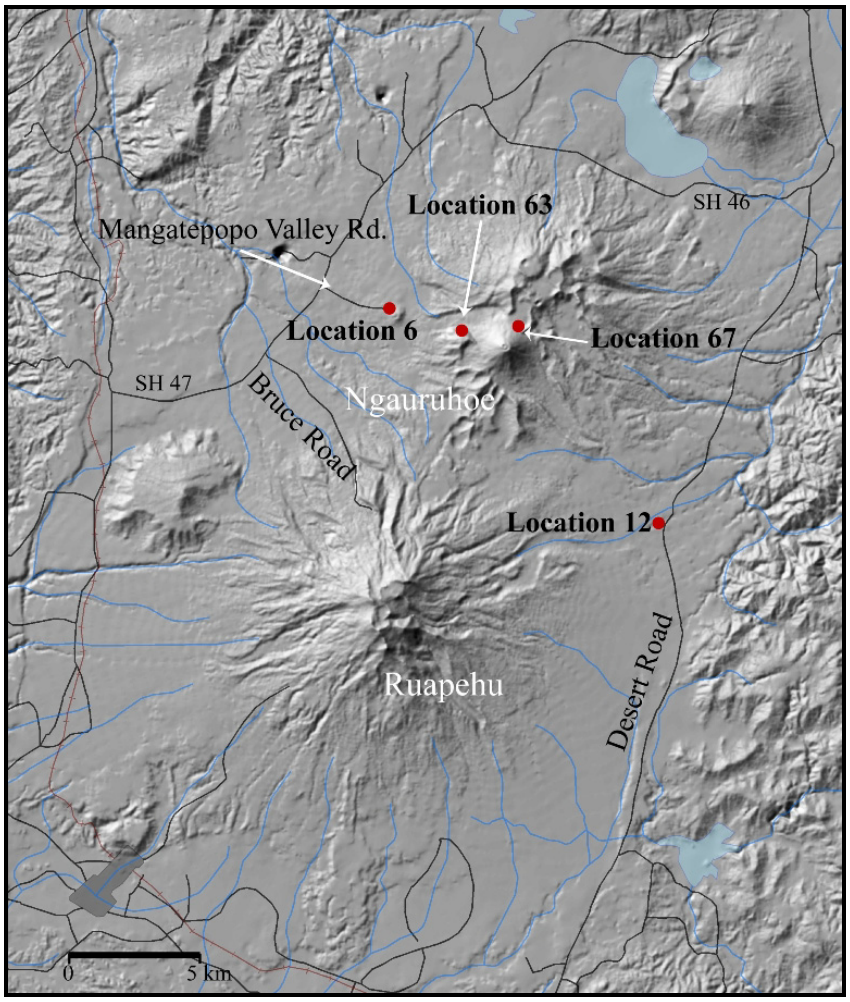

Figure 5.1.10: DEM of the TgVC showing the main locations representing Ngauruhoe's most complete tephra record.

5.1.4.1. Stage 1

Stage 1 marks the "birth" of Ngauruhoe. The first signs of tephra with Ngauruhoe chemical composition are small, isolated ash pockets and volcanic glass fragments occurring within the Papakai Formation. These units were incorporated and mixed within an accreting soil formed from medial volcanic ash and wind-blown remobilised ash (Alloway *et al.*, 1988, Cronin *et al.*, 1996a) (Fig 5.1.13A). They occur below the rhyolitic marker unit, Motutere Tephra (Table 3.1), dated at 6050 cal. yrs. B.P. (Wilson (1993); Unit H) to 7050 cal. yrs. B.P (Wilson (1993); Unit F), leading to the conclusion that Ngauruhoe is at least of this age. Alternatively, these deposits may reflect proto-Ngauruhoe eruptives. If, however, proto-Ngauruhoe was destroyed during the 12 100 to 11 170 cal. yrs. B.P. Mangamate Formation eruptions, as seems most likely, it is

possible that the present Ngauruhoe cone may have started growing immediately afterward. If so, its eruptions were not explosive or large enough to produce recognisable fall deposits until *c.* 4700 cal. yrs. B.P. Glass compositions of the preceding Mangamate Formation (Fig. 5.1.11), derived in part from vents beneath present Ngauruhoe as well as other locations (Topping, 1973; Donoghue *et al.*, 1991; Nairn *et al.*, 1998) span a wider spectrum of K_2O/FeO-ratios than known Ngauruhoe-sourced tephras of the Mangatawai Formation, and support the assumption of Ngauruhoe being older than deposits of the Motutere Tephra.

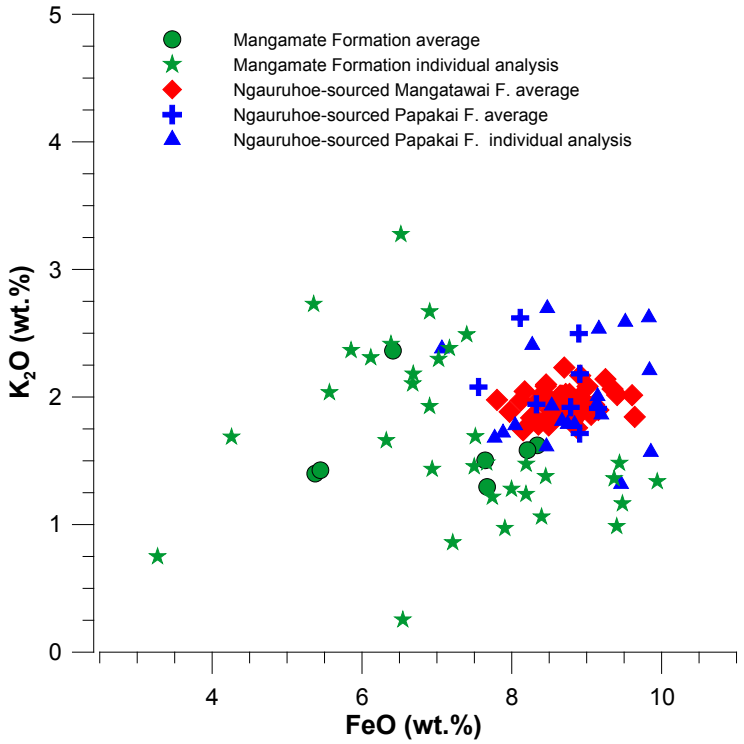

Figure 5.1.11: Major element chemistry of volcanic glasses of interpreted earliest Ngauruhoe-sourced tephras (blue) below the Motutere Tephra within the Papakai Formation in comparison to tephras of the Mangamate Formation (green) and Ngauruhoe-derived tephras younger than 3592 ± 89 cal. yrs. B.P. in the Mangatawai Formation (red). Average means the average of 10 major element analyses of volcanic glasses.

Stage 1 spans approximately 3200 years from the birth of Ngauruhoe until 3694 ± 133 cal. yrs. B.P. Eruption magnitude increases over this period, although apparent frequency appears to be constant. At least three distinctive tephras with Ngauruhoe glass chemistry occur within the Papakai Formation medial ash between the rhyolitic Hinemaiaia Tephra (unit K; Wilson, 1993) (5120 ± 150 cal. yrs. B.P.) and Stent Tephra (4323 ± 174 cal. yrs. B.P.), also described as unit Q in Wilson (1993) (Figure 5.1.12 A).

These sit within a package of more than four separate tephras that were collectively mapped by Donoghue (1991) as Ruapehu-sourced Black Ash 2. Only the uppermost of these units is now considered to be from Ruapehu. At distal profiles along the Desert Road the tephras are characterised by greasy, fine-grained, brownish-grey thin beds and laminae where the actual number of eruptive units represented is difficult to resolve (Figure 5.1.12B). Here, the lowest tephra is an isolated 15 mm-thick, dark grey fine ash that is locally iron-stained. The middle tephra is typically a 35-50 mm thick, pocketing and consist of greasy brownish grey to dark grey ash, which may combine deposits from several small and closely-spaced eruptions or eruptive pulses. The upper most of the three Ngauruhoe tephras is a 15 mm thick, semi-continuous and consist of brownish grey to dark grey fine ash. Soil accumulation rates suggest the oldest of these tephras has an age of 4714 cal. yrs. B.P. (Appendix 5) defining the oldest age of Ngauruhoe based on discrete deposits.

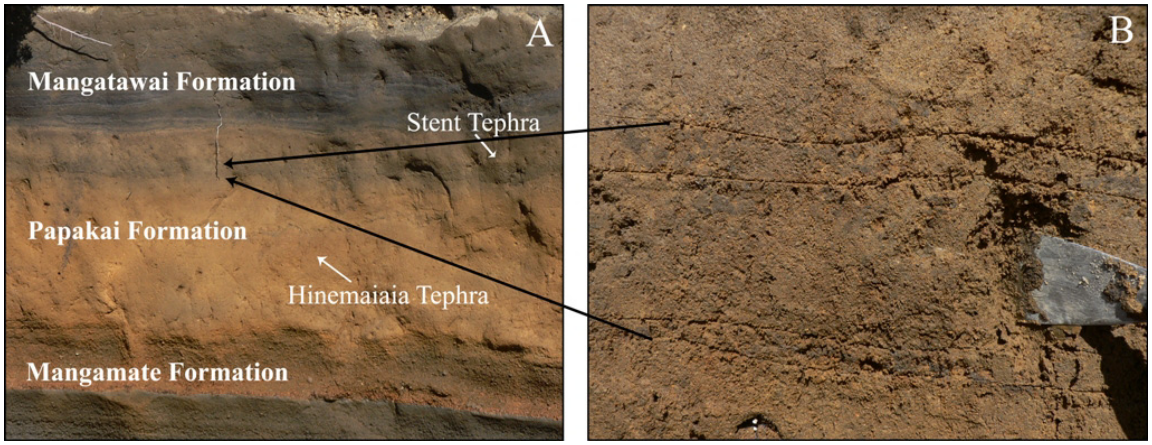

Figure 5.1.12: A) Papakai Formation between Mangatawai and Mangamate Formation at Location 12 along the Desert Road and B) a close-up view of the three discrete tephras derived from Ngauruhoe within the Papakai Formation at this site.

On the western side of Ngauruhoe, at Reference Location 6, 4.6 km downwind of the crater and 15.5 km north-west of Loc. 12, Stage 1 is represented by only a single distinctive Ngauruhoe-sourced tephra. It is a distinctive medium to coarse orange stained scoriaceous ash bed (Figure 5.1.13), up to 80 mm thick and is informally named Mangatepopo lapilli. The unit contains lapilli fragments up to 18 mm in diameter. So far this tephra layer has not been correlated to any other location analysed in this study.

This tephra occurs below the base of the previously mapped Mangatawai Formation (MtF), thus giving a minimum age of 3523 cal. yrs. B.P. The Stent Tephra does not occur in this sequence. Assuming this implies that the sequence is not old enough to preserve the Stent, then the Ng-derived tephra must be younger than 4323 cal. yrs. B.P. Ngauruhoe-glass has been found interspersed within two further ash layers beneath, implying Ng-sourced micro-tephras were deposited here.

Figure 5.1.13: Orange stained Ngauruhoe-sourced tephra (Mangatepopo lapilli) from late Stage 1, *c.* 3600 cal. yrs. B.P. at Loc. 6, 4.6 km west of Ngauruhoe.

5.1.4.2. Stage 2

Stage 2 represents a period of high-frequency and large magnitude activity from Ngauruhoe volcano. At least 38 tephra units were deposited during this phase, interspersed by a very few, thin weathering surfaces and breaks where soil could develop (Figure 5.1.14). This sequence clearly encompasses the greatest frequency of large-scale eruptions from Ngauruhoe and the highest magnitude of explosive pyroclastic eruptions known from this volcano. This location may represent the distal record of the main construction phase of the Ngauruhoe cone.

Figure 5.1.14: Finely bedded tephras of Stage 2 at Loc. 12, on the Desert Road, representing the largest-magnitude eruption phase of Ngauruhoe and possibly correlating to the major period of cone growth.

Stage 2 tephras are distinctive, firm, fine-medium, pale grey, grey and purplish-black ash beds grouped into depositional units. They often display variable thickness, reflecting underlying relief, and some units may be discontinuous. In some locations along the Desert Road the pocketing and locally over-thickened deposition pattern may indicate the local re-deposition of tephra in hollows, or clearings between the trees or shrubs that were known to be growing densely in this area at the time (McGlone and Topping, 1977). The individual tephras range between 1 and 30 mm in thickness. Of those rare units that exceed 30 mm in thickness, most are accumulations of several separate tephras (i.e. erupted ate different time), as indicated by internal bedding accompanied by rapid changes in grain size, sorting and particle-size distribution. Correlation of individual units in this sequence is extremely difficult because of the overall similarity of their lithofacies. The undulated bedding may indicate particle cohesion and the presence of water or steam during eruption and deposition. The contacts between individual tephras are usually clear and very sharp, but, because there are many very thin beds with gradational or similar colours and/or grain-sizes, boundaries between units are difficult to distinguish. Some units have wavy bedding or poorly developed cross-bedding, which indicates lateral movement either during deposition (i.e., from a pyroclastic surge), or wind/water driven post-depositional remobilisation (Figure 5.1.15 A). The fine and relatively uniform grain size of most

units suggests that the latter process is more likely. Features such as rip-ups and sharp discordant boundaries at some contacts also imply syn- or post-depositional erosion or bioturbation. The highly variable colours of the Stage 2 tephras may represent different eruption styles and/or different modes of deposition. Several layers have a pale grey to yellowish base and grade up into dark grey to black ash. This changes in colour is discussed further in Chapter 7. Accretionary lapilli of up to 5 mm diameter occur in rare poorly sorted tephras up to 16 km from source (Figure 5.1.15 B). They are extremely fragile in nature and are easily destroyed during sample processing, cleaning and sieving. Their presence imply high moisture levels in the parent plumes of these tephras, where moist, fine particles aggregate into spherical pellets with their size depending on the length of time they were held within plumes (Fisher and Schmincke, 1984; Francis and Oppenheimer, 2004). Accretionary lapilli are typical for phreatomagmatic eruptions (Fisher and Schmincke, 1984; Freundt and Rosi, 2001). Additional evidence for high moisture levels during the eruption of these tephras include very fine spherical vesicles (0.01-0.5 mm) that are preserved within most tephras (Figure 5.1.15 C and D). The largest vesicles found are up to 1.5 mm in diameter. In rare layers isolated vesicles are elongate due to compaction. Vesicles form in fine-grained deposits when they are emplaced in a hot and wet state. Escape and coalescence of the gas in bubbles causes deformation of the cohesive ash.

A further distinctive feature of the stage 2 tephras, especially east of Ngauruhoe, is the abundance of pale yellow leaves and leaf impressions within the tephras. These are dominantly from NZ beech trees, *Nothofagus sp.* (Figure 5.1.15 E and F). Leaves at the base of tephra units most likely represent normal tree litter covered by ash fall, whereas those at the top of tephra units probably dropped following an eruption due to poisoning or coating by ash. In several layers leaves occur throughout the entire tephra layer, which could indicate that the layer represents a gradual accumulation of tephra from repeated explosive eruptions over days to weeks.

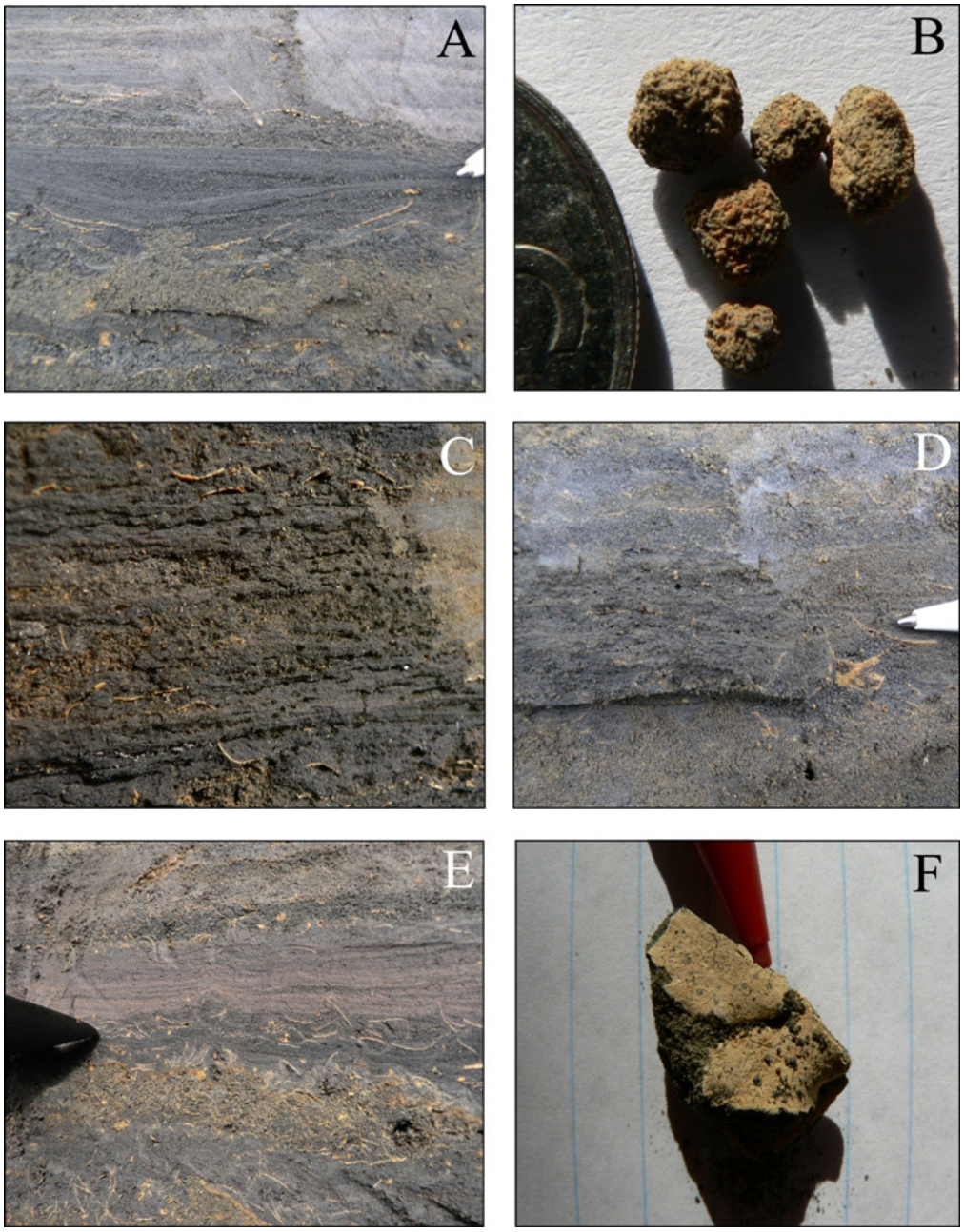

Figure 5.1.15: A) Lensoid, wavy and low-angle cross bedding, with rip-up textures at the base; B) accretionary lapilli from within stage 2 Ngauruhoe tephras; C+D) vesicles preserved within tephras with diameters from 0.01-1.5 mm; E+F) interbedded organic material, especially leaves of *Nothofagus sp.* (New Zealand beech) trees.

Two distinctive purplish grey layers within Stage 2 are the only near-universally recognisable tephras from Ngauruhoe (Fig. 5.1.16). They are so distinctive in colour and texture that they can be correlated throughout the entire Tongariro National Park area and surrounding area based on their field properties. Their purple colour probably represents an oxidative reaction of iron or manganese formed during eruption and is akin to red-oxidised basaltic scoria. It is also possible that the purple colour reflects

alteration of Fe II and III after deposition. Pyroclastic deposits from Vulcano, in the Aeolian (Lipari) Islands of southern Italy, show a range of reddening processes through alteration processes after emplacement (Capaccioni and Coniglio, 1995). Since the colour of the Ngauruhoe marker units is universal across a range of sites with individual drainage and climate characteristics, a syn-eruptive origin of the colour appears more likely. Both tephras were mapped in detail with thickness measurements made carefully to avoid any obvious locations of secondary accumulation or erosion.

Figure 5.1.16: Distinctive purple-grey marker tephras within the Mt. Ngauruhoe Stage 2 sequence. The upper pale purple marker is the most readily correlated around the Tongariro National Park and it surrounds. It comprises at least 10 stacked fine tephras. The lower dark purple unit is the deposit of an apparently single event.

On the western side of Ngauruhoe (Loc. 6), Stage 2 is represented by 37 individual tephra and tephra units, a remarkably similar number to that to the east. Eleven of these show mixed chemical signatures, with particles derived from Ngauruhoe, Ruapehu and Red Crater. This mixing could result from sampling units that are collective accumulations of several small-scaled eruptions, closely spaced in time. The historic record shows that this could be common, with Ruapehu and Ngauruhoe having often erupted near simultaneously (Gregg, 1960b). The Ngauruhoe-sourced tephras are 2-20 mm thick and range from very fine to medium ash of light grey to black colour. These

units also pinch and swell over very short distances. Several packages of tephra units could be correlated to the eastern Location 12, especially in the lower part of the sequence. Tephras from the upper part of Stage 2 could not be clearly correlated, even with collective packages having a few distinctive features such as colours and multiple layering.

At a very proximal location (Loc. 67), on the northern slopes of Ngauruhoe, at least 42 Ngauruhoe tephras (and 13+ Ruapehu units) can be chemically identified beneath the Taupo Pumice (Figure 5.1.17). Individual tephras range between 5 and 440 mm thick and vary from fine ash to scoriaceous lapilli, with some units including bombs. The thicker beds are composed of dark greyish-brown and black scoriaceous, highly vesicular and coarse-grained lapilli, indicative of dry magmatic fragmentation (Heiken, 1972; Heiken and Wohletz, 1985; Cashman *et al.*, 2000) (Figure 5.1.18 A). By contrast, the thinner tephras are typically finer-grained pale grey, pale yellow, dark grey and black containing denser blocky particles, indicative of more explosive and possibly phreatomagmatic, vulcanian style eruptions (Figure 5.1.18 B) (for classification see Chapters 7 and 8). The paler colours probably indicate higher levels of alteration and/or the involvement of weathered country rock material in the eruption.

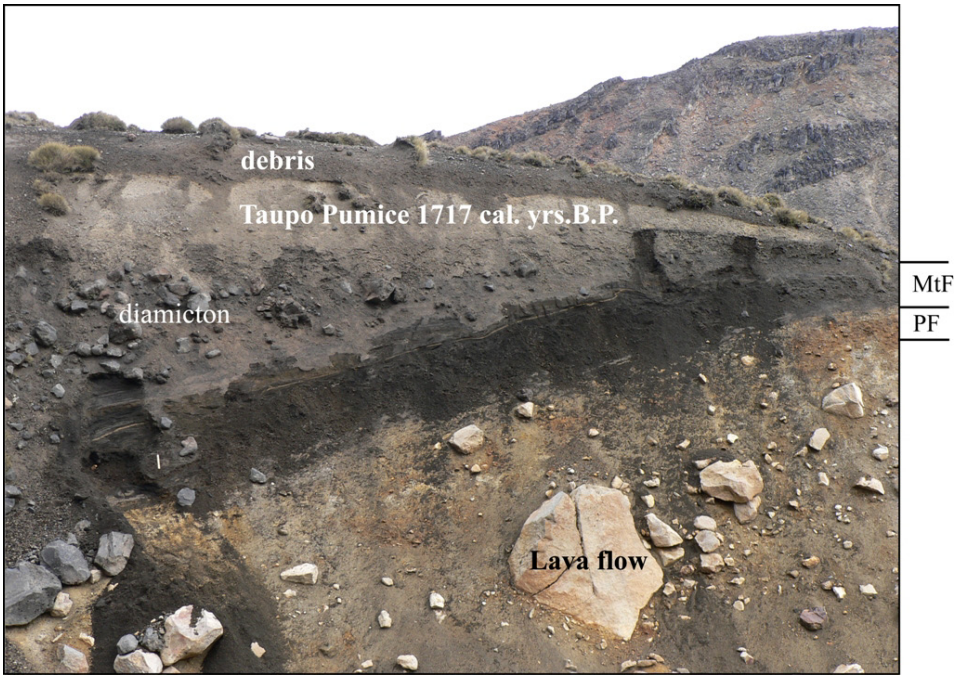

Figure 5.1.17: Location 67, showing Ngauruhoe- and Ruapehu-sourced tephras beneath the Taupo Pumice. The autobrecciated lava flow beneath the tephras is also Ngauruhoe-sourced. The thickness of the this location from the lava flow (large block) to top is~ 2.6 m.

Figure 5.1.18: Location 67, (A) the dark purple layer appears here as > 0.4 cm thick scoriaceous lapilli horizon, (B) pale purple layers are fine-medium ash.

At Loc. 67, the Taupo Pumice provides a minimum age of 1717 cal. yrs. B.P. The base of the section contains a strongly weathered fine medial ash soil (Papakai Formation), above a lava flow. The lava (Figure 5.1.17) was not mapped by Hobden *et al.* (2002),

but probably belongs to her Group 1, describing the earliest lavas erupted from Ngauruhoe, which, according to the new tephra dating, could extend back to ~6900 cal. yrs. B.P. (Matutere Tephra, Unit G) Based on the occurrence of Papakai Formation below, together with the presence of several Ruapehu tephras at the base of the sequence, Loc. 67 is considered to represent the entire stratigraphic range of Stages 2 and 3. At least 26 tephras and tephra units occur within the Stage 2 part of the profile, including 15 Ngauruhoe tephras, 6 from Ruapehu and 6 layers with glass shards from both sources.

The base of the Stage 2 tephra package is newly dated at 3694 ± 133 cal. yrs. B.P. (NZA 30052) and its top at 2810 ± 70 cal. yrs. B.P. (NZA 32435). Hence, over this period, explosive eruptions (much larger than any recorded in historical events, based on thickness and distribution) occurred at roughly 20 year-intervals. The frequency of smaller events is likely much higher, because detailed textural, macro-photography and micro-sedimentology analysis shows that several of the tephra units could also be interpreted as the combined deposits of several very thin tephras from eruptions closely spaced in time.

5.1.4.3. Stage 3

Stage 3 marks a return to intermittent production of eruptions from Ngauruhoe as shown in Stage 1, along with a decrease in the magnitude of explosive eruptions. Tephras of this stage occur between 2810 ± 70 cal. yrs. B.P. (NZA 32435) and the eruption of the distinctive Taupo Pumice, 1717 cal. yrs. B.P. (Lowe *et al.,* 2008). At location 12, Stage 3 is represented by three tephra packages, separated by four major soil/weathering horizons that successively increase in thickness from the bottom to the top (Figure 5.1.19). This appears to indicate a steady decrease in eruption frequency and/or magnitude. Some of the tephras of this Stage were not deposited as macro-units at distal profiles, which also imply that the eruptions were of lower magnitude. In general, the tephras of Stage 3 are more strongly weathered than Stage 2 tephras. In Stage 2, successive tephras were rapidly buried by subsequent tephras and hence were quickly isolated from surface weathering processes by burial, in contrast to the slower burial units of Stage 3.

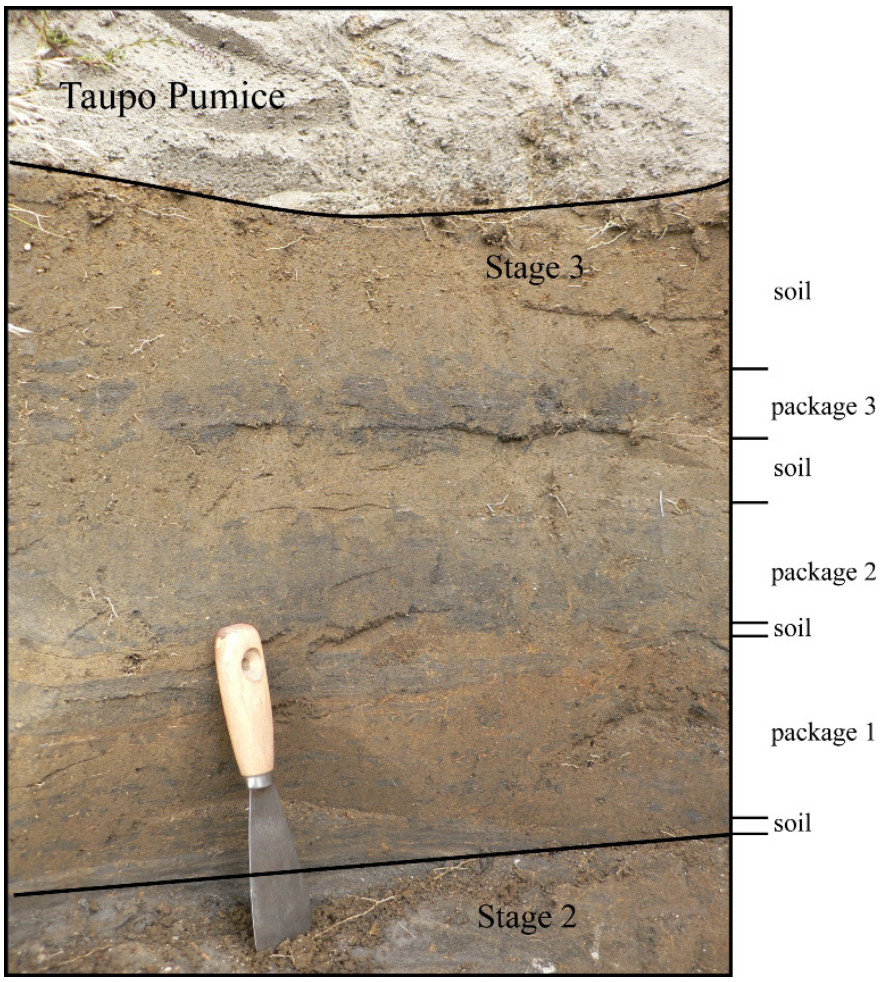

Figure 5.1.19: Tephra packages of Stage 3 at Location 12.

The lowermost package of Stage 3 consists of at least eleven very fine to fine-grained, pale–grey to black weathered individual ash beds. The boundaries between the 5-25 mm thick individual tephras are distinguished by variations in colours, grain size and other sedimentary features. Fossil leaves and roots are interbedded, but the deep root systems of recent plants can also be seen, which makes radiocarbon dating within this stratigraphic range very difficult due to potential contamination with recent carbon. The middle stage 3 package includes four dark grey to black ash units, although strong weathering masks whether these may be composites of several tephra units. The contacts between individual layers are unclear although individual beds can be distinguished by the grade of weathering and colour. No distinctive leaf horizons were identified and organic material is dominated by recent root systems and individual leaf fragments. The upper part of this middle tephra package was radiocarbon dated at 2766 ± 226 cal. yrs. B.P. (NZA 32436). The uppermost tephra package consists of two dark-

grey to black weathered tephra units. As in the central package, weathering and indistinct boundaries mean that these are likely to combine the deposits of several eruptions. Spherical vesicles 0.5 mm in diameter occur in both tephras. No organic material is found in these units. Accretionary lapilli were not found in any of the tephras of Stage 3, which indicates either drier eruption conditions or that accretionary lapilli were more poorly preserved in the more slowly accumulating soil conditions of the time.

At Loc. 6 on the western side of Ngauruhoe the same three tephra packages can be identified with variations in the number of individual tephras within each package. In addition, and as for Stages 1 and 2, tephras at this site contained many particles from both Ruapehu and Ngauruhoe. One additional Ngauruhoe tephra was found at Location 6, below the Taupo Pumice. This unit is irregularly bedded fine black ash that is partly eroded by the overlying Taupo Pumice Ignimbrite.

At Loc. 67, Stage 3 tephras occur immediately below the Taupo Pumice Ignimbrite (1717 cal. yrs. B.P.) and above a distinctive thin fine medial ash paleosol (Fig. 5.1.20 A). This sequence contains 19 Ngauruhoe tephras, 6 tephras from Ruapehu and three mixed units. The uppermost unit is a 0.4 m-thick coarse lapilli unit, similar to the dark purple (DP) layer in the Stage 2 tephras below (Figure 5.1.20 B). This uppermost tephra of Stage 3 can also be found at Loc. 6, although it is not represented as a macroscopic layer at Loc. 12. The paleosol horizons within the Stage 3 sequence at Loc. 67, although thinner than the low-elevation sites, can be directly correlated to those at Locations 6 and 12.

Figure 5.1.20: Stage 3 Ngauruhoe Tephras (and interbedded Ruapehu tephras) at location 67, above a thin but prominent paleosol also found at Locations 6 and 12. Tephras show contrast between (A) light grey - black fine to coarse ash from phreatomagmatic or vulcanian eruptions and (B) dark brown to black scoria from violent strombolian eruptions.

5.1.4.4. Stage 4

Stage 4 is characterised by frequent but very small explosive eruptions continuing into the historical record. Stage 4 began following the 1717 cal. yrs. B.P. Taupo Pumice eruption, which completely transformed the landscape, rendering the forested area into a grass and shrub-land (McGlone and Topping, 1983). Stage 4 corresponds to the previously recognised Ngauruhoe Formation (Topping, 1973), which has a type locality on the Desert Road, south of Mangatawai Stream. Donoghue *et al.* (1997) re-evaluated this site and considered that Topping had mainly included tephras derived from Ruapehu. In several examined exposures in the vicinity of the now obscured original type location, including one site only 100 m to the east, no discrete tephras are seen in this stratigraphic interval. The soil/medial ash above the Taupo Pumice representing ~1700 years is up to 440 mm thick. The medial ash profile was split vertically into six channel samples, each representing a time interval of ~315 years, if the accretion rate of the entire soil was constant. Chemical analysis of glass shards show that Ngauruhoe-

sourced micro-tephras occur within the lowermost third of the soil, approximately between 1100 and 1700 cal. yrs. B.P., as well as within the uppermost sample, representing accumulations over the last 300 years. This implies a possible break in Ngauruhoe-sourced explosive eruptions of around 1000 years. To confirm this possible pause in eruption activity, channel sampling of this soil horizon at other locations would be required.

Following the extremely violent ignimbrite emplacement from the plinian Taupo Pumice eruption, most soil/sediment sequences are eolian and alluvial sands and gravels. This means that there were few favourable depositional sites for preservation of fine-grained and thin tephra layers, comparable to the earlier sequences (McGlone and Topping, 1983, Purves, 1990, Donoghue, 1991). Topping (1974) describes pocketing discrete Ngauruhoe-sourced, post-Taupo tephras in proximal areas, such as below lava flows within the Oturere Valley at the eastern side of Red Crater. In this study two field locations were examined in the same area, along the northern side of the Oturere lava flow confirming that macroscopic andesitic tephras are present above the Taupo Pumice.

One further outcrop even more proximal to the vent was sampled in this study. This exposure occurs on the slopes of Pukekaikiore, immediately west of Mt. Ngauruhoe at Loc. 63. Here, the tephras are ash in grain size, rapidly coarsening to lapilli upslope. This sequence does not extend down as far as the Taupo Pumice, which is stratigraphically deeper. The most distinctive tephra in this sequence is a white, very fine-grained ash in mid-section (Fig. 5.1.21). A layer of similar appearance has been recognised at four other locations within the TgVC: at Pukeonake (Loc. 77), Bruce Road (Loc. 20), northern edge of Oturere lava flow (Loc. 65) and Ohakune Mountain Road. The geochemistry of glass and titanomagnetite from this layer, at all locations, shows clearly that it is a single tephra, sourced from Mt. Taranaki. It correlates directly via its chemistry to the 295 cal. yrs B.P. Burrell lapilli (Chapter 4, Druce, 1966; Platz, 2007; Turner, 2008). This is an important and distinctive marker horizon providing age control in younger Ngauruhoe tephra sequences.

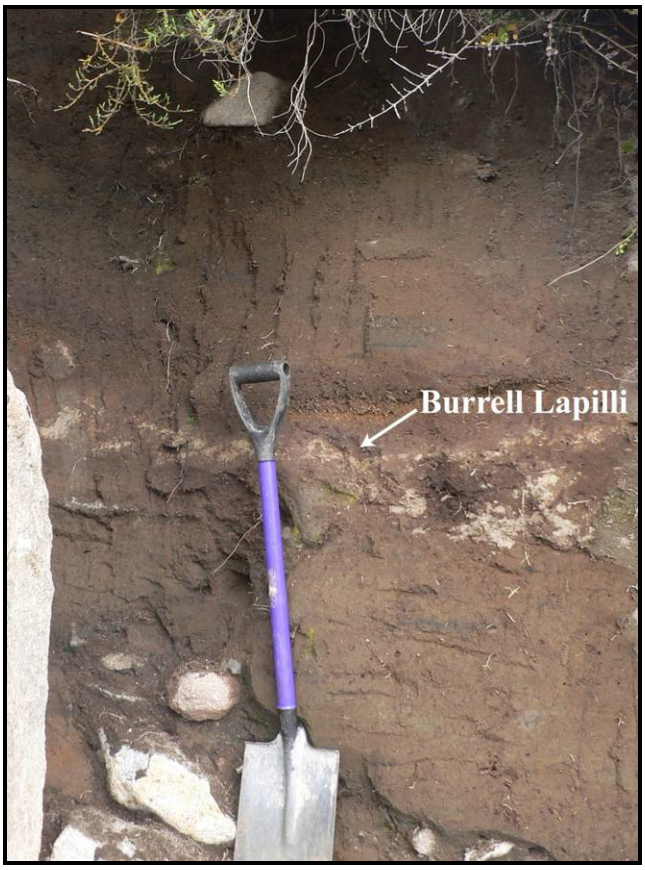

Figure 5.1.21: Location 63 at the northern face of Pukekaikiore showing a white, very fine grained tephra, which was identified as the Taranaki-sourced Burrell lapilli (295 cal. yrs. B.P.).

At Loc. 63, eight discrete fine-medium ash layers of between 10-85 mm thickness were identified as being derived from Ngauruhoe (Figure 5.1.22). These continuous beds are partly weathered with original dark grey to black colours. Five Ngauruhoe tephras occur below the 295 cal. yrs. B.P. Burrell Tephra, one immediately below it, but the others occur only 0.8 m further down in the profile. The absence of Ngauruhoe tephras further deeper in the section corresponds well to the apparent gap in the record of tephras from the channel sampling of the type section as previously described. In addition to overlying units, in the lowermost part of this section four further tephra-like layers occur that contain glass consistent with up to three sources, Ngauruhoe, Ruapehu and Red Crater. These could represent cumulative deposits of several small eruptions from these sources, or wind-blown tephra material. There are no stratigraphic indicators for the age of the base of this exposure; based on rough calculations of average inter-tephra soil accretion rates from the upper profile and soil compaction rates for the lower part, the entire section could extend back for ~1000 cal. yrs. B.P. (for age calculations see section 5.1.5). Above the Burrell Lapilli in Location 63, three discrete Ngauruhoe-

derived tephras occur, which are fresh, grey to dark grey fine ash layers, 20-35 mm thick. A further six mixed tephra-like layers also occur in this part of the profile.

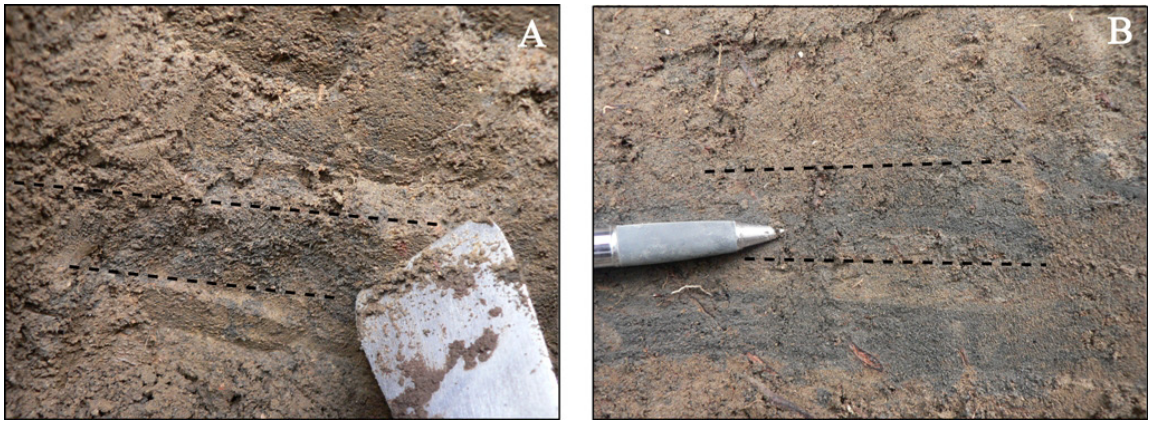

Figure 5.1.22: Individual Ngauruhoe-sourced tephras of Stage 4 at Location 63 with A) oldest tephra at this location *c.* 1000 cal. yrs. B.P. and B) tephra stratigraphically above the 295 cal. B.P. Burrell Lapilli.

Figure 5.1.23: Stratigraphic columns of four main locations representing all 4 stages of pyroclastic deposits sourced from Ngauruhoe

5.1.5. New ages for Ngauruhoe tephras

From earlier work (Topping, 1973; Donoghue *et al.*, 1995) the age of Ngauruhoe is based on the radiocarbon date 2568 ± 508 cal. yrs. B.P.; [NZ 186 R199/2] (Fergusson and Rafter, 1959). This sample comprised mainly leaves from the lower 75 mm of the Formation at its type location, north of Mangatawai Stream. Re-examination of this location indicates that the sample would have combined material from within at least 6 to 10 individual tephras, which may span a considerable period of time.

In the course of this study, eleven new samples of organic material such as leaves and microfossils (pollen) were collected from single tephra layers, or 10-15 mm thick horizons within them, for ^{14}C-dating from Loc.12 (Table 5.1.1). The purpose was to constrain the ages of Stages 2 and 3 and to confirm the age of the oldest Ngauruhoe tephras. Considerable variation in dating results occurred within these samples, depending in part on the fraction analysed by Accelerated Mass Spectroscophic dating methods at the Rafter Radiocarbon Laboratory, Lower Hutt.

The base of the "Mangatawai Formation" in this location is most likely to be 3500-3700 cal. yrs. B.P. (samples 2, 3; Table 5.1.1), around 1000 years older than the previous (bulk) estimation. This also corresponds to the Stage 1/2 transition. The distinctive dark purple tephra, also considered to be one of the largest eruptions from Ngauruhoe, was consistently dated at both Loc. 12 and 78 at 2800-2900 cal. yrs. B.P. (samples 5, 6, Table 5.1.1). The Stage 2/3 transition most likely occurred soon afterwards at ~2800 cal. yrs. B.P. (sample 9; Table 5.1.1).

Several of the dates in Table 5.1.1 are out of stratigraphic context, with one clearly contaminated by old carbon (sample 10), maybe due to windblown charcoal interbedded within the underlying Kawakawa Formation, two others apparently also possibly contaminated with older carbon (samples 7 and 8) and one sample seemingly too young (sample 1). The small sample sizes available for analysis from this site and the range in materials that could be dated probably contribute to this variability. The dates considered to be reliable are based on the key correlation of the two dates from separate

locations on the dark purple marker horizon. These provided the basis for selecting which of the other dates were most stratigraphically realistic.

Table 5.1.1: New C^{14}-dates from within tephra sequences at Location 12 as well as two samples (407 22a and 407 3a) from a nearby site (Loc. 78) along the Waihohonu Track ~ 200 m west of the Desert Road. Dates in italics are not considered reliable, and those with tick marks in the last column represent the most likely stratigraphically consistent ages.

No.	Depth in mm	Descriptions	New ^{14}C-ages in B.P.	New ^{14}C-ages in cal. yrs. B.P.	Material analysed	Used in this study
11	645-655	sample 407 58, central package of stage 2	2738 ± 75 yrs. B.P. (NZA 32436)	2766 ± 216 cal. yrs. B.P.	small amount of pollen and plant material	✓
10	*762-772*	*sample 407 53 lower package of stage 2*	*18 325 ± 100 yrs. B.P. (NZA 31249)*	*21 757 ± 405 cal. yrs. B.P.*	*Very small amount of organic material*	
9	833-843	sample 407 46, top layer of stage 2	2748 ± 45 yrs. B.P. (NZA 32435)	2810 ± 70 cal. yrs. B.P.	small amount of pollen and plant material	✓
8	*936-946*	*sample 407 35,*	*3236 ± 25 yrs. B.P. (NZA 29905)*	*3407 ± 55 cal. yrs. B.P.*	*leaves*	
7	*998-1006*	*sample 407 26, fine medium ash above the pale purple tephra unit*	*3305 ± 50 yrs. B.P. (NZA 32433)*	*3487 ± 125 cal. yrs. B.P.*	*small amount of pollen and plant material*	
6	1040-1047	sample 407 22, dark purple layer	2851 ± 30 yrs. B.P. (NZA32312)	2889 ± 101 cal. yrs. B.P.	leaves	✓
5		sample 407 22(a)	2815 ± 30 yrs. B.P. NZA 32956	2860 ± 85 cal. yrs .B.P.	leaves	✓
4	1134-1152	sample 407 15	3250 ± 50 yrs. B.P. (NZA31248)	3415 ± 144 cal. yrs. B.P.	bulk, pollen	✓
3	1203-1225	407 9, oldest Ng-sourced tephra within the MF	3470 ± 40 yrs. B.P. (NZA 30052)	3694 ± 133 cal. yrs. B.P.	fossil, bulk	✓
2	1335-1340	sample 407 3, close to base of MF, Ruapehu-sourced	3330 ± 50 yrs. B.P. (NZA 32433)	3508 ± 121 cal. yrs. B.P.	small amount of pollen and plant material	✓
1		*Sample 407 3(a)*	*2701 ± 40 yrs. B.P.* (NZA 33057)	*2783 ± 67 cal. yrs.* B.P.	*plant* fragments	

Below this sequence, within the Papakai Formation, at least three Ngauruhoe tephras occur between the Hinemaiaia Tephra (Unit K; Wilson, 1993) (5120 ± 150 cal. yrs B.P.) and the Stent Tephra/Unit Q (4323 ± 174 cal. yrs. B.P.; Wilson (1993). These units occur also above the Ruapehu-sourced Black Ash 1 (Donoghue *et al*., 1995) which is dated as at least 5562 ± 268 cal. yrs. B.P. [NZ7532].

Based on non-conflicting radiocarbon dates and marker tephra ages at Location 12, it is possible to calculate a preliminary age model for 116 discrete andesitic tephras and tephra units. These discrete ash units occur collectively within 20 tephra packages, which are separated by soil horizons. The intervals between successive radiocarbon dates ranges from 44 to 1269 cal. yrs. (Figure 5.1.23). It is assumed that accretion of medial ash (between recognisable macroscopic tephras) was constant between successive radiocarbon dated levels. From this sequence, the accumulation rates over all date-controlled intervals longer than 100 years appear to be remarkably constant at 0.133 mm/year. However, when macroscopic tephra accumulation rates are high and significant intervals of the profile are bracketed by dates <100 years apart, estimated accumulation rates are highly variable. Thus it is difficult to constrain how much time is encompassed within sequences containing many tephra units because any medial ash is included within them, especially when soil thickness <1 mm cannot be recognized with confidence in the field. While there are sub-millimetre medial-ash layers on top of tephras it is hard to say whether these are true soil horizons or just the weathered upper parts of tephras. Based on the accumulation rates, ages for individual tephras can be assigned with errors derived from the constraining radiocarbon ages. The ages are presented in Chapter 8 and Appendix 5 and 6.

Location 67, at South Crater, is overlain by the Taupo Pumice (1717 cal. yrs. B.P.) but there are no dated units or marker tephras below this to constrain a stratigraphic age. The Ruapehu-sourced units in the sequence could be correlated to those in Location 12 (Figure 5.1.23) where there is one Ruapehu tephra almost directly below Taupo Pumice and several others deeper in the sequence, below a radiocarbon date of ~3700 cal. yrs. B.P. (sample 3; Table 5.1.1). These relationships suggest that the Location 67 sequence spans 2000 years and represents both Stages 2 and 3.

At the Pukekaikiore proximal site (Loc. 63) the only dated horizon is the Burrell Lapilli at 295 cal. yrs. B.P. sourced from Mt. Taranaki and located mid-section. Above this distinct tephra the profile is non-compacted. Therefore all tephra ages younger than Burrell Lapilli were calculated using a constant soil accumulation rate (2.7 mm/year). However, below the Burrell tephra, the profile becomes increasingly compacted with depth. Hence, constant soil accretion (Neall, 1977) for this part of the profile is an unrealistic assumption. The simplest model to calculate the ages for all individual tephras for this part of the profile is given by a direct correlation of soil compaction (P) and depth (D), such as:

$$P = D^x \text{ or } x = \log_D P . \quad (1)$$

The most likely soil compaction rate x was determined by comparing the known cal. yrs. B.P. ages from the Tufa Trig Profile at Loc 56 (Chapter 6.3.) and calculated cal yrs. B.P. ages from the lower part of Location 63 profile using equation 1. There is only one value of compaction rate (x = 1.0336), which gives a very good correlation between both profiles. Based on this compaction rate, the oldest tephra of this profile at Loc. 63 has an age of 981 cal. yrs. B.P.

All calculated ages for each of the individual tephras at Location 12 and 63 are presented in Appendix 5.

5.1.6. Lithological componentry of Ngauruhoe tephras

The componentry of Ngauruhoe tephras is characterised by three main lithologies: crystals (xeno- and juvenile phenocrysts), volcanic glass fragments, and accidental lithics (from wall rock or sub-volcanic country rocks). The ratios of these particles within any tephra are dependent on magma composition, the pre-eruption storage interval, fragmentation processes, as well as transportation and deposition mechanisms. Secondary effects may also relate to environmental processes such as changes in wind strength and direction and rain, as well as post-depositional diagenetic processes.

The ratios and quantities of clinopyroxene (cpx), orthopyroxene (opx), plagioclase (plg), olivine (ol), hornblende (hb), light and dark volcanic glasses and lithics were determined by point counting (see Chapter 2). To achieve a representative result, at least 300 grains and, where possible, 500 grains of particle-size fractions 1-2 mm, 0.5 μm-1 mm, 250-500 μm were examined for each tephra sample. The point count analyses are presented in Appendix 4.

Crystals

The ferromagnesian mineral assemblage of distal TgVC tephras is characterised by opx + cpx ± ol ± hb (Lowe, 1988; Donoghue, 1991) (Chapter 3). The Ngauruhoe sourced tephras examined here have assemblages that are mainly pyx > plg > ol, but if the pyroxene is further subdivided into orthopyroxene and clinopyroxene the mineral assemblage is plg > opx > cpx > ol. Phenocrysts are common in grain size fractions up to 1-2 mm, as well as being present as microlites in glasses. Minor amounts (<2%) of titanomagnetite and chrome spinel were also found in all samples, primarily in fractions <125 μm, but also as microlites. Plagioclase is ubiquitous (4-21%) and occurs as clear and white crystals with small spherical to elongate glass inclusions. The crystals are commonly coated by transparent, light brown glass. Pyroxenes (opx+cpx) are also ubiquitous, ranging between 0.7 and 30% and are the dominant mineral phase in 77% of the analysed samples. Orthopyroxene is dominant (86%), is dark brown and ranges from fresh angular to rounded in form. Clinopyroxene is pale to dark green, occurring mostly in an elongate, euhedral monoclinic crystal form with broken and rounded edges. The cpx also contains common glass and Fe-Ti-oxide inclusions. Olivine occurs in about 66% of Ngauruhoe-sourced tephras in very minor amounts (0.2 to 2.4 %), usually as clear to pale green broken and rounded crystal fragments.

Volcanic Glass

Andesitic glass is defined according to Fisher and Schmincke (1984) as colourless glass shards and pumice with oriented microlites (small crystals) and elongate, ovoid – tubular vesicles and is is higher in silica than basaltic glasses lower in than dacitic and rhyolitic glasses with average SiO_2 between 53 and 63 %. There are two different kinds

of glass: sideromelane and tachylite. Sideromelane is a microlites poor glass, which indicates a generally rapid cooling of the melt and can be vesiculated or vesicle free (Nemeth and Martin, 2007). In contrast, tachylite is typically formed under slower cooling rates and is characterised by an abundance of microlites within the shards.

In this study, volcanic glass makes up 39 to 93% of all analysed tephras. It exhibits a range of colours and shapes, as further discussed in Chapter 7. Glass was classified into dark/black (tachylite) and brown/pale (sideromelan) glass. About 66% of the tephras contain greater proportions of black glass, known as tachylite.

Accidental and cognate lithics

Accidental lithics are clasts derived from subvolcanic basement and may be of any composition (Fisher and Schmincke, 1984). Within the TgVC the lithics are derived from upper Paleozoic rocks (Graham *et al.*, 1988), Pliocene (Opoitian and Waitotaran stages) and upper Miocene (Kapitean stage) sediments (Grant, 2006). Furthermore, silicic xenoliths were identified, which are probably derived from the lower crust (Ian Smith, pers. com.) Cognate lithics are magmatic fragments derived from previous magmas of the same volcano (Fisher and Schmincke, 1984; Nemeth and Martin, 2007).

Lithics are present in all analysed samples and range between 0.3 and 37 %, depending on the eruption style, as discussed further in Chapter 7. Most accidental lithics found were rounded. Up to 43% of analysed samples contained apparently recycled scoria, presumably from the crater walls.

Accretionary lapilli

In several Ngauruhoe-sourced samples of Stage 2 (Mangatawai Formation) up to 0.5 mm small spherical accretionary lapilli were found. They occur in poorly sorted and fine-grained ash layers and were found up to 16 km from Ngauruhoe. Their rarity could be explained by their fragile nature and destruction during the process of cleaning and sieving.

Figure 5.1.24 shows that the smaller the size fraction the more the sample becomes enriched in crystals, which can be explained by both, the high fragmentation of the crystals and the fragmentation of the microlites-rich glass shards.

The componentry of distal (Location 12) and proximal (Loc. 63 and 67, and crater rim of Ngauruhoe) locations also show variation in two size classes (Figures 5.1.25). Despite the small number of samples analysed at proximal locations, these tend to be more lithic rich in both the 500 µm to 1 mm and 250 micron to 500 µm size fractions.

The variation in glass, crystal and lithic components and their dependence on eruption style will be detailed in Chapter 7.

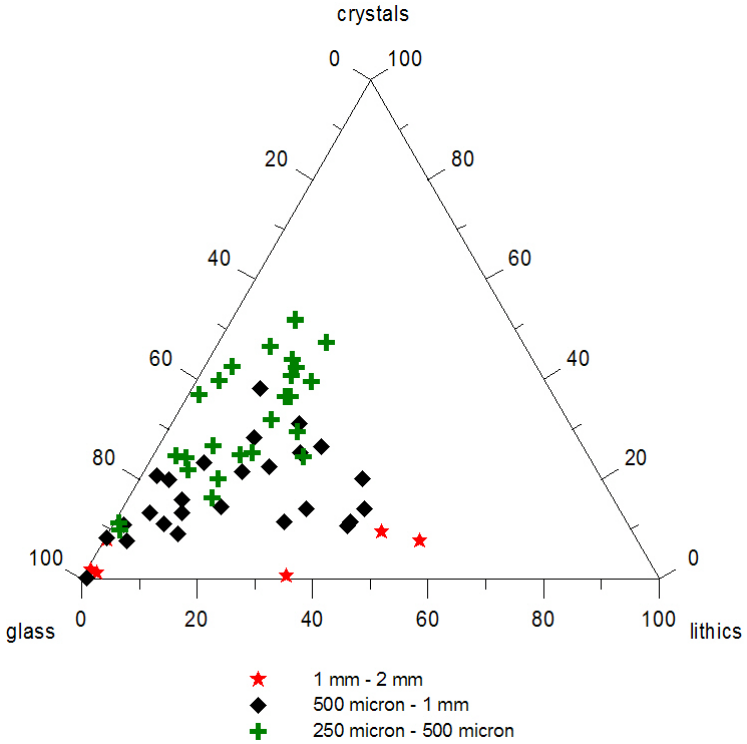

Figure 5.1.24: Discrimination plot of the main components glass, lithics and crystals for Ngauruhoe-sourced tephras and three different size fractions in wt%. The glass values are in all samples very high while the crystal content increases with smaller size fractions and the lithic content increase in coarser size fractions.

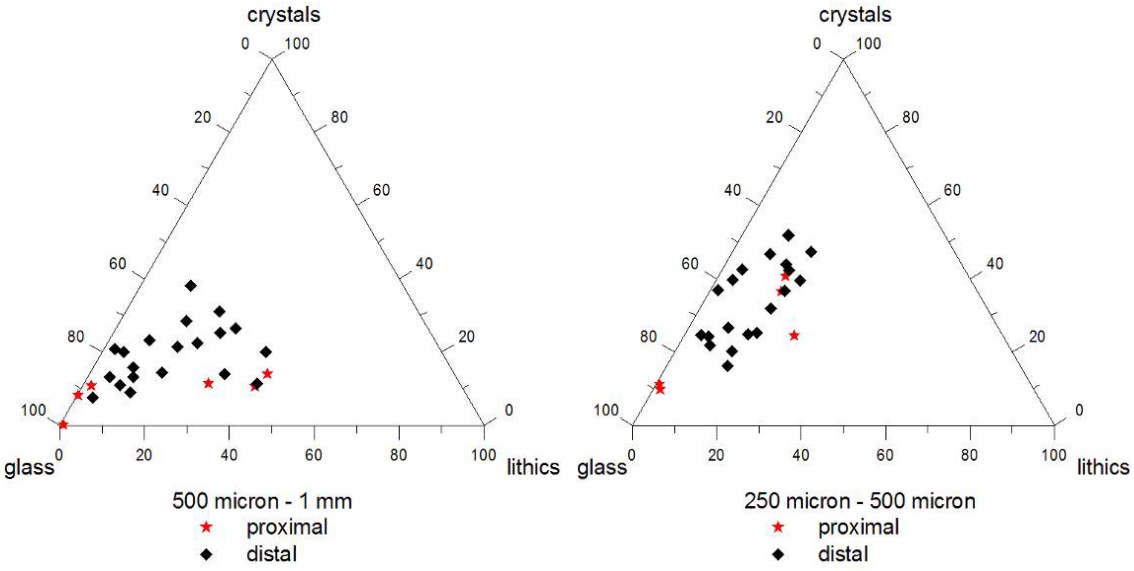

Figure 5.1.25: Discrimination plot of the main components for two size fractions showing the relation of the componentry for proximal and distal exposures.

5.1.7. Geochemistry

All chemical analyses from the Ngauruhoe tephras were obtained from volcanic glass using the electron microprobe at Auckland University for major elements. Tephras from Locations 12, 63, 67 as well as from the crater rim were analysed to represent the most complete tephra record covering all four Stages of Ngauruhoe's activity (Figure 5.1.23). An additionally 12 Ngauruhoe glass samples were analysed using Inductively Coupled Plasma Mass Spectrometry (ICP-MS) for Sr-isotopes at University of Melbourne.

The chemical composition of magma upon its eruption is a function of a variety of processes, including assimilation, fractionation and mixing, that operate over a range of depths/pressures, temperatures and volatile contents from source to surface. When analysing tephras, the examination of these magmatic processes is often hindered by the uncertainty of sampling representative proportions of crystals and glass from the magma, especially for fine-grained and distal deposits (Shane, 2000). Because of this, proxies are used to infer parental magmatic processes, primarily via the compositions of volcanic glass and a range of mineral phases. Here glass and titanomagnetite compositions are used, although, as discussed in Chapter 4, the glass analyses are considered to be the most reliable.

Previous geochemical studies characterising andesitic tephras within the TgVC were described in Chapter 4. Of these, Topping (1974), Kohn and Neall (1973), Kohn and Topping (1978), Lowe (1988) and Cronin *et al.* (1996d), attempted to distinguish Taranaki-sourced tephras from TgVC-derived tephras using titanomagnetite compositions. In addition, glass compositions have proven very reliable for identifying individual rhyolitic tephras, although typically it has been used in conjunction with mineralogy and other stratigraphic constraints (Lowe, 1988; Lowe, 1989; Froggatt and Rogers, 1990; Donoghue, 1991). In recent geochemical studies in this area, trace element compositions of Ngauruhoe lavas were used by Hobden *et al.* (1999) to model magma evolution below the TgVC.

5.1.7.1. Major element chemistry of volcanic glass

The major element composition of volcanic glass delivers information about the composition of the melt prior to eruption. This composition is therefore strongly dependent on degassing, oxidisation and crystallisation processes (Gardner *et al.*, 1998). Ngauruhoe glass is rich in microlites, which occur due to rapid decompression of magma and/or degassing of the melt (Hammer *et al.*, 1999; Cashman and Blundy, 2000). These microlites mostly consist of plagioclase, pyroxene and some titanomagnetite, and their content and size is reflected in the residual glass composition. Additionally Ngauruhoe tephras contain common plagioclase and pyroxene phenocrysts with traces of olivine and rare Fe-Ti oxides. Formation of these phases has mostly occurred prior to the eruption (although late-stage growth may have continued on their outer rims), hence they will have had an earlier influence on the eventual glass composition that is likely overshadowed by the late-stage crystallisation.

In general, the chemical variation in major element composition is very narrow for Ngauruhoe-sourced tephras, particularly in comparison to Ruapehu (Figures 5.1.26). Tephras from the two sources plot in separate compositional fields, implying no direct link between these neighbouring magmatic systems.

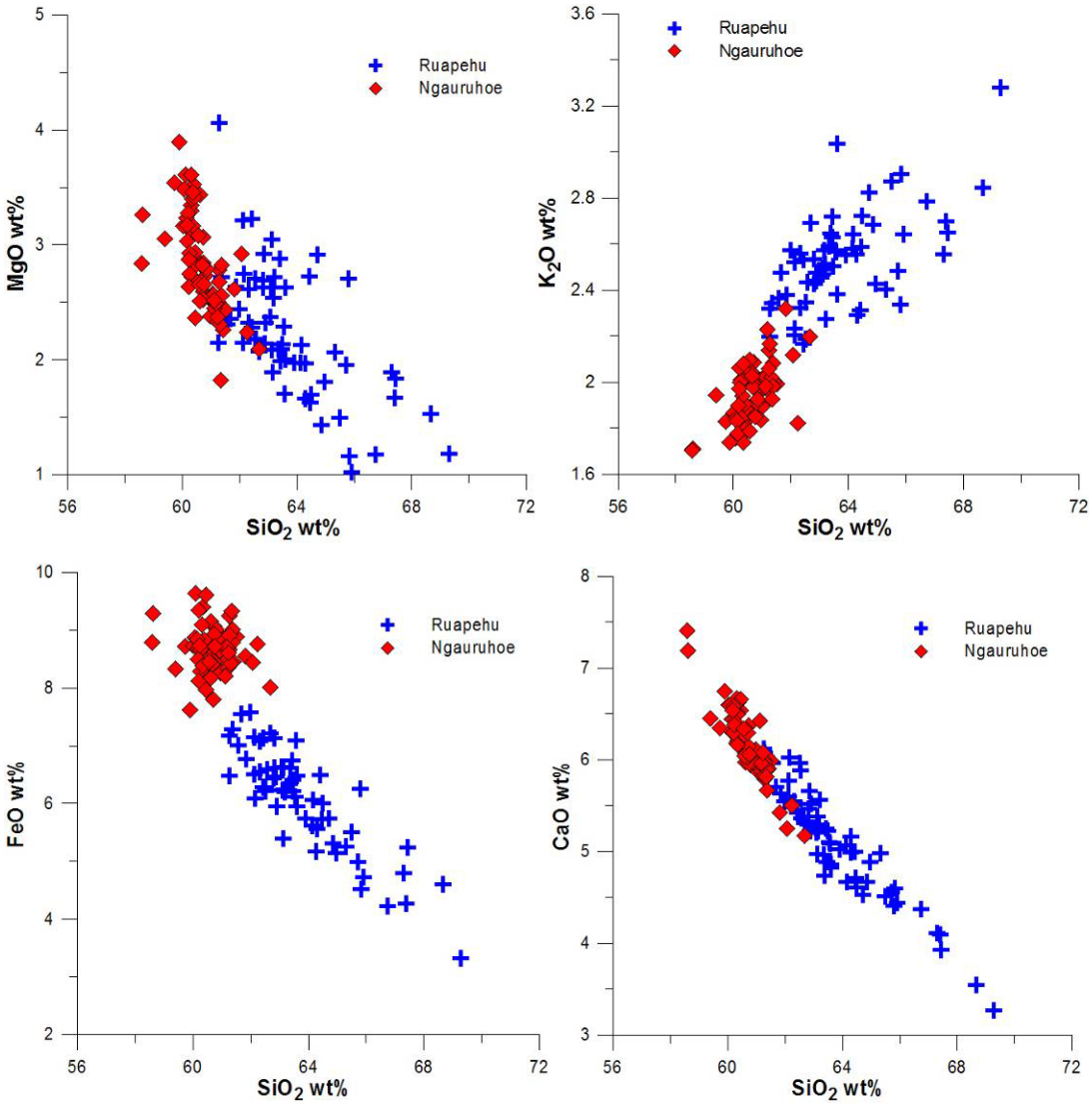

Figure 5.1.26: Major oxides vs. SiO_2 in comparison between Ngauruhoe vs. Ruapehu.

Back-scattered SEM images of the analysed glasses demonstrate the high volumetric content of microlites (Figures. 5.1.27 and 5.1.28). According to Platz *et al.* (2007), andesitic glass is difficult to analyse using a de-focussed electron beam due to the "contamination" of microlites. However, since a defocused beam is necessary to reduce the loss of Na and other light elements during analysis (Froggatt, 1983), microlite contamination is an important consideration. In this study, microlites could be avoided in the glass analyses, dominantly by watching the Al_2O_3 content during the analyses process. When Al_2O_3 was >17 wt%, these analyses were interpreted as being contaminated by plagioclase microlites and discarded. Similarly, analyses that contained Fe-Ti oxide microlites were also easily recognised.

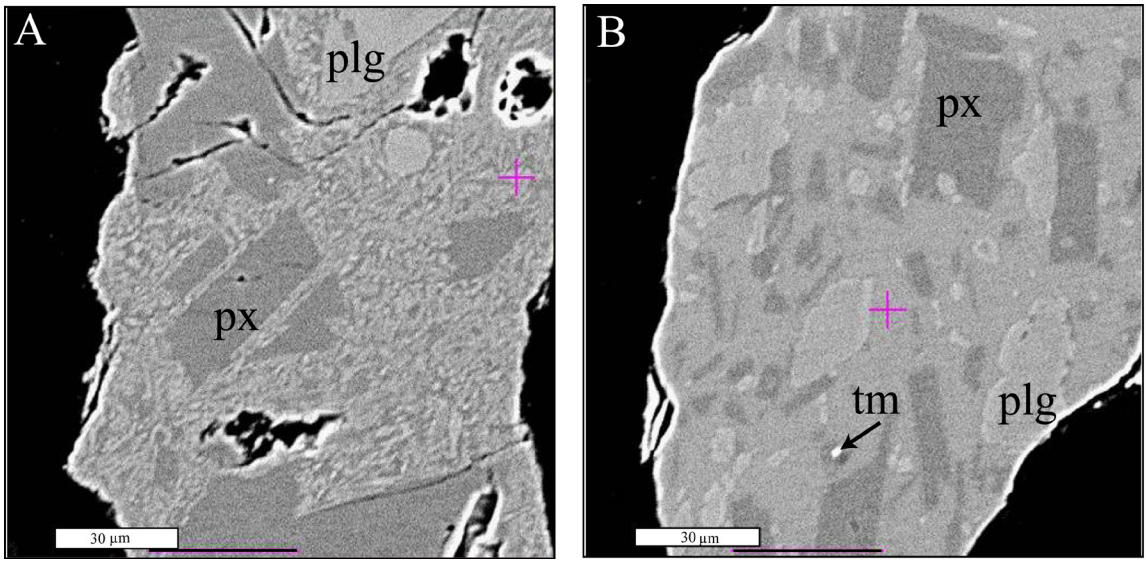

Figure 5.1.27: Back-scattered images of volcanic glass sourced from Ngauruhoe showing numerous microlites mainly consisting of (A) plagioclase and pyroxene but also (B) titanomagnetites.

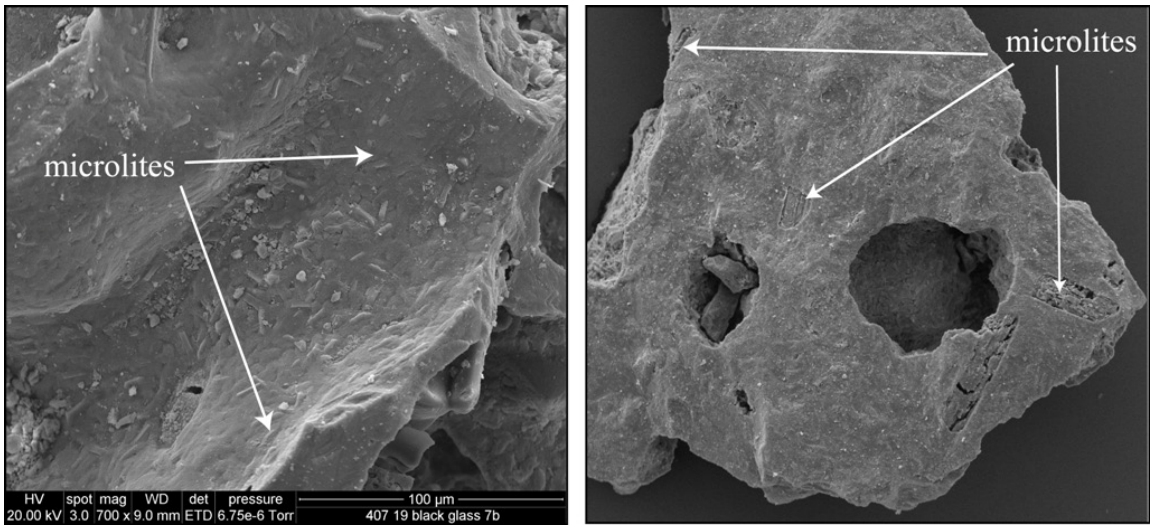

Figure 5.1.28: SEM-images of two glass shards sourced from Ngauruhoe containing numerous microlites.

The oxides of MgO, FeO (7.19 – 9.64 wt%) and TiO_2 (1.0 - 1.5 wt%) show similar trends when plotted against SiO_2 (Figures 5.1.29 A-C). The most distinctive features are that Stage 1 and 4 compositions span a wider range in SiO_2, CaO and alkali oxide contents in comparison to those erupted during Stages 2 and 3. This appears to reflect a larger variation in late-stage crystallisation, which may indicate highly variable magma rise rates and different residence times in shallow-level storage or conduit/dyke systems. In addition, it appears that the compositions are strongly influenced by late stage crystallisation of primarily plagioclase and pyroxene microlites (Figure 5.1.30)

along with titanomagnetites (Figure 5.1.31). By contrast, the Stage 2 and 3 tephras show narrower ranges in SiO_2, CaO, K_2O and Na_2O contents and variability is expressed primarily in broad ranges of MgO, FeO(total) and TiO_2 contents. This may indicate relatively uniform rise rates and consistent conduit residence times during Stages 2 and 3, along with compositional control expressed by late stage titanomagnetite-dominated microlite crystallisation.

The stratigraphic data imply that Stages 2 and 3 involved rapid, successive and relatively large-scale eruptions, implying a higher average magma flux than during either Stage 1 or 4. This high eruption rate is consistent with the glass chemistry information showing little variation and thus short residence times in shallow levels. On the other hand, eruptions during Stage 1 were intermittent with larger repose periods between them. This may have been a Stage when the conduit/feeding system was not well developed, leading to variations in shallow-crustal residence times before eruptions. Late Stage 4 is characterised by small-scale eruptions and these magmas appear to also have highly complex rise histories, perhaps due to their small volume, forming isolated batches spatially separated within the conduit feeding system. This is similar to the model proposed by Hobden *et al.* (1999) for the development of the Ngauruhoe cone construction based on lava flow analyses.

CaO shows a consistent negative trend against increasing SiO_2 (Figure 5.1.29 D), which may indicate fractionation of calcic plagioclase and clinopyroxene from these magmas. The alkalis show positive correlation with increase of SiO_2 (Figures 5.1.29 E, F, G). At Stages 2 and 3 Na_2O may have been involved in the crystallisation fractionation of more sodic plagioclase. Throughout all four Stages, SiO_2 remained within a narrow range of andesitic glass compositions (Figure 5.1.29 H).

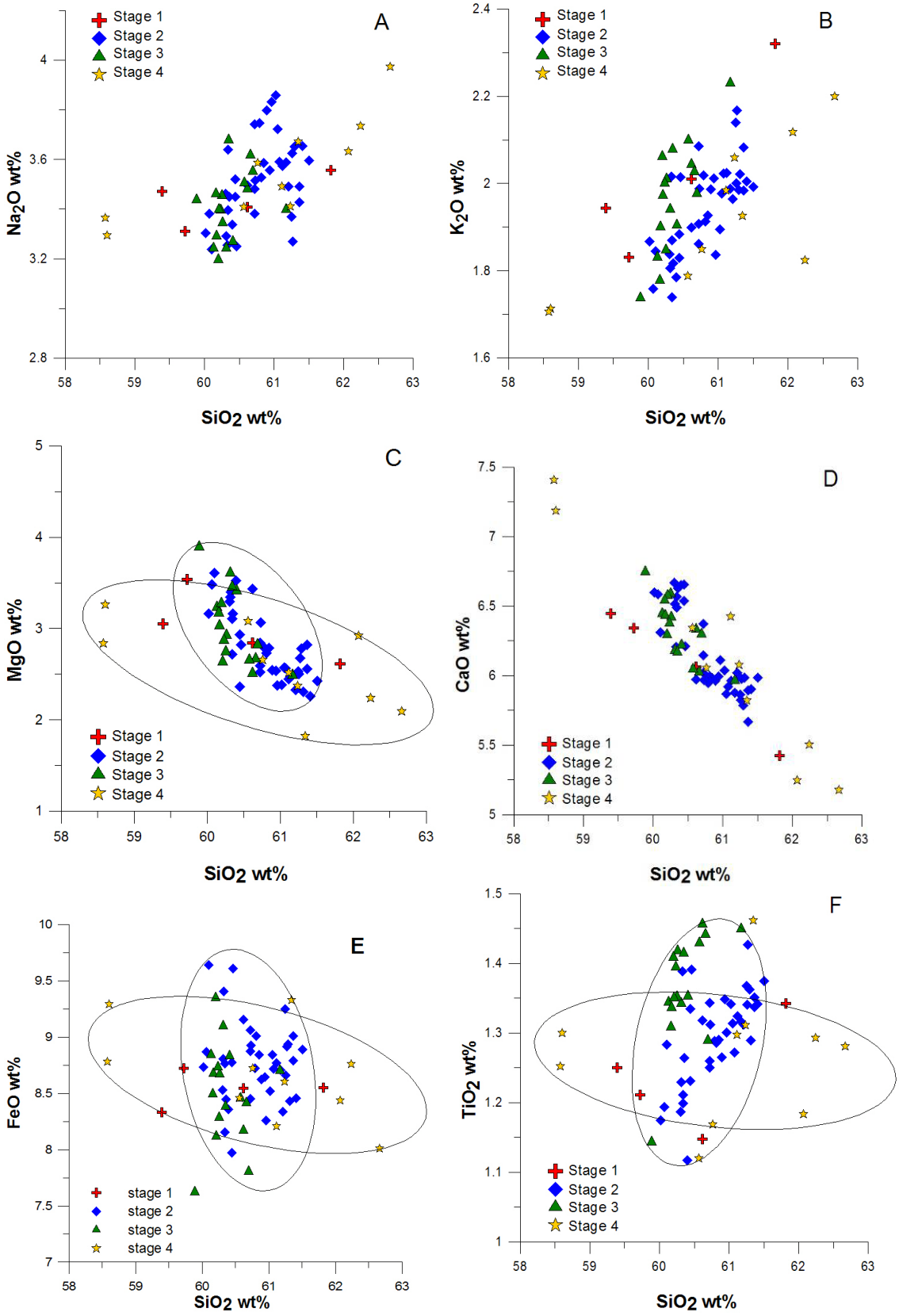
A
Stage 1
Stage 2
Stage 3
Stage 4
Na2O wt%
SiO2 wt%
B
K2O wt%
C
MgO wt%
D
CaO wt%
E
FeO wt%
stage 1
stage 2
stage 3
stage 4
F
TiO2 wt%

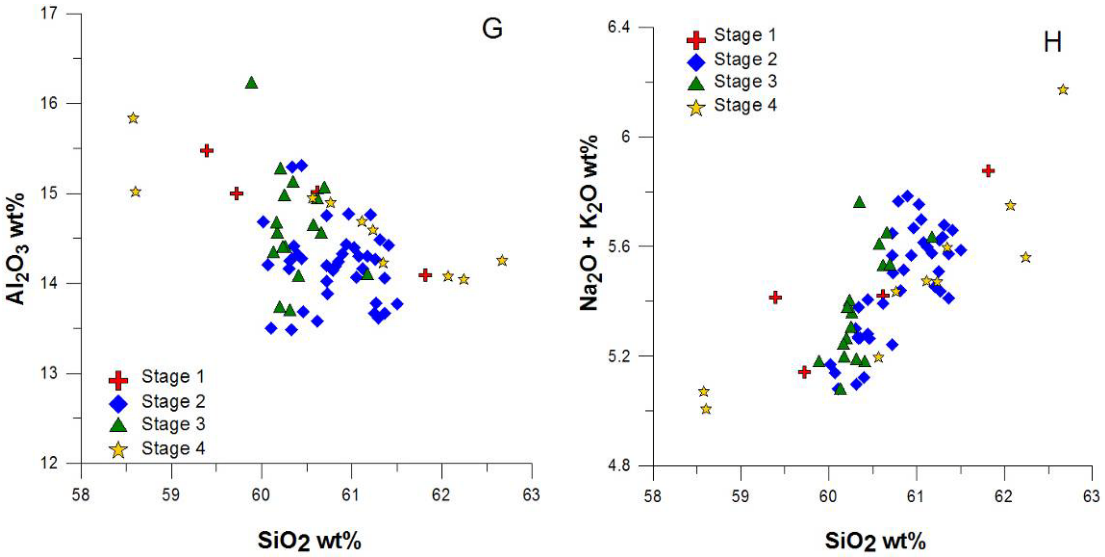

Figure 5.1.29: Electron microprobe analyses of major oxides plotted against SiO_2 wt% for volcanic glasses sourced from Mt. Ngauruhoe.

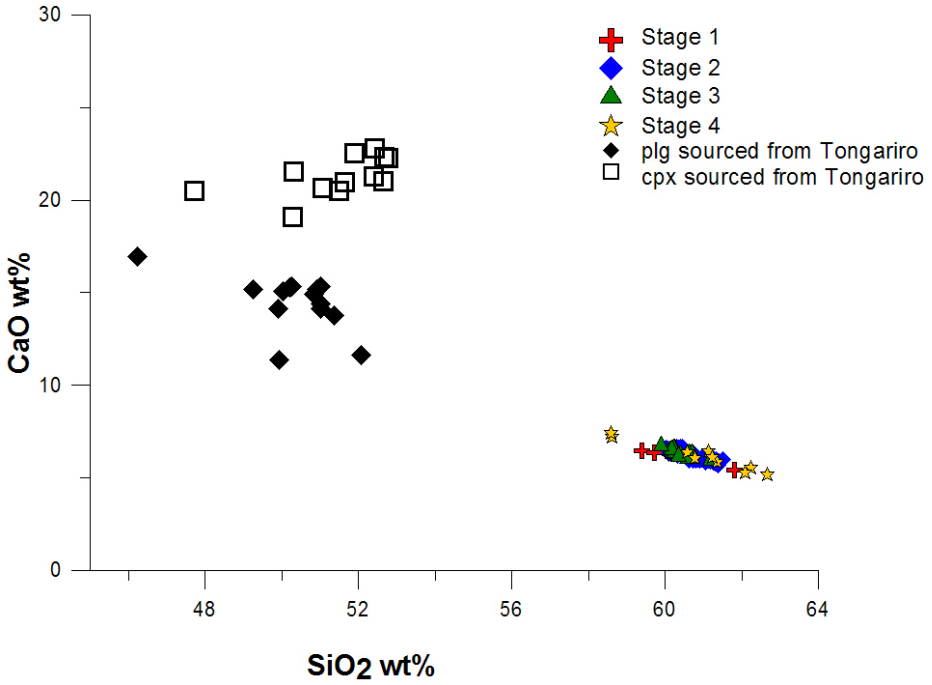

Figure 5.1.30: Major oxide analysis SiO_2 vs. FeO of Ngauruhoe-sourced glasses in comparison to EMP-analysis of pyroxene sourced from Tongariro, illustrating a crystallisation fractionation of plagioclase and partially clinopyroxene. (pyroxene data from Donoghue (1991) and plagioclase data from Hitchcock (2005).

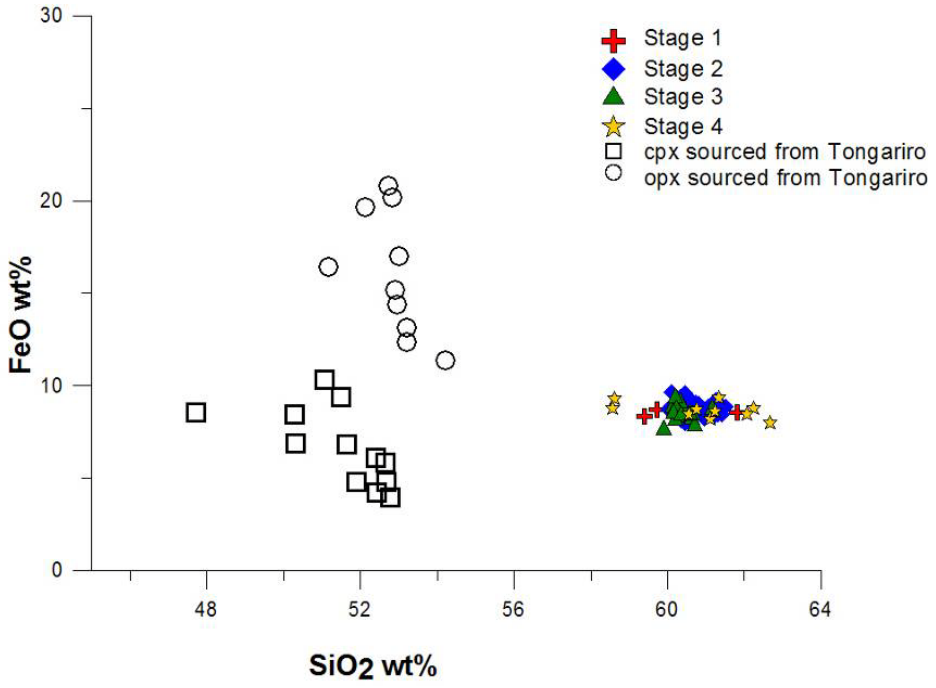

Figure 5.1.31: Major oxide analysis SiO_2 vs. FeO of Ngauruhoe-sourced glasses in comparison to EMP-analysis of pyroxene sourced from Tongariro, illustrating a crystallisation fractionation of clinopyroxene (pyroxene data from Donoghue (1991)).

The plots in Figure 5.1.32a and b, illustrate the chemical variation of the major oxides throughout the known history of Mt. Ngauruhoe. The gaps between these clusters of points represent time breaks by weathered tephras or distinctive soil horizons, as described in section 5.1.4. All oxides show very uniform ranges in values over the last ~5000 cal. yrs. B.P., which allows the confident distinction of Ngauruhoe sourced-tephras from those of other vents of the TgVC. This also implies that the magmatic system has been stable over the last 5000 years.

Focussing only on Stages 2 and 3 (Figure 5.1.33), SiO_2 and Na_2O wt.% increase at around 2890 cal. yrs. B.P. and decrease at 2810 cal. yrs. B.P.; MgO and CaO show a corresponding opposite change at these times. The first of these changes occurs with the largest eruption known from Ngauruhoe (dark purple layer) and finishes at the end of the large-scale eruptions of Stage 2.

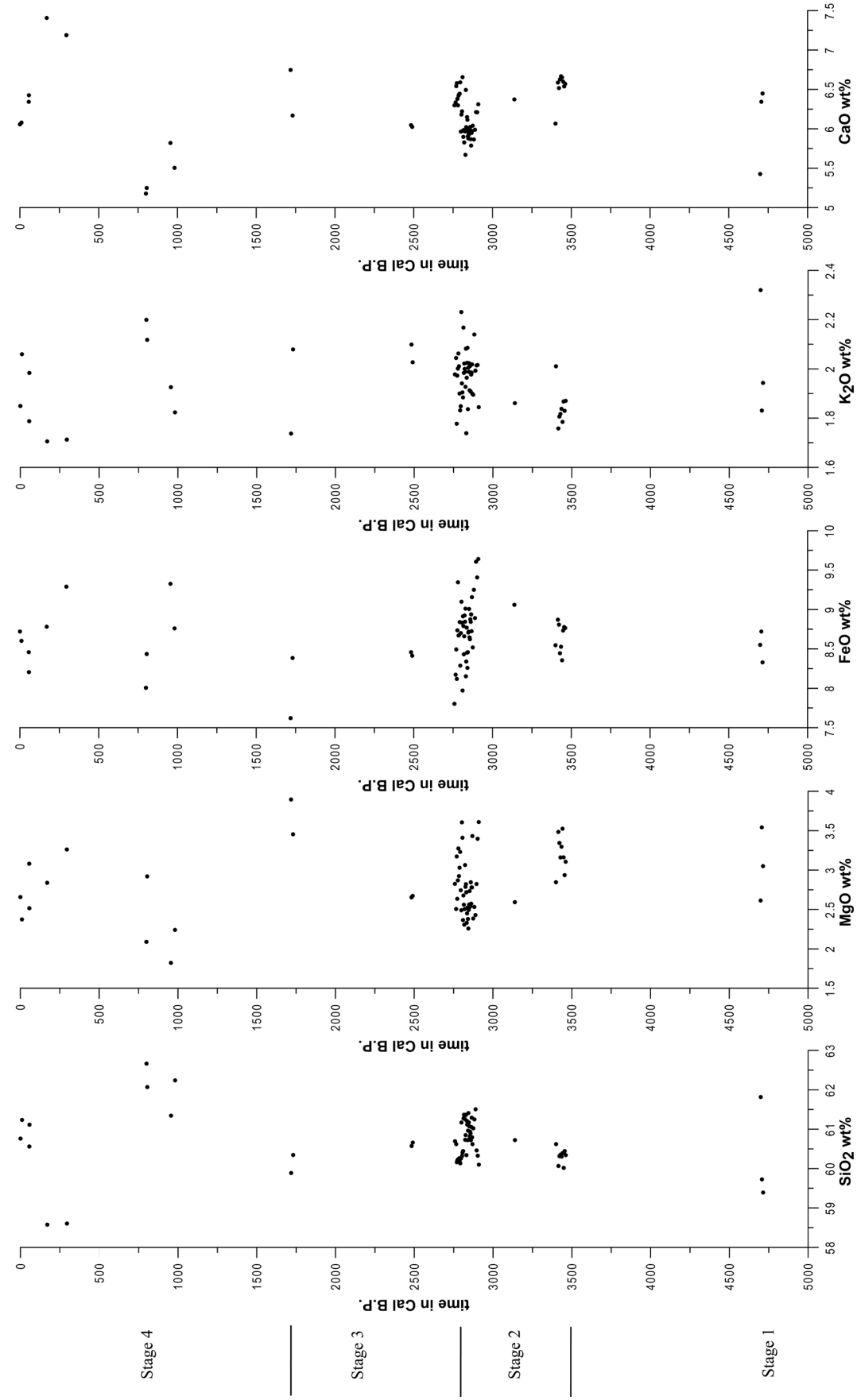

Figure 5.1.32a: Major oxides vs. time throughout the complete tephrochronological record from Ngauruhoe

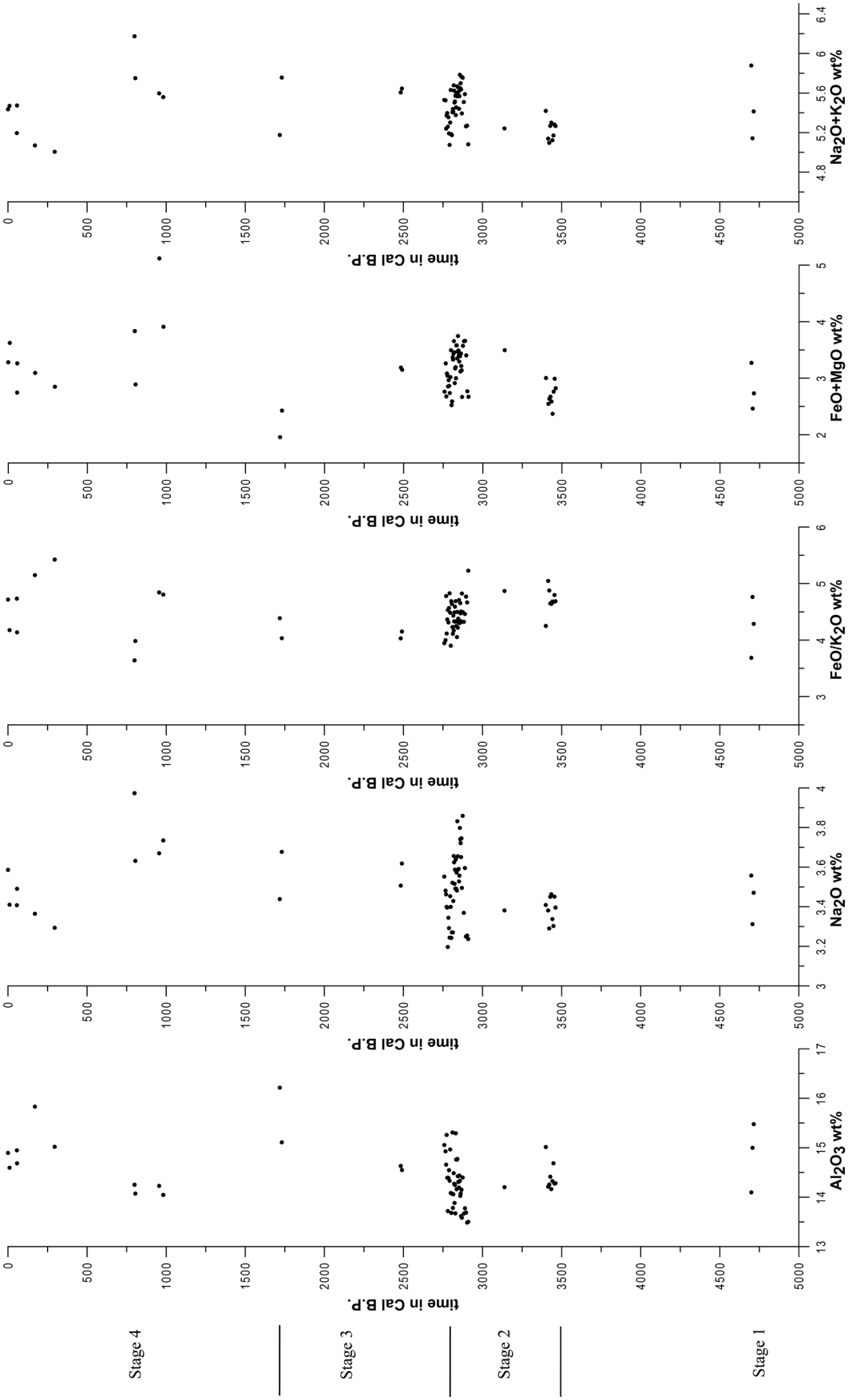

Figure 5.1.32b: Major vs. time throughout the complete tephrochronological record from Ngauruhoe

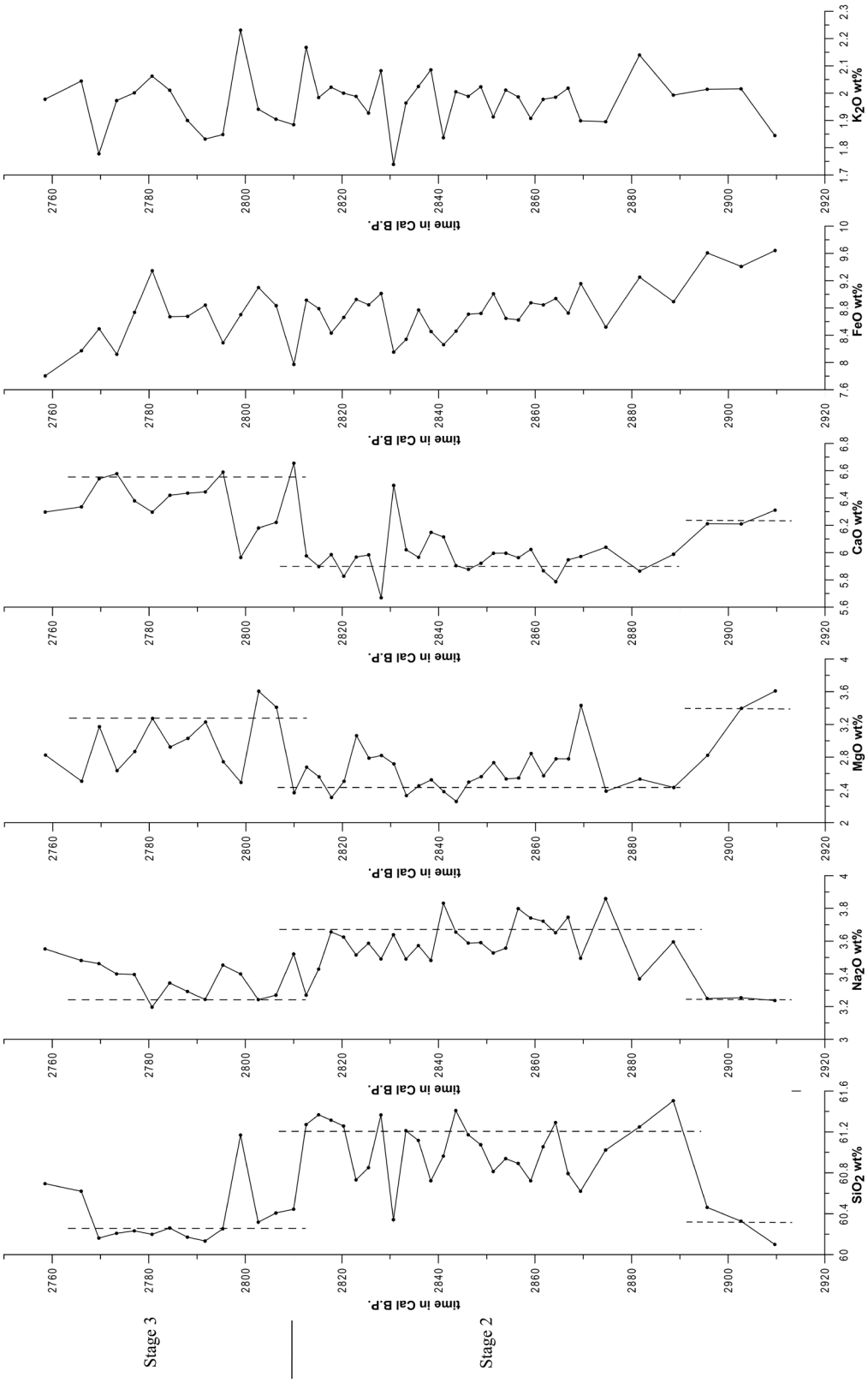

Figure 5.1.33: Major element composition of the distal profile at Location 12 in the time range from 2910 – 2760 cal yrs B.P. representing the upper part of stage 2 and lower part of stage 3

5.1.7.2. $^{87}Sr/^{86}Sr$-Isotopes

To help interpret the magma generation conditions and the subsequent processes that magmas underwent as they rose through the crust to eruption, $^{87/86}$Sr-isotopes of 12 selected samples representing the stratigraphic range of Ngauruhoe tephras were analysed, (Table 5.1.3). $^{87}Sr/^{86}Sr$ is stored in the mantle and the crust, and evolves over time (Rollinson, 1993). The $^{87}Sr/^{86}Sr$ values of MORB ranges between 0.70240 to 0.70256 in the Pacific area (Saunders *et al.*, 1988) and 0.70356 to 0.70750 for young volcanic arcs (McDermott and Hawkesworth, 1991). The estimated $^{87}Sr/^{86}Sr$ for bulk Earth varies between 0.7045 and 0.7052 and depleted-mantle values range between 0.7026 to 0.70321 (Rollinson, 1993). Magmas passing through the crust may interact with the host rocks, with the degree of assimilation depending on their residence time. Magmas with very high $^{87}Sr/^{86}Sr$ ratios have experienced large degrees of crustal assimilation, whereas those passing rapidly through the crust in days to a few months have near-mantle values.

Table 5.1.2: $^{87}Sr/^{86}Sr$-analysis of selected samples through Ngauruhoe's tephrochronological record arranged in chronological order.

Stage	Age in cal yrs B.P.	Location	Stratigraphic position	$^{87}Sr/^{86}Sr$-values	Sample number
4	1954 A.D.	Ngauruhoe crater	Within the crater lower part	0.705429	Janine 1954
4	56	Loc. 63 Pukekaikiore		0.705048	208 54
4	295	Loc. 63 Pukekaikiore	Just below Burrell Lapilli	0.704954	208 97
4	955	Loc. 63 Pukekaikiore		0.704727	208 65
3	1717	Loc. 67 South crater	Just below Taupo Pumice	0.705227	308 55
3	2493	Location 12/Desert Rd.		0.704794	407 60
3	2768	Location 12/Desert Rd.		0.70478	407 56
3	2808	Location 12/Desert Rd.		0.704792	407 47
2	2865	Location 12/Desert Rd.		0.704886	407 26
2	3416	Location 12/Desert Rd.		0.704831	407 14
1	4170	Loc. 6 Mangatepopo Valley car park	below MtF, top part of PF	0.705526	606 30
1	5590	Location 12/Desert Rd.	Black ash 2	0.705407	108 58

Age calculations presented in section 5.1.4.

Stage 1 and the 1954 sample (Stage 4) (Table 5.1.3 Figure 5.1.34) show the highest $^{87}Sr/^{86}Sr$-values, indicating the strongest levels of interaction with the crust. This is

consistent with their major element chemistry as described above. All samples analysed from Stage 2 show relatively low $^{87}Sr/^{86}Sr$ ratios, implying rapid passage through the crust to eruption. This finding corresponds both with the depositional and chronological evidence of extremely frequent and large eruptions during the period of highest magma-production known from Ngauruhoe and with the narrow range in major element chemistry described above. As described in sections 5.1.4.3 and 5.1.4.4., the youngest tephras of Stages 3 and 4 are only deposited in proximal areas, indicating low eruption volumes and is probably related to many isolated small magma batches. Sample 308 55 represents the youngest tephra from Stage 3 (location 67 at South Crater) and its high $^{87}Sr/^{86}Sr$-value indicates a strong crustal involvement. Tephras of Stage 4 show a trend in $^{87}Sr/^{86}Sr$-values that imply greater interaction with the crust over time.

Overall, 3 cycles are recognisable in the isotope ratio plot (Figure 5.1.34). The youngest two cycles begin with lower $^{87}Sr/^{86}Sr$-values (0.704727), indicating a possible pulse of fresh magma input from the mantle with little crustal involvement. Following this, magma evolves in the crust and $^{87}Sr/^{86}Sr$ ratios of erupted magmas rise to higher ratios (0.705526 w%). The oldest tephras known from Ngauruhoe (~4700 cal yrs B.P.) are interpreted as the end of such a recharge-evolution cycle and could be associated with the Mangamate Tephras sourced from 'proto'-Ngauruhoe.

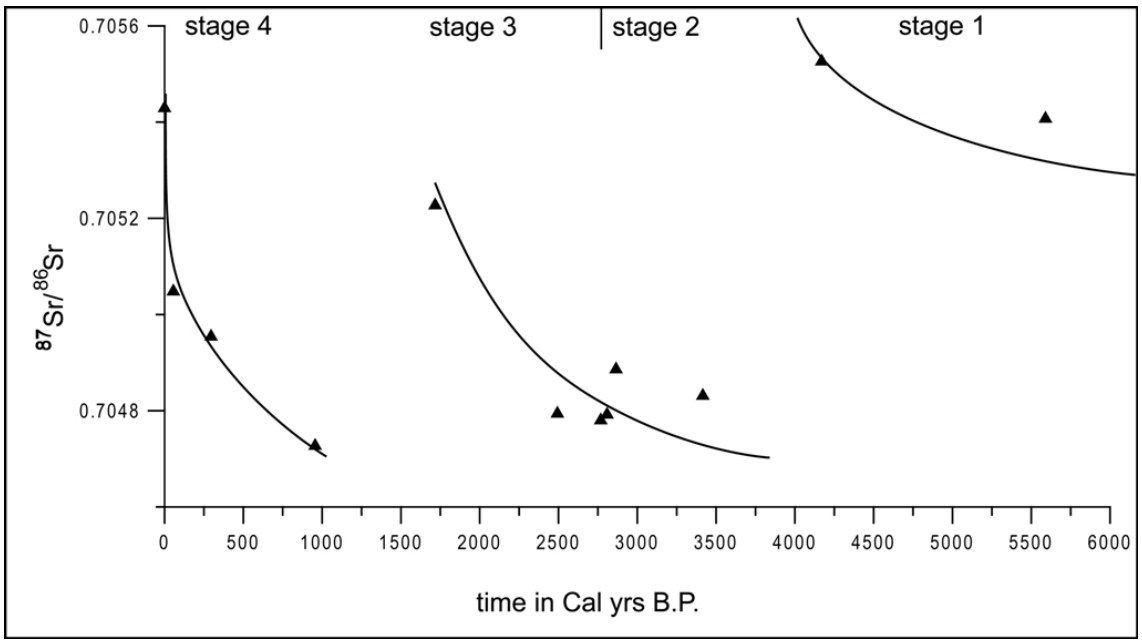

Figure 5.1.34: $^{87}Sr/^{86}Sr$-isotope analyses of selected Ngauruhoe-sourced tephras over time. Continuous lines represent possible cycles in crustal involvement of the magmatic system beneath Ngauruhoe.

Hobden *et al.* (1999, 2002) distinguished five groups of lavas from Ngauruhoe. Group 1 includes the oldest lava flows that predate the Taupo Pumice eruption. Group 2 flows were erupted on the north-western flanks of Ngauruhoe and combine lavas erupted both before and after the Taupo Pumice event. Groups 3 and 4 were erupted post-Taupo, and Group 5 represents historical events erupted between 1870 and 1975.

Ages for Groups 3-5 defined by Hobden (1997) and Hobden *et al.* (2002) remain valid. The newly defined age of Ngauruhoe in this study means that Group 1 and 2 lavas extend to older ages than earlier thought. Group 1 was considered by Hobden *et al*. (2002) to correlate to the oldest tephra of the Mangatawai Formation, which is here now correlated to Stage 2. Group 2 lavas could not be accurately correlated to the new stratigraphy, but recognising that they were dominantly erupted before the Taupo Pumice, they are here assigned an age of ~ 2800 cal. yrs. B.P., overlapping with the transition from stage 2 and 3 in the tephra record.

The $^{87}Sr/^{86}Sr$-isotope analyses of the lava flows overlap with equivalently aged tephras (Figure 5.1.35). The oldest lavas show very low $^{87}Sr/^{86}Sr$-ratios, indicating little crustal involvement and rapid magma ascent. Group 2 lavas, on the other hand, show a wider range in $^{87}Sr/^{86}Sr$ isotope composition. This may relate to the imprecision in the age determinations for these flows. The lower value could, for example, be from an older unit (overlapping with Group 1) and the highest value could be closer to the age of the Taupo Pumice. Group 3 lavas, erupted after the Taupo Pumice have higher $^{87}Sr/^{86}Sr$ ratios, similar to those tephras below the Taupo Pumice at Loc. 67 (stage 3), indicating longer periods of crustal storage and assimilation.

Overall, the Group 1-3 lavas and the corresponding stage 2-3 tephras show a trend of increasing crustal involvement over a period of at least 1700 years. A new apparent cycle with a similar, although steeper, evolutionary trend over *c*. 1000 years is displayed by the Group 4-5 lavas and Stage 4 tephras. This steeper evolutionary trend corresponds with smaller erupted volumes over this period; these potentially show the influence of crustal assimilation more strongly.

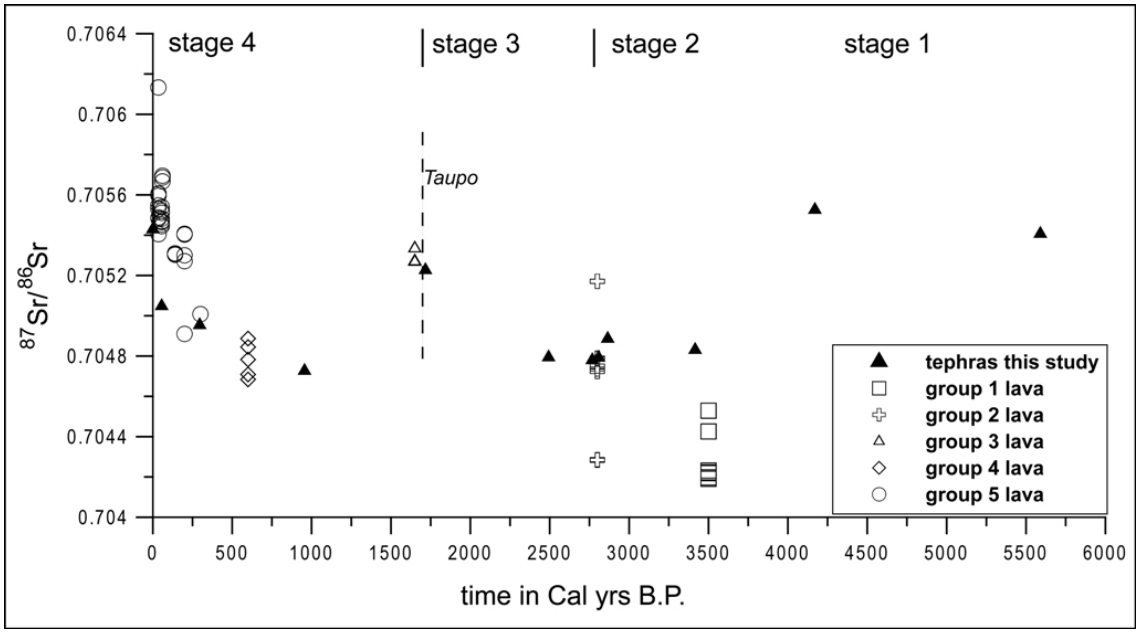

Figure 5.1.35: $^{87}Sr/^{86}Sr$-isotope analyses of selected Ngauruhoe-sourced tephras and lavas over time. Tephra data are from this study, while Group 1-5 lava data are from Hobden *et al*. (1999; 2002).

5.2. Red Crater

5.2.1. Introduction

Red Crater (1886 m) is one of the youngest vents of Mt. Tongariro and is situated 2.8 km north-east of Ngauruhoe (Figure 5.2.1). The cone is formed of scoria and agglutinate (Thompson *et al.*, 1966; Topping, 1974). Intruding dykes of basaltic andesite composition are exposed on the eastern and southern inner crater walls. The Red Crater vent system is assumed to have been active since ~10 ka (Bardsley, 2004) and its historic activity is summarised by Gregg (1960b), starting with eruptions in 1855. In 1890 lava flows were erupted into the northern Oturere Valley and lavas flowed into Oturere Valley, Central and South Craters possibly during eruptions in 1893 (Speight, 1908 in Gregg (1960b). The latest eruption from Red Crater (RC) possibly occurred in April 1926 according to Thompson (1926) in Gregg (1960b), although Johnston (1997) considers this event to have been from Ngauruhoe. Hence, the last proven eruption from Red Crater occurred in 1911 (Gregg, 1960; Thompson *et al.*, 1966) with a series of phreatic explosions widening the crater area and forming a line of explosion pits.

Lava flows derived from Red Crater were divided by Topping (1974) into 2 groups: six flows emplaced before the Taupo Pumice eruption and five following it. According to Bardsley (2004), the six pre-Taupo lava flows also predate the scoria cone. The oldest, the andesitic Oturere lava flow, is the largest at 6.5 km long, and between 370 to 640 million m^3 in volume (Hobden, 1997; Stevens, 2002). According to Topping (1974), this lava flow has an age between 11 135 cal. yrs. B.P. (Mangamate Tephra is not exposed on top of the flow) and 2568 ± 508 cal. yrs. B.P (Fergusson and Rafter, 1959). Five lava flows were deposited after the Taupo Pumice and Topping concluded that the lava flow into the northern Oturere valley is the oldest, followed by that into the south-western extension of Oturere flow, Central Crater and finally the flow into South Crater. The post-Taupo lava flows may have been erupted during the late 19^{th} century as described above. The younger lava flows are basaltic 53.0-53.7 wt% SiO_2, while the

older units are andesitic (59.1 – 61.1 wt% SiO_2; Hobden, 1997). An average magma production rate from Red Crater was calculated by Hobden (1997) to be 0.1 km^3/ka.

Figure 5.2.1: Red Crater in the foreground and Ngauruhoe in the background as seen from the north-east, the lava flow in the right foreground is one of the late 19th Century lava flows from Red Crater.

Topping (1974) described at least two tephras derived from Red Crater within the upper Oturere Valley: a greyish brown medium to very coarse lapilli within the Ngauruhoe Formation, and a red, medium and coarse ash within the Mangatawai Formation. In addition, Topping (1974) described several white and yellow distinctive hydrothermal-clay-rich marker horizons within the Oturere Valley and assumed them to be phreatic tephras sourced from Emerald Lakes and/or Red Crater. The Emerald Lakes are small explosion craters north-east of Red Crater (Figure 5.2.2.).

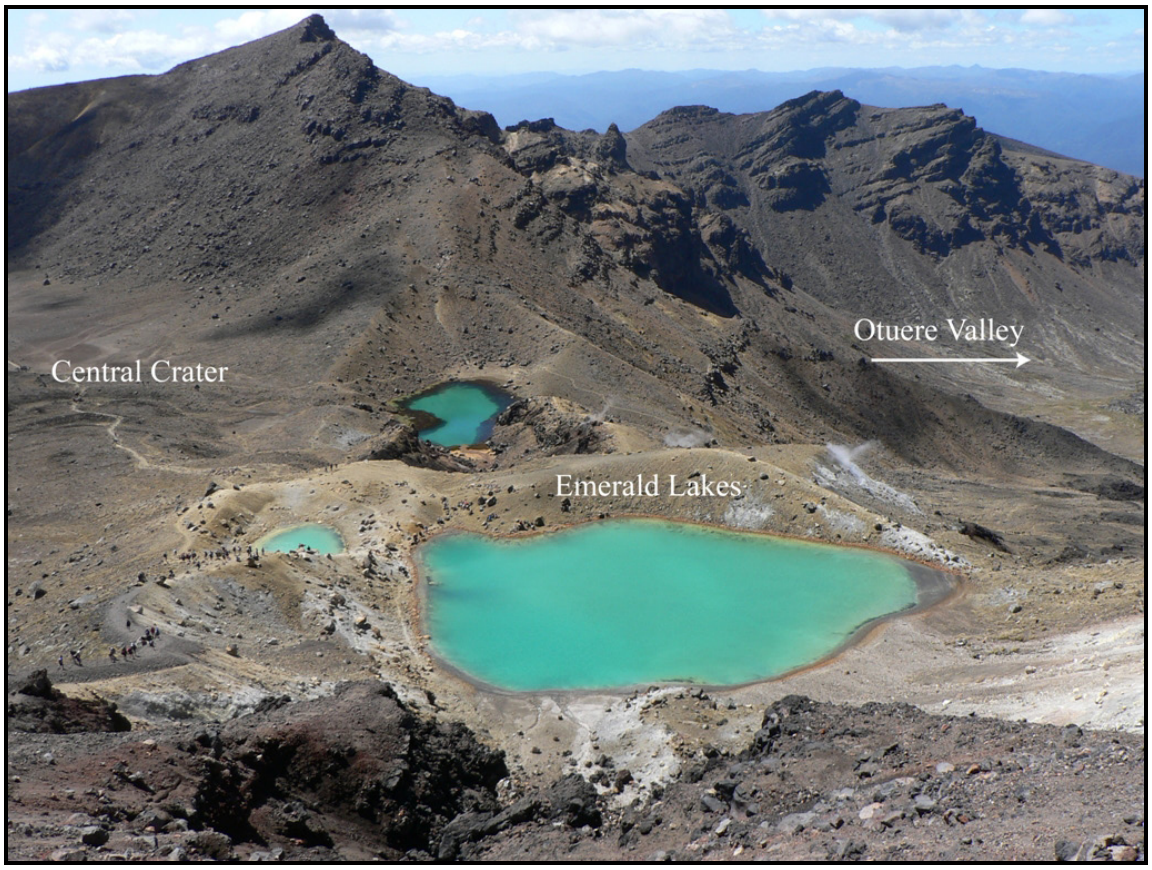

Figure 5.2.2: Emerald Lakes explosion craters as seen from Red Crater.

5.2.2. Red Crater tephra sequence

In this study, discrete tephras derived from Red Crater (RC) were found in soil sequences on the northern face of Pukekaikiore (Loc. 63) interbedded between the Ngauruhoe and Tufa Trig Formations (Figure 5.2.4.). In total 14 RC tephras were recognised. One unit was erupted prior to the 295 cal. yrs. B.P. Burrell Lapilli (Mt Taranaki). The other 13 tephras were erupted post-Burrell Lapilli with calculated ages shown in Appendix 5. The tephras vary between 3 and 95 mm thick, although the thickest are strongly weathered and appear to be accumulated deposits from several eruptions. Depending on the grain size and apparent eruption style (Chapter 7), the colours of the tephras range from white to light grey with grain sizes varying from very fine to coarse ash; some units contain up to 10 mm diameter lapilli (Figure 5.2.3).

Figure 5.2.3: Three discrete tephras sourced from Red Crater. The lower tephra indicates an initial phreatomagmatic stage shown by a light grey 2-3 mm thick tephra. The upper two tephras indicate a transition into a drier magmatic eruption (Chapter 7).

In addition to these units, RC-sourced glass fragments also occur in older deposits at Loc.12, mainly within the Mangatawai Formation Stages 2 and 3 units. The oldest identified Red Crater-sourced tephras are around 2880 cal. yrs. B.P.

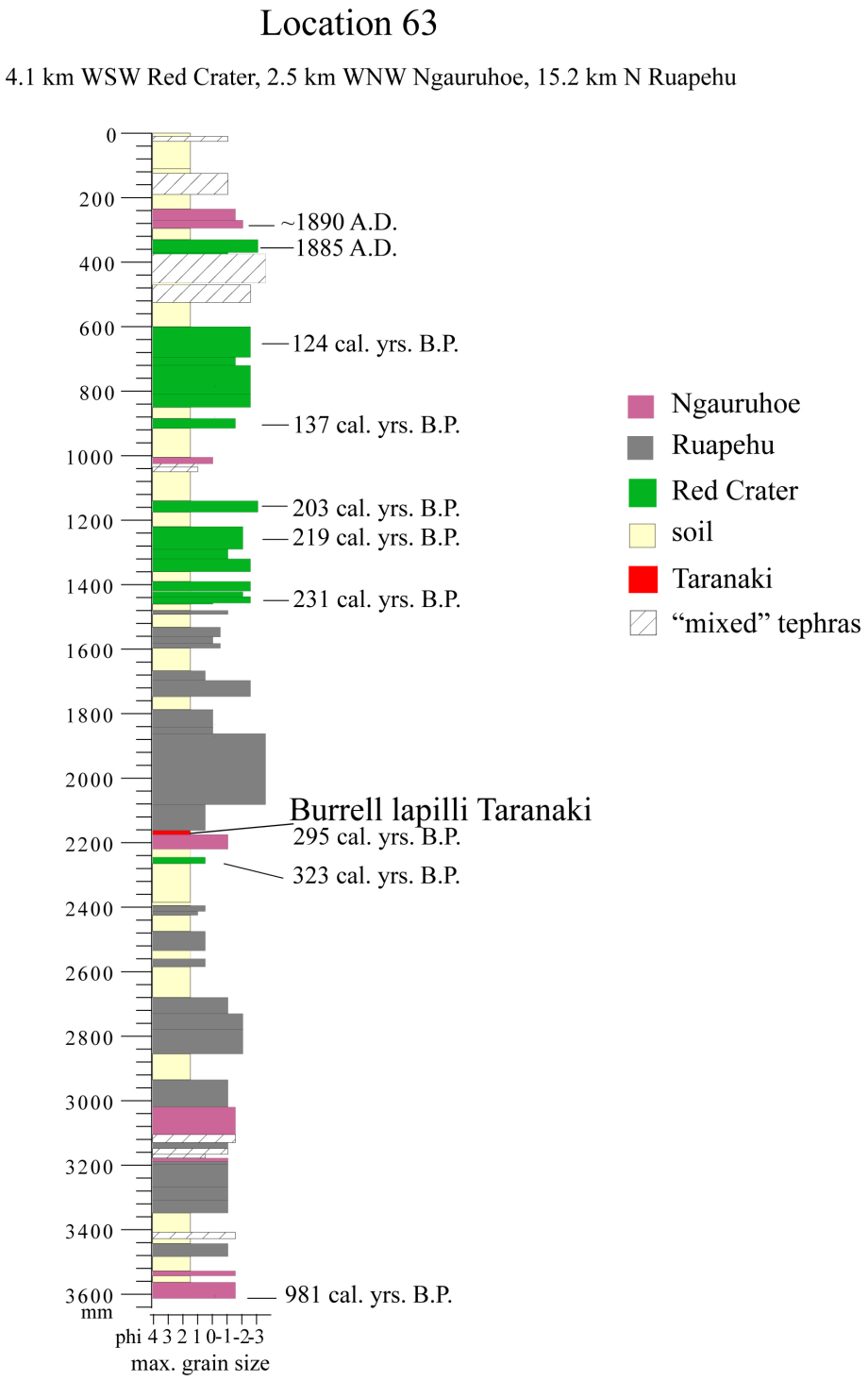

Figure 5.2.4: Stratigraphic profile of Location 63 at Pukekaikiore. Red Crater-sourced tephras are drawn in green while other TgVC-sourced tephras are shown in grey. The red tephra represents the 295 cal. yr. B.P. Burrell lapilli sourced from Mt. Taranaki. The hatched units contain glass shards from several TgVC sources (and probably indicate secondary re-distribution) while the pale yellow layers represent soil accumulations.

Within the Oturere Valley, two locations were described in post-Taupo Pumice sequences (Fig. 5.2.5). At Loc. 65 (~ 3.5 km southeast of RC, Fig. 5.2.4A) a white to pale grey, clay-rich tephra of ~50 mm thickness was identified as the 295 cal yrs B.P. Burrell Lapilli. At Loc. 66 (1.5 km east of RC) a very fine clay-rich, tephra had fresh glass with a chemical composition most similar to Ruapehu tephras (Figure 5.2.4B). At the same location, three very coarse tephras (30-200 mm thick) were identified, containing very coarse orange lapilli in a dark-grey fine-medium ash matrix. The clast sizes imply that they were derived from Red Crater.

Figure 5.2.5: (A) Loc. 65 at the northern edge of the Oturere lava flow ~ 3.5km south-east of Red Crater and 4.6 km east of Ngauruhoe. The white distinctive tephra is the 295 cal. yrs. B.P., Burrell Lapilli. (B) Loc. 66 at the northern edge of Oturere lava flow 1.5 km east of Red Crater and ~3.5 km north-east of Ngauruhoe. The distinct white layer here is Ruapehu-sourced, based on it geochemical composition.

5.2.3. Lithological componentry of Red Crater

Tephra from Red Crater described by Bardsley (2004) contained lava and wallrock lithic fragments and scoria clasts, along with rare quartz xenoliths, lithics with pumice inclusions and free crystals of plagioclase, hypersthene and olivine (Figure 5.2.8). Those analysed here contained plagioclase (plg), clino- and orthopyroxene and olivine. Plagioclase appears as clear and white, mostly broken crystals, in some cases with small

inclusions, and plg tends to be the most dominant crystal component in Red Crater tephras (Figure 5.2.6). The exceptions are, however, the youngest samples, where pyroxene is dominant, particularly in the smallest crystal size fractions. Both opx (hypersthene) and cpx (augite) occur, with the latter dominating in most samples. Cpx occurs as elongate euhedral crystals while opx crystals are often broken and rounded. Olivine is present only in 57% of the samples, occurring as colourless to pale green broken crystals.

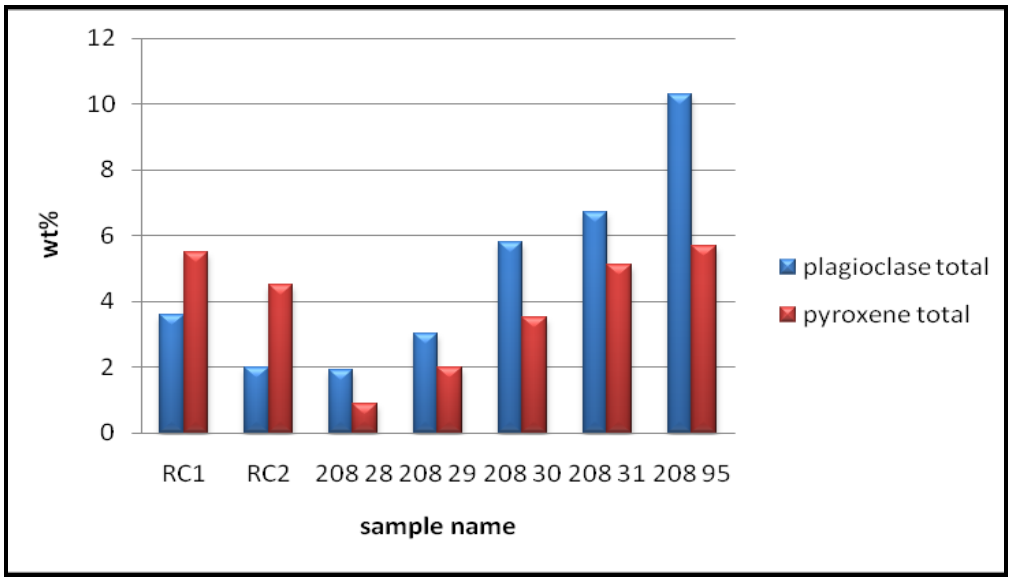

Figure 5.2.6: Plagioclase and pyroxene modal counts for Red Crater-sourced tephras. Samples RC1 and 2 are from the crater rim of Red Crater while samples 208 28 – 95 were collected at Location 63 and are in stratigraphic order from the oldest to the youngest.

Volcanic glass is the dominant component of Red Crater tephras and can be differentiated into (1) black (tachylite) and (2) clear pale-yellow to dark-brown glass (sideromelane) (Fig. 5.2.7). The ratio between lighter and darker glass appears to depend on eruption styles, as discussed further in Chapter 7. The oldest samples from Loc. 63 (Pukekaikiore) profile as well as the two youngest samples from the crater rim show higher contents of black glasses (41.8 to 54.4 vol.%) with only 2.0 to 28.9 vol.% of lighter glass, while other tephras analysed are dominated by lighter glass (>53.7 vs. <19.5 vol.%). Additionally the wt% of the black glass increases in smaller grain sizes.

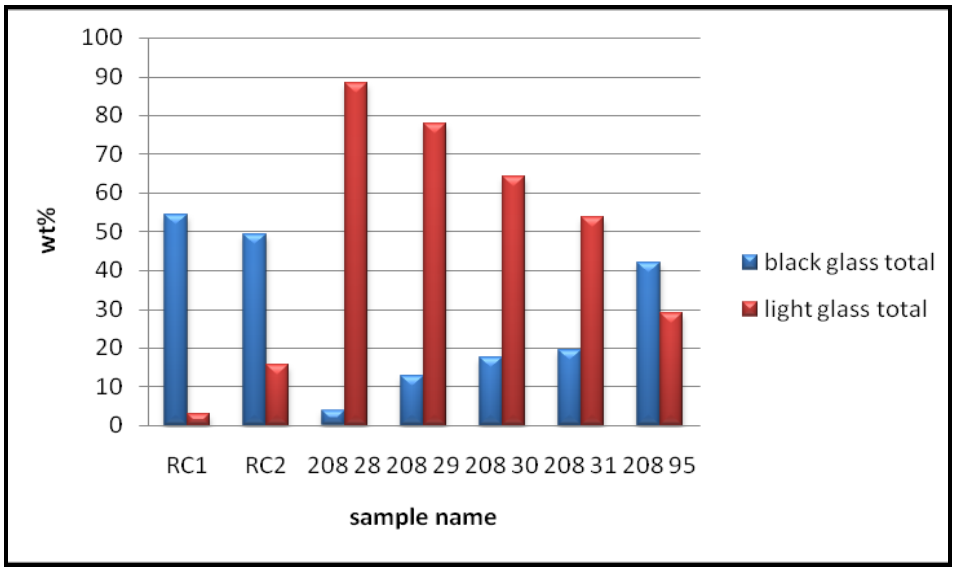

Figure 5.2.7: Modal proportions of light versus black glass in Red Crater-sourced tephras. Samples RC1 and 2 are from the crater rim of Red Crater while samples 208 28 – 95 were collected at Location 63and are in stratigraphic order from the oldest to the youngest.

Lithics are present in all of the Red Crater-sourced tephras and consist of underlying basement rocks (metagreywacke) but also cognate lithics, along with recycled glass and scoria.

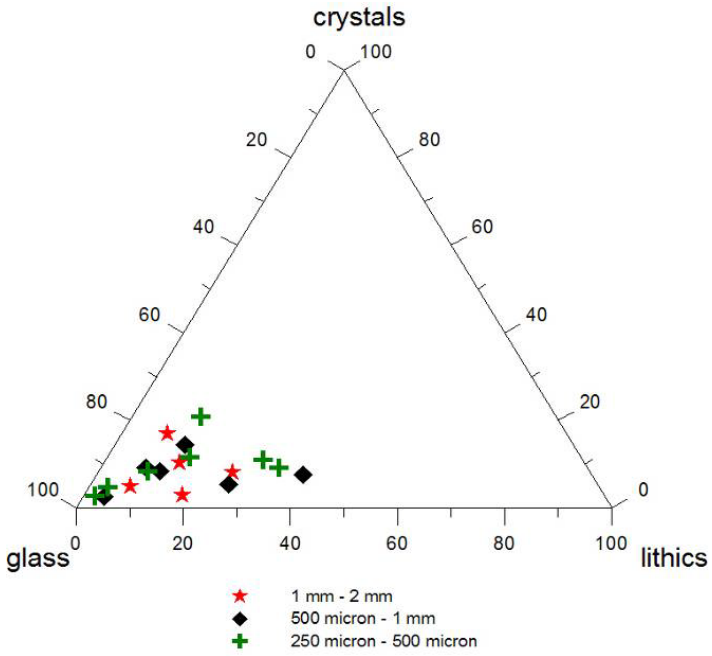

Figure 5.2.8: Discrimination plot of the main components glass, lithics and crystals for Red Crater-sourced tephras for three different size fractions in wt%. The glass values are the most dominant component in all samples and all fractions.

5.2.4. Geochemistry

The major element composition of eruptions produced from of Red Crater was obtained from volcanic glass of prehistoric eruptions and compared to crater-wall deposits that are likely to be of historic age. Red Crater sourced tephras have only been identified at Loc. 63 on the northern face of Pukekaikiore.

5.2.4.1. Major elements

The glass analysed from Red Crater contains a large proportion (possibly up to 60% by volume) of microlites that consist mainly of plagioclase and pyroxene. The crystallisation thus can influence the composition of the residual glass.

The major oxide values of glasses from historic tephras (samples from the crater rim) are higher but along a similar trend to those of prehistoric eruptions, with the exception of Na_2O (Fig. 5.2.9). The trends of MgO, CaO and Al_2O_3 abundances indicate fractionation of clinopyroxene and olivine (Figure 5.2.9 C-E).

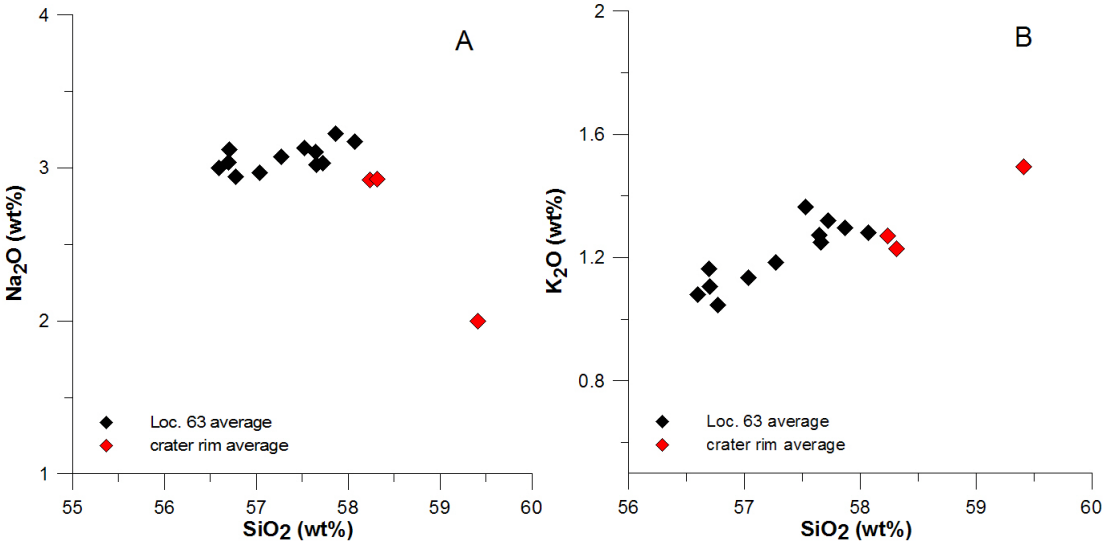

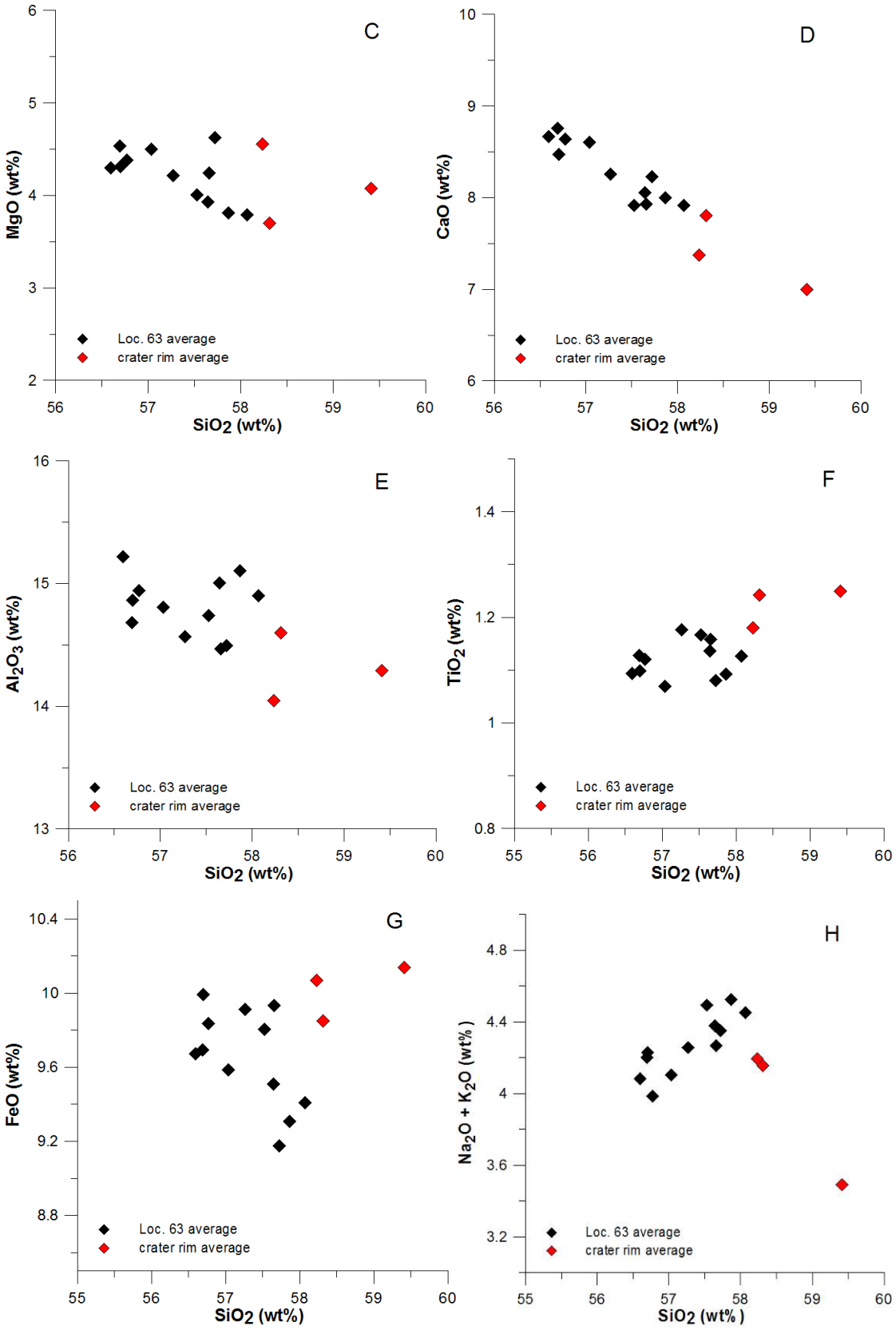

Figure 5.2.9: Major oxide composition of volcanic glass sourced from Red Crater.

The tephras sourced from Red Crater at Pukekaikiore were deposited between approximately 320 cal. yrs B.P. and 1911 A.D. (Fig. 5.2.10). These indicate a single trend of magma evolution over time from Red Crater, although strong variations imply that eruptions are generated from isolated and individual small magma pockets with differing evolutionary paths.

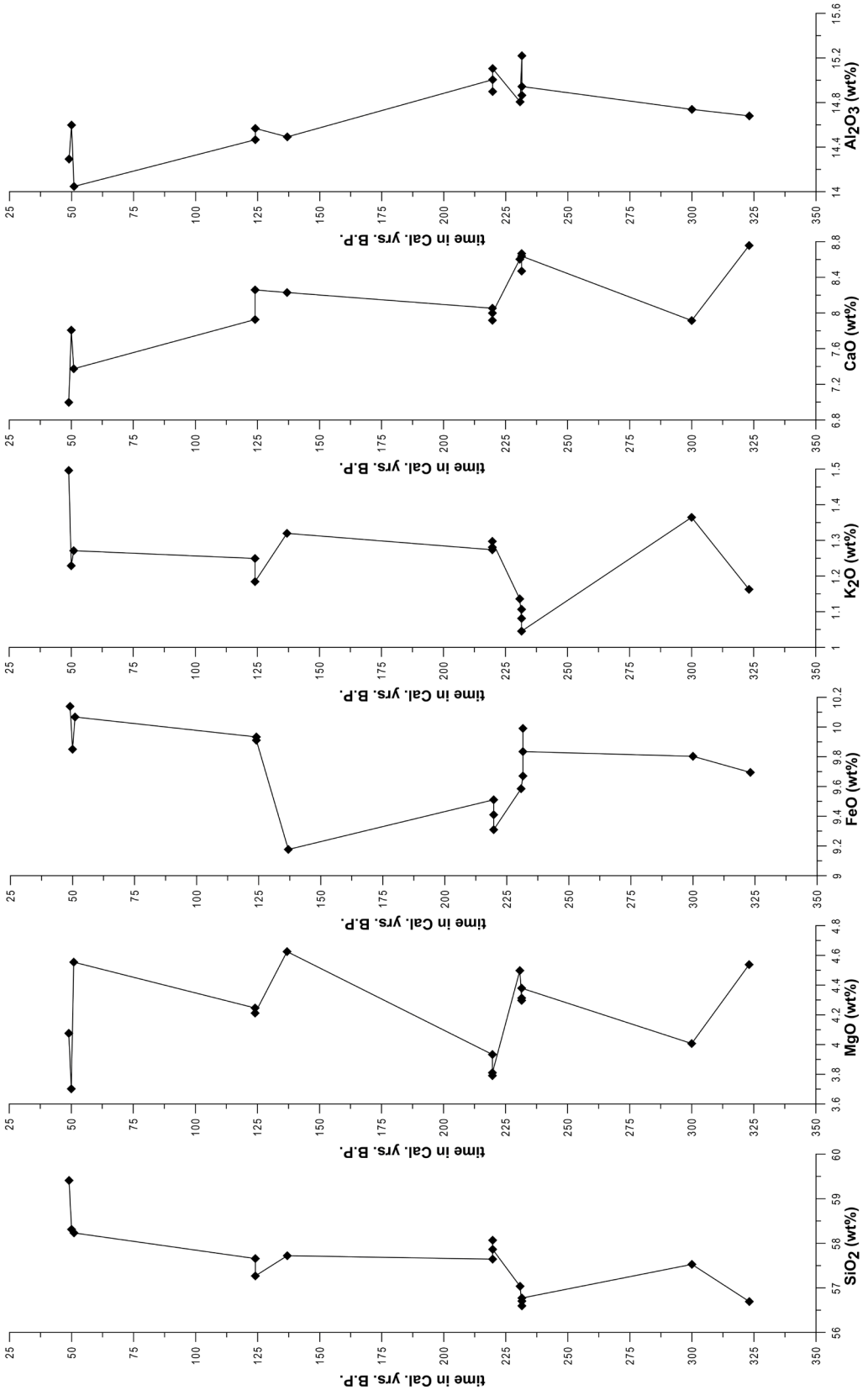

Figure 5.2.10: Major element chemistry of volcanic glass from discrete tephras of Red Crater over time (Loc. 63)

5.3. Te Maari Craters

5.3.1. Introduction

The Te Maari Craters are situated on the north-eastern slope of Mt. Tongariro and consist of at least three craters which become younger towards the south. The lower Te Maari Crater is a circular 400-500 m wide and 60-80 m deep depression at an altitude of 1345 m (northern rim) to 1420 m (southern rim) and is surrounded by a series of up to six concentrically distributed lava sheets, individually up to 4 m thick (Figure 5.3.1) (Basher, 2005). Topping (1974) described a lava flow north of the lower Te Maari Crater, which terminates at a set of older explosion craters. Here, the Waimihia Tephra (probably actually the Stent Tephra, see Chapter 3) and parts of the Papakai Formation overlie the flow, suggesting an age of the lava between 11 165 ± 31 to 6834 ± 44 cal. yrs. B.P. Several eruptions of this vent were observed in the last few hundred years by Maori (Cowan, 1927) and the first written records are of a steam or ash eruption in 1839, probably from lower Te Maari Crater, as observed by J.C. Bidwill (Gregg, 1960b).

Figure 5.3.1: Lower and upper Te Maari Craters view to the north-east toward Lake Rotoaira and beyond to Lake Taupo.

The upper Te Maari Crater was formed during an eruption in 1869, and was subsequently modified by a further event in 1886 (Gregg, 1960b). In 1890 this crater consisted of three "small and irregular-shaped craters", "from which steam was constantly rising" (Hill, 1891). Further eruptions of the upper Te Maari Crater occurred in 1892, 1893 with a final event recorded in November 1896. According to Thompson, 1928), a later eruption occurred in 1928 releasing black "steam". The 1890's eruptions formed the present 200 m-wide and 50 m-deep funnel shaped crater (Figures 5.3.2. and 5.3.3.). It is surrounded by a pyroclastic apron consisting of a grey to black, (altered in parts to red, orange, yellow and white), bedded agglutinated deposits, lapilli beds and poorly sorted angular breccia deposits passing down to a reddish grey, massive breccia deposit containing up to 2-3 m dense lava clasts (Hobden, 1997). In the crater centre is a hydrothermally altered vent structure (Basher, 2005). The pyroclastic apron overlies lava flows with multiple overlapping lobes distributed towards the north-west and into the lower Te Maari Crater. Dendrochronology revealed a maximum age for these lava flows as being at 1528 A.D., and a minimum age is from the oldest log from an overlying mudflow dated at 1764 A.D. (Topping 1974). The lava flows are all andesitic with SiO_2-compositions ranging between 57.5 to 60.2 wt% (Hobden, 1997). In thin-section, the upper Te Maari Crater breccias contain plagioclase > pyroxenes > glass, with the un-weathered glass typically being black (Basher, 2005).

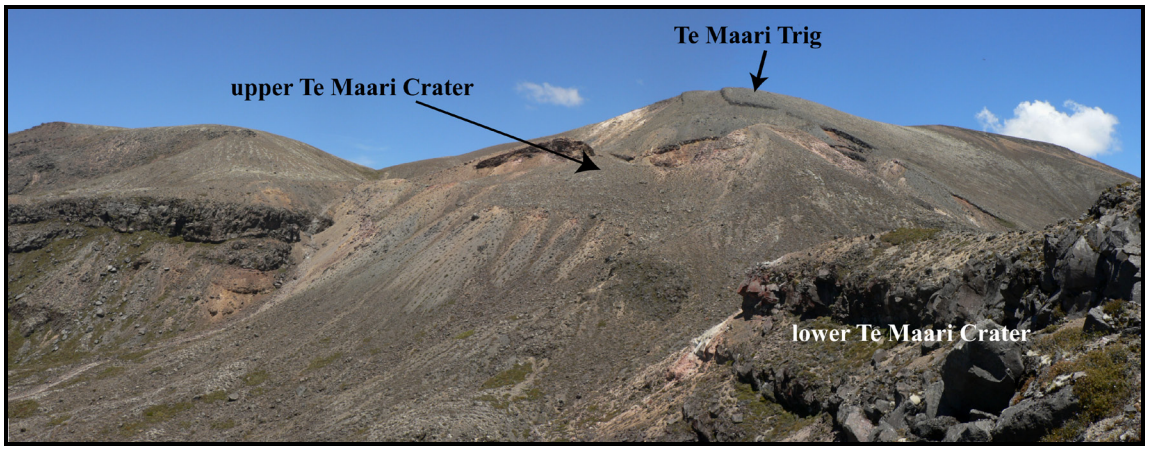

Figure 5.3.2: The lower Te Maari Crater in foreground left, viewed from the north. The upper Te Maari Crater is arrowed and spatter-fed lava flows from this have draped the surface into the lower crater.

Figure 5.3.3: Ash eruption of the upper Te Maari Crater probably during the 1890's (image: with permission from Museum of New Zealand Te Papa Tongarewa, Patrick Marshall Collection Reference: LS.004557).

Approximately 200-400 m north and down-slope of the lower Te Maari Crater, a third Te Maari crater is viewable consisting of a line of up to seven explosion pits along a fissure feature (Figure 5.3.4) (Gregg, 1960b; Topping, 1974; Basher, 2005). Nothing is known about the age of these features.

Figure 5.3.4: View down to the explosion pits, north of the lower Te Maari Crater (facing northward).

Tephras derived from the Te Maari Craters were described by Topping (1974) within the Mangatawai and Ngauruhoe Formations. In addition, he also interpreted the Rotoaira Lapilli as being sourced from Te Maari, implying that the lower craters have a possible minimum age of 16 501 ± 939 cal. yrs. B.P. [NZ1559] (Topping, 1973). New results from Basher (2005) and Griffin (2007) suggest that North Crater is a more likely source for the Rotoaira Lapilli. Nairn *et al.* (1998) postulated that two members of the Mangamate Formation could be associated with the Te Maari Craters: the Poutu Lapilli (11 165 ± 31 cal. yrs. B.P. (oxcal)) and the Te Rato Lapilli (11 242 ± 578 cal. yrs. B.P. (oxcal)). The thickest deposits of the Te Rato Lapilli were identified immediately east of the lower Te Maari Crater and lie beneath breccias that may represent part of the Poutu Lapilli episode (Nairn *et al.*, 1998).

5.3.2. Results of this study

To complete analysis of all the known recent tephra sources in the TgVC, Te Maari lapilli deposits and pyroclastic-surge deposits were sampled from the eastern part of the pyroclastic apron surrounding the upper Te Maari Crater (Figure 5.3.5).

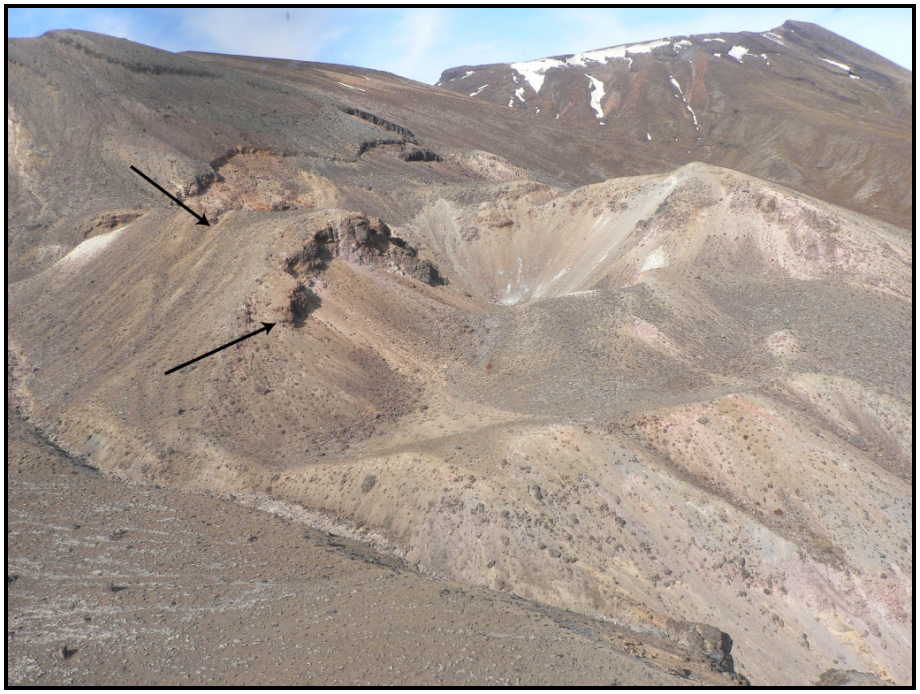

Figure 5.3.5: Upper Te Maari Crater seen from the north-east. Arrows represent the locations sampled.

This was probably formed between 1892 and 1896, as described above. The deposits consist of a series of orange-brown, strongly weathered units, which each show a basal clast-supported angular coarse-medium lapilli (>20 cm) to thin (0.5-3 cm), firm, laminated, and matrix-supported, fine-medium ash (Figure 5.3.6 A+B). These appear to reflect alternations between scoria fall and surge/fine ash-fall deposits (Figure 5.3.6 C+D).

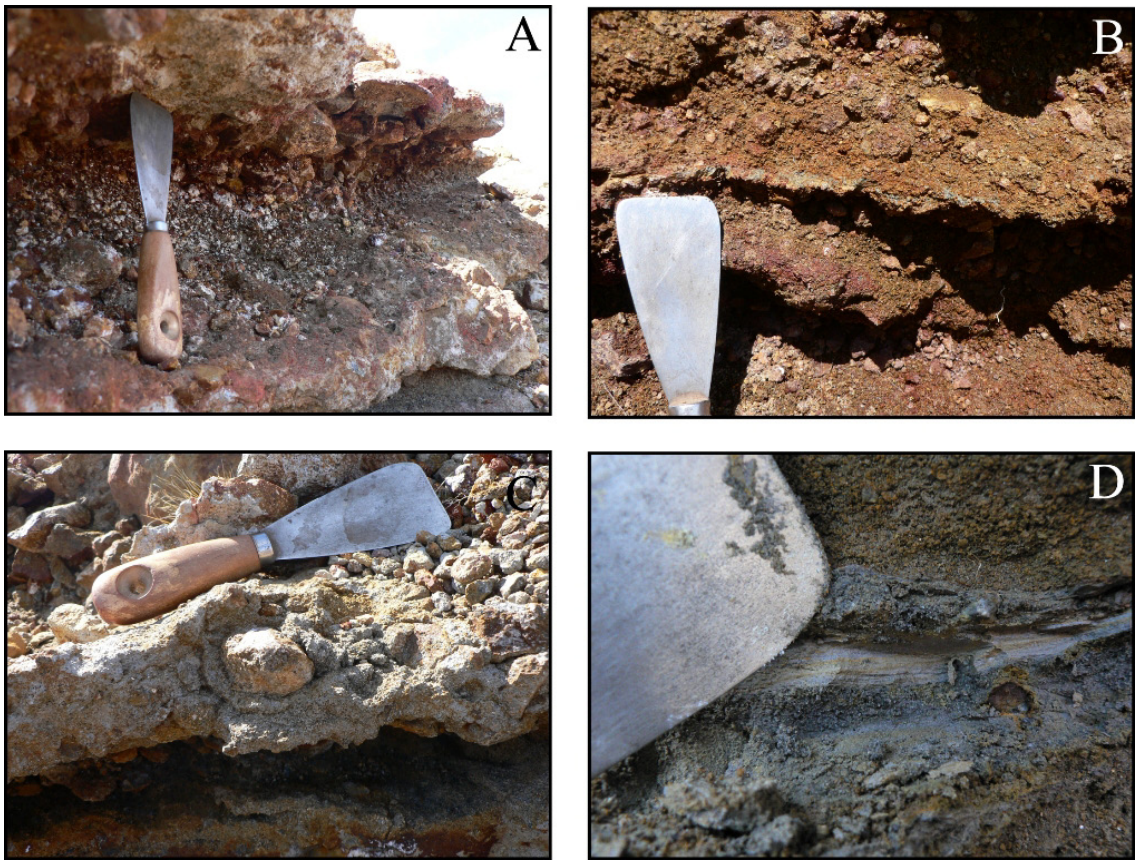

Figure 5.3.6: Pyroclastic deposits surrounding the upper Te Maari Crater, (A and B) show alternating deposits of coarse clast-supported lapilli and laminated compact, matrix-supported fine ash: (C) weathered poorly sorted, fine-medium ash, faintly laminated on a fine scale and containing bomb/block bedding sags; (D) dune-like bedding of a fine-medium ash, pyroclastic-surge deposit.

5.3.2.2. Geochemistry

Volcanic glass was handpicked and analysed using the electron microprobe at University of Auckland. The upper Te Maari Crater pyroclastic deposits have distinctively higher SiO_2 contents than the other active TgVC volcanoes, ranging between 63.7 to 78.5 wt% (Figure 5.3.7), the latter tending toward values typically

found in rhyolitic glass. In addition, the FeO/K_2O-plot used here for chemical discrimination of the tephra sources within the TgVC, shows a similar composition to Mt. Taranaki (Figure 5.3.8). One sample is an exception, showing typical andesitic values of 10 wt% FeO and 2.7 wt% K_2O which may be an accidental lithic or may indicate that a large range in magma compositions was erupted from this site.

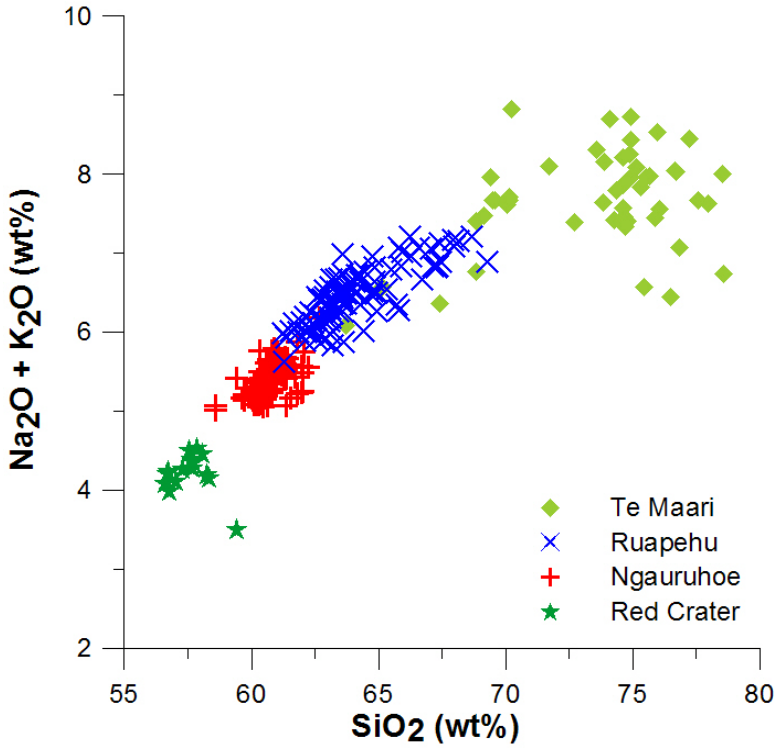

Figure 5.3.7: Total alkali silica discrimination diagram (after Le Maitre *et al.*, 1989) of analysed volcanic glasses showing rhyolite composition of the upper Te Maari Crater in comparison to the basaltic andesite to andesite composition of Red Crater, andesite for Ngauruhoe and andesite to dacite for Ruapehu.

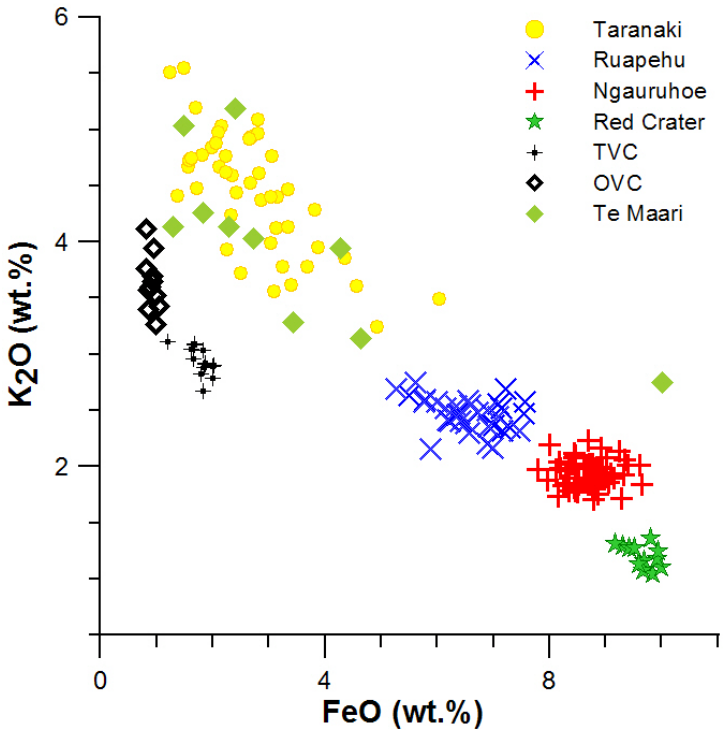

Figure 5.3.8: Volcanic glass chemistry of major elements from the four andesitic volcanoes Taranaki (yellow), Ruapehu (blue), Ngauruhoe (red) and Red Crater (green) in comparison to new and published data (see references in body text) from two rhyolitic centres TVC and OVC (black). The light green diamonds represent new results from Te Maari Crater illustrating the similarity to Mt. Taranaki-derived tephras.

The discrimination diagrams shown in Figures 5.3.9A-H, show the SiO_2 vs. the major elements analysed from the upper Te Maari Crater in contrast to the andesitic vents of the TgVC and Taranaki and the rhyolithic Taupo Volcanic Centre (TVC). In all diagrams the Te Maari samples show two batches of different magma compositions. These batches indicate a rapid transition from andesitic towards dacitic and rhyolitic composition and therefore more differentiated and evolved magma. As previous noted, the more andesitic sample (as seen in Figures 5.3.8. and 5.3.9. C, F and G) seems to be an accidental analysis of a recycled glass of older Tongariro tephras.

In comparison to the other vents of the TgVC, Taranaki and the TVC, this last eruption of Te Maari is most similar to the rhyolitic major element compositions of different tephras sourced from the TVC. Furthermore, the chemical trends in FeO, CaO, K_2O of Te Maari seems to evolve parallel to Taranaki without major overlapping, and are offset to higher oxide abundances at a given SiO_2. Also noticeable is the wider variation in the

Te Maari compositions, especially K_2O, Na_2O and MnO, while the andesitic sources tend to be more grouped and in a gradual transition from north to the south (changes in width of the rift system (TVC) and from the TgVC towards Taranaki.

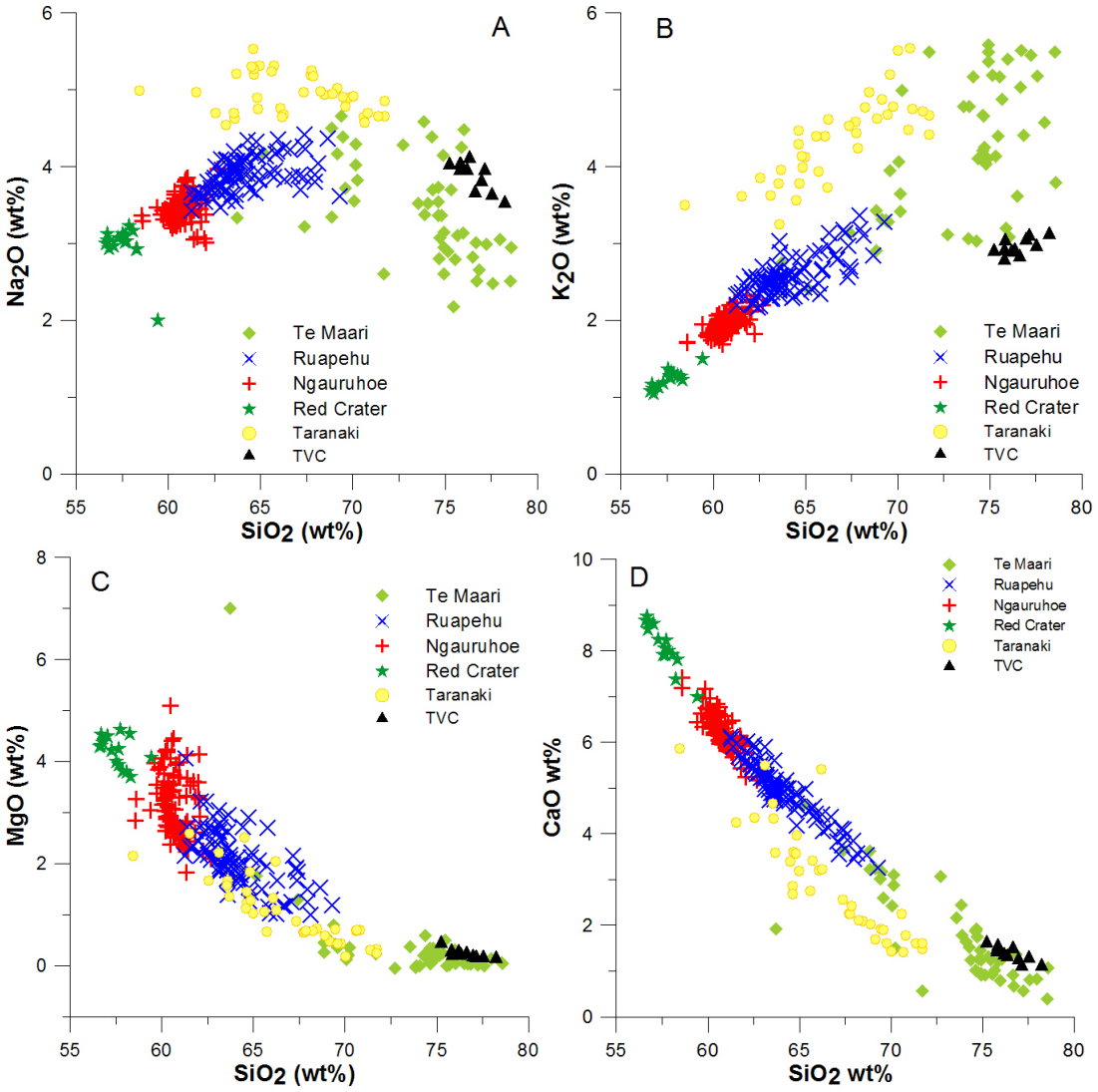

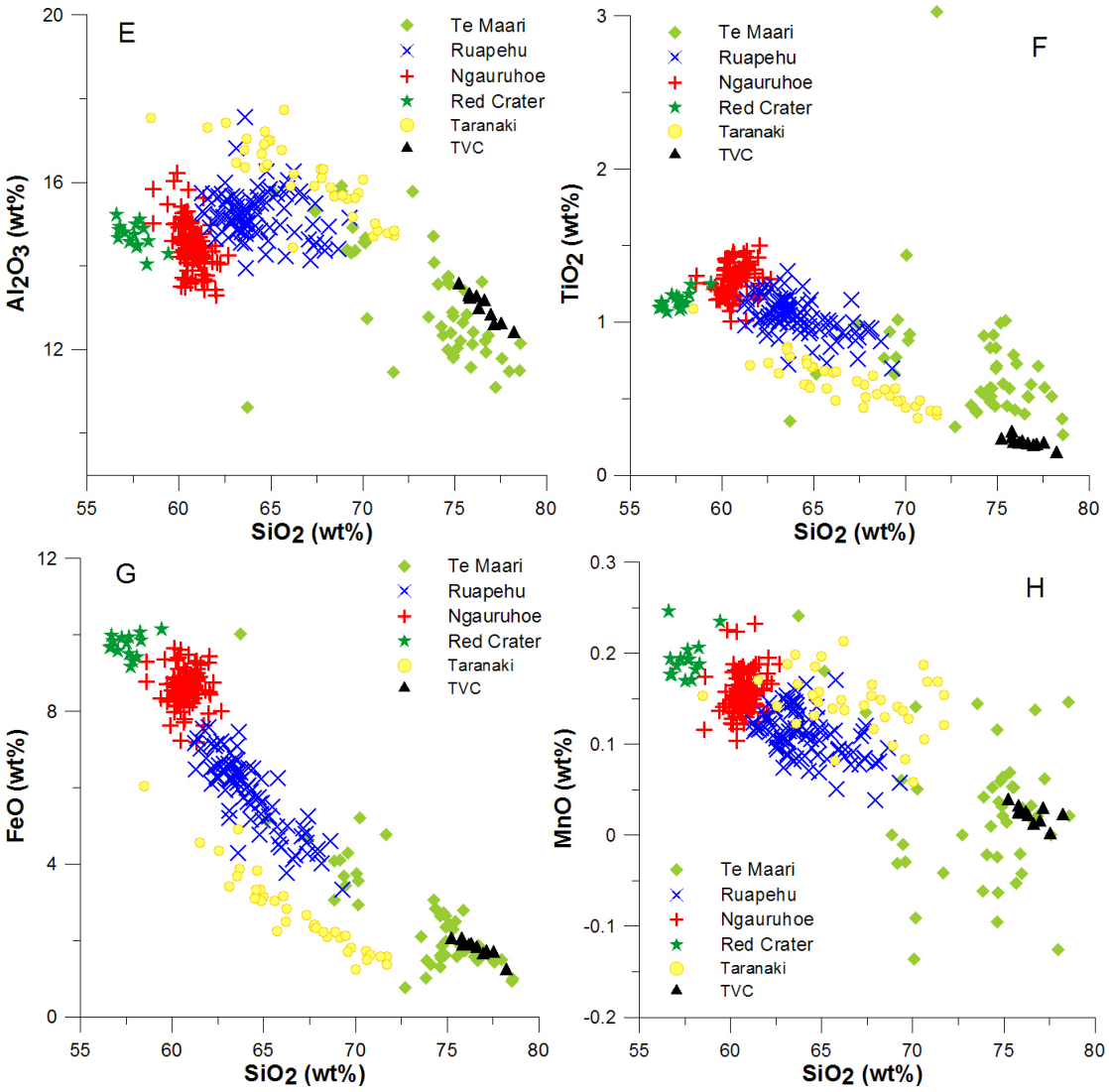

Figure 5.3.9: A-H: Average (Chapter 2) of major element composition vs. SiO_2 of volcanic glass comparing upper Te Maari with Ruapehu, Ngauruhoe and Red Crater but also to Taranaki and the TVC.

The results of the chemical major element analysis of the volcanic glass, lead to the conclusion that the last eruption from the upper Te Maari Crater was of a high silicic glass composition. The analysed glass shards look on the other hand andesitic, similar to Taranaki-sourced glass, with lots of microlites and a more blocky and compact shape unlike the fragile pumiceous clear and microlites poor rhyolitic glass shards of the TVC. This appearance and the chemical composition indicate a slow transition from an andesite to a rhyolite and imply a longer residua time in the crust. The high amount of microlites indicates a rapid decompression and fast ascent of the magma which could be caused by a tectonical shift within the rift system with a sudden release of the evolved magma batch.

As above noted, lavas from the Te Maari Craters are of andesitic composition. But lavas of dacitic compositions are described from the TgVC by Hackett (1985) for Ruapehu-sourced lava flows of the Mangawhero and Whakapapa Formations, by Hobden (1997), of lava flows from Tama 1 (Lower Tama Lake) with an age of 216 ± 14 ka - c.273 ka and Tama 2 (Upper Tama Lake) with an age of 209 ± 16 to 203 ± 11 ka and also by Griffin (2005) with a dacitic composition of North Crater lavas.

Chapter 6

Late Holocene tephras of Mt. Ruapehu

6.1. Introduction

Mt. Ruapehu (2797 m) is situated in the centre of the North Island of New Zealand and is the largest stratovolcano of the Tongariro Volcanic Centre (Figure 6.1.1). The present estimated volume of Mt. Ruapehu is 110 km^3 (Hackett, 1985; Hackett and Houghton, 1989) and the volcano is surrounded by a ring plain with an approximate volume of 100 km^3. The ring plain consists of pyroclastic, laharic and epiclastic deposits (Cole *et al.*, 1986; Hackett and Houghton, 1989) containing the most detailed stratigraphic record of the eruption history from Mt. Ruapehu. Throughout the period of historical observation, the active vent of Ruapehu has always been located beneath the c. 10 million m^3 Crater Lake. Donoghue *et al.* (1997) inferred that Crater Lake has existed for at least 3000 years.

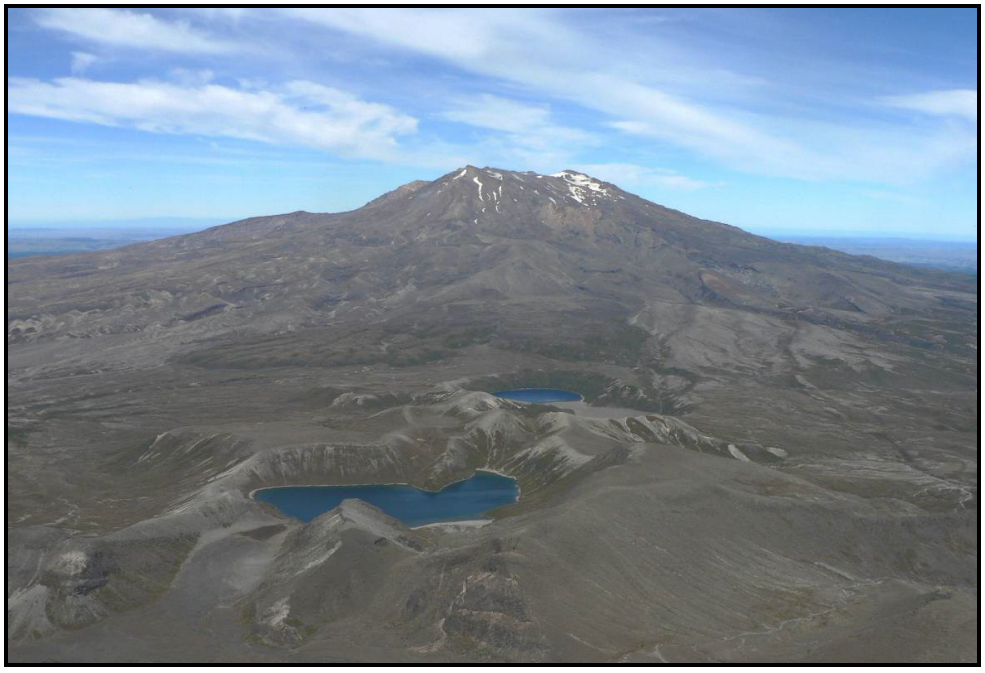

Figure 6.1.1: Ruapehu as seen from the north, with Tama Lakes in the foreground.

Four cone-building periods have been recognized in the history of Mt. Ruapehu (Hackett, 1985) (Table 6.1.1.). Te Herenga Formation comprises the oldest lavas (andesite) and pyroclastic breccias, making up the northern and north-western flanks of the volcano. The second oldest sequence is of a similar nature and make up the Wahianoa Formation which occurs on the south-eastern flanks. The Mangawhero Formation is exposed around the summit (except in the south-east), including basaltic to dacitic lava flows, and pyroclastic deposits that form the summit peak of Tahurangi. The youngest mapped units, the Whakapapa Formation, comprises lava flows (andesitic to dacitic) as well as pyroclastic-fall and -flow deposits (Hackett, 1985).

Table 6.1.1: Age in ka for Ruapehu cone-building formations.

Formation	Ages (ka yrs B.P.) Stipp, (1968)	Ages (ka yrs B.P.) Hackett (1985)	Ages (ka yrs B.P.) Hackett & Houghton (1989)	Ages (ka yrs B.P.) Lecointre *et al.* (1998)	Age (ka yrs. B.P.) Gamble *et al.* (2003)	Location
Whakapapa		0-15	0-15	0-14.7	???	summit and flanks of modern cone
Mangawhero	24	*c.*60-15	15-60	14.7 - 64	~23 Mangawhero B	north-eastern summit region Ohinepango+ Mangatoetoenui catchments
	36				~50 Mangawhero A	sout-west (Turoa skifield) Summit region
Wahianoa		*c.*60-120	60-100	64 - 120	120-150	south-east
Te Herenga	230	>*c.*130	>120	120 - >160	183-205 and suggesting 250	north and north-west

The oldest known activity from the TgVC is evidenced by andesitic pebbles identified within the O'Leary Conglomerate at the base of the Brunswick Formation (300.000 yrs B.P.) in the Wanganui Basin (Fleming, 1953; Pillans, 1990). According to Parish (1994) these pebbles have a mineralogical and chemical composition similar to that of Mt. Ruapehu eruptions.

6.1.1. Previous work

The first detailed mapping around the Ruapehu area was carried out by Grange *et al.* (1938), whose results were incorporated into maps published by Gregg (1960a). Grindley 91960), also produced a geological map of the area and identified and distinguished several groups of lava flows and lahar deposits around Ruapehu. Five lahar formations were defined: Murimotu, Hautapu, Waimarino and Rangipo of Pliocene age, and the informal unit 'Lahars of the Whangaehu River', which were produced in the Holocene. Gregg (1960b) summarised reports and observations of the historic eruptions from Ruapehu until 1959, while some particular events were described in more detail by Cotton (1945), Oliver (1945) and Reed (1945). Eruptions which have occurred since 1961 were described by Healy *et al.* (1978), Nairn *et al.* (1979), Cronin *et al.* (1996b; 1997a; 1998) and Kilgour *et al.* (2008; 2010).

Mt. Ruapehu edifice was first subdivided into formations by Hackett (1985), as described above. Later, the lavas were examined and subdivided into six petrological types (Cole *et al.*, 1986; Graham and Hackett, 1987), using geochemical and mineralogical compositions.

Cronin *et al.* (1997d) increased the number of rhyolitic tephras identified in the region, improving the local stratigraphic constraints. Donoghue (1991) and Cronin (1996) then developed stratigraphies of pyroclastic and epiclastic deposits on the ring plains surrounding the TgVC volcanoes. The youngest part of the stratigraphic record was defined by Donoghue *et al.* (1997) as the Tufa Trig Formation, comprising tephras sourced from Ruapehu post-1717 cal. yrs. B.P.

Most of the volcanic history of Mt. Ruapehu has been gleaned from the ring plain. Purves (1990) examined the lahar stratigraphy east of the volcano, defining five units of lahar deposits: Te Heuheu, Tangatu, Manutahi, Mangaio and Onetapu Formations. From this work and further mapping, Donoghue (1991) created hazard maps for the eastern ring plain, and Hodgson (1993) examined the record of lahars in detail along the Whangaehu River. Lahars generated from Ruapehu were examined from many perspectives following the 1995 eruptions of the volcano (e.g., Cronin *et al.*, 1997c;

Lecointre *et al.*, 1998 and Lecointre *et al.*, 2004a). Unusual mixtures of ice, snow, water and pyroclastic debris formed "snow or ice slurry lahars" during eruptions of Ruapehu where pyroclastic surges passed over and eroded glaciers and snowpack in 1995-96 (Cronin *et al.*, 1996b; Manville *et al.*, 1998; Rosenberg, 2000 and Lube *et al.*, 2009). Lahar research has continued in recent years with numerical mass-flow modelling for improvement of lahar hazard zones (Procter, 2009), updating risk assessment for skiers (Leonard *et al.*, 2008), examination of lahar behaviour in motion (Manville and Cronin, 2007), and detailed evaluation of geomorphic changes during large scale lahars (Procter *et al.*, 2010).

After Hackett (1985), only a few masters and bachelors thesis projects were carried out on mapping specific parts of the Ruapehu cone (e.g. Hales, 2000; Mitchell, 1997). Of these, Procter (2003) re-mapped and described the geology of the south-eastern sector of the volcano. Detailed petrological and geochemical work has continued with studies of Gamble *et al.* (1999; 2003) and Price *et al.* (2005) developing age and evolution models for Mt. Ruapehu magmas. Price *et al*. (2005) developed a model of a complex magma plumbing system beneath the volcano, where individual small magma batches undergo isolated assimilation, fractionation and crystallisation processes before erupting.

Numerous studies were carried out on the 1995-1996 eruptions of Mt Ruapehu. These include the physical volcanology of the eruptions (Cronin *et al.*, 1997c; Hurst and Turner, 1999; Cronin *et al.*, 2003; Bonadonna and Houghton, 2005; Bonadonna *et al.*, 2005b), along with environmental, agricultural and societal impacts (Coote *et al.*, 1997, Cronin *et al.*, 1997a; Cronin *et al.*, 1998; Cronin *et al.*, 2003; Hickling *et al.*, 1999 and Johnston *et al.*, 2000). Important to the dynamics of these and smaller subsequent eruptions is the omnipresent Crater Lake, and its underlying hydrothermal system (Hurst *et al.*, 1991, Christenson and Wood, 1993, Christenson *et al.*, 2010).

6.1.2. Historic eruptions

Ruapehu's historic eruption record starts from 1861 and includes 51 episodes of activity (Gregg, 1960b; Barberi *et al.*, 1992; Christenson and Wood, 1993; Werner *et al.*, 2006) (Figure 6.1.2). The eruption styles have been dominantly explosive, including phreatic and phreatomagmatic events when Crater Lake is present, along with strombolian and sub-plinian eruptions with no lake water or when there were high mass-eruption rates. The only effusive activity was recorded in 1861 and 1945. The eruption activity of Ruapehu seems to have increased since 1945, with a decrease in intensity of one VEI-magnitude.

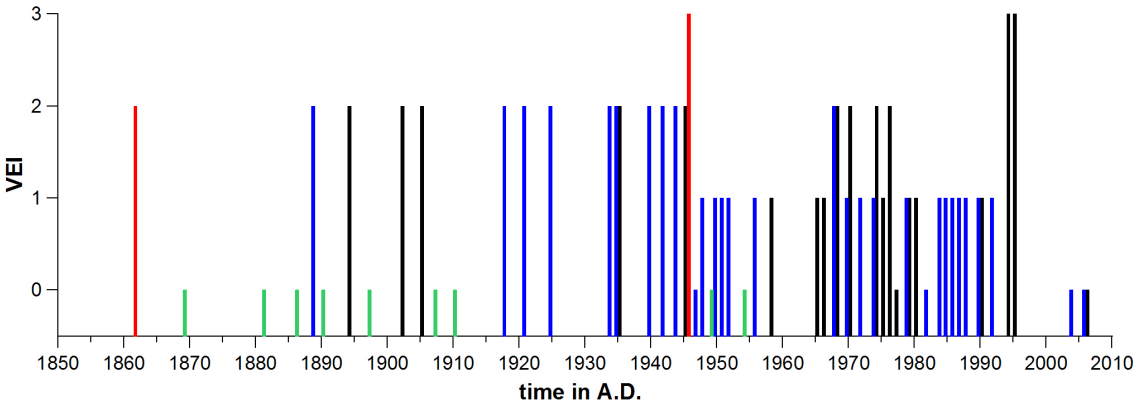

Figure 6.1.2: Magmatic/phreatomagmatic (black) and phreatic eruptions (blue) extrusive events (red),and addition crater lake steaming events (green) at Ruapehu between 1961 and 2007. References: Gregg (1960b); Barberi *et al.* (1992); Christenson and Wood (1993); Werner *et al.* (2006)Werner *et al.*, 2006 and GVP (www.volcano.si.edu)**.**

The first event of note observed from Ruapehu was on 13 February 1861, when a major lahar occured in the Whangehu River (Gregg, 1960b). Over the following years Ruapehu's Crater Lake was observed to be periodically steaming and short-lived phreatic and phreatomagmatic eruptions were reported most commonly when they were associated with ashfall or lahars (*e.g.*, 1903). The only event that has had a major effusive phase (except for possible dome-extrusion events in 1861 and 1996) was in 1945 (Cotton, 1945, Oliver, 1945, Reed, 1945, Beck, 1951) (Figures 6.1.3A and B). The 1945 eruption started on 8 March with steam rising from the Crater Lake and by 19 March a lava dome appeared within Crater Lake, before disappearing in an explosion the following day. On 7 May a larger tholoid appeared, along with explosive eruptions

ejecting rocks and fine ash over the next few days (Johnston, 1997). In the last week of June very fine sulphur-rich ash fell in Ohakune and by July the tholoid had started to fill the entire crater width (Figure 6.1.3A). The explosive activity increased in late August to September, when ash fell as far as Whakatane (193 km north-east), Hawkes Bay (140 km east and south-east) and Wanganui (~80 km to the south-west). By 16 September part of the crater floor had collapsed. After sporadic explosions and periods of quiet, the activity reached its maximum on 6 November (Beck, 1951), before declining over December and January 1946 and being followed by further sporadic ash eruptions between April to June 1946 and March to May 1947. According to Johnston (1997) the last reported ash fall was recored in Napier and Hastings on 6 December 1945, with the the latest explosion occuring on 15 December.

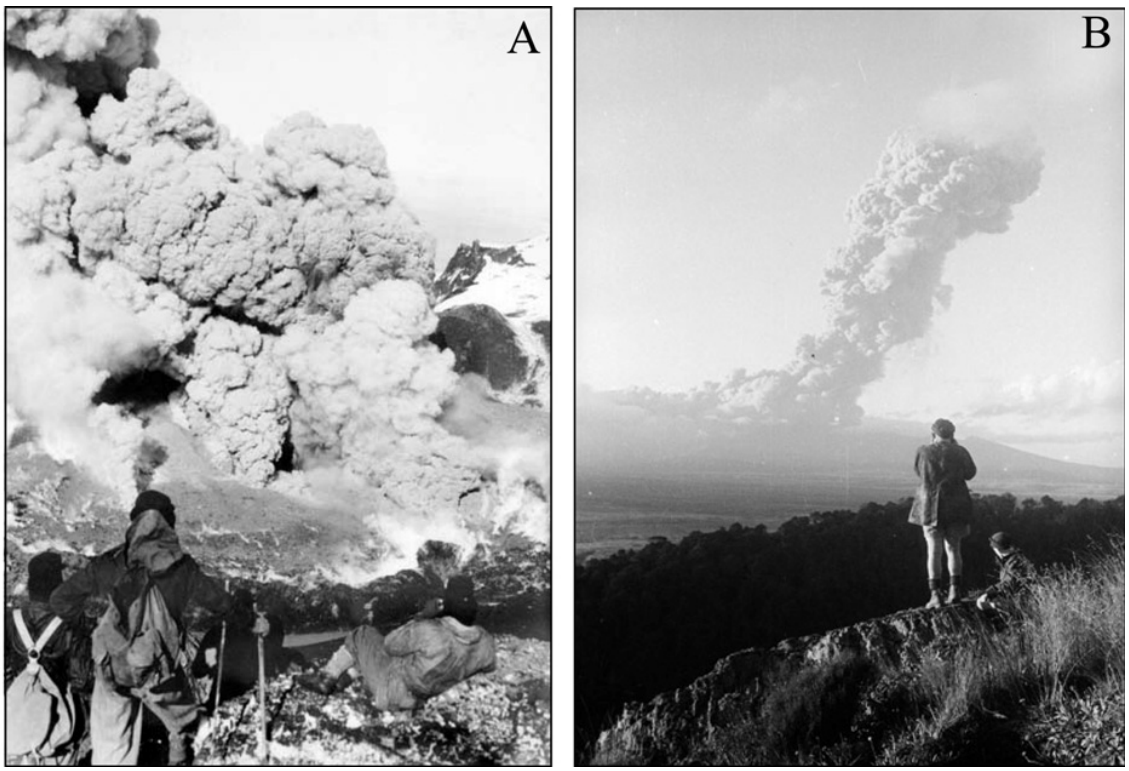

Figure 6.1.3: Ruapehu eruption 1945, A) lava dome within the crater in August 1945 with permission from "© Institute of Geological and Nuclear Sciences Limited [1945]" B) eruption cloud spreading over central North Island Image: with permission from the Alexander Turnbull Library, reference: 708-35mm-F, photographed by Bruce Valentine Davis.

On the 24th December 1953 the greatest New Zealand railway disaster occurred at Tangiwai, south-east of Mt. Ruapehu (Figures 6.1.4). At 8 pm local time, ice of the outer crater wall collapsed, releasing 340 000 m^3 of water into the Whangaehu River

(Healy, 1954). The lahar reached the Tangiwai Railway Bridge around two hours later (Gregg, 1960b, Neall, 1996) filling the channel to a depth of 7 m and with a peak discharge of 850 m^3/s (Healy, 1954). The flow destroyed the bridge supports immediately as the Wellington-Auckland express attempted to cross. The bridge collapsed under the train, and the engine and several carriages were swept downstream, killing 151 people. Five-ton blocks of concrete from the bridge were transported up to 55 m (Stilwell *et al.*, 1954), while one carriage was carried 2.4 km downstream (Neall, 1996). After this disaster, a lahar warning system was installed *c.* 12 km upstream of Tangiwai (the On Track Flood Gauge), which is still in use today.

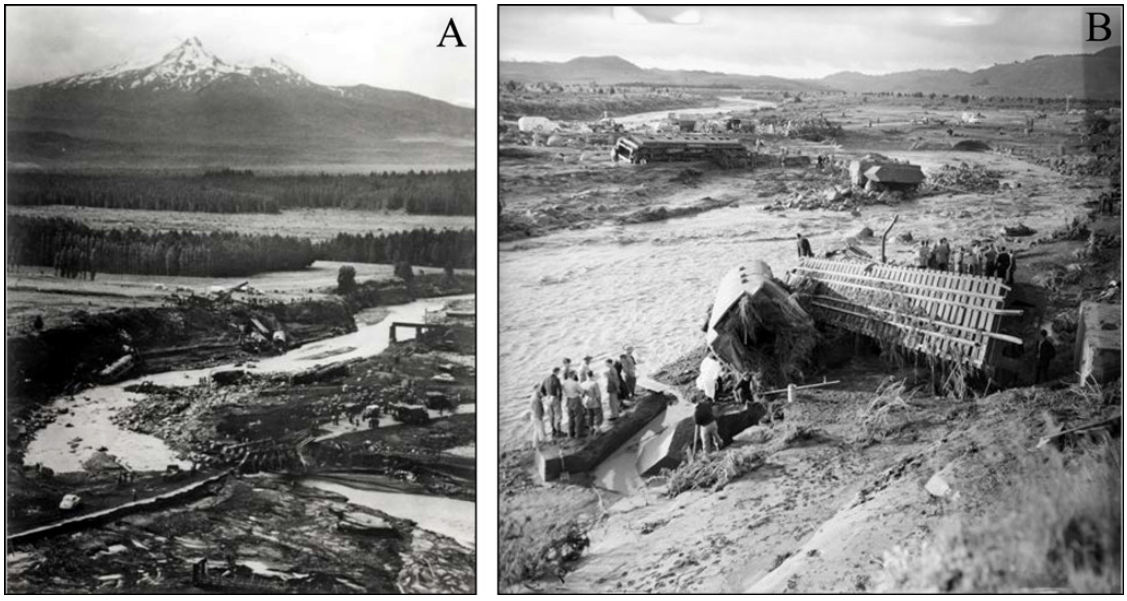

Figure 6.1.4: A) The lahar-destroyed bridge at Tangiwai on the 24th of December 1953 and Ruapehu in the background (image: Fairfax Sunday Newspapers New Zealand Limited) and B) the remains of the Wellington-Auckland express and the railway track on the 25th of December downstream of Tangiwai (with permission from the Alexander Turnbull Library, Morrie Peacock Collection (PAColl-4875), reference:MP-0059-10, photograph by Morrie Ronald Peacock).

Between 1959 and 1995, Ruapehu erupted 15 times with phreatomagmatic eruptions occurring in 1966, 1969, 1971, 1972, 1976 and 1978, and phreatic eruptions in 1968, 1973, 1975, 1979, 1980, 1982, 1988, 1989 and 1990 (Nairn *et al.*, 1979; Hackett and Houghton, 1989; Barberi *et al.*, 1992, Christenson and Wood, 1993). In some cases it has been difficult to determine if fresh magma has been involved in some of these smaller eruptions (e.g., 2007; Christenson *et al.,* 2010), and some of the historically listed phreatic events may have also been phreatomagmatic.

On the night of 22 June 1969, at around 0030hrs a phreatomagmatic eruption occurred from beneath Crater Lake. An initial blast occurred towards the north-west, generating several ice slurry lahars down the Whangaehu glacier (east) and into the Whakapapanui (north-west), Whakapaiti (north) and Mangaturuturu valleys (west). These were followed by an eruption that expelled up to 30% of Crater Lake. The Whakapapa ski-field on the north-western slope of Ruapehu was covered by a thick muddy ash layer (Healy *et al.*, 1978, Williams, 1989).

On the 24th April 1975 at 0350 hrs a large phreatomagmatic eruption occurred on Mt. Ruapehu which was first recognized when a lahar, travelling down the Whakapapanui stream, reached the Whakapapa Ski field at 0430 hrs. Large lahars occurred down into the Whakapapaiti, Mangaturuturu and Whangaehu Rivers. The lahar in the Whangaehu River reached the Tangiwai railway bridge at 0459 hrs, and reached 5 m above normal stream level. During this eruption sequence the entire summit area was covered with grey ash and lake sediment. Three days later, a further eruption produced a surge around Crater Lake, a lahar in the Whangaehu River and a fall deposit over the summit plateau. A dark ash column was observed up to 1000 m above the crater rim which drifted away to the north (Nairn *et al.*, 1979).

The eruption episode in 1995 began with phreatic eruption on 18 September. Further successively larger phreatomagmatic eruptions created snow-slurry lahars, surges and fall deposits, gradually emptying Crater Lake until 10 October. On 11 October a major sustained sub-plinian eruption began, that over 5 hours emptied the remaining water from Crater Lake (Figures 6.1.5 and 6.1.6). Up to 40 million m^3 of ash was distributed as far as Gisborne (220 km north-east). Another, 2-3 hour-long sub-plinian eruption occurred on 14 October, producing 5 million m^3 of ash that fell in a narrow south-east-oriented fan, beyond the east coast in Hawkes Bay (>150 km away) (Cronin *et al.*, 1997a; 1998; 2003).

In June 1996, after partial refilling of Crater Lake, a second cycle of eruptions started with phreatomagmatic explosions leading to a sustained sub-plinian eruption for several hours on 17 June. This event distributed c. 5 million m^3 ash over 300 km northward

toward Rotorua (Cronin *et al.*, 2003). Strombolian eruptions followed after this until 9 September 1996 (Figures 6.1.7 A and B).

Ash deposits from the 1995 and 1996 eruptions were analysed in this study for comparison to deposits from earlier in the stratigraphic record. The results of these studies are presented below and in Chapter 7.

Figure 6.1.5: "Cockscomb or Cockstails"-like phreatomagmatic eruption of Mt Ruapehu on 23.11.1995, (photographer: Megan Smith).

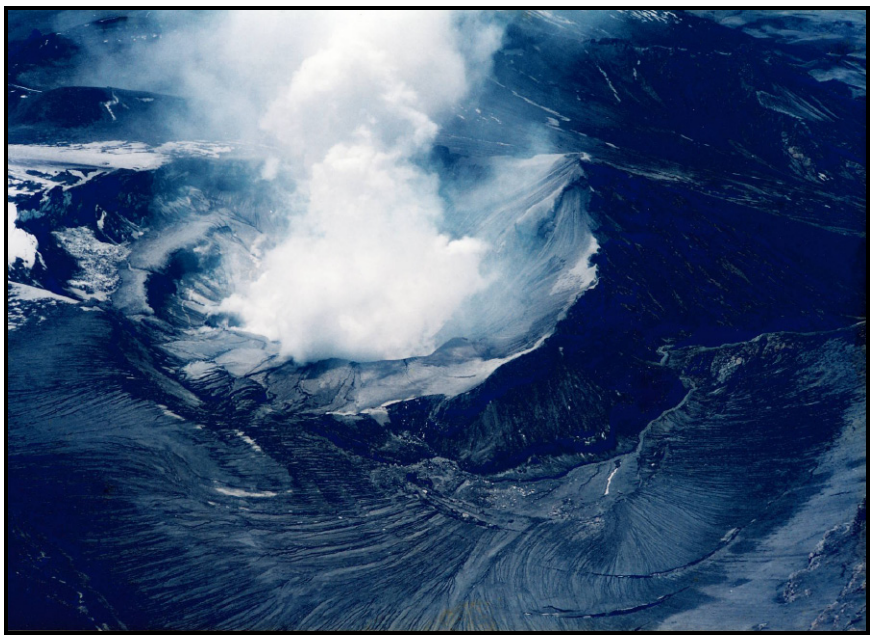

Figure 6.1.6: Ruapehu crater area the end of November 1995, in the foreground the outlet from the Crater Lake into the Whangaehu River, (Photo curtsey of Eckhard Möbis, private collection).

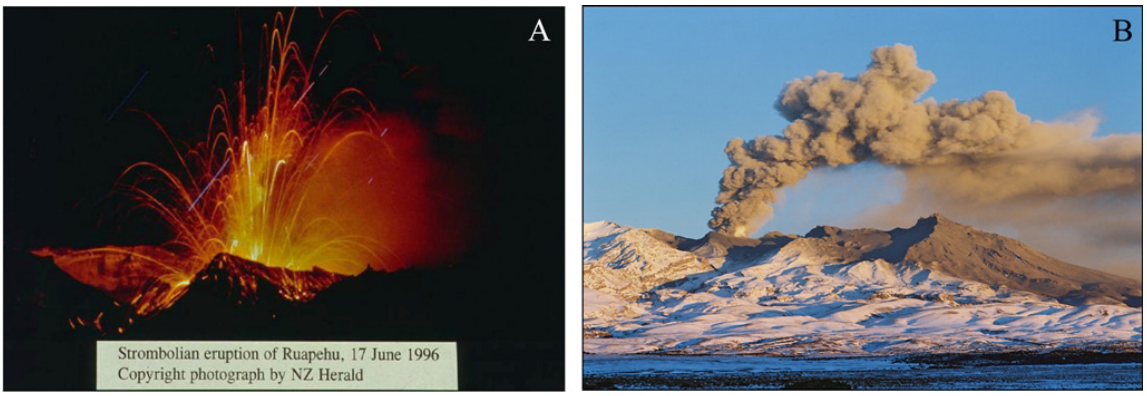

Figure 6.1.7: Strombolian eruption of Mt. Ruapehu on 17 June 1996 (images: NZ Herald (A) and eruption of Mt. Ruapehu as seen on the 19 June 1996 (B) with permission from "© Institute of Geological and Nuclear Sciences Limited [2010]", (photographer Lloyd Homer).

On 18 March 2007, heavy rain caused erosion of the outer part of the tephra dam retaining in Crater Lake. This led to a small overflow, followed by rapid down-cutting and a collapse of the tephra dam at 1118 hrs (NZST) (Massey *et al.*, 2009). In total 1.3 x 10^6 m^3 of water was released into the Whangaehu River and travelled 155 km into the Tasman Sea (Procter *et al.*, 2010), creating one of the largest lahars from Mt. Ruapehu in the last 100 years (Manville and Cronin, 2007; Figure 6.1.8). Over the first 5 km, 2.5 to 3.1 million m^3 of boulders, gravel and sand were eroded and entrained from below and alongside the channel, increasing the lahar volume from 1.3 to 4.4 million m^3 as it passed a monitoring site 6.9 km from source (Procter *et al.*, 2009).

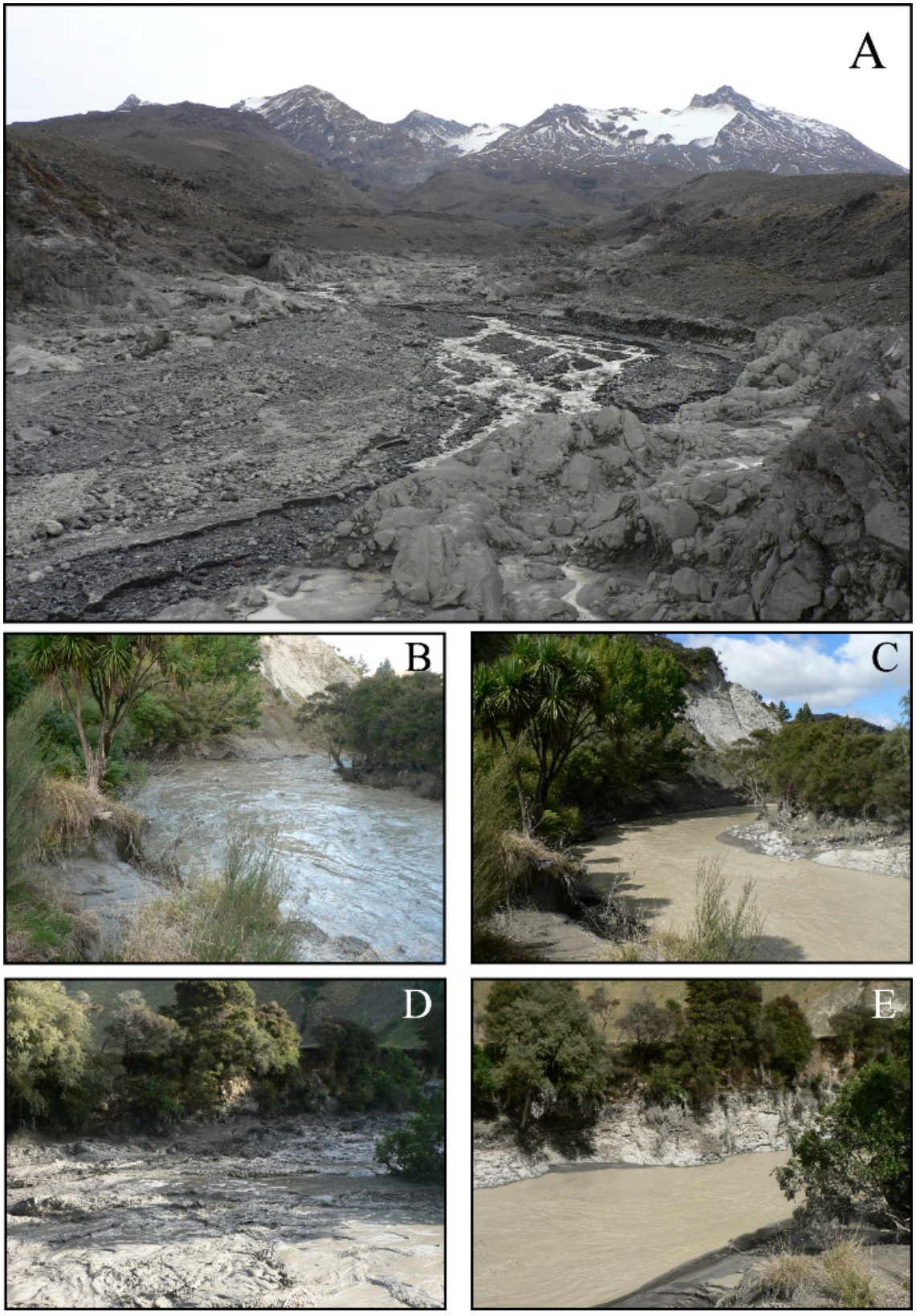

Figures 6.1.8: (A) View from the bridge at the Round the Mountain Track (6.9 km downstream of Crater Lake) immediately following the 18 March 2007 Ruapehu lahar. (B) The lahar at Colliers Bridge 82.6 km along the Whangaehu River. (C) The site shown in (B) post-lahar. (D) Another view of the lahar at Colliers Bridge, compared to the post event view in (E).

On 25 September 2007 at 2026 hrs NZDT a small phreatomagmatic eruption occurred from beneath Crater Lake (Christenson *et al.*, 2010; Kilgour *et al.*, 2010). This 60 s-long event generated a 4.5 km high steam column (Kilgour *et al.*, 2008), base surges and ashfall that blanketed a 2.5 km^2 area with ash and lapilli (Lube *et al.*, 2009). Several ice/snow-slurry lahars were generated from surges travelling across the Whakapapa and Whangaehu Glaciers (Figure 6.1.9). Two hikers were caught in the surge blast while sleeping in the Dome Shelter, 600 m north of the vent. One of the hikers was seriously injured by a large boulder from the surge (Kilgour *et al.*, 2010).

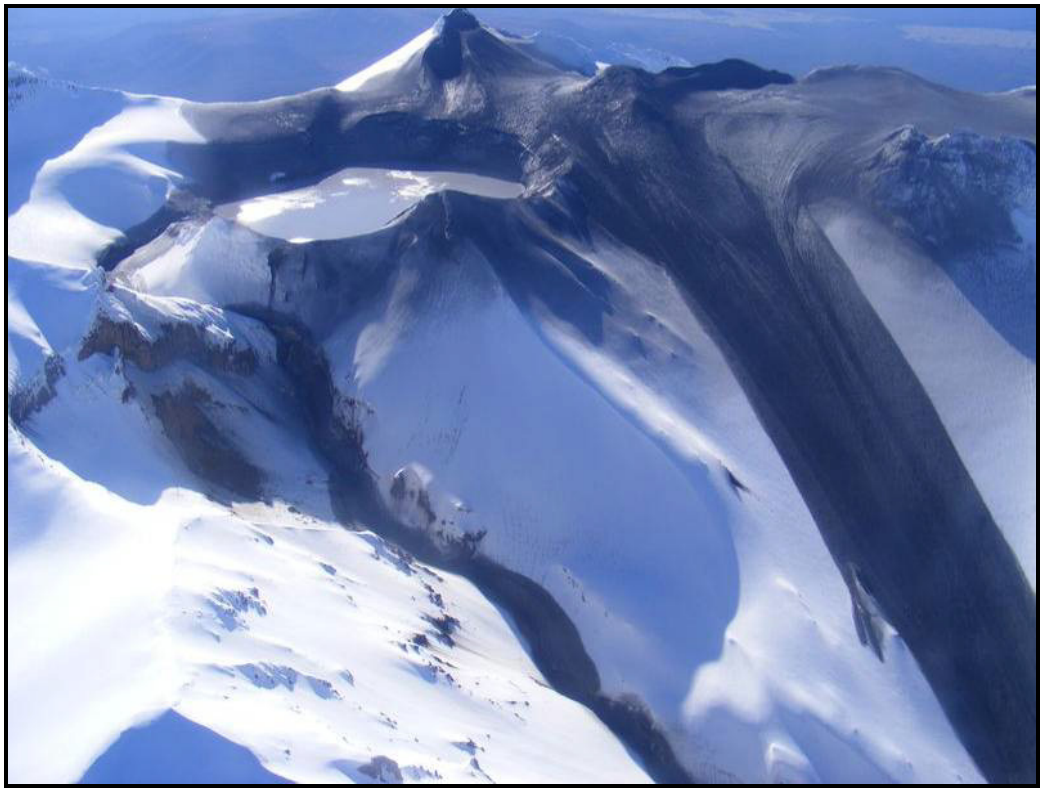

Figure 6.1.9: Phreatomagmatic eruption of Mt Ruapehu in 2007, showing the distribution of the surge deposit and the lahars generated through the eruption onto the Whangaehu Glacier (right) and the Whangaehu River catchment (left), (photographer: Károly Németh).

6.2. Holocene tephrochronological record of Ruapehu

From >26 600 to 12 000 cal. yrs. B.P., Mt. Ruapehu produced many large-scale sub-plinian eruptions with volumes of 0.1-0.5 km^3 (Topping, 1973; Donoghue *et al.*, 1999; Natalia Pardo, pers. com.), from which the deposits are mapped as the Bullot Formation (Donoghue *et al.,* 1995). In the following 12 000 cal. yrs B.P., Ruapehu tephra eruptions have been 1-10% of the size of the Bullot Formation events, and have been sporadic sub-plinian, and more often of smaller magnitude with vulcanian and strombolian events. Some of these tephras have been grouped within the 1717 cal. yrs. B.P. to present, Tufa Trig Formation (Donoghue *et al.*, 1997). Tephras between 1717 and 12000 cal. yrs. B.P. have only been described as informal units, such as Orange lapilli (1 and 2) and Black ash (1 and 2), within medial ash deposits defined as the Papakai Formation (Donoghue *et al.*, 1995).

In the following section, new findings on tephras derived from Mt. Ruapehu are presented, particularly from the time range *c.* 12 000 cal. yrs. B.P. to 1717 cal. yrs. B.P. This work is based upon four key exposures on the ring plain and a sediment core from Lake Rangatauanui, south of Ohakune.

6.2.1. Tephrochronological record of Ruapehu on the ring plain

The volcaniclastic deposits sourced from Mt. Ruapehu and Mt. Tongariro are preserved within the ring plain surrounding both volcanoes (Topping, 1974; Donoghue, 1991; Cronin, 1996). In this study, three time intervals are used to describe Ruapehu-sourced tephras on the ring plain. These correspond to the ages of the previously defined tephra formations: Papakai Formation (medial ash from all TgVC sources), Mangatawai Formation (tephras with Ngauruhoe source) and Tufa Trig Formation (tephras with Ruapehu source). Reference locations (Figure 6.2.1) used for this study include Location 6 at the car park in Mangatepopo Valley, Location 12 along the Desert Road, Location 56 east of Tufa Trig (Reference Section 2 in Donoghue (1991)), Location 63 on the northern face of Pukekaikiore, Location 67 on the northern slopes of Ngauruhoe

and Location 73 in the NZ-Army Training Area on Paradise Road at the first junction north of the shelter at Mangaio Stream.

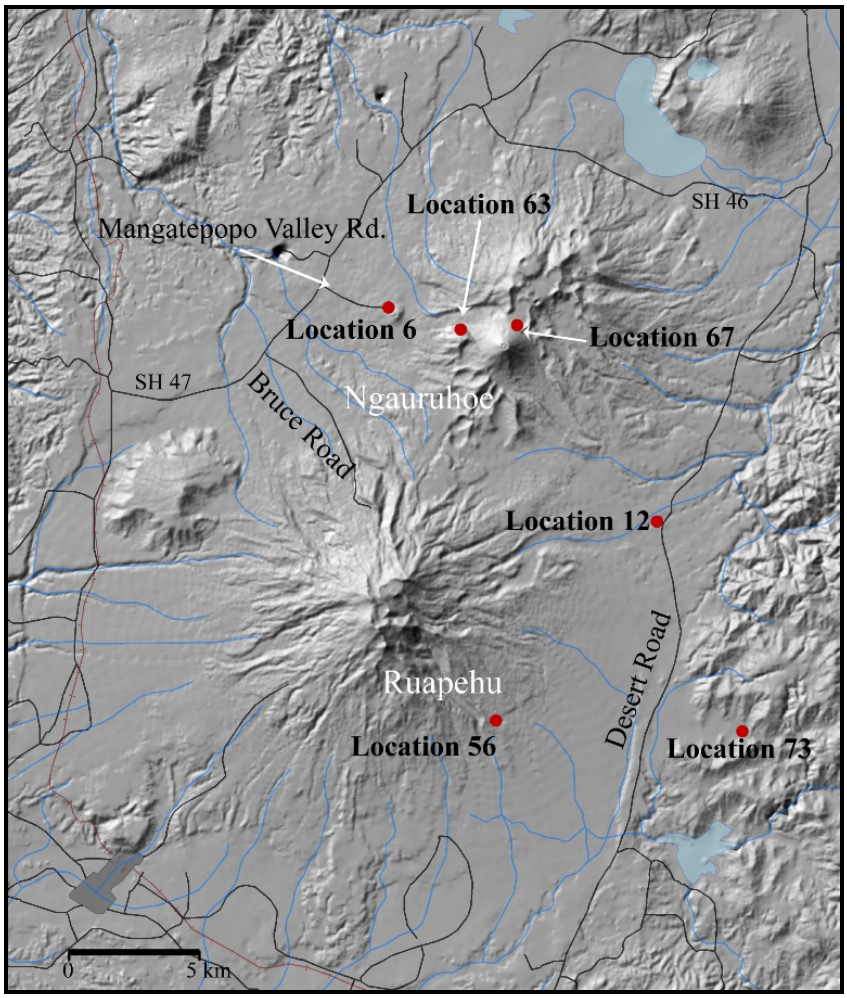

Figure 6.2.1: DEM of the TgVC showing the main locations representing Ruapehu's most complete tephra record over the last 12 000 cal. yrs. B.P.

6.2.1.1. 12 000 to 3500 cal. yrs. B.P.

Within the stratigraphic range between *c.* 12 000 and *c.* 3500 cal. yrs. B.P., four Ruapehu-sourced tephras were defined by Donoghue (1991): Orange lapilli 1 and 2 between the rhyolitic TVC-sourced Motutere Tephra (dated between 6050 to 7050 cal. yrs. B.P. (Wilson, 1993)) and Hinemaiaia Tephra (dated between 5250 to 5950 cal. yrs. B.P. (Wilson, 1993)) and Black ash 1 and 2 between Hinemaiaia and Waimihia Tephras. In Chapter 3 (section 3.2.1), the unit previously recognised as the Waimihia

Tephra has been re-defined as the TVC-source Stent Tephra (dated at 4323 ± 174 cal. yrs. B.P.).

At Loc. 12, five Ruapehu-sourced tephras were identified within the Papakai Formation by their distinctive chemistry (see Chapter 4; Figure 6.2.2). The oldest of these occurs in pockets of pale-dark grey fine ash, 50 mm below the Motutere Tephra, and 20 mm above the Tongariro-sourced Poutu Tephra (11,165 ± 31 cal. yrs. B.P). About 10 mm above the Motutere Tephra, a 45 mm-thick unit of orange lapilli occurs, containing up to 20 mm lapilli, sprinkled within fine ash of a similar colour. It could not be clearly established whether this tephra is orange lapilli 1 or 2 of Donoghue *et al*. (1995). Her "Black ash 1" was recognised as a discontinuous 5 mm-thick dark-grey/black fine ash, occurring 10 mm above the Hinemaiaia Tephra units. This black ash is a distinctive marker horizon within the Papakai Formation. About 200 mm above the Hinemaiaia Tephra and 2 mm above Ngauruhoe-sourced Stage 1 tephras (Chapter 5), a 20 mm-thick dark grey to black pocketing fine ash occurs. Its stratigraphic position indicates that it correlates to the Black ash 2 of Donoghue *et al.* (1995). The youngest Ruapehu-sourced tephra in this time range occurs 15 mm above the Stent Tephra as small pockets of fine grey ash.

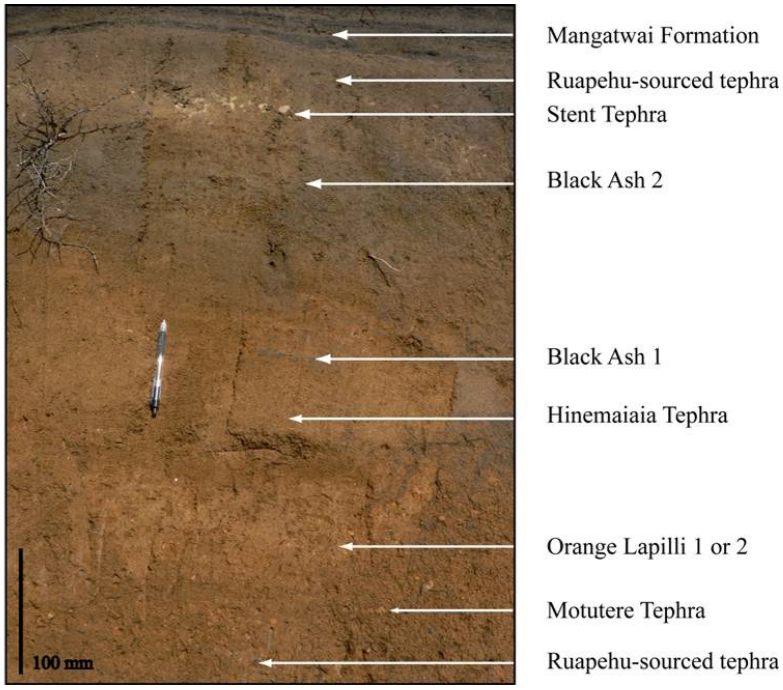

Figure 6.2.2: Ruapehu-sourced tephras within the Papakai Formation at Location 12, Desert Road.

About 15 km north of Ruapehu (Loc. 6), four tephra units derived from Ruapehu are identified within the Papakai Formation. All units occur below Ngauruhoe Stage 2 tephras (see Chapter 5). The oldest and the youngest tephra units, both 10 mm thick, show glass chemistry of both Ruapehu and Ngauruhoe suggesting that, either both volcanoes were active at the same time, several tephras were sampled and analysed collectively, or that they are partly reworked deposits. The second oldest and purely Ruapehu-sourced tephra (Figure 6.2.3A) is 50 mm thick and consist of pockets of greasy, strongly weathered bluish dark-grey ash, which may represent deposits from several individual eruptions from Ruapehu. About 50 mm above, the penultimate unit is another distinct dark-grey fine ash bed (Figure 6.2.3B).

Figure 6.2.3: Ruapehu-sourced tephras at Loc. 6 within the upper part of the Papakai Formation with A) the second oldest and purely Ruapehu-sourced tephra unit and B) a probably individual Ruapehu-sourced tephra deposited above unit shown in photo A.

6.2.1.2. 3500 to 1717 cal. yrs. B.P.

The time interval between 3500 and 1717 cal. yrs. B.P. corresponds to the time range of the Mangatawai Formation (MtF) (Topping, 1973). Nine Ruapehu tephras were identified at Loc. 12 in this interval (Figure 6.2.3A). Eight of these occur at the base of the MtF (Figure 6.2.3.B), the other occurs 10 mm below the Taupo Pumice (Figure 6.2.3.C). This stratigraphy implies that no Ruapehu tephras are represented here during Ngauruhoe's Stage 2 and lower Stage 3 (over a time period of ~1650 years). The tephras are fine to very-fine ash and differ mainly in colours that range from white to grey to black (Figure 6.2.3.B). Individual deposits can only be correlated over short

distances; none form widespread marker beds. The basal Ruapehu tephras show a restricted distribution, the lowermost 4 tephras thin markedly toward the north.

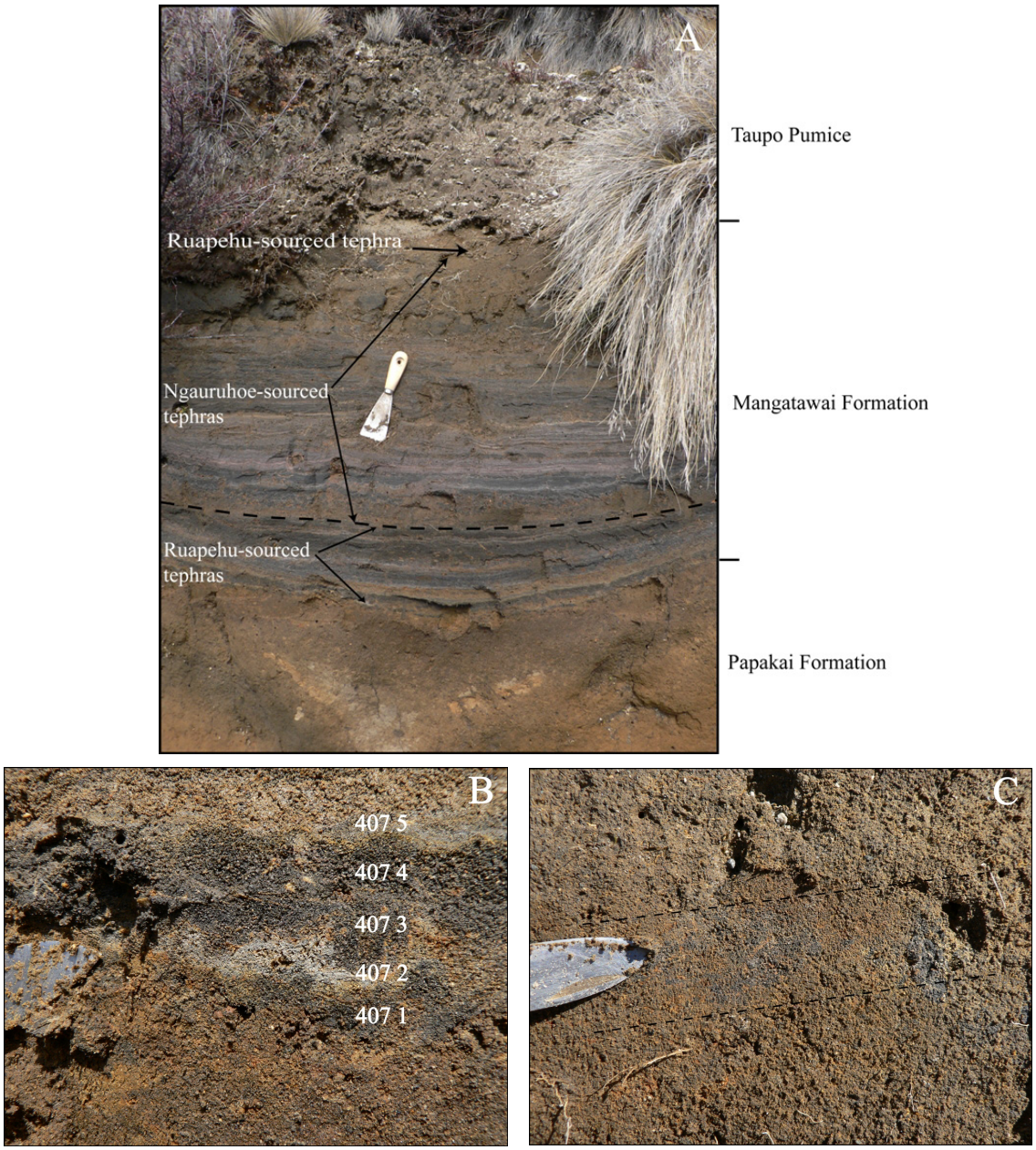

Figure 6.2.4: Ruapehu-sourced tephras at Location 12: (A) Ruapehu sourced tephras at the base and at the top of the MtF at Loc 12. B) five layers interbedded within the base of the Mangatawai Formation, and C) a single Ruapehu-sourced tephra interbedded within the top of the formation.

At Location 6, three discrete Ruapehu-sourced tephras have been identified within this time period. Two tephras occur at the base of the MtF and one discontinuous tephra at the top. These tephras appear as 5 and 7 mm thick grey-black fine-grained ash which pinch and swell over a very short distance of several cm and appear less discrete as the

Ruapehu-sourced tephras at Location 12. The main characteristic of this location, north of Ruapehu, is several "mixed" deposits (17), containing ash from Ngauruhoe and Ruapehu within the Ngauruhoe Stages 2 and 3. In contrast at Location 12, which is situated within the main wind direction towards the north-east, no tephras sourced from Ruapehu has been identified between the same time interval, leading to the impression of Ruapehu being in a non-eruptive stage. These "mixed" tephras at Location 6, may indicate Ruapehu was regularly active and distributing ash northwards during the main eruptive phases of Ngauruhoe (Chapter 5).

On the northern slope of Ngauruhoe (Loc. 67), 12 Ruapehu tephras occur in this time range, and Ruapehu ash is also being mixed into nine further Ngauruhoe units. At the base of this exposure, above a Ngauruhoe lava, and the yellowish-brown greasy medial ash of the Papakai Formation three discrete and six "mixed" deposits occur. The discrete units are 20 to 100 mm thick, strongly weathered and greasy fine ash (Figure 6.2.5). The tephras at the top of this interval are, by contrast, fresh 3 to 40 mm grey to black, fine to medium ashes.

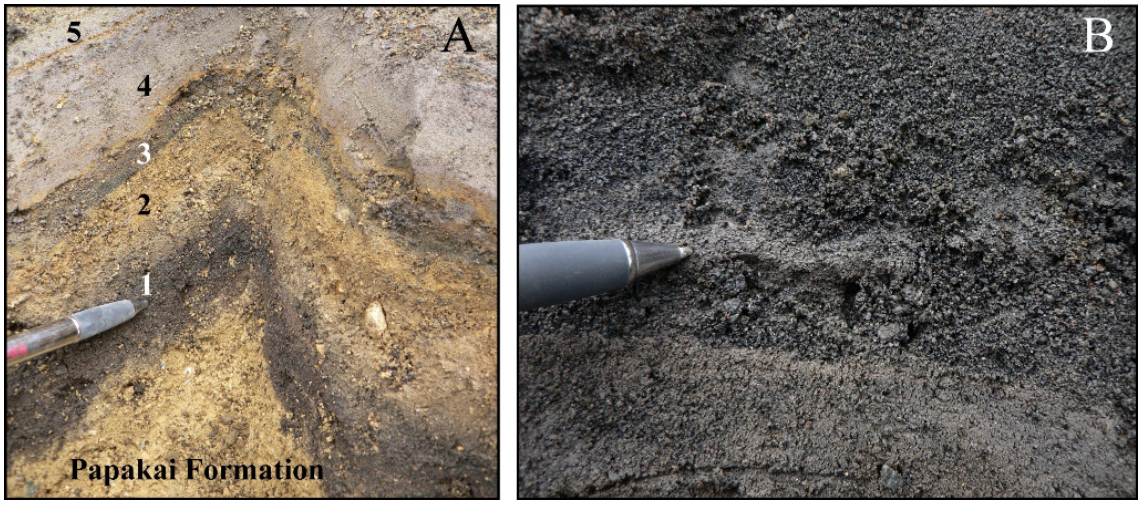

Figure 6.2.5: Location 67. (A) Ruapehu-sourced tephras (1-4) and deposits containing volcanic glasses from several sources (5) at the base of the exposure, and (B) Ruapehu-sourced tephras towards the top of the exposure at the same location.

6.2.1.3. 1717 cal. yrs. B.P. to present

Ruapehu-derived tephras deposited after the large 1717 cal. yrs. B.P. Taupo eruption are grouped within the Tufa Trig Formation, which contains at least 19 units (Donoghue *et al.*, 1997). The violent pyroclastic flows of the this Taupo-sourced event had a major impact on the vegetation of the TgVC area and destroyed most of the forest cover (McGlone and Topping, 1983). The remaining grass, tussock and scrubland was also burnt several times by Maori and European settlers transiting the area (Silvester *et al.*, 2009). Due to the high winds and the coarse-grained, rapidly draining soils, desert-like conditions hinder the development of stable vegetation and hence discourage the preservation of tephras. These are best found within dunes of Makahikatoa Sands that have been stabilised by shrubby vegetation (Purves, 1990).

In this study, members of the Tufa Trig Formation were identified at many locations around the TgVC. At Location 56 (Reference section 2 of Donoghue (1991)), east of Tufa Trig, at least 17 members of the Tufa Trig Formation are exposed in dunes of Makahikatoa Sands (Fig. 1.8 and 6.2.6, 6.2.10). At this site, the oldest tephra defined is Tf2, a distinct 80 mm-thick, pale-yellow to grey, medium to coarse scoriaceous lapilli bed (Figure 6.2.7A). The most distinctive members of the Tufa Trig Formation are Tf5, Tf8 and Tf14 (Figures 6.2.7 D to F). Tf5 occurs as a medium to coarse-grained black ash, also containing lithic lapilli. Tf8 is situated in the central part of the profile as a coarse dark grey and black discontinuous ash layer, containing brownish pumice lapilli at its base. Tf14 is less distinctive, occurring as a 20 mm-thick continuous black, medium ash, underlying a 30 mm pale grey fine–medium ash, which is also very distinctive, but was not described by Donoghue *et al.* (1995). Tf15, Tf16 and Tf18 appear as discontinuous 10-30 mm thick pale gray–black, fine ash units separated by 40-140 mm sand/medial ash. At this site several members of the TTF show a characteristic 2-3 mm (up to 12 mm), discontinuous, white to pale grey, very fine ash base, which is interpreted to represent the initial phases of each eruption (see Chapter 7).

In this study, between Tf5 and Tf15 an additional six tephras were identified, that had not been described by Donoghue *et al.* (1997). These six tephras are so far not mapped

and remain informal, but have been ascribed an informal symbol based to their stratigraphic position to other named members. For example, one of the additional tephras was identified above Tf4 and has therefore been informally named Tf4a. Further unnamed tephras are informally named Tf6a, Tf7a, Tf9a, Tf10a and Tf14a.

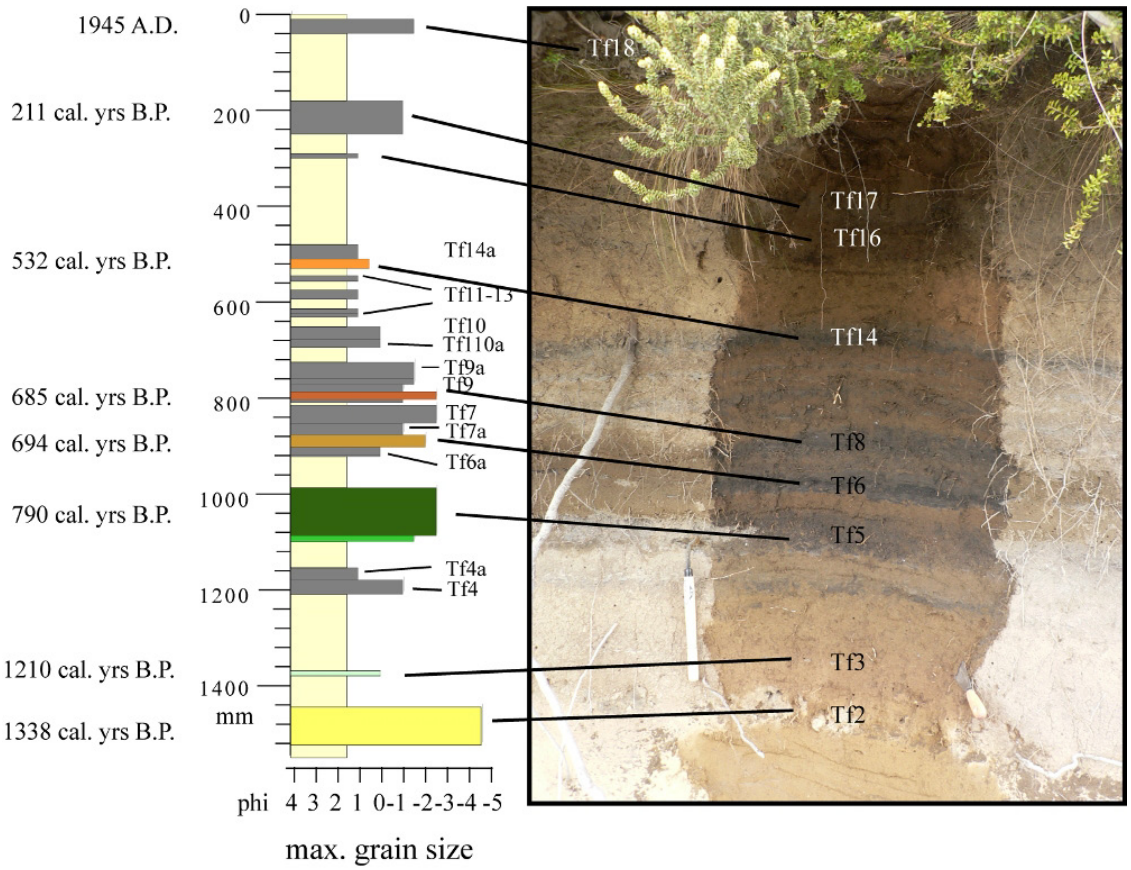

Figure 6.2.6: Stratigraphic column of the Tufa Trig Formation at Loc. 56 (Ref. Sect 2 (Donoghue *et al.* 1997)) illustrating the positions of the marker horizons Tf2, Tf5, Tf8 and Tf14 and also showing the new informally named tephra units Tf4a, Tf6a, Tf7a, Tf9a, Tf10a and Tf14a.

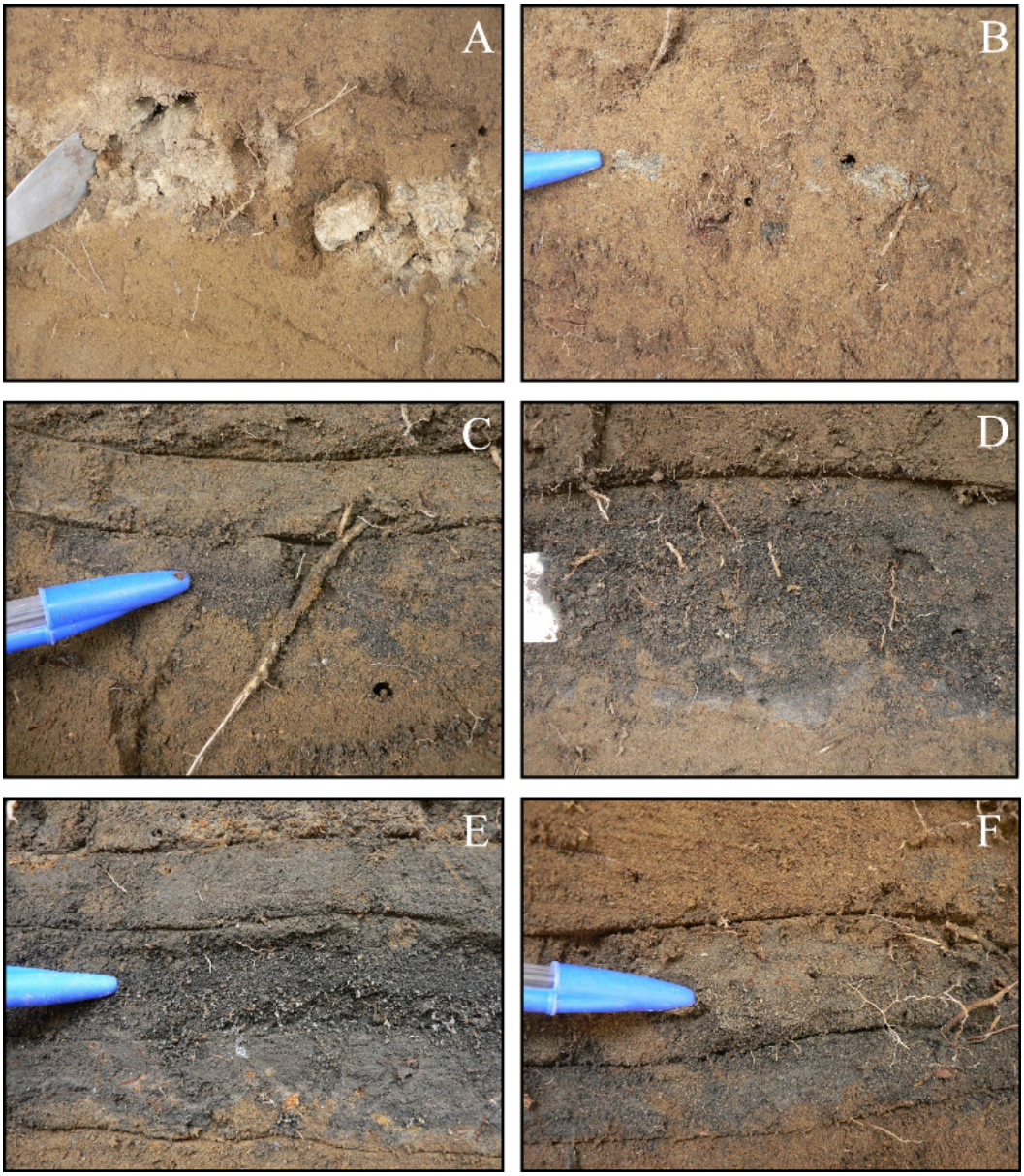

Figure 6.2.7: Individual tephras sourced from Ruapehu within the Tufa Trig Formation at Location 56 with (A) the distinctive pumiceous Tf2, (B) pale grey unit Tf3, (C) Tf4 and an additional unnamed tephra above (informally named Tf4a), (D) the distinctive member Tf5 including the pale grey base, (E) the prominent marker unit Tf8 including the probable Tf6 and Tf7 below, as well as Tf9 above and (F) the TF 14(darker grey) and an unnamed beige tephra above (informally named Tf14a).

Around 15 km north-east of Loc 56, at Loc. 12 on the Desert Road, at least eleven Ruapehu-sourced tephras are exposed above the Taupo Pumice (Figure 6.2.9A). The tephras mainly consist of 10-30 mm-thick, dark-grey to black, fine to medium ash. Several of the tephras show a distinctive 1 to 2 mm white to pale-grey very fine ash basal layer. Tf5 occurs as the thickest unit, in the central part of the profile.

Location 63, at Pukekaikiore, contains 24 Ruapehu-sourced tephras in this age range, with 10 occurring above the Taranaki-sourced Burrell lapilli (295 cal. yrs. B.P.) (Figures 6.2.9 B and 6.2.10). Those below the Burrell lapilli are mainly discontinuous pale grey to grey fine ash beds, 10 to 80 mm-thick. The thickest of these units appear to represent multiple Ruapehu eruptions. The two units above the Burrell lapilli are distinct, the oldest being a purplish fine to medium ash, overlain by a 100 mm-thick, medium to coarse orange and black ash and fine lapilli (Figure 6.2.7). Above these, the remaining Ruapehu tephras are typically grey to black fine ash beds, varying in thickness between 10 to 60 mm. Some of the individual tephras show a 2 mm, very fine pale basal ash (Figure 6.2.7D). As described in section 5.1.5, the age of this profile is calculated at ~1000 cal. yrs. B.P. indicating a much higher eruption rate than that calculated by Donoghue *et al.* (1995; 1997). This suggests that the majority of Ruapehu tephra have been distributed by southerly winds to the north of Crater Lake, rather than to the south-east where the type locality occurs.

At Loc. 73, ~16 km east of Ruapehu (Fig. 2.2), eleven Ruapehu tephras were identified including Tf1, Tf2 and Tf5. Charcoal found in Tf1 and Tf2 was radiocarbon dated (see Section 6.3).The uppermost tephra here is likely to be Tf14.

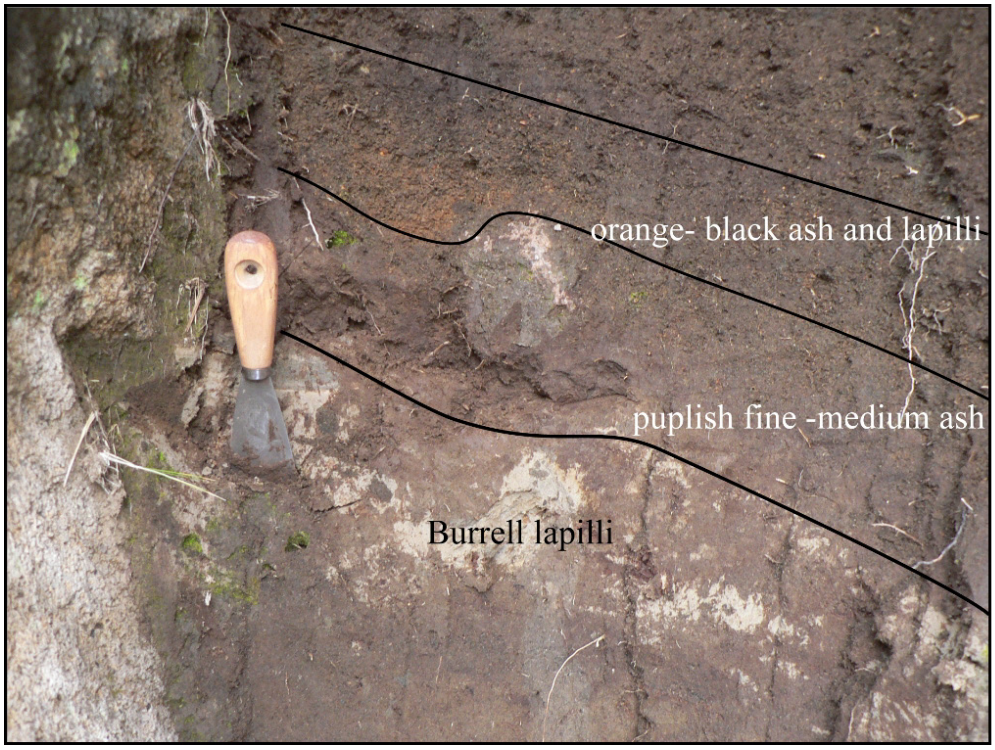

Figure 6.2.8: Two distinct Ruapehu-sourced tephras above the Burrell lapilli (Taranaki) at Location 63.

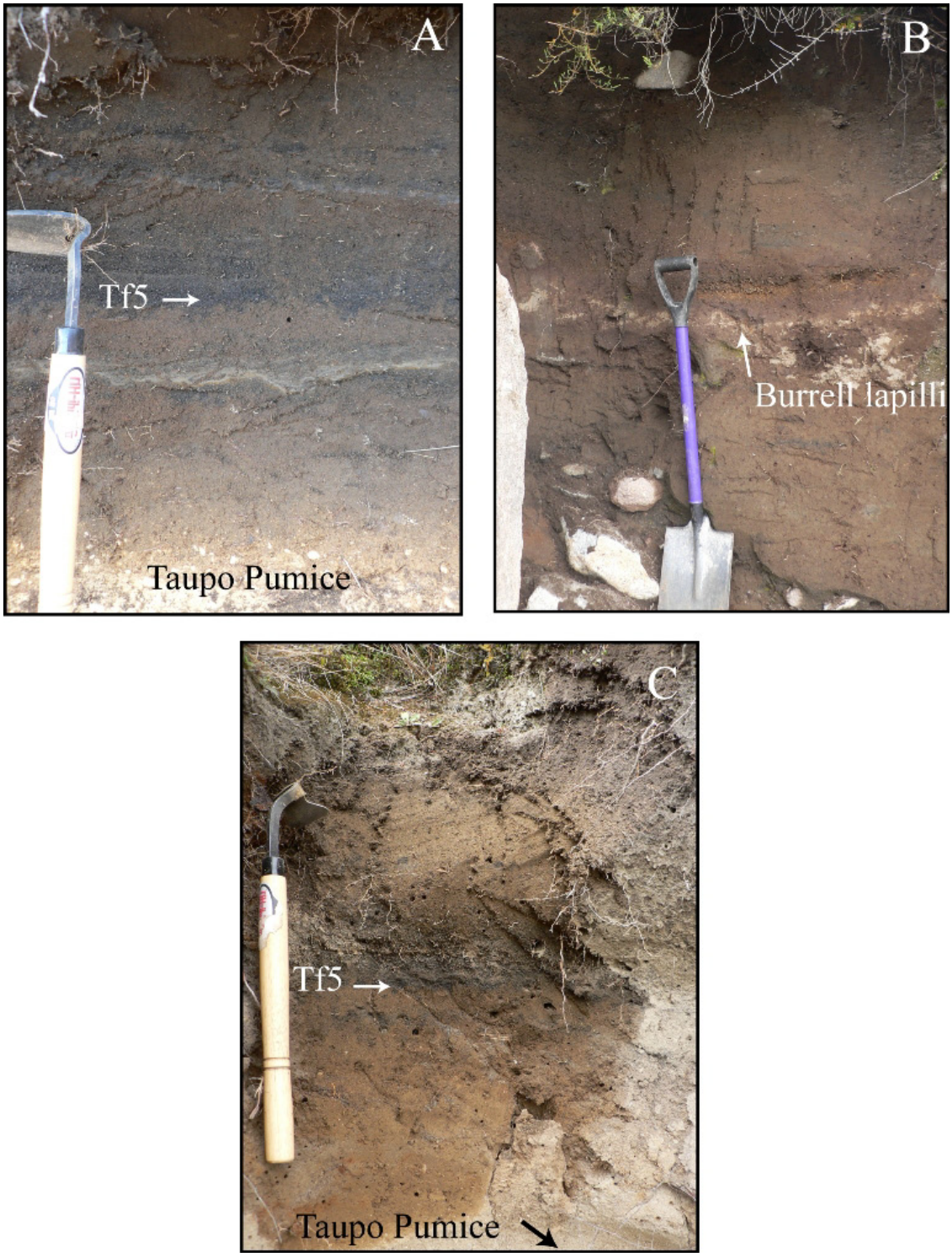

Figure 6.2.9: Exposures of the Tufa Trig Formation within the TgVC at (A) Location 12 at the Desert Road, (B) Location 63 at the northern slope at Pukekaikiore and (C) at Location 73 on Paradise Road, NZ Army Training Area.

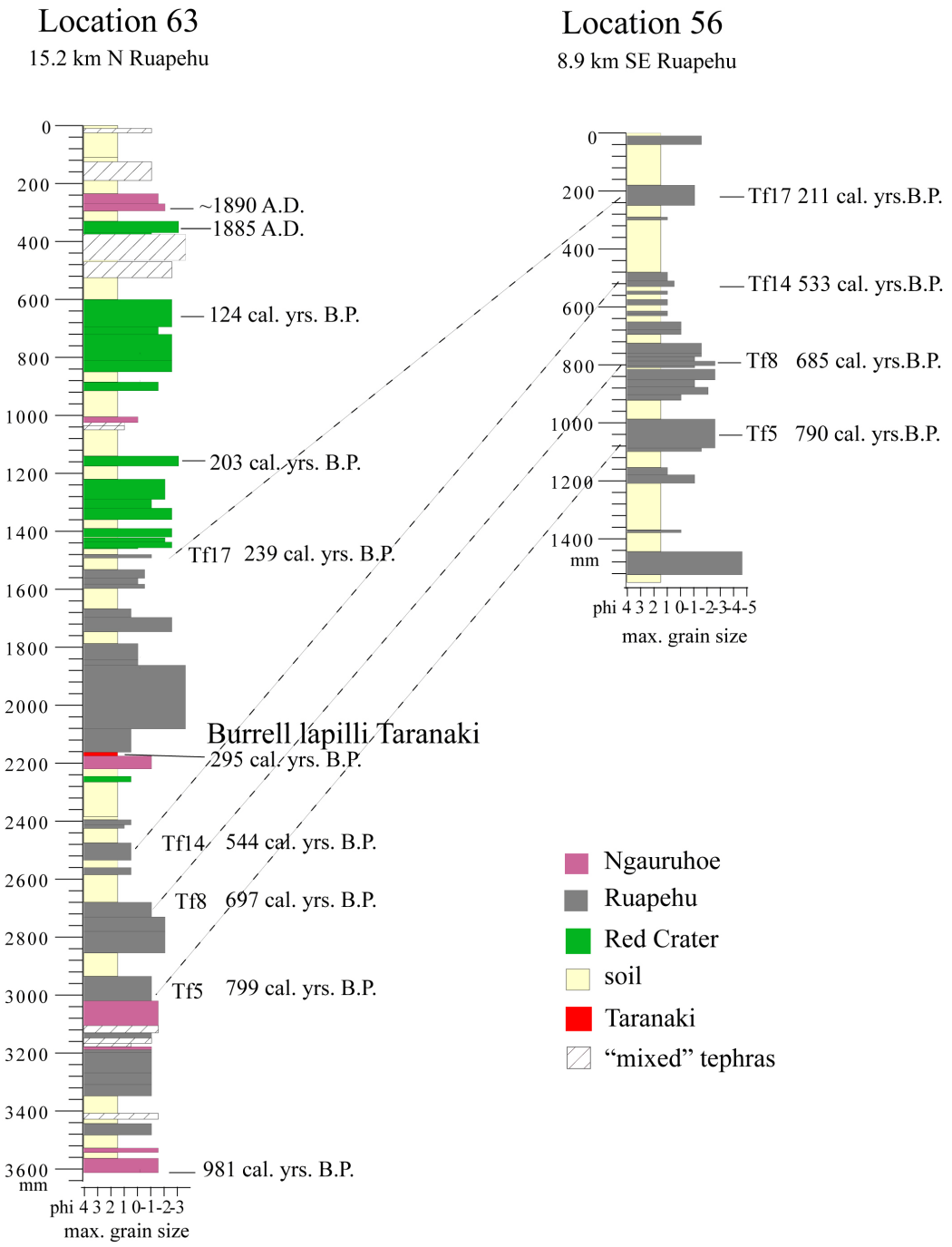

Figure 6.2.10: Stratigraphic profiles of Locations 63 and 56 representing and correlating members of the Tufa Trig Formation. Most ages are based on calculations of soil accumulation rates (Appendix 5), except Burrell lapilli and Tf5 at Location 56.

6.2.2. Tephra record of Lake Rangatauanui sediments

About 23 km south-west of Ruapehu, several tuff rings and explosion craters occur in the Ohakune township area (Gorton, 1968; Cole *et al.*, 1986). Houghton and Hackett (1984) described deposits of strombolian and phreatomagmatic eruptions from these centres. Their age of these centres is not well constrained, but all of them have the Kawakawa Tephra (27,097 ± 957 cal. yrs. B.P.; Lowe *et al.,* 2008) in their cover beds. Lakes Rangatauanui and Rangatauaiti, south of Ohakune, are not mentioned in these papers, and their deposits are not well exposed, hence their ages are unknown.

Lake Rangatauanui is located 2.5 km south-west of Ohakune, around 90 km south-west of Lake Taupo and 114 km east of Mt Taranaki. The lake has a constant water depth of 4 m, is 152 m-wide (north-south) and 253 m-long (east-west) (Figures 6.2.11 and 6.2.12).

Figure 6.2.11: Lake Rangatauanui south-west of Mt. Ruapehu.

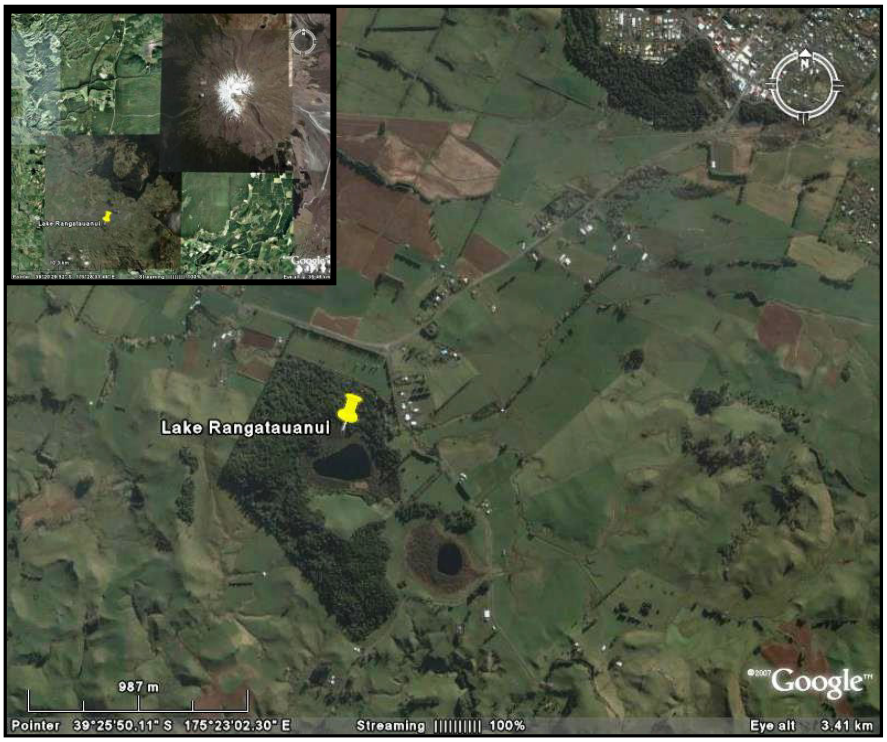

Figure 6.2.12: Lake Rangatauanui south-west of Ohakune (upper right hand corner), image from Google Earth 2008.The smaller images shows the position of Lake Rangatauanui to Ruapehu.

Five cores were collected along the long-axis of the lake. They all contained the same visible stratigraphic sequence, with a maximum depth reached of 4.5 m. This shallow depth of sediment suggests an apparently flat base to the lake, with it being filled by in-washed tuff or volcanic loess from the inner crater walls. The cores were x-rayed to determine mineral layers within the organic-rich sediment and to determine which of the cores had the most complete tephra record. Core 4 contained 100 individual tephras, with grain sizes ranging from fine ash to fine lapilli. Volcanic glass shards and titanomagnetite grains for each layer were separated and analysed with the electron microprobe for their major oxide compositions. Nine 1 cm-thick slices of organic sediment were radiocarbon dated (Table 6.3.2) with the maximum age obtained near the base of the core at *c*. 22 500 cal. yrs. B.P.

As described in Chapter 2, ten individual glass shards and titanomagnetite crystals were analysed with the EMPA for each of the 100 tephras. A definitive single identification was obtained for 66 of the samples (39 showing 10/10 classified, 12 with 9/10, six with 8/10 and nine with 7/10). The remaining 34 samples showed six or less classified as a single source. These “mixed”-deposits could in many cases be caused by contamination

by sampling very thin and closely spaced tephras from different sources or by eruptions from different volcanoes occurring in close succession under the slow deposition rates in the lake (c. 0.18 mm/yr). If it took over five years to accumulate only 1 mm of organic sediment (based on sediment accumulation rates of the lake), co-deposition of closely timed eruptions from separate volcanoes is highly likely. They could also represent natural contamination by coarse wind-blown glass shards, which may be more likely during the cold/dry and low-vegetation periods of the last Glacial Maximum (c. 25-14 ka B.P. Pillans *et al.*, 1993). The glass chemistry (see Chapter 4 and Appendix 2) showed that the tephras within Lake Rangatauanui are derived from Mts. Ruapehu Tongariro, and Taranaki, along with units from the Taupo (TVC) and Okataina Volcanic Centres (OVC) (Figure 6.2.13 and listed in Appendix 5).

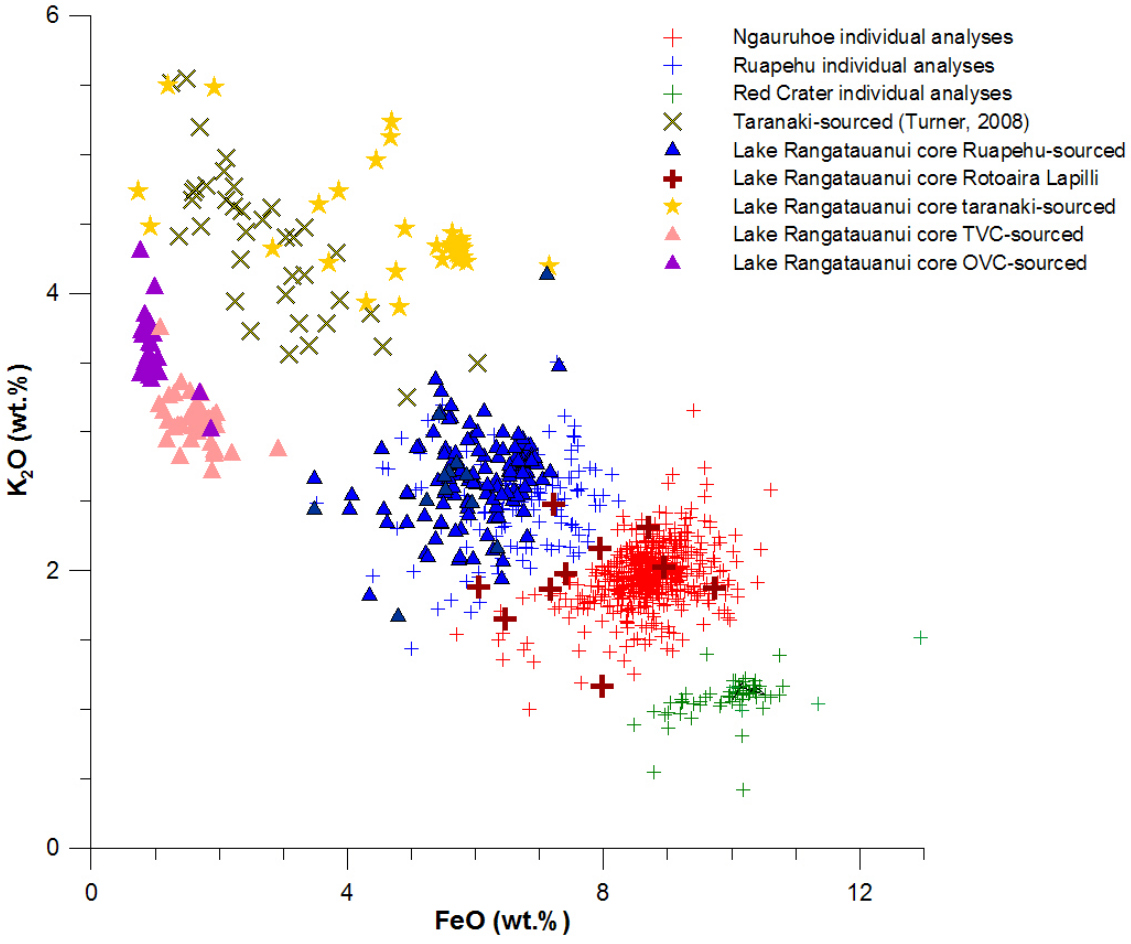

Figure 6.2.13: Major oxides of volcanic glasses as measured by electron microprobe on samples from Lake Rangatauanui, compared to tephras from known sources. Note, the Rotoaira Lapilli was probably sourced from North Crater, Tongariro volcano (Griffin, 2007).

Rhyolitic Tephras

Eleven rhyolitic tephras were correlated to known units from the Taupo and Okataina Volcanic Centres based on their stratigraphic positions, radiocarbon ages and glass chemistry (five with 10/10 shards, four with 9/10 shards and 3 with 8/10 shards). Six of these units are sourced from the TVC:

- Taupo Pumice (1779 ± 45 cal. yrs. B.P.), (Unit Y, (Wilson, 1993))
- Stent Tephra (4407 ± 417 cal. yrs. B.P.), (Unit Q, (Wilson, 1993))
- Motutere Tephra (6907 ± 250 cal. yrs. BP) (Unit F, (Wilson, 1993))
- Opepe Tephra (10 095 ± 275 cal. yrs. B.P.) (Unit E, (Wilson, 1993))
- Poronui Tephra (10 167 ± 251 cal. yrs. BP) (Unit C (Wilson, 1993))
- Karapiti Tephra (17517 ± 987 cal. yrs. B.P.) (Unit B, (Wilson, 1993)).

Several TVC-sourced glass shards were also interbedded in andesitic tephras in the age ranges between 10 032 ± 237 and 12 864 ± 212 cal. yrs. B.P. near to the Opepe and Poronui Tephras and in an older range. These may be micro-tephras from TVC, recognising that Wilson (1993) shows many locally distinguishable tephras from TVC that had not been earlier described or distinguished. For example, the "Motutere Tephra" was remapped in proximal areas to show 3 individual tephras erupted over a period between 6050 and 7050 cal. yrs B.P. (Wilson, 1993). Typically the most widely distributed of these, were the basis for defining the original formation names used by workers up to Lowe *et al.,* (2008). Correlations to the south by Topping and Kohn (1973) and Donoghue (1991) were made using these previous definitions, whereas here it is recognised that the "named" units seen in the north, may or may not correlate directly with those in the TgVC. This has led to several re-assignments of rhyolite markers (e.g. Stent vs. Waimihia Tephra, see Chapter 3).

Five tephras derived from the Okataina Volcanic Centre were identified as belonging to the following formations:

- Mamaku Tephra (8075 ± 94 cal. yrs. B.P.)
- Rotoma Tephra (9516 ± 25 cal. yrs. B.P.)
- Waiohau Tephra (13 681 ± 259 cal. yrs. B.P.)
- Rerewhakaaitu Tephra (17 891 ± 339 cal. yrs. B.P.)

- Okareka Tephra (20 430 ± 1015 cal. yrs. B.P.).

Four further tephras have Okataina glass shards as a minor component, three stratigraphically between the Mamaku and Rotoma Tephras and another near the Rerewhakaaitu Tephra. These could represent re-dispersed glass shards and the older one could even represent the Rotorua Tephra (15 425 ± 325 cal. yrs. B.P.), which has been also recognised in the TgVC by Cronin *et al.* (1997d).

Andesitic Tephra

The tephras with andesitic composition within the Lake Rangatauanui core are derived locally from Mts. Ruapehu and Tongariro, as well as from the 114 km distal source of Mt. Taranaki.

Above the Taupo Pumice (1717 cal. yrs. B.P), 10 Ruapehu tephras were identified. The calculated ages from the core, compared to those on the TgVC ring plain allow the possible chrono-correlation of Tf4, 5, 8, 10 and 14 to the Rangatauanui core. In the time range of the Mangatawai Formation, two Ruapehu tephras were identified, compared to at least 12 on TgVC ring-plain sequences. Over the depositional time range of the Papakai Formation, a further six Ruapehu tephras are identified, compared to eight in the TgVC ring plain. Below the Poronui Tephra (11 190 ± 80 cal. yrs. B.P.) in the time range of the Bullot Formation, 30 Ruapehu tephras were recognised in the core and an additional two layers have significant components of Ruapehu glass. This compares to at least 23 major tephras occurring in the same time frame on the eastern ring plain (Donoghue *et al.,* 1995).

A distinctive Tongariro volcano-sourced tephra was identified just above a sample dated at 15 438 ± 315 cal. yrs. B.P. and is here correlated to the Rotoaira Lapilli (dated at 16 501 ± 939 cal. yrs. B.P.) produced from North Crater (Griffin, 2007). In 17 further tephras possible Tongariro-sourced glass was identified as a very minor component (1-2 shards); however, it is recognised that the two compositional fields overlap a little (Figures 4.6 and 6.2.12) and these may simply be extreme compositions of the Ruapehu glass population. Rare Tongariro glass shards occur below the Rotoaira Lapilli, and may

correlate to earlier Tongariro eruptions as recognised by Shane *et al*. (2008). Other horizons with Tongariro volcano-sourced glass shards above the Rotoaira Lapilli have no recognised correlatives. The extremely large Mangamate Formation tephras from Mt. Tongariro, along with the Pahoka Lapilli are possibly only seen as trace components (2-3 shards) with Ruapehu-dominated tephras between 10 830 and 8250 cal. yrs. B.P. in the core. Furthermore, two tephras just beneath the TVC-sourced Stent Tephra contain Tongariro glass shards, which may correlate to the oldest distinct tephra sourced from Mt. Ngauruhoe described in Chapter 5.

Taranaki-derived tephras can be distinguished via their titanomagnetites using the electron microprobe determined oxides, FeO and Al_2O_3 (Figure 6.2.14). In addition, they can be separated using glass compositions (see Chapter 4).

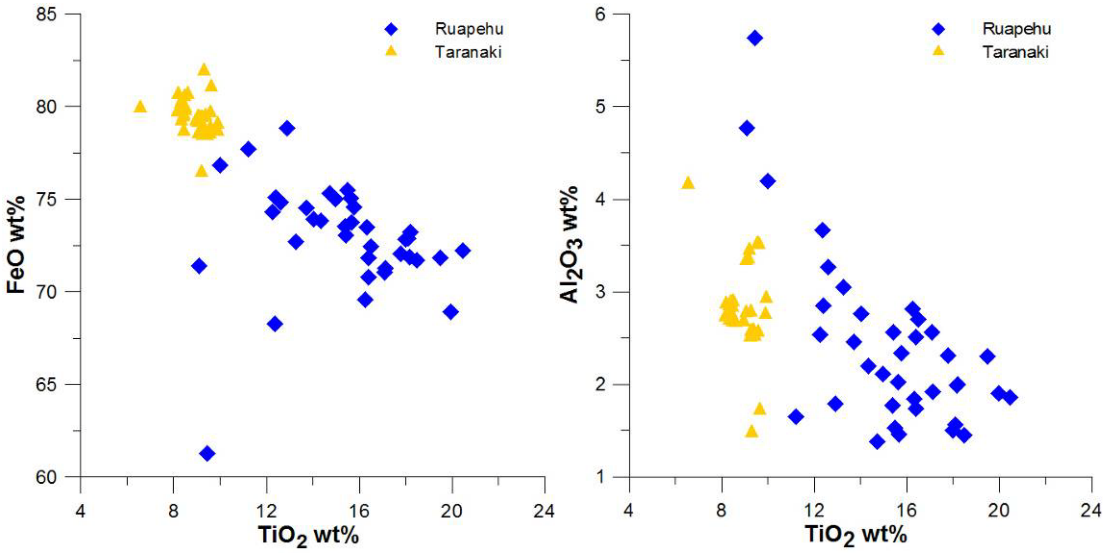

Figure 6.2.14: Major oxide analysis vs. TiO_2 of titanomagnetites sourced from Mt. Ruapehu (blue) and Mt. Taranaki (yellow).

Taranaki tephras are also distinguished from the local-sourced andesites in being typically very thin (1-20 mm) and containing only minor proportions (<5%) of volcanic glass but are enriched in clinopyroxene and plagioclase. Additionally, titanomagnetites are larger and prominent in the Taranaki tephras and easier to extract.

In total 39 tephras were recognised within the core, where 16 tephras had 6 or more/10 glass shards sourced from Taranaki and also titanomagnetites from the same source. The remaining 23 tephras in the core contain titanomagnetite of a clear Taranaki source,

but glass that could also be Ruapehu or TVC sourced. These are dominantly in the period of major large-scale and frequent Ruapehu activity, represented by the Bullot Formation (Donoghue *et al.,* 1995). They are also in the period where Taranaki is known to have had major, frequent and large scale tephra eruptions. Recognising that the pure Taranaki tephras have such little glass, these units most likely represent thin Taranaki tephras falling into sediment accumulating with additions of other wind blown glass shards derived from Ruapehu and TVC. The following Taranaki tephras were recognised:

- Maketawa Tephra (1943 ± 210 to 3286 ± 404 cal. yrs. B.P.)*
- Manganui Tephra (3277 ± 59 to 3317 ± 49 cal. yrs. B.P.)
- Inglewood Tephra (3910 ± 224 to 4060 ± 231 cal. yrs. B.P.)
- Korito Tephra (3893 ± 248 to 4647 ± 230 cal. yrs. B.P.)
- Mangotiki Tephra (~4959 ± 80 cal. yrs. B.P.)
- Tariki Tephra (5256 ± 71 to 5370 ± 65 cal. yrs. B.P.)
- Waipuku Tephra (5754 ± 163 to 6025 ± 255 cal. yrs. B.P.)
- Kaponga Tephra (6089 ± 91 to 12 166 ± 130 cal. yrs. B.P.)
- Konini Tephra unit b (12076 ± 660 cal. yrs. B.P.)
- Mahoe Tephra (12874 ± 189 to 13266 ± 95 cal. yrs. B.P.)
- Kaihouri Tephra (15 472 ± 421 to 22 363 ± 184 cal. yrs. B.P.)
- Paethai Tephra (23 068 ± 398 to 24 128 ± 247 cal. yrs. B.P.)
- Poto Tephra (24 586 ± 278 to 27399 ± 488 cal. yrs. B.P.)

Note, all dates from Alloway *et al.,* (1995) yrs. B.P. recalculated in OxCal to cal. yrs. B.P. except Maketawa Tephra* (Franks, 1984).

Table 6.2.1: Tephras in the Rangatauanui core containing Taranaki-sourced titanomagnetite and/or glass of same origin with their correlation to known tephras of the Taranaki ring plain from Alloway *et al*. (1995); Turner *et al.* (2008a and b). Note: here all ages obtained from the spline fit described in section 6.3.

Tephra core nb.	Depth in mm	cal. yrs. B.P.	Possible correlation
1	66	384±388	Burrell Lapilli
13	379	2325±258	Maketawa Tephra
16	632	3551±145	Manganui Tephra
18	684	3769±153	Inglewood Tephra
22	920	4941±506	Korito or Mangotiki Tephra
23	982	5297±424	Tariki Tephra
24	1066	5970±310	Waipuku Tephra
25	1081	6070±324	Waipuku Tephra
26	1105	6087±324	Waipuku or Kaponga Tephra
29	1270	7357±101	Kaponga tephra
30	1324	7604±79	Kaponga tephra
31	1364	7748±88	Kaponga Tephra
34	1450	8171±136	Kaponga Tephra
38	1666	9499±30	Kaponga Tephra
40	1750	9926±233	Kaponga Tephra
41	1774	9974±229	Kaponga Tephra
42	1798	10032±237	Kaponga Tephra
45	1835	10204±280	Kaponga Tephra
46	1945	10830±255	Kaponga Tephra
47	1966	10941±226	Kaponga Tephra
49	2062	11747±339	Kaponga Tephra
51	2185	12753±168	Konini Tephra
52	2201	12864±212	Mahoe Tephra
53	2230	13009±241	Mahoe Tephra
64	2799	17246±1281	Kaihouri Tephra
66	2830	17517±987	Kaihouri Tephra
67	2851	17598±884	Kaihouri Tephra
69	2918	17703±737	Kaihouri Tephra
71	3003	18095±575	Kaihouri Tephra
73	3215	19044±998	Kaihouri Tephra
75	3328	19727±1135	Kaihouri Tephra
76	3378	19897±1121	Kaihouri Tephra
77	3450	20168±1189	Kaihouri Tephra
81	3625	21196±906	Kaihouri Tephra
91	4038	23038±603	Paetahi Tephra
93	4136	23434±763	Paetahi Tephra
94	4155	23494±803	Paetahi Tephra
96	4301	24397±672	Paetahi Tephra
100	4510	25681±971	Poto Tephra

6.3. New Ages for Ruapehu tephras

In the course of this study three new ^{14}C-dates of Ruapehu-sourced tephras have been obtained (Table 6.3.1). The oldest provides clarity around ages of Ruapehu-sourced tephras that were formerly miss-identified as Ngauruhoe-sourced units and included at the base of the Mangatawai Formation. The following two provide new ages for the Tufa Trig Formation units, Tf1 and Tf2.

Table 6.3.1: New ^{14}C-dates for Ruapehu-sourced tephras.

No.	Descriptions	New ^{14}C-ages in B.P	New ages in cal. yrs. B.P.	Material analysed	Sample location
4	Tf 2	1490 ± 30 (NZA 29921)	1338 ± 45 cal. yrs. B.P.	charcoal	Loc 73
3	Tf 1	1713 ± 25 (NZA 29887	1555 ± 135 cal. yrs. B.P.	charcoal	Loc 73
2	sample 407 3, close to base of MF,	3330 ± 50 yrs B.P. (NZA 32433)	3508 ± 121 cal. yrs. B.P.	small amount of pollen and plant material	Loc 12
1	*Sample 407 3(a)*	*2701 ± 40 yrs B.P. (NZA 33057)*	*2783 ± 67 cal. yrs. B.P.*	*plant fragments*	Loc 78

Note: sample one (italic) has been considered unreliable and was not used further in this study

Donoghue *et al.* (1995) dated the Tufa Trig Formation unit Tf5 between 790 ± 119 and 611 ± 65 cal. yrs. B.P. using bracketing peat in the Ngamatea swamp, south of Waiouru. Ages of other Tf-named members and other recognised Ruapehu tephras in this study were estimated using soil and sediment accumulation rates in the sections studied. The thickness of single tephra units in these profiles has been subtracted for these accumulation rate calculations, whereas multiple layered tephras that represent a long eruption sequence were assigned an age of 1 year. Estimated error for these averaged accumulation rate measurements is considered to be smaller than ± 5 mm depth, considering that identifiable tephras are easily recognised down to 2 mm in profile. This measurement error is considerably less than the associated errors on the radiocarbon dates which are applied across all of the age estimations made. At Location 56, new radiocarbon dates and the position of the dated Tf5 show that the accretion rate of this accumulating soil (Alloway *et al.*, 1988; Cronin *et al.,* 1996a) changes over time. Using

the age of Tf2 (1338 ± 45 cal. yrs. B.P.) and the maximum age of Tf5 (790 ± 119 cal. yrs. B.P.), an average soil accretion rate of 1.95 yrs/mm or 0.51 mm/yr can be calculated. In comparison, post Tf5 an average accumulation rate is higher at 1.45 yrs/mm or 0.69 mm/yr. This post Tf5 rate is probably an overestimation, because the upper part of the soil profile is naturally less compact and contains higher volumes of organic material/humus that has already broken down in deeper levels (Birkeland, 1974). This age model leads to the possible correlation of Tf18 to the well known 1945 Ruapehu eruption that produced considerable widespread tephra (Johnston *et al.*, 2000).

Lake Rangatauanui

In total nine radiocarbon dates were obtained from the core at Lake Rangatauanui providing the basis for an age model for the 100 individual tephras within the core (Table 6.3.2). In addition, 11 rhyolitic tephras, sourced from the Taupo and Okataina Volcanic Centres and 13 andesitic Taranaki-derived tephras were clearly identified, which provide further age control (Fig 6.3.1).

Table 6.3.2: List of radiocarbon dates analysed from the core at Lake Rangatauanui. All dates were obtained using the AMS method at Rafter Radiocarbon Laboratory (Wellington, NZ) on bulk organic-rich sediment samples collected as 10 mm slices of the core.

Soil	Depth in mm	Lab-code	Age in ^{14}C yrs B.P.	Age in cal. yrs. B.P.
S-1*	90-111	NZA-29191	1885 ± 35	1718 ± 107
S-2	635-670	NZA29186	3325 ± 30	3487 ± 88
S-3	1429-1440	NZA29190	7403 ± 40	8165 ± 141
S-4	1980-1994	NZA29188	9581 ± 35	10 881 ± 210
S-5	2121-2185	NZA29187	10,377 ± 40	12 309 ± 249
S-6*	2737-2799	NZA29173	13,046 ± 60	15 438 ± 315
S-7	3076-3215	NZA29172	13,406 ± 65	15 945 ± 392
S-8*	3500-3612	NZA 29171	13,522 ± 70	16 089 ± 400
S-9	3933-3988	NZA 29175	18,880 ± 100	22 404 ± 186

Note: *ages rejected on the basis of known tephrostratigraphy in the core.

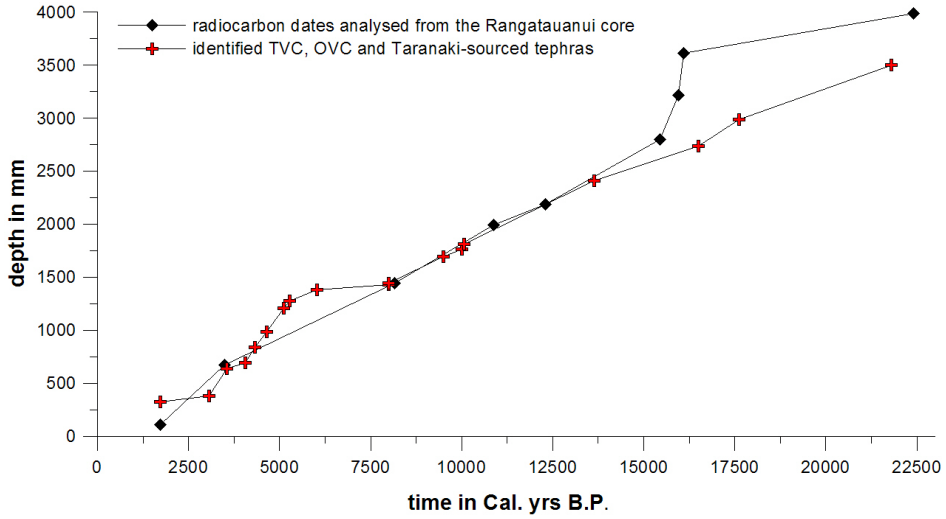

Figure 6.3.1: Depth-age curve of dated organic rich sediment sub-samples and the identified rhyolitic and andesitic tephras described above.

To determine an age model, both sources of time control were used. Recognising that there are time errors in ^{14}C-dates and uncertainties around identification of some individual distal tephras, the two information sources were critically compared. In three instances, ^{14}C ages were considered questionable. The youngest date (S1) of 1718 ± 107 cal. yrs. B.P. occurs at 198 mm above the unmistakeable Taupo Pumice of 1717 cal. yrs. B.P. Hence this ^{14}C date was not used. The S6 and S8 dates were also not used, because they were out of sequence with several marker tephras, even using available error ranges.

Table 6.3.3: Dated tephras and radiocarbon dates used to create the spline fit.

Depth	Age in B.P.	Description
309	1850 ±0	Taupo Pumice (TVC)
635	3325 ±30	dated soil (S2)
820	3940 ±70	Stent Tephra (TVC)
1419	7250 ±20	Mamaku Tephra (OVC)
1678	8530 ±10	Rotoma Tephra (OVC)
1809	9050 ±40	Opepe Tephra (TVC)
1980	9581 ±35	dated soil (S4)
2121	10377 ±40	dated soil (S5)
2400	11850 ±60	Waiohau Tephra (OVC)
2723	13800 ±300	Rotoaira Lapilli (TgVC)
2985	14700 ±110	Rerewhakaaitu Tephra (OVC)
3933	18880 ±100	dated soil (S9)

A piecewise cubic Hermite interpolating polynomial fit was used on the most reliable age horizons (Fritsch and Carlson, 1980; Turner *et al.*, 2008a; Table 6.3.3). All of these horizons have associated errors that are assumed to be normally distributed. From this model all unknown units can be assigned an age with an associated error. Using a Monte Carlo approach and repeating the age assignment process 1000 times (while maintaining stratigraphic order) the most likely ages with associated errors were derived (e.g., see method applied in Turner *et al.,* (2008a); Figures 6.3.2. and 6.3.3.; Appendix 5).

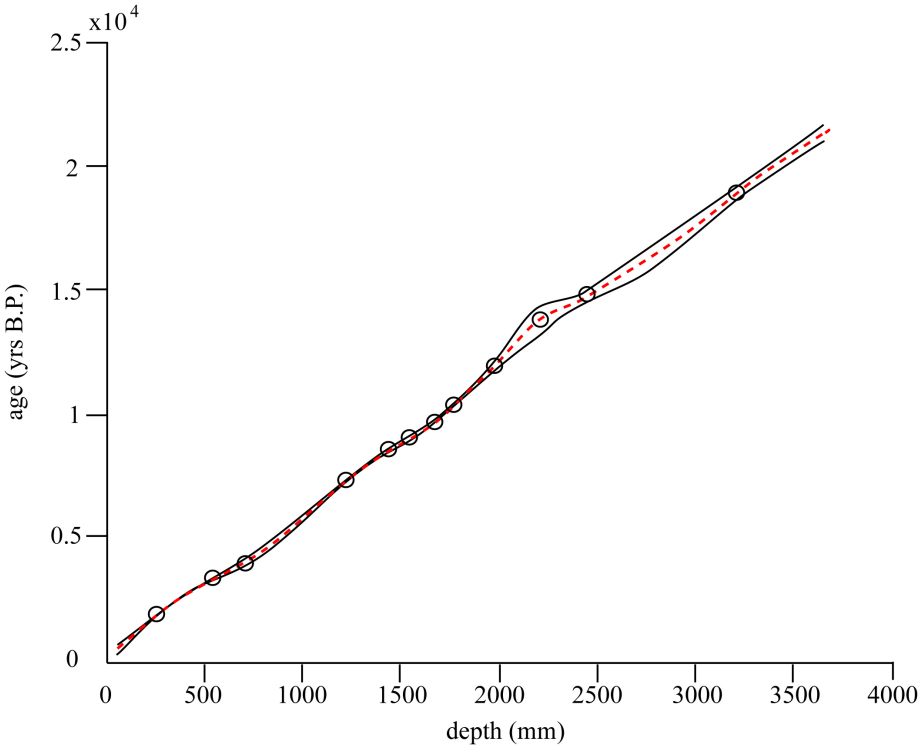

Figure 6.3.2: Depth age curve as spline fit of the Rangatauanui core (red) with associated errors (black) in yrs. B.P. for dated tephras in Table 6.3.3.

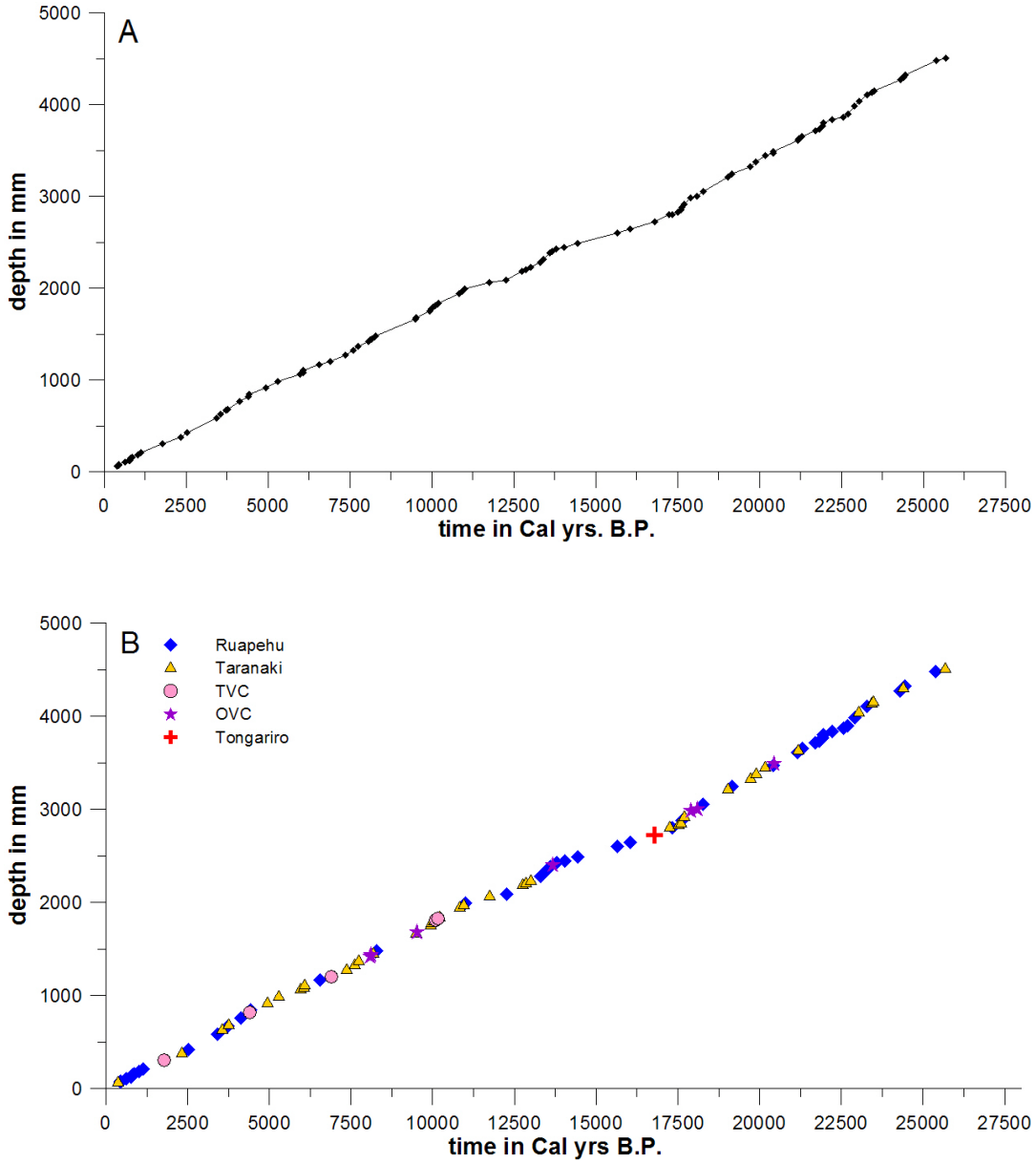

Figure 6.3.3: Depth-age spline-fit curve (in cal. yrs. B.P.) for the Rangatauanui core, showing the (A) ages of all tephra units within it; (B) showing the different sources of individual tephras.

6.4. Lithological componentry of tephras sourced from Ruapehu

Ruapehu tephras are characterised by crystals, volcanic glass fragments, and accidental lithics. The crystals are represented by clinopyroxene (cpx), orthopyroxene (opx), plagioclase (plg), along with rare hornblende (hb) and olivine (ol). Both, black glass

(opaque in plane-polarised light) and transparent (in plane polarised light) glass occurs. The latter ranges in colour under plane-polarised light from light to dark brown glass. Lithics comprise both accidental and cognate fragments. For particle-size fractions of 1-2 mm, 0.5-1 mm, 0.25-0.5 mm, 300 to 500 grains were counted (Appendix 4).

Crystals

The ferromagnesian mineral assemblage of Ruapehu tephras from the Tufa Trig and Bullot Formations are described as being opx > cpx with trace ol and trace hb in finer fractions (Donoghue, 1991). Plagioclase is often the dominant mineral phase, occurring as clear and white crystals (3-15 modal%), while pyroxene ranges between 1.2 to 27.1% with both cpx-dominant (55%) and opx-dominant units occurring. In rare cases the pyroxenes are coated with black or dark brown glass. Dark brown to black hornblende crystal fragments occur in 74.2 % of all analysed samples ranging between 0.6 to 5.8 %. Olivine is present as small pale green to pale brown broken crystals in 45% of samples, from 0.1 to 0.8 modal%. No major variation occurs in mineral proportions within the different size fractions analysed (Figure 6.4.1).

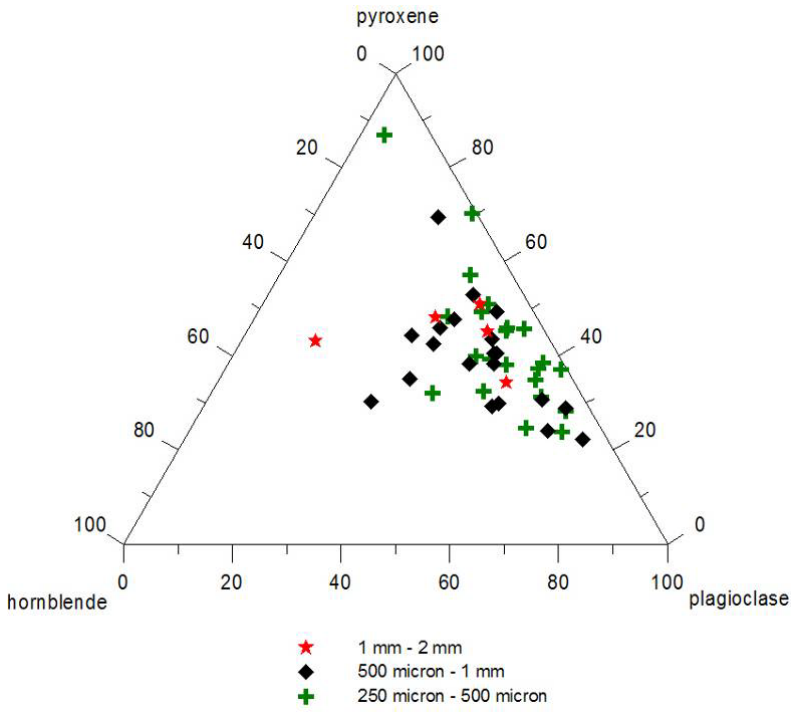

Figure 6.4.1: The ratio of the major modal minerals in tephras sourced from Mt. Ruapehu.

Volcanic glass

The shape and appearance of volcanic glass depends on the eruption style (Heiken, 1972; Sheridan and Wohletz, 1983; Wohletz, 1983; Heiken and Wohletz, 1985). The presence of Crater Lake on Mt. Ruapehu has been interpreted to have a major influence on the amount and appearance of the volcanic glass in its tephras (e.g., Donoghue *et al*., 1997; Cronin *et al.,* 2003). In 58% of the analysed Ruapehu-sourced tephras, volcanic glass is the dominant component (43.4 to 81.2 modal %). The exceptions are samples analysed from the Ruapehu 2007 eruption, where only 2 to 6% of the erupted material was juvenile volcanic glass. Both black and light/translucent glass occurs in all samples, and in 52% of them the latter is dominant.

Accidental and cognate lithics

Lithics are present in all analysed samples (1 to 42%) comprising rounded and sub-angular fragments of the Mesozoic basement rock (metagreywacke) as well as cognate clasts that are mainly recycled material from the hydrothermal vent system beneath Crater Lake (Christenson and Wood, 1993).

Accretionary lapilli and sulphur pellets

In tephras erupted from Ruapehu in 1995-96, accretionary lapilli occur up to 2 mm in diameter, being mostly spherical shaped with some being partly elongate (Cronin *et al.,* 2003). No accretionary lapilli have been found in older Ruapehu tephras of this study, although they are common in some units of the Bullot Formation (Pardo, 2009 pers. comm.). Also present in the 1995 and 2007 eruptions were up to 2 mm grey spherules of elemental sulphur (Cronin *et al.,* 2003; Christenson *et al.,* 2010). Sulphur was also the most abundant vug-filling mineral in ballistic clasts from the September 2007 Ruapehu eruption and is thought to form a molten pool at the base of the lake (Christenson *et al.,* 1993; 2010).

The ternary ratio of glass, lithics and crystals can be used to divide Ruapehu tephras into 2 groups: glass-rich and lithic-rich types (Figure 6.4.2). These two groups

distinguish dominantly magmatic vs. phreatomagmatic/phreatic eruption styles which are influenced by Crater Lake and vent-hydrothemal systems on the volcano (see Chapter 7). Crystals increase in content in finer grain-size fractions, which reflects their natural size and that phreatomagmatic fragmentation processes are common.

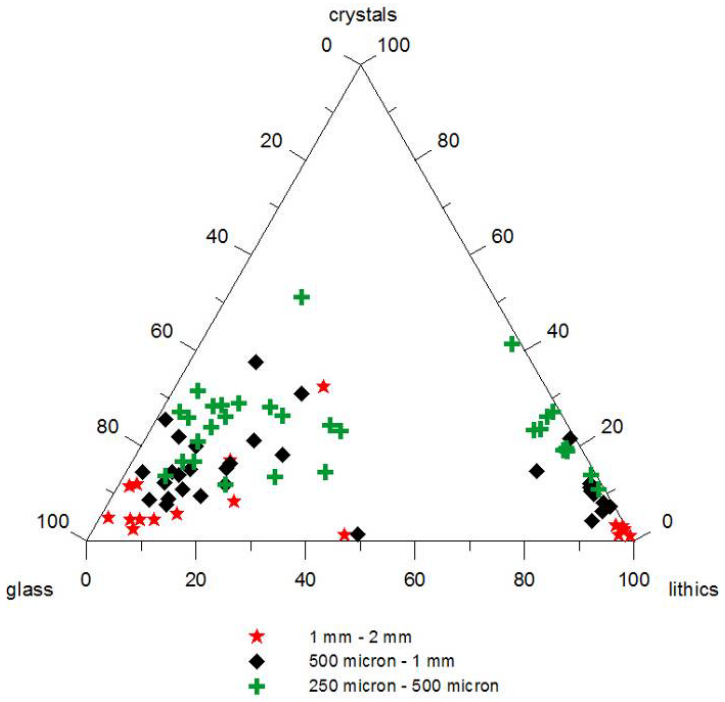

Figure 6.4.2: Discrimination plot of glass, lithic and crystal modal fractions for three different size ranges. Note the clear distinction of two groups of tephras that are either glass or lithic-dominant.

6.5. Geochemistry

Geochemical analyses of Ruapehu-sourced tephras are focused on volcanic glass for tephra correlation purposes, as described in Chapter 5. Glass composition in andesitic tephras is dependent on the conditions just prior and during the eruption (Platz *et al.*, 2007). Back-scattered scanning electron microscope images of Ruapehu sourced glasses show that they are commonly enriched in microlites, which also has a major influence on residual glass compositions (Figures 6.5.1 and 6.5.2). Price *et al.* (2005) suggested a complex plumbing system beneath Ruapehu, where magma evolves in many small and isolated bodies before erupting. The glass chemistry analysed in this study supports this

theory and emphasises that late-stage microlite growth may also generate a wide variation in major oxides in glass compositions.

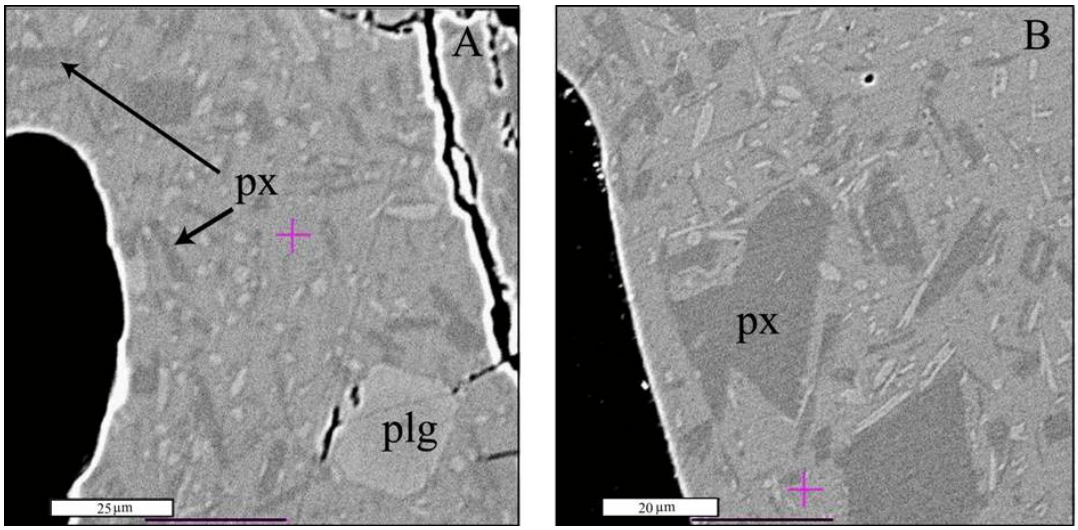

Figure 6.5.1: Microlites within volcanic glass from Ruapehu-sourced tephras.

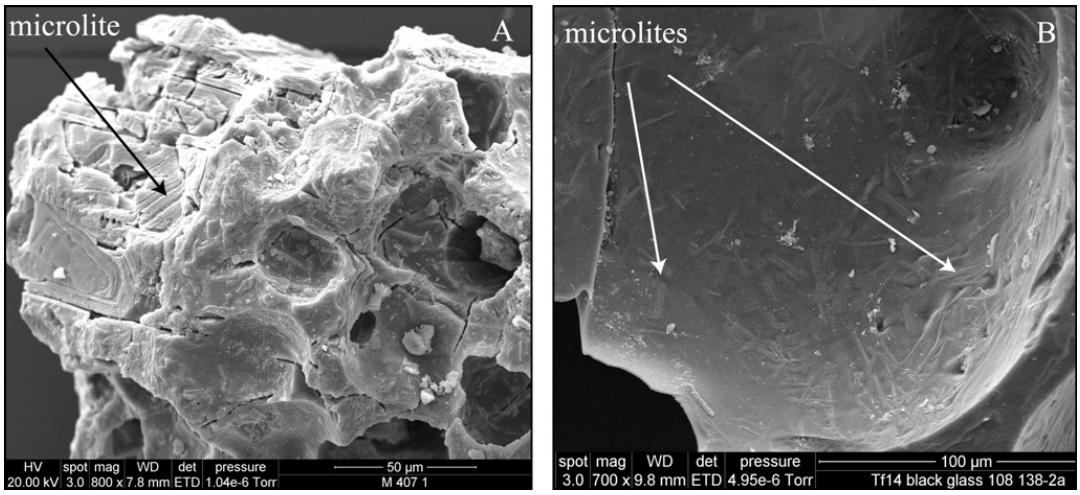

Figure 6.5.2: SEM-images of volcanic glass sourced from Ruapehu showing A) microlites which are exposed through weathering and B) are just under the surface, covered by a thin glass "skin".

In general, no major chemical differentiation has occurred over time in glass compositions from Ruapehu since the early Bullot Formation (Figures 6.5.3 A-H and Figures 6.5.6a+b and 6.5.7). As described in Chapter 5.1.7, the chemical composition of the glass reflects mainly the last stage of the melt prior to the eruption and shows the results of crystallisation fractionation of microlites within the volcanic glass as well as ongoing growth of many of the phenocryst phases. The overall ranges in compositions reflect variations in the relative components of the major microlites forming: i.e., plg, opx, cpx, and tm (Figures 6.5.4 and 6.5.5).

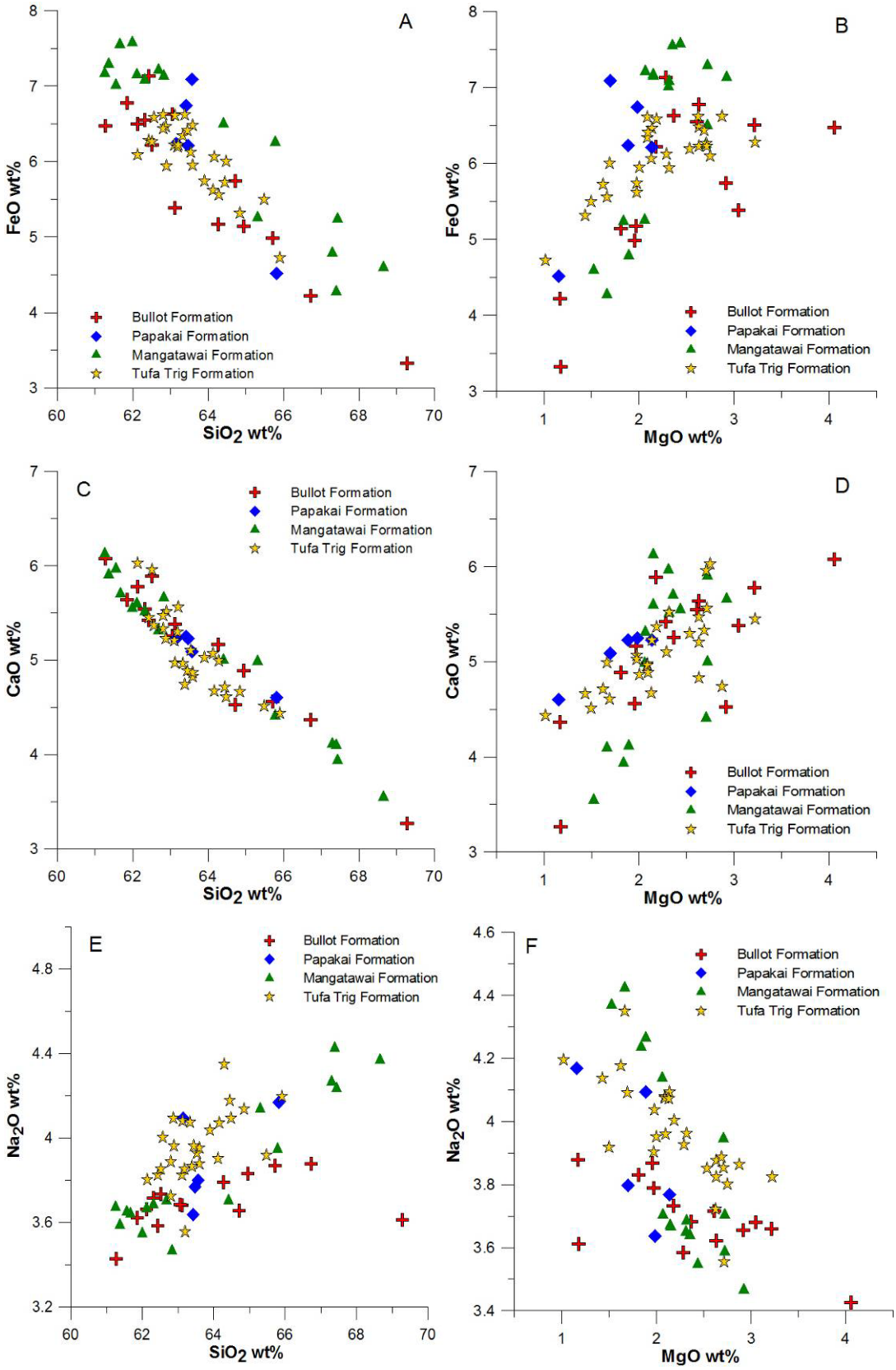
A
FeO wt%
SiO2 wt%
B
FeO wt%
MgO wt%
C
CaO wt%
SiO2 wt%
D
CaO wt%
MgO wt%
E
Na2O wt%
SiO2 wt%
F
Na2O wt%
MgO wt%
Bullot Formation
Papakai Formation
Mangatawai Formation
Tufa Trig Formation

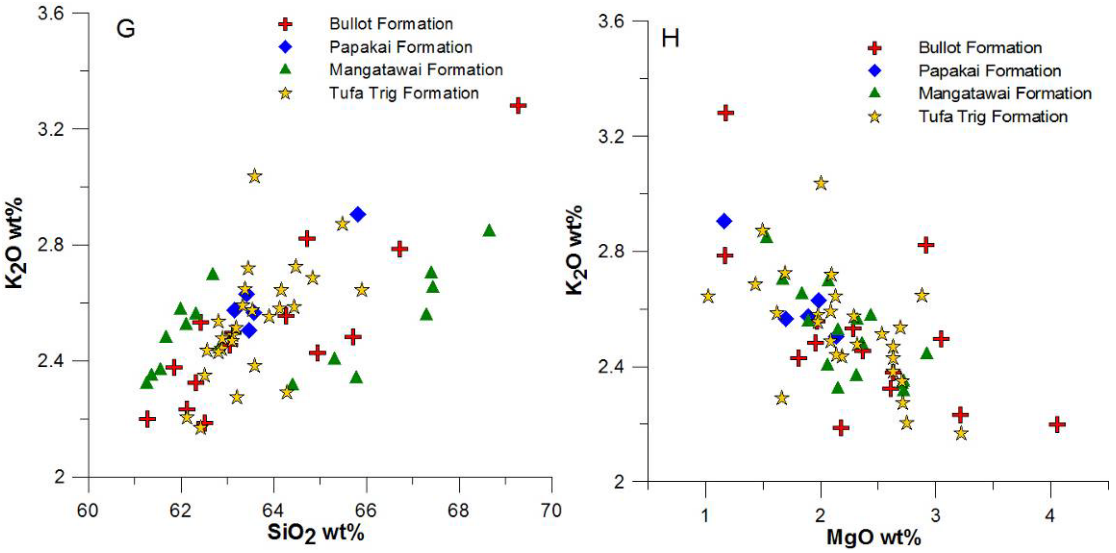

Figure 6.5.3: Electron microprobe-determined major oxides plotted against SiO_2 wt% (left) and MgO wt% (right) for volcanic glasses sourced from Mt Ruapehu over the last c. 20 ka.

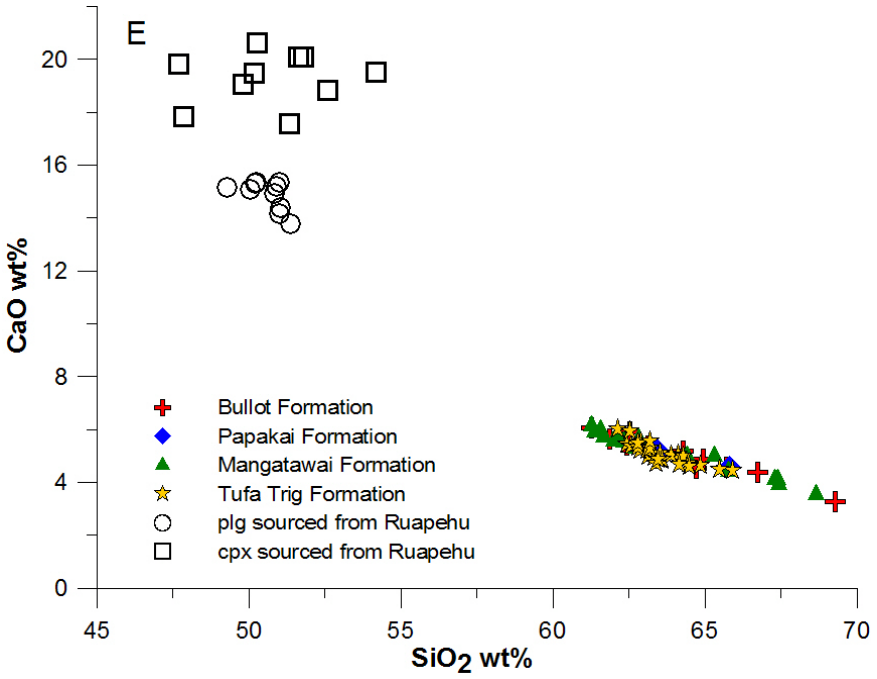

Figure 6.5.4: Major oxide analysis SiO_2 vs. CaO, of glasses in comparison to EMP-analysis of pyroxene and plagioclases sourced from Ruapehu, illustrating that crystallisation fractionation of clinopyroxene and plagioclase could generate some of the narrow trend seen in glass analyses (pyroxene data from Cronin (1996)).

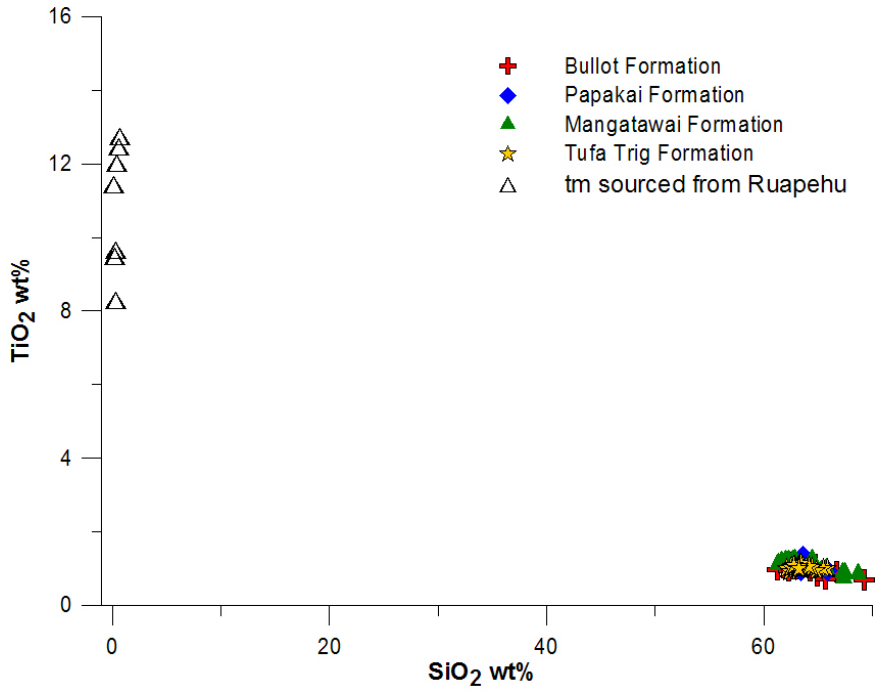

Figure 6.5.5: Major oxide analysis SiO_2 vs. TiO_2, glasses in comparison to EMP-analysis of titanomagnetites from Ruapehu-sourced tephras from the Mangatawai Formation at Location 12, illustrating that even minor crystallisation of this phase could have a major influence on the residual glass composition.

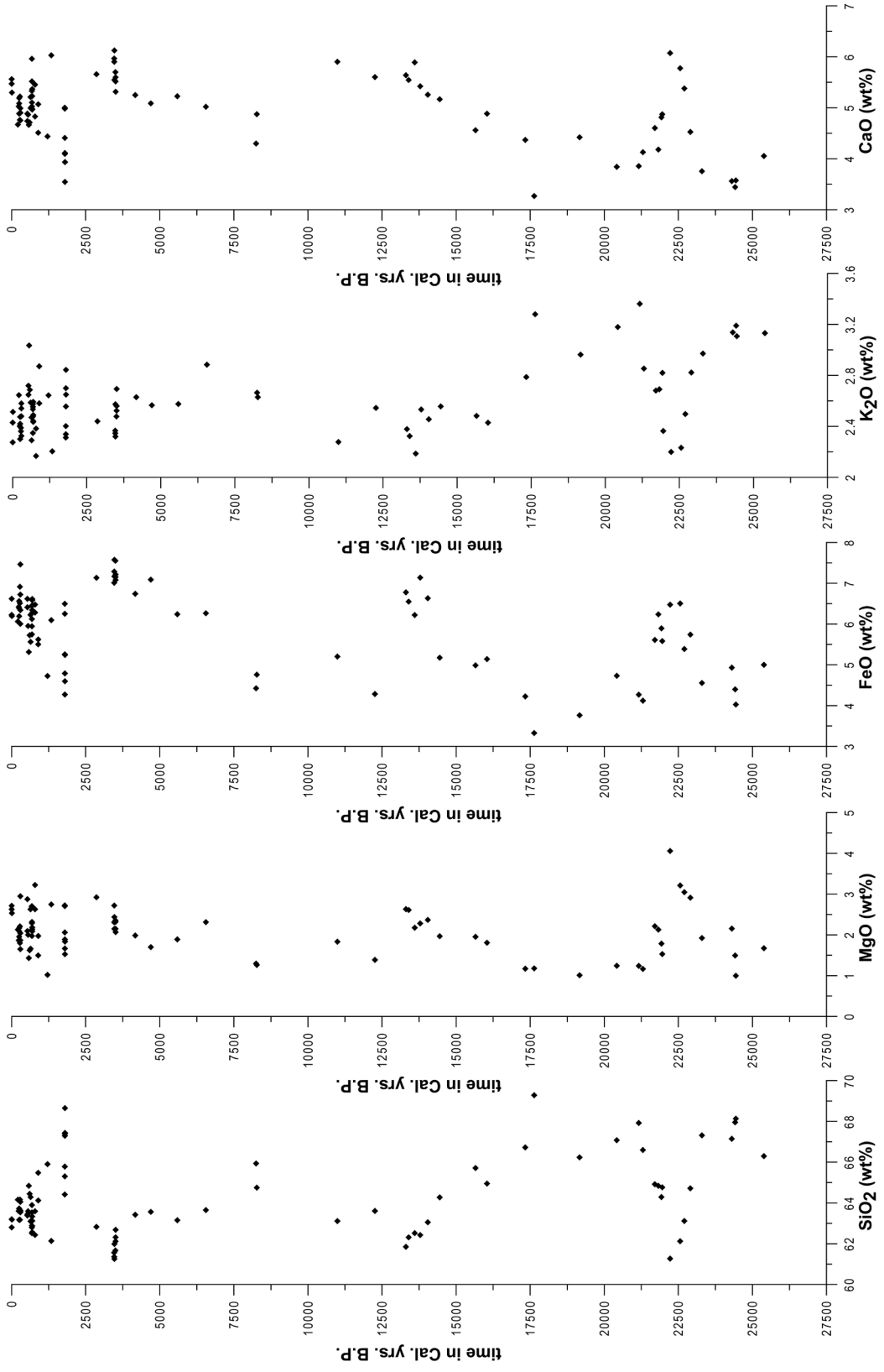

Figure 6.5.6a: Major oxide glass chemistry of Mt Ruapehu tephras over time.

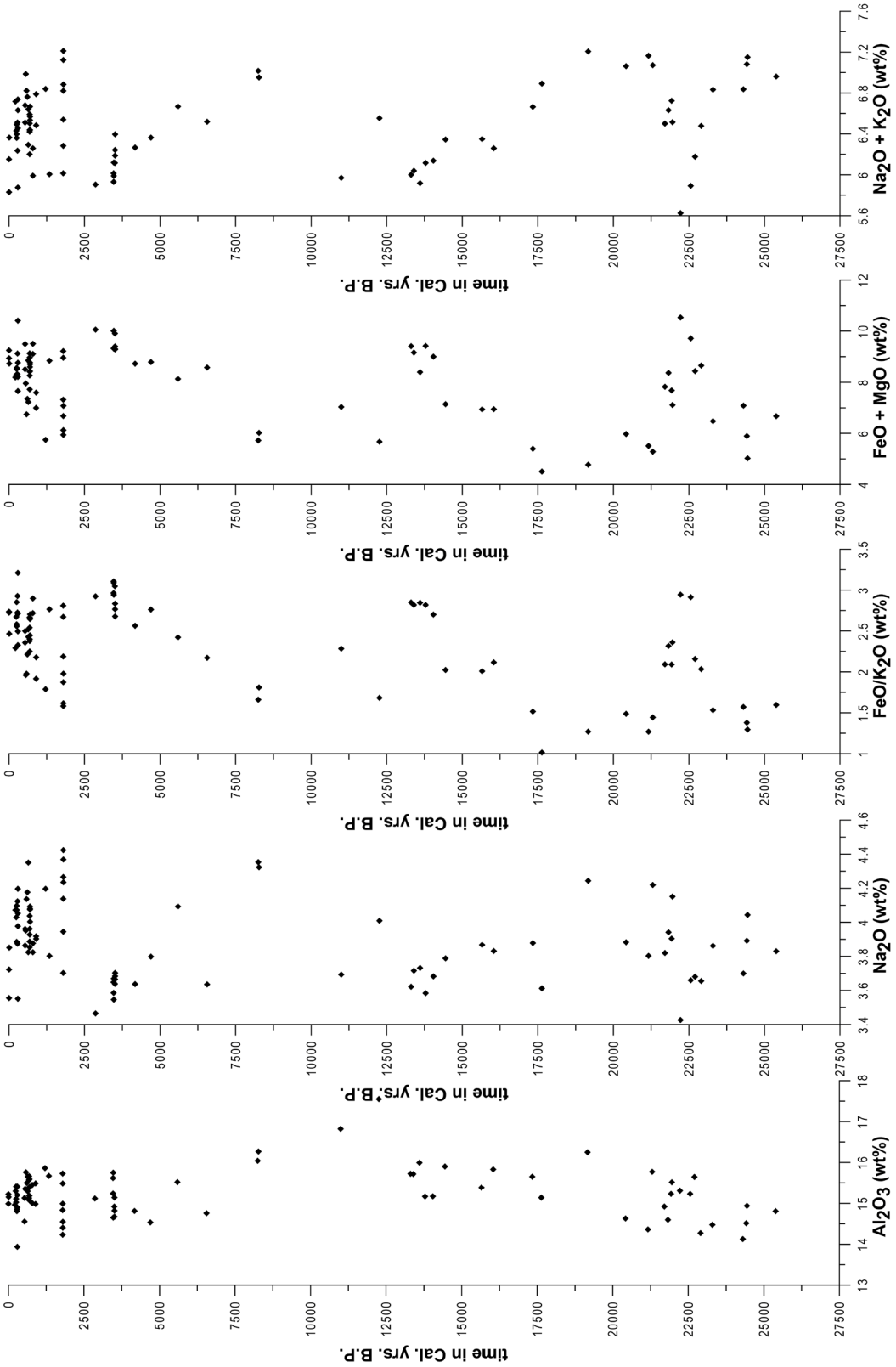

Figure 6.5.6b: Major oxide glass chemistry of Mt Ruapehu tephras over time.

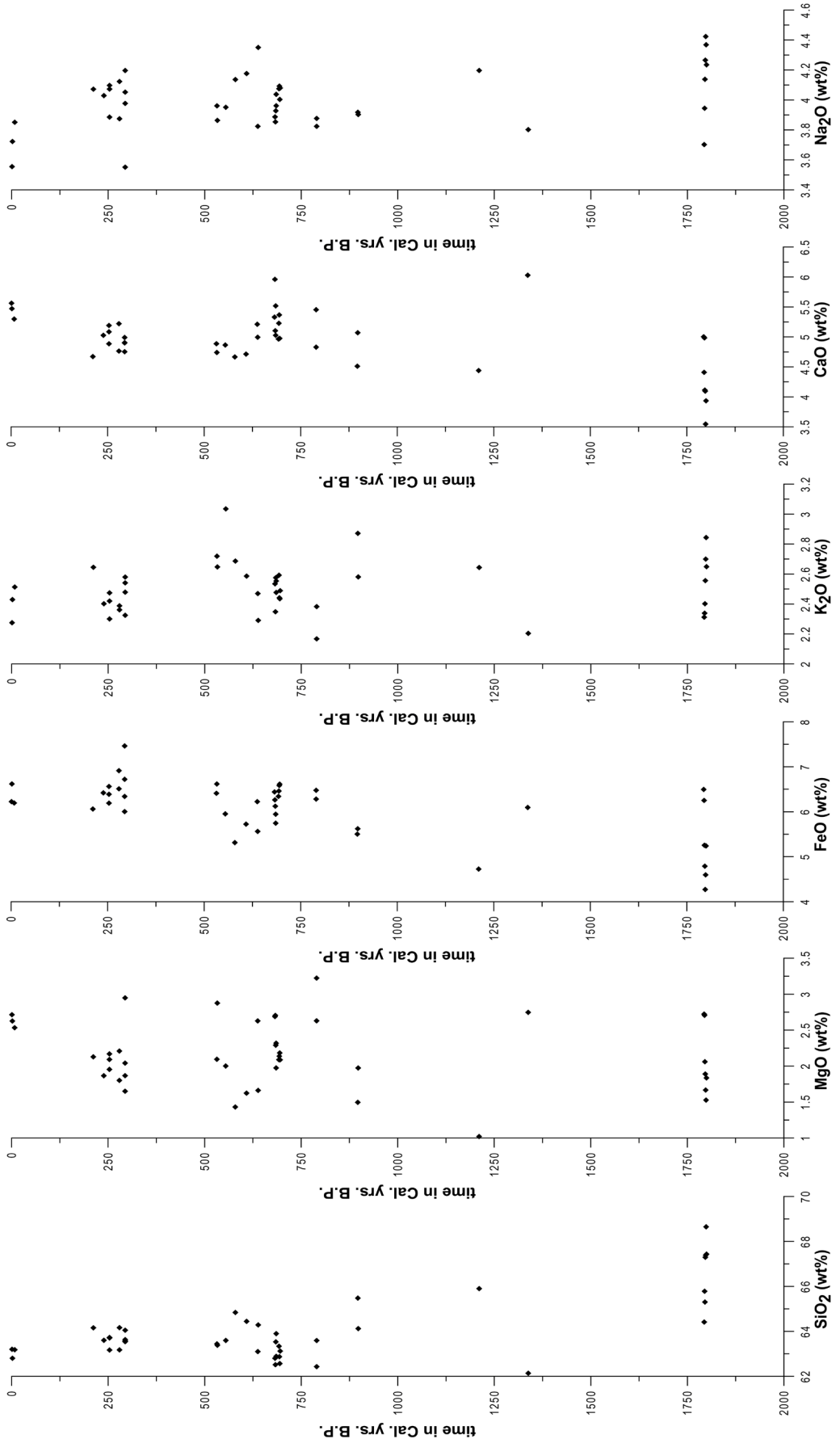

Figure 6.5.7: Major oxide glass chemistry of Mt Ruapehu tephras over the last ~2000 cal. yrs. B.P.

Chapter 7

Explosive eruption styles of the Tongariro Volcanic Centre volcanoes during the last 12 000 cal. yrs. B.P.

7.1 Introduction

Since the late 1830s, numerous eruptions of Ngauruhoe, Ruapehu, Red Crater and Te Maari have been observed and described. According to Hobden (1997), around 95% of the observed eruptions from TgVC were entirely explosive. Ruapehu eruptions have been influenced by the presence of the Crater Lake, which results in magma-water interaction, particularly during the initial phases of pyroclastic eruptions. Observed Ruapehu eruptions have been phreatic and phreatomagmatic, although magmatic, strombolian to sub-plinian eruptions have also occurred during longer periods of activity (Gregg, 1960b; Nairn *et al.*, 1979; Cronin *et al.,* 2003). Ngauruhoe, on the other hand has no permanent glaciers or water bodies in its active crater, and its eruption behaviour is more controlled by magmatic flux and gas content (Gregg, 1956; Nairn *et al.*, 1976).

In the first part of this chapter, observations and deposits from historical eruptions are illustrated and described, leading to provide a comparison and a contrast with prehistoric tephra deposits from TgVC in the latter half of the chapter.

7.1.1. Terminology and definitions

Eruption styles

Walker (1973) classified a range of eruption styles based on area of dispersion (D) and degree of fragmentation (F) of their tephra deposits. Hawaiian and strombolian eruptions have the lowest D and F values, whereas subplinian and plinian events have much higher tephra dispersal and fragmentation. With addition of water, phreatomagmatic eruptions result, including small-scaled events emerging from under water (surtseyan), to more violent phreatomagmatic eruptions, equivalent to plinian events in dispersal, but with much higher fragmentation in the resultant tephras. Vulcanian eruptions are not well classified, but are assumed to occupy intermediate values of D and F.

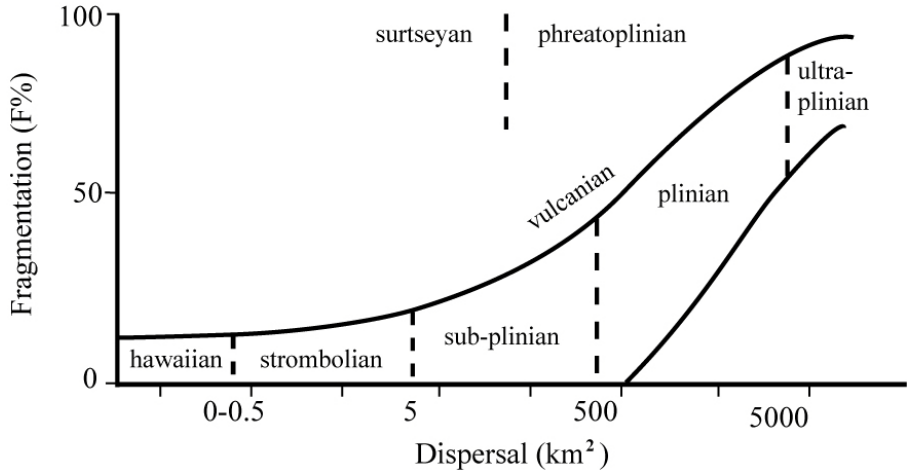

Figure 7.1: A classification diagram for eruptions styles based on their tephra fragmentation index (F) and dispersal area (D), as defined by Walker (1973).

Since this time, many attempts have been made to re-classify and more strongly discriminate the differences between eruption styles, based on observational criteria and deposit and pyroclast characteristics. In the following section, the terms usage of these in this study is explained.

Strombolian eruptions

These involve repeated discrete explosions of low magnitude, and are typical of low-viscosity magmas with low mass-eruption rates (Blackburn *et al.*, 1976; Vergniolle and

Mangan, 2000). They often produce ballistics and incandescent showers of pyroclasts which, under high eruption rates, build up scoria and spatter cones, at times leading to lava flows. Fragmentation and ejection of magma is driven primarily by magma volatiles exsolving from the low-viscosity basaltic melts. Column heights and volumes are low (0.1-5 km) and products often include bread-crust bombs, scoria and lapilli to coarse-grained ash, indicating a low degree of fragmentation. At the vent, the deposits are commonly agglutinated due to rapid deposition of still-hot spatter. Such eruptions may last several seconds to hours (Cas and Wright, 1988), or may be semi-continuous, as in the case of Stromboli (Italy) and Yasur (Vanuatu). The Volcanic Explosivity Index (VEI) of strombolian events is mainly 1-2 (Newhall and Self, 1982). Typical examples of strombolian eruptions are obviously documented at Stromboli, Italy (Rosi *et al.*, 2000) as well as Heimaey, Iceland (Self *et al.*, 1974), Etna, Sicily (Polacci *et al.*, 2006), Eifel, Germany (Houghton and Schmincke, 1989) and White Island, New Zealand (Houghton and Nairn, 1991). Strombolian activity was observed during the 1948-49, 54-55 and 1974 eruptions of Ngauruhoe (Allen, 1948; Gregg, 1956; Lube *et al.*, 2007).

Violent Strombolian eruptions

The term "violent strombolian" was defined by MacDonald (1972) to describe explosive eruptions that are more violent than the *sensu stricto* strombolian, but do not fit the criteria of vulcanian eruptions. According to Walker (1973), violent strombolian eruptions involve more viscous magmas and "repeated clogging of the vent". They may also be related to the contact of magma with groundwater. Walker describes violent strombolian tephras as bridging the properties between strombolian and surtseyan deposits. Pioli *et al.* (2008) have revised the definition of violent strombolian eruptions and describe them as pulsatory, producing eruption columns between 2 and 6 km high, with fine ash as well as lava flows. Wong and Larsen (2010) defined a transition between violent strombolian and subplinian eruptions at an eruption column height of 10 km, a dispersal of >150 km^2, and a mass discharge rate of $>10^6$ kg/s. Examples of violent strombolian eruptions are recorded at Paricutin, Mexico (Pioli *et al.*, 2008), Vesuvius, Italy (Arrighi *et al.*, 2001), Okmok, Alaska (Wong and Larsen, 2010) and Lathrop Wells, USA (Valentine *et al.*, 2005; Valentine *et al.*, 2007).

Vulcanian eruptions

These are characterised by repeated, brief, violent explosions that often produce pyroclastic density currents and shock waves (Morrissey and Mastin, 2000, Self *et al.*, 1979). They deposit blocks and bread-crusted bombs near the vent, plus highly fragmented ash. Vulcanian eruption column heights may range between 3 and 15 km, with VEI's of 2-3 (Newhall and Self, 1982). These kinds of eruptions are common for andesitic volcanoes where the conduit system is obstructed by a dome or degassed magma plug, and where contact with external water is common. Typical examples for these eruptions are known from Ngauruhoe, New Zealand (Nairn and Self, 1978), La Fossa volcano, Italy (Frazzetta *et al.*, 1983), Sakurajima, Japan (Yokoo *et al.*, 2009), Galeras, Colombia (Stix *et al.*, 1997), Soufrière Hills, Montserrat (Formenti *et al.*, 2003), and Arenal, Costa Rica (Fundali and Melson, 1971).

Sub-plinian eruptions

The key difference of this type of eruption from the above-described styles is a sustained magma discharge, rather than brief unsteady bursts. They can be small to highly energetic events that often produce high, convective eruption columns (<20 km), pyroclastic density currents and widely dispersed tephra falls (e.g., Cioni *et al.*, 2000), with VEI's of 4-5 (Newhall and Self, 1982). Examples for this type of eruption have been described at Hekla, Iceland in 1970 (Thorarinsson and Sigvaldason, 1972), Vesuvius, Italy (Sulpizio *et al.*, 2005), Mt St. Helens, USA (Scandone and Malone, 1984); Pinatubo, Philippines (Koyaguchi and Ohno, 2001) and Furnas volcano, Azores (Cole *et al.*, 1995)

Magma fragmentation mechanisms

Fragmentation of a "dry" magma is controlled by its volatile content, viscosity, crystallinity and composition, as well as ascent, degassing, and decompression rates. Rapid exsolution of magmatic volatiles related to rapid decompression and/or syneruptive crystallisation results in magmatic fragmentation (Cashman *et al.*, 2000, Cashman and Blundy, 2000). Fragmentation of the magma is caused by formation of a magma foam as bubbles grow; this becomes unstable and breaks apart upon rapid decompression (Sparks, 1978; Cashman *et al.*, 2000; Dingwell, 2001). Energy, gas and

heat released during fragmentation generates a convective eruption column (Cashman *et al.*, 2000).

When external water comes in contact with hot magma, vapour films may rapidly build and collapse, generating an explosive phreatomagmatic interaction that is a highly efficient magma fragmentation mechanism (Sheridan and Wohletz, 1983, Morrissey *et al.*, 2000, Wohletz, 2002). The effectiveness of this process relates to the geometry of the contact, mixing conditions, water supply and the local magma:water mass ratio (Wohletz and Heiken, 1991). In most eruptions, pyroclasts are influenced by a combination of magmatic and phreatomagmatic fragmentation mechanisms.

Phreatic eruptions

Phreatic or steam-driven eruptions are caused by the sudden depressurisation of hot magmatic steam and/or volatiles, without directly involving any magma (Ollier, 1974; Sheridan and Wohletz, 1983; Barberi *et al.*, 1992; Germanovich and Lowell, 1995). Therefore, during these eruptions no juvenile material is ejected. In general, phreatic eruptions are localised phenomena associated with degassing volcanoes and within solfatara areas of volcanoes (Barberi *et al.*, 1992). Examples of phreatic eruptions are described from Ruapehu, New Zealand (Nairn *et al.*, 1979), Aso, Japan (Yokoi *et al.*, 1996), Shiveluch, Russia (Ponomareva *et al.*, 1998), Etna, Italy (Branca and Del Carlo, 2005) and Dieng, Indonesia (Le Guern *et al.*, 1982).

7.2 Eruption styles of historical events from Ngauruhoe and Ruapehu volcanoes

Deposits of observed eruptions provide a valuable opportunity to understand the mechanisms creating tephras from prehistoric eruptions. The following section will focus on the descriptions and deposits of the 1954-55 and 1974-75 Ngauruhoe eruptions, and eruptions occurring from Ruapehu in 1995-96 and 2007.

7.2.1 Eruptive styles of historical Ngauruhoe eruptions

Eruptions from Ngauruhoe have been observed and documented since 1839 and are summarised in Gregg (1960b). The most commonly described are small strombolian and vulcanian eruptions (VEI 1-3), producing eruption columns up to 11 km high, as well as occasional pyroclastic density currents (PDCs) and lava flows. The 1954-1955 eruptions were among the most significant of this volcano. These involved major fire-fountaining that generated 11 lava flows, along with strombolian eruptions that produced several ash-fall events. The recent inner cone of Ngauruhoe was formed by the 1954-1955 eruption series (Figure 7.2.2). Between 1955 and 1974 at least seven brief explosive (vulcanian?) eruptions occurred (Hobden *et al*. 2002). The 1974 eruption was the best observed, distributing very fine ash from an eruption column of 3.7 km height as far as Taumarunui (45 km north-west), although the deposit was only 25 mm thick near the crater (Self, 1975).

The eruption sequence that began on 12 February 1975 is one of the best described from Ngauruhoe. The initial eruption columns were 600-1400 m above the crater. Volcanic ash was deposited c. 10-15 km away on the Desert Road (based on unpublished reports of Otway and Hewson, 1975, held at GNS). The largest eruption occurred on 19 February starting with “cannon-like” explosions producing shockwaves (Nairn and Self, 1978; Morrissey and Mastin, 2000). A vulcanian eruption column rose up to 6 km before partial collapses generated pyroclastic flows into the Mangatepopo Valley to the north-west (Nairn, 1976; Lube *et al.*, 2007). The lower part of the column (150-200 m) was primarily a fountaining of lava spatter, creating an agglutinate around the crater rim (Figure 7.2.1A), some thin rootless lava flows and several pyroclastic flows where the agglutinate collapsed (Lube *et al,* 2007). Later (1810 hrs), the column rose up to 11 km causing wide distribution of a thin fine ash layer (Figure 7.2.1B). The interior of the column partially collapsed generating pyroclastic avalanches onto the north-western and western slopes. At 1920 to 2008 hrs the same day the intensity of the eruption waned until it finally stopped during the night.

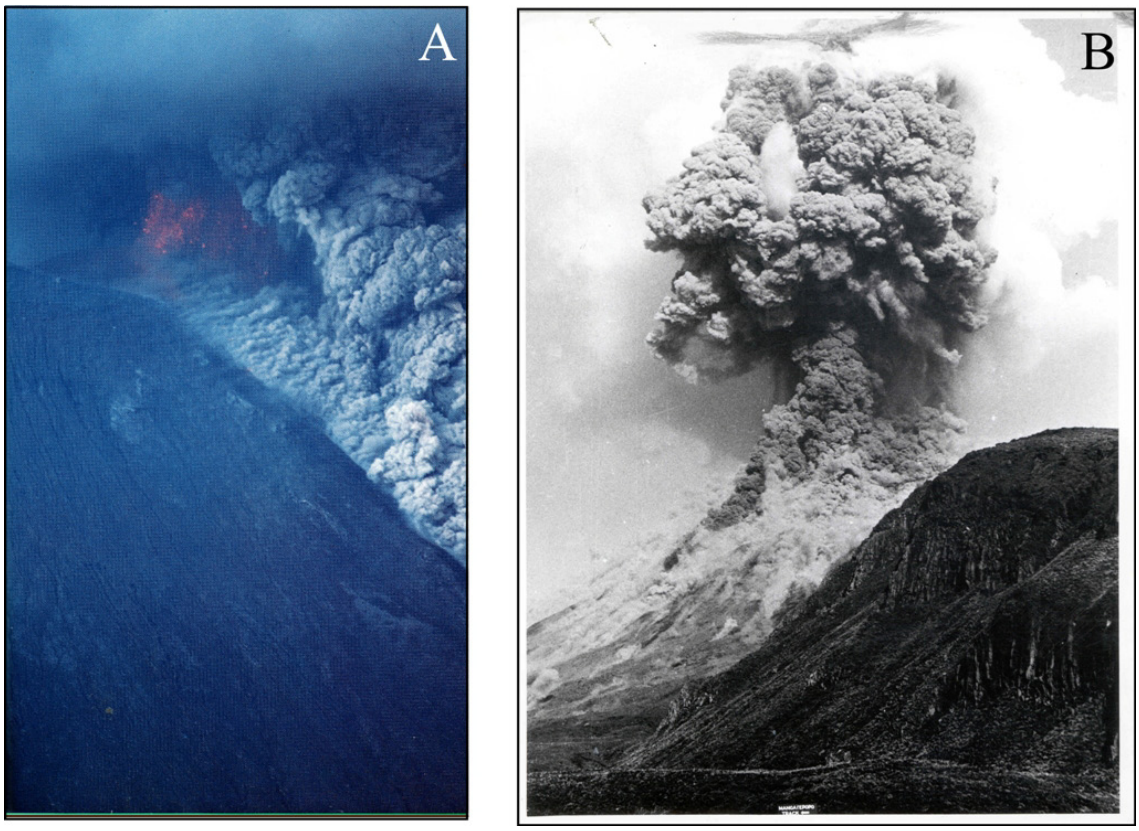

Figure 7.2.1: Ngauruhoe eruption 19 February 1975. A) Ejected lava spatter within the lower eruption column in the mid morning, creating an agglutinate on the crater rim (photographer: Herb Spannagl), and B) Partly collapsing eruption column creating pyroclastic flows at 1810 hrs (photographer: Graham Hancox, GNS).

Field-characteristics of the 1954-55 and 1974-75 eruptions at Ngauruhoe's crater rim

Deposits of the 1954-55 and 1975 eruption episodes are preserved at the crater and on the north-western slopes of Ngauruhoe (Figure 7.2.2). The 1975 deposits were described in detail by Henderson (2004); Martelli (2007), and Lube *et al.* (2007), while the inner crater facies was documented by Hobden *et al.* (2002) and Krippner (2009). Krippner (2009) described five units deposited during the 1954-55 eruption episode (Figure 7.2.2) and two from the 1975 eruption (Figure 7.2.3). The 1954-55 sequence begins with strombolian and spatter deposits that are now hydrothermally altered (Unit A), passing up to strombolian scoria lapilli-bomb layers (Unit B), a ponded lava (Unit C), followed by further strombolian lapilli and ash deposits (Unit D). The Unit D beds are associated with the 1955 eruptions and the 50 cm-thick beds dip at 30̊, parallel to the outer Ngauruhoe flanks (Krippner, 2009). The Unit E consists of a pinkish-grey ash

with common outsized bombs up to 10 cm in diameter (Figure 7.2.3, right side). While interpreted by Krippner (2009) to represent a 1955 event, it is here interpreted to represent the onset of February 1975 eruptions. This passes up to Unit F, which consists of seven individual tephras varying in colour (pale grey – pinkish red) and grain size (very fine ash – blocks (up to 13 cm). Some of the units show lamination and cross bedding and are interpreted to be surge deposits produced from collapsing eruption columns and explosions. The uppermost unit (Unit G) is a ~10 m-thick agglutinate representing the main magmatic phase of the 19 February 1975 eruption. This unit is a red-brown in colour, irregularly densely welded and commonly containing 1-10 cm xenoliths of quartzite (Krippner, 2009).

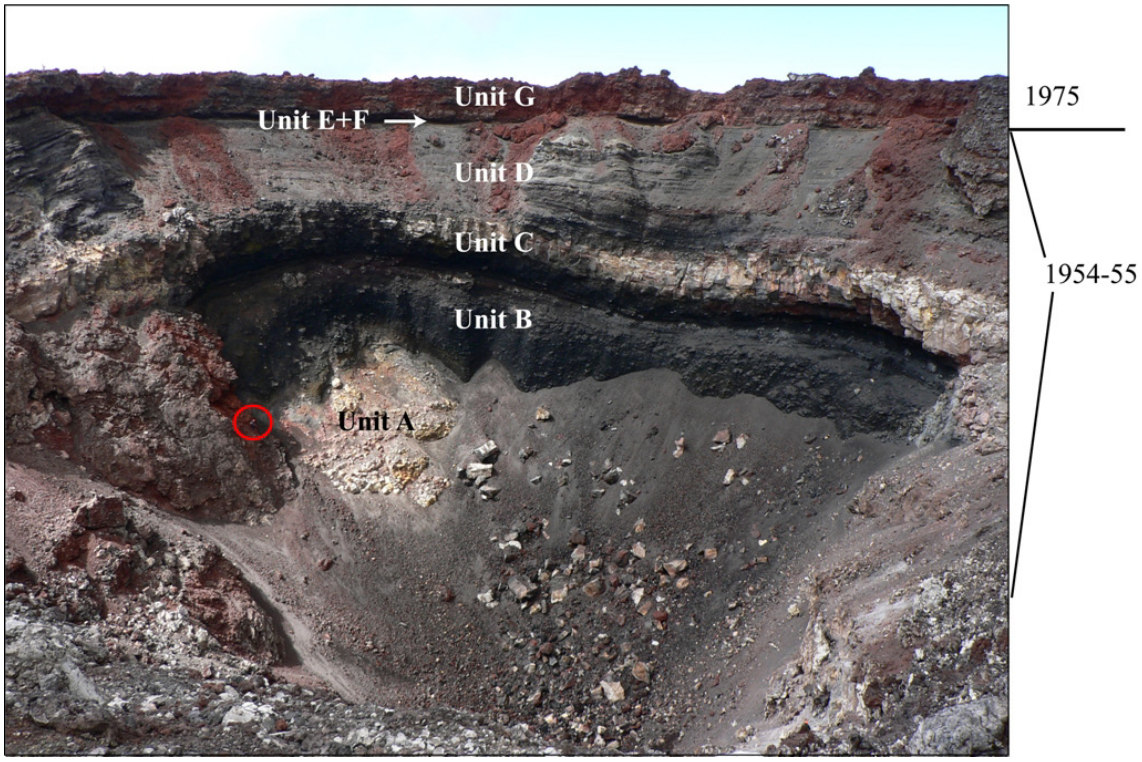

Figure 7.2.2: The inner crater facies of Ngauruhoe. The Units A-G were defined by Krippner (2009), and the red circle frames a 1.7 m tall person.

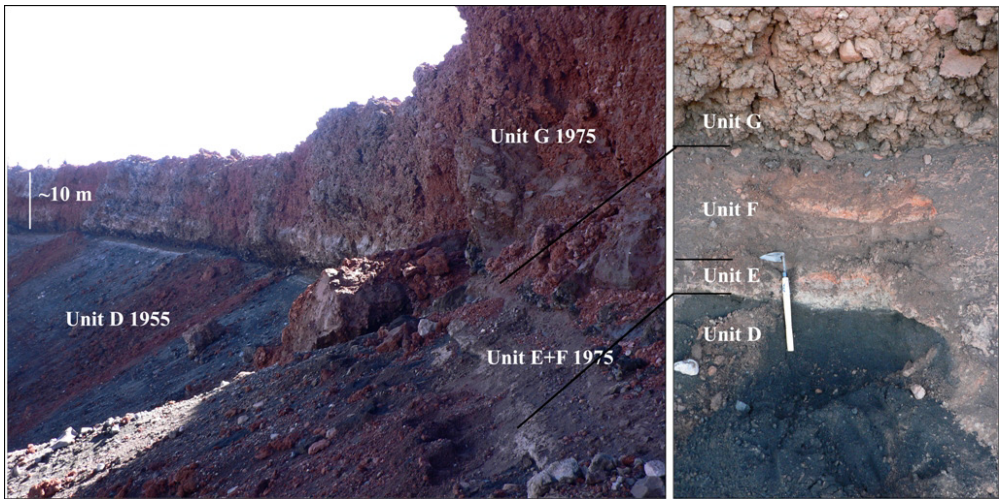

Figure 7.2.3: Inner crater wall of Ngauruhoe showing the uppermost ~15 m, which represents the final phase of the 1954-1955 eruption episode and the entire 1974-1975 sequence.

The 19 February 1975 eruption also produced bread-crust bombs transported up to 2.8 km away from the crater (Nairn and Self 1978; Krippner, 2009, Figure 7.2.4 A). At periods during the eruption the rate of agglutinate accumulation was high enough for welding and generation of rootless lava flows down the upper outer slopes and also back into the crater (Figure 7.2.4 B and C).

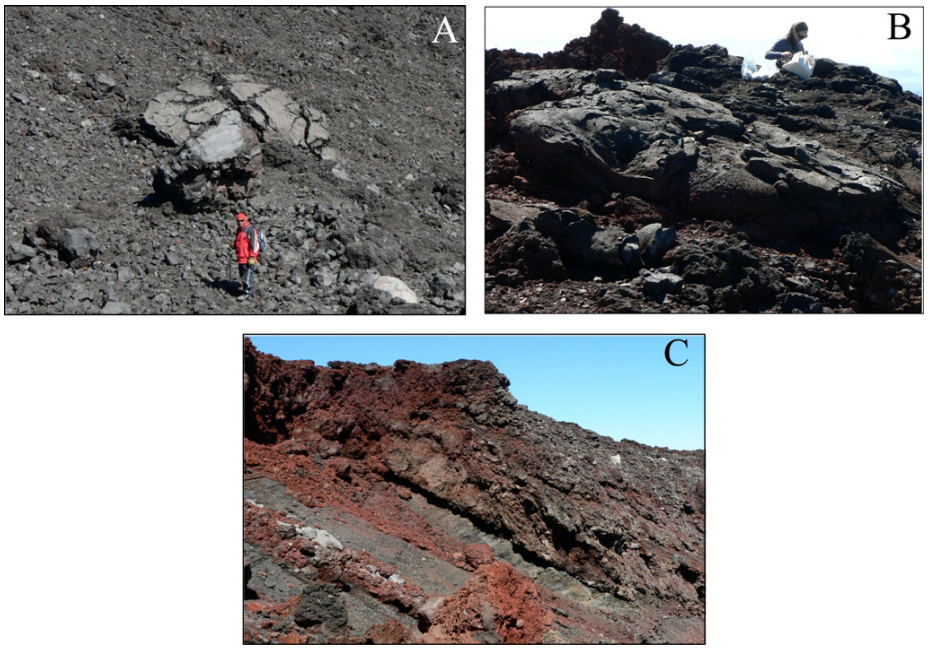

Figure 7.2.4: Characteristic features of the vulcanian and strombolian eruption phases of Ngauruhoe in 1975. A) a huge bread-crusted bomb with figure for scale, B) welded lava spatter on the crater rim and C) inward dipping rootless lava flows sourced from rapidly accumulating agglutinate.

According to Nairn and Self, 1978) fine ash deposits of the 19 February 1975 explosions were transported to the north. A well sorted, fine grained (Md= 1.1 phi) deposit containing fine scoriaceous ash and dense accidental lithic (lava), was 1 mm thick at 21 km away, along the tephra dispersal axis. At 10.5 km a well sorted coarser (Md= -0.1 phi) ash deposit accumulated up to 5 mm thickness, consisting mainly of scoriaceous fragments. Around 2 km north of Ngauruhoe, the deposits were up to 4 cm thick containing up to 20-50 mm diameter scoria lapilli.

Componentry

Krippner (2009) used thin-sections to classify the lithology of the 1954-55 and 1974-75 agglutinates and tephras (Figure 7.2.5 and 7.2.6). The 1954-55 agglutinates are dominated by a glassy matrix (groundmass) with microlites (plagioclase, pyroxene and olivine) > individual crystals (17-37 wt%) and lithics (1-45 wt%), (Figure 7.2.5 A). The lithic component consisted of mainly quartz- and metagreywacke (0.3 to 40 wt%) while the crystal contents ranged between 13-42 wt%, within which the plagioclase is the dominant phase (41-78 %) followed by opx (17- 49 wt%) > cpx (0.5 - 15 wt%) > ol (1 - 9 wt%), (Figure 7.2.5 B).

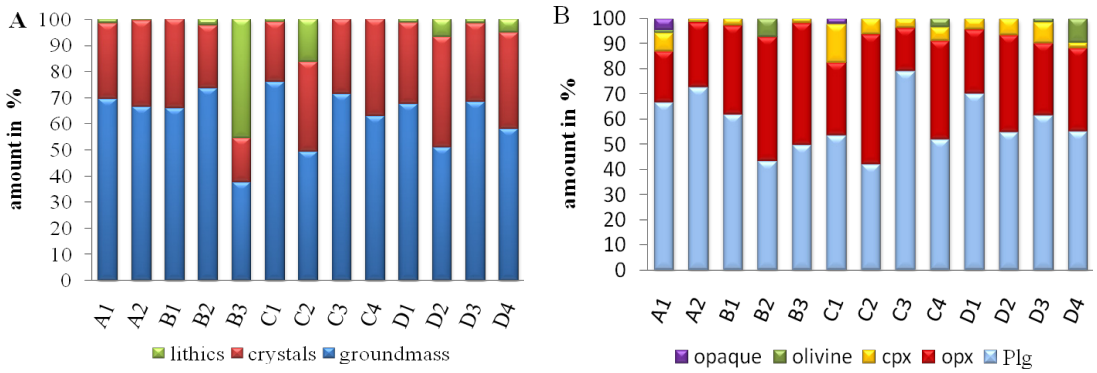

Figure 7.2.5: A) Lithics/crystal/groundmass percentage of 1954-55 depsits from Ngauruhoe's crater facies Units A-D, B) Mineral components experssed as percentage of crystal fraction. Data from Krippner (2009). Samples names correspond with Units.

Samples from Units E-F from 1975 originated from small vulcanian eruptions (VEI 1) probably between the 12 and 18 February 1975, whereas Unit G is the 19 February 1975 agglutinate (Figure 7.2.6). The crystal contents range between 17 and 33 wt% within which the crystals are mainly plg (48 - 80 wt%) >opx (18 - 46 wt%) >cpx (2 - 6

wt%) >ol (1 - 3 wt%). The lowest crystal contents are in the main Unit G phase eruptives.

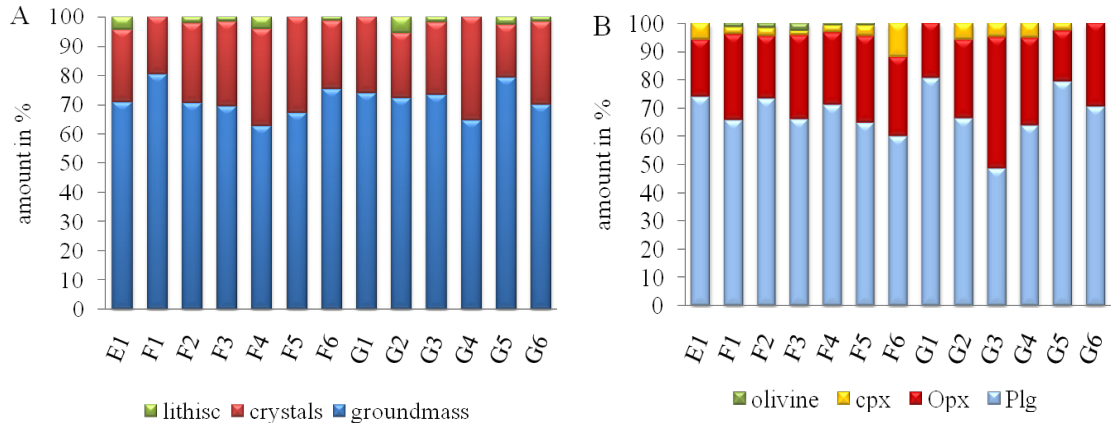

Figure 7.2.6: A) Lithics/crystal/groundmass percentage of 1975 deposits from Ngauruhoe's crater facies Units E-G, B) Mineral components experssed as percentage of crystal fraction. Data from Krippner (2009). Samples names correspond with Units.

The 1954-55 eruptives were deposited mainly by vigorous fire fountaining and intervening strombolian eruptions, whereas the 1975 deposits were mainly produced through vulcanian eruptions and fire-fountaining. The vulcanian eruption products are more vitreous and show a narrower range in crystal/groundmass/lithic ratios then the 1954-55 deposits and the vulcanian deposits are also richer in plagioclase and with lower variation in the ratios of plg > opx > cpx than the 1954-55 units (Figure 7.2.5 to 7.2.7).

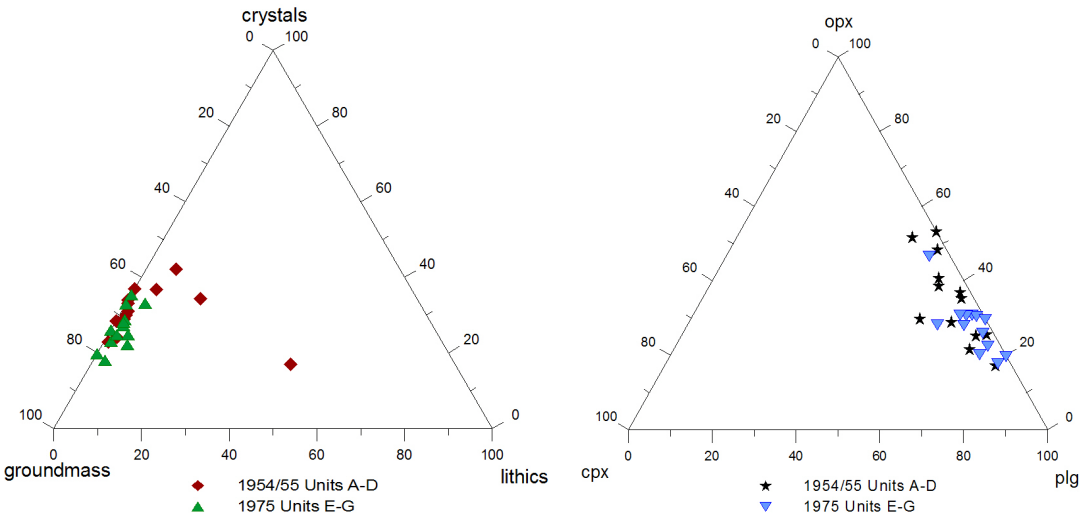

Figure 7.2.7: Ternary diagrams of main lithological components of the Ngauruhoe 1954/55 eruptions in comparison to the Ngauruhoe February 1975 eruptions, Data from Krippner (2009).

In this study, Unit B, a strombolian deposit from the 1954-55 eruptions was analysed of their componentry. This tephra contains 93 wt% volcanic glass, with both light-dark brown sideromelane glass (64 wt%), and lesser black tachylite glass. The crystal content is 5 wt% and consists mainly of plagioclase with rare pyroxene and olivine.

Grain-size analyses

Grain-size analyses were carried out with a laser particle analyser for the <2 mm fraction (Chapter 2), while coarser particles were dry hand sieved at half ϕ intervals. For eruption style classifications, four samples of the crater facies were analysed (Fig. 7.2.8). The 1955 sample is unimodal, poorly sorted and negatively skewed and was probably produced through fire fountaining at the final stages of the 1955 eruption series. The oldest and youngest analysed samples of the 1975 eruptions are characterised by bimodal histograms and very poorly sorted deposits. The high contents of very fine ash (0-13 ϕ) combined with coarse fragments (-1 to -4 ϕ) indicates that these represent combined deposition from both surges and ballistics. The other 1975 sample is also poorly sorted but unimodal, which is more consistent with a fall deposit from a more established column during the mid-phases of the eruption.

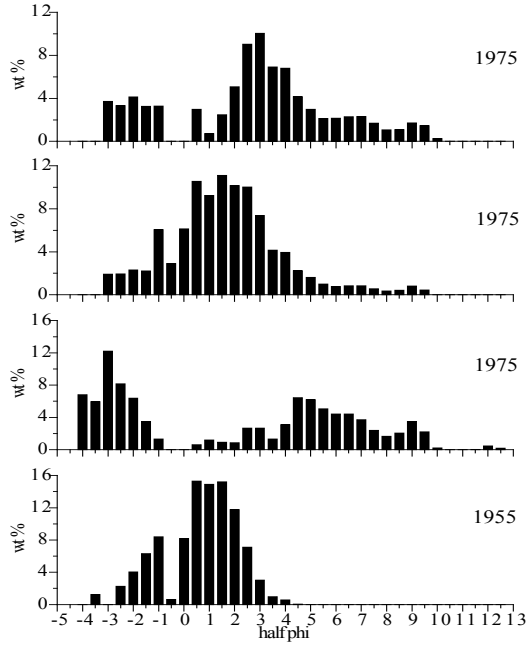

Figure 7.2.8: Grain size histograms of Unit D (1955 eruption), and three stratigraphic levels within Unit F (1975 eruption) in stratigraphic sequence.

Particle-shape analyses

Particle-shape analyses are useful to understand eruption style, fragmentation, transport and alteration mechanisms (Heiken and Wohletz, 1985). Samples from this study were analysed with a scanning electron microprobe (SEM) as described in Chapter 2. Crater wall Units B and D (1954-1955) along with E and F (1975) were examined. As shown above, the samples contain mainly volcanic glass which has been used to study their particle shape for eruptions style classification. The Unit B samples are characterised by irregular, drop-like and elongate glass particles with ovoid and tubular vesicles (Fig 7.2.9 A, C). These have mostly smooth surfaces with step-like fractures, but also moss-like uneven surfaces occur (Fig 7.2.9. G+J). Unit D shows a wider variety in particle shapes, including blocky (Fig. 7.2.9 E); angular to platy (Fig. 7.2.9 F), drop-like (Fig. (7.2.9 C); and irregular shapes. The particles have mostly smooth surfaces, although step-like fracture surfaces (Fig. 7.2.9 K) and chipped edges (Fig. 7.2.9 H) also occur. Two types of vesicular particles occur, those with rare, usually spherical vesicles with thick bubble walls, versus those that show abundant tubular shaped vesicles with thin bubble walls (Fig. 7.2.9 I).

The main particle textural features of the 1954-55 glass pyroclasts indicate dominantly magmatic fragmentation (c.f., Heiken and Wohletz, 1985). The drop-like and irregular grains result from surface tension effects when magma is still hot enough to behave as a fluid. This agrees with the eye-witness observations of the mainly fire-fountaining and strombolian styles of 1954-55 eruptions. The platy grains could result from surface crusting and flaking of stalled magma in the conduit (Morrissey *et al.*, 2000), or can result from broken bubble walls (Wohletz, 1983). The chipped edges and step-like fractures are signs of violent fragmentation during strombolian bursts, or may result from collisions during transport within an eruption column (Wohletz, 2001).

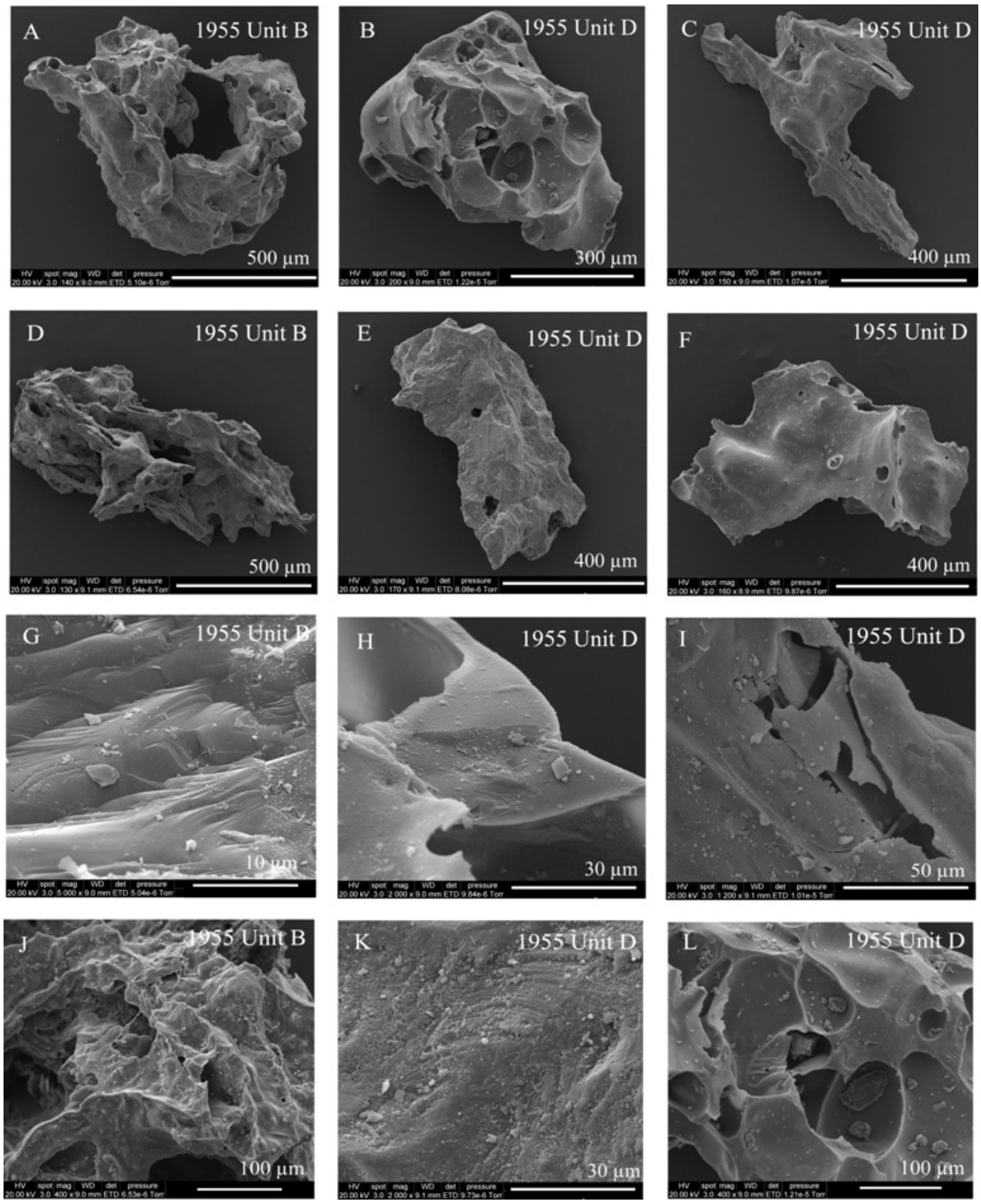

Figure 7.2.9: SEM-images of Ngauruhoe sourced glass shards of Unit B and D from the 1955 strombolian eruption, with A to D) irregular and C+D) drop-like, E) blocky, F) platy shapes and G+K) step-like fractures, H) broken edges, I) elongate vesicles with thin bubble walls, J) moss-like structures and L) round vesicles with thicker bubble walls and smooth surfaces.

The pyroclasts in Units E and F (1975) are characterised by irregular (Fig. 7.2.10 A-E); and marginally pumiceous (Fig 7.2.10 F) particle shapes with drop-like (Fig. 7.2.10 E), moss-like (Fig. 7.2.10 D+J) and also very smooth (Fig. 7.2.10 A+C) surfaces. Some particles have numerous round vesicles with variable thickness bubble walls (Fig 7.2.10 B, C+K), but other particles also have high-density tubular vesicles. Further characteristic features include adhering dust, chipped edges and rare step-like fracturing (Fig. 7.2.10 G - I+L).

The 12-19 February 1975 eruptions are commonly cited examples for vulcanian eruption styles (Nairn, 1976, Nairn *et al.*, 1976). In most cases, vulcanian eruptions are characterised as a type of phreatomagmatic eruption (Büttner *et al.*, 1999). The Unit E and F particles show evidence for two fragmentation mechanisms: phreatomagmatic (angular) and magmatic (irregular and drop-like). At vulcanian eruptions the explosion is driven by highly pressurised gas coming from the magma or phreatomagmatic interactions (Self *et al.*, 1979) and this vulcanian mechanism may also be reflected by the abundance of spherical and tubular vesicles in the analysed samples.

Conchoidal and step-like fractures as well as sharp edges of broken particles show the violence of a vulcanian eruption. Conchoidal fractures are typically associated with chilled magma upon contact with water, but here it probably represents rapid chilling upon explosive ejection into the atmosphere. Moss-like textures develop by viscous deformation under tensional stress during rapid vapour formation when vapour moves along the melt surface (Rayleigh-Taylor and Kelvin-Helmhotz instabilities) (Morrissey *et al.*, 2000). If there is water involved, it probably represents groundwater within the hydrothermal system, or that in the atmosphere encountered by the rising plume.

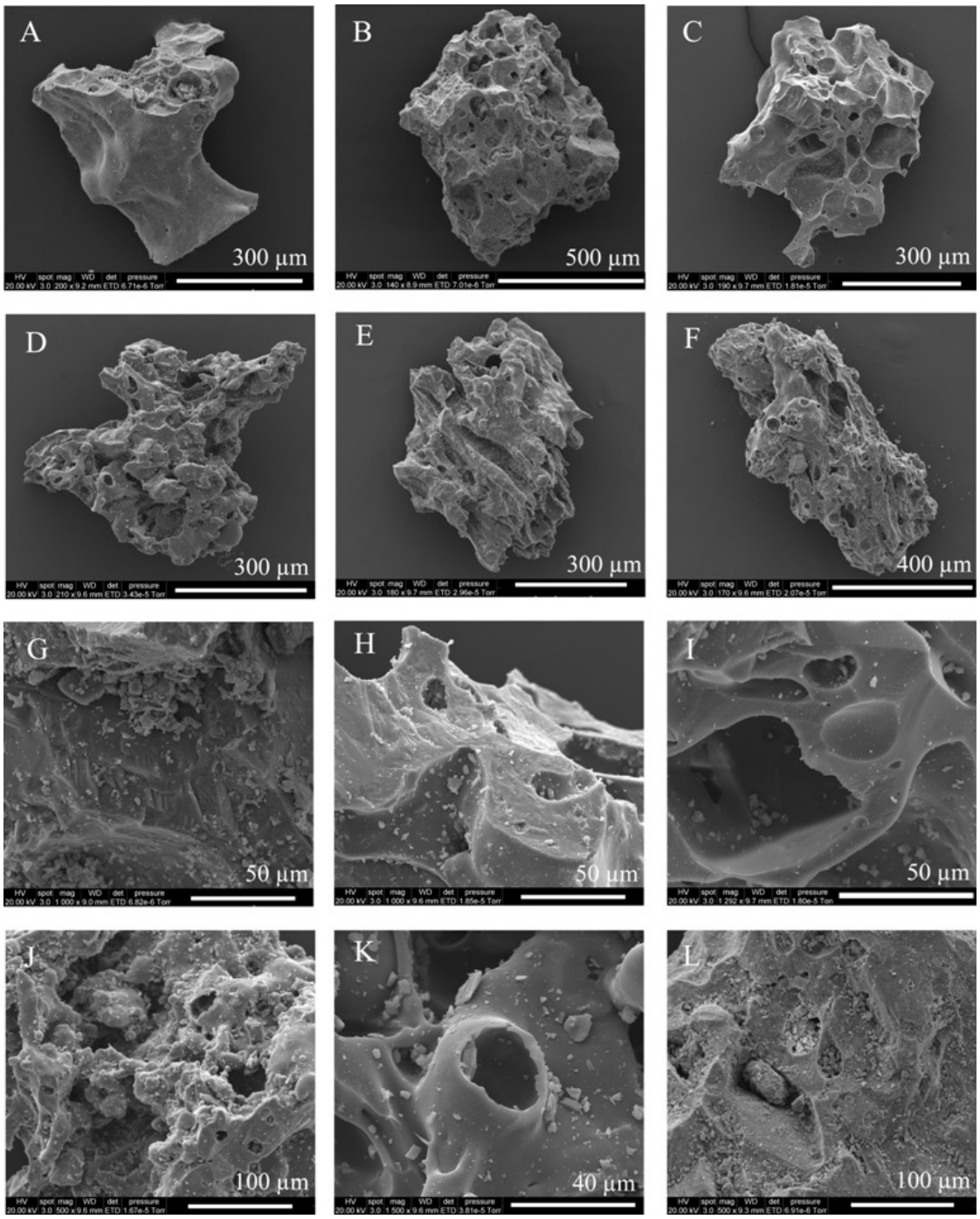

Figure 7.2.10: SEM-images of Ngauruhoe-sourced glass shards of fall deposits from the vulcanian Ngauruhoe eruption in February 1975 represented by A+ D-F) irregular and B+C) blocky shapes and G) step-like fractures, H) chipped edges, I) round vesicles with thick bubble walls, J) moss-like structures, K) smooth surfaces and vesicles with thin bubble walls and L) vesicle fillings (adhering dust). The blocky particles have fewer and round vesicles, while the irregular particles have tubular vesicles.

7.2.2 Eruption styles of historic Ruapehu eruptions

Like other volcanoes, including Popocatepetl and El Chichón, Mexico (Armienta *et al.*, 2000), Kelut, Indonesia (Badrudin, 1994), Ambae, Vanuatu (Nemeth *et al.*, 2006) and Poas volcano, Costa Rica (Rowe Jr. *et al.*, 1992) the active crater of Ruapehu has been commonly covered by the typically 10 million m^3, acidic Crater Lake (Figures 7.2.11 A+B) for at least the last 3000 years (Donoghue *et al.,* 1997). It is only removed during long continuing eruption phases such as in 1945 and 1995-96 or by break out collapses of the crater margin. Prior to the 1995 eruptions, the lake was up to 134 m deep, 500 m in diameter and oval-shaped with an area of about 0.2 km^2 (Christenson and Wood, 1993). The temperature of the lake has fluctuated between 10-60 ˚C over the last ~50 years, depending on the behaviour of the hydrothermal system beneath the lake (Hurst *et al.*, 1991). At the present time Ruapehu has two vents within the Crater Lake, a northern and a central vent (Christenson and Wood, 1993).

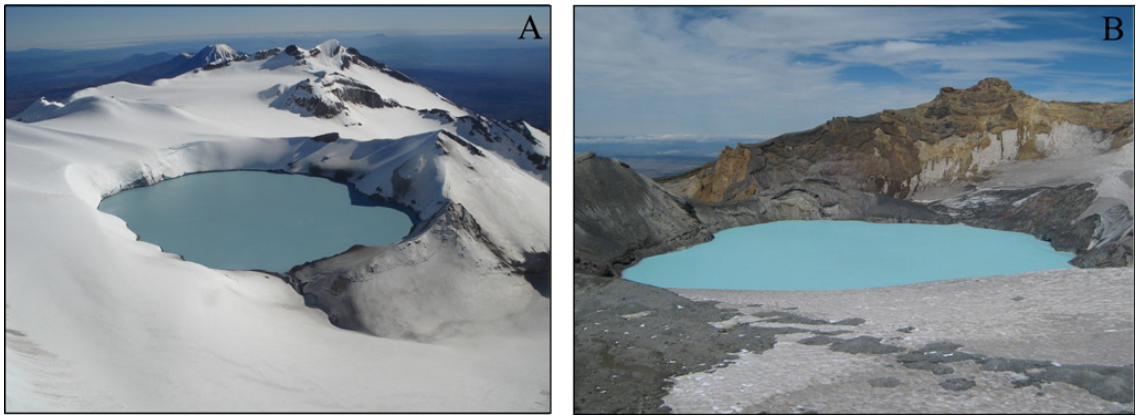

Figure 7.2.11: Ruapehu Crater Lake A) view to the north and with outlet to the Whangaehu River on the south-eastern rim in the foreground (photographer: Shane Cronin) and B) view to the south (photographer: Marco Brenna).

Ruapehu has erupted over 70 times in the last 150 years (Gregg, 1960), with 47 episodes in last 120 years (Hackett, 1989). Eruption styles have varied from steam eruptions and small phreatomagmatic explosions of VEI 0-2, up to sub-plinian explosive eruptions with VEI's >2. Detailed descriptions of historic eruptions are summarised in Gregg (1960b) and were also described by Cotton (1945), Oliver (1945), Reed (1945), Beck (1951), Healy (1978), Nairn (1979), Johnston (1995), Christenson *et*

al. (2000 and 2010), Cronin *et al*. (1996b, 1997a+c, 1998, 2003) and Kilgour *et al.* (2010).

According to Werner *et al.* (2006), Crater Lake undergoes heating, degassing and temperature change cycles that are related to a heat pipe connecting the cooling magma body with the lake. Additionally, Werner *et al.* (2006) suggest a typical regular repose period of 20-30 years between eruptions by comparing eruptive volumes with magma volume estimates from CO_2-emissions. Crater Lake has a major influence on Ruapehu's eruption behaviour (Cronin *et al.*, 2003; Hurst *et al.*, 1991; Christenson *et al.*, 2010) although it is often difficult to discriminate between phreatic and small phreatomagmatic eruptions, even when analysing ejecta lithologies (Table 7.2.1).

Table 7.2.1: Summary of historic eruption record from Mt Ruapehu showing the range in its eruption styles.

Eruption year	**Christenson *et al.* 1993**	**Barberi *et al.* 1992**	**Hackett *et al.* 1989**	**Nairn *et al.* 1979**	**Healy *et al.* 1978**	**Gregg 1960b**
1945						phreatomag.
1959						phreatic
1966	phreatomag.			phreatic	phreatomag.	
1968	phreatic?			phreatic		
1969	phreatomag.	phreatic	phreatomag.	phreatic	phreatomag.	
1971		phreatic	phreatomag.	phreatic		
1972	phreatomag.					
1973		phreatic				
1975		phreatic	phreatomag.	phreatic		
1976	phreatomag.					
1978	phreatomag.					
1979		phreatic				
1980		phreatic				
1982	phreatic	phreatic				
1988	phreatic	phreatic				
1989		phreatic				
1990		phreatic				
1995 /1996	phreatomag. /dry magmatic					

7.2.2.1. Phreatomagmatic-magmatic eruption cycles

The best documented Ruapehu eruption is the 1995-1996 eruption episode, which showed variations from phreatomagmatic to strombolian eruption styles (Figure 7.2.12). The eruption started on 18 September with phreatic eruption, which transited to a phreatomagmatic eruption on the 23 September that continued until 10 October 1995. During this time Crater Lake gradually emptied producing snow slurry lahars, hyperconcentrated flows, surges and tephras. On 11 October 1995, a major sustained sub-plinian eruption began, which over 5 hours emptied the remaining water from Crater Lake. This event produced an ash cloud 8-10 km above the crater rim, distributing 25 x 10^6 m^3 of tephra across the central and eastern North Island. On 14 October 1995 another 2-3 hour-long sub-plinian eruption occurred, producing a 10-11 km high eruption column with 5 x 10^6 m^3 tephra distributed to the south-east (Cronin *et al.*, 2003). After gas emissions between November 1995 and March 1996, a second cycle of eruptions started on the 16 June 1996. The partial refilling of Crater Lake caused initially phreatomagmatic eruptions leading to a sustained sub-plinian eruption for several hours on 17 June with an eruption column height of 7-10 km and 5 x 10^6 m^3 of tephra distributed to the north (Cronin *et al.*, 2003). Afterwards strombolian and vulcanian eruptions occurred until 9 September 1996 with ash columns typically between < 3 to 6 km high (up to 10 km on the 20 and 26 July 1996) and a maximum tephra volume of *c*. 0.01 x10^6 m^3 for the largest events.

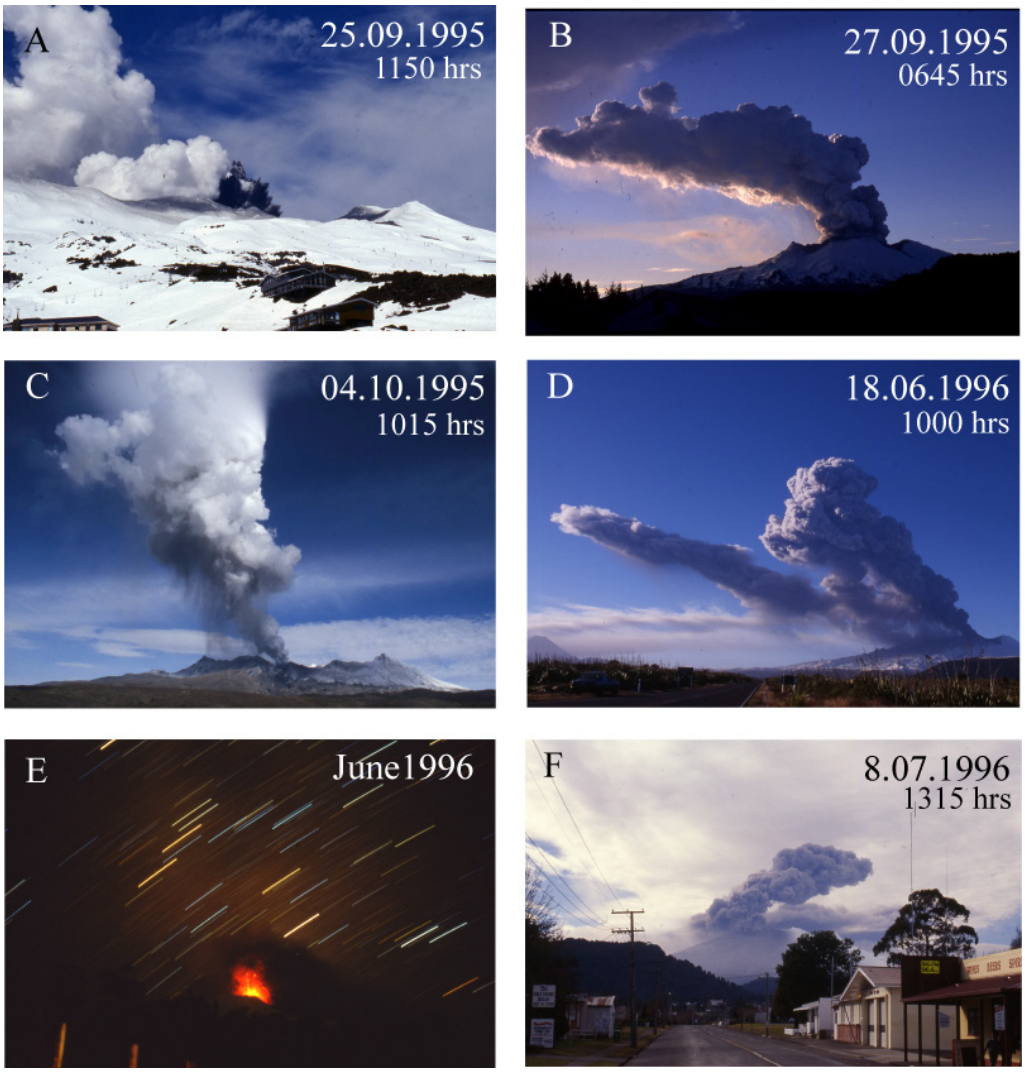

Figure 7.2.12: Eruptions from Mt Ruapehu during the 1995 to 1996 eruption episode ranging from A-C) phreatomagmatic eruptions with explosive jets to D-F) strombolian to sub-plinan eruptions including lava fountaining (photographer: Shane Cronin).

Sample selection and description

Numerous samples were collected during and after the eruptions, and are used here to gain a better understanding of the differences in particle shape, grain size, and componentry of the individual eruptions styles during the 1995-1996 eruptions. The samples were collected from *c.* 2.5 to 189 km from source (Cronin *et al.,* 2003 and unpublished data).

The samples analysed in this study where chosen by their documented eruption style, eruption date and the distance from the vent (Table 7.2.2). The samples varied in colour

from light grey (95/1, 95/3 and 96/37) to brownish dark grey (95/5; 96/46) and black (95/7, 96/19) broadly reflecting contrasting eruption styles. The light grey deposits correspond to the initial phreatomagmatic phases of eruptions, with gradual changes to darker colours as eruptions became more magmatic (Figure 7.2.13).

Table 7.2.2: Tephra samples from the Ruapehu 1995/1996 eruption episode used in this study to classify eruption types.

Sample name	Collecting area and distance from Crater Lake	Eruption style	Eruption date	Type of deposit
95/1(1	Summit D rd ; 15.8 km (+	phreatomagmatic	25.09.1995	fall out
95/3 (1	Tukino; 3.8 km (+	phreatomagmatic	25.09.1995	fall out
95/5 (1	Mgtoe D Rd; 15.1 k (+	phreatomag/magmatic	11-12.10.95	fall out
95/7(1	ECNZ aqueduct hut; 16.2 km (+	dry magmatic	14.10.1995	fall out
96/7(1	Nukuhau; 86 km (+	phreatomag./magmatic	17.06 1996	fall out
96/9 (1	Mangahuia; 14.3 km (+	magmatic/strombolian	18.06 1996	fall out
96/19 (1	Turoa; 4.1 km (+	strombolian	7.07.1996	fall out
96/37(1	Tama Lake; 9.2 km (+	phreatomag./magmatic	17.06.1996	fall out
96/46 (1	Tufa Trig; 8.7 km (+	strombolian	21.07.1996	fall out

Samples collected by: (1 Shane Cronin, Jerome Lecointre, Vince E. Neall,; Reference: (+Cronin *et al.*, 2003 and unpublished data.

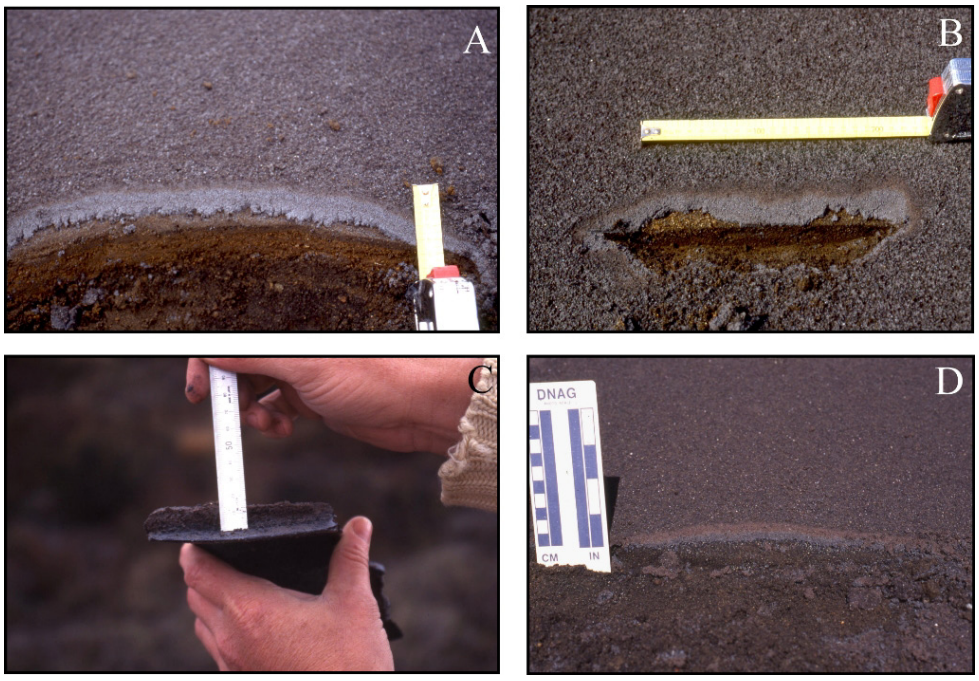

Figure 7.2.13: Deposits of the October 1995 eruptions (A and B, 11/10/95; C and D, 14/10/95) which both started with phreatomagmatic phases (light grey base) that later changed to dry magmatic eruption styles (photographer: Shane Cronin).

Componentry

The 1995-96 tephras are all composed of varying mixtures of volcanic glass (55-75 %), plagioclase, orthopyroxene and clinopyroxene (10-28 % crystals), with minor components of lithic or country rock fragments (5.5-13.5 %) and spheroids of elemental sulphur (6-9%) (Figure 7.2.14). The magmatic tephras contain similar or higher contents of lithics than the phreatomagmatic tephras, which was unexpected. The phreatomagmatic tephras show finer grain-size fractions dominated by crystal fragments.

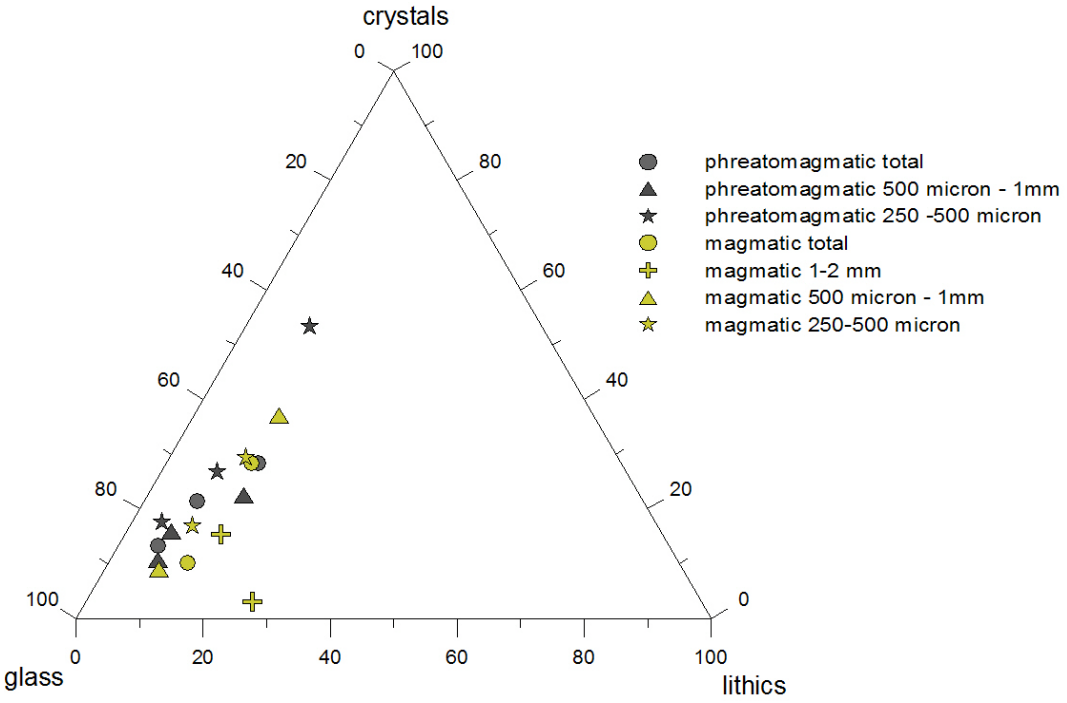

Figure 7.2.14: Componentry of phreatomagmatic and magmatic eruptions from the 1995-1996 eruption episode.

The different colours of tephras are here interpreted to be caused by the different contents of volcanic glass and by the occurrence of sulpher. Phreatomagmatic tephras contain higher contents of translucent glass (sideromelane) than the sub-plinian/magmatic eruptions (Fig. 7.2.15). The final dry phase of the October 1995 eruptions have similar glass characteristics to the phreatomagmatic phase of the June 1996 eruptions, indicating that some-degree of magma-water interaction occurred throughout the main 1995 eruption phases.

In 1995, the pyroxene (px) and plagioclase (plg) content increased as the large eruptions became more magmatic. In 1996 it was the opposite; the initial phreatomagmatic phase tephra had much higher plg and px than the equivalent 1995 phases, but in 1996 it dropped dramatically with continuing strombolian activity in July 1996.

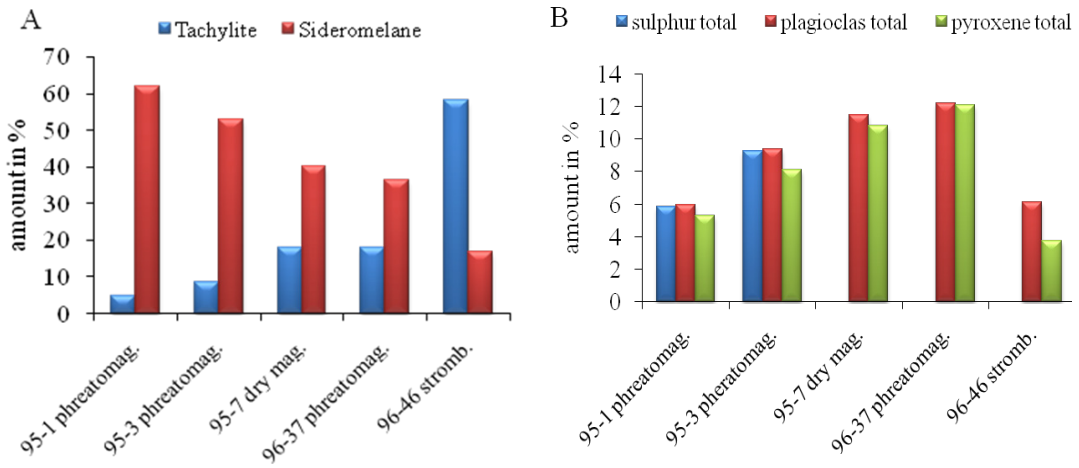

Figure 7.2.15: A. Sideromelane (light glass) vs. tachylite (black glass), and B. selected crystals and sulphur modal content over a range of different eruption styles throughout the 1995-96 eruption episode.

Grain size analyses

The grain size analyses for the Ruapehu 1995-96 samples were carried out by dry and wet sieving in half-phi steps down to 32 µm. Size fractions <32 µm are combined and analysed as one class. This <32 µm (< 4 ϕ) class is represented by a major peak apparent in all the grain size histograms (Figure 7.2.16). Without this class, all samples show a clear decreasing trend towards finer grain sizes.

The 1995 tephras become coarser from initial eruptions (25/9/95) up to the 14/10/95 (Figure 7.2.16 A-D). By contrast, the 1996 tephras, phreatomagmatic eruptions are not as fine-grained (Figure 7.2.16 E-I), while the magmatic – strombolian eruptions are finer grained.

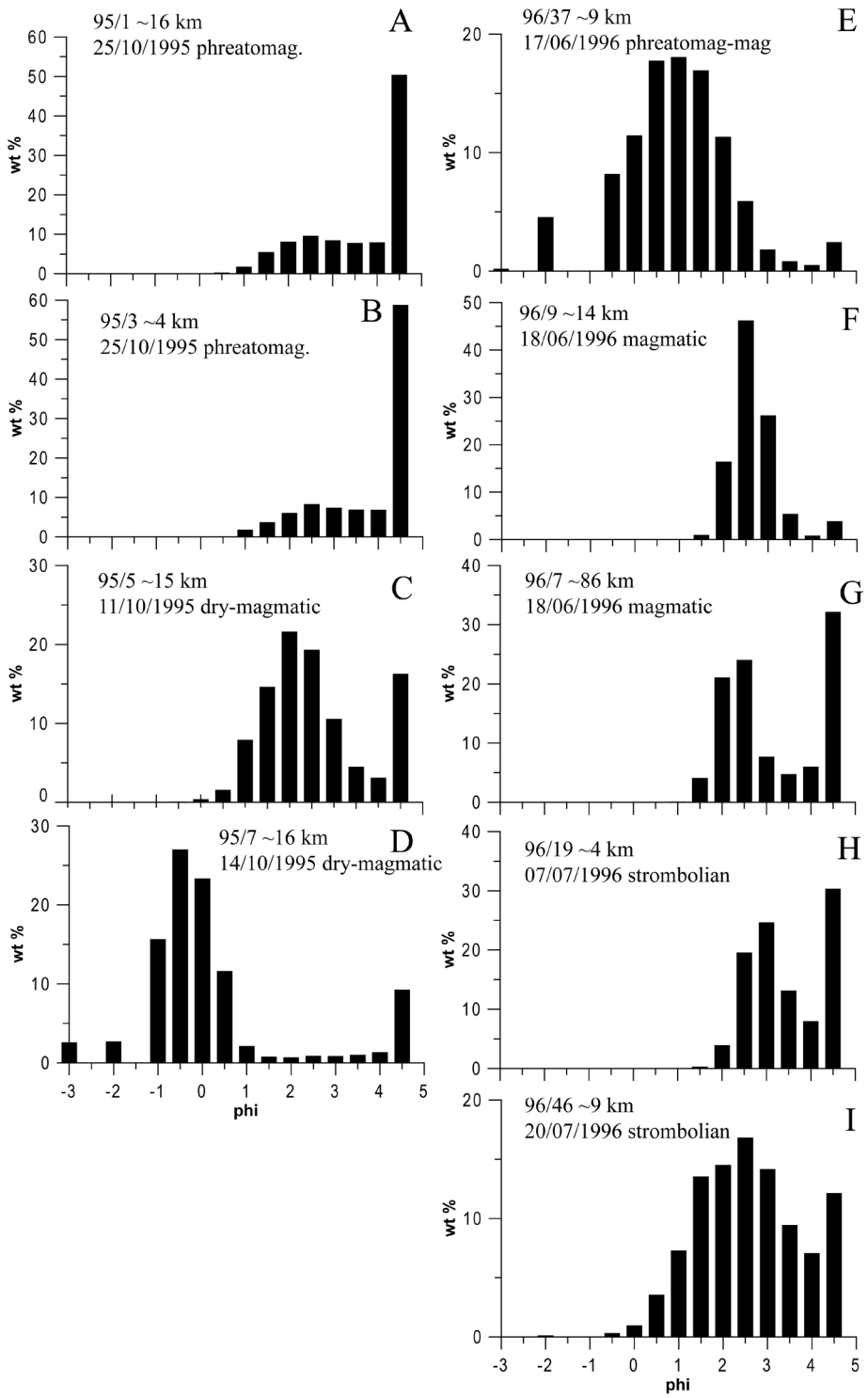

Figure 7.2.16: Grain size analyses of the 1995 (A-D) and 1996 (E-F) eruption episodes.

Particle-shapes analyses

The early Ruapehu 1995 eruptions (up until the 11 October) are mainly characterised by blocky to angular particles (Fig 7.2.17 A+D+F) consisting of only rare irregular glass shards (Fig 7.2.17 C+E+F). The spherical and ovoid vesicles can be very large, in relation to the grain size and (Fig. 7.2.17 E) are partly filled with adhering dust. Some very blocky particles do not contain any vesicles, but more irregularly shaped particles have up to ~50 % vesiculation (Figures 7.1.17 B). Some shards show smooth rounded surfaces, whereas others show conchoidal and step-like fractures (Fig. 7.2.17 K+L) with chipped edges (Fig. 7.2.17 J).

Blocky to equant shapes, low vesicularity, thick bubble walls and drop-like shapes (from fluid magma) are related to phreatomagmatism (Heiken, 1972; Sheridan and Wohletz, 1983; Dellino and La Volpe, 1995). The blocky shapes with isolated vesicles suggests the eruption of a relatively degassed magma and therefore indicates that expansion and exsolution of gas had no major role in the fragmentation process (Heiken and Wohletz, 1985; Dellino and Kyriakopoulos, 2003).

The interaction of hot magma with external water creates surface structures such as quenching cracks, conchoidal fractures and step-like fractures. Step-like fractures indicate brittle fragmentation (Büttner *et al.*, 2002). Vesicle fillings, occurrence of clay minerals, glass hydration and grain skin-formation are features of alteration processes (Freundt and Rosi, 2001), but may also be a result of very fine particles adhering in the ash cloud, due to efficient phreatomagmatic fragmentation. The clay minerals adhering to the surface of these ash particles are in this case derived from the sediments at the base of Crater Lake and within the hydrothermal system.

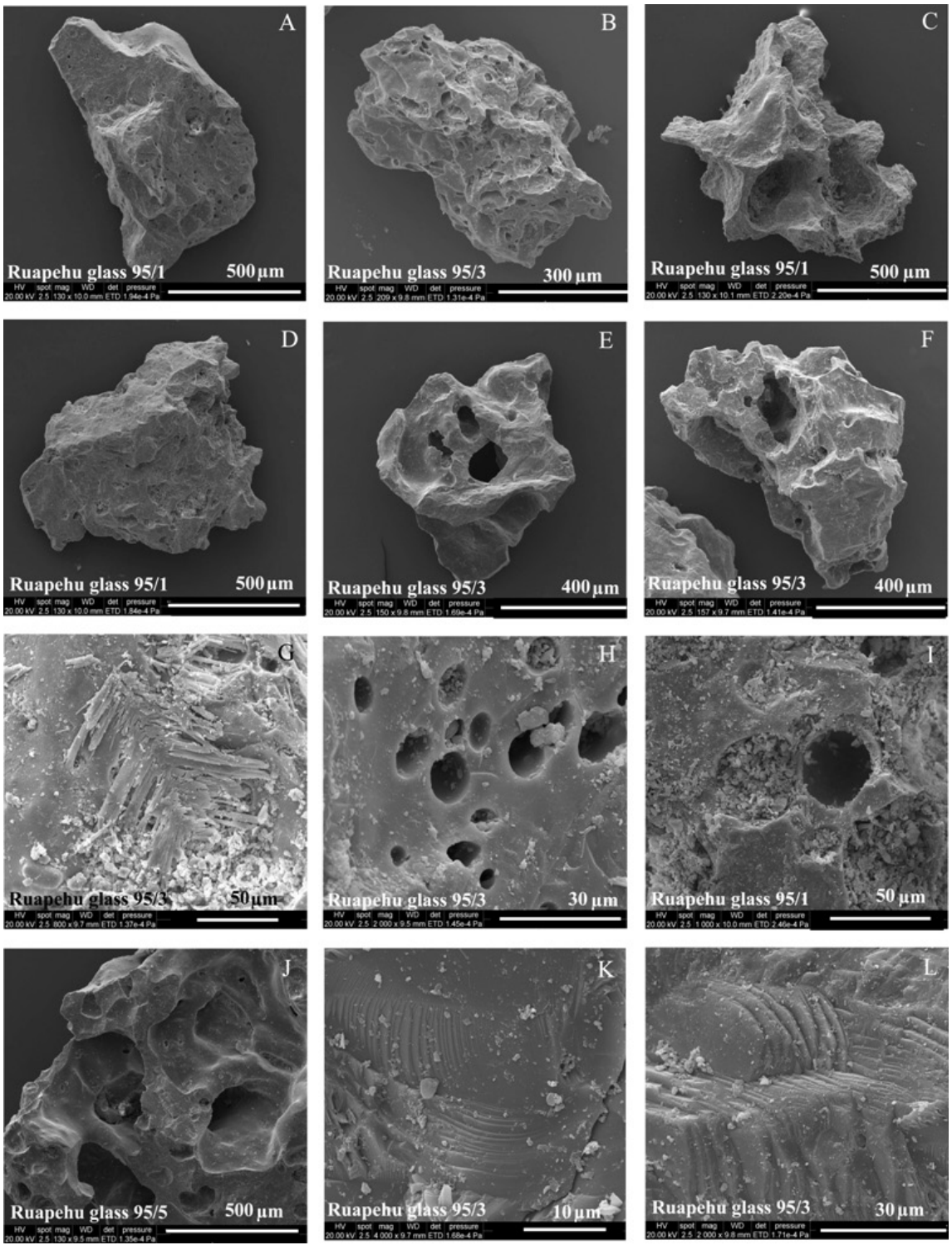

Figure 7.2.17: SEM-images of glass shards from phreatomagmatic eruptions from Ruapehu 1995 with A, B+D+F blocky and C+E) irregular shaped particles along with G) clay minerals, small round vesicles and thick bubble walls, I) vesicle fillings, J) chipped edges, K) conchoidal- and L) step-like fractures.

The 1996 tephra particles from Ruapehu have more irregular shapes and also tend toward pumiceous textures (Figures 7.2.18 A-C + E-F). They are mostly highly vesicular (>80%) with spherical, oval, tubular and contorted, variably sized vesicles and very thin bubble walls (Figures 7.2.18 A-F + I). Only in rare cases are the clasts more angular with lesser and rounded vesicles (Figure 7.2.18 D). V-shaped depressions, cracks and grooves on grain surfaces, step-like fractures and rip ups also occur.

These features are consistent with the 1996 Ruapehu eruptions being dominated by magmatic and mostly strombolian fragmentation processes (Cronin *et al.,* 2003). The abundance of spherical vesicles suggests fragmentation due to expanding and exsolution of a gas-rich magma (Dellino and La Volpe, 1995). The V-shaped depressions, cracks and grooves on grain surfaces show evidence of turbulent collisional movement, which could be a sign of more violent strombolian eruptions as previously shown from the Ngauruhoe 1954-55 deposits. Several glass shards (in particular the tachylites) have very uneven surfaces due to the high content of microlites.

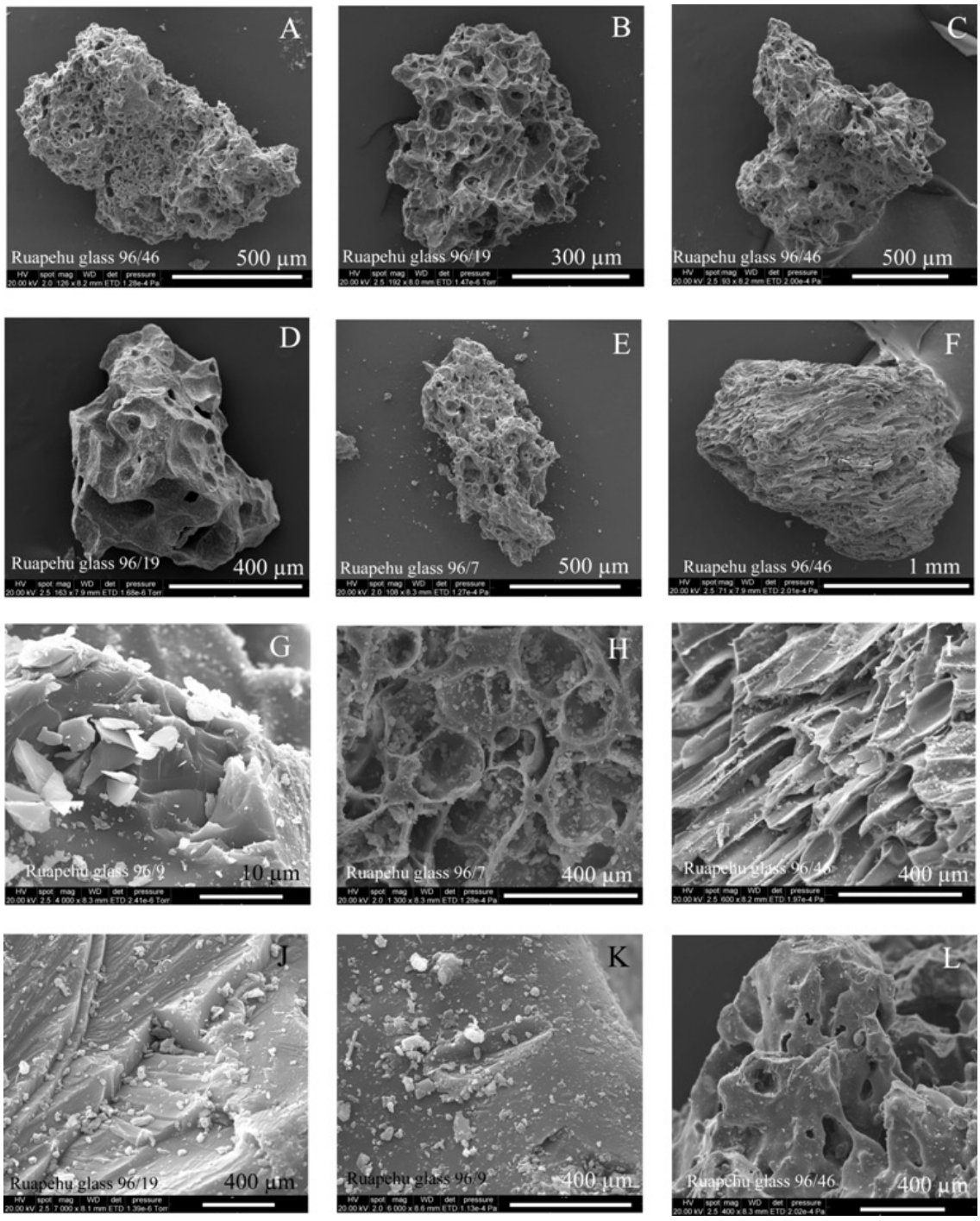

Figure 7.2.18: SEM-images of glass shards from magmatic/strombolian eruptions from Ruapehu 1996 with A-C+E-F mainly irregular and D) rare blocky shapes and G) chipped edges, H-I numerous round and elongate vesicles with thin bubble walls, J) step-like fractures, K) grooves and drop-like shapes with smooth surfaces.

7.2.2.2. 2007 Ruapehu eruption – phreatic or phreatomagmatic?

Over the last 65 years, at least 12 eruptions from Ruapehu have occurred in which apparently no juvenile material was ejected. The latest of these eruptions was on 25 September 2007. In this case, however, up to 2.4 % of juvenile material was recognised from the tephras in this study, which could be used to define this eruption as phreatomagmatic (Figure 7.2.19). Despite this fact, this eruption has an extremely low volume and is more similar to previous phreatic Ruapehu eruptions than to the phreatomagmatic eruptions described from September and October 1995. The event lasted only 60 seconds, producing a 4.5 km high steam column above the crater (Kilgour *et al.*, 2008). It also generated a 1.5 km^2 surge which covered only an area of 2.5 km^2 in ash and lapilli fall (Lube *et al.*, 2009) with associated ice-slurry lahars onto the Whakapapa and Whangaehu Glaciers (Figures 7.2.20A-F). In this study, material of the surge and fall deposits, as well as from the ice-slurries was analysed.

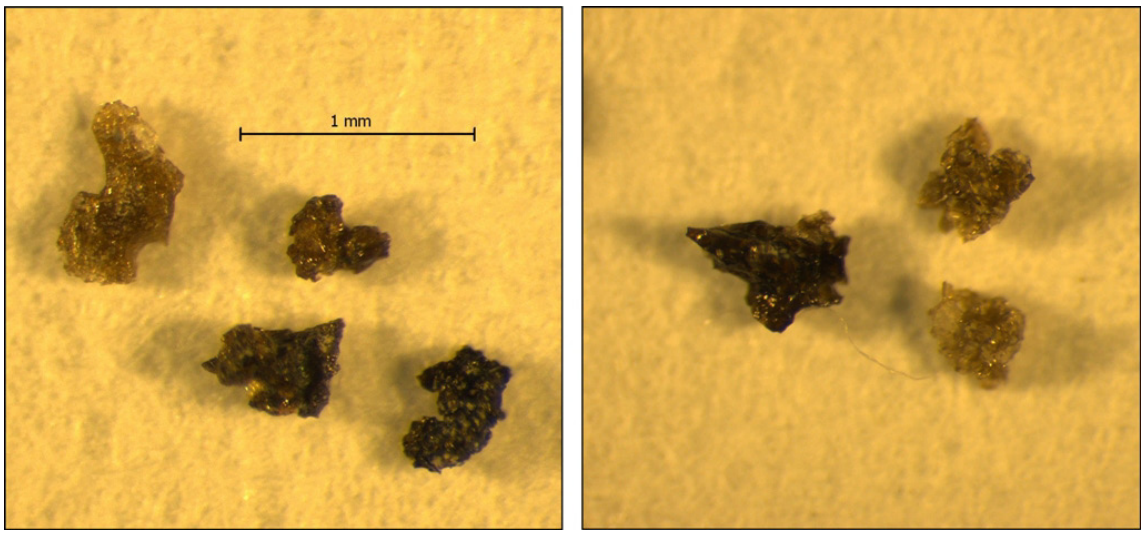

Figure 7.2.19: Juvenile volcanic glass identified within tephras from the 25 September 2007 Ruapehu eruption.

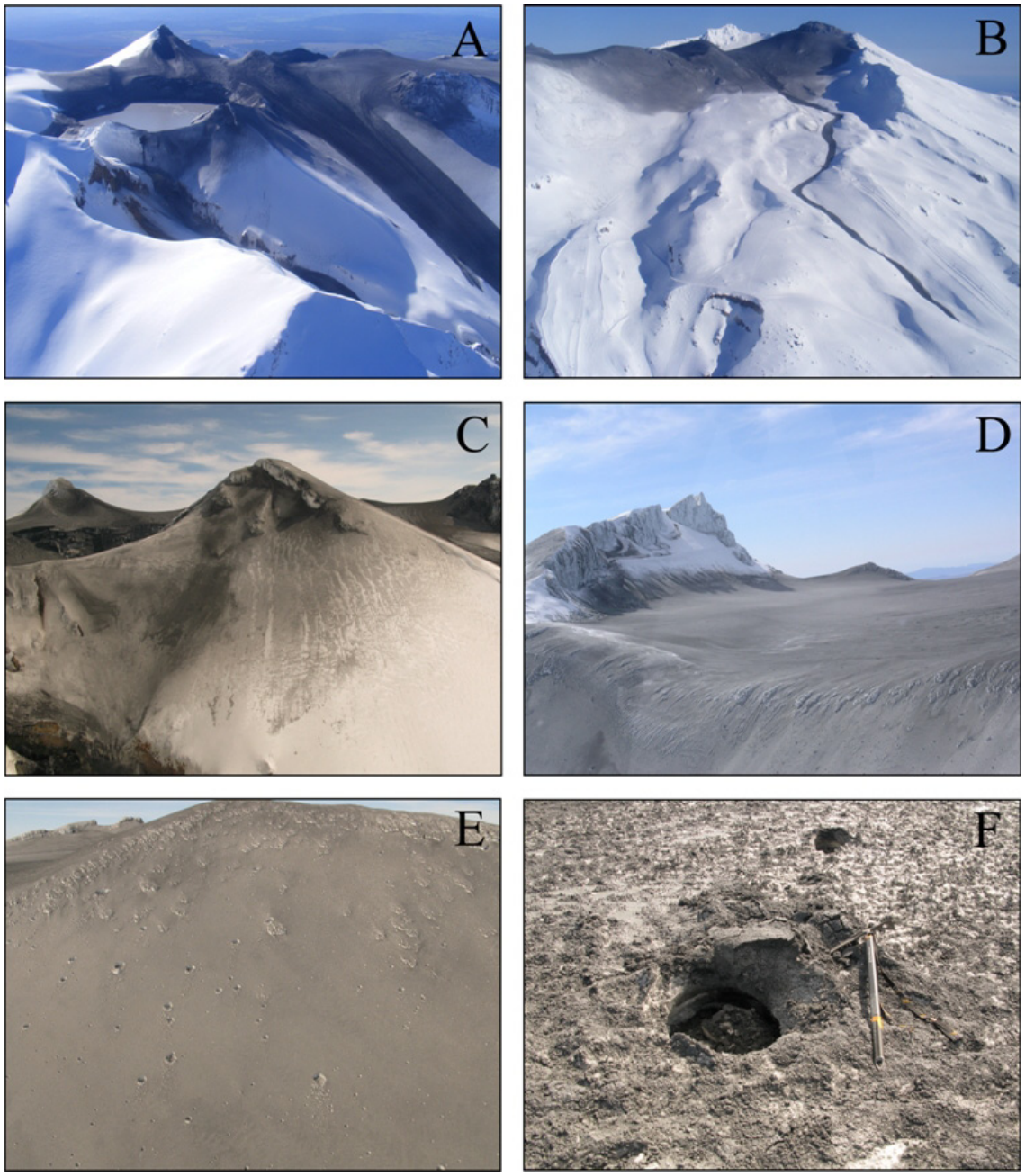

Figure 7.2.20: Phreatomagmatic eruption of Mt. Ruapehu 2007, (A) view from the south-east showing the surge deposit towards the north and two snow/ice-slurry lahar deposits on the Whangaehu Glacier and Whangaehu River valley (photographer: Károly Németh) (B) view from the north at Whakapapa Ski-field also showing a snow slurry lahar deposit (photographer: Károly Németh), (C) fall deposits north-west of Crater Lake (photographer: Gert Lube) (D) surge deposit on the northern plateau (photographer: Shane Cronin) and (E+F) bombs and impact craters on the snow (photographer: Gert Lube).

Sample description

In total eight samples were collected from this eruption, in different areas around the crater rim and from different stages of the eruption (Table 7.2.3; Figure 7.2.21). The samples collected from the Mangatoetoenui Glacier could be wind-reworked material from the surge or ice slurry deposits.

Tab. 7.2.3: Samples collected to characterise the 25 September 2007 Ruapehu eruption.

Sample number	Dist. to centre of Crater Lake	Area	Type of deposit
S1*	0.6 km	Dom Shelter (N)	surge
S2*	0.6 km	Dom Shelter (N)	surge
S3(1	~1.1 km	Summit plateau (NE)	surge
F1(1	~2 km	Mangatoetoenui-Glacier (ENE)	fall out
F2(1	~2.4 km	Mangatoetoenui-Glacier (ENE)	fall out
F3(3	~1.5 km	western slope Whakapapa Gl. (N)	fall out
W1(2	~3 km	Whakapapa Glacier (N)	ice slurry
E1(1	~0.7 km	Top of Whangaehu-Glacier (E)	ice slurry

Samples were taken by: * Harry Keys and Geoff Kilgour (1 Gert Lube & Shane Cronin, (2 Jon Procter and Anke Zernack, (3 Anja Möbis.

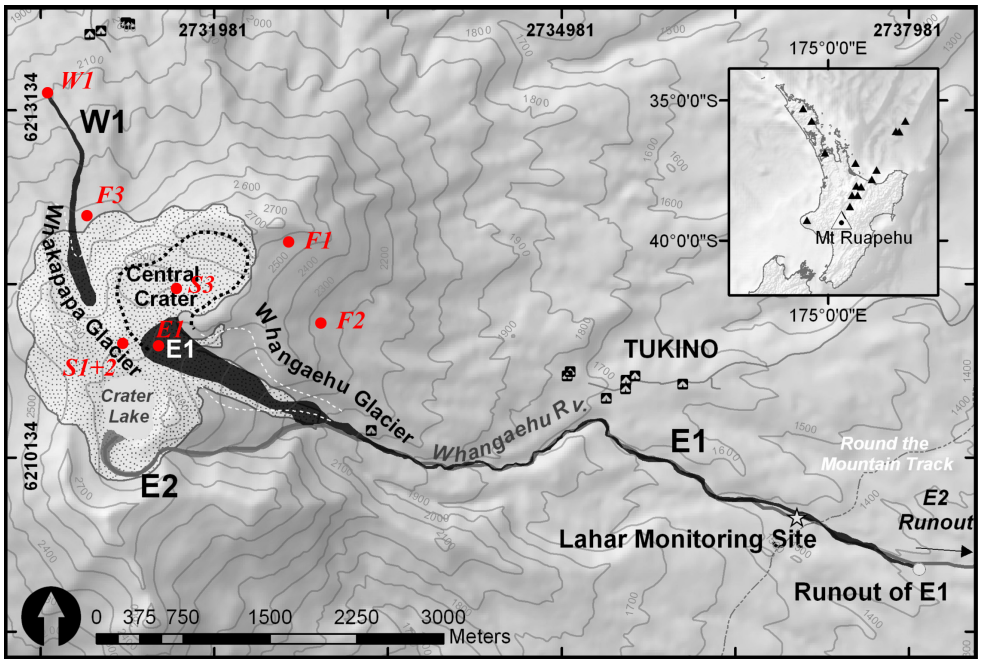

Figure 7.2.21: Map of the Ruapehu crater area and the lahar path into the Whangaehu river to the east, showing the sample locations for the here analysed samples (red).

Componentry

The deposits of the 2007 Ruapehu eruption consist mainly of non-juvenile lithics (46-77%) which is in very strong contrast to the 1995-96 units (Figure 7.2.22). The only similarity between the 2007 and 1995-96 deposits is that crystals are stronger represented in the smaller grain-size fractions. Grain-size histograms from surge and ice-slurry deposits are poorly sorted and bimodal, while the fall deposit is moderately well sorted and unimodal (Fig. 7.2.24). The juvenile material classifies this eruption as phreatomagmatic, but Christenson *et al.* (2010) indicates that the eruption was initially gas-driven and not through magma and therefore more phreatic and only later progressed into a phreatomagmatic eruption. The magma at a shallow level was however disrupted by this event and essentially brought along as an accessory. In this case, it is highly debatable as to whether this event could be classified as phreatic or phreatomagmatic.

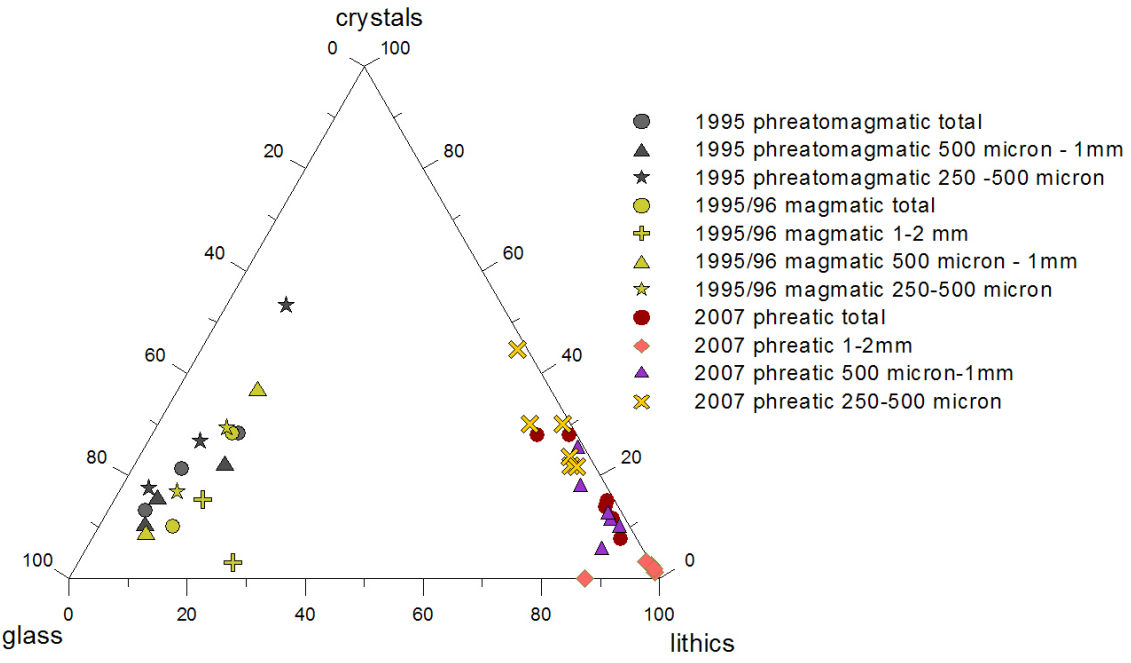

Figure 7.2.22: Lithic, crystal and glass componentry of the deposits from the Ruapehu 2007 eruption in comparison to the Ruapehu 1995-96 eruptive deposits.

One of the most important discriminators between phreatomagmatic and phreatic eruptions is whether or not juvenile material is involved. To determine juvenile vs. non-

juvenile content is in most cases very difficult because fragmented crystals could be either. For this reason crystals were counted separately. The 2007 pyroclastic products are poor in juvenile components compared to the 1995-96 tephras, indicating that only a minor amount of fresh magma was involved in this eruption (Figure 7.2.23).

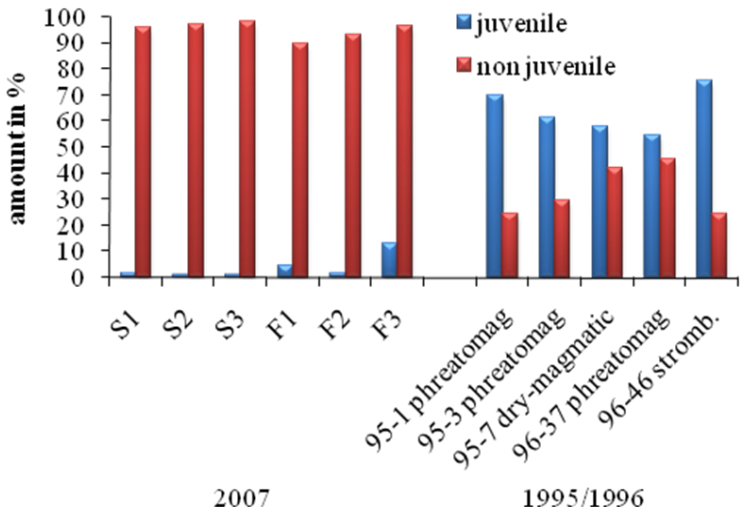

Figure 7.2.23: Juvenile vs non-juvenile componentry comparing the phreatomagmatic 2007 Ruapehu eruption with the 1995-96 phreatomagmatic/magmatic Ruapehu eruptions.

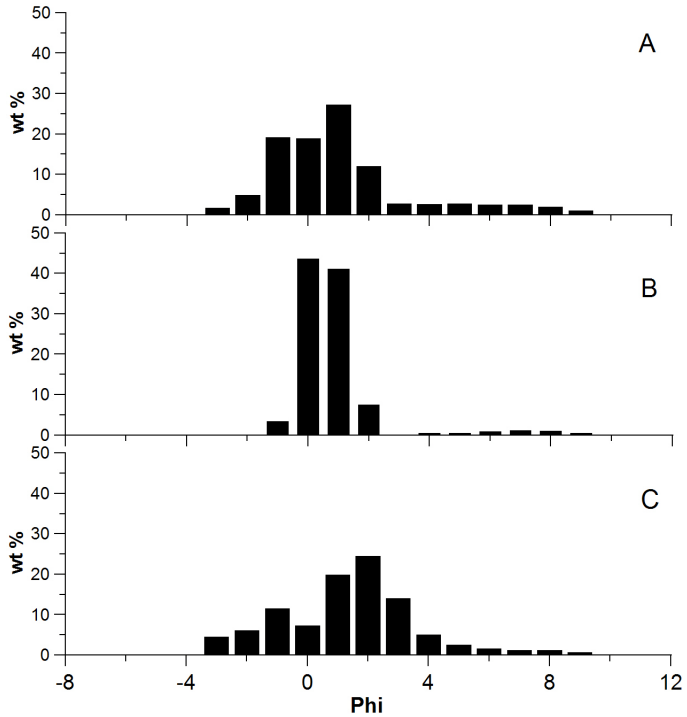

Figure 7.2.24: Grain-size histograms from samples of the 25 September 2007 Ruapehu eruption from A) deposits of the surge from the central crater, B) a fall out deposit from Whakapapa ski-field and C) in comparison, the distal end of the Whakapapa snow slurry lahar.

Particle-shape analyses

The rare glass particles of the 2007 Ruapehu eruptions are blocky to angular (Figure 7.2.25 A, B and D), with some platy and rare irregularly shaped grains (Figure 7.2.25 C, E and F). There are two types of vesicle textures; particles with concave cavities, representing margins of large bubbles, with smooth inner surfaces and thick bubble walls (Fig. 7.2.25 A, B and D); and particles with smaller numerous spherical and ovoid vesicles (Fig 7.2.25 C, E and I). Additional features include conchoidal and step-like fractures, clay mineral coatings (Fig. 7.2.25 K, H and G) and cracks (including possibly hydration cracks, Fig 7.2.25 J).

All described features are in agreement with previously described characteristics for eruptions where magma has contact with water. The mostly light coloured glass particles (sideromelane) were chilled by the interaction with Crater Lake water and contain far lower microlite contents. A further characteristic of this phreatic/ phreatomagmatic eruption was the high content of spherical and elongate elemental sulphur droplets (Fig 7.2.26 A and B). Similar sulphur droplets were identified in samples of the initial phreatomagmatic phases in 1995 and 1996 (this study; Cronin *et al*. 2003), at phreatomagmatic eruptions from El Chichón, Mexico (MacKinnon *et al.*, 1983) and Mt. Etna, Italy (Andres *et al.*, 1993).

Rounded glass globules were also identified in tephra of this eruption (Fig. 7.2.26 C and D). Such spheres are reported in several deposits such as from Kilauea, Hawaii (Meeker and Hinkley (1993), Mt. Etna, Italy (Spadaro *et al.*, 2002) and general in deposits of phreatomagmatic origin (Wohletz, 1983). According to Harpel *et al.* (2008) these spheres form due to melt quenching during disaggregation. Büttner *et al.* (2002) on the other hand describe spheres forming from experiments, where melts fragment in a ductile regime during a phase of expansion when magma interacts with water.

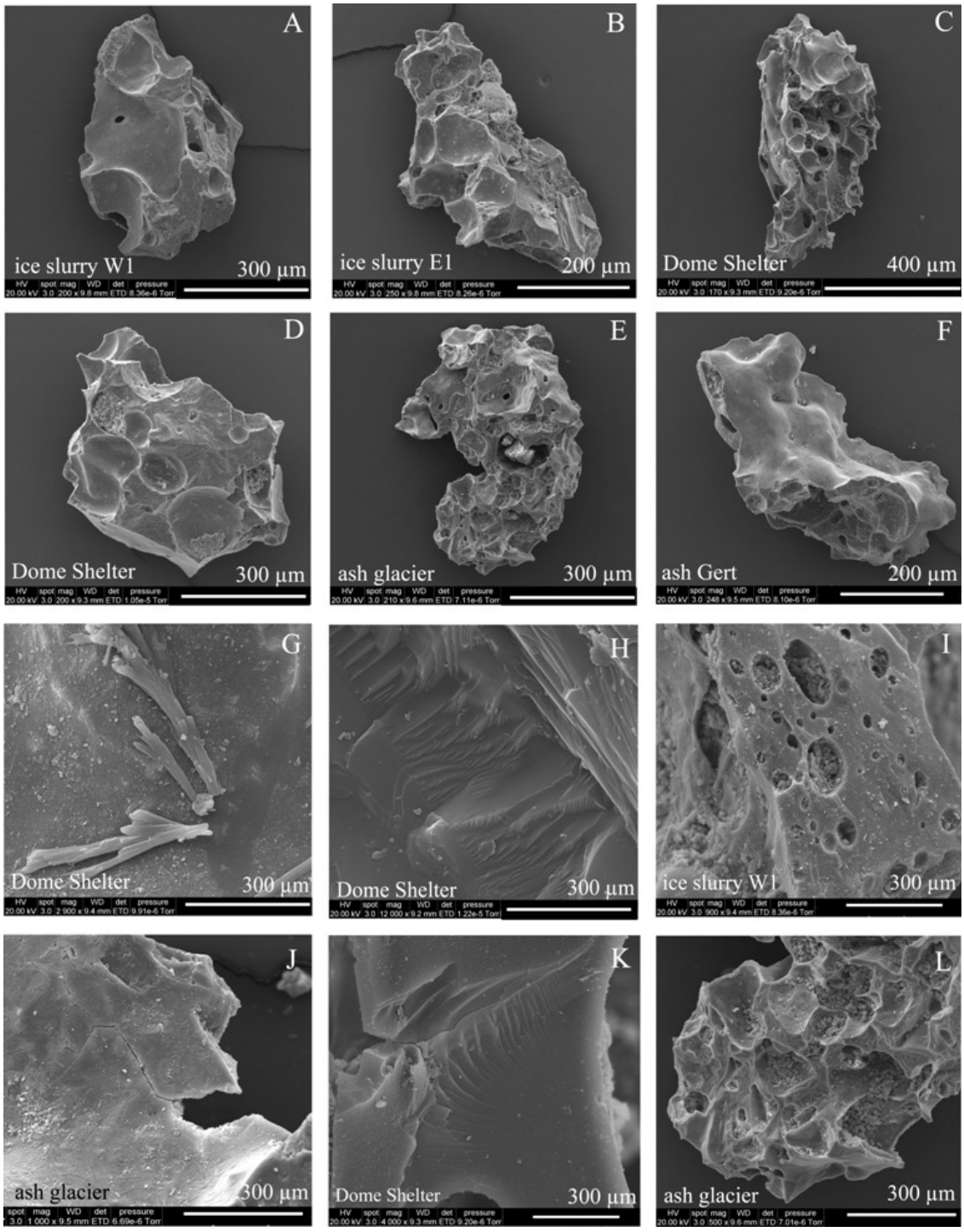

Figure: 7.2.25: SEM glass images of the 2007 Ruapehu eruption with blocky and low vesicular particles (A, B and D) and irregular (E and F) particle shapes, smoother outer surface (F), conchoidal and step-like fractures (H and K), round and ovoid vesicles with thick bubble walls (I and K) cracks (J) and clay mineral adherents (G).

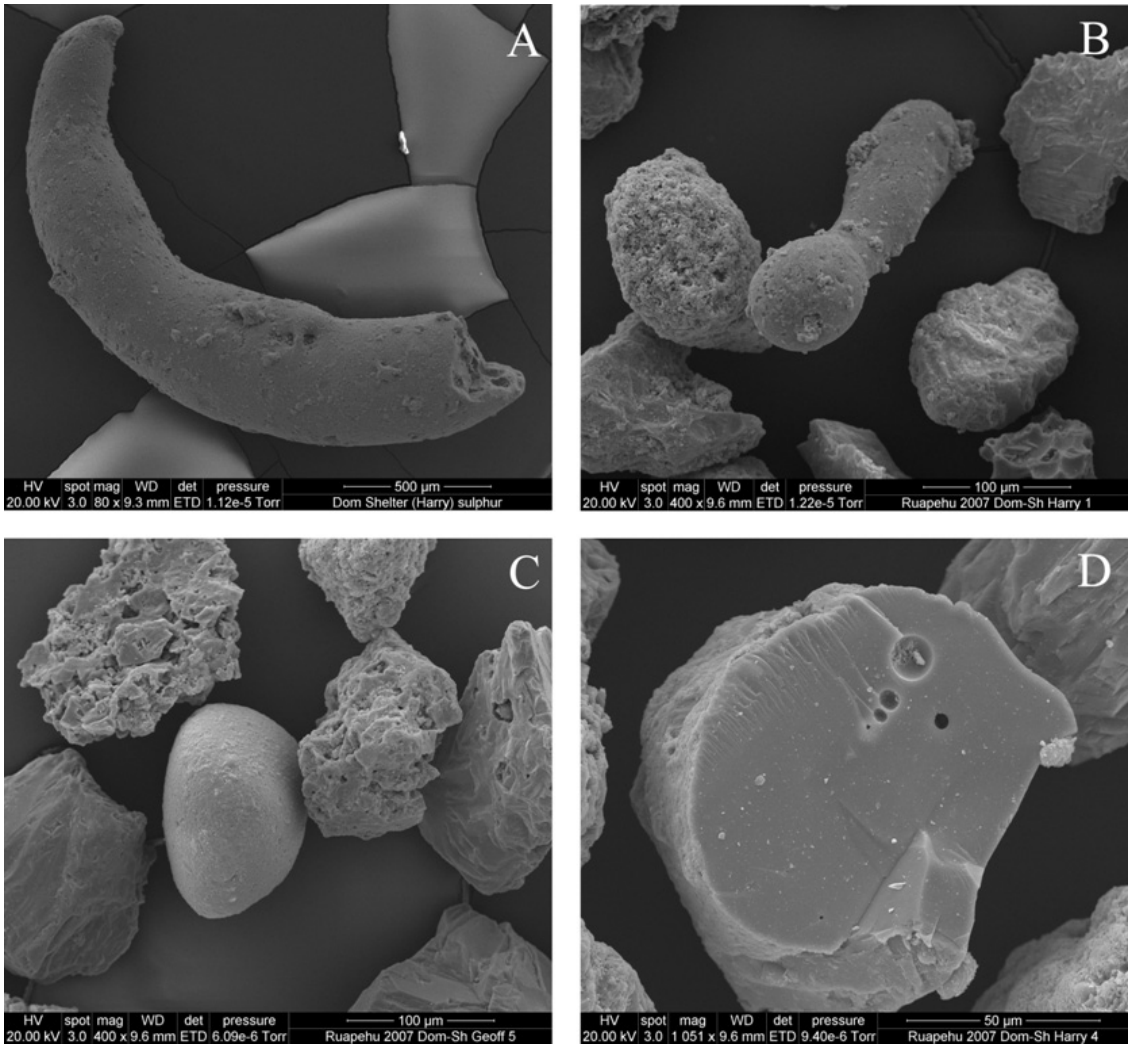

Figure 7.2.26: Spherical elemental sulphur (A and B) and solid glass spheres (C and D).

7.3. Eruption style characteristics of the TgVC over the last ~ 5000 cal. yrs. B.P.

The historical eruptions from the volcanoes of the Tongariro Volcanic Centre (TgVC) show clear characteristic features for contrasting phreatic, phreatomagmatic and magmatic eruption/fragmentation styles. This section will show the results of field observations, grain-size analyses, componentry, and particle-shape analyses of volcanic glasses from deposits of prehistoric eruptions of Ruapehu, Ngauruhoe and Red Crater, which were compared to tephras of historic eruptions from same sources.

In the course of this study two kinds of tephras were identified in Holocene sequences; deposits of single events or deposits representing an eruption episode with several related events. An individual tephra is defined as a bed accumulated during a single eruptive event lasting hours to days, without any major time breaks. Composite tephras, which represent an eruption episode with several events, were also recognised from all of the TgVC volcanoes. These composite tephras here usually characterise a gradual change from a phreatomagmatic to magmatic eruption or vice versa.

The identification of eruption styles from prehistoric eruptions is often complicated due to weathering, soil formation processes and reworking. Here, grain-size analyses, componentry/lithology, particle shape and glass chemistry have been used to try to distinguish eruption styles.

7.3.1. Field observations

Single Holocene TgVC tephra deposits range in thickness between 0.5 to 5 cm on the ring plain (medial and distal areas), with thicknesses up to 440 cm measured in proximal sites near Ngauruhoe. Deposits pinch and swell over short distances due to the relief and vegetation (Chapters 1 and 5). The colours of the tephras range from grey to black, and depend on the componentry.

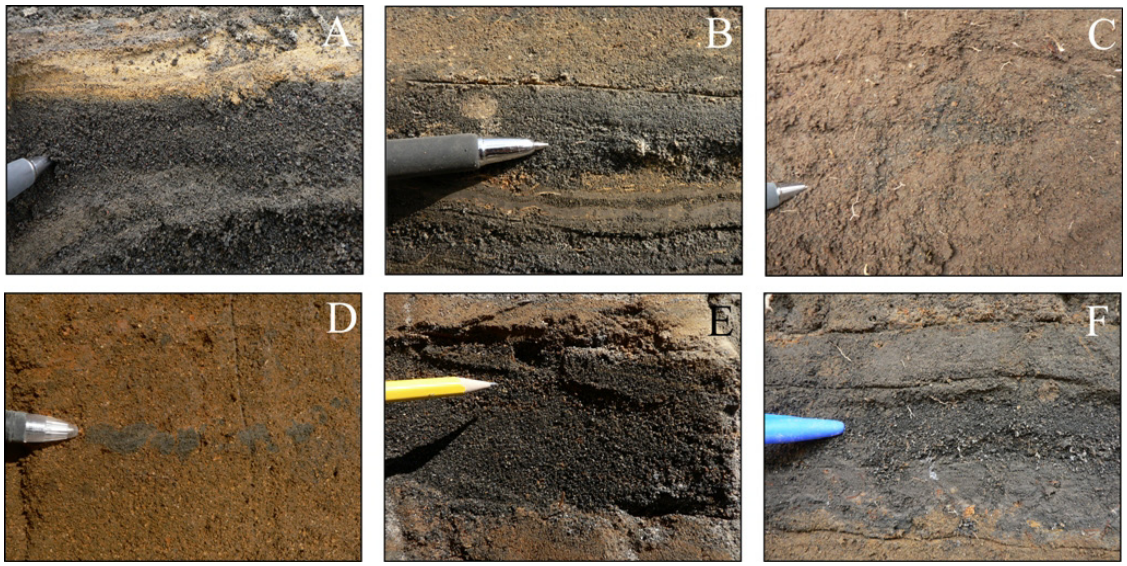

Figure 7.3.1: Individual tephras from A) Ngauruhoe at Loc. 67 (MtF, proximal) and B) from Ngauruhoe at Loc. 12 (MtF, distal), C) strongly weathered individual Red Crater tephra at Loc 63 (Ngauruhoe Form., medial) and D-F) individual Ruapehu-sourced tephras with D) from Loc 12 (Papakai Form., distal), E) at Loc 40 (Tufa Trig Form., medial) and Loc 56 (F, Tf8, medial).

Tephras representing a composite unit of an eruption episode are very common for Ruapehu units, but also have been observed in tephras derived from Ngauruhoe (mainly at Stage 2) and Red Crater. They are characterised by having a thin white layer at the base of a thicker dark grey to black tephra (Figure 7.3.2 A-F). The white – light grey, greasy fine ash is generally 1 to 5 mm thick, and in rare cases up to 10 mm. In most cases this layer is discontinuous and was deposited on uneven surfaces. Above this occurs, a much thicker (5 to 100mm) dark grey to black, fine–medium ash. In rare cases the fine-grained lower part can be of similar thickness to the upper part (e.g. pale purple Ngauruhoe tephra Figure 7.3.2 F).

During the 1995 Ruapehu eruptions a similar deposit stratigraphy was observed (Figure 7.2.13), including a white fine ash at the base and a darker, coarser ash above. This reflected the observed change in eruptive style from a phreatomagmatic (white base) into a dry-magmatic eruption (darker top). De Astis *et al.* (1997) describes similar tephras from Fossa caldera (Vulcano Island, Italy). Barberi *et al.* (1989) and Rolandi *et al.* (1993) also show that the Vesuvius 79 A.D., 1631 and 1906 tephras have similar contrasts in componentry and grain-sizes between the phreatomagmatic and magmatic-phase eruptives.

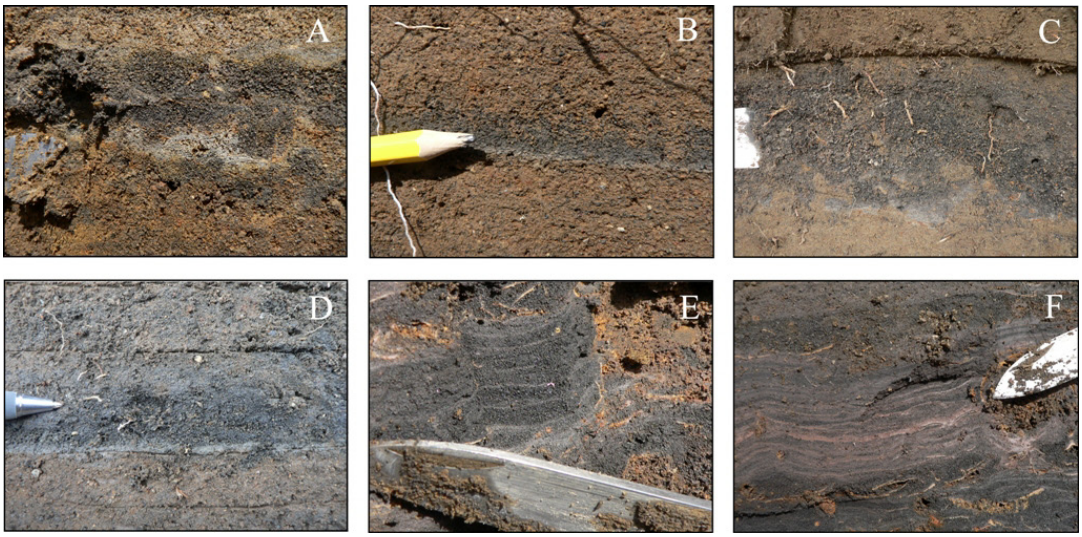

Figure 7.3.2: Distinctive thin white ash layers at the base of thicker dark grey – black ash deposits sourced from (A) Ruapehu, at Location 12 at the base of the Mangatawai Formation, (B) Location 19 and (C) at Location 56; both within the TF, (D) from Red Crater at the Loc. 63 within the Ngauruhoe Formation and (E+F) from Ngauruhoe at Location 12 within Stage 2 (MtF).

7.3.2. Tephra lithology/componentry

As shown for the historic eruptions of the TgVC, the componentry can be useful for identification of prehistoric eruption styles. Magmatic and phreatomagmatic eruptions are mainly distinguished by the ratio of sideromelane vs. tachylite glass in the tephras, while phreatic eruptions produce tephras with a higher lithic content.

In all the prehistoric tephras analysed, glass dominates (Figure 7.3.4A). The crystal fraction includes plg > opx > cpx, with the widest range shown by the prehistoric Ngauruhoe tephras (Figure 7.3.4B). Ruapehu and Red Crater tephras (individual) in comparison are in stronger agreement with the 1995-96 eruption crystal componentry. The samples with highest pyroxene contents also contain the highest glass contents, which are mainly dominated by tachylite, suggesting magmatic-gas driven fragmentation and eruption styles (Figure 7.3.5).

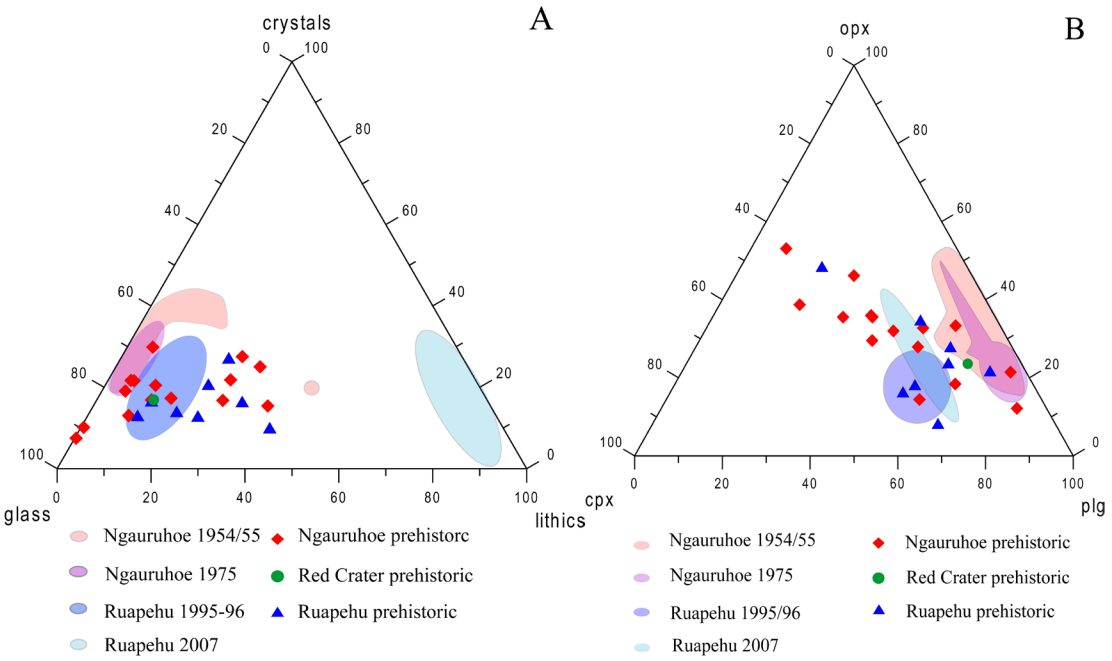

Figure 7.3.4: Componentry of tephras from TgVC analysed in this study with A) the main lithology groupings, while B) shows the dominant mineralogy.

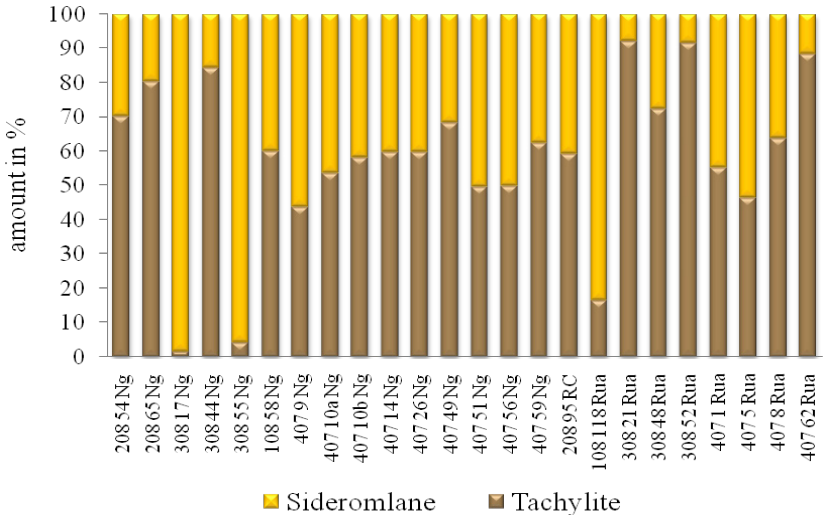

Figure 7.3.5: Propotions of sideromeline versus tachylite glass from individual tephras of prehistoric eruptions from the TgVC. Ng=Ngauruhoe, RC=Red Crater and Rua=Ruapehu. The samples are collected from Locations 12, 56, 63 and 67 (Appendix 1).

Despite the frequent occurrence of pale fine basal layers, they could not easily be sampled due to their thin and discontinuous nature. For six tephra sets analysed, the

basal layers do have higher glass contents, while the coupled upper layers have higher crystal concentrations (Figure 7.3.6).

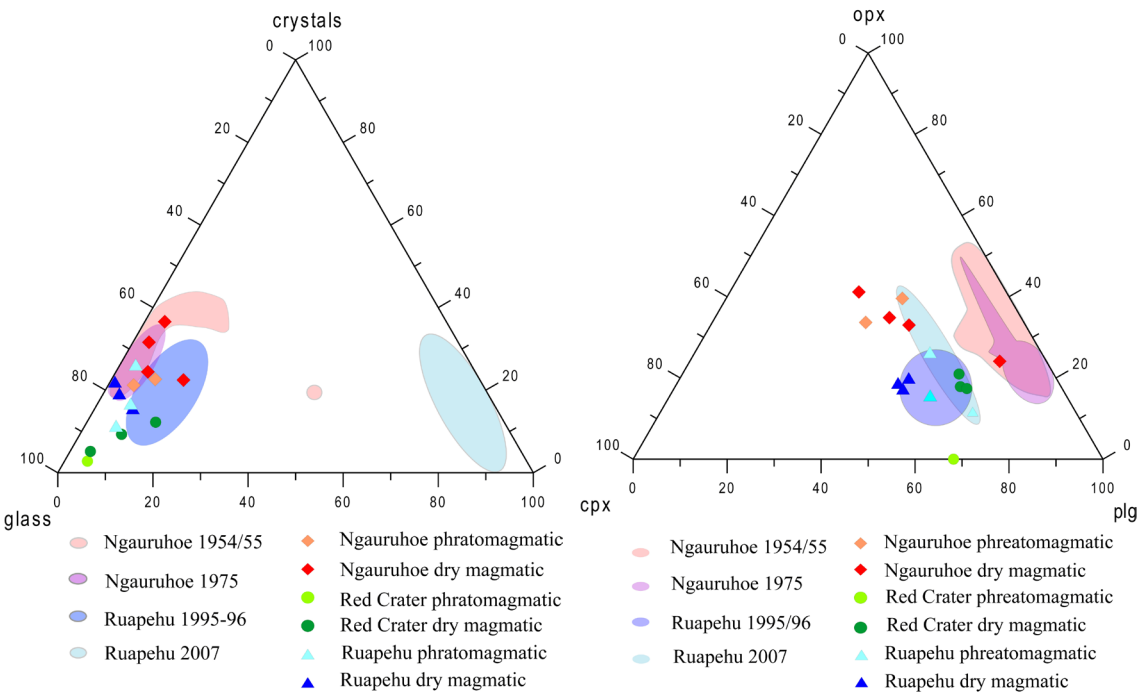

Figure 7.3.6: Componentry (total) of prehistoric eruptions representing a wet-dry eruption cycle from Ruapehu (blue), Ngauruhoe (red) and Red Crater (green) in comparison to historic eruptions from Ngauruhoe 1954/55 (pink shading) and 1975 (purple shading) and Ruapehu 1995/96 (dark blue) and 2007 (light blue). Left side: main components glass vs. lithics vs. crystals and right side; plg vs. opx vs. cpx.

Six tephra sets were analysed as illustrated in Figure 7.3.7, where the 1st bar (left) shows the glass proportions sideromelane and tachylite of the white basal layer and the 2nd bar shows this glass ratio of the coupled upper black layer. The first Ruapehu set (from the base of the Mangatawai Formation) and the last set sourced from Red Crater show that the amount of light glass decreases from old to young, while the amount of dark glass increases. This gradual transition suggests changes in eruption conditions over time. A similar trend occurs with 1995-96 Ruapehu eruptions (Figure 7.3.8), where the eruption started with phreatomagmatism and evolved over time into a dry magmatic strombolian eruption. Sets 2-5 (Figure 7.3.7), which also show a pale white ash base, display the opposite, where the amount of light glass increases from the basal to the top layer. This observation currently cannot be explained.

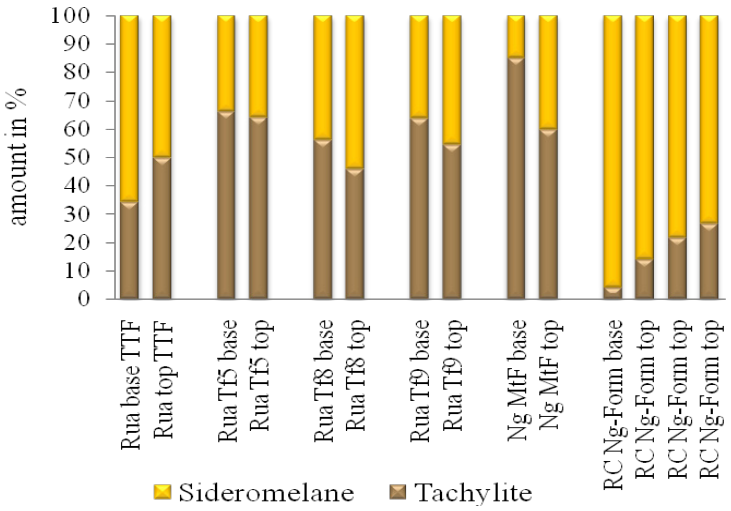

Figure 7.3.7: Point counts of sideromelane (light glass) and tachylite (black glass) from four sets of Ruapehu (Rua)-sourced tephras, one set from Ngauruhoe (Ng) and one set derived from Red Crater (RC). The set comprises a minimum of 2 tephras where the basal layer is very thin (mm), lighter and finer grained than the darker, thicker and coarser top layer. Samples were taken from Locations 12, 56 and 63 (Appendix 1).

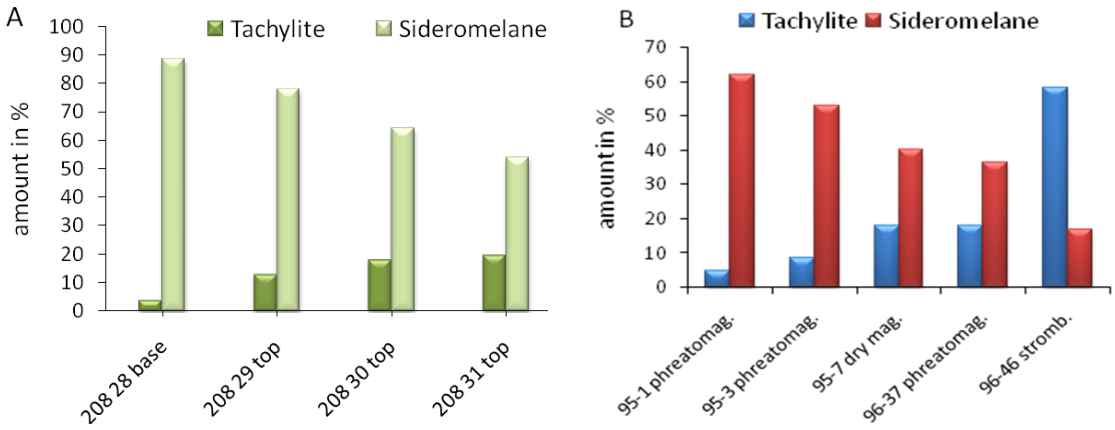

Figure 7.3.8: Ratio of **s**ideromelane (light glass) vs. tachylite (black glass) A) Analyses of from four successive tephras sourced from Red Crater. Samples are in the order from the oldest (left) to the youngest (right). B) Analyses from the 1995-96 eruption episode.

7.3.3. Grain-size analyses

The Holocene TgVC tephras analysed are fine-coarse ashes and are generally poorly sorted with unimodal distributions in proximal areas passing to polymodal in distal sites. The distal distributions may relate to local effects such as wind and/or are a result

of particles flushed out of tephra plumes by rain. The thin basal layers, where sampled, are all considerably finer-grained and poorer sorted than the upper ash units (Figure 7.3.9).

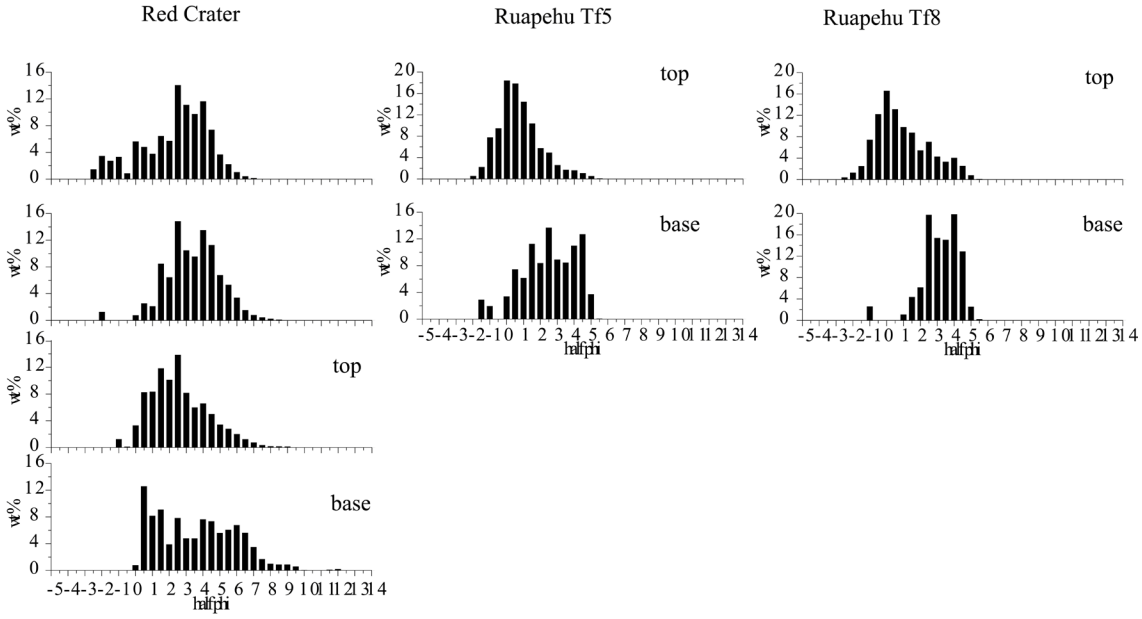

Figure 7.3.9: Examples of grain size histograms at half ϕ intervals from Red Crater and Ruapehu (Tf5 and Tf8) tephras. The lower diagrams represent the pale, thin and very fine basal ash layer, while the upper diagrams represent the darker, thicker and coarser upper portion.

7.3.4. Particle-shape analyses

All samples of prehistoric eruptions from Ruapehu and Ngauruhoe show both sideromelane and tachylite glasses. The tachylite glass is generally blocky, whereas sideromelane is mostly either irregularly or droplet-shaped with smooth surfaces and elongate and contorted vesicles with thin walls (Figure 7.3.10 A-L). The tachylites have rare, round and very large vesicles in relation to the particle size. In some cases surface pits were observed on some of the smooth surfaces (Figures 7.3.11 A-L).

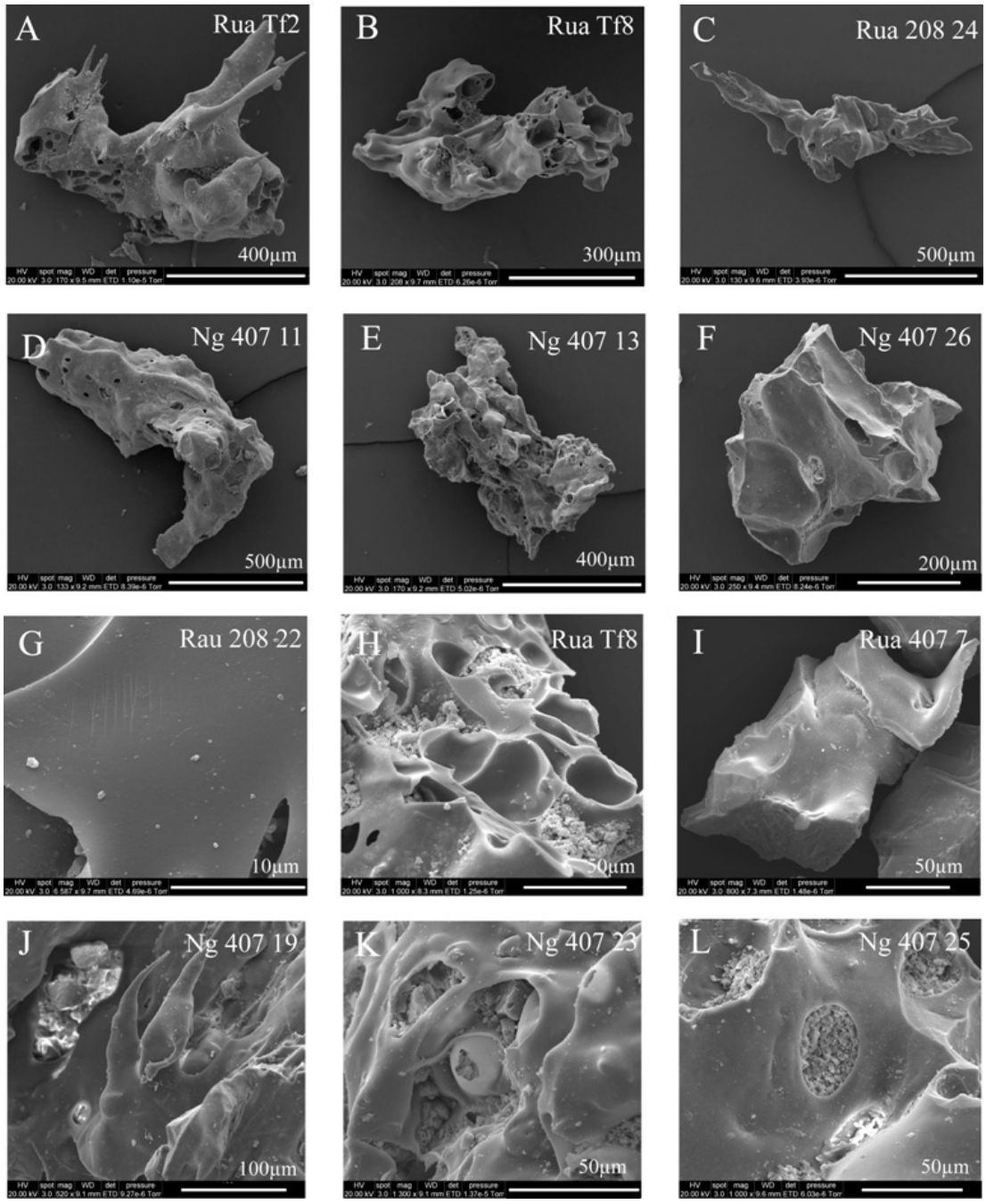

Figure 7.3.10: SEM-images of light brown glasses (sideromelane) from Ruapehu and Ngauruhoe tephras. Images show sideromelane particles from various individual tephras, with irregular (A-F) and partly drop-like (A+C+J) shape. The sideromelanes have often smooth surfaces (G+I), round vesicles with thin bubble walls (H+K) and rare vesicle fillings (L).

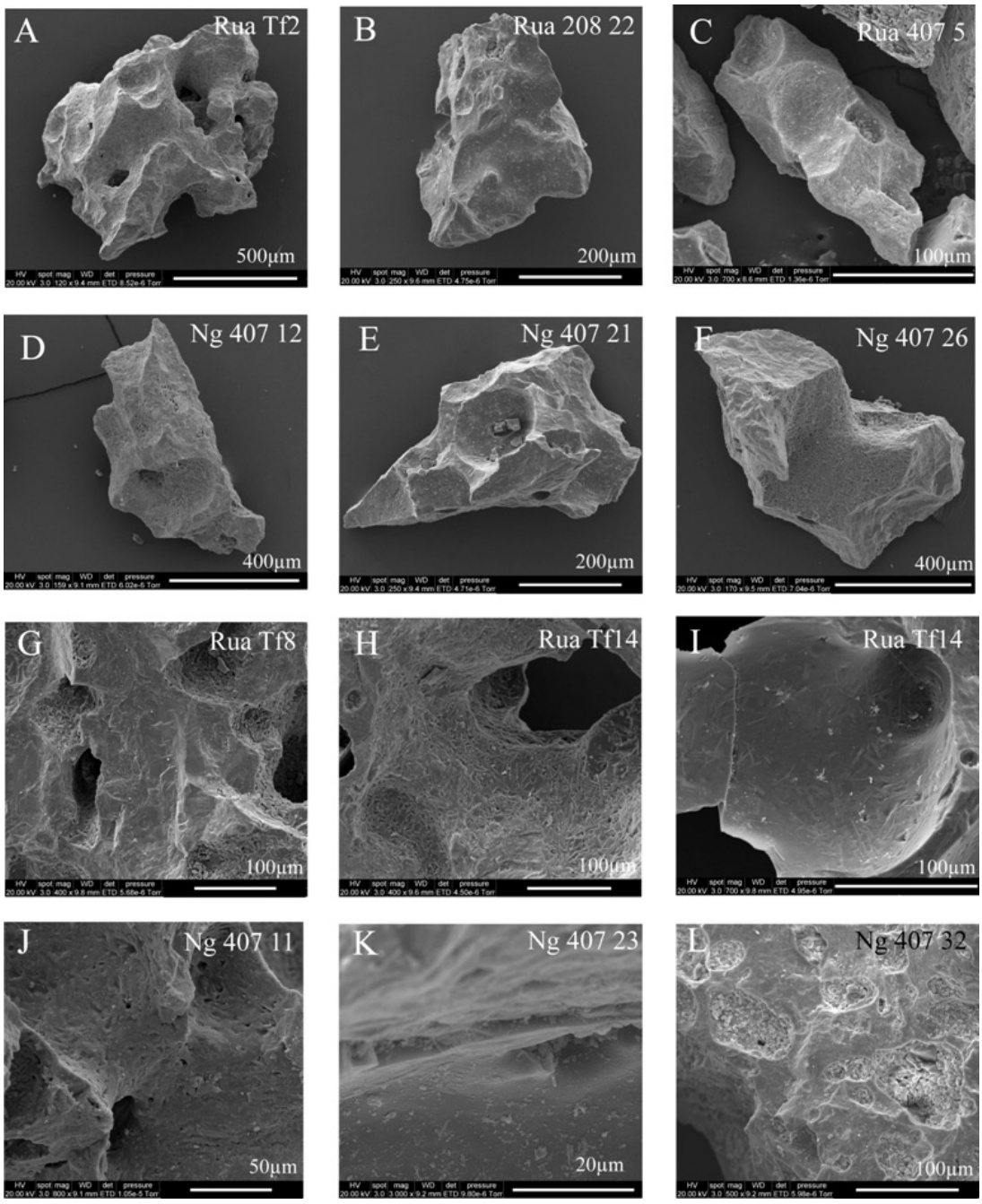

Figure 7.3.11: SEM-images of tachylites from Ruapehu and Ngauruhoe tephras with A-F) blocky shaped particles and sharp edges. Characteristic surface features of tachylites including glass coated microlites (G-I), large vesicles (E-H), chemical pitting (J+K), brittle fractures (F) and adhering dust (L).

Ash particles from all three volcanoes show characteristics such as those described above for historic Ruapehu and Ngauruhoe eruptions, including conchoidal-fractures and moss-like surface textures, hydration cracks, adhering clay minerals, and low vesiculation; features which can be related to phreatomagmatic eruptions (Wohletz and Krinsley, 1982; Dellino and Volpe, 1996) (Figures 7.3.12 A, E, G, H and J). The cracks

may be formed just after fragmentation due to sudden cooling and quenching (Büttner *et al.*, 1999). They evolve from hairline breaks in a surface skin, which may pull apart and roll up. Chipped edges (Figure 7.3.12 I) and conchoidal fractures are caused by collision and brittle fragmentation (Wohletz and Krinsley, 1982; Freundt and Rosi, 2001). Hollow glass spheres were identified only within Ruapehu samples and may be produced by phreatic or phreatomagmatic eruptions due to rapid cooling upon interaction with water (Figure 7.3.12 K). Pele's hair fragments, which are produced during fire fountaining (Fig. 7.3. 12 C), were identified in Red Crater and Ngauruhoe tephras. Glass particles from Ruapehu and Ngauruhoe showed corrosion of the particle surface, which may be caused by chemical alteration (c.f., Wohletz and Krinsley, 1982) or weathering. Ruapehu and Ngauruhoe samples also show mainly particles with low vesicularities (Figure 7.2.12 D and F) that may reflect rapid decompression or a earlier degassed magma. Such higher density clasts are common in vulcanian eruptions resulting from high crystalline microlite contents (Cashman and Blundy, 2000; Cashman *et al.*, 2000), also likely caused by a rapid decompression.

Both Ruapehu and Ngauruhoe tephras show characteristic features that are most likely related to vulcanian and phreatomagmatic eruption styles, although the evidence is more convincing in the former. Red Crater tephras, show contrasting textures, indicating a more magmatic-gas driven expansion and fragmentation process.

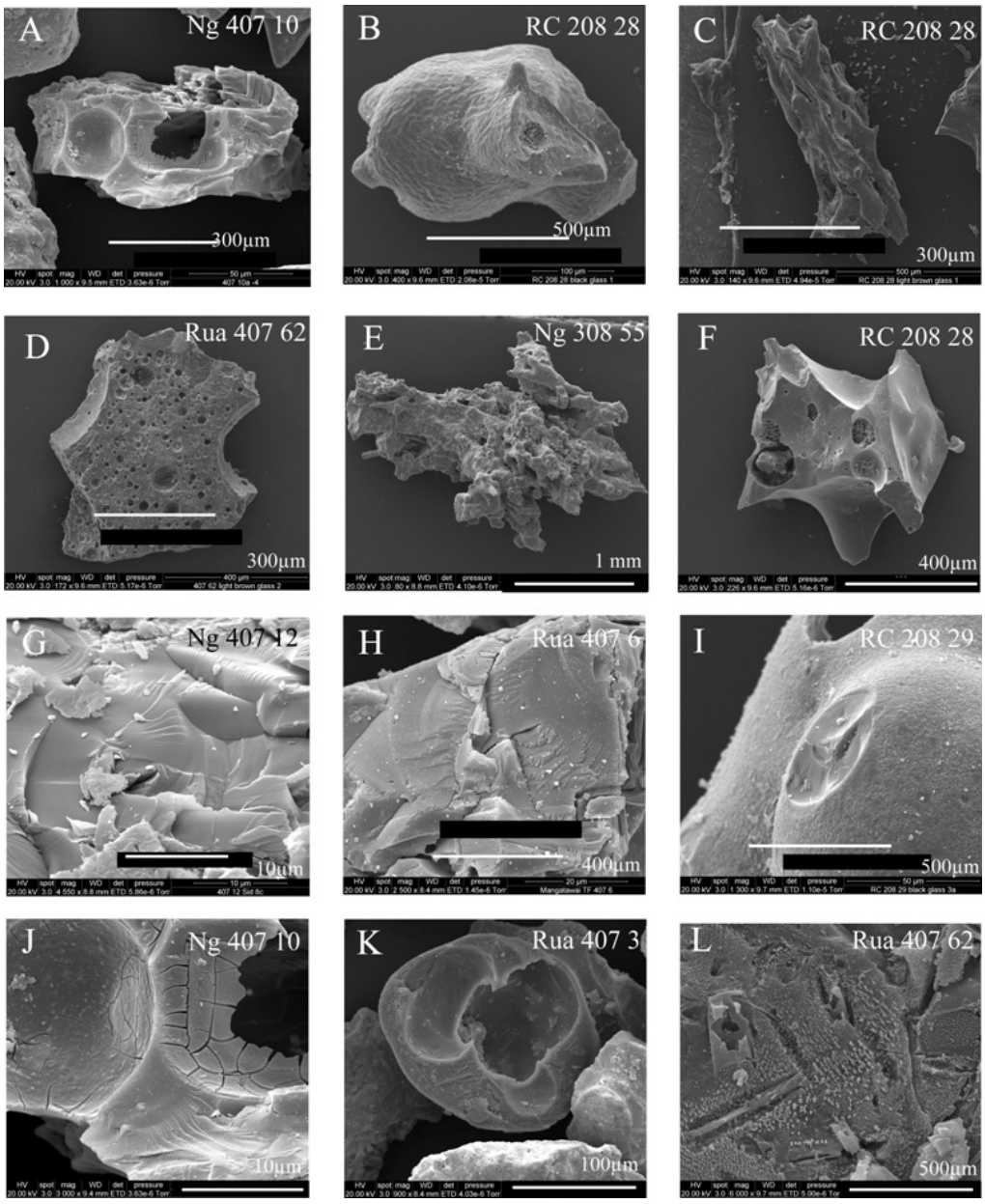

Figure 7.3.12: SEM-images of particles from individual prehistoric tephras from Ruapehu and Ngauruhoe and Red Crater with A+F) block particles with large vesicles, B) chemical pitting, C) Pele's hair, D) blocky particle with numerous small spherical vesicles and thick bubble walls, E+F) irregular shaped particle, G-H) conchoidal fractures, I) chipped surfaces, J) hydration cracks, K) hollow glass sphers, L) possible clay mineralisation.

The pale fine-grained basal ash layers, where present, show particles with characteristics of phreatomagmatic eruptions, such as blocky shapes, low vesicularity, step-like, moss-like and conchoidal fractures and hydration cracks (Figure 7.3.13). By contrast, the darker and thicker top ash layers show characteristic features of magmatic eruptions such as irregular shape, high vesicularity, Pele's hair and smooth surfaces

(Figure 7.3.14). Chipped edges with conchoidal and step-like fractures were probably produced through more violent strombolian eruptions.

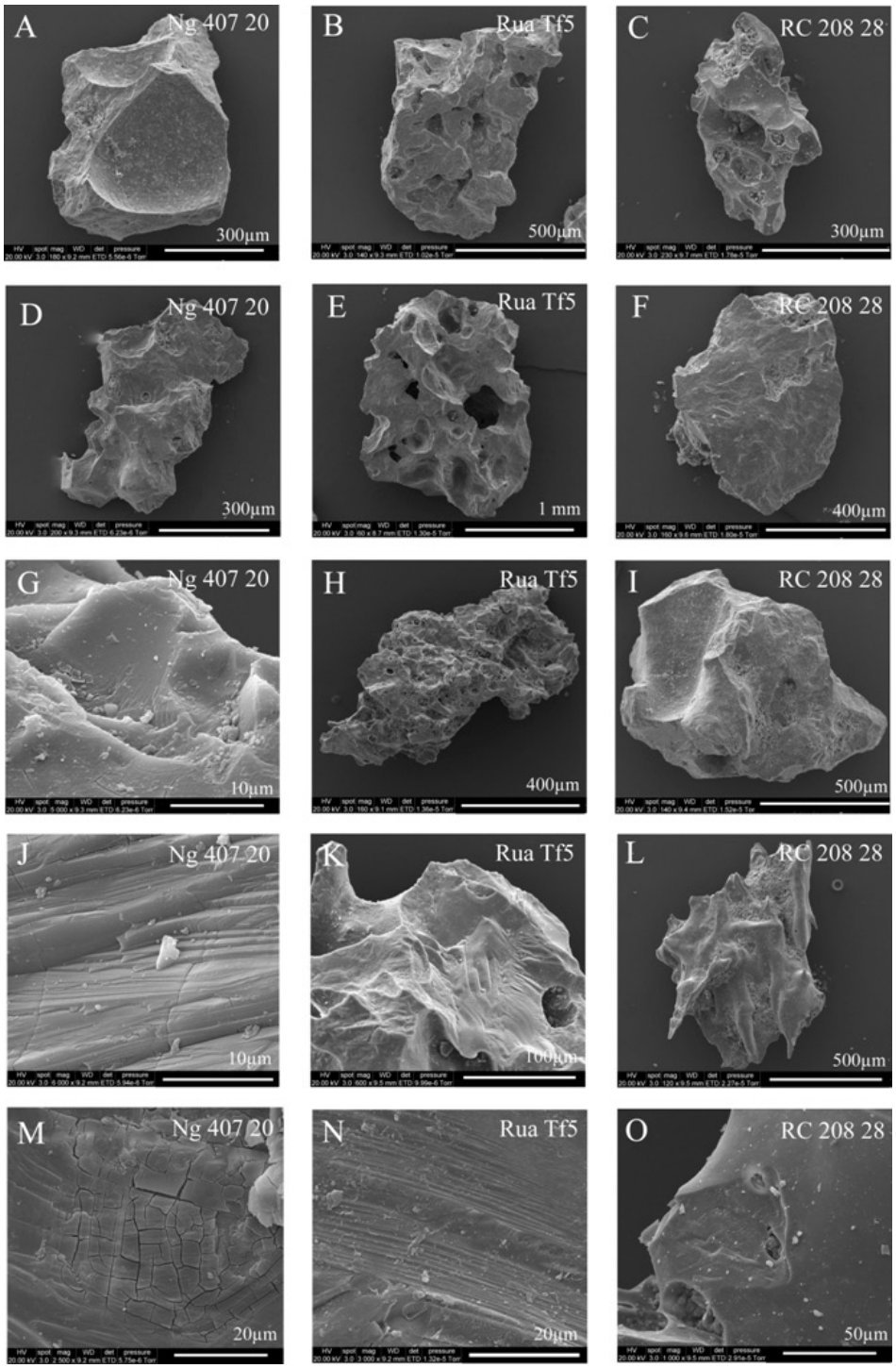

Figure 7.3.13: SEM-images of the basal white tephras sourced from prehistoric eruptions from Ruapehu, Ngauruhoe and Red Crater. Characteristic features are A-F+I) blocky particles with few large round vesicles, G+O) chipped edges, H) moss-like structures, J+N) step-like- and K) conchoidal fractures, L) irregular shaped, drop-like particles and M) hydration cracks.

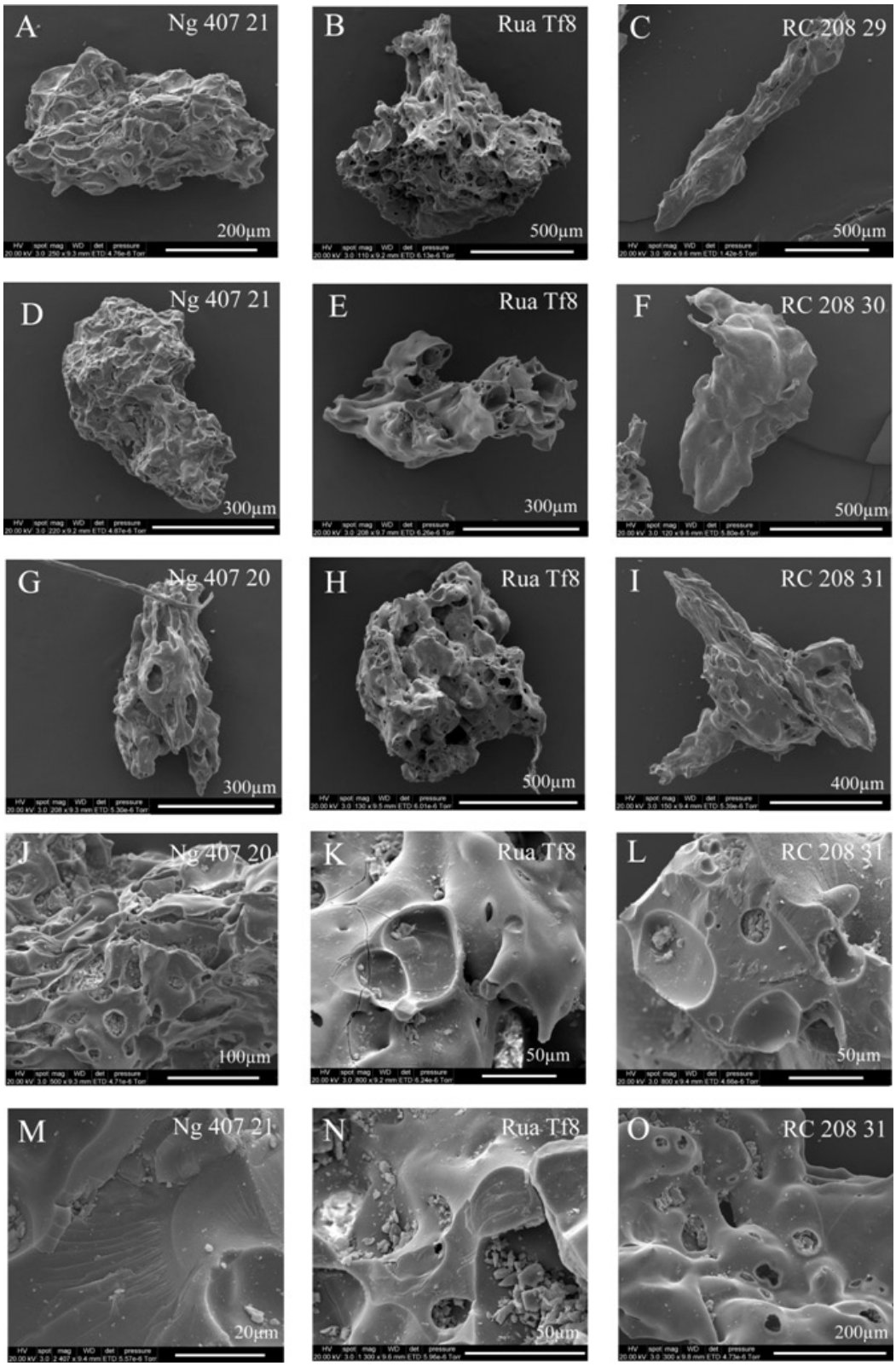

Figure 7.3.14: SEM-images of the darker and thicker top layer of tephras derived from prehistoric eruptions from Ruapehu, Ngauruhoe and Red Crater. Characteristic features are A-I) irregular shape particles, C) Pele's hair, I) drop-like shape, H+J) high vesicularity, K+L+O) smooth surfaces, M) conchoidal fractures, and N) chipped edges.

7.4. Summary

Analysing eruption styles of observed eruptions from Ruapehu and Ngauruhoe, allowed, in the case of the TgVC, an identification of eruption styles from prehistoric eruptions produced during the last 12 000 cal. yrs. B.P.

The volcanoes of the TgVC have produced a range of magma-fragmentation mechanisms, ranging from phreatic, phreatomagmatic to magmatic, with associated eruption styles varying from surtseyan, strombolian, vulcanian to sub-plinian. A combination of textural and lithological criteria is needed to distinguish each eruption style from their resulting tephra.

Overall there is a general trend for an initial phreatomagmatic eruption phase that is followed by phases during which there are dominantly magmatic-gas driven fragmentation mechanisms. This trend suggests the rapid consumption of a shallow, small source of water, such as within a snow or water-filled crater, or eruptions through a glacier. The initial phreatomagmatic events may be violent enough to have induced further decompression and volatile exsolution, generating or accelerating subsequent dry explosive pulses/phases. Ruapehu is known to have had a Crater Lake for at least 3000 years (Donoghue *et al*., 1997) which provides such patterns of influence (Cronin *et al.,* 2003). The phreatomagmatic eruptions from Ruapehu are characterised by very fine, thin white ash layers, mainly composed of blocky volcanic glass particles and crystals. The particles show characteristic phreatomagmatic-induced surface features such as hydration cracks, step-like, moss-like and conchoidal fractures along with less rounded, partly filled vesicles having thick bubble walls. The tephras from magmatic and strombolian eruptions, on the other hand, are typically coarser grained and thicker and have higher proportions of dark tachylite glass. The particles are often of irregular and droplet-shaped with smooth surfaces and a high ovoid or tubular vesicularity.

Ngauruhoe and Red Crater tephras appear to be dominantly produced by magmatic eruptions with similar features to the same eruptive styles at Ruapehu, as explained above. There are, however, a large number of Ngauruhoe tephras that appear to be the

result of vulcanian eruptions where ash is highly fragmented and dominated by volcanic glass and crystals, with more subtle expression of features that are similar to ash from phreatomagmatic eruptions.

The results presented here give rise to the assumption that it is possible to analyse tephra deposits from prehistoric eruption worldwide and compare these to deposits of observed eruptions, to classify prehistoric eruption styles and for building a complete picture of the eruptive history from a volcano.

Chapter 8

Frequency/volume/magnitude relationships and physical volcanology of the Holocene explosive eruptions in the Tongariro Volcanic Centre

Very little is known about the eruption frequency, styles, magnitude and fragmentation processes from the volcanoes of the TgVC; existing knowledge principally stems from the observed historic eruptions of the last ~170 years.

Through chemical fingerprinting of tephras from the three individual volcanoes Ruapehu, Ngauruhoe and Red Crater, the first structured analysis is now possible of the physical volcanology of explosive eruptions from the Centre. This chapter reviews the new data on pyroclastic eruption frequencies and grain size analysis of Ruapehu, Ngauruhoe and Red Crater, together with eruption volume, and eruption column height calculations for Ngauruhoe-sourced tephras.

8.1. Eruption frequency

One of the main aims of this study was to determine the eruption frequency of Ngauruhoe, Ruapehu and Red Crater during the last ~12 000 cal. yrs. B.P. The determination of eruption frequency requires making a clear distinction between discrete tephras and those depositional units containing traces of pyroclasts from mixed source. The eruption frequency was compiled from a combined record of the deposits at several dispersed locations. Age-estimations at each site were made by calculating soil accumulation rates in relation to radiocarbon dates and/or known tephra marker bed ages. In cases where the stratigraphy of the profiles overlapped, the highest frequency

record was chosen to establish the most complete composite sequence. Since many historic eruptions are not preserved in the geological record they are discussed separately.

8.1.1 Explosive eruption frequency for Ngauruhoe

As shown in previous chapters, the eruption history of Ngauruhoe extends from at least 4700 cal. yrs. B.P., with the oldest discrete tephras from this source being identified at Location 12. To reconstruct the eruption frequency for Ngauruhoe, the characteristics of discrete tephras at Locations 12, 67 and 63 were used to define a four-stage history (Figure 8.1.1). Stage 1 is represented by tephras within the Papakai Formation that have a Ngauruhoe source. Then followed a 1200 yr. interval, in which no Ngauruhoe tephras were large enough to be preserved along the Desert Road (~10-15 km from source). Then Stage 2 commenced, representing the main phase of explosive activity at Ngauruhoe with around 600 yrs of semi-continuous eruptions starting at c. 3400 cal. yrs. B.P. During the last 100 years of Stage 2 (2900-2800 cal. yrs. B.P.) the highest frequency of large explosive eruptions from Ngauruhoe occurred, reaching one event per 1.6 years. The onset of Stage 3 is heralded by increasingly sporadic, but still highly explosive eruptions extending up until 1717 cal. yrs. B.P, to the stratigraphic boundary of the distinctive Taupo Pumice. From this point onward, Stage 4 ensues, characterised by a steady decline in the magnitude of known activity until the present day, with discrete Ngauruhoe tephras recognised only at proximal Loc. 63 at Pukekaikiore. Within the last ~1000 years eight distinct Ngauruhoe tephras are known; four between 800-1000 cal. yrs. B.P. and four eruptions over the last 300 years (Fig. 8.1.2).

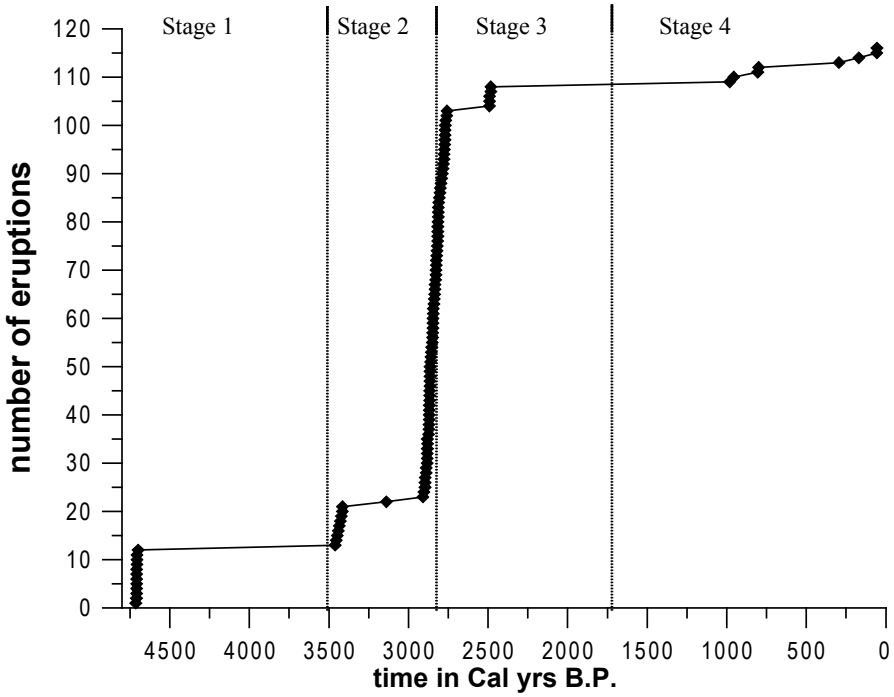

Figure 8.1.1: Cumulative frequency curve for known distinct explosive eruptions (VEI≥ 2) from Mt. Ngauruhoe since 4700 cal. yrs. B.P.

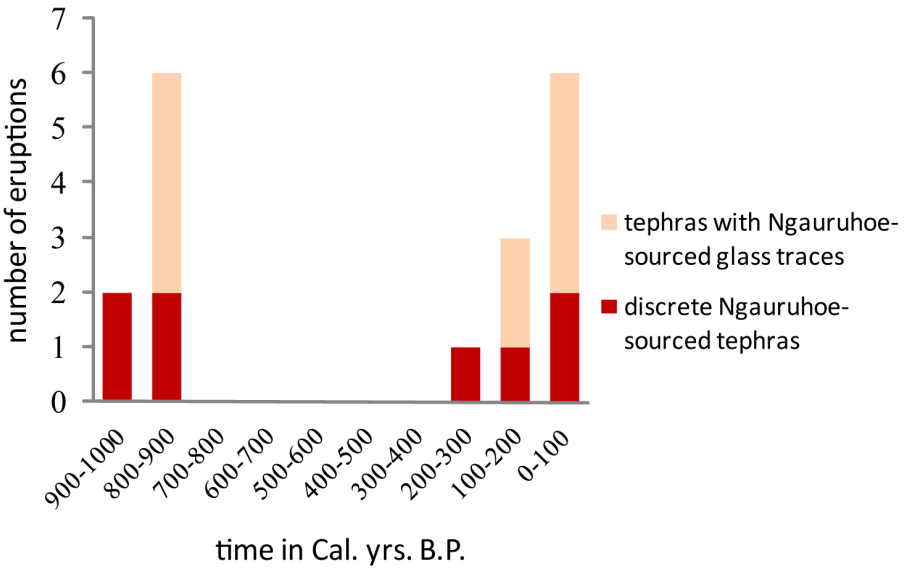

Figure 8.1.2: Eruption frequency for Ngauruhoe over the last 1000 years (latter part of Stage 4). Red bars represent eruptions of discrete tephras while pink bars represent tephras containing traces of Ngauruhoe-source pyroclasts.

The larger pauses in activity imply that Ngauruhoe was not producing large-scale tephra eruptions during these times, but chemical analysis of volcanic glasses from paleosols, and trace amounts of Ngauruhoe pyroclasts within other tephras, reveals that Ngauruhoe

was probably more frequently active than indicated by the recognisable tephras. Some gaps in the record, however, may be real representations of a hiatus in activity (e.g., 800-300 cal. yrs. B.P.). Traces of Ngauruhoe-sourced glass in some of the paleosols and other tephra deposits also suggest a slight increase in frequency of small-scale explosive activity over the last 300 years.

Over 52% of the large-scale explosive eruptions from Ngauruhoe occurred over a single ~100 year period between 2800-2900 cal. yrs. B.P. (Figure 8.1.1).

8.1.2 Explosive eruption frequency for Red Crater

Discrete tephras sourced from Red Crater were only identified at the proximal Location 63, with the positively identified tephra at 323 cal. yrs. B.P. (Figure 8.1.3). The peak of activity is characterised by seven eruptions between 300-200 years. Since then, the activity of Red Crater has steadily decreased.

Traces of possible Red Crater-sourced tephras were also found in deposits between 800-900 cal. yrs. B.P. (2 events) and 2700-3000 cal. yrs. B.P. (15 events). Interestingly, 10 possible early Red Crater eruptions are implied from trace ash particles between 2800 and 2900 cal. yrs. B.P., which was within the period of Ngauruhoe's greatest activity.

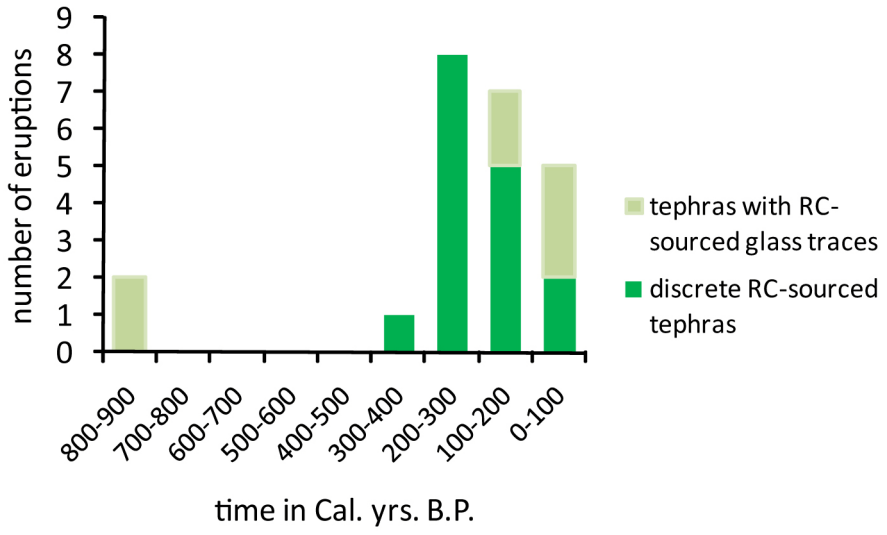

Figure 8.1.3: Eruption frequency of Red Crater over the last 1000 years. Green bars represent eruptions of discrete tephras while pale green bars represent tephras containing traces of Red Crater eruptions.

8.1.3 Explosive eruption frequency for Ruapehu

Mt. Ruapehu has been active for over 300 000 years (Parish, 1994), although its tephrochronological record is described in detail for only the last ~26 000 years. To add to this record, the tephra stratigraphic record at Locations 12, 56 and 63 and Lake Rangatauanui has been collated and integrated into the pre-existing stratigraphy. 30 explosive eruptions from Ruapehu are preserved between 26 000-12 000 cal. yrs. B.P. in the Lake Rangatauauni cores, representing a minimal record because the lake is located far from the typical dispersal axes of most eruptions. It is known that the largest eruptions of Mt. Ruapehu occured in the period c. 26 000-12 000 cal. yrs. B.P., (Donoghue *et al.,* 1995). A relatively high frequency of eruptions occured between 23 000 to 21 000 cal. yrs. B.P., declining to a steady rate over the next 8000 years, before the next high frequency period between 15 000 and 13 000 cal. yrs. B.P. Following this, the volumes of eruptions reduced by an order of magnitude or more (Donoghue *et al.,* 1995). From 13 000 to 3500 cal. yrs. B.P., 12 distinct tephras are recorded, after which the frequency of tephra preservation increases to the present day (Fig. 8.1.4). In particular, the maximum frequency occurs between 600 and 700 cal. yrs. B.P. In addition to distinct tephras sourced from Ruapehu, traces of Ruapehu-sourced pyroclasts occur within Ngaruruhoe and Red Crater-sourced tephras, indicating (assuming they are not reworked) an even higher eruptive frequency between 800 and 900 cal. yrs. B.P. and over the last 150 years (Figure 8.1.5).

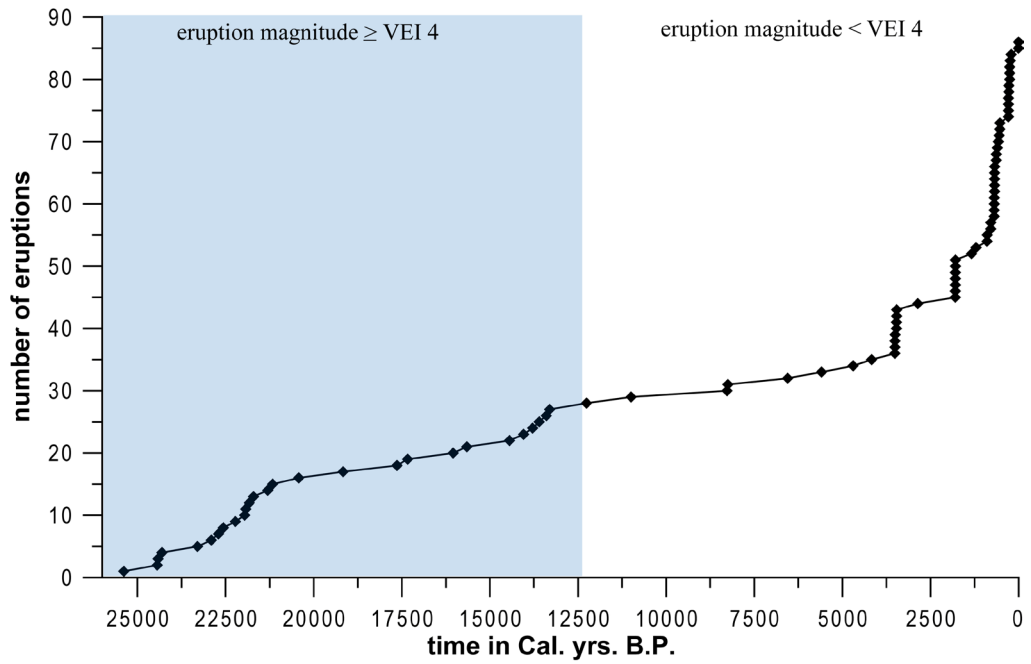

Figure 8.1.4: Cumulative frequency curve for descrete (VEI ≥ 2) known explosive eruptions from Mt. Ruapehu since 26 000 cal. yrs. B.P.

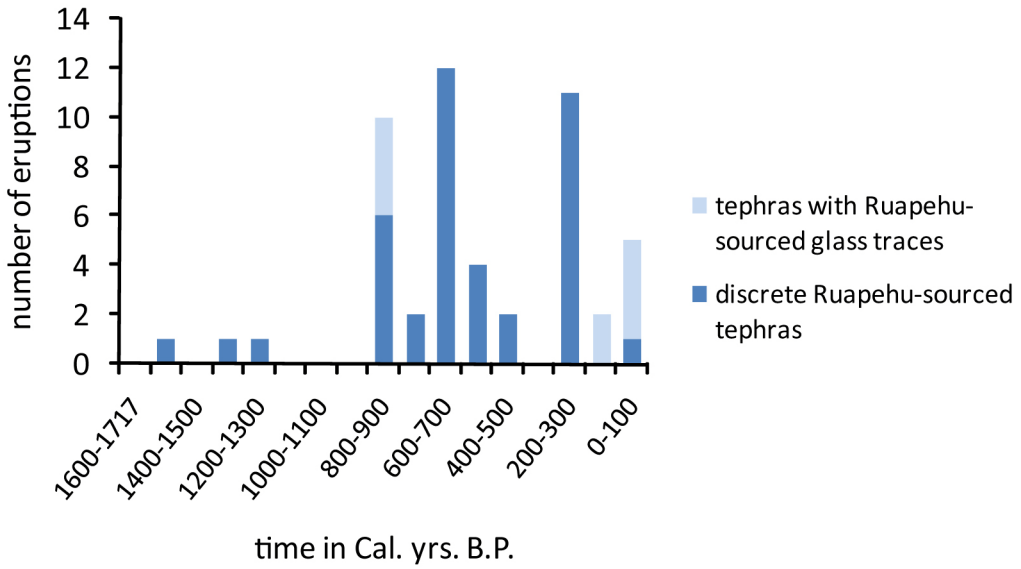

Figure 8.1.5: Frequency of explosive eruptions from Ruapehu post 1717 cal. yrs. B.P. in 100 yr intervals, representing tephras of the Tufa Trig Formation. Blue bars represent discrete tephras, while pale blue bars represent tephras containing traces of Ruapehu pyroclasts.

Over the last *c.* 12 000 cal. yrs. B.P., the largest four Ruapehu eruptions: Orange lapilli 1 and 2 and Tufa Trig members Tf1 and Tf2 appear most similar in their pumice lithology to the high-magnitude events of the earlier Bullot Formation. They differ from other Ruapehu tephras, within the PF, MtF and TTF, by their colour, grain size and very

likely by their eruption magnitude. These occurred at *c.* 5500, *c.* 5300, 1555 and 1338 cal. yrs B.P.

8.1.4 Comparison of TgVC source eruption frequencies

8.1.4.1. Prehistoric eruptions

Comparing the eruption frequency of all three volcanoes shows that Ruapehu has experienced an apparent gradual increase in activity over the last 26 000 cal. yrs B.P., while Ngauruhoe activity has been sporadic and is clustered into three main periods. Ruapehu's activity declined when Ngauruhoe had its most productive eruption phase between c. 3400 – 2700 cal. yrs. B.P. Ruapehu's activity then increased only once the eruption frequency of Ngauruhoe declined (Figures 8.1.6 and 8.1.7). Positively identified tephras of Red Crater were only recognised over the last c. 300 years.

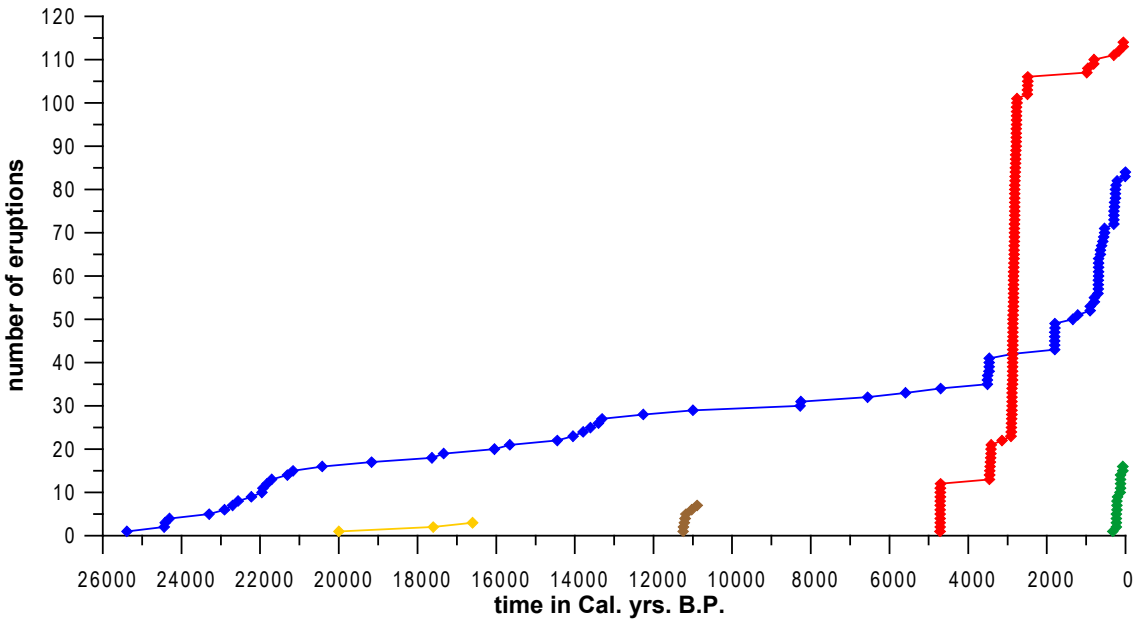

Figure 8.1.6: Cumulative explosive eruption frequency from Ruapehu (blue), Ngauruhoe (red), Red Crater (green), Tongariro Mangamate Formation (brown) and Tongariro, Rotoaira lapilli (yellow) over the last 26 000 cal. yrs. B.P. The ages for the Mangamate tephra are from Nairn *et al.,* (1998) and ages from the two younger Rotoaira lapilli are from Shane *et al.* (2008). The age of the oldest Rotoaira lapilli is stratigraphically positioned between the Rerewhakaaitu Tephra (OVC at 17625 ± 425 cal. yrs. B.P.) and Kawakawa Tephra (TVC, 27 097 ± 957 cal. yrs. B.P.), and is here estimated at c. 20 000 ca. yrs. B.P.

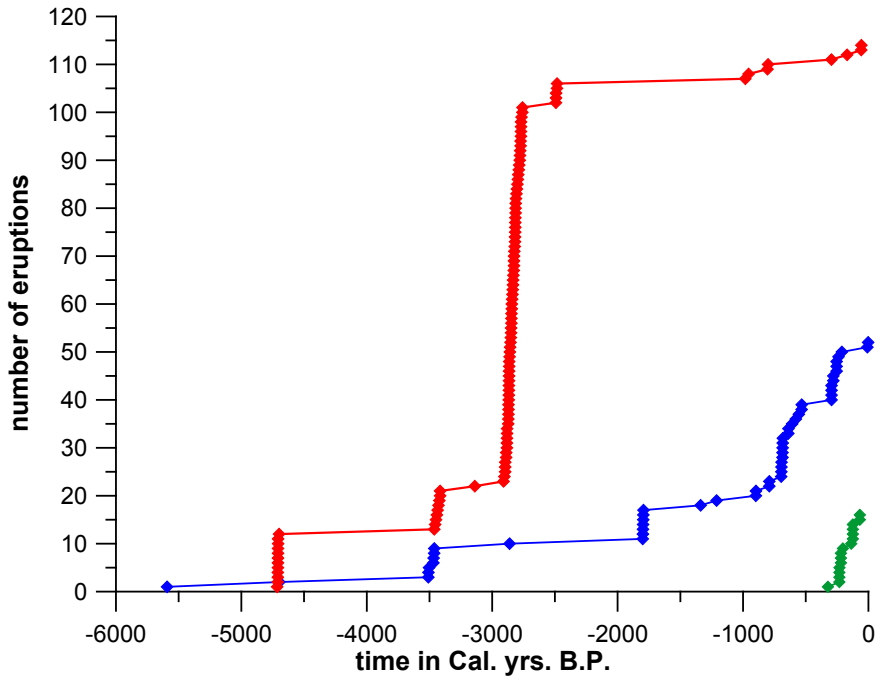

Figure 8.1.7: Cumulative explosive eruption frequency from Ruapehu (blue), Ngauruhoe (red) and Red Crater (green) over the last ~6000 cal. yrs. B.P.

For the older part of the record, where mainly VE≥ 4 tephras are reliably mapped, the cumulative curve of all three sources combined generally shows a steady rate of activity over 22 000 cal. yrs. B.P. (between 26 000 and ~ 4000 cal. yrs. B.P.) mainly with tephras sourced from Ruapehu (Bullot and Papakai Formation). There are slight increases in activity rate, the main one being between 12 000 and 11 000 cal. yrs. B.P. when the tephras of the Tongariro-sourced Mangamate Formation were erupted (Figure 8.1.8).

Over the last 4000 cal. yrs. B.P. the eruptions analysed of TgVC appear to have all been < VEI 4 and show a higher frequency than previously thought. In addition to a probable better preservation over this period, the increased rate of explosive activity is mainly associated with the development of a new edifice, Mt. Ngauruhoe. This volcano had its greatest influence on the TgVC explosive eruption frequency between 3400 and ~ 2700 cal. yrs. B.P.

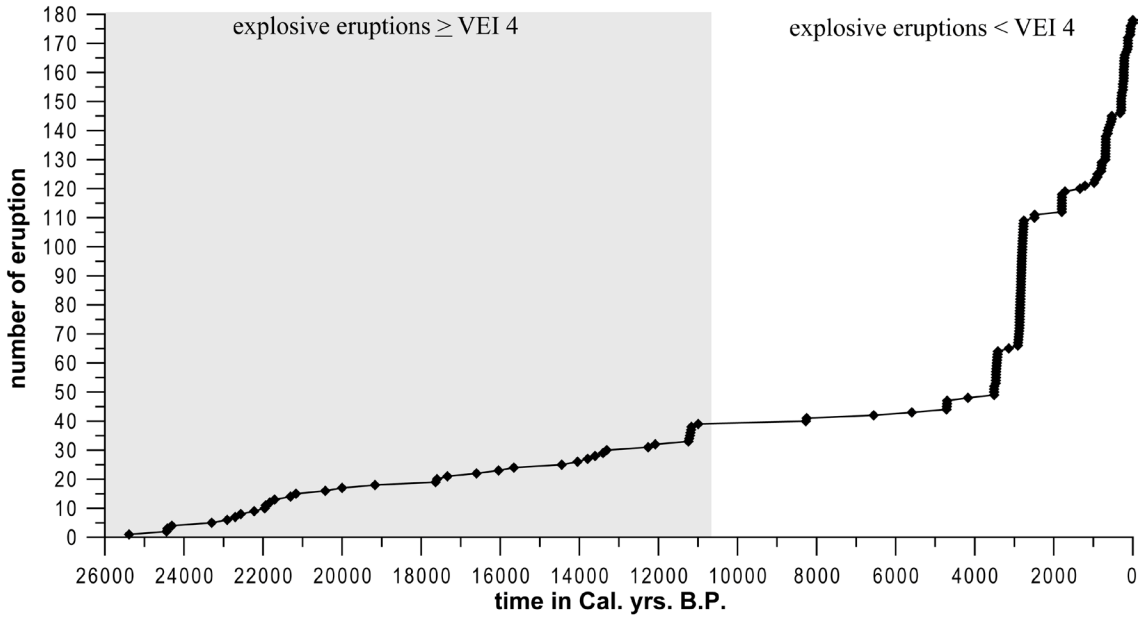

Figure 8.1.8: Cumulative explosive eruption frequency from all known explosive eruptions of the TgVC over the last 26 000 cal. yrs B.P. The shaded grey area illustrates that tephras in this area are of a VEI ≥ 4 (New studies in this area (person comm. Pardo) reveal also eruptions < VEI 4 occurred between 26 000 and 12 0000 cal. yrs. B.P.).

After the Taupo ignimbrite eruption, Ngauruhoe and Red Crater tephras are missing from the record between 1700 and 1000 cal. yrs. B.P. This absence may be due to not finding a suitable exposure for this period, recognising that the landscape was completely devastated by the ignimbrite and was very unstable thereafter (Purves, 1990). Since 1000 cal. yrs. B.P., the activity of Ngauruhoe has been steady at low levels with 1-2 larger VEI 2-3 eruptions per century. Discrete tephra eruptions from Red Crater since ~350 cal yrs B.P. appear to have peaked between 300-200 cal., yrs. B.P, and declined thereafter. By contrast, Ruapehu has been more frequently active over this time with up to twelve larger eruptions per century.

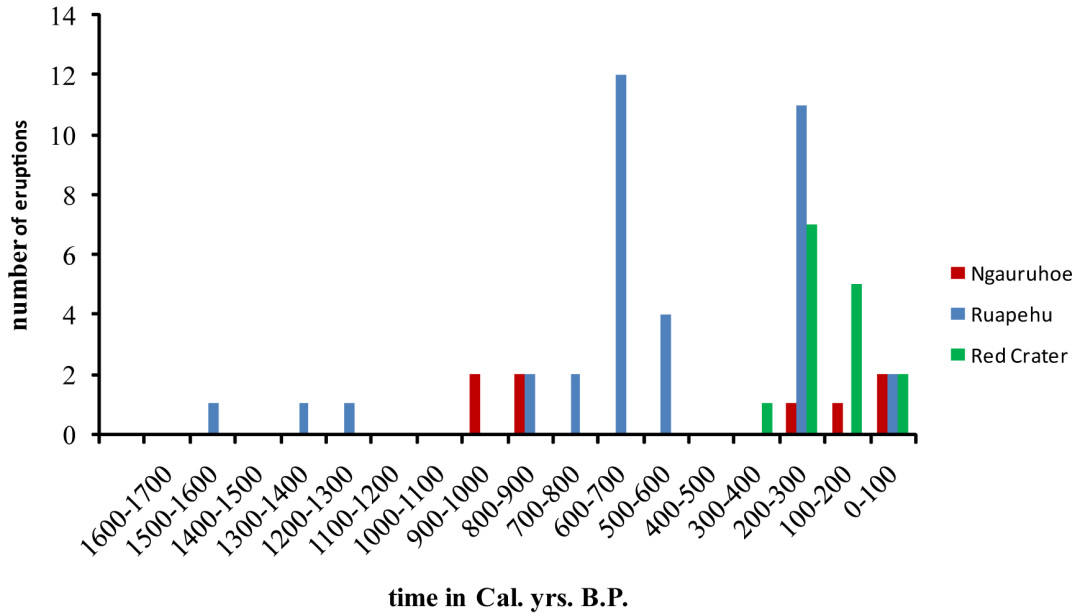

Figure 8.1.9: Eruption frequency from Ngauruhoe, Red Crater and Ruapehu over the last 1700 cal. yrs. B.P. in 100 yr. intervals.

8.1.4.2. Historic eruptions

The historic record of Ruapehu, Ngauruhoe and Red Crater show many explosive events from all three volcanoes over the last ~150 years (Figure 8.1.10). As described in Chapter 5, Ngauruhoe has produced 58 eruptions since 1839, and is thus still cited as one of the most active volcanoes of the last century. Ruapehu has produced 53 eruptions since 1861, although many of these have been very minor. It is difficult to compare this eruption record with that of the geological record, because most of the historical TgVC eruptions have left little or no trace of tephras in soil sequences.

Age calculations of discrete tephras from Loc 63 show that the two youngest Ngauruhoe tephras may be sourced from two large eruptions during the late 1890s. The two youngest Red Crater tephras in this record are also likely to have been generated by eruptions in the early 1890s. For Ruapehu, the two Tufa Trig members Tf18 and Tf19 are correlated to the 1945 and 1995-96 eruptions respectively. The historic record shows that over short periods of time, sometimes months or weeks, activity occurred from both Ngauruhoe and Ruapehu. This observation may be an analogue for the older part of the

geological record that has glass and pyroclasts combined from more than one volcanic source.

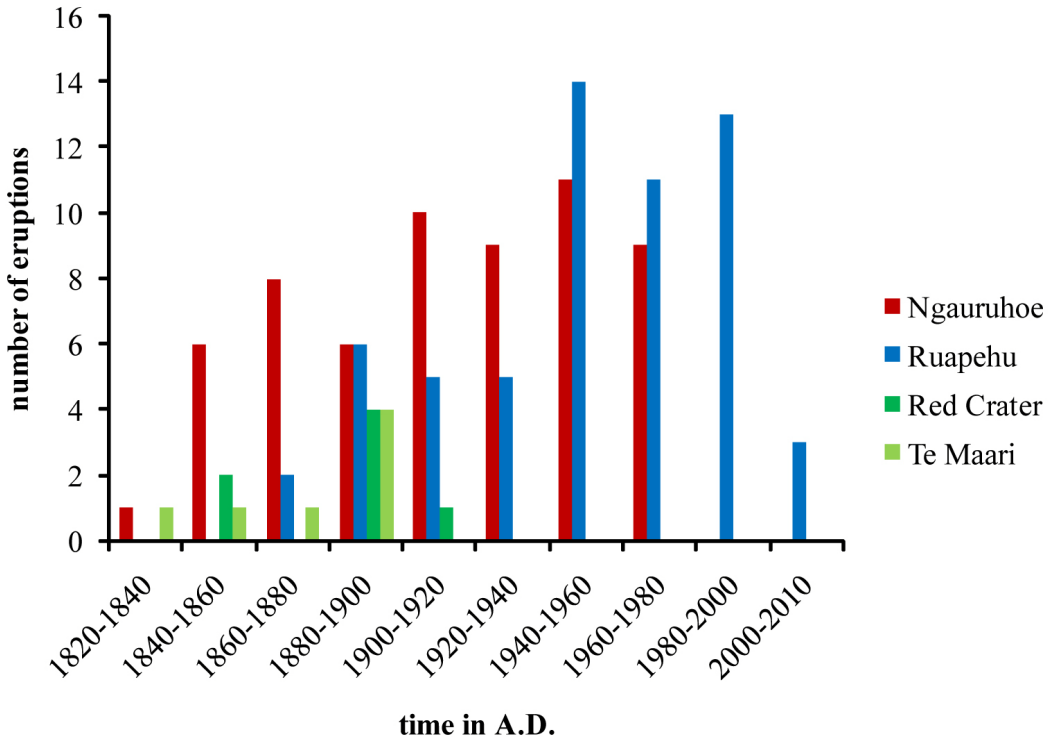

Figure 8.1.10: Historic eruption record of Ngauruhoe, Ruapehu and Red Crater (Gregg, 1960b; Hobden 2002 and Global Volcanism Program, Smithsonian Institution).

8.2. Volume calculations

From a hazard perspective, the distribution and thickness of tephras produced by explosive eruptions is an important parameter. Tephras are most commonly mapped in terms of lines of equal thickness termed "isopachs". Interpreting isopachs for tephra fall out fans is important for calculating tephra volumes because these provide a means to rank the relative magnitude of eruptions. Several approaches have been tried over the last 40 years to calculate tephra volumes. These methods have mainly focussed on > VEI 3 eruptions, whereas the ranking of smaller eruptions, especially those observed in historical times, has been made by a range of other parameters such as eruption column height and ash-distribution (Newhall and Self, 1982).

8.2.1. Previous work

As pointed out in Chapter 7, Walker, 1973) attempted to classify eruption types and magnitudes by using the ratio between the area of dispersal (D) and degree of fragmentation (F). The dispersal area is calculated by using the $0.01T_{max}$ isopach, where T_{max} is the maximum thickness of the deposit. Fragmentation, on the other hand, is an empirical measurement of the ratio of material <1 mm and is approximated by finding the point at which the $0.1T_{max}$ isopach crosses the dispersal axis.

Walker (1980; 1981) also calculated the volume of the ultra-plinian Taupo Pumice eruption based on an alternative method using crystal concentrations. For this eruption 80% of the fall deposits were estimated to have been deposited at sea, east of New Zealand, hence only part of the deposit was available for isopach and grain size analyses. Three assumptions were made to calculate the volume: a) that crystals fall closer to the vent than similar sized pumices (due to their higher density), hence crystals do not occur in the finest and most widely distributed deposit; b) that large pieces of pumice represent the original magma and can be used to obtain the original ratio of vitric components to crystals; and c) that parts of the magma are fragmented to a particle size equal or finer to the largest phenocryst erupted (~2 mm) (Walker, 1981). To calculate the volume, Walker used the on-land mass of free crystals of <2 mm, and plotted the mass per unit area to obtain an estimate of the theoretical offshore "missing" vitric component.

Rose *et al.* (1973) outlined another method to calculate tephra volume using a plot of log(area) vs. log(thickness). This relationship is able to be approximated by two straight line segments. However, this method simplifies the fact that there is an exponential dependence of thickness on area. Hence, such plots normally describe a curve, rather than two straight lines and Fierstein and Nathenson (1992) showed that this line-approach is very sensitive to the extrapolation to infinity of the thickness and area of the outer isopach.

Fierstein and Nathenson (1992) analysed several methods proposed to calculate tephra volumes. The trapezoid rule, used by e.g. Froggatt (1982), is a simple numerical integration approximation to calculate the area under a curve and is expressed by:

$$\Delta V_{n+1} = T_{n+1}\left(A_{n+1} - A_n\right) + \frac{1}{2}\left(T_n - T_{n+1}\right)\left(A_{n+1} - A_n\right)$$

$$= \frac{1}{2}\left(T_{n+1} + T_n\right)\left(A_{n+1} - A_n\right), \qquad (1)$$

where T is the thickness and A the area under the curve represented as a rectangle and capping triangle (trapezoid). The problem in this calculation is being able to interpolate the thickness toward the vent (T_{max}) and also to account for material outside the outer known isopach. Log-log scale plots approximated by straight lines proposed by Rose *et al.* (1973) were extended by applying the relationship of LogT vs. $A^{1/2}$ (Pyle, 1989). This latter relationship assumes that isopachs are elliptical, because eruption clouds are usually strongly influenced by one dominant wind direction. Fierstein and Nathenson (1992) used Pyle's method but integrated the area of an isopach as an independent variable, leading to the relationship:

$$V = \frac{2T_0}{k^2}, \qquad (2)$$

where T is the thickness and is extrapolated to A=0, and k is the single slope of the line on a Log$T$ versus $A^{1/2}$ plot. For a plot with two straight-line segments, Fierstein and Nathenson (1992) derived the following equation:

$$T = T_0 \exp\left(-kA^{1/2}\right), \qquad (3)$$

to calculate the fit for the proximal segment where T_0 is the thickness at A=0 and k is the slope of the regression line. The distal segment is calculated by:

$$T = T_1 \exp\left(-k_1 A^{1/2}\right) \qquad (4)$$

The integration over both segments yields the volume of tephra and is calculated by the equation:

$$V = \int_0^{A_{ip}^{1/2}} 2T_0 \exp\left(-kA^{1/2}\right)A^{1/2}dA^{1/2} + \int_{A_{ip}^{1/2}}^{\infty} 2T_1 \exp(-k_1 A^{1/2})A^{1/2}dA^{1/2}$$
$$= \frac{2T_0}{k^2} - \frac{2T_0}{k^2}\left[\left(kA_{ip}^{1/2}+1\right)\exp\left(-kA_{ip}^{1/2}\right)\right] + \frac{2T_1}{k_1^2}\left[\left(k_1 A_{ip}^{1/2}+1\right)\exp\left(-k_1 A_{ip}^{1/2}\right)\right] \quad (5)$$

where A_{ip} is the value of $A^{1/2}$ at the interception of the two straight segments, T_0 and k are the intercept and slope of the line in the near-vent region, and T_1 and k_1 are the intercept and slope of the distal segment. T_1 is also extrapolated towards A=0.

In general Fierstein and Nathenson (1992) suggest the use of the LogT vs. $A^{1/2}$ relationship, because it allows extrapolation of the thickness towards infinity. Naturally with more detailed isopachs, all of these methods work better.

Legros (2000) proposed a simple method to calculate the minimum volume where only one isopach is available, based on the assumption that the thickness of a tephra decays exponentially away from the vent:

$$V_{\min} = \frac{\exp(2)}{2}TA = 3.69TA\,, \quad (6)$$

with T being the thickness of the isopach and A the area it encloses.

Sulpizio (2005), on the other hand, believed that volume calculations with one isopach must be treated with care, because the volume calculations can change drastically by just changing the one variable T by as little as 1 mm. Sulpizio (2005) described three methods to extrapolate the thickness to infinity on a LogT versus $A^{1/2}$ plot and compares them to one other. These methods include (1) the ellipse method, which is applicable to eruptions producing scattered thicknesses with at least two segments in a logT vs. $A^{1/2}$ plot. According to Sulpizio (2005), this method delivers good results where isopachs are greater than 1 cm. (2) The method of $A_{ip}^{1/2}$ with one distal isopach shows a good result

if "the thickness of the distal isopach is less than the half thickness at break-in-slope distance" (Sulpizio, 2005). When only proximal data are available, the third method (3) can be used when at least two isopachs are known; using the k_1 vs. $A_{ip}^{1/2}$ relationship, distal data are obtained by empirical correlations.

Bonadonna and Houghton (2005) used the well documented and sampled eruption from Ruapehu on the 17 June 1996 to calculate total grain size distributions and the eruption volume. The authors used the LogT vs. area$^{1/2}$ method to calculate the volume which shows a three segment plot and also calculate the volume using a power-law fit on a semi-log plot vs. area$^{1/2}$. Both calculations give a similar volume of 4 x 10^6 m^3.

The power law fit is:

$$T = T_{pl} A^{1/2(-m)}, \tag{7}$$

and the integration over equation 7 yields the volume of tephra

$$V = \int_0^{\infty} 2T_{pl} \frac{A^{1/2(2-m)}}{2-m}$$
$$= \frac{2T_{pl}}{2-m}\left(C^{2-m} - B^{2-m} \right), \tag{8}$$

where T_{pl} is the constant, m the power law coefficient, and B and C are two arbitrary integration limits.

Problems and difficulties in calculating tephra volumes

Difficulties in calculating a total tephra volume are mainly due to imperfect preservation of thin tephras at distal locations where they are vulnerable to bioturbation and erosion. Often the proximal deposits are not complete because of erosion on the higher non vegetated flanks of volcanoes or due to vent collapses. According to Fierstein and Nathenson (1992), the isopach of zero thickness should be also included into all

mathematical calculations, however defining it is extremely difficult and depends on the method of extrapolation of the field data to infinity.

One of the most important hindrances for volume calculations is the lack of field exposures, especially for prehistoric eruptions. The additional problem in this study was uniquely correlating individual tephras from site to site, due to variations in thickness, erosion, depositional conditions and similarity in field appearance and chemistry. This lack of data can also be exacerbated if inaccessible areas such as water or mountains occur in the dispersal area and if only few proximal data points are available. This causes non-linearity of the function linking T and A (Bonadonna and Houghton, 2005).

8.2.2. Volume calculations for tephras sourced from Ngauruhoe

The collection of field data on tephras exclusively derived from Mt. Ngauruhoe has been challenging because of the small size of eruptions that produced very fine-grained and thin ash deposits (ranging between 1-30 mm). The presence of forest and shrub vegetation at the time of deposition has also led to major variations thicknesses at any one location. Tephras deposited after the Taupo Pumice Ignimbrite emplacement are even more poorly preserved.

To quantify most accurately the volume of eruptions from Mt. Ngauruhoe over the last ~4500 years, the two most distinctive tephra units were analysed in more detail. This included the dark purple layer (DP) as the largest apparent single eruption from Mt Ngauruhoe, and the pale purple layer (PP), a package containing at least 14 individual eruptions, too thin (1-3 mm each at Loc 12) to sample individually or to correlate as single eruptions. These two units were mapped and analysed in detail, with careful measurement of thicknesses which avoided obvious areas of secondary accumulation, or erosion.

8.2.2.1. Single tephra volume calculations

The dark purple (DP) tephra is recognised at a maximum distance of ~30 km south of the vent within Karioi Forest and ~23 km south-east of the vent at Paradise Road (NZ-Army training area). Isopachs show an elliptical distribution with the main dispersal axis towards the south to south-east (Figure 8.2.1). Thicknesses measurements were used to draw six isopachs (Table 8.1), where the thickest isopach is represented by a 0.44 m-thick coarse scoria lapilli at Loc. 67 on the northern slope of Ngauruhoe.

Table 8.2.1: Isopach data for the dark purple (DP) tephra

T (mm)	A (km^2) dispersal	$A^{1/2}$ (km)
440	5.00	2.24
30	92.06	9.59
20	263.69	16.24
10	493.06	22.20
7	718.13	26.80
5	1055.55	32.49

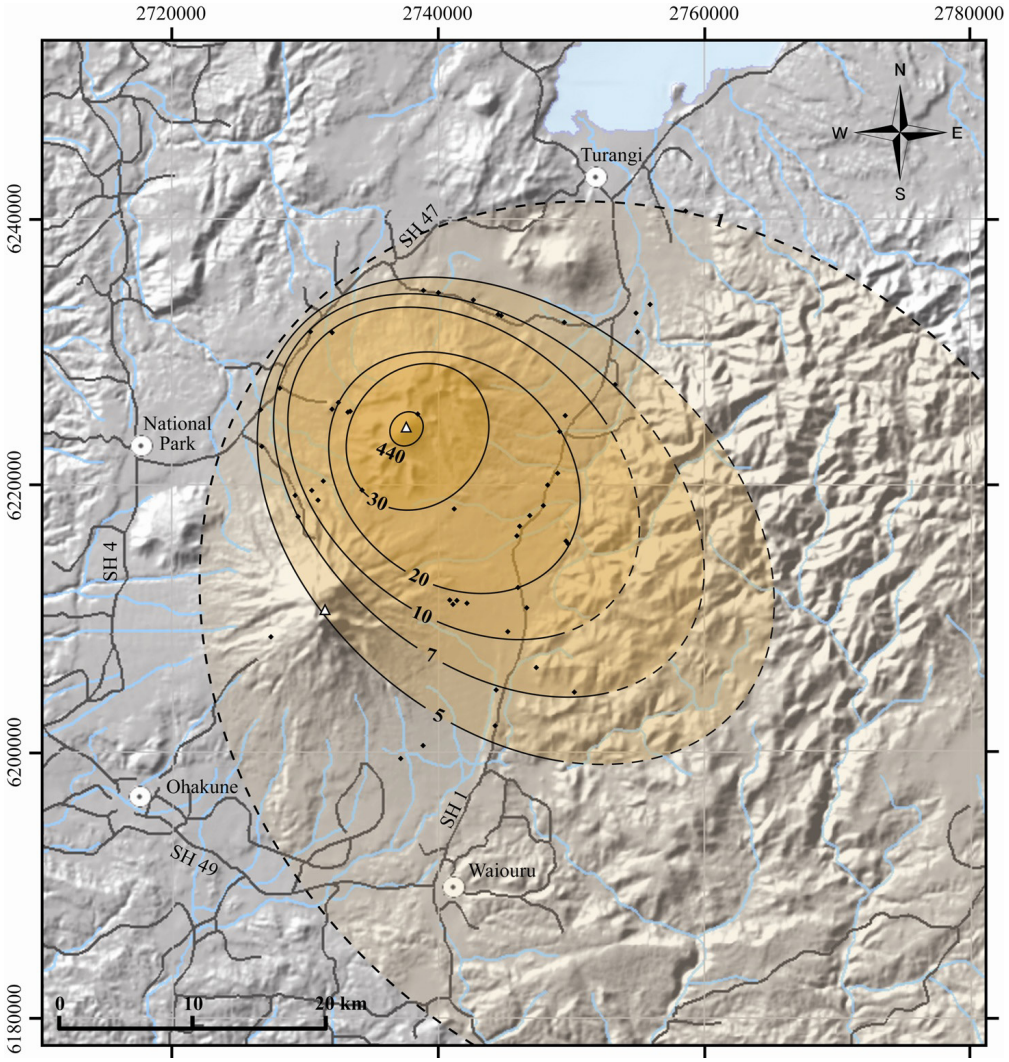

Figure 8.2.1: Isopach map extrapolated for the distinctive Ngauruhoe-sourced dark purple (DP) tephra, dots indicate locations of measured thicknesses. Thickness in mm.

To calculate the minimum volume of the eruption producing the DP-tephra, the LogT vs. $A^{1/2}$ (Fierstein and Nathenson, 1992) and the power-law fit on a semi-log plot vs. $A^{1/2}$ applied by Bonadonna and Houghton (2005) were used.

The first method (Figure 8.2.2) has a proximal line segment that is only represented by two proximal isopachs. The inner isopach may represent the direct fall from only the thrust region of the eruption column (e.g., Self, 1975); the second isopach, however, was probably deposited from the outer umbrella region of the plume. The distal segment includes five isopachs that plot linearly.

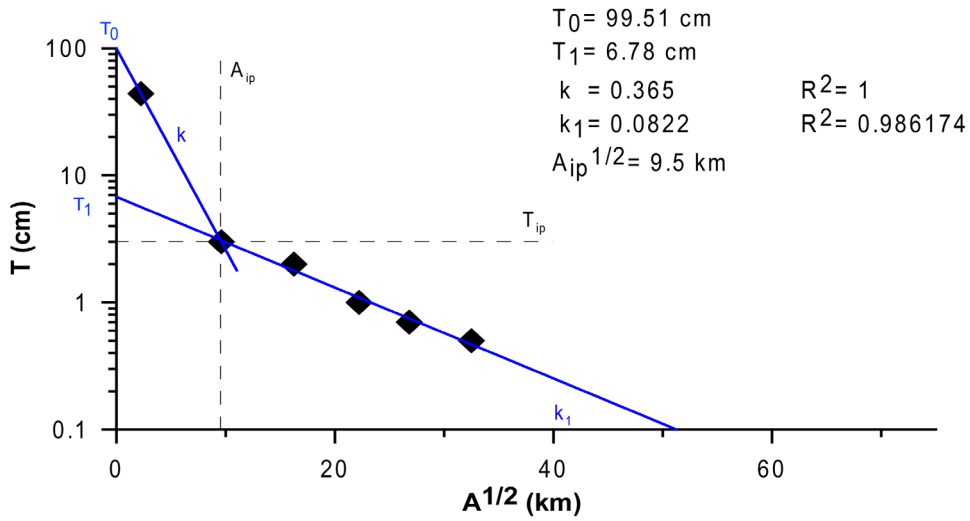

Figure 8.2.2.: LogT vs. $A^{1/2}$ for isopachs mapped of the dark purple (DP) layer.

Using the Bonadonna and Houghton (2005) semi- logT plot vs. $A^{1/2}$ Power-law method, the volume integration limit B (eq. 7) was calculated by:

$$B = \left(\frac{T_0}{T_{pl}}\right)^{\left(-\frac{1}{m}\right)} = 1.4km \qquad (9)$$

while C (eq. 7) was defined as the value of $A^{1/2}$ at a thickness T = 1 mm, which yields C = 73 km, resulting in the plot of Figure 8.2.3.

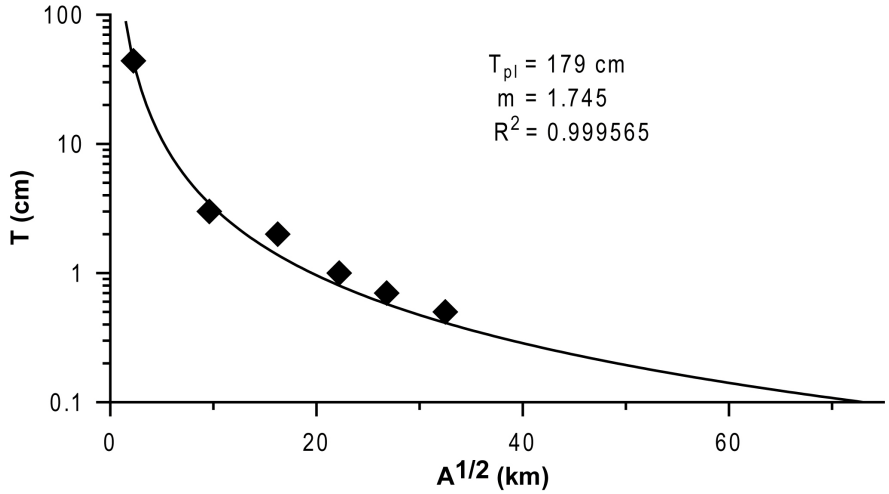

Figure 8.2.3: The power law fit method of Bonadonna and Houghton (2005) applied to the mapped isopachs of the dark purple (DP) tephra.

Both methods show good approximations to the data, but the Power-law method represents the proximal data better, whereas the exponential method appears to fit the medial-distal data better. The largest differences are at the extrapolated thickness of <3 mm, where no reliable isopach data exist to verify either fit. The resulting volume calculated for the dark purple tephra is similar for both methods; using Equation 5 (Fierstein and Nathenson, 1992) it is V = 27.6 x 10^6 m^3; with Equation 7 (Bonadonna and Houghton, 2005) V= 26.7 x 10^6 m^3 results. This is the largest single explosive eruptive unit known from Ngauruhoe.

8.2.2.2. Tephra package volume calculations

By contrast to the DP unit, the pale purple layer (PP) has broadly concentric isopachs, which are consistent with its internal stratigraphy. It is composed of the deposits of at least 10 closely timed eruptions, under a range of varying wind directions (Figure 8.2.4). At the most proximal Loc. 67, the unit occurs as a set of continuously stacked 10-40 mm-thick, bedded fine-coarse ash units.

Table 8.2.2: Isopach data for the pale purple tephra unit

T (mm)	A (km^2)	$A^{1/2}$ (km)
100	11.73131	3.4251
40	93.23122	9.655631
30	330.8087	18.18815
20	591.5919	24.32266
15	794.0196	28.17835
10	981.5082	31.32903

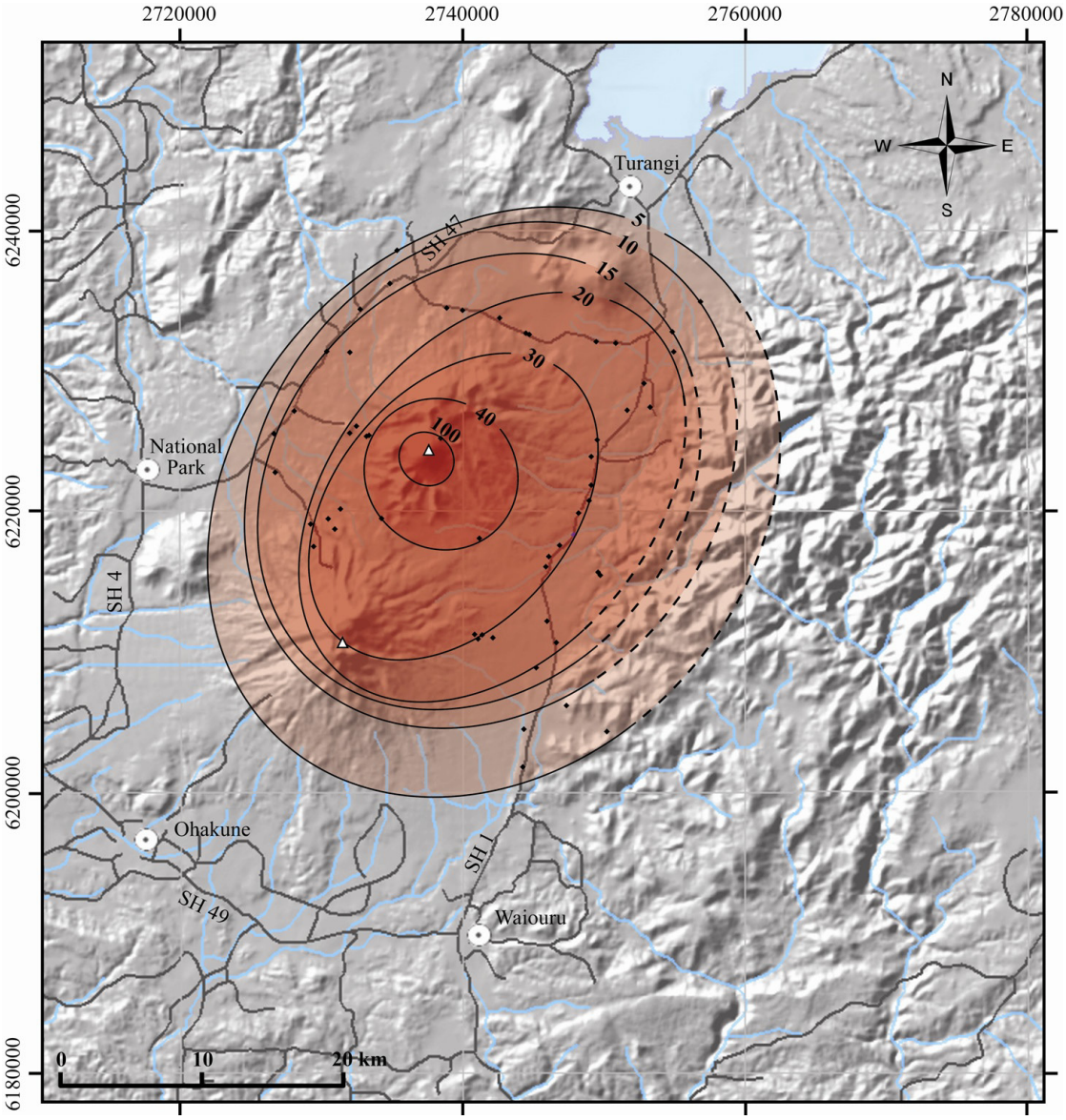

Figure 8.2.4: Isopach map of the Ngauruhoe-sourced pale purple (PP) tephra unit.

Six isopachs could be drawn for the pale purple tephra (Table 8.2). The LogT vs. $A^{1/2}$ relationship is unusual in not following a normal thinning behaviour (Figure 8.2.5). This is very consistent with the package being a composite unit of several eruptions. The thickness of the PP unit may therefore depend more closely on the number of individual tephras accumulated at given measured location, and this correlation between the two parameters is shown in Figure 8.2.5.

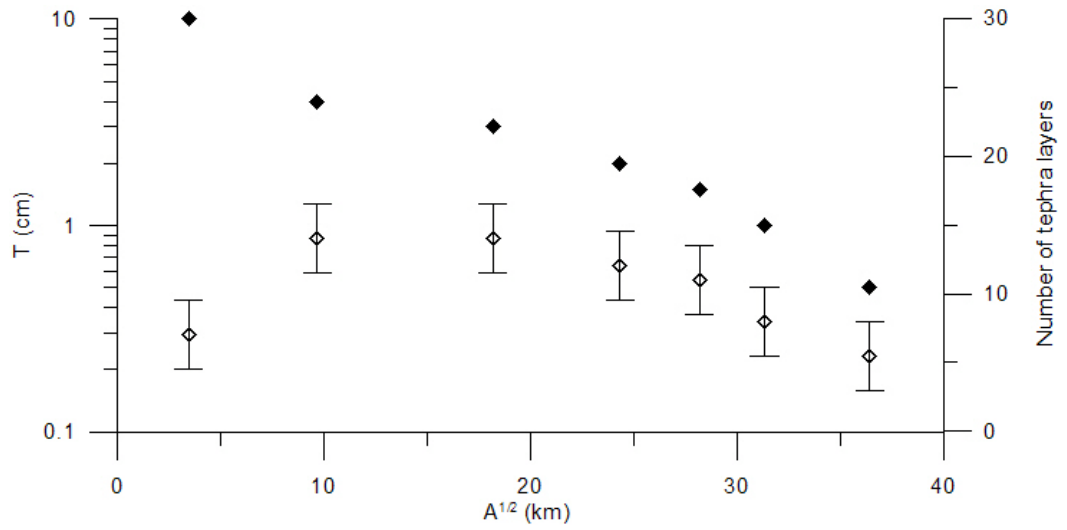

Figure 8.2.5: LogT vs. $A^{1/2}$ plot for isopach data of pale purple layer (filled diamonds). Open diamonds show average number of tephra layers that make up the pale purple (PP) layer in each isopach vs. $A^{1/2}$.

Interestingly, if T vs. $A^{1/2}$ is plotted on a linear scale, the data align onto two prominent linear segments (Figure 8.2.6).

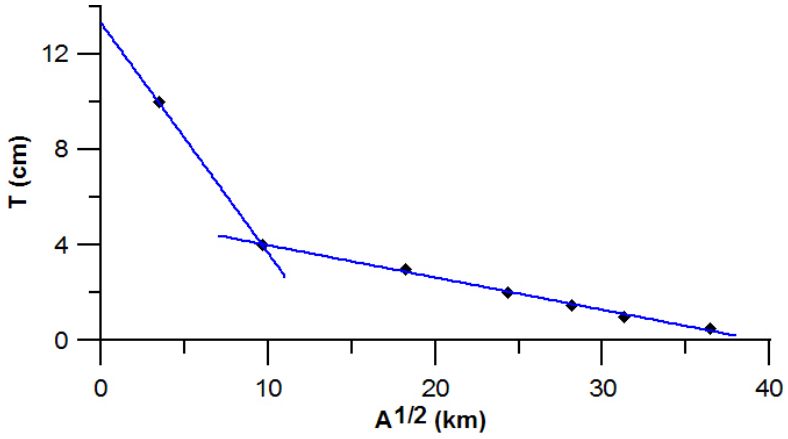

Figure 8.2.6: Thickness versus $A^{1/2}$ of mapped isopachs of the pale purple (PP) layer.

The integration of these two segments is straightforward and yields the total composite volume of 30.9 $x10^6$ m^3 for the PP-layer. The volume of individual layers within the PP unit can be calculated as a ratio of isopach thickness T over the average number of tephra layers within it. The single-tephra data are similarly well represented by a single power law and two straight-line segments on a semi-log graph (Figure 8.2.7).

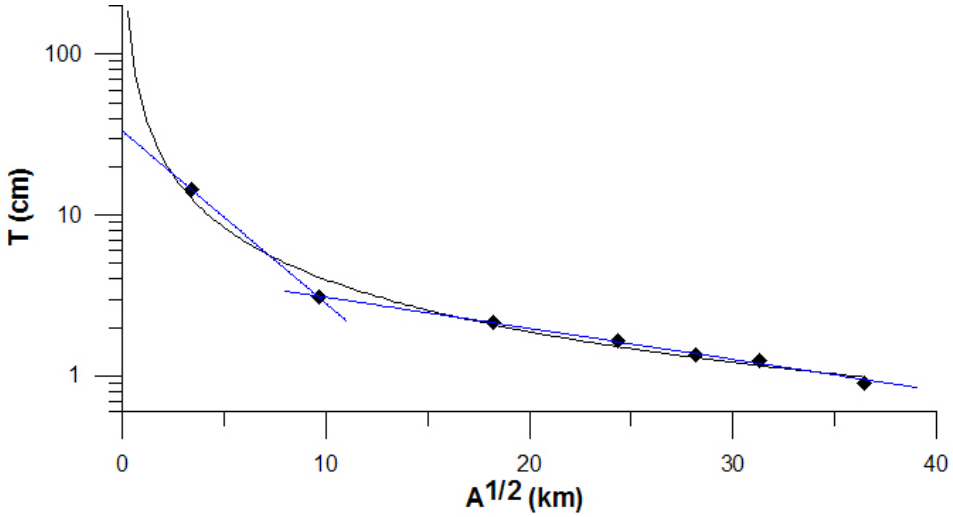

Figure 8.2.7: LogT vs. $A^{1/2}$ of one individual tephra within the pale purple (PP) unit. The black curve represents a best-fit Power-law regression to the data, while the two blue lines represent exponential fits to segments 1 and 2.

8.2.2.3. Volume calculations for all Ngauruhoe-sourced tephras

To be able to evaluate changes in eruption magnitude from Mt. Ngauruhoe over time and relate these to the eruption frequency, it is necessary to calculate the volume of individual eruptions from tephras of all four stages of its known pyroclastic activity. Reliable and relatively complete isopachs for two individual tephras (DP tephra and the 1974 tephra) and one composite unit are available. These can be used to calibrate volume calculations for other individual Ngauruhoe tephras mapped in the same dispersal area. The DP-layer represents the largest eruption known from Ngauruhoe whereas the 1974 unit is an approximation of one of the smallest in the range. The 28-29 March 1974 ash plume was carried towards the north-west as far as Taumarunui (43 km north-west). The ash deposits had a maximum fresh-fall thickness of 25 mm immediately below the rim of the active crater, quickly thinning towards the north (Figure 8.2.8). The bulk volume was calculated at 0.74 x 10^6 m^3 (with isopachs extrapolated to 0.1 mm thickness) (Self, 1975). It was also recognized at the time that this volume was a minimum, since a finer-grained portion was probably "lost" in the

wider dispersal of dust for several hundred km, beyond the thinnest isopach. In addition, blocks and bombs around the active vent were not taken into account.

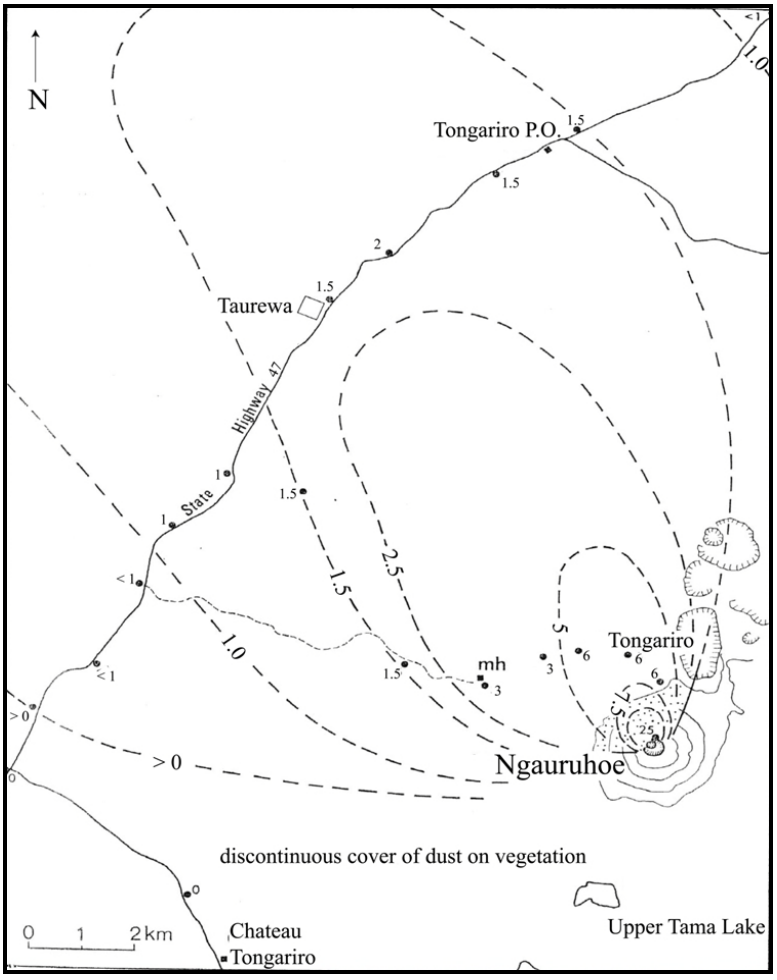

Figure 8.2.8: Isopach map of the eruption from Ngauruhoe on 28–29 March 1974. The thickness is in mm. (after Self, 1975).

Volume calculations were made for all other Ngauruhoe-sourced tephras using tephra thickness measurements at two locations representing the most complete stratigraphic record of Ngauruhoe tephras at Loc. 12 and 63. Location 12 contains tephras of Stages 1-3 and $A_{Loc\ 12}{}^{1/2}$ shows that it belongs to the start of the medial-distal linear segment known for the DP and PP layers. Location 63 contains Ngauruhoe tephras of deposited in Stage 4 (over the last ~ 1000 cal. yrs. B.P.) and is proximal to source preserving many small tephra units.

The following assumptions were made to enable the calculations:

1. all eruptions show similar distal thinning rate (i.e., slope k_1 is constant for all eruptions). While this may not hold true, there is little control on its potential variability.
2. V_p/V_t is constant (Vp is the volume under the proximal segment and Vt is the volume under the distal segment (Sulpizio, 2005)).

This gives rise to the following:

$$-k_1 = \frac{\ln T_1 - \ln T_{Loc12}}{A_{Loc12}^{1/2}} \tag{10}$$

$$\ln T_1 = -kA_{Loc12}^{1/2} + \ln T_{Loc12} \tag{11}$$

$$T_1 = \exp\left(-k_1 A_{Loc12}^{1/2} + \ln T_{Loc12}\right), \tag{12}$$

where T_{Loc12} is the thickness of individual tephras at Location 12 and $A_{Loc\ 12}{}^{1/2}$ is the distribution of the individual tephras at Location 12. The combined volume (V_{tot}) of an individual tephra is that calculated from a single line segment of the distal component (Equation 2) added together with an estimate of the proximal component V_p. V_p is estimated by applying the V_p/V_t ratio known from the DP tephra as a constant multiplier, hence

$$V_{tot} = V_p + V_t, \tag{13}$$

where, $V_p = 0.15(V_t)$.

The collective volume for all of the Ngauruhoe tephras is 952 x 10^6 m^3, which equals ~43% of the cone volume (c.f., Hobden *et al.,* 2002). The total eruptive volume from Ngauruhoe therefore amounts to 3-3.2 km^3 (calculated volumes presented in Appendix 5).

The greatest volumetric eruptive rate from Ngauruhoe occurred between c. 2900 to 2700 cal. yrs. B.P. when 57% of the total pyroclastic fall volume was produced (Figures 8.2.9). This relates closely to the eruptive frequency and magnitude from the volcano.

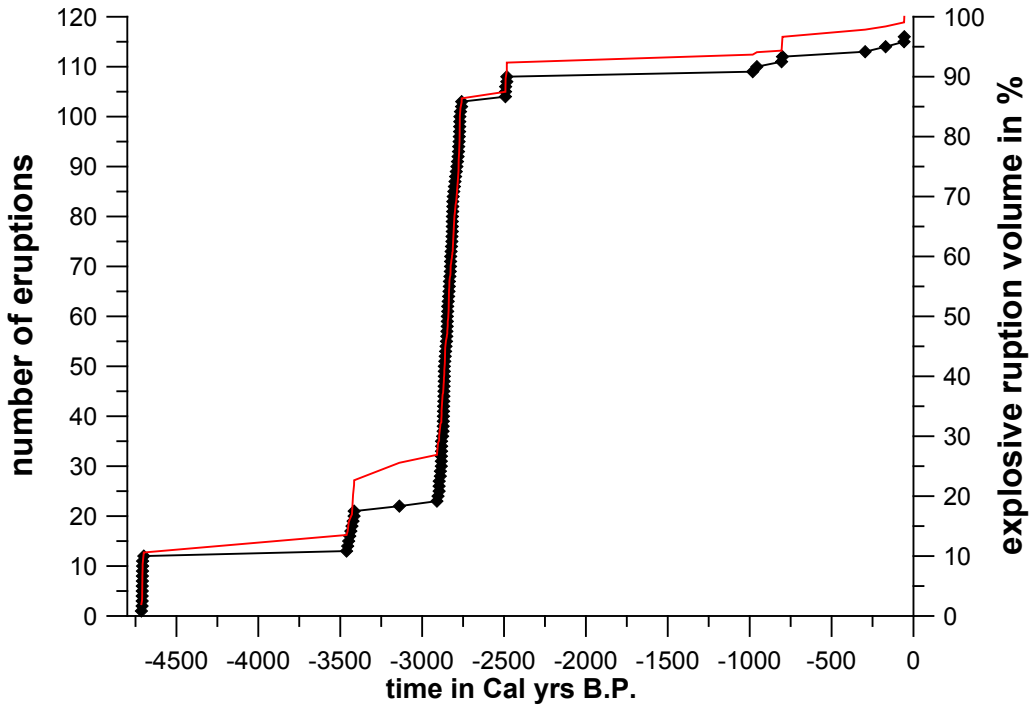

Figure 8.2.9: Cumulative curve of volume proportion (red) of pyroclastic tephra deposits from Ngauruhoe in comparison to the explosive eruption frequency (black).

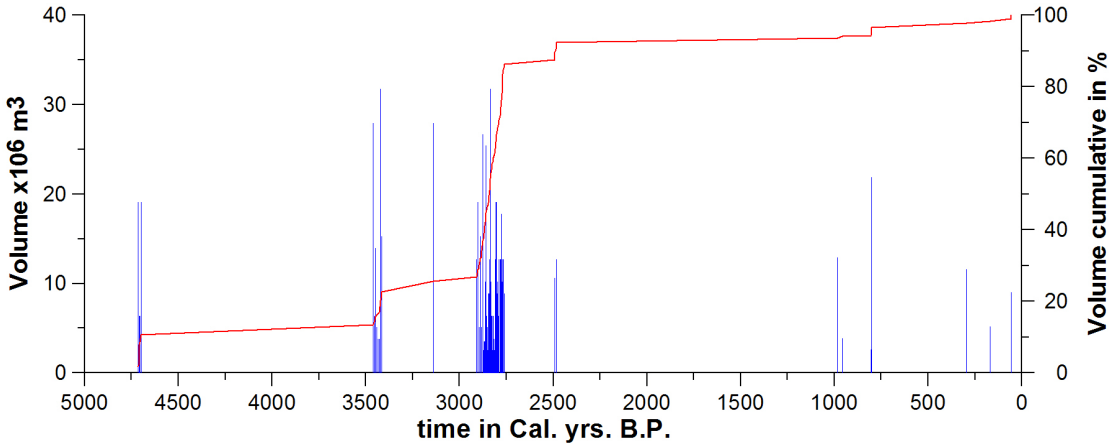

Figure 8.2.10: Volume of individual tephras over time (blue bars) in comparison to the cumulative volume in % (red line) for Ngauruhoe volcano.

8.3. Calculations of eruption column heights

The behaviour, shape, height, duration and collapse of eruption columns have been studied over several decades and are described with numerous equations and illustrations. The initial shape and height of an eruption column is driven primarily by the energy and mass-eruption rate (Sparks and Wilson, 1976; Schmincke, 2000). Later, the primary influence is the atmospheric wind pattern.

An eruption column is composed of two parts, the gas thrust and the convective region (Sparks and Wilson, 1976). Settle (1978) described the eruption column height as a function of the convective buoyancy of a mixture of volcanic gas, entrained air and fine pyroclasts. It is also dependent on the thermal energy generated by cooling of the gases and the pyroclastic material. Settle (1978) suggested that the maximum column height is correlated with the mass ejection rate of tephra.

Wilson *et al.* (1978) defined the column height as a function "of vent radius, gas content of eruption products, and the efficiency of conversion of thermal energy contained in juvenile material to potential and kinetic energy during the entrainment of atmospheric air" where:

$$H_T = 8.2\dot{Q}^{1/4}, \tag{14}$$

when H_T is the column height and $\dot{Q}$ is the released energy at the vent region. $\dot{Q}$ is dependent on bulk density (density of pyroclasts and magmatic gas), velocity, specific heat, temperature of the erupted fluid, and temperature to which the erupted products cool. The equation only applies for eruption columns that are not disturbed by wind.

Sparks (1986) calculated column heights by including the variable of the proportion of entrained solids into the expanding cloud. The expansion of the cloud (H_B) increases with mass eruption rate and the initial temperature. H_T is related to H_B by the equation:

$$H_T = 1.32(h_0 + H_B), \quad (15)$$

where h_0 is the focal depth (a function of discharge rate of the magma).

Sparks *et al.* (1992) showed that the eruption column height is related to the tephra thickness "half-distance" by using Walker's (1973) dispersal index (D) as a function of the eruption column height. Additionally Sparks *et al*. (1992) showed that the tephra grain size distribution with distance is a function of the column height and dispersion (Figure 8.3.1). Thus one can deduce the latter parameters by interpolating from the resultant tephra deposits.

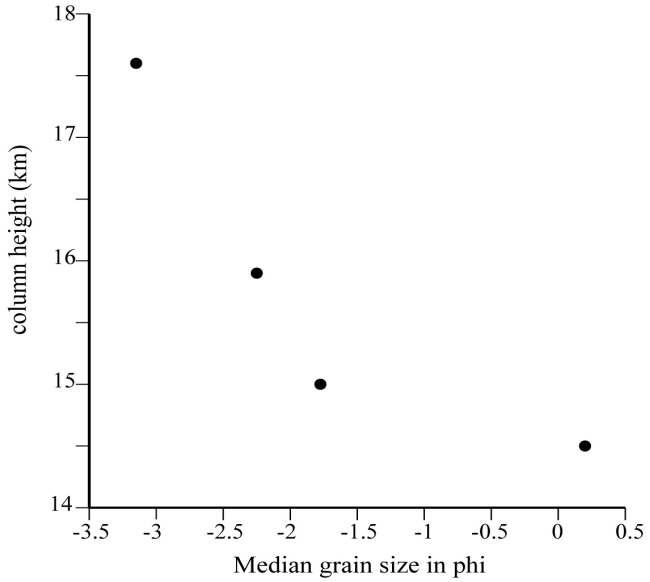

Figure 8.3.1: Column height vs. median grain size for dispersal index (D) of 500 km^2 plinian/subplinian boundary from Walker's (1973) classification (from Sparks *et al.* (1992)).

Bonadonna *et al.* (1998) suggested that the column height can be related to the position of the break-in-slope found in tephra isopach thicknesses. This correlation between H_T and the distance of the break-in-slope is also shown in Figure 8.3.2. Better results are obtained when the most proximal and distal points of the distal break-in-slope are extrapolated and are described by the equation:

$$H_t \approx 12 + 0.3A_{BS}^{1/2}, \quad (16)$$

(For 12 km < H_t < 45 km).

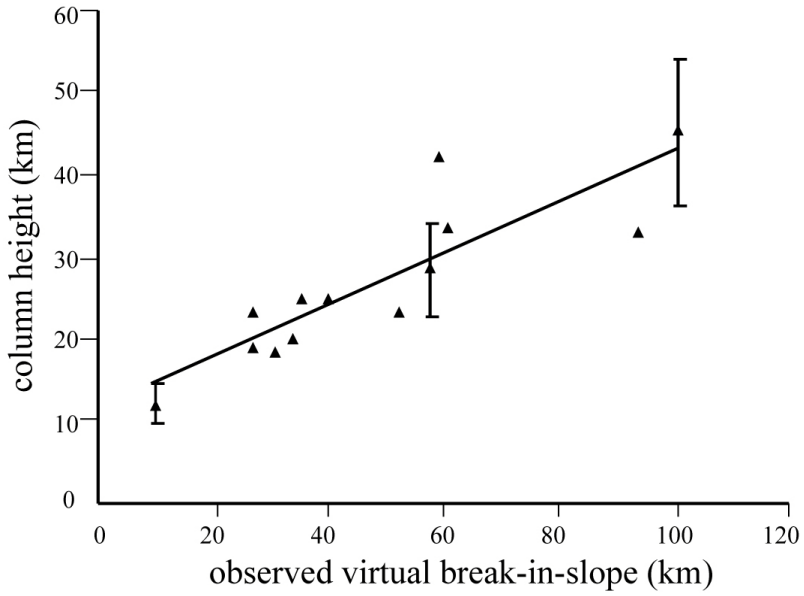

Figure 8.3.2: The eruption-column height (observed or estimated) vs. position of the break in slope with distance from source (A_{ip}). Column height is estimated within 20% error bars, after Bonadonna *et al.* (1998).

Sulpizio (2005) defined a relationship between column height and the break in slope obtained from the LogT vs. $A^{1/2}$ (after Bonadonna *et al.*, 1998) when at least two isopachs are available, and this allows an easy calculation of the column height. These calculations have, according to Sulpizio, an accuracy of ± 20% in 94% of the cases analysed. The calculation is based on the empirical relationship between proximal tephra deposit thinning rate and column height with the best fit at:

$$H_t = 7.6k^{-0.47} \qquad R = 0.90 \tag{17}$$

The eruption column height was also classified, depending on the eruption style, in a similar fashion to the Walker's 1973 classification of dispersal and fragmentation (Cas and Wright, 1988; Figure 8.3.3) to ascertain eruption style.

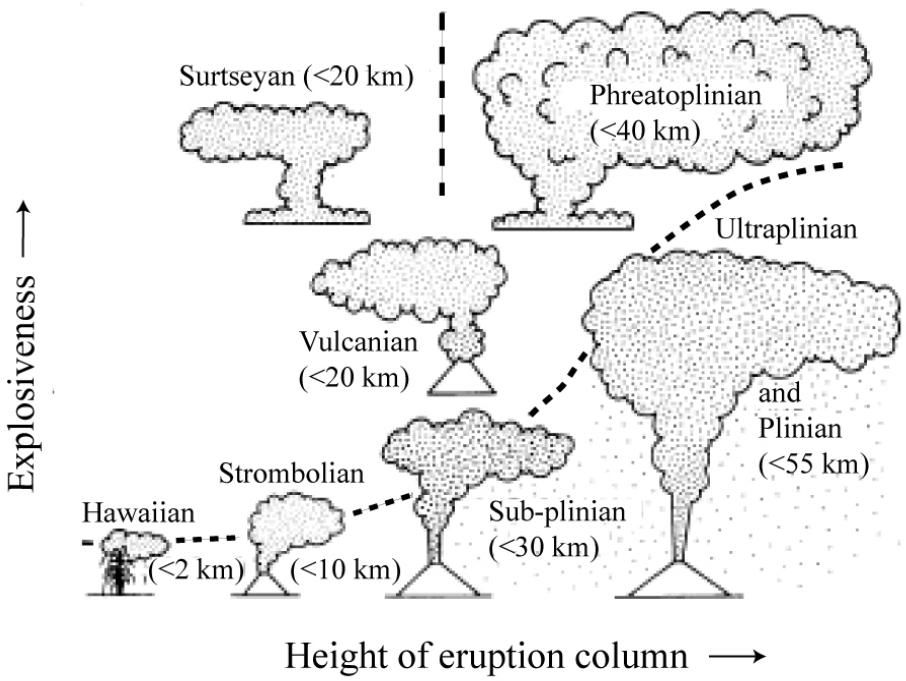

Figure 8.3.3: Eruption column height in contrast to eruption styles (after Cas and Wright (1988)).

8.3.1. The eruption column height of Ngauruhoe eruptions

To calculate the eruption column height for individual eruptions from Ngauruhoe, the two most reliable methods were applied: Bonadonna *et al.* (1998) and Sulpizio (2005). The method of Sparks *et al.* (1992) does not yield useful estimates of eruption column heights for the small-volume, but highly fragmented and widespread tephras produced by Ngauruhoe. For instance, the thickness half-distance for the dark purple (DP) layer is around 20 km. Following Sparks *et al.* (1992) the corresponding column height would be around 40 km, which seems an over-estimate. The distance of break-in-slope (A_{ip}) for the dark purple tephra = 9.5 km. According to equation 16 defined by Bonadonna *et al.* (1998) the corresponding column height would be 14.8 km. Equation 17 from Sulpizio (2005), gives a height of 12.2 km.

To calculate the column height of the composite pale purple (PP) layer it was necessary to identify the distance of the break-in-slope, which depends on the distribution and thickness of individual component tephras. As shown in Figure 8.2.7, the LogT vs. $A^{1/2}$

of an individual tephra within the pale purple unit is characterised by a two line-segment. Only the Bonadonna *et al.* (1998), equation 16 method could be applied, where $A_{BS}^{1/2}$ encloses the smallest isopach (at 9.4 km). This leads to a maximum column height estimate of ~13 km for an individual tephra within the pale purple unit.

Eruption column heights vs. volume

An apparent exponential relationship exists between tephra volumes and eruption column heights at Ngauruhoe (Fig 8.3.4 and 8.3.5). Eruptions with high column heights and high volumes (Group A on Fig. 8.3.4) such as the DP tephra and Mt St Helens 1980 are sub-plinian. The individual PP tephra units, Hekla and Mayon have eruption columns of ~10 km and low volumes, likely relating to violent strombolian- vulcanian type eruptions (Group B on Fig 8.3.4.); (Fig. 8.3.6B). Many of the historical events from Ngauruhoe, such as 1974, are characterised by low eruption column heights and low volumes, consistent with strombolian eruptions (Group C on Fig. 8.3.4.); (Fig. 8.3.6A).

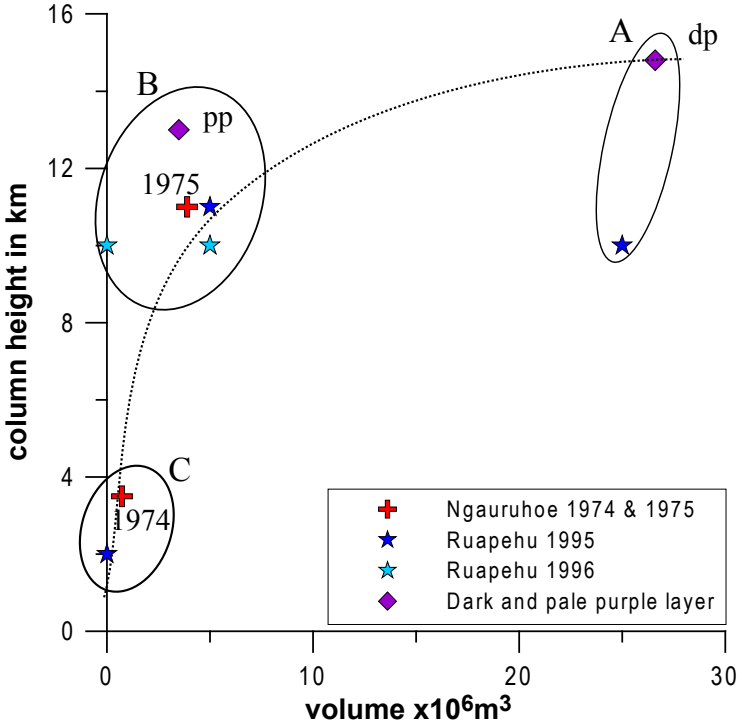

Figure 8.3.4: Column height vs. volume of selected eruptions from Ruapehu (Cronin *et al.* 2003) and Ngauruhoe (Sparks (1975); Nairn and Self (1978).

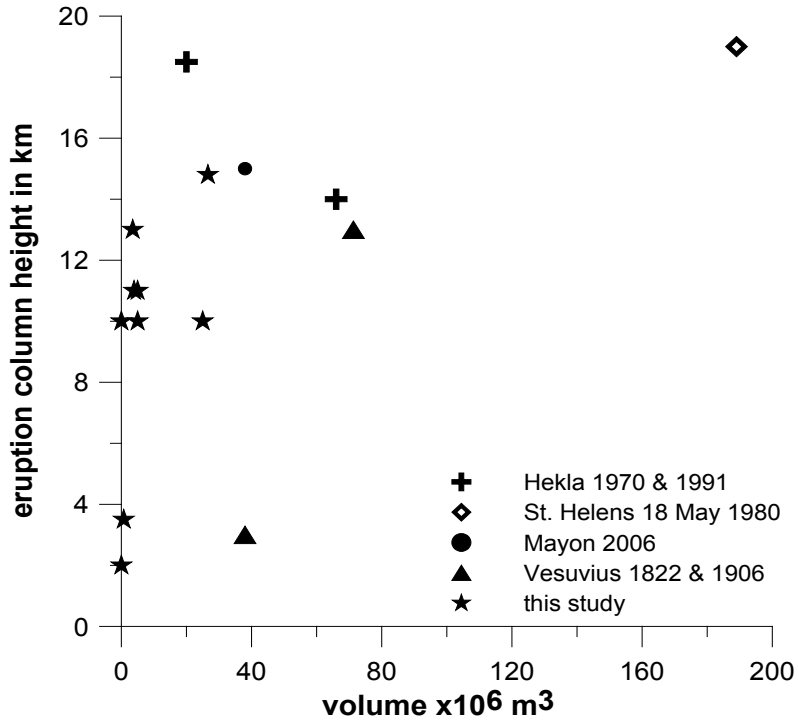

Figure 8.3.5: Column height vs. volume of Ruapehu and Ngauruhoe eruptions compared with selected examples from Hekla, Vesuvius, Mayon and Mt St. Helens. References: Hekla: Sulpizio (2005); Mt St Helens: Carey *et al.* (1990); Sulpizio (2005); Mayon: (Global Volcanism Program); Vesuvius: Arrighi *et al.* (2001).

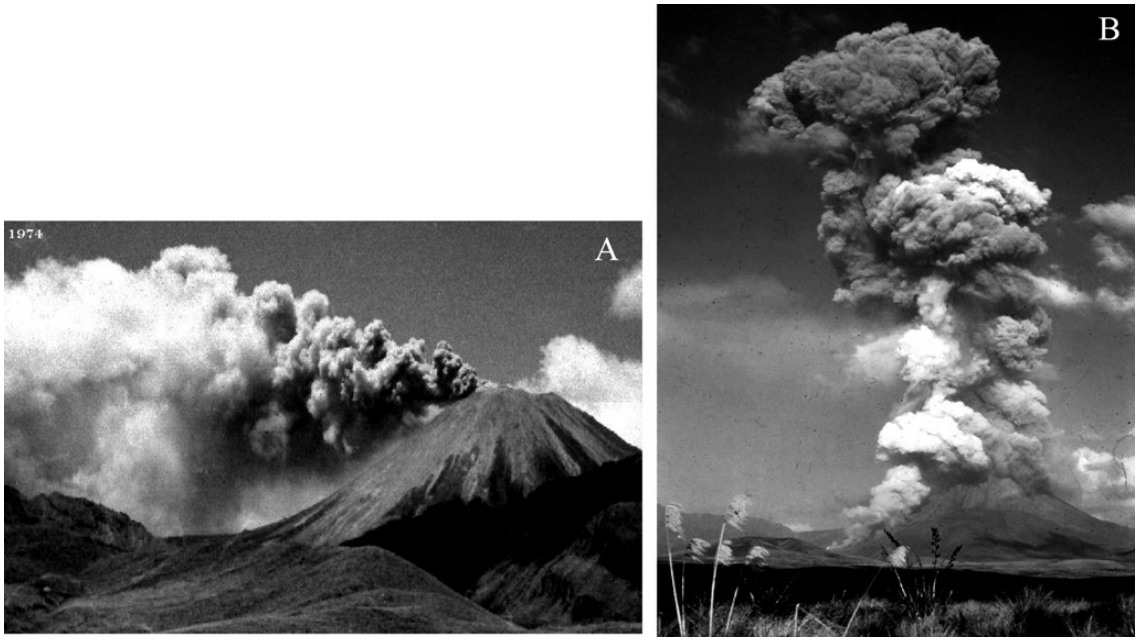

Figure 8.3.6: A) Ngauruhoe eruption in 1974 showing a weak plume being blown towards the north and B) eruption column from Ngauruhoe on the 19 February 1975 (images: private collection John A. Krippner).

8.4. Volcanic Explosivity Index (VEI)

To classify the magnitude of a volcanic eruption, Newhall and Self (1982) developed the Volcanic Explosivity Index (VEI) and also explained its use and limitations. Studies prior to the VEI used descriptive terms such as the thermal and kinetic energy, column heights, estimated volumes of lavas and pyroclasts and ballistic trajectories (Tsuya, 1955; Yokoyama, 1956; Yokoyama, 1957; Hedervari, 1963). Lamb (1970) estimated the atmospheric "dust" resulting from approximately 250 eruptions by using temperature records, atmospheric opacity and volcanological report (such as volumes), giving volcanic eruptions an indication of their relative size. Walker (1980) suggested five parameters to describe the scale of explosive eruptions: magnitude (from the volume of the ejecta), intensity (volume of the ejecta over time), dispersive power (estimated from the column height), violence (kinetic energy) and the destructive potential. Newhall and Self (1982) took the approach of classifying the magnitude of a volcanic eruption by using only volcanological data. The VEI combines the estimate of "Walker's magnitude and/or intensity and/or destructiveness and/or disperse power violence and energy release rate". The scale distinguishes eight categories on a logarithmic scale (Table 8.4.1). Newhall and Self (1982) calculated the VEI of over 8000 historical eruptions. For eruptions not having associated descriptions, a default VEI 2 was applied. This was in order to compensate between the rich information around historic eruptions and the lack of it for older pre-historic events i.e. "all VEI values from 1-4 prior to a certain date in each region have been upgraded by 1 VEI unit", unless there was other information. All data calculated by Newhall and Self are presented in Simkin *et al.* (1981).

Table 8.4.1: Volcanic Explosivity Index applied after Newhall and Self (1982)

VEI	0	1	2	3	4	5	6	7	8
volume in m^3	$< 10^4$	$> 10^6$	$> 10^7$	$> 10^8$	10^9	10^{10}	$> 10^{11}$	$> 10^{12}$	$> 10^{13}$
Classification	Hawaiian	Hawaiian /Strombolian	Strombolian/ Vulcanian	Vulcanian/ Peléan	Peléan/ Plinian	Plinian	Plinian/ Ultra-Plinian	Plinian/ Ultra-Plinian	Ultra-Plinian
Description	non-explosive	gentle	explosive	severe	cata-clysmic	parox-ysmal	colossal	super-colossal	mega-colossal
Column height in km	<0.01	0.1-1	1-5	3-15	10-25	> 25 km	> 25 km	> 25 km	> 25 km

The VEI is also based on the assumption that intensity and magnitude of a volcanic eruption are related, but Pyle (2000) shows there is not a simple relationship between the two terms and magnitude need an independent logarithmic scale. The magnitude scale is defined as:

$$magnitude = log_{10} (erupted\ mass, kg) - 7, \quad (18)$$

while the intensity is defined as follows:

$$intensity = log_{10} (mass\ eruption\ rate, kg/s) + 3. \quad (19)$$

8.4.1. VEI estimations for volcanoes of the TgVC

For all discrete tephras identified from Ngauruhoe, 66.4 % of eruptions are classified VEI 2 and 33.6 % VEI 3, based on their calculated volume. Note that these are minimum values, and no historic "weighting" has been applied (c.f. Newhall and Self, 1982). During Stage 1 around 17% of eruptions had an estimated VEI of 3, while during Stages 2 and 3, when Ngauruhoe had its highest eruption frequency, as well for Stage 4, >35 % were VEI 3. Eruptions of < VEI 2 are not distinguishable in the tephrostratigraphic record.

As shown in Chapter 5, VEI's of observed eruptions from Ngauruhoe range from VEI 0 (2%), VEI 1 (6%), VEI 2 (86%) up to VEI 3 (6%). Age calculations of tephras from Loc. 63 suggest that the two youngest tephras preserved can be correlated to two Ngauruhoe eruptions during the late 1890's. Volume calculations of these two Ngauruhoe tephras at Loc. 63 (9 and 6.4 x 10^6 m^3) also suggest a VEI of 2. During this time, seven eruptions were recorded (GVP, Gregg, 1960b), of which six had a VEI 2 and one a VEI 1.

The Ngauruhoe eruption from 1974 had a volume of 0.74 x 10^6 m^3 and its eruption column height rose to ~3.5 km (Self, 1975). This implies a VEI of 1 based on volume, and a VEI 2 according to its eruption column height. No tephra from this eruption is

distinguishable within the geological record. The 1975 Ngauruhoe eruption had a minimum bulk volume of 3.4 x10^6 m^3 (Nairn and Self, 1978), composed of 2.4 x10^6 m^3 fall deposit and 1-1.5 x10^6 m^3 pyroclastic-flow deposit (Lube *et al.*, 2007). The eruption column height rose to 11 km. This eruption was classified as VEI 3 by the Smithsonian Institution (GVP), presumably based on the eruption column height, but its volume falls into a VEI 2 category. No medial fall deposits are preserved.

The Ruapehu eruptions between 1995 and 1996 show a range of volumes between <0.01 and 25 x 10^6 m^3 (Cronin *et al*. 2003; Table 8.4.2). The eruption column heights ranged between <1 and 11 km, leading to VEI estimates of 1-3 depending on volume or eruption column height.

Table 8.4.2: Details of eruptions between 1995 and 1996 (modified after Cronin *et al*., 2003), including VEI estimations depending on column height or eruption volume.

Eruption date	Eruption type	column height (H) in km	Tephra volume (x 10^6 m^3)	Distribu-tion in km	Applied VEI for H	Applied VEI for volume
23 Sep 1995	phreatomag.	10	<0.01	12	3	0
4 Oct 1995	phreatomag.	<5	<0.01	15	2	0
11-12 Oct1995	phreatomag./ magmatic	8-10	25	>220	3	3
14 Oct1995	dry-magmatic?	<5	<0.01	>140	2	0
15-17 Oct '95	dry magmatic	1-2	<0.01	3	1	0
17 June 1996	phreatomag./ magmatic	7-10	5	>300	3	2
18 June 1996	magmatic/ strombolian	2-5	1	>70	2	2
8 July 1996	strombolian	3-5	*c.* 0.1	>50	2	1
26 July 1996	strombolian	9-10	*c.* 0.01	120	3	0

The physical parameters of historic eruptions are often very well determined but in the case of Ruapehu and Ngauruhoe, VEI estimates from volume vs. eruption column height are discordant. This poses concern when evaluating the true VEI of pre-historic eruptions based on the preserved tephra record. In Stages 2 and 3 of Ngauruhoe's tephra record the thinnest identified eruptions (1-2 mm thickness at 11 km distance from

source) have volumes ranging between 1.27 to ~ 5 x 10^6 m^3, which results in a classification of VEI 2. The eruption column heights estimated for these eruptions are around 13 km. Based on comparison to the much smaller observed historical eruptions, these column height estimates may be a little low, but certainly the VEI estimates are too low. In this case, the rule applied by Newhall and Self (1982) is probably appropriate, and the VEI's calculated from tephra volumes should be inflated by 1 category.

8.5. Fragmentation and dispersal characteristics

8.5.1. Grain-size distributions

Grain-size analyses have been studied to classify individual tephras sourced from Ruapehu, Ngauruhoe and Red Crater according to their eruption style, fragmentation and distribution (also see Chapter 7). A laser particle analyser was used for the <2 mm fraction (Chapter 2) while coarser particles were dry hand sieved in half-phi intervals.

Grain size histograms

Tephras from Ngauruhoe have been compared from three different locations (Loc. 12, 63, 67) which show the variation in grain size at different distances (Figure 8.5.1). Most of the units have a broadly unimodal distribution and are mainly positively skewed. They show sub-modes at 1.5 and 2.5 ϕ that are confirmed by optical microscope observation to represent the natural size of mainly plagioclase phenocrysts. Nearer to source, the grain size is coarser, but by 2.5 km the main grain size mode is similar to deposits found at 11 km distance (~3ϕ). At the distal site, grain-size distribution becomes polymodal.

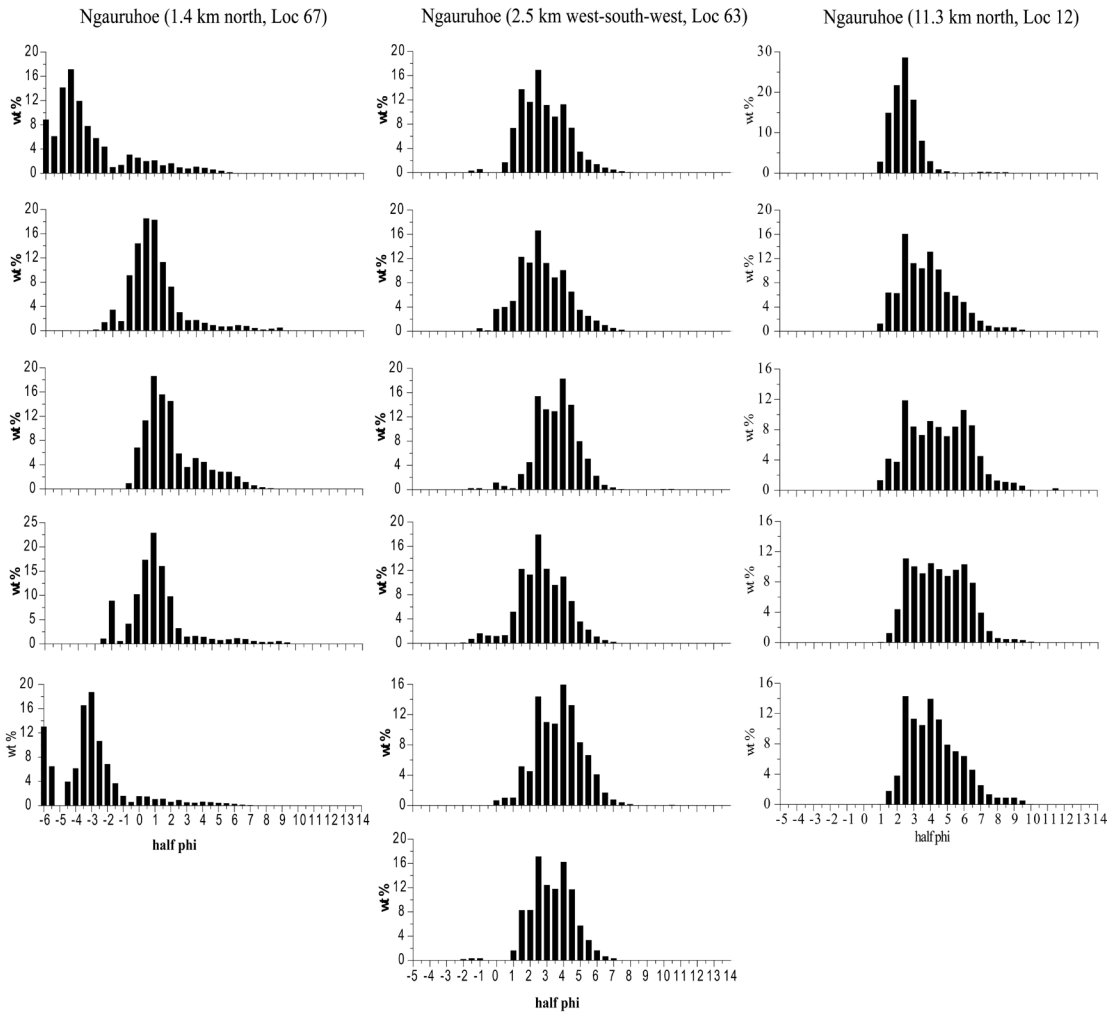

Figure 8.5.1: Grain-size histograms showing half phi vs. wt% of tephras from Ngauruhoe at different distances from source.

Grain-size histograms from Ruapehu are in general more complicated than those from Ngauruhoe. At all three locations, and therefore at different distances, a wide variety of grain sizes are present, ranging from very coarse particles to very fine grained tephras which could be caused by being located on different parts of the dispersal axis for Ruapehu eruptions.

Ruapehu histograms show examples of unimodal and polymodal distributions with a poorer sorting than Ngauruhoe tephras and mainly positive or symmetrical skewness (Figure 8.5.2).

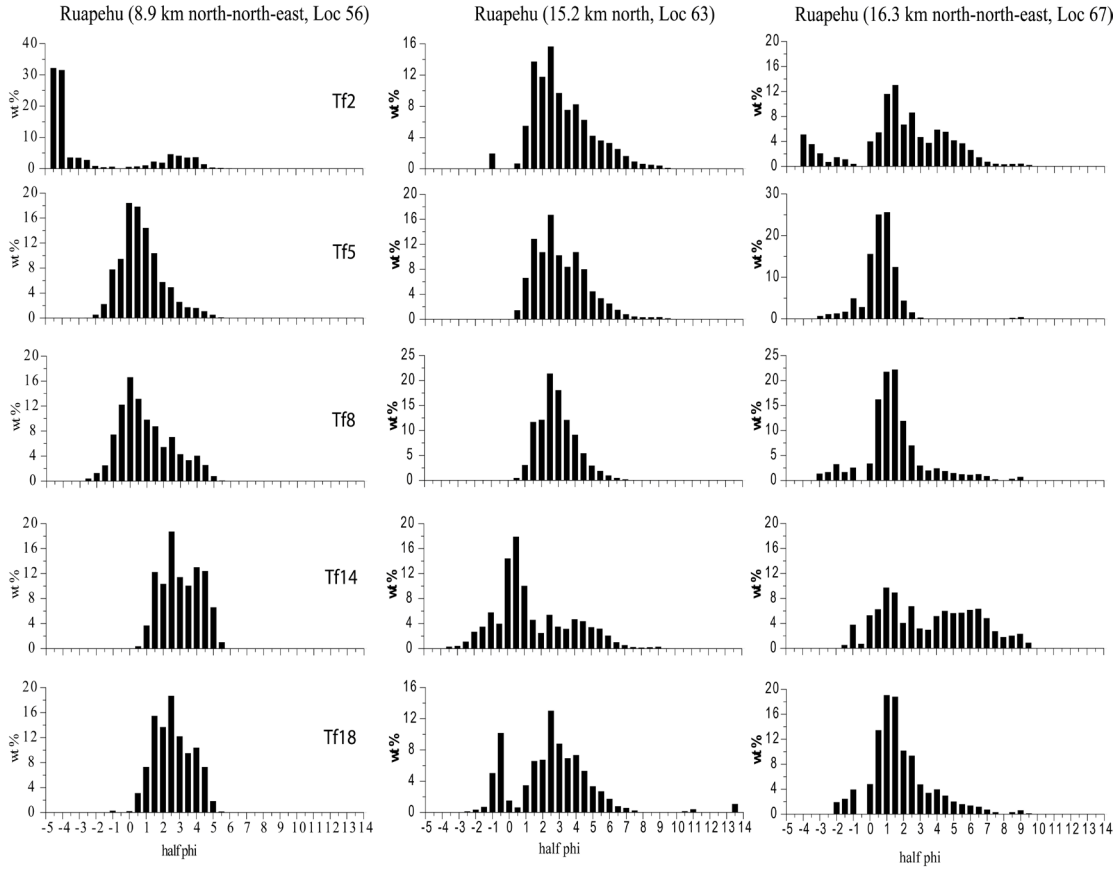

Figure 8.5.2: Grain-size histograms showing half phi vs. wt% of tephras from Ruapehu at different distances from source.

At equivalent distances from source (Figure 8.5.3) Ruapehu tephras are coarser grained than Ngauruhoe tephras and with a broader, at times more complex distribution. Ruapehu's grain-size histograms are more unimodal to bimodal while the Ngauruhoe-sourced tephras are more polymodal.

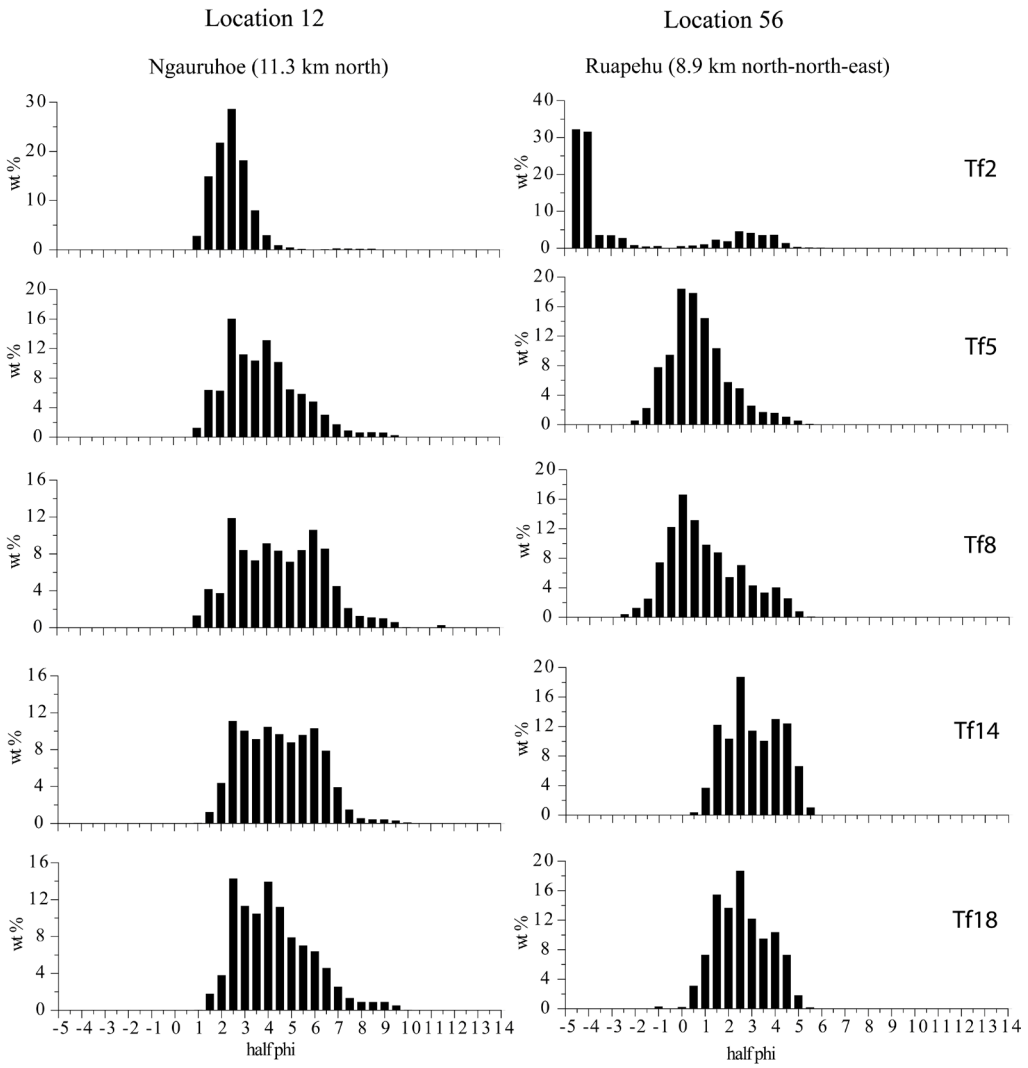

Figure 8.5.3: Grain-size histograms showing phi vs. wt% of tephras from Ngauruhoe at Location 12 and Ruapehu at Location 56.

Tephra grain-size distributions at any given site depend on the fragmentation process, column height and wind strength/direction. Diagenesis and weathering may also overprint the characteristics of these primary processes. The tephras analysed here were derived from sub-plinian, violent strombolian, vulcanian and phreatomagmatic eruptions (see Chapter 7), all producing very highly fragmented ash. Most tephras are moderately well to poorly sorted and fall into the typical boundaries of pyroclastic-fall deposits and also in the lower half of in general more poorly sorted pyroclastic flow-deposits (Figure 8.5.4).

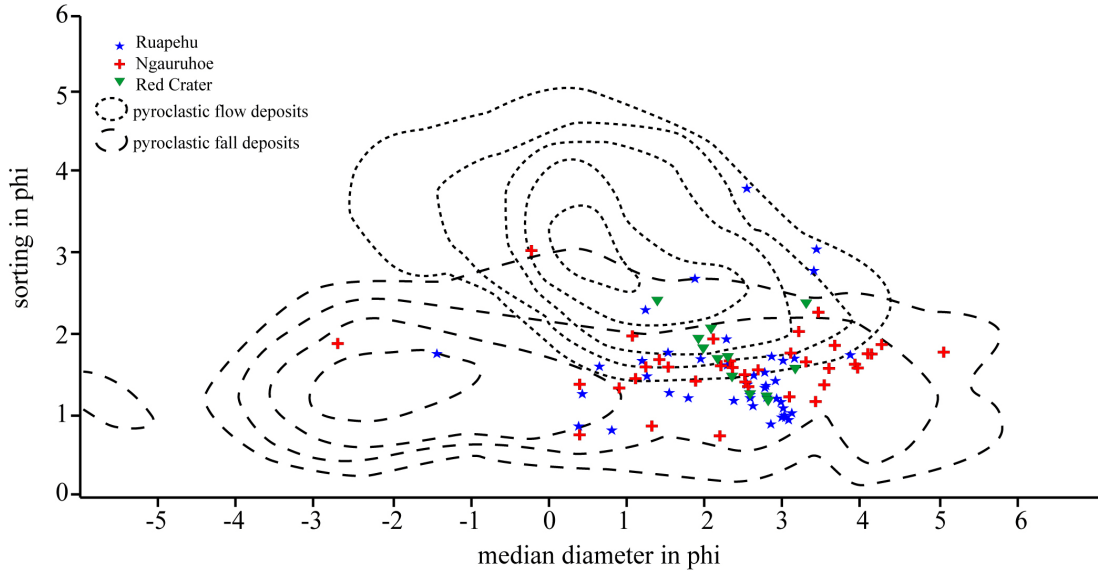

Figure 8.5.4: Medium diameter vs. sorting of Ruapehu, Ngauruhoe and Red Crater in comparison to fields for pyroclastic flow and fall deposits from Walker (1971).

Due to the highly fragmented and fine-grained nature of these tephras they are at times as poorly sorted as some pyroclastic-flow deposits (Figure 8.5.4). They are also typically finer grained and more poorly sorted than strombolian and phreatomagmatic tephras from White Island and Vesuvius and fall most closely into the finer end of the range of tephras from Paricutin (1943-1952) (Pioli *et al.*, 2008). Samples obtained from White Island are from proximal locations, with finer distal material carried out to sea (Houghton and Nairn, 1991). Secondary processes such as weathering could contribute to the increased fine-grained nature of tephras analysed in this study.

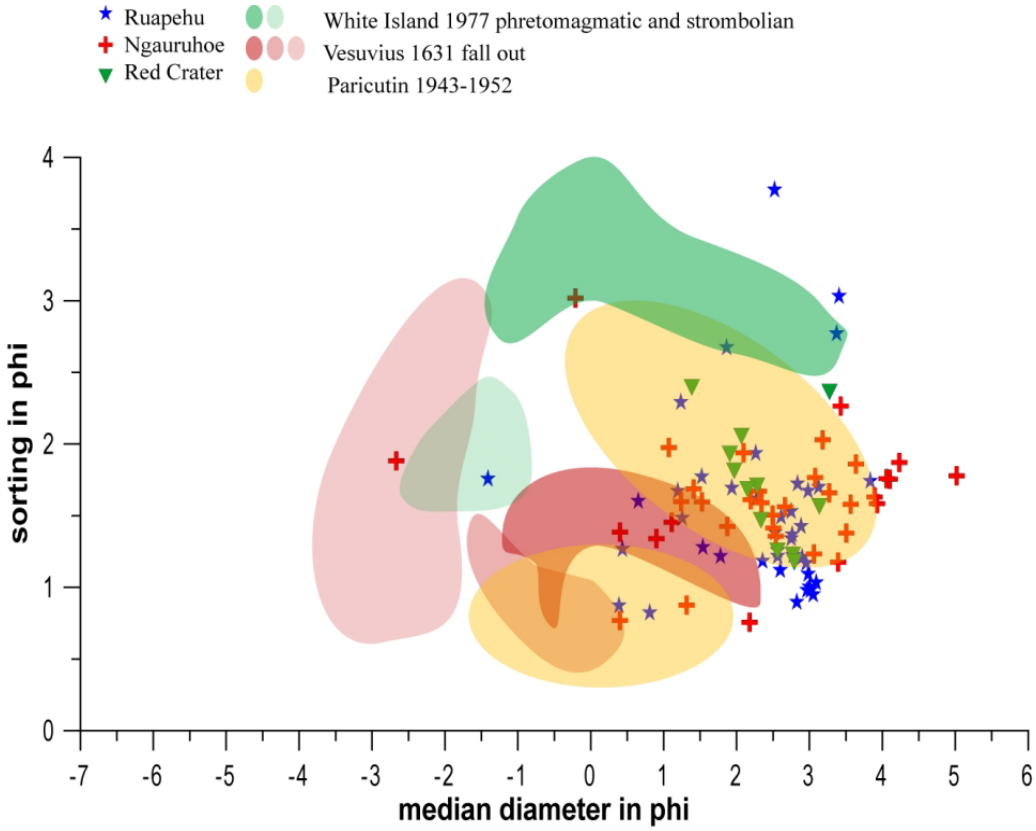

Figure 8.5.5: Medium diameter vs. sorting of TgVC-sourced tephras in comparison to White Island tephras (green), Vesuvius (red) and Paricutin (yellow), darker green and red represent phreatomagmatic eruptions while lighter green and red are strombolian eruptions. The yellow Paricutin elipses represent a violent strombolian style. References: Houghton and Nairn (1991), Rolandi *et al.* (1993), Pioli *et al.* (2008).

The dark purple (DP) and pale purple (PP) tephras

An isopleth map of the DP tephra (Figures 8.5.6) shows a nearly circular distribution of isopleths with finer grain-sizes (< 500 µm) extended towards the south-east. A secondary centre of coarsening is observed in this direction with particles up to 1 mm in size. These unique isopleths pattern can only be explained by a change to strong wind conditions during the eruption where strong north-westerlies carried larger and heavier particles farther than it would have been the case during weaker wind conditions. An analogue example of a similar grain-size distribution was observed after the 14 October 1995 Ruapehu eruption. The isopach and isopleths of this eruption showed an absence of tephra deposited between the vent and a point ~ 9 km to the south-east. These

patterns were explained by strong north-westerly winds decapitating the plume from the vent and carrying it to the south-east, the upward thrust buoying the particles before they could fall out at a farther distance (Prof. V. E. Neall, pers. com., 2010).

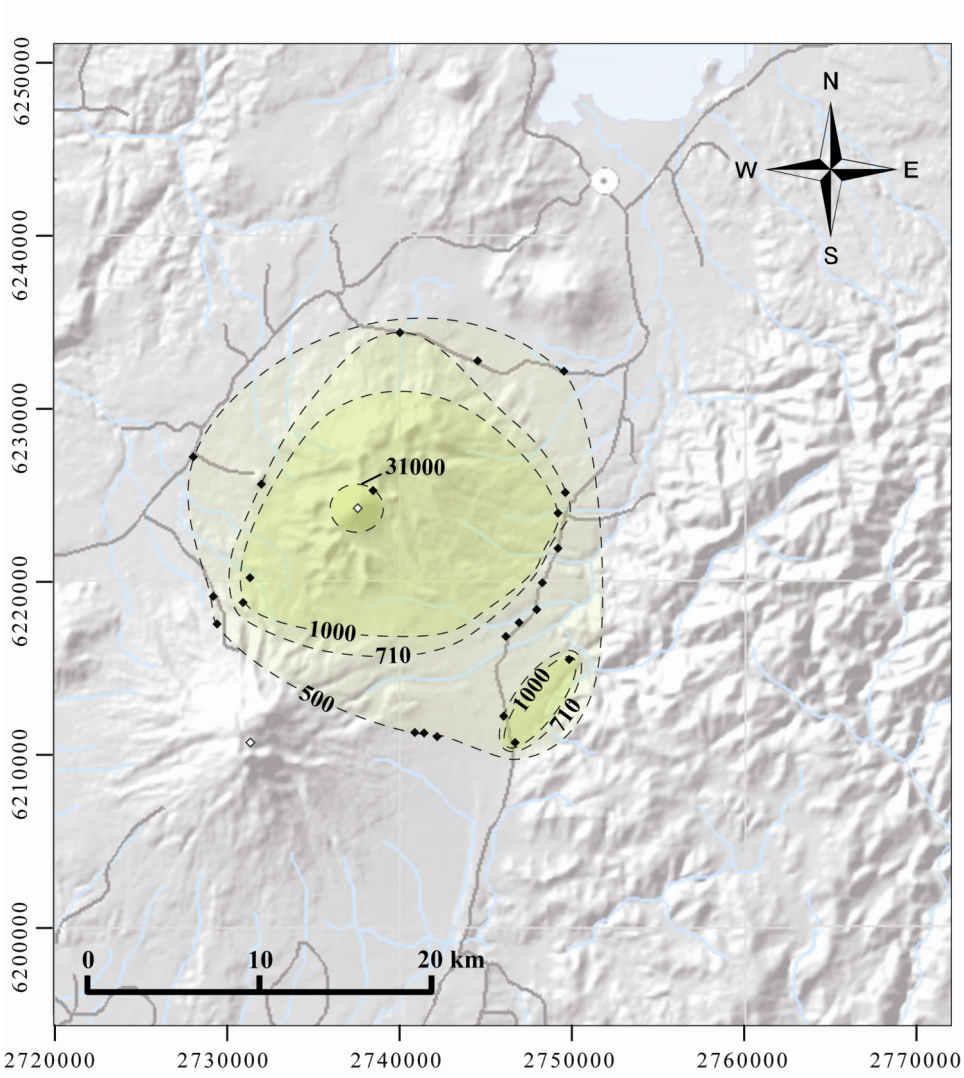

Figure 8.5.6: Isopleth map of the dark purple tephra. The isopleths are shown in µm.

For the PP unit package, the isopleths indicate three possible depositional lobes, with a strong ESE lobe, and weaker NE and NW lobes. These lobe patterns are similar to the distribution of the Ruapehu 1995-1996 major tephra lobes and corresponds to the typical range in wind directions for the region (Cronin *et al.,* 2003; Thompson, 1984).

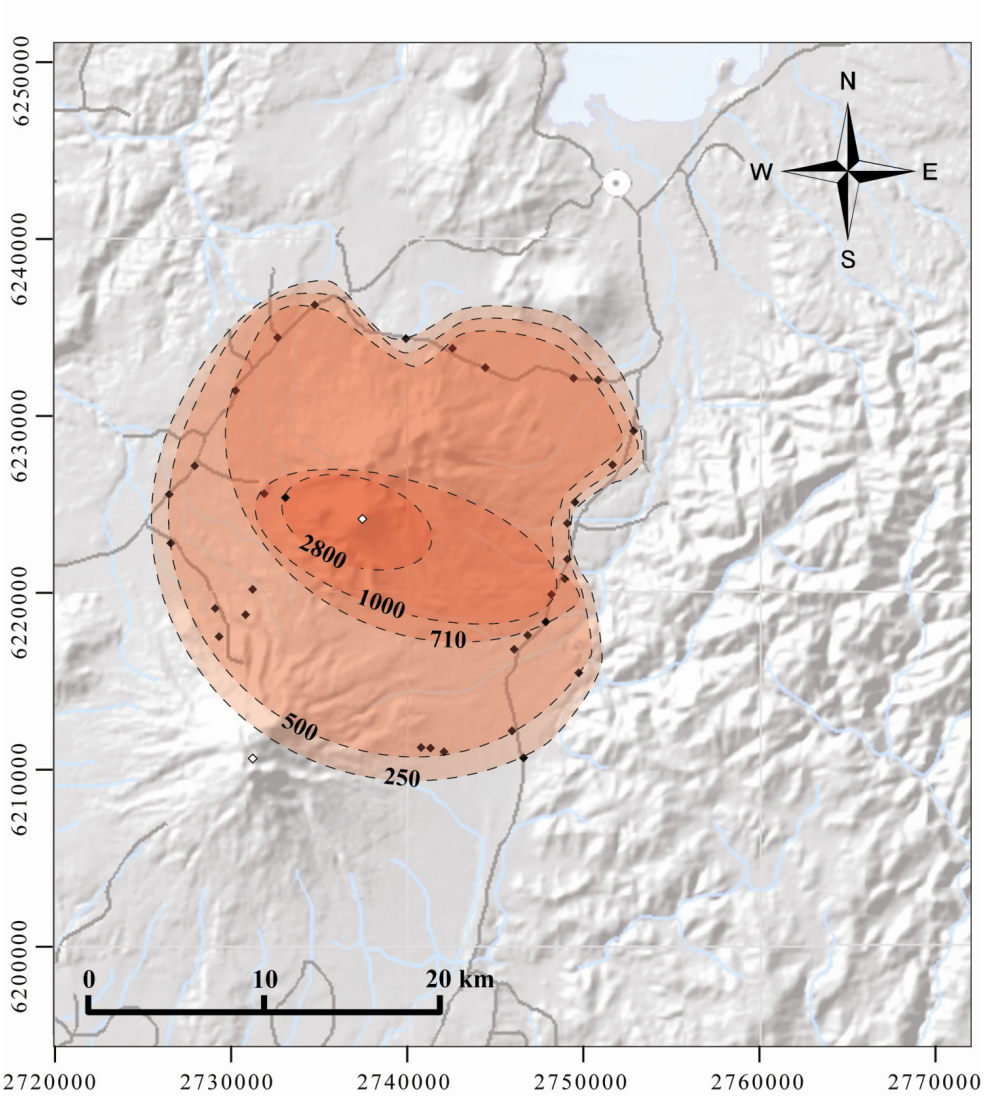

Figure 8.5.7: Isopleth map of the pale purple tephra package. The isopleths are shown in µm.

The DP-tephra rapidly fines (Figure 8.5.8), from 1.4 to 5.7 km from source, but then is similar from 10.9 km out to at least 16.3 km, improving only in its sorting. A secondary mode is recognisable at around 2 ϕ, representing the crystal (plagioclase and pyroxene) content. The composite PP-unit, made up of several smaller ash falls, shows a similar pattern in proximal areas only and has generally more complex medial to distal distributions.

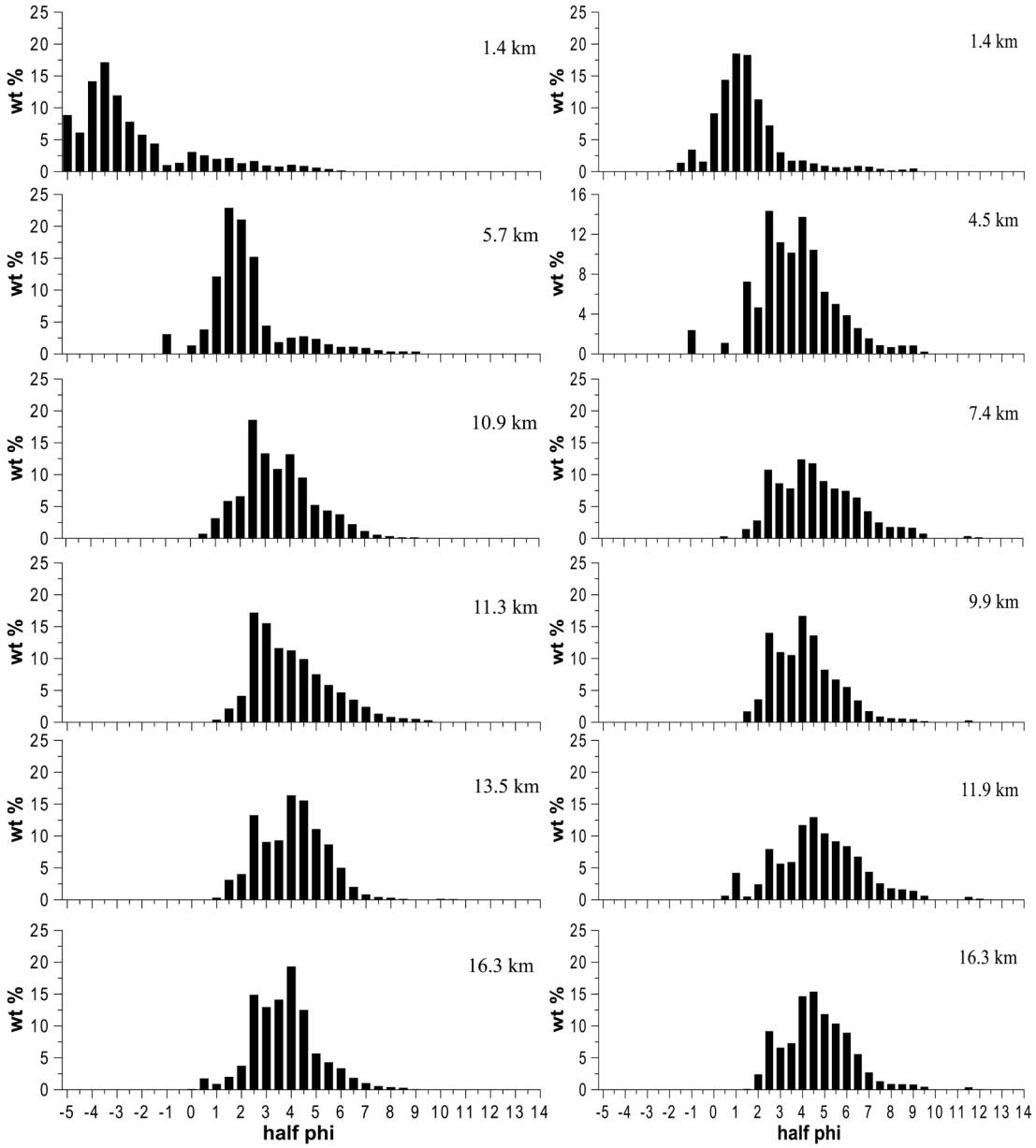

Figure 8.5.8: Grain-size distributions for the dark purple (DP) tephra (left) and the pale purple (PP) (right) unit with distance from source.

The median diameter vs. sorting follow typical patterns of pyroclastic-fall deposits (Walker, 1971) (Figure 8.5.9). Both PP and DP-layers fine until c. 8 km from source, after which the median diameter remains constant until at least 16 km (Figure 8.5.10A). The DP-tephra shows a constant improvement in sorting with distance, while the PP-unit remains poorly sorted throughout (Figure 8.5.10B).

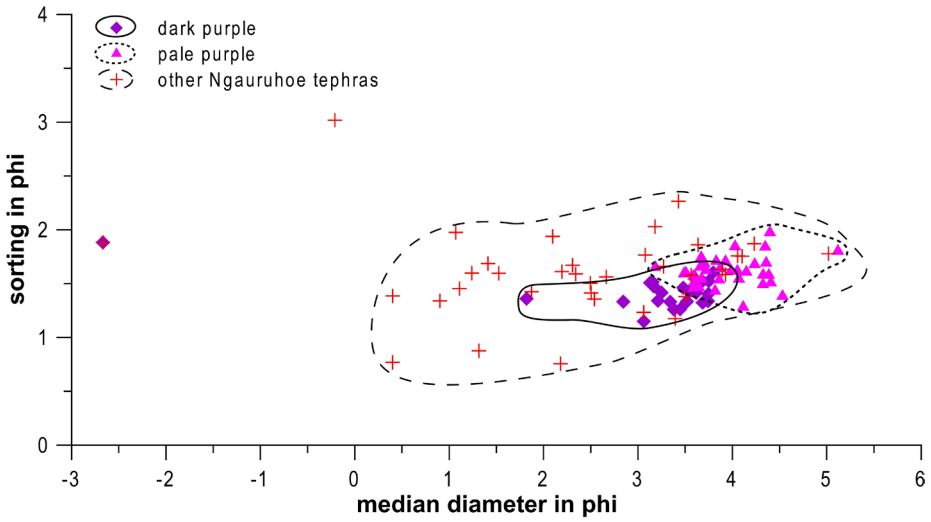

Figure 8.5.9: Median diameter vs. sorting for the dark purple (DP) tephra and pale purple (PP) unit in comparison to other Ngauruhoe-sourced tephras.

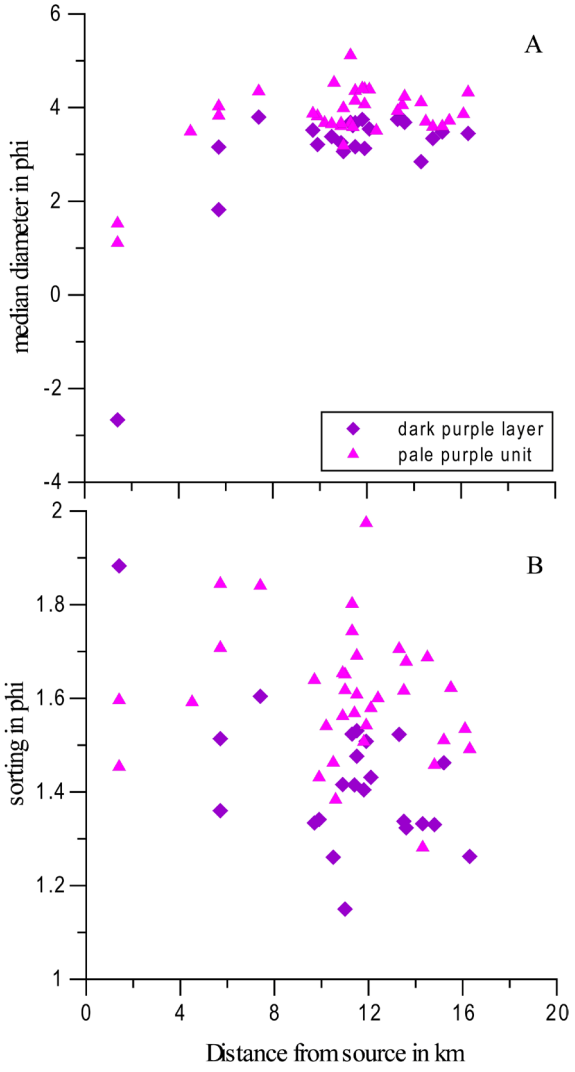

Figure 8.5.10: Median diameter (A) and sorting (B) vs. distance from source.

Due to their poor sorting and fine grainsize, the DP and PP-tephras cannot be readily classified using standard approaches that assume primarily magmatic fragmentation (e.g., on the Walker's (1973) dispersal vs. fragmentation plots both units fall into the phreatoplinian field, Figure 8.5.11). These are highly fragmented tephras, where >95 wt% of grains are < 1 mm and estimates of dispersal at 0.01% of T_{max} are around 1000 km^2 for PP and ~500 km^2 for DP. This was also pointed out by Self (1975) with a very thin tephra from the 1974 Ngauruhoe eruption.

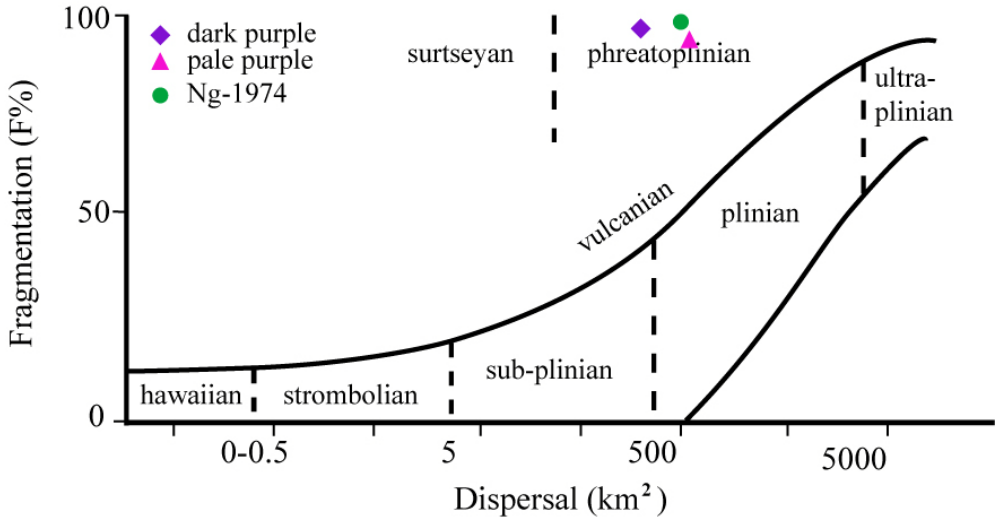

Figure 8.5.11: Fragmentation vs. dispersal after Walker (1973), where three of the analysed tephras from Ngauruhoe fall due to the high grade of fine ash falsely into the phreatoplinian filed.

These results point out a gap in our standard classification of eruption styles, when they are applied to small-scaled eruptions, where possibly both magmatic and phreatomagmatic fragmentation mechanisms are at work. Similar eruptions are regularly observed at locations such as Paricutin (Mexico), Mayon (Philippines), Sakurajima (Japan), Arenal (Costa Rica), Galeras (Colombia) and Yasur (Vanuatu), but the resulting deposits are usually poorly preserved, and the very fine-grained and thin tephras are difficult to correlate.

The dispersal information shown here from the TgVC tephras enables the construction of extended fields for hawaiian and strombolian-scaled events, which probably reflect a phreatomagmatic component to the fragmentation mechanism (i.e., vulcanian

eruptions). The tephra deposits from the volcanoes of the TgVC (Figure 8.5.12, red area) show similar thickness to strombolian and hawaiian eruptions and are thinner than plinian, phreatoplinian and subplinian eruptions. The dispersal of the TgVC-tephras shows in contrast the opposite behaviour with approximate distributions to phreatoplinian tephras. Demonstrating that such small-scaled events (VEI 1-4) can be much more broadly dispersed than previously assumed, these frequent, small-scaled, explosive eruptions play a bigger role in hazard evaluation at volcanoes producing vulcanian eruptions.

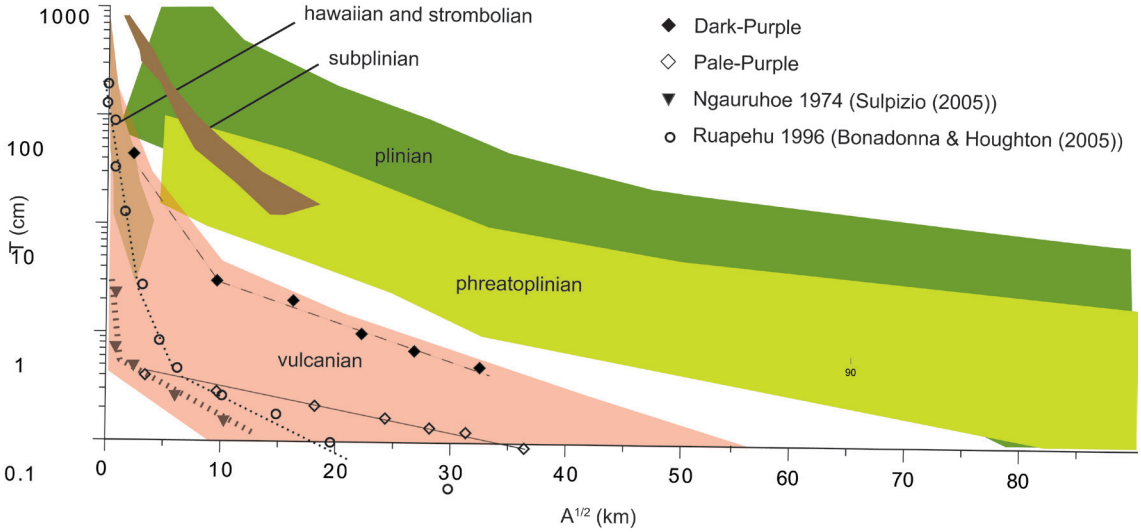

Figure 8.5.12: LogT vs. $A^{1/2}$ plot of the DP, one unit from within PP, as well as Ngauruhoe 1974 and Ruapehu 1996 tephras, defining here a new field (red) for "vulcanian" eruptions that contrasts to areas defined for plinian, subplinian, hawaiian and strombolian eruptions by Houghton *et al.* (2000) and Wehrmann (2005).

Chapter 9

Discussion and conclusion

9.1. Summary of key findings

The Tongariro Volcanic Centre (TgVC) is situated at the south-western termination of the Taupo Volcanic Zone (TVZ); it is characterized by andesitic volcanism and is dominated by the edifices of Ruapehu and Tongariro. The tephrochronological record of these two volcanoes is well constrained for the largest eruptions (>VEI 4) going back to around 26 000 cal. yrs. B.P. (Topping, 1973; Donoghue *et al*., 1995; Cronin, 1996). The initial objective of this study was to untangle the stratigraphy of the smaller tephras, particularly through the Holocene sequence. These small units had been, at times mapped collectively into tephra formations which obscured their relationship to their source vents (Table 9.1). Through studying the smaller-scaled eruptions the study aimed to reveal new constraints on the physics of eruption processes and develop a more robust and complete record of eruption frequency, magnitude (volume, eruption column height) and style from the volcanoes of the centre (Table 9.1.). This, in turn, can be used to underpin an improved understanding of future volcanic hazards of the Central North Island of New Zealand and also how such volcanoes behave worldwide.

The Late Pleistocene tephra stratigraphy of the TgVC is represented by the Bullot, Mangamate, Papakai, Mangatawai, Ngauruhoe and Tufa Trig Formations. In the case of the Papakai and Mangatawai Formations, individual tephras were collectively grouped from several volcanic sources. To untangle the complex stratigraphy of 1-30 mm thick, fine-grained and otherwise non-distinguishable tephra beds, the major-oxide composition of volcanic glass shards were analysed. Four eruptive sources were distinguished: Ruapehu, Ngauruhoe, Red Crater and upper Te Maari Crater. Tephras pre-12 000 cal. yrs. B.P. were less well discriminated using this method, due to a wider

range in their chemical compositions. This tephrochronological approach was used to establish the first detailed stratigraphy and eruption frequency model for each of the TgVC volcanoes over the last 12 000 cal. yrs. B.P.

New radiocarbon analyses of interbedded organic material in the basal tephras of the Mangatawai Formation show an age of 3508 ± 121 cal. yrs. B.P. extending the previous age estimates of these tephras (c.f., Fergusson and Rafter, 1959) by around 1000 years. The oldest recognised discrete tephras sourced from Ngauruhoe volcano were identified within the upper part of the Papakai Formation, also demonstrating that the volcano is older than previously considered (Topping, 1973; Donoghue *et al*., 1995). Calculations of soil accumulation rates between further new radiocarbon dates (Chapter 5) and rhyolitic marker tephras within the Papakai Formation reveal that the oldest identifiable Ngauruhoe tephra is ~ 4710 cal. yrs. B.P., almost doubling the previously assumed age (2568 ± 508 cal. yrs. B.P.) for this volcano. Chemical analyses of glasses below the Motutere Tephra (thought to equate to Unit G of Wilson, 1993) also have Ngauruhoe composition, suggesting that Ngauruhoe could even have started evolving before 6900 cal. yrs. B.P.

The detailed stratigraphic record of Ngauruhoe is split into Stages 1 to 3 (pre-Taupo Pumice Formation) and the post-1700 cal. yrs. B.P., Stage 4. Ngauruhoe's major explosive eruptive phase occurred during Stage 2, between 3200 and 2700 cal. yrs. B.P., during which time the largest eruptions (VEI 3-4) were produced. The typically finely bedded and fine-ash grade tephras are very difficult to correlate over wide areas, and only two distinctive purple tephras could be traced widely. The isopach and isopleth maps of these units, along with observations of historical eruptions from this area were used to constrain the physical volcanology of Ngauruhoe eruptions and to estimate eruption volumes and column heights for individual prehistoric events. The dark purple-DP unit is identified to be the largest known eruption of Ngauruhoe, with the widest distribution, a minimum erupted volume of 26.6 x 10^6 m^3 and a probable eruption column height of ~14.8 km.

Red Crater is situated north-east of Ngauruhoe and is the youngest active vent of Mt Tongariro. The oldest erupted unit attributed to Red Crater is the Oturere lava flow, east

of the crater, which is assumed to have an age of at least ~ 4000 cal. yrs. B.P., based the oldest cover-bed being upper Papakai Formation. The glass major element chemistry of Red Crater-sourced tephras suggests that larger pyroclastic eruptions began between 2900 and 2800 cal. yrs. B.P., as indicated by scattered glassy pyroclasts found interbedded within Ngauruhoe-sourced tephras. Discrete Red Crater tephras were recognised only in proximal locations and estimated to be <323 cal. yrs. B.P. on age.

Te Maari Craters, on the north-eastern flanks of Mt Tongariro, encompass two complex craters and at least seven explosion pits. The last eruptions occurred in 1896 from the upper Te Maari Crater. The surge and fall deposits on the eastern crater rim have dacitic glass compositions, similar to the highly evolved Taranaki-sourced glasses.

Ruapehu has been one of the most active volcanoes of New Zealand over the last ~40 years, with its latest phreatomagmatic eruption occurring in September 2007. The Late Pleistocene tephrostratigraphic record is represented by tephras of the Bullot, Papakai, Mangatawai and Tufa Trig Formations. Tephras were analysed from Ruapehu in this study from the ring plain (up to 12 000 cal. yrs. B.P.) and sediment cores from Lake Rangatauanui, near Ohakune (up to ~26 000 cal. yrs. B.P.). The eruptions of Ruapehu were apparently influenced by a crater lake since at least 3000 cal. yrs. B.P. (Donoghue *et al.,* 1997), leading to phreatic and phreatomagmatic eruptions up to the scale of subplinian events. Results from this study have updated the frequency records of this volcano and recognised that a crater lake may have been an even longer-lived feature of this volcano.

Table 9.1: Overview of the new tephrostratigraphical record found within the TgVC in comparison to previous work of Topping (1973) and Donoghue (1991). *italic:* rhyolitic tephras from the TVC and OVC.

Previous work		**This study**				
Formation	**Members**	**Formation**	**Members**			**Age in cal. yrs**
			Ruapehu	**Ngauruhoe**	**Red Crater**	**B.P.**
Tufa Trig Formation	Tf19	Tufa Trig Form.	Tf19			1995 AD
Ngauruhoe Formation		Ngauruhoe Form.		Unit A-G		1954/55, 1975
Tufa Trig Formation	Tf18	Tufa Trig Form	Tf18			1945 AD
Ngauruhoe Formation		Ngauruhoe Form.		Nh 5-6		*c.* 1890 A.D.
					RC 10-16	*c.*140 to *c.* 70
				Nh 4		*c.* 170
					RC 2-9	*c.* 200 to *c.* 230
Tufa Trig Formation	Tf16-Tf17		Tf16-Tf17			*c.* 270 to *c.* 210
			6 unnamed			*c.* 290
Kaharoa Tephra		Burrell lapilli (Taranaki)				1655 AD
Ngauruhoe Formation		Ngauruhoe Form.		Nh 3		1654 AD
					RC-1	323
Tufa Trig Formation			2 unnamed			*c.* 480
Tufa Trig Formation	Tf5-Tf15	Tufa Trig Form.	Tf6-Tf15			*c.* 700 to *c.* 530
			Tf5			790
Ngauruhoe Formation		Ngauruhoe Form		Nh 2		*c.* 800
Tufa Trig Formation	Tf4	Tufa Trig Form	Tf4			*c.* 895
Ngauruhoe Formation		Ngauruhoe Form.		Nh 1		*c.* 980
Tufa Trig Formation	Tf1-Tf3	Tufa Trig Form.	Tf3			*c.* 1210
			Tf2			1338
			Tf1			1555
Taupo Pumice		*Taupo Pumice*				1717
Mangatawai Tephra Form.		Mangatawai Form	Mw 62			*c.* 1790.
				Mw 9-61		*c.* 3694 to *c.* 2485
			Mw 1-8			*c.* 3520 to *c.* 3470
Papakai Formation		Papakai Form.		Mangatepopo lapilli		
			1 unnamed			*c.* 4170
Waimihia Tephra		*Stent (Unit Q)*				4323
	Black Ash 2		Black ash 2			*c.* 4170
				Pp 1-3		*c.* 4710
	Black Ash 1		Black ash 1			5592
Hinemaiaia Tephra		*Unit K?*				5120
	Orange lapilli 2		Orange lapilli 2			
	Orange lapilli 1		Orange lapilli 1			
Motutere Tephra		*Unit G*				6907
			1 unnamed			
Mangamate Formation		Mangamate Form.				11 244 to 10 891
	Poutu Lapilli					10891
	Wherapu Tephra					11 173
	Ohinepango Teph.					min 11 173
	Waihohonu Lap.					
	Oteuere Tephra					
	Te Rato lapilli					11 241
Pahoka Tephra						min 11244
Bullot Formation		Bullot Form.				*c.* 26 000 to 11 244

9.2. Conclusions

One of the main findings of this study has been the identification of chemical variation between Ruapehu, Ngauruhoe and Red Crater. This chemical fingerprint characterises the pyroclastic deposits of each volcano and for the first time provides a basis on which to establish an eruption frequency over Ngauruhoe's and Red Craters **entire** life span and Ruapehu's younger explosive eruption record of the last ~ 25 000 cal. yrs. B.P. The chemical variations, defining this fingerprint, suggest that the three volcanoes have discrete behaviour patterns with individual magma batches apparently derived from non-communicating crustal magma storage zones beneath both Mts. Tongariro and Ruapehu (Hobden *et al*., 1999; Price *et al.,* 2005). Furthermore, the chemical variations follow topographical features with an evolved andesitic-dacitic composition from Ruapehu glasses in the south trending towards a more primitive basaltic-andesitic (Ngauruhoe) and basaltic (Red Crater) glass composition to the north-east. This chemical variation could be caused by the propagating rift system which narrows at its southern end, where magma has a lower ascent rate allowing interaction with the crust and evolution of the magma. Towards north-east, the rift system of the TVZ widens allowing magma to migrate more quickly through the crust without major magma-crust interactions and reach the surface in a more primitive condition.

The eruption frequencies from all three volcanoes are only based on discrete tephras and therefore exclude the numerous eruptions such as that from Ngauruhoe 1974, which were too small to leave a record within the geological record. This means that the explosive eruption frequencies identified in this study, only deliver the minimum of the actual explosive activity for each of the volcanoes. This study, however, shows at least two kinds of eruption frequency within the TgVC. Ruapehu and Tongariro changed their eruption magnitude and styles around 12 000 cal. yrs. B.P. from mainly larger scale, sub-plinian eruptions of the Bullot and Mangamate Formations (VEI ≥4) to vulcanian to strombolian eruptions of smaller magnitude (VEI ≤3) and only rare subplinian events. Since 12 000 cal. yrs. B.P. the explosive eruptions from Ruapehu increase steadily. VEI's of historical Ruapehu eruptions range from 1 to 3. Examples are the well known eruptions from 1945 (Tf18) and 1995/96 (Tf19). Field observations show that both the 1945 and 1995-96 events left deposits of ≤ 30 mm thickness. Tf5, in

comparison, erupted at 790 cal. yrs. B.P., reaches 100 mm-thick at the same locations, and is considered to be the largest eruption from Ruapehu over the last ~1400 cal. yrs. B.P. So far no complete isopach map could be constructed from this eruption, hence no volume and eruption column heights are known. In addition to a typical dark grey to black, fine to coarse ash, Ruapehu produced four distinctive orange pumice lapilli units within the Late Holocene, the Orange lapilli 1 and 2 within the Papakai Formation as well as Tf1 and 2 at the base of Tufa Trig Formation. The lapilli are very similar to those from members of the sub-plinian Bullot Formation units, however, the Holocene pumice units are of similar magnitude to the typical grey ash-producing eruptions. The grey, highly fragmented tephras are attributed to phreatomagmatic eruption styles and considered as evidence for the presence of a crater lake (Donoghue *et al.,* 1997). The orange pumice lapilli layers represent the same erupted magma volume as their grey-ash counterparts but their highly contrasting fragmentation and textural properties indicate the absence of a crater lake. This in turn implies a time when the summit area was free of water/ice, and possibly indicates times when major Holocene lava eruptions took place (i.e., episodes producing Whakapapa Formation lavas; Hackett, 1985). The frequency of VEI≥3 eruptions from Ruapehu increased dramatically over the last ~1700 cal. yrs. B.P. Periods of high-eruption frequency at Ruapehu also appear to correspond to relative quiet at Ngauruhoe although for smaller events in the historic record, Ruapehu erupted simultaneously, or in the same year as Ngauruhoe on 25 occasions.

In contrast to Ruapehu, Ngauruhoe shows a different pattern in activity and therefore its eruption frequency. This study has allowed the analyses of an entire life span of a volcano which helps to understand the birth, growth and also possible death of a single andesitic cone. Ngauruhoe's initial activity (main part of Stage 1) was interpreted to be dominantly effusive, and probably began after the Mangamate Formation eruptions of Tongariro, around 11 150 cal. yrs. B.P. Traces of Ngauruhoe glass shards show that this effusive phase, with very small explosive eruptions lasted approximately 6350 years, building the foundations for the high strato-cone. The first significant explosive eruptions began at around 4700 cal. yrs. B.P., possibly in relation to an increase in the cone height. Larger and more frequent explosive eruptions started from ~3400 cal. yrs. B.P. (Stage 2) and the climactic phases of pyroclastic activity occurred between 2900

and 2800 cal. yrs. B.P. with mainly VEI 3-4 eruptions. In this 100 year-interval, 37% of the total known tephra volume was erupted from Ngauruhoe. Following this, a decrease in eruption frequency and magnitude occurred (Stage 3). After the eruption of the Taupo Pumice Ignimbrite (1717 cal. yrs. B.P.), eruption magnitudes further declined. This decline in eruption magnitude is also reflected by slightly more evolved magmas. The last 35 years of quiet, represents the longest known historical pause in activity from Ngauruhoe (Hobden *et al.*, 1999). Similar intervals between prehistoric eruptions appear common, although it is noted that the prehistoric events are much larger in scale.

Small chemical variations over time in the Ngauruhoe tephras (Hobden *et al.*, 1999, this study), can be explained by increased residence times of magmas within the crust, or to declining magma production/flux rates. Hobden *et al*. (1999) showed that historical lava flows were derived from an open system characterised by small (< 0.1 km^3) and short-lived (≤ 1 ka) magma batches. $^{87}Sr/^{86}Sr$ analyses from volcanic glass and lavas exhibit three broad cycles of magma production throughout Ngauruhoe's history. Cycles are characterised by initial low $^{87}Sr/^{86}Sr$ values that rise to a maximum over ≥ 2000 years. This represents a change from initially high magma ascent rates from deep in the system that gradually decrease, allowing magmas to interact for longer with the crust in later parts of the cycle. The oldest two Ngauruhoe tephras indicate part of an early cycle. The first complete cycle is shown within Stage 2 to 3 tephras, starting with the largest known pyroclastic eruptive phase from Ngauruhoe and completed after the Taupo Pumice eruption (Hobden, 1997). The beginning of the latest cycle began sometime before 982 cal. yrs. B.P., whereas the 1975 eruptives show high Sr-values typical for the end of a cycle. This may imply that the latest 35 year pause in eruptions will be followed by recharge of new magma into the system. If so, the eruption magnitudes of future events could be considerably larger than those seen in the historic record.

Mt. Tongariro consists of several overlapping vents and apart from Ngauruhoe, two other vents are currently active, Red Crater and the upper Te Maari Crater. Red Crater is a relatively small pyroclastic construct, but has produced several lava flows over the last ~4000 years (Figure 9.1), providing a minimum age for its activity. The main tephras from Red Crater were emplaced only during the last ~400 years, although minor pyroclastic activity has occurred since at least 2900 cal. yrs. B.P. The structure and

activity style of Red Crater, with lava flows emplaced over the last ~4000 cal. yrs. B.P., parallels that of the early phases of Ngauruhoe (Stage 1), leading to the possibility that Red Crater could develop into a larger, more explosive and more frequent eruption centre over time. If this is the case, it is very likely that observed Red Crater eruptions are at the lower end of the eruption magnitude than of those which might be produced from Red Crater in the future.

Figure 9.1: The cone of Red Crater in contrast to the larger cone of Ngauruhoe to the south. (photographer: Hans Aeschilmann).

The Te Maari craters, situated on the north-eastern slope of Mt. Tongariro are the most north-eastern eruption vent of a ~23 km-long TgVC-alignment stretching northward from Ruapehu. The glass chemistry from Holocene pyroclastic eruptives becomes more primitive along this alignment toward the north-east. The latest eruption of Te Maari Craters in the late 1890s however, produced high-silica glass (SiO_2 69-76 wt%), similar to that of Taranaki-derived tephras, while the associated lava flows are more of a basaltic-andesitic composition. This difference could indicate that the magma has undergone significant shallow-level assimilation-fractional crystallisation processes before erupting or could also indicate a partial melting of the crust and/or mixing of magmas. That eruptives with high silica glass composition occur in the TgVC was little known, but if this also indicates a high degree of explosivity and has major implications for hazard evaluation in the TgVC.

The eruption history of all three active Tongariro cones delivers an interesting insight of the eruption behaviour of a volcano with multiple vents. The activity of Mt. Tongariro over the last 12 000 cal yrs. B.P. has been dominated by the initial effusive and later explosive eruption episodes from Mt. Ngauruhoe. Red Crater seems to have been active since at least 4000 cal yrs. B.P., the same time span in which Ngauruhoe delivered explosive eruptions. An important question is whether active vents of Mt. Tongariro follow a certain pattern where the behaviour of one vent, e.g. Red Crater's birth with effusive eruptions, depends on the behaviour of another, such as Ngauruhoe becoming more explosive. While Ngauruhoe's activity and magnitude declines, Red Crater could become more explosive and more frequently active. The distinctive glass compositions for each of the analysed volcanoes from the TgVC implies independent magma plumbing systems, which has also been concluded from petrological studies of lavas in this area. Independence between magma feeding systems may imply no systematic pattern of eruptions between volcanoes of the TgVC. However, the new detailed pre-historic eruption record developed in this thesis shows that there is at least an antithetic relationship between major bursts of explosive activity of Ngauruhoe versus Ruapehu. Such patterns and any other apparent relationships between co-occurrence of eruptions from TgVC should form part of any future probabilistic hazard assessment.

Numerous andesitic volcanoes worldwide produce frequent small-scaled eruptions (VEI 1-4) such as Arenal (Costa Rica), Etna (Italy), Fuego (Guatemala) Galeras (Colombia), Kanlaon (Philippines), Kliuchevskoi (Kamchatka), Lascar (Chile), Llaima (Chile), Masaya (Nicaragua), Mayon (Philippines), Merapi (Indonesia), Okmok (Alaska), Pavlov (Alaska), Popocatépetl (Mexico), Rabaul (Papua New Guinea), Sakurajima (Japan), Semeru (Indonesia), Stromboli (Italy), Yake-dake (Japan) and Yasur (Vanuatu), and this shows the importance and the demand of studying these small eruptions. In countries like Indonesia and Philippines, Japan, Vanuatu, people live close to volcanoes because of limited space in the mostly densely populated areas but also because the soils are very fertile. Volcanic eruptions in these areas not only cause the largest damage to surrounding landscape but also have the biggest impact on people's lives (Blong, 1984, Johnston *et al.*, 2000; Cronin and Sharp, 2002).

The results of this study, using the tephrochronological record of the TgVC over the last 12 000 cal yrs. B.P., give an idea how andesitic stratovolcanoes individually behave over their entire life span or a certain time period, but is seems also possible to get an insight of how volcanic centres grow and how volcanoes of such a centre depend and/or relate to each other.

9.3. Future work

The results of this study provide a new fundamental basis upon which probabilistic hazard assessments can be made for the TgVC. Along with shedding light on the birth, development and apparent waning of activity at Ngauruhoe and insights into the other volcanoes, these new data also raises further questions on how the TgVC-volcanoes and their magma systems behave.

The three main questions for people who live in the Central North Island of New Zealand, and with the decision makers, utilities companies and businesses are: Which volcano(es) will erupt next? When will it happen? And how will it affect us?

1. To forecast the next eruption within the TgVC, it is important to understand, amongst other things, its historic and prehistoric eruption behaviour and frequency. This study has improved the Holocene tephrochronological record of the TgVC volcanoes, but this has been limited by the difficulty of correlating individual tephra units, as well as the lack of preservation of deposits from smaller scaled eruptions (≤ VEI 2) and the lack of suitable deposition sites for precise radiocarbon dating. The stratigraphy and frequency of Ngauruhoe sourced tephras as well as age calculations based on the stratigraphy at Loc. 63 suggest that a gap in the stratigraphy occurs between 1717 and 981 cal. yrs. B.P. In this time frame, immediately following the landscape-altering Taupo eruption, no exposure was clearly identified with tephras representing any of the volcanoes from the TgVC. Future work should seek out new sites to study the detailed stratigraphy immediately above the distinctive Taupo Pumice, especially sites that contains both Ngauruhoe and Ruapehu-derived tephras. This would lead to a more complete

eruption frequency and tephrostratigraphic record for both volcanoes. In addition, extending the detailed tephrochronology study back in time would help to understand the broad overall activity rate at these volcanoes. In particular, hazard studies need to take into account the transition (and the reasons for it) that occurred between the high-frequency and high-magnitude Bullot Formation activity and the smaller scaled volcanism that followed.

2. A direct follow-up activity from this tephrochronological work should be to develop appropriate statistical models from the tephra magnitude and frequency data to produce a probabilistic eruption forecast for the TgVC volcanoes using methods such as in Bebbington (2008) and Turner *et al.* (2008a). This would require consideration of alternative means of combining the historical and the stratigraphic eruption record. This task remains difficult for the TgVC, because of the apparent differences in magnitude between observed events and the absence of useful deposits to compare with the pre-historic ones.

3. As shown in Chapters 5 and 8, only two tephra units sourced from Ngauruhoe could be correlated. For Ruapehu, tephra correlations were only established for Tufa Trig Formation Members Tf5, Tf6, Tf8 and Tf14 (Donoghue, 1991; Donoghue *et al.*, 1995). This could be possibly improved by the application of trace-element geochemistry, but this would be an expensive and extremely time-consuming task. Also, to further understand the eruption mechanisms at work during these small-scaled eruptions additional field-based studies will likely yield few new results. Other methodologies must be applied to the existing deposits, including attempting numerical modelling of eruption plumes and "inverse" application of tephra dispersal models to specific well-preserved deposit sequences (Connor *et al.*, 2001; Bonadonna *et al.*, 2005a).

4. Strontium isotopic analyses were carried out on only 12 Ngauruhoe-sourced tephras, but these showed interesting and apparently systematic variations in the magma-crust interaction over the life of this volcano. This indicates that the volcanism type and scale may be correlate with the deep magmatic processes. Extending this isotopic study to further Ngauruhoe and Red Crater tephras may

provide new light on the details of magma storage and recharge below the TgVC and help understand the differences between Tongariro and Ruapehu volcanic and magmatic systems.

5. Magma fragmentation mechanisms of the post 12 000 cal. yrs. B.P. tephras from the TgVC appear to be the result of a complex range in combinations of phreatomagmatic and magmatic processes. These tephras are typically very fine grained, implying some degree of phreatomagmatism, although the relative influences of external water and magmatic gases remain poorly known. To address this, melt inclusions within phenocrysts (and perhaps the phenocrysts themselves) as well as residual volcanic glass could be analysed for volatile contents using techniques such as Fourier Transform Infrared (FTIR) Spectroscopy. This may help to elucidate original magma compositions and explain changes upon rise, crustal storage and during eruption.

6. What generates changes between periods of dominantly effusive versus explosive volcanism? For Ngauruhoe and possibly also Red Crater, the initial stages of volcanism were effusive and they evolved to produce more explosive eruptions. Is the size or geometry of a cone responsible, in particular the height of a cone above the surrounding landscape? By analysing the volatile content in detail of eruptive products from early to late stages in the evolution of Ngauruhoe, it may be possible to understand the extra evolution and degassing required for magmas to erupt from a high cone compared to when little or no edifice was present.

7. Red Crater is located at the highest point of the “Tongariro Crossing” one of the most-walked day tracks in New Zealand. The results of this thesis show that Red Crater is possibly only the very early stages of a volcano that can potentially produce larger and more violent eruptions (> VEI 2). This hazard potential suggests that a more comprehensive study of Red Crater is warranted.

Bibliography

Allan, A.S.R., Baker, J.A., Carter, L. and Wysoczanksi, R.J., (2008). Reconstructing the Quaternary evolution of the world's most active silicic volcanic system: insights from an ~1.65 Ma deep ocean tephra record sourced from Taupo Volcanic Zone, New Zealand. Quaternary Science Reviews, 27(25-26): 2341-2360.

Allen, L.R., (1948). Activity at Ngauruhoe, April-May 1948. New Zealand Journal of Science and Technology, 30: 187-193.

Allen, L.R., (1949). The eruption of Ngauruhoe, February-March, 1949. New Zealand Science Review, 7(10): 180-183.

Alloway, B., Neall, V.E. and Vucetich, C.G., (1995). Late Quaternary (post 28,000 year B.P.) tephrostratigraphy of northeast and central Taranaki, New Zealand. Journal of Royal Society of New Zealand, 25(4): 385-458.

Alloway, B.V., Neall, V.E. and Vucetich, C.G., (1988). Localised volcanic loess deposits in North Taranaki, North Island, New Zealand. In: D.N. Eden and R.J. Furkert (Editors), Loess-Its distribution, geology and soils, Rotterdam, pp. 1-6.

Alloway, B.V., (1989). The late Quaternary cover bed stratigraphy and tephrochronology of north-eastern and central Taranaki, New Zealand. Unpublished Ph.D. Thesis, Massey University, Palmerston North.

Alloway, B.V., Lowe, D.J., Chan, R.P.K., Eden, D. and Froggatt, P., (1994). Stratigraphy and chronology of the Stent Tephra, a C-4000 year-old distal silicic tephra from Taupo-Volcanic-Centre, New-Zealand. New Zealand Journal of Geology and Geophysics, 37(1): 37-47.

Andreastuti, S.D., Alloway, B.V. and Smith, I.E.M., (2000). A detailed tephrostratigraphic framework at Merapi Volcano, Central Java, Indonesia: implications for eruption predictions and hazard assessment. Journal of Volcanology and Geothermal Research 100: 51-67.

Andres, R.J., Kyle, P.R. and Chuan, R.L., (1993). Sulphur dioxide, particle and elemental emissions from Mount Etna, Italy during July 1987. Geologische Rundschau 82(4): 687-695.

Armienta, M.A., De la Cruz-Reyna, S. and Macías, J.L., (2000). Chemical characteristics of the crater lakes of Popocatepetl, El Chichon, and Nevado de Toluca volcanoes, Mexico Journal of Volcanology and Geothermal Research, 97(1-4).

Arrighi, S., Principe, C. and Rosi, M., (2001). Violent strombolian and subplinian eruptions at Vesuvius during post- 1631 activity. Bulletin of Volcanology, 63: 126-150.

Badrudin, M., (1994). Kelut volcano monitoring: Hazards, mitigation and changes in water chemistry prior to the 1990 eruption. Geochemical Journal, 28(3): 233-241.

Ballance, P.F., Ablaev, A.G., Pushchin, I.K., Pletnev, S.P., Birylina, M.G., Itaya, T., Follas, H.A. and Gibson, G.W., (1999). Morphology and history of the Kermadec trench-arc-backarc basin-remnant arc system at 30 to 32 degrees S:

geophysical profile, microfossil and K-Ar data. Marine Geology, 159(1-4): 35-62.

Barberi, F., Cioni, R., Rosi, M., Santacroce, R., Sbrana, A. and Vecci, R., (1989). Magmatic and Phreatomagmatic Phases in Explosive Eruptions of Vesuvius as Deduced by Grain-Size and Component Analysis of the Pyroclastic Deposits. Journal of Volcanology and Geothermal Research, 38(3-4): 287-307.

Barberi, F., Bertagnini, A., Landi, P. and Principe, C., (1992). A review on phreatic eruptions and their precursors. Journal of Volcanology and Geothermal Research, 52(4): 231-246.

Bardsley, C.J., (2004). Physical volcanology of Red Crater, Tongariro. Unpublished M.Sc. Thesis, University of Waikato, Hamilton, 209 pp.

Basher, R., (2005). Physical Volcanology and future volcanic risk from Te Maari Craters, Tongariro. Unpublished M.Sc. Thesis, University of Waikato, Hamilton, 160 pp.

Baumgart, I.L., (1954). Some ash showers of the Central North Island. N.Z. Journal of Science and Technology, B35: 456-467.

Bebbington, M.S. and Lai, C.D., (1996). Statistical analysis of New Zealand volcanic occurrence data. Journal of Volcanology and Geothermal Research, 74(1-2): 101-110.

Bebbington, M.S., (2008). Incorporating the eruptive history in a stochastic model for volcanic eruptions. Journal of Volcanology and Geothermal Research, 175(3): 325-333.

Beck, A.C., (1951). Volcanic activity at Mt. Ruapehu from August to December, 1945. New Zealand Journal of Science and Technology, B31(5): 1-13.

Bibby, H.M., Caldwell, T.G., Davey, F.J. and Webb, T.H., (1995). Geophysical evidence on the structure of the Taupo Volcanic Zone and its hydrothermal circulation. Journal of Volcanology and Geothermal Research, 68(1-3): 29-58.

Bibby, H.M., Risk, G.F. and Caldwell, T.G., (2002). Long offset tensor apparent resistivity surveys of the Taupo Volcanic Zone, New Zealand. Journal of Applied Geophysics, 49(1-2): 17-32.

Bildwill, J.C., (1841). "Rambles in New Zealand". 1st ed. Orr, London: 104 pp.

Birkeland, P.W., (1974). Pedology, weathering and geomorphological research. Oxford University Press, New York, 285 pp.

Blackburn, E.A., Wilson, L. and Sparks, R.S.J., (1976). Mechanisms and dynamics of strombolian activity. Journal of the Geological Society London, 132: 429-440.

Blong, R.J., (1984). Volcanic Hazards- A source book on the effects of Eruptions. Academic Press, Sydney, 424 pp.

Boddington, T., Perkins, C.J. and Gubbins, D., (2004). Isolated deep earthquakes beneath the North Island of New Zealand. Geophys. J. Int., 158: 972-982.

Bonadonna, C., Ernst, G.G.J. and Sparks, R.S.J., (1998). Thickness variations and volume estimates of tephra fall deposits: the importance of particle Reynolds number. Journal of Volcanology and Geothermal Research, 81(3-4): 173-187.

Bonadonna, C., Connor, C.B., Houghton, B.F., Connor, L., Byrne, M., Laing, A. and Hincks, T.K., (2005a). Probabilistic modelling of tephra dispersal: Hazard assessment of a multiphase rhyolitic eruption at Tarawera, New Zealand. Journal of Geophysical Research, 110.

Bonadonna, C. and Houghton, B.F., (2005). Total grain-size distribution and volume of tephra-fall deposits. Bulletin of Volcanology, 67(5): 441-456.

Bonadonna, C., Phillips, J.C. and Houghton, B.F., (2005b). Modelling tephra sedimentation from a Ruapehu weak plume eruption. Journal of Geophysical Research-Solid Earth, 110(B8).

Bourdier, J.L., Boudon, G. and Gourgaud, A., (1989). Stratigraphy of the 1902 and 1929 nuée-ardente deposits, Mt. Pelée, Martinique Journal of Volcanology and Geothermal Research, 38(1-2): 77-96.

Branca, S. and Del Carlo, P., (2005). Types of eruptions of Etna volcano AD 1670–2003: implications for short-term eruptive behaviour. Bulletin of Volcanology, 67(8): 732-742.

Büttner, R., Dellino, P. and Zimanowski, B., (1999). Indentifying magma-water interaction from surface features of ash particles. Nature, 401: 688-690.

Büttner, R., Dellino, P., La Volpe, L., Lorenze, V. and Zimanowski, B., (2002). Thermohydraulic explosions in phreatomagmatic eruptions as evidenced by the comparison between pyroclasts and products from molten fuel coolant interaction experiments. Journal of Geophysical Research 107: 2277.

Capaccioni, B. and Coniglio, S., (1995). Varicolored and Vesiculated Tuffs from La-Fossa Volcano, Vulcano Island (Aeolian Archipelago, Italy) - Evidence of Syndepositional Alteration Processes. Bulletin of Volcanology, 57(1): 61-70.

Carey, S., Sigurdsson, H., Gardner, J.E. and Criswell, W., (1990). Variations in column height and magma discharge during the May 18, 1980 eruption of Mount St. Helens Journal of Volcanology and Geothermal Research, 43(1-4): 99-112.

Carter, L., Nelson, C.S., Neil, H.L. and Froggatt, P.C., (1995). Correlation, dispersal, and preservation of the Kawakawa Tephra and other late Quaternary tephra layers in the Southwest Pacific Ocean. New Zealand Journal of Geology and Geophysics, 38: 29-46.

Cas, R.A.F. and Wright, J.V., (1988). Volcanic Successions: modern and ancient. Academic Division of Unwin Hyman Ltd., London, pp. 528 pp.

Cashman, K. and Blundy, J., (2000). Degassing and crystallization of ascending andesite and dacite. Philosophical Transactions of the Royal Society of London Series a-Mathematical Physical and Engineering Sciences, 358(1770): 1487-1513.

Cashman, K.V., Sturtevant, B., Papale, P. and Navon, O., (2000). Magmatic Fragmentation. In: H. Sigurdsson (Editor), Encyclopedia of Volcanoes. Academic Press, pp. 421-430.

Cassidy, J., Ingham, M., Locke, C.A. and Bibby, H., (2009). Subsurface structure across the axis of the Tongariro Volcanic Centre, New Zealand. Journal of Volcanology and Geothermal Research, 179(3-4): 233-240.

Chinn, T.J., (2001). Distribution of the glacial water resources of New Zealand. J. Hydrology (NZ), 40(2): 139-187.

Christenson, B.W. and Wood, C.P., (1993). Evolution of a vent-hosted hydrothermal system beneath Ruapehu Crater Lake, New-Zealand. Bulletin of Volcanology, 55(8): 547-565.

Christenson, B.W., Reyes, A.G., Young, R., Moebis, A., Sherburn, S., Cole-Baker, J. and Britten, K., (2010). Cyclic processes and factors leading to phreatic eruption events: Insights from the 25 September 2007 eruption through Ruapehu Crater Lake, New Zealand. Journal of Volcanology and Geothermal Research, 191(1-2): 15-32.

Cioni, R., Marianelli, P., Santacroce, R. and Sbrana, A., (2000). Plinian and subplinian eruptions. In: H. Sigurdsson (Editor), Encyclopedia of Volcanoes. Academic Press, San Diego, pp. 477-495.

Cloud, P.E., (1951). The 1949 Eruption of Ngauruhoe. The Scientific Monthly, 72(4): 241-251.

Cole, J.W., (1978). Andesites of Tongariro Volcanic Centre, North Island, New-Zealand. Journal of Volcanology and Geothermal Research, 3(1-2): 121-153.

Cole, J.W., Graham, I.J., Hackett, W.R. and Houghton, B.F., (1986). Volcanology and Petrology of Quaternary Composite Volcanoes of Tongariro Volcanic Centre, Taupo Volcanic Zone. In Smith, I.E. (Ed.): The Royal Society of New Zealand Bulletin 23: 224 – 250.

Cole, P.D., G., Q., Wallenstein, N., Gaspar, J.L., Duncan, A.M. and Guest, J.E., (1995). An historic subplinian/phreatomagmatic eruption: the 1630 AD eruption of Furnas volcano, São Miguel, Azores Journal of Volcanology and Geothermal Research, 69(1-2): 117-135.

Connor, C.B., Hill, B.E., Winfrey, B., Franklin, N.M. and La Femina, P.C., (2001). Estimation of volcanic hazards from tephra fallout. Natural Hazards Review, 2(1): 33-42.

Coote, G.E., Cutress, T.W. and Suckling, G.W., (1997). Uptake of fluoride into developing sheep teeth, following the 1995 volcanic eruption of Mt. Ruapehu, New Zealand. Nuclear Instruments & Methods in Physics Research Section B-Beam Interactions with Materials and Atoms, 130(1-4): 571-575.

Cotton, C.A., (1944). Volcanoes as Landscape Forms. Whitecombe and Tombs, 1st edition, Christchurch, 416 pp.

Cotton, C.A., (1945). Ruapehu in 1945. N.Z. Sci. Rev., 3: 3-4.

Cowan, J., (1927). "The Tongariro National Park, New Zealand". Tongariro National Park Board, Wellington: 156 pp.

Cronin, S.J., (1996). Late quaternary volcanic stratigraphy within a portion of the north-eastern Tongariro Volcanic Centre. Unpublished Ph.D. Thesis, Massey University, Palmerston North, 147 pp.

Cronin, S.J., Neall, V.E. and Palmer, A.S., (1996a). Investigation of an aggrading paleosol developed into andesitic ring-plain deposits, Ruapehu volcano, New Zealand. Geoderma, 69(1-2): 119-135.

Cronin, S.J., Neall, V.E., Lecointre, J. and Palmer, A.S., (1996b). Unusual "snow slurry" lahars from Ruapehu volcano, New Zealand, September 1995. Geology, 24(12): 1107-1110.

Cronin, S.J., Wallace, R.C. and Neall, V.E., (1996d). Sourcing and identifying andesitic tephras using major oxide titanomagnetite and hornblende chemistry, Egmont volcano and Tongariro Volcanic Centre, New Zealand. Bulletin of Volcanology, 58(1): 33-40.

Cronin, S.J., Hedley, M.J., Smith, R.G. and Neall, V.E., (1997a). Impact of Ruapehu ash fall on soil and pasture nutrient status .1. October 1995 eruptions. New Zealand Journal of Agricultural Research, 40(3): 383-395.

Cronin, S.J., Neall, V.E., Lecointre, J.A. and Palmer, A.S., (1997c). Changes in Whangaehu river lahar characteristics during the 1995 eruption sequence, Ruapehu volcano, New Zealand. Journal of Volcanology and Geothermal Research, 76(1-2): 47-61.

Cronin, S.J., Neall, V.E., Palmer, A.S. and Stewart, R.B., (1997d). Methods of identifying late Quaternary rhyolitic tephras on the ring plains of Ruapehu and Tongariro volcanoes, New Zealand. New Zealand Journal of Geology and Geophysics, 40(2): 175-184.

Cronin, S.J., Hedley, M.J., Neall, V.E. and Smith, R.G., (1998). Agronomic impact of tephra fallout from the 1995 and 1996 Ruapehu Volcano eruptions, New Zealand. Environmental Geology, 34: 21-30.

Cronin, S.J. and Sharp, D.S., (2002). Environmental impacts on health from continuous volcanic activity at Yasur (Tanna) and Ambrym, Vanuatu. International Journal of Environmental Health Research 12: 109-123.

Cronin, S.J., Neall, V.E., Lecointre, J.A., Hedley, M.J. and Loganathan, P., (2003). Environmental hazards of fluoride in volcanic ash: a case study from Ruapehu volcano, New Zealand. Journal of Volcanology and Geothermal Research, 121(3-4): 271-291.

Darby, D. and Meertens, C.M., (1995). Terrestrial and GPS measurements of deformation across the Taupo back arc and Hikurangi forearc regions in New Zealand. Journal of Geophysical Research, 100: 8221-8231.

Darragh, M., Cole, J., Nairn, I. and Shane, P., (2006). Pyroclastic stratigraphy and eruption dynamics of the 21.9 ka Okareka and 17.6 ka Rerewhakaaitu eruption episodes from Tarawera Volcano, Okataina Volcanic Centre, New Zealand. New Zealand Journal of Geology & Geophysics, 49: 309-328.

De Astis, G., Dellino, P., De Rosa, R. and La Volpe, L., (1997). Eruptive and emplacement mechanisms of widespread fine-grained pyroclastic deposits on Vulcano Island (Italy). Bulletin of Volcanology, 59: 87-102.

Dellino, P. and La Volpe, L., (1995). Fragmentation Versus Transportation Mechanisms in the Pyroclastic Sequence of Monte-Pilato Rocche-Rosse (Lipari, Italy). Journal of Volcanology and Geothermal Research, 64(3-4): 211-231.

Dellino, P. and Volpe, L., (1996). Image processing analysis in reconstructing fragmentation and transportation mechanisms of pyroclastic deposits. The case of Monte Pilato-Rocche Rosse eruptions, Lipari (Aeolian islands, Italy). Journal of Volcanology and Geothermal Research, 71: 13-29.

Dellino, P., Isaia, R., La Volpe, L. and Orsi, G., (2001). Statistical analysis of textural data from complex pyroclastic sequences: implications for fragmentation processes of the Agnano-Monte Spina Tephra (4.1 ka), Phlegraean Fields, southern Italy. Bulletin of Volcanology, 63(7): 443-461.

Dellino, P. and Kyriakopoulos, K., (2003). Phreatomagmatic ash from the ongoing eruption of Etna reaching the Greek island of Cefalonia. Journal of Volcanology and Geothermal Research, 126: 341-345.

DeMets, C., Gordon, R.G., Argus, D.F. and Stein, S., (1994). Effect of recent revisions to the geomagnetic reversal time scale on estimates of current plate motions. Geophysical Research Letters, 21: 2191-2194.

Dingwell, D.B., (2001). Magma degassing and fragmentation: Recent experimental advances. In: A. Freundt and M. Rosi (Editors), From magma to tephra. Elservier, Amsterdam, pp. 318.

Donoghue, S.L., (1991). Late Quaternary volcanic stratigraphy of the south-eastern sector of the Mount Ruapehu Ring Plain, New Zealand. unpublished PhD Thesis, Massey University, Palmerston North, 336 pp.

Donoghue, S.L., Stewart, R.B. and Palmer, A.S., (1991). Morphology and Chemistry of Olivine Phenocrysts of Mangamate Tephra, Tongariro Volcanic Centre, New-Zealand. Journal of the Royal Society of New Zealand, 21(3): 225-236.

Donoghue, S.L., Neall, V.E. and Palmer, A.S., (1995). Stratigraphy and Chronology of Late Quaternary Andesitic Tephra Deposits, Tongariro-Volcanic-Centre, New-Zealand. Journal of the Royal Society of New Zealand, 25(2): 115-206.

Donoghue, S.L., Neall, V.E., Palmer, A.S. and Stewart, R.B., (1997). The volcanic history of Ruapehu during the past 2 millennia based on the record of Tufa Trig tephras. Bulletin of Volcanology, 59(2): 136-146.

Donoghue, S.L., Palmer, A.S., McClelland, E., Hobson, K., Stewart, R.B., Neall, V.E., Lecointre, J. and Price, R., (1999). The Taurewa Eruptive Episode: evidence for climactic eruptions at Ruapehu volcano, New Zealand. Bulletin of Volcanology, 61(4): 223-240.

Druce, A.P., (1966). Tree-ring dating of recent volcanic ash and lapilli, Mt. Egmont. N.Z. Journal of Botany, 4: 3-41.

Eden, D.N. and Froggatt, P.C., (1996). A 6500-year-old history of tephra deposition recorded in the sediments of Lake Tutira, eastern North Island, New Zealand. Quaternary International, 34-6: 55-64.

Electricity Corporation of New Zealand Limited, (1994). Tongariro, a guide to the Tongariro power Scheme, Wellington.

Ewart, A., (1963). Petrology and petrogenesis of the Quaternary pumice ash in the Taupo area, New Zealand. Journal of Petrology, 4(3): 392-&.

Ewart, A., (1967). Pyroxene and magnetite phenocrysts from Taupo Quaternary rhyolitic pumice deposits, New Zealand. Mineralogical Magazine and Journal of the Mineralogical Society, 36(278): 180-&.

Ewart, A., (1971). Notes on chemistry of ferromagnesian phenocrysts from selected volcanic rocks, Central Volcanic Region. New Zealand Journal of Geology and Geophysics, 14(2): 323-&.

Fergusson, G.J. and Rafter, T.A., (1959). New Zealand ^{14}C Age Measurements-4. New Zealand Journal of Geology and Geophysics, 2: 208-241.

Fierstein, J. and Nathenson, M., (1992). Another look at the calculation of fallout tephra volumes. Bulletin of Volcanology, 54(2): 156-167.

Fisher, R.V., Smith, A.L. and Roobol, M.J., (1980). Destruction of St. Pierre, Martinique, by ash-cloud surges, May 8 and 20, 1902. Geology, 8(10): 472-476.

Fisher, R.V. and Schmincke, H.U., (1984). Pyroclastic Rocks. Springer Verlag, Berlin, Heidelberg, New York, Tokyo, 472 pp.

Fleming, (1953). The geology of Wanganui subdivision. New Zealand Geological Survey bulletin, 52: 362 pp.

Formenti, Y., Druitt, T.H. and Kelfoun, K., (2003). Characterisation of the 1997 Vulcanian explosions of Soufriere Hills Volcano, Montserrat, by video analysis. Bulletin of Volcanology, 65(8): 587-605.

Francis, P. and Oppenheimer, C., (2004). Volcanoes. Oxford University Press, New York, 521 pp.

Franks, A.M., (1984). Soils of Eltham County and the Tephrochronology of Central Taranaki. Unpublished PhD Thesis, Massey Univeristy, Palmerston North.

Frazzetta, G., Lavolpe, L. and Sheridan, M.F., (1983). Evolution of the Fossa Cone, Vulcano. Journal of Volcanology and Geothermal Research, 17(1-4): 329-360.

Freundt, A. and Rosi, M., (2001). From Magma to Tephra. Elsevier, Amsterdam, Lausanne, New York, Oxford, Shannon, Singapore, Tokyo, 318 pp.

Friedrich, W.L., Kromer, B., Friedrich, M., Heinemeier, J., Pfeiffer, T. and Talamo, S., (2006). Santorini Eruption radiocarbon dated to 1627-1600 B.C. Science 28.

Fritsch, F.N. and Carlson, R.E., (1980). Monotone piecewise cubic interpolation. SIAM J Numer Anal, 17: 238-246.

Froggatt, P., (1983). Toward a comprehensive upper Quaternary tephra and ignimbrite stratigraphy in New Zealand using electron-microprobe analysis of glass shards. Quaternary Research, 19: 188-200.

Froggatt, P.C., (1981a). Stratigraphy and nature of Taupo Pumice Formation. New Zealand Journal of Geology and Geophysics, 24(2): 231-248.

Froggatt, P.C., (1981b). Motutere Tephra Formation and re-definition of Hinemaiaia Tephra Formation, Taupo Volcanic Centre, New Zealand. New Zealand Journal of Geology and Geophysics, 24(1): 99-105.

Froggatt, P.C., (1981c). Karapiti Tephra Formation - a 10000 years BP rhyolitic Tephra from Taupo. New Zealand Journal of Geology and Geophysics, 24(1): 95-98.

Froggatt, P.C., (1982). Review of methods of estimating rhyolitic tephra volumes - applications to the Taupo volcanic Zone, New Zealand. Journal of Volcanology and Geothermal Research, 14(3-4): 301-318.

Froggatt, P.C. and Lowe, D.J., (1990). A Review of Late Quaternary silicic and some other tephra formations from New-Zealand - their stratigraphy, nomenclature, distribution, volume, and age. New Zealand Journal of Geology and Geophysics, 33(1): 89-109.

Froggatt, P.C. and Rogers, G.M., (1990). Tephrostratigraphy of high-altitude peat bogs along the axial ranges, North Island, New-Zealand. New Zealand Journal of Geology and Geophysics, 33(1): 111-124.

Fundali, R.F. and Melson, W.G., (1971). Ejecta velocities, magma chamber pressure and kinetic energy associated with the 1968 eruption of Arenal Volcano. Bulletin of Volcanology, 35: 383-401.

Gamble, J.A., Wood, C.P., Price, R.C., Smith, I.E.M., Stewart, R.B. and Waight, T., (1999). A fifty year perspective of magmatic evolution on Ruapehu Volcano, New Zealand: verification of open system behaviour in an arc volcano. Earth and Planetary Science Letters 170: 310-314.

Gamble, J.A., Price, R.C., Smith, I.E.M., McIntosh, W.C. and Dunbar, N.W., (2003). 40Ar/39Ar geochronology of magmatic activity, magma flux and hazards at Ruapehu volcano, Taupo Volcanic Zone, New Zealand. Journal of Volcanology and Geothermal Research 120, 120(3): 271-287.

Gardner, C.A., Cashman, K.V. and Neal, C.A., (1998). Tephra-fall deposits from the 1992 eruption of Crater Peak, Alaska: implications of clast textures for eruptive processes. Bulletin of Volcanology, 59(8): 537-555.

Germanovich, L.N. and Lowell, R.P., (1995). The Mechanism of Phreatic Eruptions. Journal of Geophysical Research-Solid Earth, 100(B5): 8417-8434.

Gill, J.B., Morris, J.D. and Johnson, R.W., (1993). Timescale for producing the geochemical signature of Island-Arc-Magmas - U-Th-Po and Be-B systematics in recent Papua-New-Guinea lavas. Geochimica Et Cosmochimica Acta, 57(17): 4269-4283.

Gorton, M.P., (1968). A description of a group of explosion craters at Ohakune. Unpublished Bsc (Hons.) Thesis, Victoria University, Wellington.

Gow, A.J., (1968). Petrographic and petrochemical studies of Mt Egmont andesites. New Zealand Journal of Geology and Geophysics, 11(1): 166-&.

Graham, I.J. and Hackett, W.R., (1987). Petrology of calc-alkaline lavas from Ruapehu volcano and related vents, Taupo Volcanic Zone, New Zealand. Journal of Petrology, 28: 531-567.

Graham, I.J., Grapes, R.H. and Kifle, K., (1988). Buchitic metagreywacke xenoliths from Mt. Ngauruhoe, Taupo Volcanic Zone, New Zealand. Journal of Volcanology and Geothermal Research, 35(3): 205-216.

Graham, I.J., Cole, J.W., Briggs, R.M., Gamble, J.A. and Smith, I.E.M., (1995). Petrology and petrogenesis of volcanic rocks from the Taupo Volcanic Zone: a review. Journal of Volcanology and Geothermal Research, 68: 59-87.

Grange, L.I. and Williamson, J.H., (1930). Tongariro Subdivision. N.Z. Geological Survey 24th Annual Report: 10-3.

Grange, L.I., (1931). Volcanic Ash showers: a geological reconnaissance of volcanic ash showers of the central part of the North Island. N.Z. Journal of Science, 12: 228-240.

Grange, L.I. and Taylor, N.H., (1933). Report on soil surveys for 1932-1933. N.Z. Department of Scientific and Industrial Research, Annual Report 1932-33.

Grange, L.I., Williamson, J.H. and Hurst, J.A., (1938). Geological maps of Tongariro Subdivision, to accompany. N.Z. Geological Survey Bulletin, 40: 4 sheets.

Grant, S., (2006). Tertiary and Quaternary volcanics interface at Mt. Ruapehu, North Island, New Zealand. Unpublished B.Sc.-Honours Thesis, Massey University, Palmerston North.

Green, J.D. and Lowe, D.J., (1985). Stratigraphy and development of c.17000 year old Lake Maratoto, North Island, New Zealand, with some inference about postglacial climate change. New Zealand Journal of Geology and Geophysics, 28(4): 675-699.

Greenway, R.D., (1998). The restless Land; Stories of Tongariro National Park-World Heritage Area. Tongariro/Taupo Conservancy, Department of Conservation and Tongariro National History Society, Turangi, 156 pp.

Gregg, D.R., (1956). Eruption of Ngauruhoe 1954-55. N.Z.J. Sci. Tech, B37: 675-688.

Gregg, D.R., (1960a). The Geology of Tongariro Subdivision. N.Z. Geological Survey Bulletin 40.

Gregg, D.R., (1960b). Volcanoes of Tongariro National Park N.Z. DSIR Information Series 28. Department of Scientific and Industrial Research, 82 pp.

Griffin, A.M., (2007). Products and processes of cone-building eruptions from North Crater, Tongariro. Unpublished M.Sc.- Thesis, University of Waikato, Hamilton.

Grindley, G.W., (1960). Geological map of New Zealand, 1st ed., 1: 250 000, Sheet 8, Taupo. D.S.I.R., Wellington.

Gromme, S., (1982). Origin of natural remnant magnetization of tephra from the 1979 Surtsey drill hole, Iceland. Surtsey Research Progress Reports: 111-116.

Hackett, W.R., (1985). Geology and petrology of Ruapehu volcano and related vents. Unpublished Ph.D. Thesis, Victoria University, Wellington, 312 pp.

Hackett, W.R. and Houghton, B.F., (1989). A Facies Model for a Quaternary Andesitic Composite-Volcano - Ruapehu, New-Zealand. Bulletin of Volcanology, 51(1): 51-68.

Hales, T.C., (2000). The geology of the summit area, Mt. Ruapehu. Unpublished BSc.(Hons) Thesis, Massey University, Palmerston North, 123 pp.

Hammer, J.E., Cashman, K.V., Hoblitt, R.P. and Newman, S., (1999). Degassing and microlite crystallization during pre-climactic events of the 1991 eruption of Mt. Pinatubo, Philippines. Bulletin of Volcanology, 60: 355-380.

Harlen, L., (1999). From 'useless' lands to world heritage: a history of tourism in Tongariro National Park. Unpublished MSc.-Thesis Thesis, Massey University, Palmerston North 141 pp.

Harpel, C.J., Kyle, P.R. and Dunbar, N.W., (2008). Englacial tephrostratigraphy of Erebus volcano, Antarctica. Journal of Volcanology and Geothermal Research, 177(3): 549-568.

Healy, J., (1954). Origin of flood and Ruapehu lahars In: Tangiwai Railway Disaster. Report of Board of Inquiry. Government Printer, Wellington, N.Z.: 6-8 and 28-31.

Healy, J., (1964). Stratigraphy and Chronology of late Quaternary Volcanic Ash in Taupo, Rotorua, and Gisborne Districts, Part1. New Zealand Geological Survey, 73: 1-42.

Healy, J., Lloyed, E.F., Rishworth, D.E.H., Wood, C.P., Glover, R.B. and Dibble, R.R., (1978). The eruption of Ruapehu, New Zealand, on 22 June 1969. DSIR Bulletin, 217: 1-80.

Hector, J., (1887). Presidential Address. Transaction of the New Zealand Institute 19: 461-470.

Hedervari, P., (1963). On the energy and magnitude of volcanic eruptions. Bulletin of Volcanology, 25: 373-385.

Heiken, G., (1972). Morphology and Petrography of Volcanic Ashes. Geological Society of America Bulletin, 83(7): 1961-&.

Heiken, G. and Wohletz, K.H., (1985). Volcanic Ash. University of California Pres, Berkeley, Los Angeles, London, 246 pp.

Henderson, C., (2004). Pyroclastic flow deposits of the 1975 eruption of Mt. Ngauruhoe. Unpublished BSc (Hons) Thesis, Massey University, Palmerston North.

Hickling, J., Clements, M., Weinstein, P. and Woodward, A., (1999). Acute health effects of the Mount Ruapehu (New Zealand) volcanic eruption of June 1996. International Journal of Environmental Health Research, 9(2): 97-107.

Hill, (1891). Tongariro, Ngauruhoe and Ruapehu as Volcanic Cones, Rep. 3rd Meet. A'asian Ass. Advanc. Sci. pp. 162-172. In: Gregg, D.R., 1960b. Volcanoes of Tongariro National Park N.Z. DSIR Information Series 28. Department of Scientific and Industrial Research, 82 pp.

Hitchcock, D.W., (2005). The 9.7 B.P. Poutu Lapilli eruption (TgVC), and impacts of a similar future eruption. Unpublished M.Sc. Thesis, University of Canterbury, Canterbury, 189 pp.

Hobden, B.J., Houghton, B.F., Lanphere, M.A. and Nairn, I.A., (1996). Growth of the Tongariro volcanic complex: New evidence from K-Ar age determinations. New Zealand Journal of Geology and Geophysics, 39(1): 151-154.

Hobden, B.J., (1997). Modelling magmatic trends in time and space: eruptive and magmatic history of Tongariro Volcanic Complex, New Zealand. Unpublished Ph.D. Thesis, University of Canterbury, Christchurch, 508 pp.

Hobden, B.J., Houghton, B.F., Davidson, J.P. and Weaver, S.D., (1999). Small and short-lived magma batches at composite volcanoes: time windows at Tongariro volcano, New Zealand. Journal of Geological Society, London, 156: 865-868.

Hobden, B.J., Houghton, B.F. and Nairn, I.A., (2002). Growth of a young, frequently active composite cone: Ngauruhoe volcano, New Zealand. Bulletin of Volcanology, 64(6): 392-409.

Hodgson, K.A., (1993). Late Quaternary lahars from Mount Ruapehu in the Whangaehu River Valley, North Island, New Zealand. Unpublished Ph.D. Thesis, Massey University, Palmerston North, 256 pp.

Horrocks, M. and Ogden, J., (2000). Evidence for Late glacial and Holocene tree-line fluctuations from pollen diagrams from the Subalpine zone on Mt Hauhangatahi, Tongariro National Park, New Zealand. Holocene, 10(1): 61-73.

Houghton, B.F. and Hackett, W.R., (1984). Strombolian and phreatomagmatic deposits of Ohakune Craters, Ruapehu, New-Zealand - a complex interaction between external water and rising basaltic magma. Journal of Volcanology and Geothermal Research, 21(3-4): 207-231.

Houghton, B.F. and Schmincke, H.U., (1989). Rothenberg Scoria Cone, East Eifel - a complex strombolian and phreatomagmatic volcano. Bulletin of Volcanology, 52(1): 28-48.

Houghton, B.F. and Nairn, I.A., (1991). The 1976-1982 strombolian and phreatomagmatic eruptions of White Island, New-Zealand - eruptive and depositional mechanisms at a wet volcano. Bulletin of Volcanology, 54(1): 25-49.

Houghton, B.F., Wilson, C.J.N. and Pyle, D.M., (2000). Pyroclastic fall deposits. In: H. Sigurdsson (Editor), Encyclopedia of Volcanoes. Academic Press, pp. 555-570.

Howorth, R. and Ross, A., (1981). Holocene tephrostratigraphy and chronology at Tiniroto, Cook County. in: Howorth, R.; Froggatt, P.C.; Vucetich J.D.; Collen, J.D. (Eds): Proceedings of tephra Workshop, June 30th- July 1st 1980, pp 41-50 Publication N° 20 of Geology Department, Victoria University of Wellington.

Hurst, A.W., Bibby, H.M., Scott, B.J. and McGuinness, M.J., (1991). The heat-source of Ruapehu Crater Lake - deductions from the energy and mass balances. Journal of Volcanology and Geothermal Research, 46(1-2): 1-20.

Hurst, A.W. and Turner, R., (1999). Performance of the program ASHFALL for forecasting ashfall during the 1995 and 1996 eruptions of Ruapehu volcano. New Zealand Journal of Geology and Geophysics, 42(4): 615-622.

Itoh, H., Yoshida, M., Harada, N., Kusunoki, M. and Ui, T., (2004). Volcanic hazard assessment of the possible disasters using numerical simulations at Tokachidake volcano, Central Hokkaido, Northern Part of Japan.

Jamieson, K.M., (1974). Management of Contorta Pine regeneration in Karioi forest for production. New Zealand Journal of Forestry 19(1): 93-101.

Johnston, D.M. (1995). Ruapehu awakens, the 1945 eruption of Ruapehu, Massey University, Palmerston North, 28pp

Johnston, D.M., (1997). Physical and social impacts of past and future volcanic eruptions in New Zealand. Unpublished Ph.D.-Thesis, Massey University, Palmerston North

Johnston, D.M., (1997). Did Red Crater erupt in 1926? Geological Society of New Zealand Newsletter, 114: 15-16.

Johnston, D.M., Houghton, B.F., Neall, V.E., Ronan, K.R. and Paton, D., (2000). Impacts of the 1945 and 1995-1996 Ruapehu eruptions, New Zealand: An example of increasing societal vulnerability. Geological Society of America Bulletin, 112(5): 720-726.

Julian, S.R., Westgate, J.A., Daniels, J.M., Rancourt, D.G. and Sullivan, P., (1988). A comparison of the titanomagnetites produced by several volcanoes in Iceland. Hyperfine Interactions, 41(1): 807-810.

Kilgour, G., de la Pasqua, F., Jolly, A., Christenson, B. and Jolly, G., (2008). Directed blast deposits of the 25 September 2007 phreatic eruption at Mount Ruapehu, New Zealand, Geosciences 08, Joint annual conference, Wellington.

Kilgour, G., Manville, V., Della Pasqua, F., Graettinger, A., Hodgson, K.A. and Jolly, G.E., (2010). The 25 September 2007 eruption of Mount Ruapehu, New Zealand: Directed ballistics, surtseyan jets, and ice-slurry lahars. Journal of Volcanology and Geothermal Research, 191(1-2): 1-14.

Kohn, B.P., (1970). Identification of New Zealand Tephra-Layers by emission spectrographic analysis of their Titanomagnetites. Lithos, 3: 361-368.

Kohn, B.P., (1973). Some studies of New Zealand Quaternary pyroclastic rocks. Unpublished Ph.D. Thesis, Victoria University Wellington, 340 pp.

Kohn, B.P. and Neall, V.E., (1973). Identification of Late Quaternary tephras for dating Taranaki lahar deposits. New Zealand Journal of Geology & Geophysics, 16(3): 781-792.

Kohn, B.P. and Topping, W.W., (1978). Time-space relationships between Late Quaternary rhyolitic and andesitic volcanism in southern Taupo Volcanic Zone, New-Zealand. Geological Society of America Bulletin, 89(8): 1265-1271.

Koyaguchi, T. and Ohno, M., (2001). Reconstruction of eruption column dynamics on the basis of grain size of tephra fall deposits 2. Application to the Pinatubo 1991 eruption. Journal of Geophysical Research, 106: 6513-6533.

Krippner, J.B., (2009). Ngauruhoe inner crater, volcanic processes of the 1954-1955 and 1974-1975 eruptions. Unpublished M.Sc. Thesis, University of Waikato, Hamilton, 185 pp.

Lamb, H.H., (1970). Volcanic dust in the atmosphere; with a chronology and assessment of its meteorological significance. Philosophical Transactions of the Royal Society London, 266: 425-533.

Lardy, M. and Tabbagh, A., (1999). Measuring and interpreting heat fluxes from shallow volcanic bodies using vertical temperature profiles: a preliminary test. Bulletin of Volcanology, 60: 441-447.

Le Guern, F., Tazieff, H. and Faivre-Pierret, R., (1982). An example of health hazard: people killed by gas during a phreatic eruption: Dieng Plateau (Java, Indonesia) Feb.20 1979. Bulletin of Volcanology, 45: 153-156.

Le Maitre, R.W., Batemann, P., A., D., Keller, J., Lameyre, J., Le Bas, M.L., Sabine, P.A., Scmid, R., Sorensen, H., Streckeisen, A., Woolley, A.R. and Zanettin, B., (1989). A classification of igneous rocks and glossary of terms. Blackwell Scientific Publications, Oxford, UK.

Lecointre, J.A., Neall, V.E. and Palmer, A.S., (1998). Quaternary lahar stratigraphy of the western Ruapehu ring plain, New Zealand. New Zealand Journal of Geology and Geophysics, 41(3): 225-245.

Lecointre, J.A., Hodgson, K.A., Neall, V.E. and Cronin, S.J., (2004a). Lahar-triggering mechanisms and hazard at Ruapehu Volcano, New Zealand. Natural Hazards, 31: 85-2004.

Lecointre, J.A., Neall, V.E., Wallace, R.C., Elliot, M.B. and Sparks, R., (2004b). Late quaternary evolution of the Rotoaira Basin, northern Tongariro ring plain, New Zealand. New Zealand Journal of Geology and Geophysics, 47(3): 549-565.

Legros, F., (2000). Minimum volume of a tephra fallout deposit estimated from a single isopach. Journal of Volcanology and Geothermal Research, 96(1-2): 25-32.

Leonard, G.S., Johnston, D.M., Paton, D., Christianson, A., Becker, J. and Keys, H., (2008). Developing effective warning systems: Ongoing research at Ruapehu volcano, New Zealand. Journal of Volcanology and Geothermal Research, 172(3-4): 199-215.

Lipman, P.W. and Mullineaux, D.R., (1981). The 1980 eruptions of Mount St. Helens, Washington. United States Government Printing Office, Washington, D.C., 844 pp.

Lirer, L., Munno, R., Postiglione, I., Vinci, A. and Vitelli, L., (1997). The A.D. 79 eruption as a future explosive scenario in the Vesuvian area: evaluation of associated risk. Bulletin of Volcanology 59: 112-124.

Lowe, D.J., (1980). Origin and composite nature of late Quaternary air-fall deposits, Hamilton Basin, New Zealand., Unpublished M.Sc-Thesis, University of Waikato, Hamilton.

Lowe, D.J., (1986). Revision of the age and stratigraphic relationship of Hinemaiaia Tephra and Whakatane Ash, North Island, New Zealand, using distal occurrences in organic deposits. New Zealand Journal of Geology and Geophysics, 29(1): 61-73.

Lowe, D.J. and Hogg, A.G., (1986). Tephrostratigraphy and chronology of the Kaipo Lagoon, an 11.500 year-old montane peatbog in Urewera National Park, New Zealand. Journal of Royal Society of New Zealand, 16: 25-41.

Lowe, D.J., (1988). Stratigraphy, age, composition, and correlation of Late Quaternary tephras interbedded with organic sediments in Waikato Lakes, North Island, New-Zealand. New Zealand Journal of Geology and Geophysics, 31(2): 125-165.

Lowe, D.J., (1989). Distinguishing rhyolitic and andesitic Tephras of soil parent materials for series definition. N.Z. Soil News, 37(4): 90-93.

Lowe, D.J., Shane, P.A.R., Alloway, B.V. and Newnham, R.M., (2008). Fingerprints and age models for widespread New Zealand tephra marker beds erupted since 30,000 years ago: a framework for NZ-INTIMATE Quaternary Science Reviews, 27: 95-126.

Lube, G., Cronin, S.J., Platz, T., Freundt, A., Procter, J.N., Henderson, C. and Sheridan, M.F., (2007). Flow and deposition of pyroclastic granular flows: A type example from the 1975 Ngauruhoe eruption, New Zealand. Journal of Volcanology and Geothermal Research, 161(3): 165-186.

Lube, G., Cronin, S.J. and Procter, J.N., (2009). Explaining the extreme mobility of volcanic ice slurry flows, Ruapehu volcano, New Zealand. Geology, 37(1): 15-18.

Lundstrom, C.C., Gill, J., Williams, Q. and Perfit, M.R., (1995). Mantle melting and basalt extraction by equilibrium porous flow. Science, 270(5244): 1958-1961.

MacDonald, G.A., (1972). Volcanoes. Prentice-Hall inc., Englewood Cliffs, New Jersey, 510 pp.

MacKinnon, I.D.R., Gooding, J.L., McKay, D.S. and Clanton, U.S., (1983). The El Chichón stratospheric cloud: Solid particulates and settling rates. Journal of Volcanology and Geothermal Research, 23(1-2): 125-146.

Manville, V., Hodgson, K.A. and White, J.D.L., (1998). Rheological properties of a remobilised-tephra lahar associated with the 1995 eruptions of Ruapehu volcano, New Zealand. New Zealand Journal of Geology and Geophysics, 41: 157-164.

Manville, V. and Cronin, S.J., (2007). Break-out Lahar from New Zealand's Crater Lake. EOS, 88(43): 441-442.

Martelli, K.M., (2007). Computer Modelling of the potential hazard from scoria and asf flows on Mt. Ngauruhoe, Tongariro Volcanic Centre, New Zealand. Unpublished Ph.D. Thesis, Massey University, Palmerston North, 160 pp.

Massey, C.I., Manville, V., Hancox, G.H., Keys, H.J., Lawrence, C. and McSaveney, M., (2009). Out-burst flood (lahar) triggered by retrogressive landsliding, 18 March 2007 at Mt. Ruapehu, New Zealand—a successful early warning. Landslides, Springer Verlag 2009.

Mathews, W.H., (1967). A contribution to geology of Mount Tongariro Massif, North Island, New Zealand. New Zealand Journal of Geology and Geophysics, 10(4): 1027-&.

McDermott, F. and Hawkesworth, C.J., (1991). Th, Pb and Sr isotopic variations in young island arc volcanics and oceanic sediments. Earth and Planetary Science Letters, 104: 1-15.

McGlone, M.S. and Topping, W.W., (1977). Aranuian (Postglacial) Pollen diagrams from Tongariro Region, North Island, New Zealand. New Zealand Journal of Botany, 15(4): 749-&.

McGlone, M.S. and Topping, W.W., (1983). Late Quaternary vegetation, Tongariro Region, Central North Island, New Zealand. New Zealand Journal of Botany, 21(1): 53-76.

Meeker, G.P. and Hinkley, T.K., (1993). The structure and composition of microspheres from the Kilauea Volcano, Hawaii. American Mineralogist, 78(7-8): 873-876.

Mitchell, A., (1997). Geology of Scoria Flat. unpublished B.Sc (Hons) Thesis, Massey University, Palmerston North, 25 pp.

Moebis, A., Cronin, S.J., Lube, G., Neall, V.E. and Nemeth, K., (2008). Fingerprinting of volcanic glasses unravels the volcanic history of Ngauruhoe volcano, New Zealand, abstract at the annual joint conference of the Geological and Geophysical Societies of New Zealand, Wellington.

Molloy, L., (1998). Soils in the New Zealand landscape, the living mantle. Mallinson Rendel Publisher Ltd, Wellington.

Morrissey, M., Zimanowski, B., Wohletz, K. and Buettner, R., (2000). Phreatomagmatic Fragmentation. In: H. Sigurdsson (Editor), Encyclopedia of Volcanoes. Academic Press, San Diego, pp. 431-445.

Morrissey, M.M. and Mastin, L.G., (2000). Vulcanian eruptions. In: H. Sigurdsson (Editor), Encyclopedia of volcanoes. Academic Press, San Diego, pp. 463-475.

N.Z. Meteorological Service Miscellaneous Publications 145, (1973).

N.Z. Meteorological Service Miscellaneous Publications 177, (1980).

Nairn, I.A., (1976). Atmospheric Shock-Waves and Condensation Clouds from Ngauruhoe Explosive Eruptions. Nature, 259(5540): 190-192.

Nairn, I.A., Hewson, C.A.Y., Latter, J.H. and Wood, C.P., (1976). Pyroclastic eruptions of Ngauruhoe Volcano, central North Island, New Zealand, 1974 January and March. In: R.W. Johnson (Editor) Volcanism in Australasia. Elsevier, Amsterdam, pp 385-405.

Nairn, I.A. and Self, S., (1978). Explosive eruptions and pyroclastic avalanches from Ngauruhoe in February 1975. Journal of Volcanology and Geothermal Research, 3(1-2): 39-60.

Nairn, I.A., Wood, C.P. and Hewson, C.A.Y., (1979). Phreatic eruptions of Ruapehu - April 1975. New Zealand Journal of Geology and Geophysics, 22(2): 155-170.

Nairn, I.A., Kobayashi, T. and Nakagawa, M., (1998). The similar to 10 ka multiple vent pyroclastic eruption sequence at Tongariro Volcanic Centre, Taupo Volcanic Zone, New Zealand: Part 1. Eruptive processes during regional extension. Journal of Volcanology and Geothermal Research, 86(1-4): 19-44.

Nakagawa, M., Nairn, I.A. and Kobayashi, T., (1998). The similar to 10 ka multiple vent pyroclastic eruption sequence at Tongariro Volcanic Centre, Taupo Volcanic Zone, New Zealand - Part 2. Petrological insights into magma storage and transport during regional extension. Journal of Volcanology and Geothermal Research, 86(1-4): 45-65.

Nakagawa, M., Wada, K., Thordarson, T., Wood, C.P. and Gamble, J.A., (1999). Petrologic investigations of the 1995 and 1996 eruptions of Ruapehu volcano, New Zealand: formation of discrete and small magma pockets and their intermittent discharge. Bulletin of Volcanology, 61(1-2): 15-31.

Neall, V.E., (1972). Tephrochronology and tephrostratigraphy of western Taranaki (N108-109), New Zealand. New Zealand Journal of Geology and Geophysics, 15: 507-57.

Neall, V.E., (1977). Genesis and Weathering of Andosols in Taranaki, New Zealand. Soil Science, 123(6): 400-408.

Neall, V.E., Stewart, R.B. and I.E.M., S., (1986). History and petrology of the Taranaki volcanoes. In: Smith, I.M.E. (ed) Late Cenozoic volcanism. Royal Society of New Zealand Bulletin, 23: 251-263.

Neall, V.E., (1996). Hydrological disasters associated with volcanoes. In: V.P. Singh (Editor), Hydrology of disasters. Kluwer Academic Publisher, Dordrecht, pp. 395-425.

Neall, V.E., (2006). Volcanic soils, in Land Cover and Land Use (Ed. Willy Verheye), in Encyclopedia of Life Support Systems (EOLSS), developed under the auspices of the UNESCO, EOLSS Publishers, Oxford, UK. (http://www.eolss.net).

Neall, V.E. and Trewick, A., (2008). The age and origin of the Pacific islands: a geological overview. Philosophical Transactions of the Royal Society B, 363: 3293-3308.

Nemeth, K., Cronin, S.J., Charley, D., Harrison, M. and Garae, E., (2006). Exploding lakes in Vanuatu - "Surtseyan-style" eruptions witnessed on Ambae Island. Episodes, 29(2): 87-92.

Nemeth, K. and Martin, U., (2007). Practical Volcanology, Lecture notes for understanding volcanic rocks from field based studies. Geological Institute of Hungary, Budapest, 221 pp.

Newhall, C.G. and Self, S., (1982). The Volcanic Explosivity Index (VEI) - an Estimate of Explosive Magnitude for Historical Volcanism. Journal of Geophysical Research-Oceans and Atmospheres, 87(NC2): 1231-1238.

Newhall, C.G., Bronto, S., Alloway, B., Banks, N.G., Bahar, I., del Marmol, M.A., Hadisantono, R.D., Holcomb, R.T., McGeehin, J., Miksic, J.N., Rubin, M., Sayudi, S.D., Sukhyar, R., Andreastuti, S., Tilling, R.I., Torley, R., Trimble, D. and Wirakusumah, A.D., (2000). 10,000 Years of explosive eruptions of Merapi Volcano, Central Java: archaeological and modern implications. Journal of Volcanology and Geothermal Research 100: 9-50.

Odell, N.E., (1955). Mount Ruapehu, New Zealand, Observations on its Crater Lake and Glaciers. Journal of Glaciology.

Oliver, R.L., (1945). Further Activity of Mt. Ruapehu May-July, 1945. N.Z. Journal of Science and Technology: 24-33.

Ollier, C.D., (1974). Phreatic eruptions and maars. In: L. Civetta, and et.al. (Editor), Physical Volcanology. Elsevier, New York, pp. 289-310.

Oppenheimer, C., Bani, P., Calkins, J.A., Burton, M.R. and Sawyer, G.M., (2006). Rapid FTIR sensing, of volcanic gases released by strombolian explosions at Yasur Volcano, Vanuatu. Applied Phys.B 85: 453-460.

Pardo, N., Macias, J.L., Giordano, G., Cianfarra, P., Avellan, D.R. and Bellatreccia, F., (2009). The ~1245 yr BP Asososca maar eruption: The youngest event along the Nejapa–Miraflores volcanic fault, Western Managua, Nicaragua. Journal of Volcanology and Geothermal Research, 184: 292-312.

Parish, A., (1994). Petrology and Provenance of the O'Leary Conglomerate, North East Wanganui, New Zealand. Unpublished B.Sc. Thesis, Thesis, Victoria University of Wellington, Wellington, 89 pp.

Parson, L.M. and Wright, I.C., (1996). The Lau-Havre-Taupo back-arc basin: A southward-propagating, multi-stage evolution from rifting to spreading. Tectonophysics, 263(1-4): 1-22.

Pillans, B., (1990). Late Quaternary marine terraces South Taranaki-Wanganui. New Zealand Geological Survey Miscellaneous series map, 18: 47 pp.

Pillans, B., McGlone, M., Palmer A, Mildenhall, D., Alloway, B. and Glenn Berger, G., (1993). The last glacial maximum in central and southern North Island, New Zealand: a paleoenvironmental reconstruction using the Kawakawa Tephra Formation as a chronostratigraphic marker Palaeogeography, Palaeoclimatology, Palaeoecology, 1(3-4): 283-304.

Pioli, L., Erlund, E., Johnson, E., Cashman, K., Wallace, R., Rosi, M. and Granados, H.D., (2008). Explosive dynamics of violent Strombolian eruptions: The eruption of Paricutin Volcano 1943-1952 (Mexico). Earth and Planetary Science Letters, 271(1-4): 359-368.

Platz, T., (2007). Understanding aspects of andesitic dome-forming eruptions through the last 1000 yrs. of volcanism at Mt. Taranaki, New Zealand. Unpublished Ph.D.- Thesis, Massey University, Palmerston North, 265 pp.

Platz, T., Cronin, S.J., Smith, I.E.M., Turner, M.B. and Stewart, R.B., (2007). Improving the reliability of microprobe-based analyses of andesitic glasses for tephra correlation. The Holocene, 17(5): 573-583.

Polacci, M., Corsaro, R.A. and Andronico, D., (2006). Coupled textural and compositional characterization of basaltic scoria: Insights into the transition from Strombolian to fire fountain activity at Mount Etna, Italy Geology, 34(3): 201-204.

Ponomareva, V.V., Pevzner, M.M. and Melekestsev, I.V., (1998). Large debris avalanches and associated eruptions in the Holocene eruptive history of Shiveluch Volcano, Kamchatka, Russia Bulletin of Volcanology, 59(7): 490-505.

Price, R.C., Stewart, R.B., Woodhead, J.D. and Smith, I.E.M., (1999). Petrogenesis of high-K arc magmas: Evidence from Egmont Volcano, North Island, New Zealand. Journal of Petrology, 40(1): 167-197.

Price, R.C., Gamble, J.A., Smith, I.E.M., Stewart, R.B., Eggins, S. and Wnight, I.C., (2005). An integrated model for the temporal evolution of andesites and rhyolites and crustal development in New Zealand's North Island. Journal of volcanology and geothermal research, 140(1-3): 1-24.

Procter, J.N., (2003). The quaternary geology of the southeastern sector of Ruapehu volcano. Unpublished Ms.S Thesis, Massey University, Palmerston North.

Procter, J.N., (2009). Towards improving volcanic mass flow hazard assessment at New Zealand stratovolcanoes. Unpublished Ph.D. Thesis, Massey University, Palmerston North, 302 pp.

Procter, J.N., Cronin, S.J., Fuller, I.C., Lube, G. and Manville, V., (2010). Quantifying the geomorphic impacts of a lake-breakout lahar, Mount Ruapehu, New Zealand. Geology, 38: 67-70.

Pullar, W.A. and Heine, J.C., (1971). Ages, inferred from 14C dates, of some tephra and other deposits from Rotorua, Taupo, Bay of Plenty, Gisborn and Hawke's Bay districts, Proceedings of Radiocarbon Users Conference, Wellington, pp. 119-138.

Pullar, W.A., Birrell, K.S. and Heine, J.C., (1973). Named tephras and tephra formations occurring in Central North-Island, with notes on derived soils and buried paleosols. New Zealand Journal of Geology and Geophysics, 16(3): 497-518.

Purves, A.M., (1990). Landscape Ecology of the Rangipo Desert. Unpublished Ph.D.-Thesis, Massey University, Palmerston North, 277 pp.

Pyle, D.M., (1989). The Thickness, Volume and Grainsize of Tephra Fall Deposits. Bulletin of Volcanology, 51(1): 1-15.

Pyle, D.M., (2000). Size of volcanic eruptions. In: H. Sigurdsson, B.F. Houghton, W.F. Mc Donough, H. Rymer and J. Stix (Editors), Encyclopedia of volcanoes. Academic Press, San Diego, pp. 263-270.

Rankin, P.C., (1973). Correlation of Volcanic Glasses in Tephras and Soils Using Microelement Compositions. New Zealand Journal of Geology and Geophysics, 16(3): 637-641.

Reed, J.J., (1945). Activity at Ruapehu, March-April 1940. N.Z. Journal of Science and Technology: 17-23.

Reyners, M., Eberhart-Phillips, D., Stuart, G. and Nishimura, Y., (2006). Imaging subduction from the trench to 300 km depth beneath the central North Island, New Zealand, with Vp and Vp/Vs. Geophysical Journal International, 165(2): 565-583.

Rolandi, G., Barrella, A.M. and Borrelli, A., (1993). The 1631 Eruption of Vesuvius. Journal of Volcanology and Geothermal Research, 58(1-4): 183-201.

Rollinson, H.R., (1993). Using Geochemical Data: Evaluation, Presentation, Interpretation. Longman Group Uk Limited, 352 pp.

Rose, W.I., Bonis, S., Stoiber, R.E., Keller, M. and Bickford, T., (1973). Studies of volcanic ash from two recent Central American eruptions. Bulletin of Volcanology, 37: 338-364.

Rosenberg, M.D., (2000). The Whakapapaiti lahar: a snow-rich debris flow fro th 23rd September 1995 eruption of Mt Ruapehu,. Science Report of Geological & Nuclear Sciences, 30: 34 pp.

Rosi, M., Bertagnini, A. and Landi, P., (2000). Onset of the persitsent activity at Stromboli volcanoe (Italy). Bulletin of Volcanology, 62: 294-300.

Rowe Jr., G.L., Ohsawa, S., Takano, B., Brantley, S.L., Fernandez, J.F. and Barquero, J., (1992). Using Crater Lake chemistry to predict volcanic activity at Poás Volcano, Costa Rica Bulletin of Volcanology, 54(6): 494-503.

Rowland, J.V. and Sibson, R.H., (2001). Extensional fault kinematics within the Taupo Volcanic Zone, New Zealand: soft-linked segmentation of a continental rift system. New Zealand Journal of Geology & Geophysics, 44: 271-283.

Ruapehu Alpine Lifts Limited, (2009). Annual report. 26 pp.

Sarna-Wojcicki, A.M., Shipley, S., Waitt, R.B., Dzurisin, D. and Wood, S.H., (1981). Areal Distribution, thickness, mass, volume, and grain size of air-fall ash from the six major eruptions of 1980. In: P.W. Lipman and D.R. Mullineaux (Editors), The 1980 eruptions of Mount St. Helens, Washington, pp. 577-600.

Saunders, A.D., Norry, M.J. and Tarney, J., (1988). Origin of MORB and chemically depleted mantle reservoirs: trace element constraints. Journal of Petrology, Special Lithosphere Issue: 415-445.

Scandone, R. and Malone, S.D., (1984). Magma supply, magma discharge and readjustment of the feeding system of Mt. St. Helens during 1980. Journal of Geothermal Research 23: 239-262.

Schmincke, H.U., Park, C. and Harms, E., (1999). Evolution and environmental impacts of the eruption of Laacher See Volcano (Germany) 12,900 a BP Quaternary International, 61(1): 61-72.

Schmincke, H.U., (2000). Vulkanismus. Wissenschaftliche Buchgesellschaft, Darmstadt, 264 pp.

Scolamacchia, T. and Macias, J.L., (2005). Distribution and stratigraphy of deposits produced by diluted pyroclastic density currents of the 1982 eruption of El Chichon volcano, Chiapas, Mexico. Revista Mexicana De Ciencias Geologicas, 22(2): 159-180.

Self, S., Sparks, R., Booth, B. and Walker, G.P.L., (1974). The 1973 Heimaey Strombolian Scoria deposit, Iceland. Geological Magazine, 111(6): 539-548.

Self, S., (1975). Explosive Activity of Ngauruhoe, 27-30 March 1974. New Zealand Journal of Geology and Geophysics, 18(1): 189-195.

Self, S., Wilson, L. and Nairn, I.A., (1979). Vulcanian eruption mechanisms. Nature, 277(5696): 440-443.

Self, S. and Sparks, R.S.J., (1980). Tephra Studies. D.Reidel Publishing Company.

Settle, M., (1978). Volcanic eruption clouds and thermal power output of explosive eruptions. Journal of Volcanology and Geothermal Research, 3(3-4): 309-324.

Shane, P. and Froggatt, P.C., (1992). Composition of Widespread Volcanic Glass in Deep-Sea Sediments of the Southern Pacific-Ocean - an Antarctic Source Inferred. Bulletin of Volcanology, 54(7): 595-601.

Shane, P. and Froggatt, P.C., (1994). Discriminant Function Analysis of Glass Chemistry of New Zealand and North American Tephra Deposits Quaternary Research 41(1): 70-81.

Shane, P., (1998). Correlation of rhyolitic pyroclastic eruptive units from the Taupo volcanic zone by Fe-Ti oxide compositional data. Bulletin of Volcanology, 60(3): 224-238.

Shane, P., Black, T., Eggins, S. and Westgate, J., (1998). Late Miocene marine tephra beds: recorders of rhyolitic volcanism in North Island, New Zealand. New Zealand Journal of Geology and Geophysics, 41(2): 165-178.

Shane, P., (2000). Tephrochronology: a New Zealand case study. Earth-Science Reviews 49, 49: 223-259.

Shane, P. and Hoverd, J., (2002). Distal record of multi-sourced tephra in Onepoto Basin, Auckland, New Zealand: implications for volcanic chronology, frequency and hazards. Bulletin of Volcanology, 64: 441-454.

Shane, P., Martin, S.B., Smith, V.C., Beggs, K.F., Darragh, M.B., Cole, J.W. and Nairn, I.A., (2007). Multiple rhyolite magmas and basalt injection in the 17.7 ka

Rerewhakaaitu eruption episode from Tarawera volcanic complex, New Zealand. Journal of Volcanology and Geothermal Research 164: 1-26.

Shane, P., Doyle, L.R. and Nairn, I.A., (2008). Heterogeneous andesite-dacite ejecta in 26-16.6 ka pyroclastic deposits of Tongariro Volcano, New Zealand: the product of multiple magma-mixing events. Bulletin of Volcanology, 70(4): 517-536.

Sharp, T.G., Stevenson, R.J. and Dingwell, D.B., (1996). Microlites and "nanolites" in rhyolitic glass: Microstructural and chemical characterization. Bulletin of Volcanology, 57(8): 631-640.

Sheridan, M.F. and Wohletz, K.H., (1983). Hydrovolcanism - Basic Considerations and Review. Journal of Volcanology and Geothermal Research, 17(1-4): 1-29.

Sigurdsson, H., Cashdollar, S. and Sparks, S.R.J., (1982). The eruption of Vesuvius in AD 79: reconstruction from historical and volcanological evidence. American Journal of Archaeology, 86(1): 39-51.

Silvester, W., Singers, N. and Keys, H., (2009). Use of Fire for Ecological Management in Tongariro National, Department of Conservation, Turangi.

Simkin, T., Seibert, L., McClelland, L., Melson, W.G., Bridge C., Newhall, C.G. and Latter, J., (1981). Volcanoes of the world. Hutchinson Ross, New York.

Simkin, T., Fiske, R.S. and Melcher, S., (1983). Krakatau, 1883--the volcanic eruption and its effects. Smithsonian Institution Press, Washington D.C., 464 pp.

Smith, V.C., Shane, P. and Nairn, I.A., (2005). Trends in rhyolite geochemistry, mineralogy, and magma storage during the last 50 kyr at Okataina and Taupo Volcanic Centres, Taupo Volcanic Zone, New Zealand. Journal of Volcanology and Geothermal Research, 148: 372-406.

Spadaro, F.R., Lefevre, R.A. and Ausset, P., (2002). Experimental rapid alteration of basaltic glass: Implications for the origins of atmospheric particulates. Geology, 30(8): 671-674.

Sparks, R.S.J. and Wilson, L., (1976). A model for the formation of ignimbrite by graviational column collapse. Journal of Geological Society, London, 132(4): 441-451.

Sparks, R.S.J., (1978). The dynamics of bubble formation and growth in magmas: A review and analysis. Journal of Volcanology and Geothermal Research, 3(1-2): 1-37.

Sparks, R.S.J., (1986). The dimensions and dynamics of volcanic eruptio columns. Bulletin of Volcanology, 48: 3-15.

Sparks, R.S.J., Bursik, M.I., Ablay, G.J., Thomas, R.M.E. and Carey, S.N., (1992). Sedimentation of Tephra by Volcanic Plumes .2. Controls on Thickness and Grain-Size Variations of Tephra Fall Deposits. Bulletin of Volcanology, 54(8): 685-695.

Sparks, R.S.J., Melhuish, W.H., McKee, J.W.A., Ogden, J., Palmer, J.G. and Molloy, B.P.J., (1995). C-14 calibration in the southern hemisphere and the date of the last Taupo eruption: Evidence from tree-ring sequences. Radiocarbon, 37(2): 155-163.

Speight, R., (1908). Geology. *In:* Cockayne, L., :Report on a botanical survey of the Tongariro National Park. Append. J. House Repres. N.Z. C-11: 7-13.

Spence, R.J.S., Baxter, P.J. and Zuccaro, G., (2004). Building vulnerability and human casualty estimation for a pyroclastic flow: a model and its application to Vesuvius. Journal of Volcanology and Geothermal Research 133: 321-343.

Stevens, N.F., (2002). Emplacement of the large andesite lava flow in the Oturere Stream valley, Tongariro Volcano, from airborne interferometric radar. New Zealand Journal of Geology and Geophysics, 45(3): 387-394.

Stilwell, W.F., Hopkins, H.J. and Appleton, W., (1954). Derailment of Wellington-Auckland Express at Whangaehu River bridge between Tangiwai and Karioi railways stations on 24 December 1953.,Inquiry report, Wellington, pp 3-31.

Stipp, J.J., (1968). The geochronology and petrogenesis of the Cenozoic volcanics of North Island, New Zealand. Unpublished Ph.D. Thesis, Australian National University, Canberra, 488 pp.

Stix, J., Torres, R.C., Narváez, L., G.P., C., J.A., R., M., G. and Castonguay, R., (1997). A model of vulcanian eruptions at Galeras volcano, Colombia Journal of Volcanology and Geothermal Research, 77(1-4): 285-303.

Stokes, S., Lowe, D.J. and Froggatt, P.C., (1992). Discriminant function analysis and correlation of late Quaternary rhyolitic tephra deposits from Taupo and Okataina volcanoes, New Zealand, Using glass shard major element composition. Quaternary International, 13/14: 103-117.

Stratford, W.R. and Stern, T.A., (2006). Crust and upper mantle structure of a continental backarc: central North Island, New Zealand. Geophysical Journal International, 166(1): 469-484.

Sulpizio, R., (2005). Three empirical methods for the calculation of distal volume of tephra-fall deposits. Journal of Volcanology and Geothermal Research 145: 315-336.

Sulpizio, R., Mele, D., Dellino, P. and La Volpe, L., (2005). A complex, Subplinian-type eruption from low-viscosity, phonolitic to tephri-phonolitic magma: the AD 472 (Pollena) eruption of Somma-Vesuvius, Italy Bulletin of Volcanology, 67: 743-767.

Suzuki, T., (2006). Analysis of titanomagnetite within weathered middle Pleistocene KMT tephra and its application for fluvial terrace chronology, Kanto Plain, central Japan Quaternary International, 178(1): 119-127.

Taylor, B., (2006). The single largest oceanic plateau: Ontong Java–Manihiki–Hikurangi Earth and Planetary Science Letters, 241(3-4): 372-380

Thomas, A.P.W., (1889). Notes on the Geology of the Tongariro and Taupo district. Transaction of the New Zealand Institute 21: 338-53 In: Topping W.W. (1973): Tephrostratigraphy and Chronology of Late Quaternary Eruptives from the Tongariro Volcanic Centre, New Zealand, N.Z. Journal of Geology and Geophysics(16): 397-423.

Thompson, B.N., Kermode, L.O. and Ewart, A., (1966). New Zealand Volcanology, Central Volcanic Region.

Thompson, C.S., (1984). The weather and climate of the Tongariro region. N.Z. Meteorological Service Miscellaneous Publication, 115(14): 1-35.

Thompson, J.B., (1926). Tongariro National Park, Report of the Board. Append. J. House Repres. N.Z. C-13: 7 pp.

Thompson, J.B., (1928). Tongariro National Park, Report of the Board. Append. J. House Repres. N.Z., C-13: 5pp.

Thorarinsson, S. and Sigvaldason, G.E., (1972). The Hekla eruption of 1970. Bulletin of Volcanology, 36(2): 269-288.

Tongariro Natural History Society, (1996). Common alpine and forest plants of Tongariro National Park. Tongariro Natural History Society, 44 pp.

Topping, W.W., (1973). Tephrostratigraphy and Chronology of Late Quaternary Eruptives from Tongariro-Volcanic-Centre, New-Zealand. New Zealand Journal of Geology and Geophysics, 16(3): 397-423.

Topping, W.W. and Kohn, B.P., (1973). Rhyolitic Tephra Marker Beds in Tongariro Area, North-Island, New-Zealand. New Zealand Journal of Geology and Geophysics, 16(3): 375-395.

Topping, W.W., (1974). Some aspects of Quaternary history of Tongariro Volcanic Centre. Unpublished Ph.D.- Thesis, Victoria University, Wellington.

Tsuya, H., (1955). Geological and petrological studies of volcano Fuji. Tokyo Daigaku Jishin Kenkyusho Iho, 33: 341-382.

Turner, M.B., (2008). Eruption cycles and magmatic processes at a reawakening volcano, Mt. Taranaki, New Zealand. Unpublished Ph.D.-Thesis, Massey University, Palmerston North.

Turner, M.B., Cronin, S.J., Bebbington, M.S. and Platz, T., (2008a). Developing probabilistic eruption forecast for dormant volcanoes; a case study from Mt Taranaki, New Zealand Bulletin of Volcanology, 70: 507-515.

Turner, M.B., Cronin, S.J., Stewart, R.B., Bebbington, M. and Smith, I.E.M., (2008b). Using titanomagnetite textures to elucidate volcanic eruption histories. Geology, 36(1): 31-34.

Turner, M.B., Bebbington, M., Cronin, S.J. and Stewart, R.B., (2009). Merging eruption datasets: building an integrated Holocene eruptive record for Mt Taranaki, New Zealand Bulletin of Volcanology, 71(8): 903-918.

Turner, S. and Costa, F., (2007). Measuring timescales of magmatic evolution. Elements, 3(4): 267-272.

Valentine, G.A., Krier, D., Perry, F.V. and Heiken, G., (2005). Scoria cone construction mechanisms, Lathrop Wells volcano, southern Nevada, USA. Geology, 33(8): 629-932.

Valentine, G.A., Kriera, D.J., Perrya, F.V. and Heiken, G., (2007). Eruptive and geomorphic processes at the Lathrop Wells scoria cone volcano Journal of Volcanology and Geothermal Research, 161(1-2): 57-80.

Vergniolle, S. and Mangan, M., (2000). Hawaiian and strmbolian eruptions. In: H. Sigurdsson (Editor), Encyclopedia of Volcanoes. Academic Press, San Diego, pp. 447-461.

Villamor, P. and Berryman, K., (2001). A late Quaternary extension rate in the Taupo Volcanic Zone, New Zealand, derived from fault slip data. New Zealand Journal of Geology & Geophysics, 44: 243-169.

Villamor, P. and Berryman, K.B., (2006). Evolution of the southern termination of the Taupo Rift, New Zealand. New Zealand Journal of Geology & Geophysics, 49: 1-21.

Vucetich, C.G. and Pullar, W.A., (1964). Stratigraphy and Chronology of Late Quaternary Volcanic Ash in Taupo, Rotorua, and Gisborne Districts, Part 2. New Zealand Geological Survey, 73: 43-81.

Vucetich, C.G. and Pullar, W.A., (1969). Stratigraphy and Chronology of Late Pleistocene Volcanic Ash Beds in Central North Island, New Zealand. New Zealand Journal of Geology and Geophysics, 12(4): 784-&.

Vucetich, C.G. and Pullar, W.A., (1973). Holocene Tephra Formations Erupted in Taupo-Area, and Interbedded Tephras from Other Volcanic Sources. New Zealand Journal of Geology and Geophysics, 16(3): 745-&.

Walker, G.P.L., (1971). Grain-size characteristics of pyroclastic deposits. Journal of Geology, 79(6): 696-&.

Walker, G.P.L., (1973). Explosive volcanic eruptions - a new classification scheme. Geologische Rundschau, 62: 431-446.

Walker, G.P.L., (1980). The Taupo Pumice - Product of the Most Powerful Known (Ultraplinian) Eruption. Journal of Volcanology and Geothermal Research, 8(1): 69-94.

Walker, G.P.L., (1981). The Waimihia and Hatepe plinian deposits from the rhyolitic Taupo Volcanic Centre. New Zealand Journal of Geology and Geophysics, 24(3): 305-324.

Walker, G.P.L., Self, S. and Wilson, L., (1984). Tarawera 1886, New Zealand - A Basaltic plinian fissure eruption. Journal of Volcanology and Geothermal Research, 21(1-2): 61-78.

Wallace, L.M., Beavan, J., McCaffrey, R. and Darby, D., (2004). Subduction zone coupling and tectonic block rotations in the North Island, New Zealand. Journal of Geophysical Research-Solid Earth, 109(B12).

Wehrmann, H., (2005). Volatile degassing and plinian eruption dynamics of the mafic Fontana Tephra, Nicaragua. Unpublished Ph.P. Thesis, Christian-Albrechts-Universit¨at, Kiel, 113 pp.

Werner, C., Christenson, B.W., Hagerty, M. and Britten, K., (2006). Variability of volcanic gas emissions during a crater lake heating cycle at Ruapehu Volcano, New Zealand. Journal of Volcanology and Geothermal Research, 154(3-4): 291-302.

Wiesner, M.G., Wetzel, A., Catane, S.G., Listanco, E.L. and Mirabueno, H.T., (2004). Grain size, areal thickness distribution and controls on sedimentation of the 1991 Mount Pinatubo tephra layer in the South China Sea Bulletin of Volcanology, 66(3): 226-242.

Williams, K., (1989). Volcanoes of the south wind, a field guide to the volcanoes landscape of Tongariro National Park. Tongariro Natural History Society, Wellington.

Wilson, C.J.N. and Walker, G.P.L., (1985). The Taupo Eruption, New Zealand I. General Aspects. Philosophical Transactions of the Royal Society of London. Series A, Mathematical and Physical Sciences, 314(1529): 199-228.

Wilson, C.J.N., (1993). Stratigraphy, chronology, styles and dynamics of Late Quaternary eruptions from Taupo Volcano, New Zealand. Philosophical Transactions: Physical Sciences and Engineering, 343(1668): 205-306.

Wilson, C.J.N., Houghton, B.F., McWilliams, M.O., Lanphere, M.A., Weaver, S.D. and Briggs, R.M., (1995). Volcanic and structural evolution of Taupo Volcanic Zone, New Zealand: a review. Journal of Volcanology and Geothermal Research, 68: 1-28.

Wilson, C.J.N., (2001). The 26.5 ka Oruanui eruption, New Zealand: an introduction and overview. Journal of Volcanology and Geothermal Research, 112(1-4): 133-174.

Wilson, L., Sparks, R.S.J., Huang, T.C. and Watkins, N.D., (1978). The control of volcanic column heights by eruption energetics and dynamics. Journal of Geophysical Research, 83(NB4): 1829-1836.

Wohletz, K. and Krinsley, D., (1982). Scanning Electron Microscopy of basaltic hydromagnetic ash. University of California, Los Alamaos.

Wohletz, K., (1983). Mechanisms of hydrovolcanic pyroclast formation - grain-size, Scanning Electron-Microscopy, and experimental studies. Journal of Volcanology and Geothermal Research, 17(1-4): 31-63.

Wohletz, K. and Heiken, G., (1991). Volcanology and geothermal energy,. University of California Press, Barkley, CA.

Wohletz, K., (2001). Pyroclastic surges and compressible two-phase flow. In: A. Freundt and M. Rosi (Editors), From magma to tephra. Elsevier, Amsterdam, pp. 247-312.

Wohletz, K., (2002). Water/magma interaction: some theory and experiments on peperite formation. Journal of Volcanology and Geothermal Research, 114(1-2): 19-35.

Wong, L.J. and Larsen, J.F., (2010). The Middle Scoria sequence: A Holocene violent strombolian, subplinian and phreatomagmatic eruption of Okmok volcano, Alaska. Bulletin of Volcanology, 72(1): 17-31.

Yokoi, M., Kobayashi, K., Manabe, T., Takahashi, T., Sakaguchi, I., Katsuura, G., Shigemoto, R., Ohishi, H., Nomura, S., Nakamura, K., Nakao, K., Katsuki, M. and Nakanishi, S., (1996). Mechanism of phreatic eruptions at Aso Volcano inferred from near-field broadband seismic observations. Science, 273: 642-645.

Yokoo, A., Tameguri, T. and Iguchi, M., (2009). Swelling of a lava plug associated with a Vulcanian eruption at Sakurajima Volcano, Japan, as revealed by infrasound record: case study of the eruption on January 2, 2007 Bulletin of Volcanology, 71: 619-630.

Yokoyama, I., (1956). Energetics in active volcanoes 1. Tokyo Daigaku Jishin Kenkyusho Iho, 34: 185-195.

Yokoyama, I., (1957). Energetics in active volcanoes 2-3. Tokyo Daigaku Jishin Kenkyusho Iho, 35: 75-107.

Zellmer, G.F., Sparks, R.S.J., Hawkesworth, C.J. and Wiedenbeck, M., (2003). Magma emplacement and remobilisation timescales beneath Montserrat: Insights from Sr and Ba zonation in plagioclase phenocrysts. Journal of Petrology, 44(8): 1413-1431.

List of Appendices

Appendices (on disc)

Appendix 1

List of field descriptions and photos of selected locations

Appendix 2

Electron microprobe glass and titanomagnetite analysis of

- Tufa Trig Formation
- Ngauruhoe Formation
- Mangatawai Formation
- Papakai Formation
- Mangamate Formation
- Te Maari Craters
- Mt Taranaki
- Reference samples for Ruapehu, Ngauruhoe and Red Crater

Appendix 3

Grain size analysis (LPA) of selected samples from Locations 12, 63, 67, and 68 along with samples of the dark and pale purple layers.

Appendix 4

Componentry (Point counts) of individual tephras sourced from Ruapehu, Ngauruhoe and Red Crater.

Appendix 5

Age calculations for Ruapehu, Red Crater and Ngauruhoe-sourced tephras based on soil accumulation rates, age calculations of tephras within the sediment core Lake Rangatauanui (spline fit), and volume calculations for Ngauruhoe-derived tephras.

Appendix 6

Radiocarbon dates from the Rafter Radiocarbon Laboratory at the GNS Science in Lower Hutt.

Appendix 7

Images of Scanning Electron Microscopy (SEM)

Northern Tongariro with Red Crater and three Emerald Lakes (lower left hand corner), North Crater (left side, back) and Blue Lake (right side); photographer: Eckhard Möbis.